Lecture Notes on
Topics in Accelerator Physics

Alex Chao
Stanford Linear Accelerator Center

These are lecture notes that cover a selection of topics, some of them under current research, in accelerator physics. I try to derive the results from first principles, although the students are assumed to have an introductory knowledge of the basics. The topics covered are:

1. Panofsky-Wenzel and Planar Wake Theorems
2. Echo Effect
3. Crystalline Beam
4. Fast Ion Instability
5. Lawson-Woodward Theorem and Laser Acceleration in Free Space
6. Spin Dynamics and Siberian Snakes
7. Symplectic Approximation of Maps
8. Truncated Power Series Algebra
9. Lie Algebra Technique for nonlinear Dynamics

The purpose of these lectures is not to elaborate, but to prepare the students so that they can do their own research. Each topic can be read independently of the others.

Many useful comments and help at the lecturing from Gennady Stupakov of SLAC and Jeff Holmes of ORNL are greatly appreciated.

1 Panofsky-Wenzel and Planar Wake Theorems

1.1 Concept of Wakefields

To a large degree, accelerator physics and plasma physics are quite similar. Both involve nonlinear dynamics (single-particle effects) and collective instabilities (multi-particle effects). However, there is an important difference:

$$\text{beam self fields} > \text{external applied fields} \qquad \text{(plasma)}$$
$$\text{beam self fields} \ll \text{external applied fields} \qquad \text{(accelerators)}$$

This difference means perturbation techniques are applicable to accelerators with

$$\text{unperturbed motion} = \text{external fields},$$
$$\text{perturbation} = \text{self fields, or "wakefields"}$$

In fact, in accelerator physics, a first order perturbation often suffices.

It is important to appreciate the fact that our instability analysis in accelerators is based on the validity of this perturbation technique. In particular, the concept of wakefields is based on the validity of this perturbation technique as applied to high energy accelerators – the words "high energy" are critical, as we will explain.

Consider a beam with distribution ψ. The dynamics of the evolution of ψ is described by the Vlasov equation,

$$\frac{\partial \psi}{\partial t} + \frac{\vec{p}}{m} \cdot \frac{\partial \psi}{\partial \vec{q}} + \vec{f} \cdot \frac{\partial \psi}{\partial \vec{p}} = 0$$
$$\vec{f} = e(\vec{E} + \frac{\vec{v}}{c} \times \vec{B}) \tag{1.1}$$

In case the beam is intense, the EM fields contain two contributions,

$$\vec{E} = \vec{E}_{\text{ext}} + \vec{E}_{\text{wake}}$$
$$\vec{B} = \vec{B}_{\text{ext}} + \vec{B}_{\text{wake}} \tag{1.2}$$

The wakefields (N is beam intensity)

$$(\vec{E}, \vec{B})_{\text{wake}} \propto N$$
$$(\vec{E}, \vec{B})_{\text{wake}} \ll (\vec{E}, \vec{B})_{\text{ext}} \tag{1.3}$$

are determined by the Maxwell equations where the source terms ρ and $\vec{j}$ are determined by the beam distribution ψ:

$$\rho = \int d^3p \; \psi, \qquad \vec{j} = \int d^3p \; \vec{v}\psi \tag{1.4}$$

We therefore have the situation when the beam distribution is described by the Vlasov equation whose force terms are given by the electromagnetic

fields, while the electromagnetic fields are described by the Maxwell equations whose source terms are given by the beam distribution. It is clear that a full treatment of the beam-wakefield system requires solving a coupled "Vlasov-Maxwell equation".

Most wakefields are generated by beam-structure interaction. Figure 1.1 shows no wakefields when the beam pipe is smooth and perfectly conducting, while a structure causes wakefields to be generated.
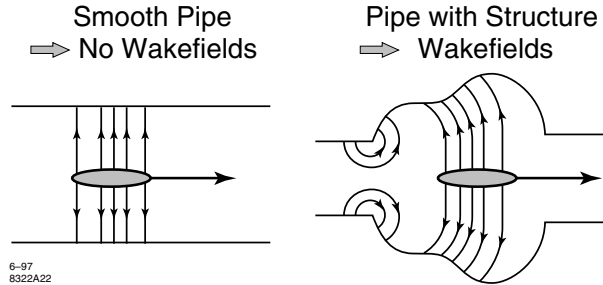

Figure 1.1: Wakefields are generated when the beam pipe is not smooth.

Beam-structure interaction is a difficult problem in general. Its solution often involves numerical solution using particle-in-cell (PIC) codes. Applying PIC codes is reasonable for small devices such as electron guns and klystrons, but becomes impractical for large accelerators.

So, can we simplify it for our purpose? The answer is yes. For *high energy* accelerators, this complication can be avoided due to two simplifying approximations. These simplifications lead to the concepts of "wake function" and "impedance".

Rigid beam approximation   The first simplification is the rigid beam approximation. At high energies, beam motion is little affected during the passage of a structure. This means one can calculate the wakefields assuming the beam shape is rigid and its motion is ultrarelativistic with $v = c$. In fact, we only need to calculate the wakefields generated by a "rigid $\cos m\theta$ ring beam" as shown in Fig.1.2, where $m = 0$ is monopole moment (net charge), $m = 1$ is dipole moment, etc. Wakefield of a general beam can be obtained by superposition of wakefields due to the ring beams with different m's and different ring radii.

Impulse approximation   The second simplification is the impulse approximation. First, let's note that we don't need to know the instantaneous $\vec{E}$ or $\vec{B}$ separately. We need only to know $\vec{f}$. Second, for high energies, we don't even need the instantaneous $\vec{f}$. We only need the integrated impulse

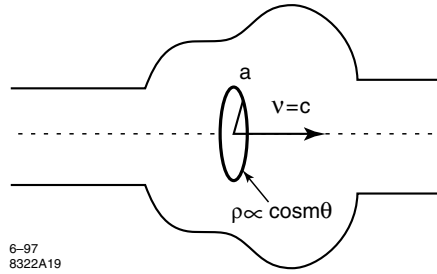$$\Delta \vec{p} = \int_{-\infty}^{\infty} dt \ \vec{f} \tag{1.5}$$

Figure 1.2: An ultrarelativistic $\cos m\theta$ ring beam going down the beam pipe in the rigid-beam approximation.

where the integration over t is performed along the *unperturbed* trajectory of the test charge e, holding D fixed. See Fig.1.3. The integration from $-\infty$ to ∞ assumes the wakefield is localized to the neighborhood of the structure in the beam pipe.
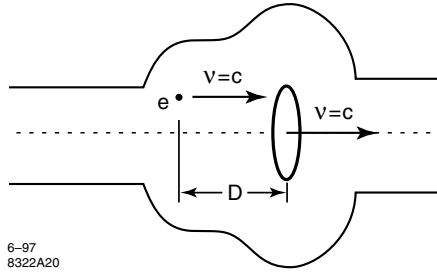

Figure 1.3: Configuration of a ring beam and a test charge that follows it. The ring beam generates a wakefield. The test charge receives a wake-induced impulse in the impulse approximation.

The instantaneous wakefields are complicated, but as we will soon see, $\Delta\vec{p}$ is much simpler and it is $\Delta\vec{p}$ that we need! Mother nature has been very kind. The quantity $c\Delta\vec{p}$ is sometimes called the "wake potential". Note that although the beam is considered to be rigid *during* the passage, the impulse will affect the subsequent beam motion *after* the passage.

Reasoning along this line turns out to be quite fruitful. In the following, I will first derive a theorem (Panofsky-Wenzel), and then consider various applications along similar lines, including the introduction of another theorem called the planar wake theorem. The Panofsky-Wenzel theorem is the basis of all beam instability analyses in high energy accelerators.

1.2 Panofsky-Wenzel Theorem

We derive the theorem in this section. Details of the derivation are different from the original paper. Maxwell equations read

$$\nabla \cdot \vec{E} = 4\pi\rho$$

$$\nabla \times \vec{B} - \frac{1}{c}\frac{\partial \vec{E}}{\partial t} = 4\pi\beta\rho\hat{z}$$

$$\nabla \cdot \vec{B} = 0$$

$$\nabla \times \vec{E} + \frac{1}{c}\frac{\partial \vec{B}}{\partial t} = 0 \qquad (1.6)$$

where we have made the important rigid beam approximation $\vec{j} = \rho\vec{v}$ and $\vec{v} = \beta c\hat{z}$.

The Lorentz force, Eq.(1.1) is given by

$$\vec{f} = e(\vec{E} + \beta\hat{z} \times \vec{B}) \qquad (1.7)$$

which leads to

$$
\begin{aligned}
\nabla \cdot \vec{f} &= e[4\pi\rho + \beta\nabla \cdot (\hat{z} \times \vec{B})] \\
&= e[4\pi\rho - \beta\hat{z} \cdot \nabla \times \vec{B}] \\
&= e\left[4\pi\rho - \frac{\beta}{c}\hat{z} \cdot \frac{\partial \vec{E}}{\partial t} - 4\pi\beta^2\rho\right] \\
&= 4\pi\frac{e\rho}{\gamma^2} - \frac{e\beta}{c}\frac{\partial E_z}{\partial t} \qquad (1.8) \\
\nabla \times \vec{f} &= e\left[-\frac{1}{c}\frac{\partial \vec{B}}{\partial t} + \beta\nabla \times (\hat{z} \times \vec{B})\right] \\
&= -e\left(\frac{1}{c}\frac{\partial}{\partial t} + \beta\frac{\partial}{\partial z}\right)\vec{B} \qquad (1.9)
\end{aligned}
$$

As mentioned, we are only interested in the impulse given by Eq.(1.5). To be more specific, we want to calculate the net kick received by a test charge e which has a transverse position (x, y) and longitudinal position D relative to the moving beam (see Fig.1.3). Both the beam and the test charge move with $\vec{v} = \beta c\hat{z}$. Eq.(1.5) is then written more precisely as

$$\Delta\vec{p}(x, y, D) = \int_{-\infty}^{\infty} dt\ \vec{f}(x, y, D + \beta ct, t) \qquad (1.10)$$

Note that $D < 0$ if the test charge is trailing the beam.

So far, we have not assumed any detailed shape of the beam. Neither have we assumed any information of the pipe boundary. We have kept β in the derivation, postponing setting $\beta = 1$ until later.

With Eq.(1.10), we have

$$
\begin{aligned}
\nabla \times \Delta \vec{p} &= \int_{-\infty}^{\infty} dt \left[\nabla' \times \vec{f}(x,y,z,t) \right]_{z=D+\beta ct} \\
&= -e \int_{-\infty}^{\infty} dt \left[\left(\frac{1}{c} \frac{\partial}{\partial t} + \beta \frac{\partial}{\partial z} \right) \vec{B}(x,y,z,t) \right]_{z=D+\beta ct} \\
&= -\frac{e}{c} \vec{B}(x,y,D+\beta ct,t) \Big|_{t=-\infty}^{t=\infty}
\end{aligned} \tag{1.11}
$$

In Eq.(1.11), ∇ refers to taking derivative with respect to coordinates (x,y,D), while ∇' refers to taking derivative with respect to coordinates (x,y,z). If the wakefield $\vec{B}$ vanishes far away from the region of interest, we have

$$
\nabla \times \Delta \vec{p} = \vec{0} \tag{1.12}
$$

which is the Panofsky-Wenzel theorem.

One might ask if the Panofsky-Wenzel theorem exhausts all the useful information contained in the Maxwell equations regarding the wake impulse. The answer to this question is no. Panofsky-Wenzel theorem, in this sense, is necessary but not sufficient. In particular, one observes that the Panofsky-Wenzel theorem (1.12) makes use of Eq.(1.9), but not Eq.(1.8). Also, Eq.(1.12) implies that $\Delta \vec{p}$ can be written as the gradient of another quantity W, but it does not say what W is. On the other hand, Maxwell equations allow expressions for W, as illustrated in Exercises 4 and 5.

We introduce W by

$$
\Delta \vec{p}(x,y,D) = -e \nabla W(x,y,D) \tag{1.13}
$$

Equation (1.17) in Exercise 2 then requires the Laplace condition (when $\beta = 1$)

$$
\nabla_\perp^2 W = 0 \qquad \text{or} \qquad \frac{\partial^2 W}{\partial x^2} + \frac{\partial^2 W}{\partial y^2} = 0 \tag{1.14}
$$

Exercise 1 Equation (1.12) is a vector equation. One can decompose it into a component parallel to $\hat{z}$ and a component perpendicular to $\hat{z}$ by taking $\hat{z} \cdot$ or $\hat{z} \times$ operations to it. Use these operations to show

$$
\nabla \cdot (\hat{z} \times \Delta \vec{p}) = 0 \tag{1.15}
$$

$$
\frac{\partial}{\partial D} \Delta \vec{p}_\perp = \nabla_\perp \Delta p_z \tag{1.16}
$$

Eq.(1.15) says something about the transverse components of $\Delta \vec{p}$. Eq.(1.16) says that the transverse gradient of the longitudinal wake potential is equal to the longitudinal gradient of the transverse wake potential.

Exercise 2 When $\beta = 1$, show that

$$
\nabla_\perp \cdot \Delta \vec{p}_\perp = 0 \tag{1.17}
$$

By setting $\beta = 1$, we have dropped the direct space-charge terms, i.e. the 1-st term on the right-hand-side of Eq.(1.8).

Solution

$$
\begin{aligned}
\nabla \cdot \Delta \vec{p} &= \int_{-\infty}^{\infty} dt \left[\nabla' \cdot \vec{f}(x,y,z,t) \right]_{z=D+ct} \\
&= -\frac{e}{c} \int_{-\infty}^{\infty} dt \left(\frac{\partial E_z}{\partial t} \right)_{z=D+ct} = e \int_{-\infty}^{\infty} dt \left(\frac{\partial E_z}{\partial z} \right)_{z=D+ct} \\
&= \int_{-\infty}^{\infty} dt \left(\frac{\partial f_z}{\partial z} \right)_{z=D+ct} = \frac{\partial \Delta p_z}{\partial D}
\end{aligned} \tag{1.18}
$$

which proves (1.17).

Exercise 3 In Cartesian coordinates, Eq.(1.15) gives $\frac{\partial \Delta p_x}{\partial y} = \frac{\partial \Delta p_y}{\partial x}$, while Eq.(1.17) gives $\frac{\partial \Delta p_x}{\partial x} + \frac{\partial \Delta p_y}{\partial y} = 0$ when $\beta = 1$. Combining these equations give $(\frac{\partial^2}{\partial x^2} + \frac{\partial^2}{\partial y^2}) \Delta p_{x,y} = 0$ if $\beta = 1$. It is clear that Panofsky-Wenzel theorem imposes strong conditions on $\Delta \vec{p}$.

Exercise 4 Use Maxwell equations and the Lorentz force equation to show that

$$
W = \int_{-\infty}^{\infty} dt (\phi - A_z)\big|_{x,y,D+ct,t} \tag{1.19}
$$

Solution With $\vec{E} = -\nabla \phi - \frac{1}{c} \frac{\partial \vec{A}}{\partial t}$ and $\vec{B} = \nabla \times \vec{A}$, we have

$$
\frac{d\vec{p}}{dt} = e(\vec{E} + \hat{z} \times \vec{B}) = -e\nabla\phi - \frac{e}{c}\frac{\partial \vec{A}}{\partial t} + e\nabla_\perp A_z - e\frac{\partial \vec{A}_\perp}{\partial z}
$$

We then use $\frac{d\vec{A}}{dt} = \frac{\partial \vec{A}}{\partial t} + (\vec{v} \cdot \nabla)\vec{A} = \frac{\partial \vec{A}}{\partial t} + c\frac{\partial \vec{A}}{\partial z}$, and integrate over t, to obtain

$$
\Delta \vec{p} = -e \int_{-\infty}^{\infty} dt (\nabla \phi - \nabla A_z) \tag{1.20}
$$

Eq.(1.19) then follows.

Exercise 5 Show that one can cast the Panofsky-Wenzel theorem in terms of relativity 4-vectors as

$$
\Delta p^\alpha = -e \frac{\partial W}{\partial x_\alpha} \quad \text{where} \quad W = \frac{1}{c} \int_{-\infty}^{\infty} d\tau A^\beta u_\beta \tag{1.21}
$$

where τ is the proper time.

Solution The 4-vectors are $x^\alpha = (ct, x, y, z)$, $u^\alpha = (\gamma c, \gamma \vec{v})$, $A^\alpha = (\phi, \vec{A})$, $p^\alpha = mu^\alpha = (E/c, \vec{p})$. Start with the 4-vector equation of motion for a relativistic particle,

$$
\frac{dp^\alpha}{d\tau} = m\frac{du^\alpha}{d\tau} = -\frac{e}{c}\left(\frac{\partial A^\beta}{\partial x_\alpha} - \frac{\partial A^\alpha}{\partial x_\beta} \right) u_\beta
$$

$$
\implies \quad \Delta p^\alpha = m\Delta u^\alpha = -\frac{e}{c}\int_{-\infty}^{\infty} d\tau \frac{\partial A^\beta}{\partial x_\alpha} u_\beta + \frac{e}{c}\int_{-\infty}^{\infty} d\tau \frac{\partial A^\alpha}{\partial x_\beta} u_\beta \tag{1.22}
$$

The second term on the RHS can be written as, using the fact that $u_\beta d\tau = dx_\beta$, $-\frac{e}{c}\int_{-\infty}^{\infty} dx_\beta \frac{\partial A^\alpha}{\partial x_\beta} = -\frac{e}{c}A^\alpha\big|_{-\infty}^{\infty} = 0$. Eq.(1.21) then follows. This result is consistent with Eq.(1.19).

It should be pointed out that Eqs.(1.19) and (1.21) are formal expressions. Explicit expressions of W still requires solving Maxwell equations for A^α, which is the difficult part. Indeed, the power of Panofsky-Wenzel theorem lies in the fact that one can obtain so much result without resorting to solving Maxwell equations in detail.

Exercise 6 As an illustration of decomposing a general beam distribution into a superposition of $\cos m\theta$-ring components, consider a point charge q located at $r = r_0$ and $\theta = \theta_0$, moving with velocity $\vec{v} = c\hat{z}$. Perform the $\cos m\theta$-ring decomposition for this beam.

Exercise 7 Panofsky-Wenzel theorem applies when the impulse is caused by a Lorentz force. Consider a particle with magnetic moment $\vec{\mu}$, which experiences a Stern-Gerlach force instead of a Lorentz force. Does the Panofsky-Wenzel theorem apply to its motion?

1.3 Cylindrically Symmetric Pipe

In cylindrical coordinates, Eq.(1.15) gives

$$\nabla \cdot [\hat{z} \times (\Delta p_r \hat{r} + \Delta p_\theta \hat{\theta})] = 0$$
$$\implies \quad \frac{\partial}{\partial r}(r\Delta p_\theta) = \frac{\partial}{\partial \theta}\Delta p_r \tag{1.23}$$

Eq.(1.16) gives

$$\frac{\partial}{\partial D}(\Delta p_r \hat{r} + \Delta p_\theta \hat{\theta}) = \left(\hat{r}\frac{\partial}{\partial r} + \frac{\hat{\theta}}{r}\frac{\partial}{\partial \theta}\right)\Delta p_z$$
$$\implies \quad \begin{cases} \frac{\partial}{\partial D}\Delta p_r = \frac{\partial}{\partial r}\Delta p_z \\ \frac{\partial}{\partial D}\Delta p_\theta = \frac{1}{r}\frac{\partial}{\partial \theta}\Delta p_z \end{cases} \tag{1.24}$$

Eq.(1.17) gives

$$\frac{1}{r}\frac{\partial}{\partial r}(r\Delta p_r) + \frac{1}{r}\frac{\partial}{\partial \theta}\Delta p_\theta = 0$$
$$\implies \quad \frac{\partial}{\partial r}(r\Delta p_r) = -\frac{\partial}{\partial \theta}\Delta p_\theta \qquad (\beta = 1) \tag{1.25}$$

Equations (1.23-1.25) are surprisingly simple. They do not contain any beam source terms. Exact shape or distribution of the beam does not matter. Neither do they depend on the boundary conditions. The boundary can be perfectly conducting or resistive metal, or it can be dielectric. The boundary does not have to be a sharply defined surface; it can for example be a gradually fading

plasma surface. The boundary also does not have to consist of a single piece. The only inputs needed for the Panofsky-Wenzel theorem are the Maxwell equations in free space and the rigid-beam and the impulse approximations.

We are now ready to consider a $\cos m\theta$ ring beam with $\vec{v} = c\hat{z}$ as in Fig.1.3. Eqs.(1.23-1.25) can be solved, and it follows that there exists a function $W_m(D)$ such that

$$
\begin{aligned}
c\Delta\vec{p}_\perp &= -eI_m W_m(D)mr^{m-1}(\hat{r}\cos m\theta - \hat{\theta}\sin m\theta) \\
c\Delta p_z &= -eI_m W'_m(D)r^m \cos m\theta
\end{aligned}
\tag{1.26}
$$

where I_m is the m-th multipole moment of the ring beam. The reader should try to derive Eq.(1.26) from Eqs.(1.23-1.25). On the other hand, the derivation can be recovered as a special case when we discuss Eqs.(1.28-1.33). Eq.(1.26) can also be derived by solvng Eq.(1.14) to obtain

$$
W = I_m W_m(D)r^m \cos m\theta
\tag{1.27}
$$

The solution (1.26) contains explicit dependences of r and θ. The dependence on D is through the *wake function* $W_m(D)$ which can be obtained only if boundary conditions are introduced. The fact that we can go so far without much details shows the power of this line of study.

When the beam pipe is cylindrically symmetric, each m-multipole component of the beam excites a wake pattern according to (1.26). Different m's do not mix.

I assume the reader is familiar with the properties of the wake function and its Fourier transform, known as the *impedance*. Suffice it to remind the reader that the rigid-beam and the impulse approximations have led to a drastically simpler Vlasov system (instead of a Vlasov-Maxwell system) to solve, and as a result one obtains a large amount of analytical results without resorting to PIC codes. Below we look for other applications along the line of the Panofsky-Wenzel analysis.

1.4 Cylindrically Symmetric Pipe With a Central Conductor

Consider now a cylindrically symmetric beam pipe except that this time there is a perfect conductor at the center. The pipe therefore has a coaxial-like geometry, as sketched in Fig.1.4. The beam has $\vec{v} = c\hat{z}$ and is necessarily ring shaped and goes around the central conductor. The beam can again be decomposed into a superposition of $\cos m\theta$ ring beams. Other than being cylindrically symmetric, the geometries of the pipe and the central conductor are arbitrary.

Everything from Maxwell equations (1.6) to the Panofsky-Wenzel theorem, Eqs.(1.12-1.25) still hold. But Eq.(1.26) needs to be changed. In obtaining Eq.(1.26) as solution to Eqs.(1.23-1.25), we have applied the condition that the solution must be well-behaved at the pipe center $r = 0$. Indeed, when $r \to 0$ in

(a)

v=c

ρ ∝ cosmθ

Central
Conductor

Beam Pipe

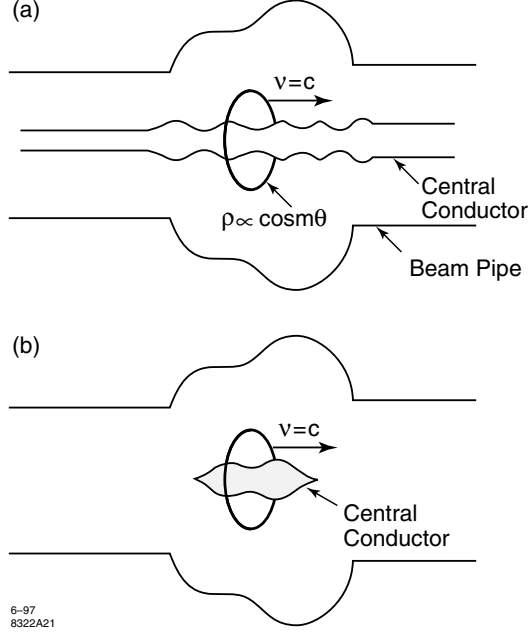(b)

v=c

Central
Conductor

6–97
8322A21

Figure 1.4: When there is a central conductor in the beam pipe.

Eq.(1.26), the wake potentials are well behaved.[1]

But with a central conductor, this condition does not have to hold and there are new modes which can be excited by the beam. As we will see, the general form of the wakefield will then be quite different from Eq.(1.26). This can be of concern because one of the techniques often used to measure the wakefield is to run a thin conducting wire down the pipe structure. The concern is then whether the thin wire has profoundly perturbed the wakefield.

With a $\cos m\theta$ beam, even with a central conductor, we can write

$$\Delta p_r = \Delta \bar{p}_r \cos m\theta, \quad \Delta p_\theta = \Delta \bar{p}_\theta \sin m\theta, \quad \Delta p_z = \Delta \bar{p}_z \cos m\theta \qquad (1.28)$$

where $\Delta \bar{p}_r$, $\Delta \bar{p}_\theta$, $\Delta \bar{p}_z$ are functions of r and D. Substituting into Eqs.(1.23-1.25), we find

$$\frac{\partial}{\partial r}(r\Delta \bar{p}_\theta) = -m\Delta \bar{p}_r, \qquad \frac{\partial}{\partial D}\Delta \bar{p}_r = \frac{\partial}{\partial r}\Delta \bar{p}_z$$

$$\frac{\partial}{\partial D}\Delta \bar{p}_\theta = -\frac{m}{r}\Delta \bar{p}_z, \qquad \frac{\partial}{\partial r}(r\Delta \bar{p}_r) = -m\Delta \bar{p}_\theta \qquad (1.29)$$

It follows that, by eliminating $\Delta \bar{p}_r$ and $\Delta \bar{p}_\theta$,

$$r\frac{\partial}{\partial r}\left(r\frac{\partial \Delta \bar{p}_z}{\partial r}\right) - m^2\Delta \bar{p}_z = 0 \qquad (1.30)$$

---

[1]The only questionable case is when $m = 0$, the r^{m-1}-dependence of $\Delta \vec{p}_\perp$ seems divergent. But when $m = 0$, the entire $\Delta \vec{p}_\perp$ vanishes because $\Delta \vec{p}_\perp \propto m$.

9

There are two solutions of Eq.(1.30) for $\Delta\bar{p}_z$ as far as its r-dependence is concerned, namely

$$\Delta\bar{p}_z = \begin{cases} r^m, \quad r^{-m}, & \text{if } m \neq 0 \\ \text{constant in } r, \quad \ln(r/b), & \text{if } m = 0 \end{cases} \quad (1.31)$$

where b is the pipe radius far away from the structure. This leads to the general solution

$$\Delta\bar{p}_z = \begin{cases} r^m W_m'(D) + r^{-m} U_m'(D), & \text{if } m \neq 0 \\ W_0'(D) + U_0'(D)\ln(r/b), & \text{if } m = 0 \end{cases} \quad (1.32)$$

where $W_m(D)$ and $W_0(D)$ are the wake functions introduced before, while $U_m(D)$ and $U_0(D)$ are a new set of modes excitable by the beam due to the presence of the central conductor. Had there be no central conductor, we re-obtain our previous results.

Having obtained $\Delta\bar{p}_z$, the other components are obtained from Eq.(1.29). Together with Eq.(1.28), we find

$$\Delta p_r = -eI_m \begin{cases} m[r^{m-1}W_m(D) - r^{-m-1}U_m(D)]\cos m\theta, & \text{if } m \neq 0 \\ \frac{1}{r}U_0(D), & \text{if } m = 0 \end{cases}$$

$$\Delta p_\theta = -eI_m \begin{cases} -m[r^{m-1}W_m(D) + r^{-m-1}U_m(D)]\sin m\theta, & \text{if } m \neq 0 \\ 0, & \text{if } m = 0 \end{cases}$$

$$\Delta p_z = -eI_m \begin{cases} [r^m W_m'(D) + r^{-m}U_m'(D)]\cos m\theta, & \text{if } m \neq 0 \\ W_0'(D) + U_0'(D)\ln(r/b), & \text{if } m = 0 \end{cases} \quad (1.33)$$

We can apply our results to the case when the central conductor is a smooth, perfectly conducting wire of radius a. For the mode $m = 0$, the condition that $E_z = 0$ along the surface of the wire leads to the condition that

$$\Delta p_z(r = a, \theta, D) = 0$$

$$\implies \quad U_0(D) = -\frac{W_0(D)}{\ln(a/b)}$$

$$\implies \quad \begin{cases} \Delta p_r = eI_0\frac{W_0(D)}{r\ln(a/b)} \\ \Delta p_\theta = 0 \\ \Delta p_z = -eI_0 W_0'(D)\left[1 - \frac{\ln(r/b)}{\ln(a/b)}\right] \end{cases} \quad (1.34)$$

with I_0 the total charge of the driving beam.

For modes $m \neq 0$, similarly, we obtain

$$U_m(D) = -a^{2m}W_m(D)$$

$$\implies \quad \begin{cases} \Delta p_r = -eI_m m W_m(D)[r^{m-1} + a^{2m}r^{-m-1}]\cos m\theta \\ \Delta p_\theta = eI_m m W_m(D)[r^{m-1} - a^{2m}r^{-m-1}]\sin m\theta \\ \Delta p_z = -eI_m W_m'(D)(r^m - a^{2m}r^{-m})\cos m\theta \end{cases} \quad (1.35)$$

Compared with Eq.(1.26), the central wire seems to perturb the wakefield pattern profoundly. The effect of a central wire in some impedance measuring devices is yet to be analyzed more carefully.

10

Exercise 8 What if the central conductor looks like Fig.1.4(b)? Is a divergence at $r = 0$ allowed in the analysis of wake potentials?

1.5   Planar Wake Theorem

Planar Structures   In order to reach higher acceleration gradients in linear accelerators, it is advantageous to use a higher accelerating RF frequency, which in turn requires smaller accelerating structures. As the structure size becomes smaller, rectangular structures become increasingly attractive because they are easier to manufacture than cylindrically symmetric ones. One drawback of small structures, however, is that the wakefields generated by the beam tend to be strong. Recently, Rosenzweig suggested that one way of ameliorating this problem is to use rectangular structures that are very flat and to use flat beams [4].

In the limiting case of a very flat planar geometry, the problem resembles a purely two-dimensional (2-D) problem as sketched in Fig.1.5. The beam is considered to be infinitely long in the horizontal x-direction; it propagates with $v = c$ in the z-direction. The beam distribution in the y-z plane is arbitrary. The environment consists of boundaries which are independent of x, but are otherwise unrestricted. We do assume, however, that the beam trajectory is entirely in free space and that it nowhere intersects the boundaries. A test charge e in the beam (or trailing the beam) also moving in the z-direction with $v = c$ samples the force due to the wakefield generated by the beam.

Proof of Theorem   Under these conditions, there is a "planar wake theorem" which states that the transverse wake potential $\Delta \vec{p}_\perp$ received by the test charge is independent of the y-positions of the beam and the test charge, and is also independent of D, the longitudinal separation between the beam and the test charge (see Fig.1.5). In addition, the theorem states that the longitudinal potential Δp_z wake kick is also independent of y, though it does not say anything about its D-dependence.

From the symmetry of the problem, we know that the only nonvanishing EM field components are E_y, E_z and B_x, and all components depend only on y, z and t (and are independent of x). We also have the condition $\vec{j} = c\rho \hat{z}$ (rigid beam approximation). The Maxwell equations then become

$$\frac{\partial E_y}{\partial y} + \frac{\partial E_z}{\partial z} = 4\pi\rho$$

$$\frac{\partial B_x}{\partial z} - \frac{1}{c}\frac{\partial E_y}{\partial t} = 0$$

$$\frac{\partial B_x}{\partial y} + \frac{1}{c}\frac{\partial E_z}{\partial t} = -4\pi\rho$$

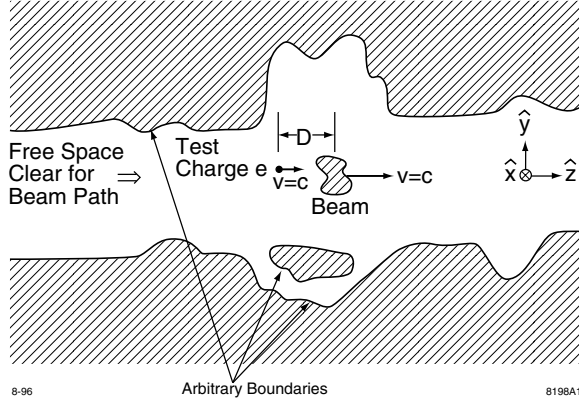$$\frac{\partial E_z}{\partial y} - \frac{\partial E_y}{\partial z} + \frac{1}{c}\frac{\partial B_x}{\partial t} = 0 \qquad (1.36)$$

11

Figure 1.5: A planar beam-environment arrangement.

and the Lorentz force components are given by

$$f_y(y, z, t) = eE_y + eB_x$$
$$f_z(y, z, t) = eE_z \tag{1.37}$$

Combining Eqs.(1.36) and (1.37), we obtain

$$\frac{\partial f_y}{\partial y} = -e(\frac{\partial}{\partial z} + \frac{1}{c}\frac{\partial}{\partial t})E_z$$

$$\frac{\partial f_y}{\partial z} = e(\frac{\partial}{\partial z} + \frac{1}{c}\frac{\partial}{\partial t})E_y$$

$$\frac{\partial f_z}{\partial y} = e(\frac{\partial}{\partial z} + \frac{1}{c}\frac{\partial}{\partial t})(E_y - B_x) \tag{1.38}$$

Note that the right hand sides of Eq.(1.38) all contain the operator $\frac{\partial}{\partial z} + \frac{1}{c}\frac{\partial}{\partial t}$.

We are interested in the wake kick $c\Delta\vec{p}$,

$$c\Delta p_{y,z}(y, D) = \int_{-\infty}^{\infty} f_{y,z}(y, D + ct, t)\, dt \tag{1.39}$$

Substituting Eqs.(1.38) into Eq.(1.39) we obtain integrals of the form

$$\int_{-\infty}^{\infty} dt \left[(\frac{\partial}{\partial z} + \frac{1}{c}\frac{\partial}{\partial t})G(z, t) \right]_{z = D+ct}$$

which in all cases equals zero, since the integrand is proportional to the total derivative $dG(D + ct, t)/dt$ and since $G(D + ct, t)$ approaches zero as $|t| \to \infty$. It therefore follows that

$$\frac{\partial \Delta p_y}{\partial y} = \frac{\partial \Delta p_y}{\partial D} = \frac{\partial \Delta p_z}{\partial y} = 0 \tag{1.40}$$

12

which proves the planar wake theorem.

Note that the boundary properties never enter into our proof of the planar wake theorem. Also note that for our problem, the wake kick is also independent of the y position of the driving beam. This is because the wakefield is a response to the primary field carried by the driving beam, and the primary field at the boundaries is independent of the y-position of the beam in a 2-D planar geometry.

> *Exercise* 9 Repeat the proof of the planar wake theorem using Eqs.(1.15-1.17) instead of starting from Maxwell equations.
> *Hint* You may be able to show $\partial \Delta p_y / \partial y = 0$ and $\partial \Delta p_y / \partial D = \partial \Delta p_z / \partial y$, but not the complete theorem.

Two Soluble Problems   There are two known 2-D planar geometries whose wakefields are exactly soluble. The boundaries in both cases are wedge-shaped, made of perfectly conducting metal, and are only on one side of the beam path [see Fig.1.6]. By solving the Maxwell equations it was found that the transverse wake kick received by the test charge due to the wakefield generated by a rod beam (*i.e.* one that is infinitely long in x and a δ-function in the y- and z-directions) of line charge density λ_0 is given by

$$c\Delta p_y(y, y_0, D < 0) = \begin{cases} 2\pi e \lambda_0 & \text{for Fig.1.6(a)} \\ \pi e \lambda_0 & \text{for Fig.1.6(b)} \end{cases} \tag{1.41}$$

where y_0 is the y-offset of the rod beam. We note that the transverse wake kick is independent of y, y_0 and D, as the planar wake theorem states. It is also interesting that the result, Eq.(1.41), does not depend on α, the wedge angle.[2] Although Eq.(1.41) applies only to a rod beam, the wake kick for a more general y-z beam distribution can be obtained by simple superposition.

The two examples in Fig.1.6 are not the only soluble cases with planar arrangement. By applying conformal mapping technique, with Schwarz-Christoffel transformation, there should be other soluble cases, including cases with metal boundaries on both sides of the beam.

Two Corollaries   The planar wake theorem has an interesting corollary when the 2-D boundaries have the additional property of up-down symmetry, as is sketched in Fig.1.7(a). In this case, the transverse wake kicks due to the upper and the lower halves of the boundaries cancel each other and the net transverse kick becomes zero. Note that the beam does not need to observe up-down symmetry and that the cancellation applies even when it has a y off-set.

To prove this corollary, let us first consider a rod beam. Since the wake kick does not depend on the y-positions of the beam and the test charge, we can choose to locate both along the symmetry axis $y = 0$ without affecting the result. But for such a configuration the transverse wake kick must vanish due to

---

[2]One would expect no wakefields when $\alpha = \pi$, but this is a singular case.
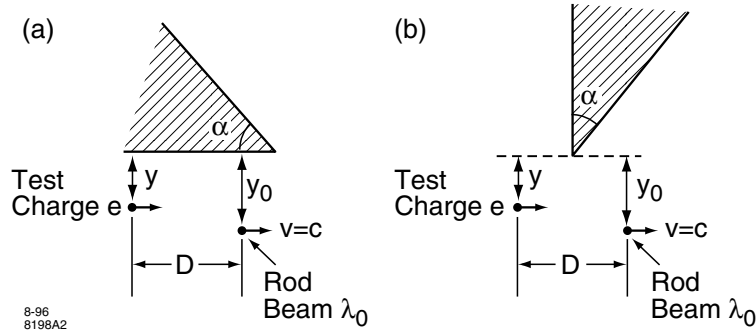
13

Figure 1.6: Two soluble planar problems.

the symmetry of the problem. Finally, we can extend this result to an arbitrary y-z beam distribution by applying superposition, and the corollary follows.

Note that the corollary applies to the total *integrated* wake kick received by the test charge. The *instantaneous* wake force is not necessarily zero. In case the boundary has translational symmetry, *i.e.* is independent of the z-position, the instantaneous transverse wake force would, of course, also vanish. Note also that the up-down symmetry of the boundary is required for the corollary to hold; the transverse wake kick is not zero due to the 2-D planar geometry alone. Two nonvanishing examples were shown already in Eq.(1.41). It vanishes only when the additional requirement of up-down symmetry is applied.

Another application of the planar wake theorem is when the boundary on one side of the beam path is a perfectly conducting plate, as sketched in Fig.1.7(b). In this case, one must have $\Delta p_z \propto \delta(D)$. To demonstrate this, consider a test charge that travels immediately next to the surface of the plate. For this test charge, F_z necessarily vanishes and thus $\Delta p_z = 0$. An application of the planar wake theorem then predicts $\Delta p_z = 0$ for a test charge with any vertical position y. The only way this can happen is when $\Delta p_z(D) \propto \delta(D)$. The reason the wake kick is not identically zero is because there must be some net loss of energy by the beam.

Questions not yet addressed   It is conceivable to hope that, by using planar beams and planar structures, one might be able to eliminate, or at least to minimize, the transverse wakefield effects (using the first corollary and Fig.1.7(a)) or the longitudinal wakefield effects (using the second corollary and Fig.1.7(b)). Before these potential applications, however, we need to address a few questions.

1. A very flat 3-D structure is not the same as a 2-D planar structure. How flat does a 3-D structure have to be before it becomes effectively 2-D planar?

2. Even in a purely 2-D structure it may turn out that an initial, slight
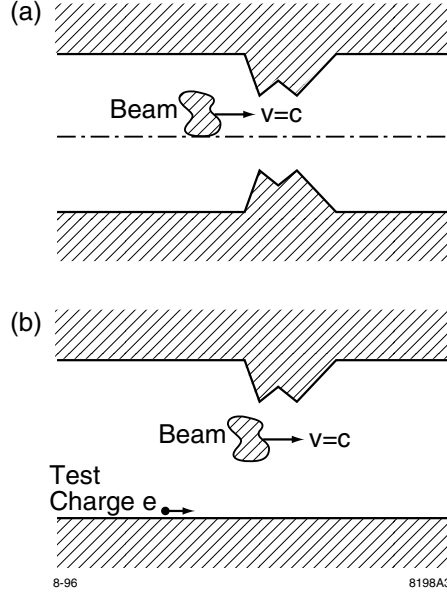
14

Figure 1.7: Two corollaries of the planar wake theorem.

un-evenness of the beam distribution in the x-direction, or a tilt of the beam in the x-y plane, leads to unstable growth as the beam propagates down the accelerator. This question requires a study of collective instabilities (see next section).

3. Although the arrangement in Fig.1.7(a) potentially solves the transverse wake problem and Fig.1.7(b) potentially solves the longitudinal wake problem, there is not one arrangement that solves both problems.

1.6 Planar Pipe with Nonplanar Beam

As a first step in analyzing beam instabilities, consider a beam, or a perturbation on the beam, with $\vec{v} = c\hat{z}$ and $\vec{j} = c\rho\hat{z}$ with

$$\rho(x, y, z) = \bar{\rho}(y, z) \cos kx \tag{1.42}$$

When $k \to 0$, we obtain the case of planar beam. It is conceivable that when $k \sim$ the planar gap size b, the instability mechanism becomes as severe as a cylindrically symmetric pipe with radius b, except for the fact that the beam density is lower in the planar case because the beam is more spread out.

The EM field and Lorentz force components can be written as

$$(E_x, B_y, B_z, f_x, \Delta p_x) = (\bar{E}_x, \bar{B}_y, \bar{B}_z, \bar{f}_x, \Delta \bar{p}_x) \sin kx$$

15

$$(E_y, E_z, B_x, f_y, f_z, \Delta p_y, \Delta p_z) = (\bar{E}_x, \bar{B}_y, \bar{B}_z, \bar{f}_y, \bar{f}_z, \Delta\bar{p}_y, \Delta\bar{p}_z) \cos kx$$

All barred quantities are independent of x. Substituting into Maxwell equations and using

$$\bar{f}_x = e(\bar{E}_x - \bar{B}_y), \qquad \bar{f}_y = e(\bar{E}_y + \bar{B}_x), \qquad \bar{f}_z = e\bar{E}_z \qquad (1.43)$$

we obtain

$$\frac{\partial \bar{f}_x}{\partial y} = e\left(\frac{\partial}{\partial z} + \frac{1}{c}\frac{\partial}{\partial t}\right)\bar{B}_z - k\bar{f}_y$$

$$\frac{\partial \bar{f}_x}{\partial z} = -e\left(\frac{\partial}{\partial z} + \frac{1}{c}\frac{\partial}{\partial t}\right)\bar{B}_y - k\bar{f}_z$$

$$\frac{\partial \bar{f}_y}{\partial y} = -e\left(\frac{\partial}{\partial z} + \frac{1}{c}\frac{\partial}{\partial t}\right)\bar{E}_z - k\bar{f}_x$$

$$\frac{\partial \bar{f}_y}{\partial z} = e\left(\frac{\partial}{\partial z} + \frac{1}{c}\frac{\partial}{\partial t}\right)\bar{E}_y + ek\bar{B}_z$$

$$\frac{\partial \bar{f}_z}{\partial y} = e\left(\frac{\partial}{\partial z} + \frac{1}{c}\frac{\partial}{\partial t}\right)(\bar{E}_y - \bar{B}_x) + ek\bar{B}_z \qquad (1.44)$$

which leads to the conditions for the wake kick,

$$\frac{\partial \Delta\bar{p}_x}{\partial y} = -k\Delta\bar{p}_y$$

$$\frac{\partial \Delta\bar{p}_x}{\partial D} = -k\Delta\bar{p}_z$$

$$\frac{\partial \Delta\bar{p}_y}{\partial y} = -k\Delta\bar{p}_x$$

$$\frac{\partial \Delta\bar{p}_y}{\partial D} = \frac{\partial \Delta\bar{p}_z}{\partial y} = ek \int dt\,\bar{B}_z \qquad (1.45)$$

One solution which avoids $\Delta p_z \to \infty$ when $k \to 0$ is

$$\Delta p_x = [(W_0 + ka_0(D))\cosh ky + (W_1 + ka_1(D))\sinh ky]\sin kx$$

$$\Delta p_y = -[(W_0 + ka_0(D))\sinh ky + (W_1 + ka_1(D))\cosh ky]\cos kx$$

$$\Delta p_z = -[a_0'(D)\cosh ky + a_1'(D)\sinh ky]\cos kx \qquad (1.46)$$

where $W_{0,1}$ are some constants, and $a_{0,1}(D)$ are some functions of D ($W_{0,1}$ and $a_{0,1}(D)$ may depend on k). When k is small, we keep to first order in k to obtain

$$\Delta p_x \approx W_0 \sin kx$$

$$\Delta p_y \approx -[W_1 + ka_1(D) + W_0 ky]\cos kx$$

$$\Delta p_z \approx -[a_0'(D) + a_1'(D)ky]\cos kx \qquad (1.47)$$

which satisfies the planar wake theorem that, when $k = 0$, Δp_y is independent of y and D, and Δp_z is independent of y. The quantities $W_{0,1}$ and $a_{0,1}(D)$ remain to be calculated by imposing proper boundary conditions.

16

References

[1] W.K.H. Panofsky and W.A. Wenzel, Rev. Sci. Instr. 27, 967 (1956).

[2] A.W. Chao, Physics of Collective Beam Instabilities in High Energy Accelerators, Wiley, 1993.

[3] S.Vaganian and H.Henke, Part. Accel. 48, 239 (1995).

[4] J. Rosenzweig, Snowmass 1996.

2   Echo Effect

This is a curious effect that can occur in a proton or heavy-ion storage ring. Consider a beam which has been stored for a long time and is in a steady state. At $t = 0$ we kick this beam by a one-turn dipole kicker. The beam's centroid then subsequently executes a betatron oscillation. Due to a spread in the betatron frequencies in the beam, the centroid signal decoheres in a relatively short time, say in 1 ms. Long after the kick, say 1 s later, the centroid signal is of course dead zero. At this point, we give the beam a quadrupole kick. Such a kick does not affect the beam centroid, and thus the beam centroid signal stays zero. The curious thing is that if we wait approximately another 1 s after the quadrupole kick, the beam centroid signal would give a sudden and pronounced blip. This sudden blip is called the echo, and is a result of the correlation and interplay between the two kicks and the detailed beam motion in the phase space.

The echo effect is well known in plasma physics (See Fig.2.1.), and was first introduced to accelerator physics by Stupakov (1992) [2].

The echo can also be observed in the longitudinal direction in which case an RF phase shift and an RF amplitude jump play the roles of the dipole and quadrupole kicks, respectively. Experimentally, longitudinal echo has been observed in the antiproton accumulator ring at FNAL and in the CERN SPS for unbunched beams. Those experiments demonstrated that echo can be effectively used for measuring an extremely weak diffusion inside the beam. Electron storage rings do not exhibit the echo effect because radiation damping and quantum excitation completely overwhelm any echo signal.

The echo effect is also influenced by the collective effects. The echo measurements should yield useful information about the wakefield and impedance of the accelerator. In the following, however, we ignore these collective effects.
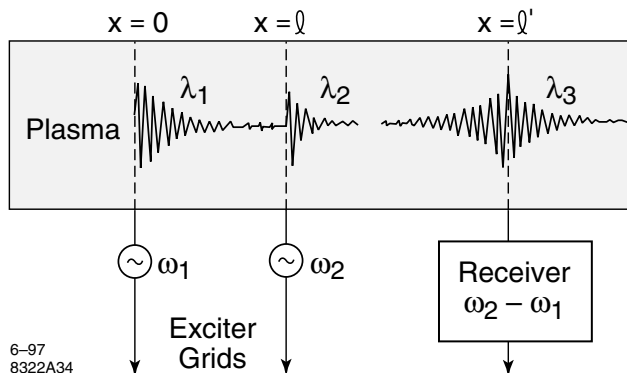

Figure 2.1: Schematic of a plasma echo experiment [1].

2.1 Transverse Decoherence

We describe the transverse dynamics using the action-angle variables J and ϕ, with

$$x = \sqrt{2J\beta}\cos\phi, \quad p = \beta x' + \alpha x = -\sqrt{2J\beta}\sin\phi$$
$$J = \frac{x^2 + p^2}{2\beta}, \quad \tan\phi = -\frac{p}{x} \qquad (2.1)$$

where β, α are the Courant-Snyder functions.

The beam receives a dipole kick at time $t = 0$. Let the kick be $\Delta p = \beta\theta$. The action of the kick is

$$x_{\text{out}} = x_{\text{in}}, \quad p_{\text{out}} = p_{\text{in}} + \beta\theta \qquad (2.2)$$

The beam distribution immediately after the kick $\psi_1(x, p)$ is related to the distribution immediately before the kick $\psi_0(x, p)$ by[3]

$$\psi_1(x, p) = \psi_0(x, p - \beta\theta) \qquad (2.3)$$

Before the kick at $t = 0$, the beam has a steady-state transverse phase space distribution. This means $\psi_0(x, p) = \psi_0(J)$ depends only on J. Immediately after the kick, the beam distribution is given by

$$\psi_1(x, p) = \psi_0\left(\frac{x^2 + (p - \beta\theta)^2}{2\beta}\right)$$
$$\implies \quad \psi_1(\phi, J) = \psi_0(J + \theta\sqrt{2J\beta}\sin\phi + \frac{1}{2}\beta\theta^2) \qquad (2.4)$$

At time $t > 0$ after the kick, the motion of individual particles is described by

$$J_{\text{out}} = J_{\text{in}}, \quad \phi_{\text{out}} = \phi_{\text{in}} + \omega(J_{\text{in}})t \qquad (2.5)$$

where $\omega(J)$ is the betatron oscillation frequency of a particle whose action is J. The dependence of ω on J is important. It gives rise to a spread in the betatron frequencies and thus the decoherence after kick.

The distribution after the kick is given by

$$\begin{aligned}
\psi_2(\phi, J, t) &= \psi_1(J, \phi - \omega(J)t) \\
&= \psi_0[J + \theta\sqrt{2J\beta}\sin(\phi - \omega(J)t) + \frac{1}{2}\beta\theta^2] \qquad (2.6)
\end{aligned}$$

The beam centroid signal is

$$\langle x \rangle = \int_0^\infty dJ \int_0^{2\pi} d\phi \; \psi_2(\phi, J)\sqrt{2J\beta}\cos\phi \qquad (2.7)$$

---

[3]Note it is $p - \beta\theta$, not $p + \beta\theta$, in the argument of ψ_0. Similar comment applies to Eq.(2.6).

We are interested in the case when the beam distribution before the kick is gaussian,

$$\psi_0(J) = \frac{1}{2\pi J_0} e^{-J/J_0} \tag{2.8}$$

and when the amplitude-dependent betatron frequency is given by

$$\omega(J) = \omega_0 + \omega' J \tag{2.9}$$

where ω_0 and ω' are constants, independent of J.

Substituting Eqs.(2.6), (2.8) and (2.9) into Eq.(2.7) and changing variable from J to $a = \sqrt{2J\beta}$, we obtain

$$\langle x \rangle(t) = \frac{1}{\beta J_0} \int_0^\infty a^2 da \ \exp\left(-\frac{a^2}{2\beta J_0} - \frac{\beta \theta^2}{2J_0}\right) \sin\left(\omega_0 t + \frac{\omega' t}{2\beta} a^2\right) I_1\left(\frac{\theta a}{J_0}\right) \tag{2.10}$$

where we have integrated over ϕ using

$$\frac{1}{2\pi} \int_0^{2\pi} d\phi \cos\phi \ e^{x\cos\phi} = I_1(x) \tag{2.11}$$

with $I_1(x)$ the Bessel function.

The integration over a can also be performed using

$$\int_0^\infty a^2 da \ e^{-Aa^2} I_1(Ba) = \frac{B}{4A^2} e^{B^2/4A} \tag{2.12}$$

We then obtain

$$
\begin{aligned}
\langle x \rangle(t) &= \beta\theta \ \mathrm{Im}\left[\frac{e^{i\omega_0 t}}{(1-i\Theta)^2} \exp\left(\frac{\beta\theta^2}{2J_0}\frac{i\Theta}{1-i\Theta}\right)\right] \\
&= \frac{\beta\theta}{1+\Theta^2} \exp\left[-\frac{\beta\theta^2\Theta^2}{2J_0(1+\Theta^2)}\right] \sin\left[\omega_0 t + \frac{\beta\theta^2\Theta}{2J_0(1+\Theta^2)} + 2\tan^{-1}\Theta\right] \\
\Theta &\equiv \omega' J_0 t
\end{aligned} \tag{2.13}
$$

Equation (2.13) also gives the beam centroid oscillation amplitude

$$\langle x \rangle^{\mathrm{ampl}}(t) = \frac{\beta\theta}{1+\Theta^2} \exp\left[-\frac{\beta\theta^2\Theta^2}{2J_0(1+\Theta^2)}\right] \tag{2.14}$$

and decoherence time

$$\tau_{\mathrm{decoh}} \approx \min\left[\frac{1}{\omega' J_0}, \frac{1}{\omega'\theta\sqrt{\beta J_0}}\right] \tag{2.15}$$

Figure 2.2 shows how the beam centroid signal decoheres. It shows $\langle x \rangle/\beta\theta$ versus Θ for $\omega_0 = 50\,\omega' J_0$, and various values of

$$u \equiv \beta\theta^2/2J_0$$

21
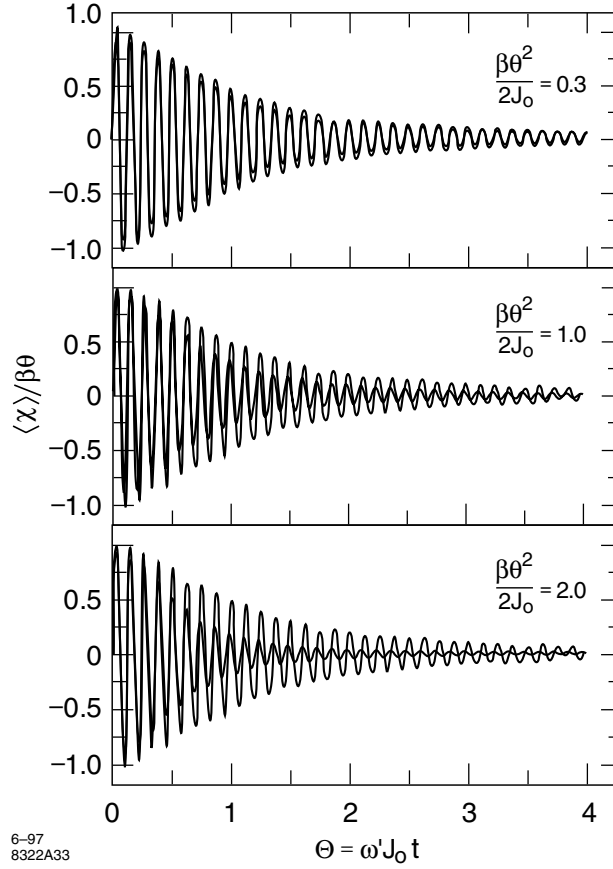
Figure 2.2: Decoherence of the beam centroid signal after a kick, for various values of the kick amplitude.

When $u \ll 1$, i.e. when the kick amplitude is much smaller than the unperturbed beam size, Eq.(2.13) can be approximated as

$$
\begin{aligned}
\langle x \rangle(t) &\approx \frac{\beta\theta}{1+\Theta^2} \sin(\omega_0 t + 2\tan^{-1}\Theta) \\
&= \frac{\beta\theta}{(1+\Theta^2)^2}[(1-\Theta^2)\sin\omega_0 t + 2\Theta\cos\omega_0 t] \\
\langle x \rangle^{\mathrm{ampl}}(t) &\approx \frac{\beta\theta}{1+\Theta^2}
\end{aligned}
\tag{2.16}
$$

There are two curves in each subfigure of Fig.2.2; the curves with the larger amplitudes are the first order approximation (2.16). When the kick amplitude

22

is not small compared with the unperturbed beam size, Eq.(2.16) over-estimates the beam centroid motion. When $u \ll 1$, the decoherence time is $\tau_{\text{decoh}} \approx 1/\omega' J_0$. When $u \gtrsim 1$, $\tau_{\text{decoh}} \approx \frac{1}{\omega' J_0} \frac{1}{\sqrt{2u}}$, according to Eq.(2.15).

Exercise 1 Find $\langle p \rangle(t)$ as the counter part to Eq.(2.13).
Hint It is algebraically simpler to compute $(\langle x \rangle + i\langle p \rangle)(t)$.

Exercise 2 The kick we considered is when the beam is kicked in angle. Does the decoherence behavior change if the kick is a sudden displacement of the beam?

Exercise 3 (a) We have concentrated on the beam centroid signal after a kick. Extend the calculation to find the time evolution of the second moments $\langle x^2 \rangle, \langle xp \rangle, \langle p^2 \rangle$. Apply to the special case with (2.8-2.9). (b) Repeat for the moment $\langle x^m p^n \rangle$.

2.2 Transverse Echo

We now let the beam decohere for a time much longer than τ_{decoh}. The beam centroid signal completely vanishes. At time $t = \tau$ with $\omega' J_0 \tau \gg 1$, we give the beam a second, one-turn, quadrupole kick,

$$x_{\text{out}} = x_{\text{in}}, \quad p_{\text{out}} = p_{\text{in}} - q x_{\text{in}} \tag{2.17}$$

where $q = \beta/f$ with f the focal length of the kicking quadrupole ($f > 0$ means focusing quadrupole).

For simplicity, we consider the dipole and the quadrupole kicks to be weak. When $u = \beta \theta^2 / 2 J_0 \ll 1$, let's first re-derive Eq.(2.16) as follows.

$$
\begin{aligned}
\psi_1 &= \psi_0(x, p - \beta\theta) \approx \psi_0(J) - \beta\theta\psi_0'(J)\frac{\partial J}{\partial p} \\
&= \psi_0(J) + \theta\psi_0'(J)\sqrt{2J\beta}\sin\phi \\
\implies \\
\psi_2 &\approx \psi_0(J) + \theta\psi_0'(J)\sqrt{2J\beta}\sin(\phi - \omega(J)t)
\end{aligned}
\tag{2.18}
$$

The first term $\psi_0(J)$ in Eq.(2.18) does not contribute to the beam centroid signal. The second term contributes

$$
\begin{aligned}
\langle x \rangle(t) &\approx \theta \int_0^\infty dJ \int_0^{2\pi} d\phi \sqrt{2J\beta} \cos\phi \; \psi_0'(J)\sqrt{2J\beta}\sin(\phi - \omega(J)t) \\
&= -2\pi\beta\theta \int_0^\infty J dJ \psi_0'(J)\sin(\omega(J)t)
\end{aligned}
\tag{2.19}
$$

Equation (2.19) holds for arbitrary $\psi_0(J)$ and $\omega(J)$. If they are given by Eqs.(2.8) and (2.9), we recover Eq.(2.16).

The decoherence time is given by $\tau_{\text{decoh}} = 1/\omega' J_0$. Physically, one might say that the decoherence time is basically given by $1/\Delta\omega$, where $\Delta\omega$ is the oscillation frequency spread of the beam. However, this physical intuition should be applied with care. See Exercise 4.

23

Apply Eq.(2.19) to a waterbag beam distribution $\psi_0(J) = \frac{1}{2\pi J_0} H(J_0 - J)$. (a) Find $\langle x \rangle(t)$ for a weak dipole kick. (b) Explain why there is no decoherence. This exercise shows that the formula $\tau_{\text{decoh}} \approx 1/\Delta\omega$ is not always valid.

At time $t = \tau$, the beam is given a weak quadrupole kick with $q \ll 1$ [see Eq.(2.27) later]. We have immediately before the kick,

$$\psi_3 = \psi_0(J) + \theta\psi_0'(J)\sqrt{2J\beta}\sin(\phi - \omega(J)\tau) \tag{2.20}$$

Immediately after the kick, we have

$$
\begin{aligned}
\psi_4(\phi, J) &\approx \psi_3(J, \phi) + qx\frac{\partial\psi_3}{\partial p} \\
&= \psi_3(J, \phi) + q\sqrt{2J\beta}\cos\phi\left[\frac{\partial J}{\partial p}\frac{\partial\psi_3}{\partial J} + \frac{\partial\phi}{\partial p}\frac{\partial\psi_3}{\partial\phi}\right] \\
&= \psi_3(J, \phi) - q\sqrt{2J\beta}\cos\phi\left[\sqrt{\frac{2J}{\beta}}\sin\phi\frac{\partial\psi_3}{\partial J} + \frac{1}{\sqrt{2J\beta}}\cos\phi\frac{\partial\psi_3}{\partial\phi}\right]
\end{aligned}\tag{2.21}
$$

From Eq.(2.20), we have

$$
\begin{aligned}
\frac{\partial\psi_3}{\partial J} &= \psi_0'(J) + \theta\frac{\partial}{\partial J}[\psi_0'(J)\sqrt{2J\beta}]\sin(\phi - \omega(J)\tau) \\
&\quad - \theta\omega'(J)\tau\psi_0'(J)\sqrt{2J\beta}\cos(\phi - \omega(J)\tau) \tag{2.22} \\
\frac{\partial\psi_3}{\partial\phi} &= \theta\psi_0'(J)\sqrt{2J\beta}\cos(\phi - \omega(J)\tau) \tag{2.23}
\end{aligned}
$$

The three terms in Eq.(2.22) have the relative magnitudes of the order of

$$1 \ : \ \sqrt{u} \ : \ (\omega'J_0\tau)\sqrt{u} \tag{2.24}$$

We have already assumed $u \ll 1$. We will consider the case when the third term dominates the beam centroid signal. The first term, when substituted into Eq.(2.21), does not contribute to the centroid signal. Therefore, the third term dominates if

$$(\omega'J_0\tau) \gg 1 \tag{2.25}$$

The quantity $\omega'J_0\tau$ is the betatron phase smear due to the frequency spread in a time period of τ. Equation (2.25) means the decoherence effect must be large, but that is just what we are interested in.

The term due to Eq.(2.23), in the scale as in Eq.(2.24), has a magnitude of $\sqrt{u}$, so is also negligible. We have thus obtained, under condition (2.25),

$$\psi_4 \approx \theta q\omega'(J)\tau J\psi_0'(J)\sqrt{2J\beta}\sin 2\phi\cos(\phi - \omega(J)\tau) \tag{2.26}$$

Note that $\psi_4 \propto \theta q$, i.e. it is proportional to both the dipole and the quadrupole kick amplitudes.

If we go back to Eq.(2.21), the condition $q \ll 1$ really requires $(\psi_4 - \psi_3) \ll (\psi_3 - \psi_0)$, or

$$(\omega' J_0 \tau) q \ll 1 \tag{2.27}$$

Combining all the conditions for the validity of our analysis, we have

$$\frac{1}{q} \gg (\omega' J_0 \tau) \gg 1, \qquad \frac{1}{\theta}\sqrt{\frac{J_0}{\beta}} \gg 1 \tag{2.28}$$

For $t > \tau$, after the quadrupole kick, the beam distribution is

$$\psi_5(J, \phi, t) = \psi_4(J, \phi - \omega(J)(t - \tau)) \tag{2.29}$$

The beam centroid is

$$
\begin{aligned}
\langle x \rangle^{\text{echo}}(t) &= \int_0^\infty dJ \int_0^{2\pi} d\phi \sqrt{2J\beta} \cos\phi \; \psi_5(\phi, J, t) \\
&\approx 2\beta\theta q\tau \int_0^\infty J^2 dJ \omega'(J)\psi_0'(J) \\
&\quad \times \int_0^{2\pi} d\phi \cos\phi \sin[2\phi - 2\omega(J)t + 2\omega(J)\tau]\cos[\phi - \omega(J)t] \quad (2.30)
\end{aligned}
$$

The integration over ϕ can be performed to yield

$$-\frac{\pi}{2}\sin[\omega(J)(t - 2\tau)] \tag{2.31}$$

This integration over ϕ is the key to the echo phenomenon. Magically, the two kicks, the frequency spread, and the particle evolution in phase space conspire to produce a recoherence in the neighborhood of time $t = 2\tau$! (Although exactly at $t = 2\tau$, the echo signal is zero.) Furthermore, the recoherence, and the fact that it occurs at $t = 2\tau$, do not depend on the exact form of $\psi_0(J)$ or $\omega(J)$!

> *Exercise 5* The integrand of the ϕ-integral in Eq.(2.30) contains four sinusoidal factors
>
> $\cos\phi \times \sin[\phi - \omega(J)t + \omega(J)\tau] \times \cos[\phi - \omega(J)t + \omega(J)\tau] \times \cos[\phi - \omega(J)t]$
>
> Trace back to find out where each factor originates from. This would give a feel for the intricate phase space dynamics we are dealing with.

After performing the ϕ-integral, we obtain

$$\langle x \rangle^{\text{echo}}(t) = -\pi\beta\theta q\tau \int_0^\infty J^2 dJ \omega'(J)\psi_0'(J)\sin[\omega(J)(t - 2\tau)] \tag{2.32}$$

Equation (2.32) is our main result. If $\omega(J)$ and $\psi_0(J)$ are given by Eqs.(2.8-2.9), the integration over J can be performed to yield

$$
\begin{aligned}
\langle x \rangle^{\mathrm{echo}}(t) &= \beta\theta q \omega' J_0 \tau \,\mathrm{Im}\left[\frac{e^{i\Phi}}{(1-i\xi)^3}\right] \\
&= \beta\theta q \frac{\omega' J_0 \tau}{(1+\xi^2)^3}[\xi(3-\xi^2)\cos\Phi + (1-3\xi^2)\sin\Phi] \quad (2.33) \\
\xi &= \omega' J_0(t-2\tau) \\
\Phi &= \omega_0(t-2\tau)
\end{aligned}
$$

The amplitude of the echo signal is

$$
\langle x \rangle^{\mathrm{echo\ ampl}}(t) = \beta\theta q \frac{\omega' J_0 \tau}{(1+\xi^2)^{2/3}} \quad (2.34)
$$

The maximum echo amplitude occurs near $t = 2\tau$, and is given by

$$
\langle x \rangle^{\mathrm{echo\ ampl\ max}} = \beta\theta q \omega' J_0 \tau \quad (2.35)
$$

Away from the peak, the echo amplitude is proportional to $\sim |t-2\tau|^{-3}$. The full width at half maximum time duration around $t = 2\tau$ of the echo is

$$
\Delta T^{\mathrm{FWHM}} = \frac{2}{\omega' J_0}\sqrt{2^{3/2}-1} \approx \frac{1.53}{\omega' J_0} \quad (2.36)
$$

This echo duration is comparable to the decoherence time τ_{decoh} after the dipole kick. One sees that both τ_{decoh} and ΔT^{FWHM} are much less than τ, while much longer than the beam betatron period $1/\omega_0$. Figure 2.3 shows a schematic of the echo signal. Figure 2.4 shows the echo signal near time $t = 2\tau$ according to Eq.(2.33), assumig $\omega_0 = 50\,\omega' J_0$.
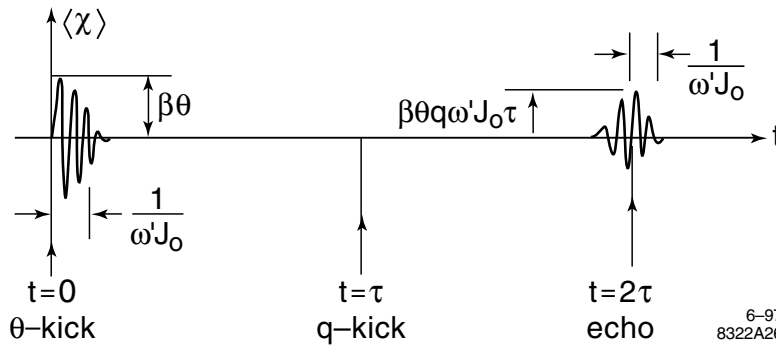

Figure 2.3: Schematic of a transverse echo experiment in a storage ring.

Exercise 6 Verify Eqs.(2.30-2.33). In passing, calculate $\langle p \rangle^{\mathrm{echo}}(t)$.
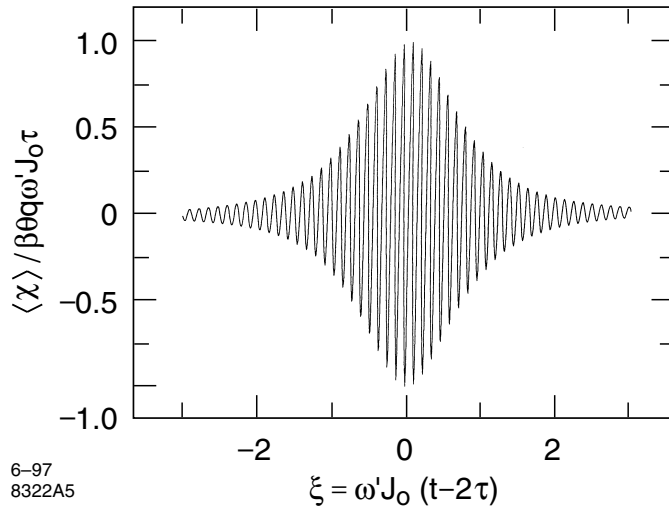
Figure 2.4: A close-in observation of the echo signal. The echo amplitude peaks at $t = 2\tau$, even though the exact value of $\langle x \rangle$ vanishes there.

Exercise 7 We showed there is an echo at $t = 2\tau$. Are there multiple echoes, for example at $t = 4\tau$, etc.?

Exercise 8 We have analyzed the problem with a quadrupole kick following a dipole kick. What happens if we reverse the order of these two kicks?

Exercise 9 There can be an echo in a linac. Give the beam at $s = 0$ a nonlinear angular kick of $\Delta x' = \theta_1 \sin k_1 x$. At $s = D$, kick the beam again by $\Delta x' = \theta_2 \sin k_2 x$. There is an echo if one observes the beam at location $s = \frac{k_1}{k_2 - k_1} D$.

Exercise 10 The ϕ-integral in Eq.(2.30) also yields a finite result if we replace the $\cos \phi$ in the integrand by $\cos 3\phi$. This means there is also an echo if we measure the sextupole moment of the beam instead of its centroid (dipole moment). Follow the procedure of the text to derive the sextupolar echo signal. When does the sextupolar echo appear? What is the magnitude of the signal?

Exercise 11 Echo signals can be superimposed.
(a) Consider two sets of kicks

> (dipole kick θ_1 at $t = -2\tau_1$, quadrupole kick q_1 at $t = -\tau_1$)
> (dipole kick θ_2 at $t = -2\tau_2$, quadrupole kick q_2 at $t = -\tau_2$)

Show that the two echo signals simply add coherently near $t = 0$ and the net amplitude is proportional to $\theta_1 q_1 \tau_1 + \theta_2 q_2 \tau_2$.
(b) Apply dipole kicks θ_0 every other turn to the beam from $t = -2T$ to $t = 0$, and apply quadrupole kicks q_0 every turn from $t = -T$ to

27

$t = 0$. There should be a very large echo signal at $t = 0$. Find this echo response.

(c) Same as (b) but when the dipole kicks are applied every turn from $t = -2T$ to $t = 0$. The dipole and quadrupole kicks in this case are therefore effectively simple step-functions.

(d) Apply dipole $(-2T < t < 0)$ and quadrupole $(-T < t < 0)$ kicks every turn, but modulate the kick strength by $\theta = \theta_0 \sin \omega_1 t$ and $q = q_0 \sin 2\omega_1 t$, where ω_1 is some modulation frequency. Find the echo response. Show that the echo amplitude is proportional to $\theta_0 q_0 T^2 / T_0$, where T_0 is the revolution time.

This exercise indicates that one can apply very weak kicks – almost at a subliminal level – for multiple number of turns and obtain a sudden huge echo.

Exercise 12 The echo set-up can be generalized. If the two kicks are m_1-th and m_2-th multipolar kicks $(m_2 > m_1)$, we should observe an $(m_2 - m_1)$-th multipolar signal at time $t = \frac{m_1}{m_2 - m_1} \tau$.

If we compare the maximum echo amplitude (2.35) to the initial kick amplitude of $\beta\theta$, we see that the echo amplitude is weaker by a factor of $q\omega' J_0 \tau$, which, according to Eq.(2.27), is much less than 1 in order for our analysis to apply. One may want to push the parameters to see how to get as big an echo signal as possible. This occurs when $q\omega' J_0 \tau$ is made to approach 1, when our analysis begins to break down.

In our analysis, we have made approximations summarized by Eq.(2.28). It is instructive to do a simulation and observe what happens in detail in the phase space. Figure 2.5 shows some of the results obtained in Ref.[3]. A gaussian beam receives a dipole kick at 0-th turn and a quadrupole kick at 20-th turn. From 0-th turn to 20-th turn the beam decoheres. By about the 30-th turn, several "clumps" develope in the beam distribution. These kinks come from an interplay of the two kicks. Each of them occurs at a specific amplitude, which are most conspiring in the sense that, with the amplitude-dependent betatron frequency, they all cohere *simultaneously* at the 40-th turn as they migrate in the phase space relative to one another.

Exercise 13 What determines the number of clumps in Fig.2.5?
Solution Examine how clumps form, and deduce that the number of clumps is equal to 2 times the number of spirals at time $t = \tau$.

Simulation also allows exploring parameters range beyond Eq.(2.28). For example, Fig.2.6 shows what happens when q is varied. Cases 1 to 3 are for small q, consistent with Eq.(2.28), and we obtain results similar to Eq.(2.34). As q is increased further, cases 4 and 5, the echo signal develops a double hump structure. The maximum echo amplitude is found to be about 40% of the initial kick amplitude (near case 3).

−1.0 −0.5 0 0.5 1.0   −1.0 −0.5 0 0.5 1.0
x (0 Turns)   x (21 Turns)

x (5 Turns)   x (30 Turns)

x (10 Turns)   x (35 Turns)

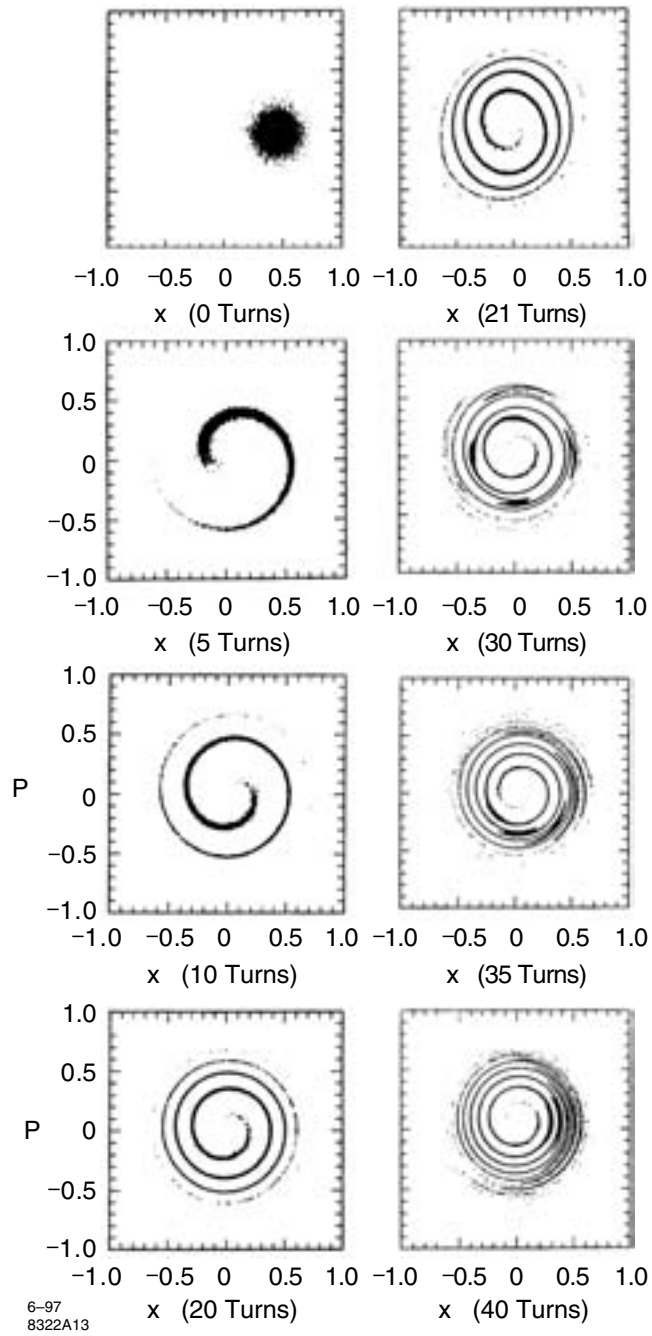x (20 Turns)   x (40 Turns)

6–97
8322A13

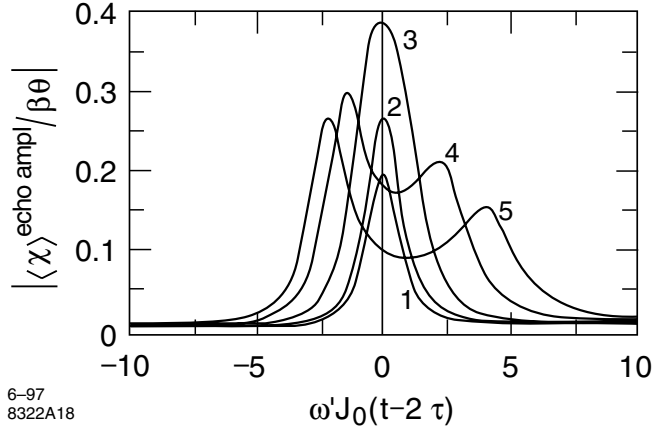Figure 2.5: Simulation of a transverse echo [3].

29

Figure 2.6: Echo amplitude signal obtained in a simulation. Curves 1 to 5 correspond to $q = 0.02, 0.03, 0.08, 0.2, 0.3$ respectively.

2.3 Transverse Echo with Diffusion

The echo mechanism involves a long term memory of the intricacies of the phase space structure. One expects that the echo signal will be affected by diffusion even when the diffusion is weak. This is turned around and becomes a great way to measure weak diffusion in storage rings.

With diffusion, the beam distribution evolves according to the diffusion equation

$$\frac{\partial \psi}{\partial t} + \omega(J)\frac{\partial \psi}{\partial \phi} = \frac{\partial}{\partial J}\left(D(J)J\frac{\partial \psi}{\partial J}\right) \tag{2.37}$$

where $D(J)$ is the diffusion coefficient.

Exercise 14 To get a feel for Eq.(2.37), show that

$$\psi = \frac{1}{2\pi(J_0 + D_0 t)}e^{-J/(J_0+D_0 t)} \tag{2.38}$$

is a solution when $D(J) + D_0$. Physically, this is simply a diffusing gaussian, with an emittance growing with time according to $\langle J \rangle = J_0 + D_0 t$.

Exercise 15 Check that $\psi_2(\phi, J, t) = \psi_1(\phi - \omega(J)t, J)$ satisfies Eq.(2.37) without diffusion.

We will solve Eq.(2.37) in the limit of weak diffusion. Specifically, we assume that the diffusion has a small effect on a time scale during which the beam decoheres. The diffusion time is roughly equal to $\tau_{\text{diff}} \approx J/D$. Requiring $\tau_{\text{diff}} \gg \tau_{\text{decoh}}$, we get

$$D \ll \omega' J^2 \tag{2.39}$$

30

In the limit of very strong diffusion, when the inequality opposite to (2.39) holds, the diffusion completely suppresses the echo effect.[4]

At time $t = 0$, the beam receives a small dipole kick. Immediately after the kick, the beam distribution is given by ψ_1 of Eq.(2.18). In the period $0 < t < \tau$, however, ψ_2 is not given by Eq.(2.18) but has to be found by solving Eq.(2.37). Change variable from ϕ to

$$v = \phi - \omega(J)t \qquad (2.40)$$

Eq.(2.37) gives

$$\frac{\partial \psi_2}{\partial t} = (\frac{\partial}{\partial J} - \omega'(J)t\frac{\partial}{\partial v}) \left[D(J)J \left(\frac{\partial \psi_2}{\partial J} - \omega'(J)t\frac{\partial \psi_2}{\partial v} \right) \right] \qquad (2.41)$$

When $\omega'Jt \gg 1$, Eq.(2.41) becomes

$$\frac{\partial \psi_2}{\partial t} \approx [\omega'(J)t]^2 D(J)J\frac{\partial^2 \psi_2}{\partial v^2} \qquad (2.42)$$

With initial condition $\psi_2(J, v, t = 0) = \psi_1(J, v)$, the solution of (2.42) for $0 < t < \tau$ is

$$\psi_2(J, v, t) = \theta\sqrt{2J\beta}\psi_0'(J) \ e^{-\frac{1}{3}D(J)J(\omega'(J))^2t^3} \sin v \qquad (2.43)$$

where we have dropped the term $\psi_0(J)$ because it does not contribute to beam centroid motion.

At $t = \tau$, the beam receives a quadrupole kick, immediately before the kick, we have

$$\psi_3(\phi, J) = \theta\sqrt{2J\beta}\psi_0'(J) \ e^{-\frac{1}{3}D(J)J(\omega'(J))^2\tau^3} \sin(\phi - \omega(J)\tau) \qquad (2.44)$$

Immediately after the kick, the perturbation ψ_4 is

$$\psi_4 \approx \theta q \omega'(J)\tau J\psi_0'(J)\sqrt{2J\beta} \ e^{-\frac{1}{3}D(J)J(\omega'(J))^2\tau^3} \sin 2\phi \cos(\phi - \omega(J)\tau) \qquad (2.45)$$

Equations (2.43-2.45) are the same as (2.18), (2.20) and (2.26) except for the extra exponential factors due to diffusion.

In the period $t > \tau$, we make a change of variable from (J, ϕ, t) to (J, v_1, t) where

$$v_1 = \phi - \omega(J)(t - \tau) \qquad (2.46)$$

in Eq.(2.37) to obtain for ψ_5

$$\frac{\partial \psi_5}{\partial t} = \left(\frac{\partial}{\partial J} - \omega'(J)(t - \tau)\frac{\partial}{\partial v_1} \right) \left[D(J)J \left(\frac{\partial \psi_5}{\partial J} - \omega'(J)(t - \tau)\frac{\partial \psi_5}{\partial v_1} \right) \right] \qquad (2.47)$$

When $\omega'J(t - \tau) \gg 1$, we have

$$\frac{\partial \psi_5}{\partial t} \approx [\omega'(J)(t - \tau)]^2 D(J)J\frac{\partial^2 \psi_5}{\partial v_1^2} \qquad (2.48)$$

---

[4]Strong diffusion is typical for electron storage rings where diffusion is caused by quantum excitations. This is why echo effect is not relevant to electron storage rings.

The solution with the initial condition $\psi_5(J, v_1 = \phi, t = \tau) = \psi_4(\phi, J)$, keeping only the term $\propto \sin(v_1 + \omega(J)\tau)$, is

$$\psi_5 = \frac{1}{2}\theta q \omega'(J)\tau J \psi_0'(J)\sqrt{2J\beta}\sin[\phi - \omega(J)t + 2\omega(J)\tau]$$
$$\times \exp\left[-\frac{1}{3}D(J)J(\omega'(J))^2((t-\tau)^3 + \tau^3)\right] \tag{2.49}$$

Substituting (2.49) into (2.30) and performing the ϕ-integration gives for the echo signal

$$\langle x\rangle^{\text{echo}}(t) = -\pi\beta\theta q\tau \int_0^\infty J^2 dJ \; \omega'(J)\psi_0'(J)\sin[\omega(J)(t - 2\tau)]$$
$$\times e^{-\frac{1}{3}D(J)J(\omega'(J))^2(\tau^3 + (t-\tau)^3)} \tag{2.50}$$

Note that the echo appears near $t \approx 2\tau$. Since we assume that diffusion is weak, the exponent in Eq.(2.50) is a slow function of time, and we can put $t = 2\tau$ in it, yielding

$$\langle x\rangle^{\text{echo}}(t) \approx -\pi\beta\theta q\tau \int_0^\infty J^2 dJ \; \omega'(J)\psi_0'(J)\sin[\omega(J)(t - 2\tau)]e^{-\frac{2}{3}D(J)J(\omega'(J))^2\tau^3}$$
$$\tag{2.51}$$

which is a generalization of Eq.(2.32).

If we assume that $\omega(J)$ and $\psi_0(J)$ are given by Eqs.(2.8-2.9), and that the diffusion coefficient is a constant, $D(J) = D_0$, the integration in (2.51) can be performed explicitly. The result is

$$\langle x\rangle^{\text{echo}}(t) = \beta\theta q \omega' J_0 \tau \; \text{Im}\left[\frac{e^{i\Phi}}{(\alpha - i\xi)^3}\right]$$
$$= \frac{\beta\theta q \omega' J_0 \tau}{(\alpha^2 + \xi^2)^3}[\xi(3\alpha^2 - \xi^2)\cos\Phi + \alpha(\alpha^2 - 3\xi^2)\sin\Phi] \tag{2.52}$$

where ξ and Φ were defined in Eq.(2.33), and

$$\alpha \equiv 1 + \frac{2}{3}D_0(\omega')^2 J_0 \tau^3 \tag{2.53}$$

When $D_0 = 0$, this reduces to (2.33). It also follows that

$$\langle x\rangle^{\text{echo ampl}}(t) = \beta\theta q \frac{\omega' J_0 \tau}{(\alpha^2 + \xi^2)^{3/2}} \tag{2.54}$$

Compared with Eq.(2.34), Eq.(2.54) is just to replace the quantity $1 + \xi^2$ by $\alpha^2 + \xi^2$ in the denominator. The difference between α and 1 can be written as

$$\alpha - 1 = \frac{2}{3}\left(\frac{D_0\tau}{J_0}\right)(\omega' J_0 \tau)^2 \tag{2.55}$$

where the factor $D_0\tau/J_0$ is just τ/τ_{diff}, i.e. the ratio of the time between the two kicks to the diffusion time. The factor $\omega' J_0 \tau$ is the betatron phase smear

due to the frequency spread, and is $\gg 1$. We see that the difference between α and 1 is typically large, thus allowing a good opportunity to measure the diffusion strength. In fact, the measurement can in principle be so accurate that it is conceivable that one can explore the diffusion coefficient as a function of J using this method.

Figure 2.7 shows the echo amplitude as a function of ξ for various values of α. When $\alpha = 1$, the curve is just the envelope of Fig.2.4. When $\alpha \neq 1$, the location of the echo is not changed, but the magnitude is reduced by a factor of α^3, indicating the sensitive dependence on diffusion.
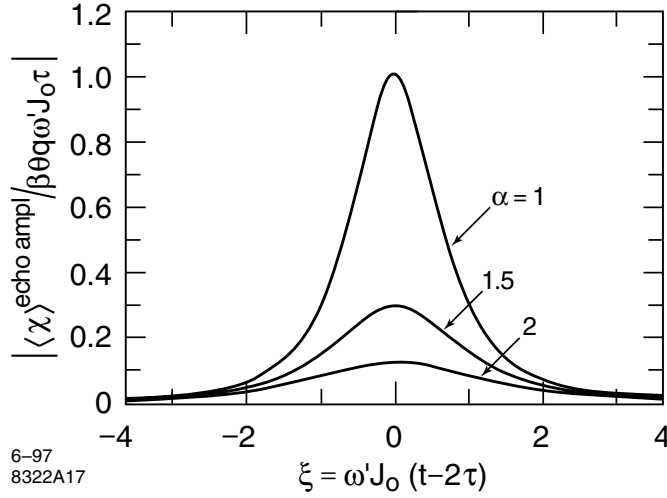
Figure 2.7: Reduction of echo amplitude when diffusion is included.

Given the diffusion coefficient D_0, one may want to maximize the echo signal by choosing τ. With

$$\langle x \rangle^{\text{echo ampl max}} = \frac{\beta \theta q \omega' J_0 \tau}{\alpha^3} \tag{2.56}$$

or, equivalently

$$\frac{\langle x \rangle^{\text{echo ampl max}}}{\beta \theta q} = \frac{\Theta}{\left[1 + \frac{2}{3} \left(\frac{D_0}{\omega' J_0^2} \right) \Theta^3 \right]^3} \tag{2.57}$$

where $\Theta = \omega' J_0 \tau \ll 1$. The quantity $D_0 / \omega' J_0^2$ in Eq.(2.57) is $\ll 1$ according to condition (2.39). Fig.2.8 shows $\langle x \rangle^{\text{echo ampl max}}$ as a function of τ. Without diffusion, $D_0 = 0$, the perturbation theory predicts a linear growth of the echo signal with the delay time τ. When $D_0 \neq 0$, the maximum value of $\langle x \rangle^{\text{echo ampl max}}$ is achieved at

$$\tau_{\max} = \left[\frac{16}{3} D_0 (\omega')^2 J_0 \right]^{-1/3} \tag{2.58}$$

33

In terms of decoherence and diffusion times, the maximum is achieved at $\tau_{\max} \sim (\tau_{\mathrm{diff}}\tau_{\mathrm{decoh}}^2)^{1/3}$. When $\tau = \tau_{\max}$, we have $\alpha = \frac{9}{8}$ and the maximum echo amplitude is given by

$$\mathrm{maximum}\left(\frac{\langle x \rangle^{\mathrm{echo\ ampl\ max}}}{\beta\theta q}\right) = \left(\frac{8}{9}\right)^3 \left(\frac{16}{3}\frac{D_0}{\omega' J_0^2}\right)^{-1/3} \qquad (2.59)$$

The full width at half maximum time duration of the echo signal is [compare Eq.(2.36)]

$$\Delta T^{\mathrm{FWHM}} = \frac{2\alpha}{\omega' J_0}\sqrt{2^{2/3}-1} \approx 1.53\frac{\alpha}{\omega' J_0} \qquad (2.60)$$

For $\tau = \tau_{\max}$, we have $\Delta T_{\mathrm{FWHM}} = 1.72/\omega' J_0$.
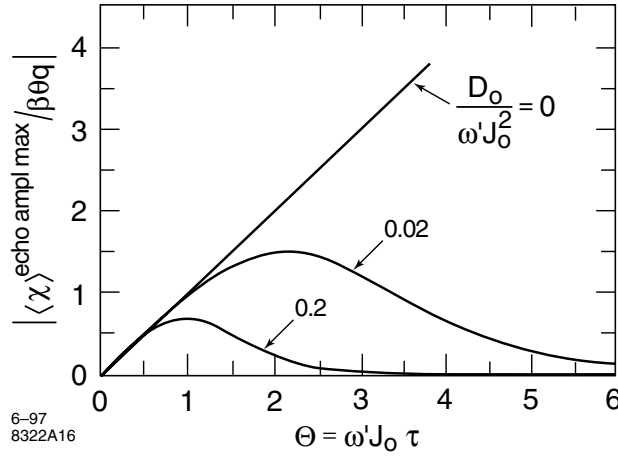
Figure 2.8: Dependence of the maximum echo amplitude when the time between the two kicks is varied. Three cases are for different strengths of the diffusion effect.

Experimentally, both quantities ω' and D_0 can be found from the echo measurements. Measurement of ΔT^{FWHM} or the decoherence time τ_{decoh} can yield information on $\omega' J_0$. If the beam emittance J_0 is known, this allows one to determine ω'. After that, D_0 can be found by measuring $\tau_{\max}$ and using Eq.(2.58), or by measuring the maximum echo amplitude and using Eq.(2.59). See the following table:

Measurement	$\rightarrow$	information
τ_{decoh}	$\rightarrow$	$\omega' J_0$
height of echo	$\rightarrow$	$\frac{\omega' J_0 \tau}{\alpha^3}$
width of echo	$\rightarrow$	$\frac{\omega' J_0}{\alpha}$
$\tau_{\max}$	$\rightarrow$	$D_0 \omega'^2 J_0$
height of echo at $\tau = \tau_{\max}$	$\rightarrow$	$\frac{D_0}{\omega' J_0^2}$
shape of echo amplitude with respect to τ	$\rightarrow$	D as a function of J

34

In some cases (e.g. with beam-beam interaction, or near a nonlinear resonance), the diffusion coefficient may be a sensitive function of J, and it may not be a good approximation to treat it as a constant. Experimentally, transverse echo gives a possibility not only to measure an average diffusion coefficient within the bunch, but also to obtain information on the dependence of diffusion strength on betatron amplitude. With $D = D(J)$, we resort to Eq.(2.51). For example, we may model the diffusion coefficient as

$$D(J) = D_n \left(\frac{J}{J_0} \right)^n \tag{2.61}$$

Equation (2.51) can be used to give

$$\langle x \rangle^{\text{echo ampl max}} = -\pi \beta \theta q \tau \int_0^\infty J^2 dJ \ \omega'(J) \psi_0'(J) e^{-\frac{2}{3} D(J) J (\omega'(J))^2 \tau^3} \tag{2.62}$$

where we have inserted $t = 2\tau$ to obtain the maximum echo amplitude.

If we assume Eqs.(2.8-2.9) for $\psi_0(J)$ and $\omega(J)$, then

$$\frac{\langle x \rangle^{\text{echo ampl max}}}{\beta \theta q} = \frac{\Theta}{2} \int_0^\infty x^2 dx \ \exp\left[-x - \frac{2}{3} \left(\frac{D_n}{\omega' J_0^2} \right) \Theta^3 x^{n+1} \right] \tag{2.63}$$

where $\Theta = \omega' J_0 \tau$. Figure 2.9 shows $\langle x \rangle^{\text{echo ampl max}}$ as a function of Θ for various values of $D_n/\omega' J_0^2$; (a, b, c, d) are for $n = (-1, 1, 2, 3)$ respectively. When $n = 0$, Fig.2.8 is reproduced.

Exercise 16 (a) Show that when $n = 0$, Eq.(2.62) reduces to (2.56). (b) A special case occurs when $n = -1$, i.e. when the diffusion is stronger for smaller J than for larger J. Show that, acccording to Eqs.(2.8-2.9),[5]

$$\langle x \rangle^{\text{echo ampl max}} = \beta \theta q \omega' J_0 \tau \ e^{-\frac{2}{3} D_{-1} (\omega')^2 J_0 \tau^3} \tag{2.64}$$

Exercise 17 Find what happens to a waterbag model $\psi_0(J) = \frac{1}{2\pi J_0} H(J_0 - J)$ with arbitrary $\omega(J)$ and $D(J)$.

2.4 Longitudinal Decoherence and Echo

The above analysis applies to the transverse motion of a bunched beam. With minor modifications, the same physics applies to the longitudinal motion of a bunched beam. For an unbunched beam, however, the dynamics is sufficiently different that we are going to treat it independently in the following sections.

---

[5]The fact that the $n = -1$ case is particularly simple can be traced to Eq.(2.37). Equation (2.37) becomes particularly simple when $D(J) \propto J^{-1}$. In fact, the longitudinal echo with diffusion has this same simplifying behavior when $D(\delta) = $ constant. See Eq.(2.91) later.
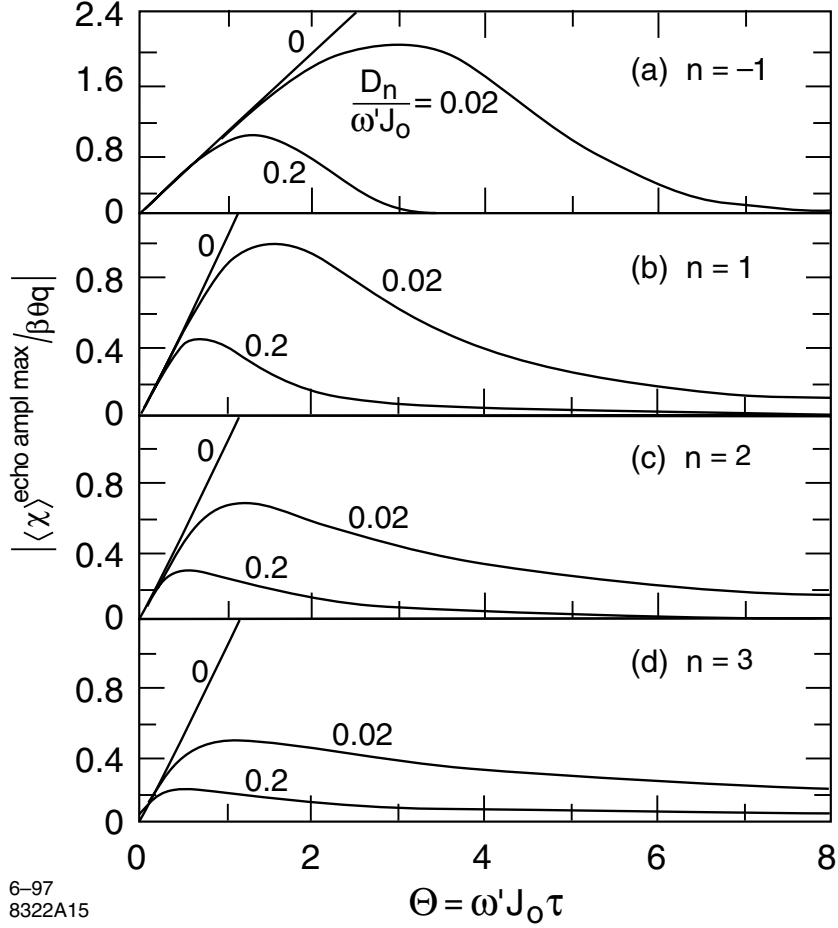
Figure 2.9: Same as Fig.2.8, but the diffusion is now modeled as in Eq.(2.61).

To study the longitudinal echo effect for an unbunched beam, we also need two kicks separated by a long time τ. Before the first kick, the beam has a phase space distribution

$$\psi(z, \delta) = \psi_0(\delta) \tag{2.65}$$

which is uniform in z. The first kick at time $t = 0$ is to impose an rf voltage energy kick

$$\Delta\delta(z) = \frac{eV_1}{E_0} \sin\left(h_1 \frac{z}{R} + \phi_1\right) \tag{2.66}$$

where E_0 is the nominal beam energy, and h_1 is the harmonic number. The application of the voltage is considered to be instantaneous in the sense that it is applied for a time much shorter than the decoherence time to be defined later in Eq.(2.76).

After the first kick, the beam begins to bunch up with harmonic number h_1, but due to the energy spread of the beam, this bunching signal decoheres

36

quickly. Long after the signal has decohered, at $t = \tau$, a second kick is then applied to the beam,

$$\Delta\delta(z) = \frac{eV_2}{E_0} \sin\left(h_2\frac{z}{R} + \phi_2\right) \tag{2.67}$$

What we will show is that, at a much later time, one will observe a sudden echo with harmonic number $|h_2| - |h_1|$ if $|h_1| < |h_2|$ and no echo if $|h_1| > |h_2|$.

Longitudinal Decoherence

We first consider the decoherence after the first kick. The single-particle equations of motion are

$$\dot{z} = -\eta c\delta, \qquad \dot{\delta} = 0 \tag{2.68}$$

where η is the phase slippage factor. Immediately after the kick, the beam distribution is

$$
\begin{aligned}
\psi_1(z,\delta) &= \psi_0\left[\delta - \frac{eV_1}{E_0}\sin\left(h_1\frac{z}{R} + \phi_1\right)\right] \\
&\approx \psi_0(\delta) - \psi_0'(\delta)\frac{eV_1}{E_0}\sin\left(h_1\frac{z}{R} + \phi_1\right)
\end{aligned}
\tag{2.69}
$$

where we have assumed the kick is weak.

After the kick, the particle coordinates are given by

$$z_2 = z_1 - \eta ct\delta_1, \qquad \delta_2 = \delta_1 \tag{2.70}$$

The beam distribution is therefore

$$
\begin{aligned}
\psi_2(z,\delta,t) &= \psi_1(z + \eta ct\delta, \delta) \\
&\approx \psi_0(\delta) - \psi_0'(\delta)\frac{eV_1}{E_0}\sin\left(h_1\frac{z + \eta ct\delta}{R} + \phi_1\right)
\end{aligned}
\tag{2.71}
$$

The beam current monitor measures

$$
\begin{aligned}
I_2(z,t) &= \int_{-\infty}^{\infty} d\delta\ \psi_2(z,\delta,t) \\
&\approx I_0 - \frac{eV_1}{E_0}\int_{-\infty}^{\infty} d\delta\ \psi_0'(\delta)\sin\left(h_1\frac{z + \eta ct\delta}{R} + \phi_1\right)
\end{aligned}
\tag{2.72}
$$

where $I_0 = \int_{-\infty}^{\infty} d\delta\psi_0(\delta)$ is the unperturbed beam current. We are of course interested only in the second term in Eq.(2.72). We shall simply drop the term I_0.

If we have a gaussian δ-distribution,

$$\psi_0(\delta) = \frac{I_0}{\sqrt{2\pi}\sigma_\delta}e^{-\delta^2/2\sigma_\delta^2} \tag{2.73}$$

37

Eq.(2.72) can be integrated to yield[6]

$$I_2(z,t) \approx I_0 \frac{eV_1 h_1 \eta ct}{E_0 R} \cos\left(h_1 \frac{z}{R} + \phi_1\right) \exp\left[-\frac{1}{2}\left(\frac{h_1 \eta ct\sigma_\delta}{R}\right)^2\right] \qquad (2.75)$$

At $t = 0$, the beam current signal is zero. This is because the beam takes some time to become bunched after the kick. The signal will continue to grow indefinitely if not due to the energy spread of the beam which causes a decoherence. The decoherence time is when it takes a σ_δ-particle to move longitudinally by a distance R/h_1, i.e.

$$\tau_{\text{decoh}} = \frac{R}{h_1 \eta c\sigma_\delta} \qquad (2.76)$$

One obtains the amplitude of the signal by dropping the cosine factor in Eq.(2.75),

$$I_2^{\text{ampl}}(t) \approx I_0 \frac{eV_1}{E_0 \sigma_\delta} \frac{t}{\tau_{\text{decoh}}} \exp\left(-\frac{t^2}{2\tau_{\text{decoh}}^2}\right) \qquad (2.77)$$

The maximum values of I_2^{ampl} occurs when $t = \tau_{\text{decoh}}$ with

$$I_2^{\text{ampl max}} = I_0 \frac{eV_1}{E_0 \sigma_\delta} \exp(-\frac{1}{2}) \qquad (2.78)$$

At $t = 0$ and $t \to \infty$, however, the beam current signal vanishes.

Longitudinal Echo

The evolution of the coordinates of a particle during the process is summarized by

$$
\begin{aligned}
\text{At } t = 0^+, &\quad \begin{cases} z_1 = z_0 \\ \delta_1 = \delta_0 + \frac{eV_1}{E_0}\sin\left(h_1\frac{z_0}{R} + \phi_1\right) \end{cases} \\[1em]
\text{At } t = \tau^-, &\quad \begin{cases} z_3 = z_1 - \eta c\tau\delta_1 \\ \delta_3 = \delta_1 \end{cases} \\[1em]
\text{At } t = \tau^+, &\quad \begin{cases} z_4 = z_3 \\ \delta_4 = \delta_3 + \frac{eV_2}{E_0}\sin\left(h_2\frac{z_3}{R} + \phi_2\right) \end{cases} \\[1em]
\text{At } t > \tau, &\quad \begin{cases} z_5 = z_4 - \eta c(t - \tau)\delta_4 \\ \delta_5 = \delta_4 \end{cases}
\end{aligned}
\qquad (2.79)
$$

What we need to do is to solve (z_0, δ_0) in terms of (z_5, δ_5), and substitute $\delta_0(z_5, \delta_5)$ into the initial distribution $\psi_0(\delta_0)$ to obtain the beam distribution at time $t > \tau$. Having obtained the beam distribution, the beam signal follows.

---

[6]Using

$$\int_{-\infty}^{\infty} \delta d\delta \, e^{-\delta^2/2\sigma_\delta^2} \sin a\delta = \sqrt{2\pi} a\sigma_\delta^3 e^{-a^2\sigma_\delta^2/2} \qquad (2.74)$$

But this is a tedious calculation, and in the following, we shall be content with the perturbation approach again as we did in the transverse case. Thus, keeping only the leading terms for the echo effect, we find

$$\psi_3(z,\delta) \approx -\psi_0'(\delta)\frac{eV_1}{E_0}\sin\left(h_1\frac{z+\eta c\tau\delta}{R}+\phi_1\right) \tag{2.80}$$

$$\begin{aligned}
\psi_4(z,\delta) &= \psi_3\left[z,\delta-\frac{eV_2}{E_0}\sin\left(h_2\frac{z}{R}+\phi_2\right)\right]\\
&\approx -\frac{eV_2}{E_0}\sin\left(h_2\frac{z}{R}+\phi_2\right)\frac{\partial\psi_3}{\partial\delta}\\
&\approx \frac{eV_1}{E_0}\frac{eV_2}{E_0}\frac{h_1\eta c\tau}{R}\psi_0'(\delta)\sin\left(h_2\frac{z}{R}+\phi_2\right)\\
&\quad \times\cos\left(h_1\frac{z+\eta c\tau\delta}{R}+\phi_1\right)
\end{aligned} \tag{2.81}$$

$$\begin{aligned}
\psi_5(z,\delta,t) &= \psi_4(z+\eta c(t-\tau)\delta,\delta)\\
&\approx \frac{eV_1}{E_0}\frac{eV_2}{E_0}\frac{h_1\eta c\tau}{R}\psi_0'(\delta)\sin\left(h_2\frac{z+\eta c(t-\tau)\delta}{R}+\phi_2\right)\\
&\quad \times\cos\left(h_1\frac{z+\eta ct\delta}{R}+\phi_1\right)
\end{aligned} \tag{2.82}$$

Knowing ψ_5, the echo beam current signal is given by

$$I^{\mathrm{echo}}(z,t) = \int_{-\infty}^{\infty} d\delta\ \psi_5(z,\delta,t) \tag{2.83}$$

Substituting Eq.(2.82) into Eq.(2.83), assuming an initial gaussian energy distribution (2.73), and performing the integration over δ, we obtain

$$\begin{aligned}
I^{\mathrm{echo}}(z,t) &= -\frac{1}{2}I_0\frac{eV_1}{E_0}\frac{eV_2}{E_0}\frac{h_1\eta^2c^2\tau}{R^2}\\
&\quad \times\Bigg\{[(h_1+h_2)t-h_2\tau]\cos\left((h_1+h_2)\frac{z}{R}+\phi_1+\phi_2\right)\\
&\quad \times\exp\left[-\frac{\eta^2c^2\sigma_\delta^2}{2R^2}((h_1+h_2)t-h_2\tau)^2\right]\\
&\quad -[(h_1-h_2)t+h_2\tau]\cos\left((h_1-h_2)\frac{z}{R}+\phi_1-\phi_2\right)\\
&\quad \times\exp\left[-\frac{\eta^2c^2\sigma_\delta^2}{2R^2}((h_1-h_2)t+h_2\tau)^2\right]\Bigg\}
\end{aligned} \tag{2.84}$$

An inspection of Eq.(2.84) shows that the echo signal occurs potentially at times $t^{\mathrm{echo}} = h_2\tau/(h_1+h_2)$ and $t^{\mathrm{echo}} = -h_2\tau/(h_1-h_2)$. However, we are interested only when $t^{\mathrm{echo}} > \tau$. By evaluating the possible signs of h_1 and h_2, one finds that an echo signal occurs only if $|h_2| > |h_1|$, and that the echo contribution to Eq.(2.84) can be re-written as

$$I^{\mathrm{echo}}(z,t) = -\frac{1}{2}\mathrm{sgn}(h_2)I_0\frac{eV_1}{E_0}\frac{eV_2}{E_0}\frac{h_1\eta^2c^2\tau}{R^2}[(|h_2|-|h_1|)t-|h_2|\tau]$$

$$\times \cos\left((|h_2| - |h_1|)\frac{z}{R} - \text{sgn}(h_1)\phi_1 + \text{sgn}(h_2)\phi_2\right)$$

$$\times \exp\left[-\frac{\eta^2 c^2 \sigma_\delta^2}{2R^2}((|h_2| - |h_1|)t - |h_2|\tau)^2\right] \qquad (2.85)$$

Dropping the cosine factor in Eq.(2.85) gives

$$
\begin{aligned}
I^{\text{echo ampl}}(t) &= -\frac{1}{2}\text{sgn}(h_2)I_0\frac{eV_1}{E_0}\frac{eV_2}{E_0}\frac{h_1\eta c\tau}{R\sigma_\delta}\,\xi e^{-\xi^2/2} \\
t^{\text{echo}} &= \frac{|h_2|\tau}{|h_2| - |h_1|} \\
\xi &= \frac{\eta c\sigma_\delta(|h_2| - |h_1|)}{R}(t - t^{\text{echo}})
\end{aligned} \qquad (2.86)
$$

Equation (2.86) for the longitudinal echo is the equivalent of Eq.(2.34) for the transverse echo.

One sees from Eqs.(2.85-2.86) that (a) the RF kick phases $\phi_{1,2}$ determine the phase of the current signal, but otherwise does not have a prominent role, (b) the echo signal has a harmonic number $|h_2| - |h_1|$, and (c) the echo amplitude vanishes at $t = t^{\text{echo}}$. Observation (c) is in contrast to the transverse echo amplitude, which reaches maximum at $t = 2\tau$ (even though the *instantaneous signal* vanishes, the *amplitude* reaches a maximum).

The echo amplitude reaches maxima when $\xi = \pm 1$, or

$$t - t^{\text{echo}} = \pm\frac{R}{\eta c\sigma_\delta(|h_2| - |h_1|)} \qquad (2.87)$$

and the maximum value reached is

$$I^{\text{echo ampl max}} = \pm\frac{1}{2}I_0\frac{eV_1}{E_0}\frac{eV_2}{E_0}\frac{h_1\eta c\tau}{R\sigma_\delta}\exp(-\frac{1}{2}) \qquad (2.88)$$

Note that the beam current signal after the first kick has harmonic number h_1, while the echo signal has harmonic number $h_2 - h_1$. Inspite of this, however, one can compare the maximum echo amplitude (2.88) with the maximum decoherence signal (2.78) and obtain

$$\frac{I^{\text{echo ampl max}}}{I_2^{\text{ampl max}}} = \frac{1}{2}\frac{eV_2}{E_0}\frac{h_1\eta c\tau}{R} \qquad (2.89)$$

Equation (2.89) is to be compared with Eq.(2.35).

The analogies between transverse and longitudinal echoes are as follows:

$$
\begin{aligned}
\frac{eV_1}{E_0} &\leftrightarrow \beta\theta \\
\frac{eV_2}{E_0} &\leftrightarrow q \\
h_1 &\leftrightarrow 1 \text{ (dipole kick)}
\end{aligned}
$$

40

$$\begin{aligned}
h_2 &\leftrightarrow 2 \text{ (quadrupole kick)} \\
\frac{\eta c}{R} &\leftrightarrow \omega' J_0 \\
t - t^{\text{echo}} &\leftrightarrow t - 2\tau
\end{aligned} \qquad (2.90)$$

Definition of ξ in Eq.(2.86) is analogous to the ξ defined in Eq.(2.33).

Exercise 18 Reference [4] contains beautiful data, reproduced as Fig.2.10, of longitudinal echo for an unbunched beam in the Antiproton Accumulator Ring at Fermilab. Compare the data with what is expected from Eqs.(2.86), (2.87) and (2.89). The parameters: $h_1 = 9, h_2 = 10, R = 70$ m, $\tau = 0.075$ s, $\eta = 0.023, E_0 = 8696$ MeV, $\Delta E = 3.2$ MeV. The two rf kicks are of the same magnitude $V_1 = V_2 = 1.5$ MV (to be checked).

Solution The following quantities can be checked: $t_{\text{peak}} = 10\tau = 0.75$ s, $\Delta t_{\text{peak}} = 2R/\eta c\sigma_\delta = 0.06$ s, $\tau_{\text{decoh}} = R/h_1\eta c\sigma_\delta = 3$ ms, $I^{\text{echo ampl max}}/I_2^{\text{ampl max}} = 0.4$. Diffusion effect is not serious in this experiment as can be checked against Fig.2.11 later.
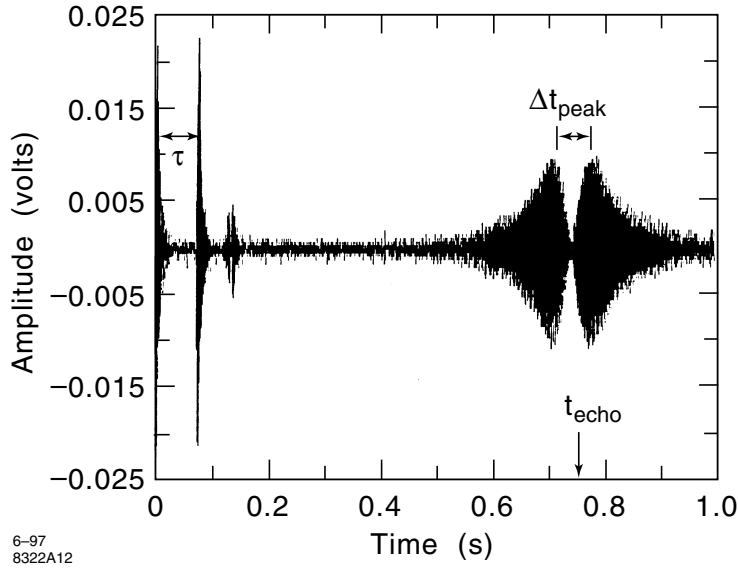

Figure 2.10: A longitudinal echo experiment at the AA ring [4]. There is a high order echo at $t = 10\tau = 0.75$ s.

2.5 Longitudinal Echo with Diffusion

We next consider what happens to the longitudinal echo when there is diffusion. The analysis follows similar steps as in the transverse case. After the first kick,

the beam distribution is still given by ψ_1 of Eq.(2.69). The distribution ψ_2, however, is not given by Eq.(2.71), but is to be solved with the diffusion equation

$$\frac{\partial \psi_2}{\partial t} - \eta c \delta \frac{\partial \psi_2}{\partial z} = \frac{\partial}{\partial \delta} \left[D(\delta) \frac{\partial \psi_2}{\partial \delta} \right] \tag{2.91}$$

In Eq.(2.91) we have assumed that the diffusion originates from noise in δ. A noise in z is not going to have a significant effect on the echo.

   Exercise 19 To get a feel for Eq.(2.91), show that

$$\psi = \frac{1}{\sqrt{2\pi(\delta_0^2 + D_0 t)}} e^{-\delta^2/(\delta_0 + D_0 t)} \tag{2.92}$$

   is a solution when $D(\delta) = D_0$. Physically this is simply a diffusing gaussian distribution with energy spread $\langle \delta^2 \rangle = \delta_0^2 + D_0 t$. Compare with Exercise 14 for similarities and differences.

   Changing variable from z to

$$v = z + \eta c t \delta \tag{2.93}$$

and Let $\psi_2 = \psi_2(v, \delta, t)$, Eq.(2.91) becomes

$$\frac{\partial \psi_2}{\partial t} = \left(\frac{\partial}{\partial \delta} + \eta c t \frac{\partial}{\partial v} \right) \left[D(\delta) \left(\frac{\partial \psi_2}{\partial \delta} + \eta c t \frac{\partial \psi_2}{\partial v} \right) \right] \tag{2.94}$$

When $\eta c t \delta \gg 1$, Eq.(2.94) becomes

$$\frac{\partial \psi_2}{\partial t} \approx (\eta c t)^2 D(\delta) \frac{\partial^2 \psi_2}{\partial v^2} \tag{2.95}$$

   The solution to Eq.(2.95), with the initial condition $\psi_2(v = z, \delta, t = 0) = \psi_1(z, \delta)$, is

$$\psi_2(v, \delta, t) \approx -\psi_0'(\delta) \frac{eV_1}{E_0} \exp \left[-\frac{1}{3} \left(\frac{\eta c h_1}{R} \right)^2 D(\delta) t^3 \right] \sin \left(h_1 \frac{v}{R} + \phi_1 \right) \tag{2.96}$$

Having obtained ψ_2, the beam distributions before and after the second RF kick are found to be the same as Eqs.(2.80) and (2.81) when there was no diffusion, except that now they both have acquired an extra exponential diffusion factor

$$\exp \left[-\frac{1}{3} \left(\frac{\eta c h_1}{R} \right)^2 D(\delta) \tau^3 \right]$$

   After the second kick, the diffusion equation for ψ_5 is

$$\frac{\partial \psi_5}{\partial t} = \left(\frac{\partial}{\partial \delta} + \eta c (t - \tau) \frac{\partial}{\partial v_1} \right) \left[D(\delta) \left(\frac{\partial \psi_5}{\partial \delta} + \eta c (t - \tau) \frac{\partial \psi_5}{\partial v_1} \right) \right] \tag{2.97}$$

where we have changed variables to $\psi_5(v_1, \delta, t)$ with

$$v_1 = z + \eta c(t - \tau)\delta \qquad (2.98)$$

If $\eta c(t - \tau)\delta \gg 1$, we have

$$\frac{\partial \psi_5}{\partial t} \approx \eta^2 c^2 (t - \tau)^2 D(\delta) \frac{\partial^2 \psi_5}{\partial v_1^2} \qquad (2.99)$$

With the initial condition $\psi_5(v_1 = z, \delta, t = \tau) = \psi_4(z, \delta)$, the solution to Eq.(2.99) is

$$
\begin{aligned}
\psi_5(z, \delta, t) \quad &\approx \quad \frac{1}{2} \frac{eV_1}{E_0} \frac{eV_2}{E_0} \frac{h_1 \eta c \tau}{R} \psi_0'(\delta) \\
&\times \exp\left[-\frac{1}{3} \frac{\eta^2 c^2}{R^2} D(\delta) \left(h_1^2 \tau^3 + (h_2 - h_1)^2 (t - \tau)^3 \right) \right] \\
&\times \sin\left[(h_2 - h_1)\frac{z}{R} + \phi_2 - \phi_1 + \frac{\eta c}{R}\delta((h_2 - h_1)t - h_2\tau) \right] (2.100)
\end{aligned}
$$

where we have assumed $h_2 > h_1 > 0$ and have kept only the echo contribution. The exponential factor in Eq.(2.100) can be replaced by its value near $t = \tau^{\text{echo}}$ with τ^{echo} given by Eq.(2.86) because it is a slow function of t, i.e.

$$
\begin{aligned}
&\exp\left[-\frac{1}{3} \frac{\eta^2 c^2}{R^2} D(\delta) \left(h_1^2 \tau^3 + (h_2 - h_1)^2 (t - \tau)^3 \right) \right] \\
\approx \quad &\exp\left[-\frac{1}{3} \frac{\eta^2 c^2}{R^2} D(\delta) \frac{h_1^2 h_2}{h_2 - h_1} \tau^3 \right] \qquad (2.101)
\end{aligned}
$$

Given ψ_5, the echo signal is given by Eq.(2.83). If we assume that the initial beam distribution is given by Eq.(2.73) and that the diffusion coefficient is a constant $D(\delta) = D_0$, we find that I^{echo} is given by the same expression (2.85) without diffusion, multiplied by the exponential factor (2.101). It then follows that

$$I^{\text{echo ampl}} = \frac{1}{2} I_0 \frac{eV_1}{E_0} \frac{eV_2}{E_0} \frac{h_1 \eta c \tau}{R \sigma_\delta} \, \xi e^{-\xi^2/2} \exp\left[-\frac{1}{3} \frac{\eta^2 c^2}{R^2} D_0 \frac{h_1^2 h_2}{h_2 - h_1} \tau^3 \right] \qquad (2.102)$$

where ξ was defined with Eq.(2.86).

The maxima of echo amplitude occur at $\xi = \pm 1$, with [compare Eq.(2.88)]

$$I^{\text{echo ampl max}} = \pm \frac{1}{2} I_0 \frac{eV_1}{E_0} \frac{eV_2}{E_0} \frac{h_1 \eta c \tau}{R \sigma_\delta} \exp(-\frac{1}{2}) \exp\left[-\frac{1}{3} \frac{\eta^2 c^2}{R^2} D_0 \frac{h_1^2 h_2}{h_2 - h_1} \tau^3 \right]$$
$$(2.103)$$

and

$$\tau_{\text{max}} = \left[\frac{(h_2 - h_1)R^2}{\eta^2 c^2 D_0 h_1^2 h_2} \right]^{1/3} \qquad (2.104)$$

43
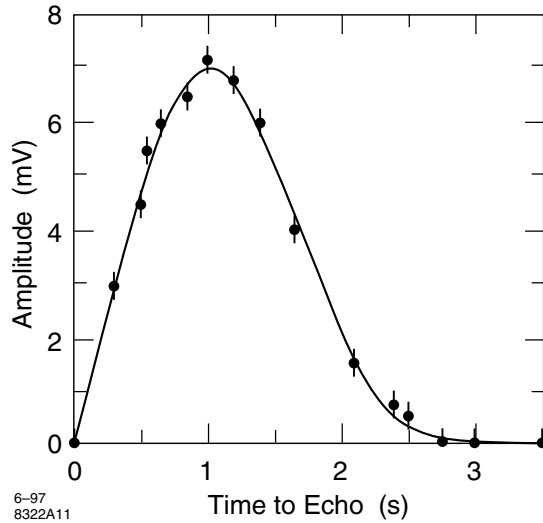
Figure 2.11: Measured maximum echo amplitude as a function of t^{echo} in the AA ring. Diffusion is playing an important role.

Exercise 20 Figure 2.11 reproduces the data in Ref.[4] when the maximum echo amplitude is measured as τ is varied. (a) Fit the data to Eq.(2.103) to find the value of D_0. (b) Show that Eq.(2.91) implies the rms energy spread diffuses according to $\frac{d}{dt}\sigma_\delta^2 = D_0$. (c) Use the result found in (a) to calculate how much time does it take the diffusion to contribute to an energy spread of 10^{-3}. This diffusion is weak, and yet it can be measured in a rather pronounced manner by the echo experiment.
Solution $D_0 = 1.3 \times 10^{-10} \, \text{s}^{-1}$.

Exercise 21 Consider a bunched beam. First kick the beam by an RF phase shift. Then kick it again by an RF amplitude jump. Analyze the echo response of this beam. This problem is more similar to the transverse case than to the longitudinal unbunched beam case.

Exercise 22 Find an expression for the echo amplitude if $D(\delta)$ is not a constant, but is $D(\delta) = D_n(\delta/\sigma_\delta)^n$. Is there any indication from Fig.2.11 that $D(\delta)$ is not a constant?

References

[1] A.Y. Wong, D.R. Baker, Phys. Rev. 188, 326 (1969).

[2] G. Stupakov, SSCL Report 579 (1992).

[3] G. Stupakov and S. Kauffmann, SSCL Report 587 (1992).

[4] L.K. Spenzouris, J.-F. Ostigy, P.L. Colestock, Phys. Rev. Lett. 76, 620 (1996).

[5] O. Bruning et al., Euro. Part. Accel. Conf. 1996.

[6] G. Stupakov and A. Chao, Part. Accel. Conf. 1997.

3 Crystalline Beams

When completed, crystalline beam research should be much more extensive than what will be presented below. Basically we could be re-doing the entire solid state physics – melting point, phonons, specific heat, heat conduction, quantum effects, spin effects – just replacing molecular force by Coulomb force. It also has the added complication that charges can radiate.

For accelerators, we ask (a) how to cool the beam sufficiently for it to crystalize (i.e. how does the beam make the phase transition from a gaseous state to a solid state), and (b) what conditions must the accelerator fulfill so as not to destroy the crystal once it is formed. For possible applications, we ask (c) what if we collide two crystalline beams, or (d) how does a crystalline beam radiate in an undulater, in a solid crystal, or in another crystalline beam.

We will first find several types of beam crystals (crystal hunting) and examine some of their properties. The procedure is not systematic and does not provide an exhaustive hunt. (A systematic hunt would use group theory.) We will then make a preliminary examination of question (b) above. What we will talk about can at best be a very small fraction of the research this topic eventually can offer.

When sufficiently cooled, a crystalline beam should exhibit significant quantum mechanical effects. We will not discuss these effects here.

Crystalization has been observed in ion traps. There has been hint of observation at Novosibirsk for a real crystalline beam in an accelerator. Crystalline beams have been observed in computer simulations. There are current efforts – not an easy task – to design storage rings to observe crystalline beams. Hopefully, as beam cooling technology advances, an exciting research field of crystalline beams will open up in front of us.

3.1 1-D Infinite Crystal

The simplest crystal is a 1-D infinite line of equally-spaced charged particles. Assume there is an infinitely strong transverse focusing so that the crystal is 1-D in z-direction. Let the spacing between charges be a.

This is a trivial lattice arrangement. But one can still ask what are the small-amplitude normal modes of this crystal. Let the longitudinal location of the nth particle be designated as $z_n = na + \Delta_n$, where Δ_n is a small displacement from its lattice site. Let each particle have mass M and charge Q. The equation of motion of the nth particle is

$$M\ddot{z}_n + \sum_{k=1}^{\infty} \frac{Q^2}{(z_n - z_{n+k})^2} - \sum_{k=1}^{\infty} \frac{Q^2}{(z_n - z_{n-k})^2} = 0, \quad \text{for all } n \qquad (3.1)$$

where the second and third terms on the LHS are Coulomb forces due to charges on each side of the nth particle. For small deviations from the lattice sites, we

linearize Eq.(3.1) to obtain

$$M\ddot{\Delta}_n + \sum_{k=1}^{\infty} \frac{2Q^2}{k^3 a^3}(2\Delta_n - \Delta_{n+k} - \Delta_{n-k}) = 0 \quad \text{for all } n \tag{3.2}$$

The eigenmode solution to Eq.(3.2) is found to be

$$\text{eigenvalue } \lambda \equiv \frac{M\omega^2 a^3}{2Q^2} = 4\sum_{k=1}^{\infty} \frac{1}{k^3}\sin^2\left(\frac{k\theta}{2}\right)$$

$$\text{eigenvector } \Delta_n = \cos(n\theta + \phi)\, e^{-i\omega t} \tag{3.3}$$

where ω is the eigenmode frequency. This eigenmode is characterized by the continous variables θ and ϕ. All modes with different ϕ values are degenerate, i.e. they all have the same eigenvalue. The mode index θ gives the snapshot phase in the mode pattern Δ_n between adjacent lattice sites. The modes with $\theta = 0$ have all charges moving in unison and the mode frequency is $\omega_0 = 0$ as one would expect because there is no restoring force. The modes with $\theta = \pi$ have charges moving with alternating displacements; they have the largest mode frequency given by[7]

$$\omega_\pi = \sqrt{7\zeta(3)\frac{Q^2}{Ma^3}} \tag{3.4}$$

where $\zeta(p)$ is the Riemann zeta-function (which occurs often in crystal beam calculations),

$$\zeta(p) = \sum_{k=1}^{\infty} \frac{1}{k^p}, \qquad \zeta(3) \approx 1.20205 \tag{3.5}$$

Figure 3.1 shows eigenvalue λ as a function of θ. When $\theta = \pi$, we have $\lambda = 7\zeta(3)/2 \approx 4.207$.

3.2 1-D Finite Crystal

Now consider a beam with a finite number N of particles in a crystalline state. In the z-direction, there is linear focusing with spring constant k_z. The first question we ask is what are the lattice locations $\{z_n, n = 1, 2, \cdots, N\}$. This maybe useful when considering cold ions in a trap. The total potential eneregy

---

[7]We have used the fact that

$$\sum_{k=1,\text{odd}}^{\infty} \frac{1}{k^p} = \sum_{k=1}^{\infty}\frac{1}{k^p} - \sum_{k=1,\text{even}}^{\infty} \frac{1}{k^p} = \sum_{k=1}^{\infty}\frac{1}{k^p} - \sum_{k=1}^{\infty}\frac{1}{(2k)^p}$$

$$= (1 - \frac{1}{2^p})\sum_{k=1}^{\infty}\frac{1}{k^p} = (1 - \frac{1}{2^p})\zeta(p)$$

In particular, this implies $\sum_{k=1,\text{odd}}^{\infty} = \frac{7}{8}\zeta(3)$.
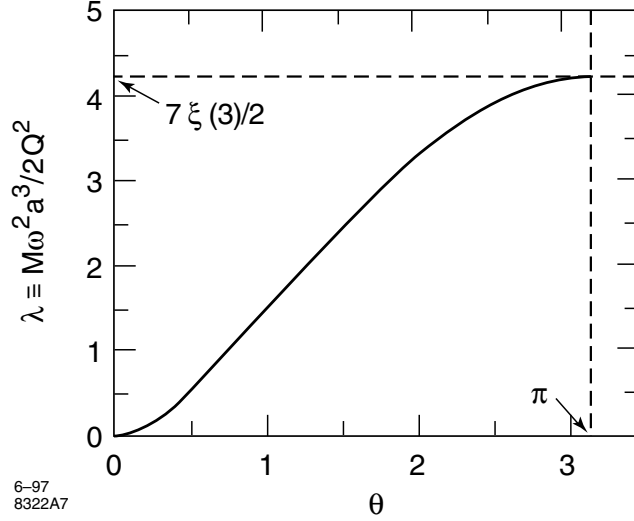
Figure 3.1: Eigenvalue λ versus eigenmode index θ for a 1-D infinite crystal.

of the beam is

$$V(z_1, z_2, \cdots, z_N) = \frac{k_z}{2} \sum_{n=1}^{N} z_n^2 + \sum_{n=1}^{N} \sum_{j>n} \frac{Q^2}{|z_n - z_j|} \qquad (3.6)$$

The lattice locations are determined by the condition that all particles in the beam are in equilibrium, or

$$\frac{\partial V}{\partial z_n} = 0 \quad \text{for all } n \qquad (3.7)$$

Equivalently one can say that V reaches a local minimum as a function of all coordinates $\{z_n, n = 1, 2, \cdots, N\}$.

Deviation from the equilibrium state is described by the equations of motion

$$M\ddot{z}_n + \frac{\partial V}{\partial z_n} = 0 \quad \text{for all } n \qquad (3.8)$$

Eq.(3.8) can be used to find small amplitude normal mode frequencies of the crystalline beam.

$\underline{N=1}$ When there is only one ion in the beam, the lattice is trivial. We have $V = k_z z_1^2/2$ and Eq.(3.7) gives $z_1 = 0$. This charge is located at the origin. It oscillates in a potential with frequency $\omega_z = \sqrt{k_z/M}$.

$\underline{N=2}$ When there are two charges, Coulomb repulsion between them separate them apart, while the external focusing keeps them together to reach an

49

equilibrium lattice arrangement. In this case,

$$V = \frac{k_z}{2}(z_1^2 + z_2^2) + \frac{Q^2}{|z_1 - z_2|} \tag{3.9}$$

and Eq.(3.7) gives two equations whose solution is

$$z_1 = -z_2 = \left(\frac{Q^2}{4k_z}\right)^{1/3} \tag{3.10}$$

One notes that the lattice size is characterized by the quantity

$$(Q^2/k_z)^{1/3} \tag{3.11}$$

There are two normal modes, a $+$ mode in which both particles oscillate in phase, and a $-$ mode in which the two particles oscillate out of phase. The small amplitude mode frequencies are found to be

$$\omega_{z+} = \sqrt{\frac{k_z}{M}}, \quad \omega_{z-} = \sqrt{\frac{3k_z}{M}} \tag{3.12}$$

$\underline{N = 3}$ The lattice locations are

$$z_1 = -z_3 = \left(\frac{5Q^2}{4k_z}\right)^{1/3}, \quad z_2 = 0 \tag{3.13}$$

The small amplitude normal mode frequencies are determined by

$$\text{Det} \begin{bmatrix} -\frac{M\omega_z^2}{k_z} + \frac{14}{5} & -\frac{8}{5} & -\frac{1}{5} \\ -\frac{8}{5} & -\frac{M\omega_z^2}{k_z} + \frac{21}{5} & -\frac{8}{5} \\ -\frac{1}{5} & -\frac{8}{5} & -\frac{M\omega_z^2}{k_z} + \frac{14}{5} \end{bmatrix} = 0 \tag{3.14}$$

$$\implies \quad \omega_z = \sqrt{\frac{k_z}{M}}, \quad \sqrt{\frac{3k_z}{M}}, \quad \sqrt{\frac{29k_z}{5M}} \tag{3.15}$$

The three normal modes respectively corresponds to (1) all three particles move in phase with the same amplitue, (2) particle 1 and 3 move out of phase, while particle 2 is stationary, and (3) particles 1 and 3 move in phase with same amplitude, while particle 2 moves opposite to them with twice the amplitude.

$\underline{N = 4}$ We find the lattice sites numerically,

$$z_1 = -z_4 \approx 1.4368 \left(\frac{Q^2}{k_z}\right)^{1/3}$$

$$z_2 = -z_3 \approx 0.4544 \left(\frac{Q^2}{k_z}\right)^{1/3} \tag{3.16}$$

50

$$z_1 = -z_5 \approx 1.7429 \left(\frac{Q^2}{k_z}\right)^{1/3}$$

$$z_2 = -z_4 \approx 0.8221 \left(\frac{Q^2}{k_z}\right)^{1/3}$$

$$z_3 = 0 \tag{3.17}$$

These lattices are shown in Fig.3.2 for $N = 1$ to 5.
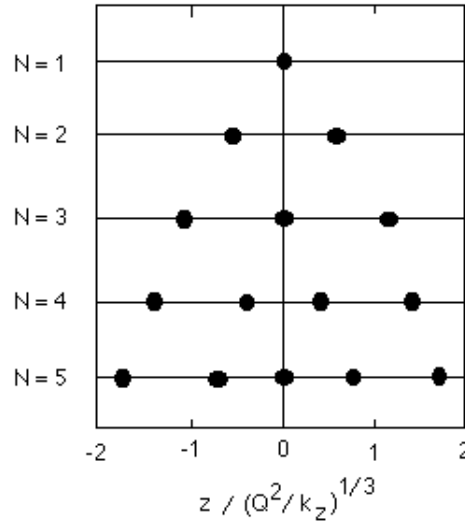
Figure 3.2: 1-D lattices for $N = 1$ to 5.

Exercise 1 What are the mode frequencies for the cases of $N = 4$ and $N = 5$ discussed above?

Solution The mode frequency ω is determined by $\det[(-\frac{M\omega^2}{k_y}+1)I + \frac{2Q^2}{k_z}A] = 0$, where matrix A has the elements

$$A_{nm} = \begin{cases} \sum_{j \neq n} \frac{1}{|z_j - z_n|^3} & \text{if } m = n \\ -\frac{1}{|z_m - z_n|^3} & \text{if } m \neq n \end{cases} \tag{3.18}$$

The fact that A is symmetric assures real eigenvalues.

Exercise 2 Show that the ratio of the two terms in the potential energy Eq.(3.6) is 1:2.

$$\frac{1}{2}\sum_{n=1}^{N}k_z z_n^2 = \frac{1}{2}\sum_{n=1}^{N}z_n(k_z z_n) = \frac{1}{2}\sum_{n=1}^{N}z_n\Big(\sum_{j\neq n}\frac{Q^2(z_n-z_j)}{|z_n-z_j|^3}\Big) = \frac{1}{2}\sum_{n\neq j}^{N}z_n\frac{Q^2(z_n-z_j)}{|z_n-z_j|^3}$$

By switching $j \leftrightarrow n$,

$$\frac{1}{2}\sum_{n=1}^{N}k_z z_n^2 = -\frac{1}{2}\sum_{n\neq j}^{N}z_j\frac{Q^2(z_n-z_j)}{|z_n-z_j|^3}$$

By adding the above and dividing by 2,

$$\frac{1}{2}\sum_{n=1}^{N}k_z z_n^2 = \frac{1}{4}\sum_{n\neq j}^{N}\frac{Q^2(z_n-z_j)^2}{|z_n-z_j|^3} = \frac{1}{4}\sum_{n\neq j}^{N}\frac{Q^2}{|z_n-z_j|} = \frac{1}{2}\sum_{n<j}^{N}\frac{Q^2}{|z_n-z_j|}$$

Q.E.D.[8]

Exercise 3 Show that as $N \to \infty$, the 1-D finite lattice length $\propto$ $(N^2 Q^2/k_z)^{1/3}$. Fitting to the $N = 5$ case, we find that the full length of the lattice is

$$L \approx 1.2 \left(\frac{N^2 Q^2}{k_z}\right)^{1/3} \tag{3.19}$$

3.3 Planar Crystal

In this case, we consider an infinitely long crystal without z-focusing, but confined transversely by a focusing in the y-direction with spring constant k_y. Focusing in the x-direction is assumed to be infinite; the crystal is in the y-z plane.

An important difference from the 1-D lattices is that now some lattice configurations can be unstable. When the linear charge density (characterized by a, the z-spacing between adjacent charges) is low, the transverse focusing is strong enough to overcome the Coulomb repulsion and to confine the crystal to a 1-D configuration, just like the 1-D infinite crystal studied earlier. As a becomes shorter, the 1-D configuration can become unstable. To illustrate this, consider a crystal with lattice sites $z_n = na$ but undergoing an oscillation with a pattern of a zig-zag in which all particles at sites with (n = even) move in one direction in y, while all particles with (n = odd) move in the opposite direction. The unperturbed lattice is sketched in Fig.3.3(a).

Consider the y-motion of the charge located at $n = 0$. The equation of motion is

$$M\ddot{y} + y\left[k_y - 4Q^2\sum_{k=1,\text{odd}}^{\infty}\frac{1}{(4y^2+k^2a^2)^{3/2}}\right] = 0 \tag{3.20}$$

---

[8]Thank to Jeff Holmes for this nice proof.
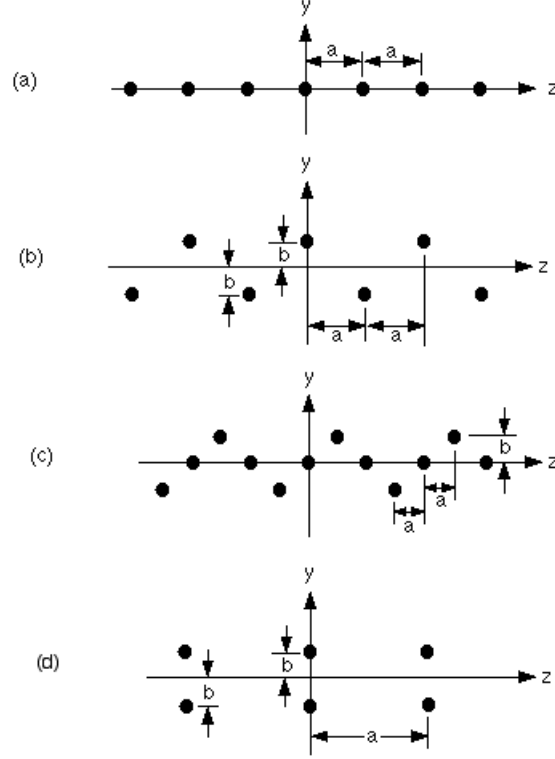
Figure 3.3: Various planar lattice configurations.

For small y, this becomes

$$M\ddot{y} + y\left[k_y - \frac{7Q^2}{2a^3}\zeta(3)\right] = 0 \qquad (3.21)$$

The y-motion of the crystal would be unstable if

$$k_y < \frac{7\zeta(3)}{2}\frac{Q^2}{a^3} \quad \text{or} \quad a < \left(\frac{7\zeta(3)}{2}\frac{Q^2}{k_y}\right)^{1/3} \qquad (3.22)$$

i.e., when the focusing is overcome by the Coulomb repulsion.

One may ask if the crystal is necessarily stable when condition (3.22) is not satisfied. The answer is we have not proved it. What we have proved is that the crystal is stable against *one type of* perturbation – the type with a zig-zag pattern. For the crystal to be stable, it must be stable against all possible perturbations, and we have not done that. However, the zig-zag pattern (we might call this the transverse π-mode) turns out to be the least stable pattern,
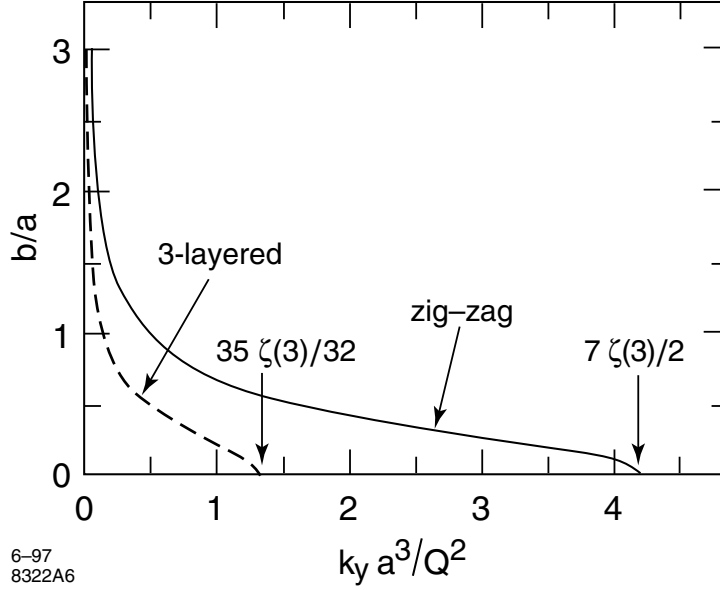
Figure 3.4: The parameter b/a as a function of $k_y a^3/Q^2$ for the zig-zag and a 3-layered lattices.

so Eq.(3.22) is the necessary and sufficient condition for the 1-D lattice to be stable.

What happens to the unstable crystal when Eq.(3.22) is satisfied? The answer is that it can not stay 1-D. The crystal has a zig-zag pattern. Designate this pattern by two layers of lattice sites

$$(y, z) = \begin{cases} (b, 2na) \\ (-b, (2n+1)a) \end{cases}, \quad n = -\infty \text{ to } \infty \tag{3.23}$$

where $2b$ is the y-spacing between the two sets of sites, and is yet to be determined. This zig-zag pattern is shown as Fig.3.3(b).

To determine b, we apply the condition that the lattice is in equilibrium. The forces have been computed in Eq.(3.20). The equilibrium condition is found to be

$$\frac{k_y a^3}{4Q^2} = \sum_{k=1,\text{odd}}^{\infty} \frac{1}{\left[4(\frac{b}{a})^2 + k^2\right]^{3/2}} \tag{3.24}$$

We need to solve it for b/a. There is a solution if and only if condition (3.22) is satisfied. The solid curve in Fig.3.4 shows b/a as a function of $k_y a^3/Q^2$.

Having a solution for b/a, however, does not guarantee the stability of the zig-zag crystal. When a decreases further, the zig-zag crystal gives way to a configuration with three lines of charges. Let the lattice sites be indexed as

$$(y, z) = \begin{cases} (b, (4n+1)a) \\ (0, 2na) \\ (-b, (4n-1)a) \end{cases}, \quad n = -\infty \text{ to } \infty \tag{3.25}$$

54

This lattice is sketched in Fig.3.3(c). The equilibrium coniditon is found to be

$$\frac{4k_y a^3}{5Q^2} = \sum_{k=1,\text{odd}}^{\infty} \frac{1}{\left[4(\frac{b}{a})^2 + k^2\right]^{3/2}} \tag{3.26}$$

The dashed curve in Fig.3.4 shows the solution of b/a for the 3-layered planar crystal.

We conclude that when $(k_y a^3/Q^2) > (7\zeta(3)/2) \approx 4.207$, the planar crystal is 1-D. When $(7\zeta(3)/2) > (k_y a^3/Q^2) > (35\zeta(3)/32)$, the crystal has the zig-zag configuration. When $(35\zeta(3)/32) > (k_y a^3/Q^2)$, a 3-layered planar crystal takes over. As a decreases more, of course, the crystal becomes increasingly complex, etc.

> _Exercise 4_ (a) Can you think of possible 2-layered arrangements other than the zig-zag? For example, how about the arrangement
>
> $$(y, z) = \begin{cases} (b, na) \\ (-b, na) \end{cases}, \quad n = -\infty \text{ to } \infty \tag{3.27}$$
>
> as shown in Fig.3.3(d)? What is the value for b/a? Under what conditions is this crystal stable? (b) Can you think of possible 3-layered arrangements other than that considered in Fig.3.3(c)?
> _Solution_ (a) Unstable against sliding the top row relative to the bottom row of particles.

3.4   3-D Infinite Cubic Crystal

Before we specialize to cubic crystal, let's consider a 3-D crystal in general.[9] Let the lattice site of the nth particle be $\vec{\ell}_n$. Let the position of the nth particle be slightly perturbed from the lattice site with

$$\vec{r}_n = \vec{\ell}_n + \vec{\Delta}_n \tag{3.28}$$

The Coulomb force seen by the nth particle is

$$\vec{F} = Q^2 \sum_{j \neq n} \frac{\vec{r}_n - \vec{r}_j}{|\vec{r}_n - \vec{r}_j|^3} \tag{3.29}$$

The fact that $\vec{\ell}_n$ are lattice sites requires that the Coulomb force in equilibrium must vanish, i.e.,

$$\sum_{j \neq n} \frac{\vec{\ell}_n - \vec{\ell}_j}{|\vec{\ell}_n - \vec{\ell}_j|^3} = \vec{0} \qquad \text{for all } n \tag{3.30}$$

---

[9]Strictly speaking, a 3-D infinite crystal beam cannot exist. Coulomb force from all other charges makes lattice sites intrinsically unstable – the summation (3.29) diverges. But here we study it as a curiosity.

For small deviations $\vec{\Delta}_n$, the linearized equation of motion (assumed to be nonrelativistic) for the nth particle is

$$
M\ddot{\vec{\Delta}}_n = Q^2 \sum_{j \neq n} \frac{\vec{\ell}_n + \vec{\Delta}_n - \vec{\ell}_j - \vec{\Delta}_j}{|\vec{\ell}_n + \vec{\Delta}_n - \vec{\ell}_j - \vec{\Delta}_j|^3} \tag{3.31}
$$

$$
\approx Q^2 \sum_{j \neq n} \frac{1}{|\vec{\ell}_n - \vec{\ell}_j|^3} \left[\vec{\Delta}_n - \vec{\Delta}_j - 3(\vec{\ell}_n - \vec{\ell}_j) \frac{(\vec{\ell}_n - \vec{\ell}_j) \cdot (\vec{\Delta}_n - \vec{\Delta}_j)}{|\vec{\ell}_n - \vec{\ell}_j|^2} \right]
$$

In a cubic crystal with lattice dimension a, we have $\vec{\ell}_i = \vec{i}a$, and Eq.(3.31) becomes

$$
M\ddot{\vec{\Delta}}_{\vec{n}} = \frac{Q^2}{a^3} \sum_{\vec{k} \neq \vec{0}} \frac{1}{|\vec{k}|^3} \left[\vec{\Delta}_{\vec{n}} - \vec{\Delta}_{\vec{n}-\vec{k}} - 3\vec{k} \frac{\vec{k} \cdot (\vec{\Delta}_{\vec{n}} - \vec{\Delta}_{\vec{n}-\vec{k}})}{|\vec{k}|^2} \right] \tag{3.32}
$$

$$
= \frac{Q^2}{2a^3} \sum_{\vec{k} \neq \vec{0}} \frac{1}{|\vec{k}|^3} \left[2\vec{\Delta}_{\vec{n}} - \vec{\Delta}_{\vec{n}-\vec{k}} - \vec{\Delta}_{\vec{n}+\vec{k}} - 3\vec{k} \frac{\vec{k} \cdot (2\vec{\Delta}_{\vec{n}} - \vec{\Delta}_{\vec{n}-\vec{k}} - \vec{\Delta}_{\vec{n}+\vec{k}})}{|\vec{k}|^2} \right]
$$

An eigenmode has a plane wave pattern

$$
\vec{\Delta}_{\vec{n}} = \vec{\theta} \cos(\vec{n} \cdot \vec{\theta} + \phi) e^{-i\omega t} \tag{3.33}
$$

where $\vec{\theta}$ and ϕ serve as mode indices. The mode frequency ω is determined by

$$
\frac{M\omega^2 a^3}{Q^2} = \sum_{\vec{k} \neq \vec{0}} \frac{1}{|\vec{k}|^3} [1 - \cos(\vec{k} \cdot \vec{\theta})] \left(3 \frac{(\vec{k} \cdot \vec{\theta})^2}{|\vec{k}|^2 |\vec{\theta}|^2} - 1 \right) \tag{3.34}
$$

For example, when $\vec{\theta} = \theta\hat{z}$, or $\theta\hat{y}$, or $\theta\hat{x}$, we have

$$
\lambda(\theta) \equiv \frac{M\omega^2 a^3}{2Q^2} = \sum_{k_z=1}^{\infty} (1 - \cos k_z \theta) F(k_z)
$$

$$
F(k_z) = \sum_{k_x=-\infty}^{\infty} \sum_{k_y=-\infty}^{\infty} g(k_x, k_y)
$$

$$
g(k_x, k_y) = \frac{2k_z^2 - k_x^2 - k_y^2}{(k_x^2 + k_y^2 + k_z^2)^{5/2}} \tag{3.35}
$$

The double summation in $F(k_z)$ is rather subtle because of the cancelation among terms, and must be handled carefully.[10] Figure 3.5 shows $\lambda(\theta)$. The cubic lattice is stable (provided it can be formed in the first place – see the previous footnote).

---

[10]We first rewrite Eq.(3.35) as

$$
F(k_z) = \sum_{k_x=0}^{\infty} \sum_{k_y=0}^{\infty} \left[g(k_x, k_y) + g(k_x + 1, k_y) + g(k_x, k_y + 1) + g(k_x + 1, k_y + 1) \right]
$$
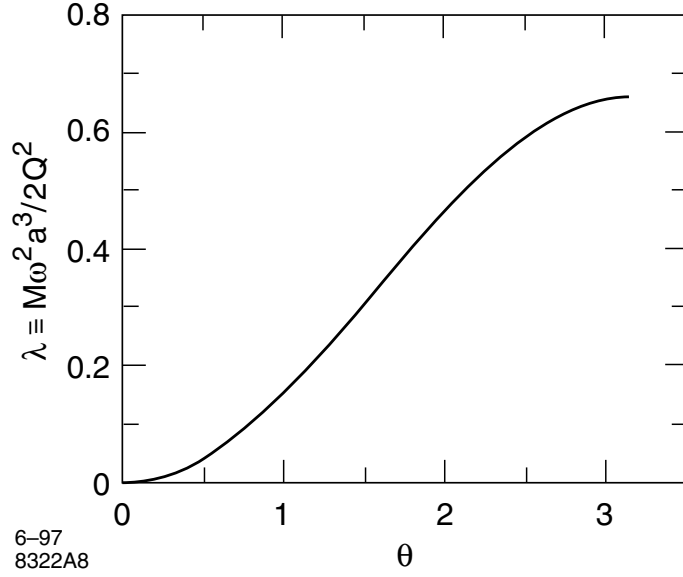
Figure 3.5: Eigenvalue λ versus eigenmode index $\vec{\theta}$ for a cubic crystal, when $\vec{\theta} = \theta\hat{x}$, or $\theta\hat{y}$, or $\theta\hat{z}$.

<u>*Exercise* 5</u> Verify that Eqs.(3.33-3.34) describe eigenmodes for the

$$
= \sum_{k_x=0}^{\infty} \sum_{k_y=0}^{\infty} \Bigg[g(k_x, k_y) + g(k_x + 1, k_y) + g(k_x, k_y + 1) + g(k_x + 1, k_y + 1)
$$
$$
-4 \int_{k_x}^{k_x+1} d\alpha_x \int_{k_y}^{k_y+1} d\alpha_y g(\alpha_x, \alpha_y) \Bigg] \tag{3.36}
$$

where in the second step we have added artificially a term which sums up to zero to help the convergence,

$$
-4 \sum_{k_x=0}^{\infty} \sum_{k_y=0}^{\infty} \int_{k_x}^{k_x+1} d\alpha_x \int_{k_y}^{k_y+1} d\alpha_y g(\alpha_x, \alpha_y)
$$
$$
= -4 \int_0^{\infty} d\alpha_x \int_0^{\infty} d\alpha_y \frac{2k_z^2 - \alpha_x^2 - \alpha_y^2}{(\alpha_x^2 + \alpha_y^2 + k_z^2)^{5/2}} \quad = \quad 0 \tag{3.37}
$$

The integral in Eq.(3.36) can be performed and we have a summation which converges much faster,

$$
F(k_z) = \sum_{k_x=0}^{\infty} \sum_{k_y=0}^{\infty} \Bigg[g(k_x, k_y) + g(k_x + 1, k_y) + g(k_x, k_y + 1) + g(k_x + 1, k_y + 1)
$$
$$
-4\{[h(k_x, k_y) - h(k_x + 1, k_y)] - [h(k_x, k_y + 1) - h(k_x + 1, k_y + 1)]\} \Bigg]
$$
$$
h(k_x, k_y) = \frac{k_x k_y (k_x^2 + k_y^2 + 2k_z^2)}{(k_x^2 + k_z^2)(k_y^2 + k_z^2)(k_x^2 + k_y^2 + k_z^2)^{1/2}} \tag{3.38}
$$

It turns out that $F(k_z)$ decreases rapidly with increasing k_z: $F(1) = 0.3274645, F(2) = 5.5496 \times 10^{-4}, F(3) = 1.03 \times 10^{-6}$, and all higher values of k_z practically vanish.

57

equation of motion (3.32).

Exercise 6 Following similar approach of the text, find the eigen-mode pattern and eigenfrequencies for the 2-D infinite square crystal with lattice sites $(x, y) = (n_x a, n_y a), n_{x,y} = \pm$integers.
Solution

$$\frac{M\omega^2 a^3}{2Q^2} = \sum_{k_z=1}^{\infty} (1 - \cos k_z \theta) \sum_{k_y=-\infty}^{\infty} \frac{2k_z^2 - k_y^2}{(k_y^2 + k_z^2)^{5/2}} \qquad (3.39)$$

Exercise 7 We concluded that the cubic lattice is stable after analyzing the case $\vec{\theta} = \theta \hat{z}$. Does this conclusion hold when we consider an arbitrary mode index $\vec{\theta}$?

Exercise 8 Repeat the analysis for a rectangular crystal with $\vec{\ell}_n = (n_x b, n_y b, n_z a)$, where a and b are the longitudinal and transverse lattice periods. Is this crystal stable?

3.5 Planar Crystal With z Focusing

We next add back z-focusing to the planar crystal discussed earlier. The beam now has a finite number of N particles. The crystal is still in the y-z plane. Let k_y and k_z be the spring constants.

Consider the case with $N = 2$. At equilibrium, they are located at $(y, z) = (y_1, z_1)$ and $(-y_1, -z_1)$ respectively, where

$$k_y y_1 = \frac{Q^2 y_1}{4(y_1^2 + z_1^2)^{3/2}}, \qquad k_z z_1 = \frac{Q^2 z_1}{4(y_1^2 + z_1^2)^{3/2}} \qquad (3.40)$$

There are two possible solutions,

$$(y_1, z_1) = \begin{cases} \left(\left(\frac{Q^2}{4k_y} \right)^{1/3}, 0 \right) \\ \left(0, \left(\frac{Q^2}{4k_z} \right)^{1/3} \right) \end{cases} \qquad (3.41)$$

We next analyze the stability around each of the possible solutions. Take the first case first. Let the two ions have displacements

$$(y_1 + \Delta_{y1}, \Delta_{z1}) \text{ and } (-y_1 + \Delta_{y2}, \Delta_{z2}) \qquad (3.42)$$

The y-motion of ion 1 is described by

$$M\ddot{\Delta}_{y1} + k_y(y_1 + \Delta_{y1}) - \frac{Q^2(2y_1 + \Delta_{y1} - \Delta_{y2})}{[(2y_1 + \Delta_{y1} - \Delta_{y2})^2 + (\Delta_{z1} - \Delta_{z2})^2]^{3/2}} = 0 \quad (3.43)$$

By linearizing with respect to Δ-quantities, and extend the analysis to the y- and z-motions of both ions, we find

$$
\begin{aligned}
M\ddot{\Delta}_{y1} + k_y(2\Delta_{y1} - \Delta_{y2}) &= 0 \\
M\ddot{\Delta}_{y2} + k_y(2\Delta_{y2} - \Delta_{y1}) &= 0 \\
M\ddot{\Delta}_{z1} + (k_z - \frac{k_y}{2})\Delta_{z1} + \frac{k_y}{2}\Delta_{z2} &= 0 \\
M\ddot{\Delta}_{z2} + (k_z - \frac{k_y}{2})\Delta_{z2} + \frac{k_y}{2}\Delta_{z1} &= 0
\end{aligned}
\tag{3.44}
$$

Note that the y- and z-motions are decoupled from each other. The y-motion has two eigenmodes,

$$
\omega = \begin{cases} \sqrt{k_y/M}, & 0 \text{ mode} \\ \sqrt{3k_y/M}, & \pi \text{ mode} \end{cases}
\tag{3.45}
$$

while for the z-motion,

$$
\omega = \begin{cases} \sqrt{k_z/M}, & 0 \text{ mode} \\ \sqrt{(k_z - k_y)/M}, & \pi \text{ mode} \end{cases}
\tag{3.46}
$$

The z-motion is unstable if $k_z < k_y$. These four modes are shown in Fig.3.6.
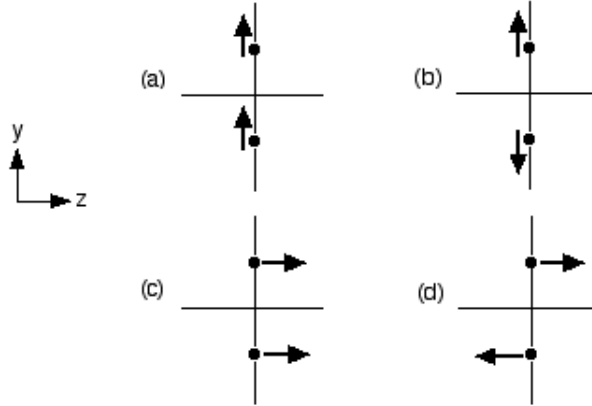
Figure 3.6: There are 8 eigenmodes for a 2-particle planar crystal with z-focusing. Four of them with the two particles on the y-axis are shown here. (a) y-motion, 0 mode. (b) y-motion, π-mode. (c) z-motion, 0 mode. (d) z-motion, π-mode. The sheering mode (d) is unstable if $k_z < k_y$. The remaining four modes are with the two particles on the z-axis.

For the second set of equilibrium coordinates in (3.41), we find its y-motion is unstable if $k_y < k_z$. We thus conclude that when $k_y > k_z$, the crystal is oriented along the z-axis. When $k_y > k_z$, the crystal is oriented along the y-axis. Ions tend to stay away from the strong focusing dimension in a crystalline beam.

There is also a degenerate case when $k_y = k_z$. The crystal can be oriented along an arbitrary direction in the y-z plane, but it is barely stable. Any shearing motion would not be focussed.

3.6 Helical Crystal

Consider the case without longitudinal focusing and the crystal is again infinitely long in z-direction. Let there be transverse focusing with spring constants k_x and k_y. We learned from Eq.(3.22) that if the longitudinal average particle spacing a is sufficiently large, the crystal is 1-D. As the line density increases (i.e. as a decreases), the 1-D crystal becomes unstable and more complicated crystal structures result.

Figure 3.7 shows one simulation result of possible crystal structures when $k_x = k_y = k$ and no longitudinal focusing [3]. The structure depends on the dimensionless linear particle density $\lambda = \frac{1}{a}(3Q^2/2k)^{1/3}$. As λ increases, one sees 1-D, zig-zag, and helical, and multi-layered helical crystals, successively. If a longitudinal focusing is introduced, one may contemplate a buckey ball crystal, and crystals with multiple 3-D shells.
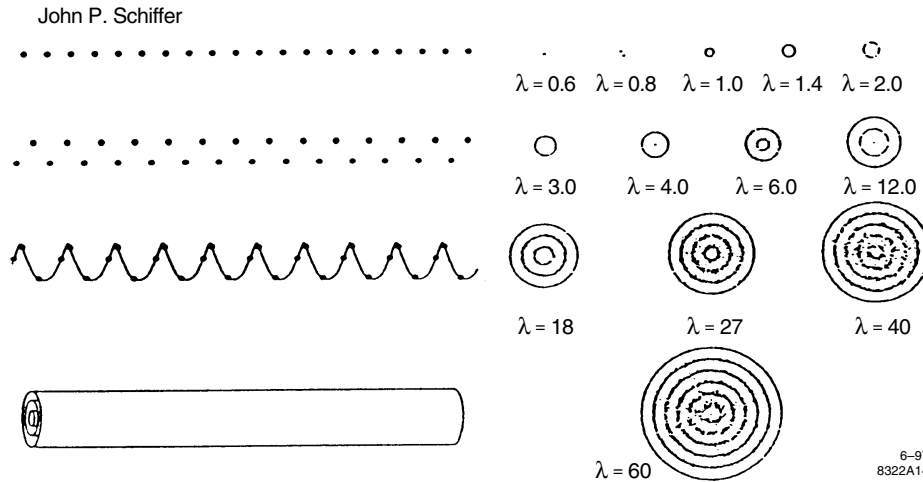
Figure 3.7: Simulation results of lattice configurations as the linear particle density λ is varied. For comparison, condition (3.22) for the instability of a 1-D crystal gives $\lambda > (3/7\zeta(3))^{1/3}$, which is consistent with the results here.

3.7 Moving Crystal

On may pursue crystal hunting some more, perhaps using group theory to be systematic. But below we will study the topic of crystal beam motion in an accelerator. Let us consider a crystal moving in the z-direction with speed βc.

To illustrate, we take a planar crystal which has a y-focusing spring constant (in the laboratory frame) k_y, while $k_x = \infty$ and $k_z = 0$.

First let us write down the electric field of a moving charge:

$$\vec{E}(\vec{r}) = \frac{\gamma Q \vec{r}}{(x^2 + y^2 + \gamma^2 z^2)^{3/2}} \tag{3.47}$$

which can also be written as

$$E_x = -\frac{\partial \Phi}{\partial x}, \quad E_y = -\frac{\partial \Phi}{\partial y}, \quad E_z = -\frac{1}{\gamma^2}\frac{\partial \Phi}{\partial z}$$

$$\Phi = \frac{\gamma Q}{(x^2 + y^2 + \gamma^2 z^2)^{1/2}} \tag{3.48}$$

Another charge moving with the same velocity along z-direction sees a Lorentz force

$$\vec{F} = -\frac{Q}{\gamma^2}\nabla\Phi \tag{3.49}$$

where we have used the fact that the magnetic and electric contributions cancel each other to introduce an extra factor of $1/\gamma^2$ to the transverse Lorentz force.

For sufficiently large a (a is in the laboratory frame), the equilibrium crystal is 1-D. To see how large a must be in order for this moving 1-D crystal to be stable, we follow what we did for the stationary planar crystal, and consider the perturbation of a zig-zag pattern. The y-motion obeys [Cf. Eq.(3.20)]

$$M\gamma c^2 y'' + y\left[k_y - \frac{4Q^2}{\gamma}\sum_{k=1,\text{odd}}^{\infty}\frac{1}{(4y^2 + \gamma^2 k^2 a^2)^{3/2}}\right] = 0 \tag{3.50}$$

It follows that a 1-D crystal is stable only if

$$a > \left(\frac{7\zeta(3)}{2}\frac{Q^2}{\gamma^4 k_y}\right)^{1/3} \tag{3.51}$$

Similarly, we find the crystal has a zig-zag pattern if

$$\left(\frac{7\zeta(3)}{2}\frac{Q^2}{\gamma^4 k_y}\right)^{1/3} > a > \left(\frac{35\zeta(3)}{32}\frac{Q^2}{\gamma^4 k_y}\right)^{1/3} \tag{3.52}$$

Exercise 9 Show Eqs.(3.51-3.52) by Lorentz transformation from the rest frame of the crystalline beam.
Solution In the beam rest frame, particle spacing is γa and spring constant is γk_y.

Equations of Motion   Equation (3.49) allows one to write down the equations of motion for one of the particles in a circular accelerator,

$$x'' + K_x x + \frac{\partial V}{\partial x} = \frac{\delta}{\rho}$$

61

$$y'' + K_y y + \frac{\partial V}{\partial y} = 0$$

$$z' = -\frac{x}{\rho} + \frac{\delta}{\gamma^2}$$

$$\delta' = -\frac{\partial V}{\partial z} \qquad (3.53)$$

where

$$V = \frac{Q^2}{Mc^2\gamma^2} \sum_k \frac{1}{[(x - x_k)^2 + (y - y_k)^2 + \gamma^2(z - z_k)^2]^{1/2}} \qquad (3.54)$$

with summation over all lattice sites k other than the site for the particle under consideration. Quantities K_x, K_y and ρ are periodic functions of s with period $C = 2\pi R$. Quantities $K_{x,y}$ are related to the spring constants $k_{x,y}$ by $K_{x,y} = k_{x,y}/M\gamma c^2$. We have considered an unbunched beam in an accelerator without rf focusing. We have also ignored the curvature of the crystal beam conforming to the circular closed orbit of the accelerator.

The Hamiltonian for the above equations of motion is

$$H = \frac{1}{2}(p_x^2 + p_y^2) + \frac{1}{2\gamma^2}\delta^2 - \frac{x\delta}{\rho} + \frac{1}{2}(K_x x^2 + K_y y^2) + V \qquad (3.55)$$

In a weak focusing synchrotron, we have

$$K_x = \frac{1 - n}{R^2}, \quad K_y = \frac{n}{R^2}, \quad \rho = R \qquad (3.56)$$

In a smooth approximation for an alternating gradient synchrotron, we may take

$$K_x = \left(\frac{\nu_x}{R}\right)^2, \quad K_y = \left(\frac{\nu_y}{R}\right)^2, \quad \rho = R \qquad (3.57)$$

Lattice Sites   Let the coordinates of the nth particle be designated as

$$x_n = X_n + \alpha_n, \quad y_n = Y_n + \beta_n, \quad z_n = Z_n + \gamma_n, \quad \delta_n = \Delta_n + \sigma_n \qquad (3.58)$$

where X_n, Y_n, Z_n, Δ_n are the lattice site coordinates, and $\alpha_n, \beta_n, \gamma_n, \sigma_n$ are small deviations from the sites. Note that each lattice site is assigned not only three space coordinates X_n, Y_n, Z_n, but also an energy deviation Δ_n. We expand V to quadratic terms in $\alpha_n, \beta_n, \gamma_n$ to obtain

$$V \approx \frac{Q^2}{Mc^2\gamma^2} \sum_{k \neq n} \frac{1}{R_{nk}} \times$$

$$\left\{ 1 - \frac{(\alpha_n - \alpha_k)(X_n - X_k) + (\beta_n - \beta_k)(Y_n - Y_k) + \gamma^2(\gamma_n - \gamma_k)(Z_n - Z_k)}{R_{nk}^2} \right.$$

$$\left. - \frac{(\alpha_n - \alpha_k)^2 + (\beta_n - \beta_k)^2 + \gamma^2(\gamma_n - \gamma_k)^2}{2R_{nk}^2} \right.$$

$$+\frac{3}{2}\left[\frac{(\alpha_n-\alpha_k)(X_n-X_k)+(\beta_n-\beta_k)(Y_n-Y_k)+\gamma^2(\gamma_n-\gamma_k)(Z_n-Z_k)}{R_{nk}^2}\right]^2\Bigg\}$$

$$R_{nk}\equiv[(X_n-X_k)^2+(Y_n-Y_k)^2+\gamma^2(Z_n-Z_k)^2]^{1/2} \tag{3.59}$$

Equation (3.53) then yields the equations for the lattice sites,

$$X_n''+K_xX_n-\frac{Q^2}{Mc^2\gamma^2}\sum_{k\neq n}\frac{X_n-X_k}{R_{nk}^3}=\frac{\Delta_n}{\rho}$$

$$Y_n''+K_yY_n-\frac{Q^2}{Mc^2\gamma^2}\sum_{k\neq n}\frac{Y_n-Y_k}{R_{nk}^3}=0$$

$$Z_n'=-\frac{X_n}{\rho}+\frac{\Delta_n}{\gamma^2}$$

$$\Delta_n'=\frac{Q^2}{Mc^2}\sum_{k\neq n}\frac{Z_n-Z_k}{R_{nk}^3} \tag{3.60}$$

In order for the beam to crystalize, we must require the lattice site coordinates to be periodic with period C.

In the smooth approximation, K_x, K_y, ρ as well as the lattice structure are independent of s. The crystal rotates around the accelerator rigidly. All primed terms on the LHS of Eq.(3.60) vanish. One must have

$$\Delta_n=\frac{\gamma^2}{\rho}X_n \tag{3.61}$$

Equation (3.61) means that a particle with $X_n\neq0$ must be associated with a Δ_n in such a way that the extra path length due to X_n is exactly compensated by the extra velocity of the particle due to Δ_n. Equation (3.60) then becomes

$$(K_x-\frac{\gamma^2}{\rho^2})X_n-\frac{Q^2}{Mc^2\gamma^2}\sum_{k\neq n}\frac{X_n-X_k}{R_{nk}^3}=0$$

$$K_yY_n-\frac{Q^2}{Mc^2\gamma^2}\sum_{k\neq n}\frac{Y_n-Y_k}{R_{nk}^3}=0$$

$$\sum_{k\neq n}\frac{Z_n-Z_k}{R_{nk}^3}=0 \tag{3.62}$$

It is conceivable that a "liquid crystal" beam can be defined when a layer of lattice slips with respect to other layers by exactly an integer multiple of the unit dimension of the lattice when the beam completes one revolution. The lattice is re-formed after each revolution. This possibility is not considered here.

1−D Lattice

A 1-D lattice trivially satisfies Eq.(3.62),

$$X_n=Y_n=0,\quad \Delta_n=0,\quad Z_n=na \tag{3.63}$$

63

Zig−zag Lattice in the $y-z$ Plane

This lattice has $X_n = 0$ and $\Delta_n = 0$. Its (Y, Z) site coordinates are given by Eq.(3.23), with [Cf. Eq.(3.24)]

$$\frac{K_y M c^2 \gamma^2 a^3}{4Q^2} = \sum_{k=1,\text{odd}}^{\infty} \frac{1}{\left[4\left(\frac{b}{a}\right)^2 + \gamma^2 k^2\right]^{3/2}} \tag{3.64}$$

Eq.(3.64) has solution only if [Cf. Eqs.(3.22) and (3.51)]

$$a < \left(\frac{7}{2}\zeta(3)\frac{Q^2}{K_y M \gamma^5 c^2}\right)^{1/3} \tag{3.65}$$

Zig−zag Lattice in the $x-z$ Plane

This zig-zag crystal is more complicated than the one in the y-z plane because x-deviations necessarily involve energy deviations. Let the crystal sites have $Y_n = 0$ and

$$(X_n, Z_n, \Delta_n) = \begin{cases} (b, 2na, \gamma^2 b/R) \\ (-b, (2n+1)a, -\gamma^2 b/R) \end{cases} \tag{3.66}$$

Substituting into Eq.(3.62) yields the condition

$$\frac{M c^2 \gamma^2 a^3}{4Q^2}\left(K_x - \frac{\gamma^2}{\rho^2}\right) = \sum_{k=1,\text{odd}}^{\infty} \frac{1}{\left[4\left(\frac{b}{a}\right)^2 + \gamma^2 k^2\right]^{3/2}} \tag{3.67}$$

Eq.(3.67) has solution only if

$$K_x > \frac{\gamma^2}{\rho^2} \tag{3.68}$$

and

$$a < \left(\frac{7}{2}\zeta(3)\frac{Q^2}{\left(K_x - \frac{\gamma^2}{\rho^2}\right)M\gamma^5 c^2}\right)^{1/3}, \quad \text{or} \quad k_x < \frac{\gamma^2}{\rho^2} + \frac{7}{2}\zeta(3)\frac{Q^2}{Mc^2 a^3 \gamma^5} \tag{3.69}$$

In the smooth approximation (3.57), Eq.(3.68) means

$$\nu_x > \gamma \tag{3.70}$$

We thus conclude that the accelerator must be operated below transition in order for the crystalline beam to form. Physically this is so that the horizontal focusing force must be greater than the centrifugal force, i.e.

$$K_x X > \frac{\Delta}{\rho} \tag{3.71}$$

When the particle line density is small enough that both Eqs.(3.65) and (3.69) are not satisfied, the crystal is 1-D. Take for example the case of a proton beam, and $\rho = 10$ m, $\gamma = 5$, $\nu_x = 10$, $K_x = \nu_x^2/\rho^2 = 1$ m^{-2}, Eq.(3.69) says that the formation of 1-D crystal requires $a > 1.4$ μm, or the number of protons in the accelerator is less than $2\pi\rho/(1.4~\mu\text{m}) = 4.5 \times 10^7$. To store more protons in a 1-D crystal, one way is to increase γ.

3.8 Perturbation from Lattice Sites

Assuming the lattice sites have been established, we next need to make sure the crystal is stable against small deviations like Eq.(3.58). Linearizing Eq.(3.53) around the lattice sites, the equations of motion become

$$
\alpha_n'' + K_x \alpha_n - \frac{Q^2}{Mc^2\gamma^2} \sum_{k \neq n} \left\{ \left[\frac{1}{R_{nk}^3} - \frac{3(X_n - X_k)^2}{R_{nk}^5} \right] (\alpha_n - \alpha_k) \right.
$$

$$
\left. - \frac{3(X_n - X_k)(Y_n - Y_k)}{R_{nk}^5}(\beta_n - \beta_k) - \frac{3\gamma^2(X_n - X_k)(Z_n - Z_k)}{R_{nk}^5}(\gamma_n - \gamma_k) \right\} = \frac{\sigma_n}{\rho}
$$

$$
\beta_n'' + K_y \beta_n - \frac{Q^2}{Mc^2\gamma^2} \sum_{k \neq n} \left\{ \left[\frac{1}{R_{nk}^3} - \frac{3(Y_n - Y_k)^2}{R_{nk}^5} \right] (\beta_n - \beta_k) \right.
$$

$$
\left. - \frac{3(X_n - X_k)(Y_n - Y_k)}{R_{nk}^5}(\alpha_n - \alpha_k) - \frac{3\gamma^2(Y_n - Y_k)(Z_n - Z_k)}{R_{nk}^5}(\gamma_n - \gamma_k) \right\} = 0
$$

$$
\gamma_n' = -\frac{\alpha_n}{\rho} + \frac{\sigma_n}{\gamma^2}
$$

$$
\sigma_n' = \frac{Q^2}{Mc^2} \sum_{k \neq n} \left\{ \left[\frac{1}{R_{nk}^3} - \frac{3\gamma^2(Z_n - Z_k)^2}{R_{nk}^5} \right] (\gamma_n - \gamma_k) \right.
$$

$$
\left. - \frac{3(X_n - X_k)(Z_n - Z_k)}{R_{nk}^5}(\alpha_n - \alpha_k) - \frac{3(Y_n - Y_k)(Z_n - Z_k)}{R_{nk}^5}(\beta_n - \beta_k) \right\} \quad (3.72)
$$

Note that, in general, horizontal, vertical and longitudinal motions are coupled. An oscillation in one dimension excites oscillations in the other dimensions.

1-D Lattice For the 1-D lattice (3.63), the y-motion is decoupled from the other two dimensions, with

$$
\beta_n'' + K_y \beta_n - \frac{Q^2}{Mc^2\gamma^2} \sum_{k \neq n} \frac{1}{R_{nk}^3}(\beta_n - \beta_k) = 0 \quad (3.73)
$$

where $R_{nk} = a\gamma|n - k|$, while the x- and z-motions are coupled,

$$
\alpha_n'' + K_x \alpha_n - \frac{Q^2}{Mc^2\gamma^2} \sum_{k \neq n} \frac{1}{R_{nk}^3}(\alpha_n - \alpha_k) = \frac{\sigma_n}{\rho}
$$

$$
\gamma_n' = -\frac{\alpha_n}{\rho} + \frac{\sigma_n}{\gamma^2}
$$

$$
\sigma_n' = -\frac{2Q^2}{Mc^2} \sum_{k \neq n} \frac{1}{R_{nk}^3}(\gamma_n - \gamma_k) \quad (3.74)
$$

Eigenmodes of y-motion are, according to Eq.(3.73), described by

$$
\beta_n = \cos(n\theta + \phi)e^{-i\omega s/c}, \quad \alpha_n = 0, \quad \gamma_n = 0, \quad \sigma_n = 0 \quad (3.75)
$$

65

where θ, ϕ are mode indices, and ω is the eigenmode frequency, [Cf. Eq.(3.3)]

$$\left(\frac{\omega}{c}\right)^2 = K_y - \xi \tag{3.76}$$

where

$$\xi \equiv \frac{4Q^2}{Mc^2a^3\gamma^5} \sum_{k=1}^{\infty} \frac{1}{k^3} \sin^2\left(\frac{k\theta}{2}\right) \tag{3.77}$$

The Coulomb force is defocusing for y-motion as seen by the fact that it shifts the mode frequencies down-ward as $\xi > 0$.

In order for the 1-D crystal to be stable against small y-perturbations, all modes in Eq.(3.76) must be stable. This means K_y must be larger than ξ for all possible values of θ. This in turn requires exactly the opposite of condition (3.65). When (3.65) is satisfied, 1-D crystal is unstable, and the next stable crystal is of course the zig-zag crystal.

Eigenmodes in the x-z motion are described by

$$\begin{aligned}
\alpha_n &= \cos(n\theta + \phi)e^{-i\omega s/c} \\
\gamma_n &= iG\cos(n\theta + \phi)e^{-i\omega s/c} \\
\sigma_n &= S\cos(n\theta + \phi)e^{-i\omega s/c}
\end{aligned} \tag{3.78}$$

Substituting Eq.(3.78) into Eq.(3.74) gives

$$\begin{aligned}
K_x - \left(\frac{\omega}{c}\right)^2 - \xi &= \frac{S}{\rho} \\
G\frac{\omega}{c} &= -\frac{1}{\rho} + \frac{S}{\gamma^2} \\
S\frac{\omega}{c} &= 2G\gamma^2\xi
\end{aligned} \tag{3.79}$$

We need to solve Eq.(3.79) for S, G, ω. The solution is

$$\begin{aligned}
S &= \frac{2\gamma^2\xi\frac{1}{\rho}}{2\xi - \frac{\omega^2}{c^2}} \\
G &= \frac{\frac{\omega}{c}\frac{1}{\rho}}{2\xi - \frac{\omega^2}{c^2}}
\end{aligned} \tag{3.80}$$

and the eigenfrequency ω satisfies

$$\left(\frac{\omega^2}{c^2} - K_x + \xi\right)\left(\frac{\omega^2}{c^2} - 2\xi\right) = \frac{2\gamma^2\xi}{\rho^2}$$

$$\implies \left(\frac{\omega}{c}\right)^2 = \frac{K_x + \xi}{2} \pm \frac{1}{2}\sqrt{(K_x - 3\xi)^2 + \frac{8\xi\gamma^2}{\rho^2}} \tag{3.81}$$

In order for the x-z motion to be stable, it is necessary that both solutions of $(\omega/c)^2$ in Eq.(3.81) are real and positive. This requires

$$K_x > \frac{\gamma^2}{\rho^2} + \xi \tag{3.82}$$

66

Since Eq.(3.82) must be satisfied for all θ, ϕ, the 1-D crystal is stable against x-z motion only if

$$K_x > \frac{\gamma^2}{\rho^2} + \frac{7}{2}\zeta(3)\frac{Q^2}{Mc^2a^3\gamma^5} \tag{3.83}$$

which we recognize is just the opposite of Eq.(3.69), as it should.

Equation (3.80) indicates that the x-, z- and δ-amplitudes have relative magnitudes of

$$A_x \;:\; A_z \;:\; A_\delta \quad = \quad \rho(2\xi - \frac{\omega^2}{c^2}) \;:\; \frac{\omega}{c} \;:\; 2\gamma^2\xi \tag{3.84}$$

This relative amplitudes would be what one observes in an accelerator when an 1-D crystalline beam is executing an x-z mode oscillation.

> *Exercise* 10 (a) Follow the text to derive the mode frequencies (3.76) for y-motion and (3.81) for x-z motion. (b) Show Eq.(3.84). What happens to the oscillation amplitudes when k_x is barely above the stability condition (3.83)? What happens when k_x is much greater than the threshold value?

Zig-zag Lattice One may proceed to analyze the stability of the zig-zag lattices and the lattice in general in a similar fashion.

References

[1] A. Rahman and J.P. Schiffer, Phys. Rev. Lett. 57, 1133 (1986).

[2] Jie Wei, Xiao-Ping Li, Andrew M. Sessler, Phys. Rev. Lett. 73, 3089 (1994).

[3] John Schiffer, Proc. 31st Eloisatron Workshop on Crystalline Beams, Erice, 1996, p.217.

[4] A.F. Haffmans, D. Maletic, A.G. Ruggiero, Part. Accel. Conf. 1995.

4   Fast Ion Instability

The vacuum chamber of an accelerator is far from under vacuum. In addition to the applied electromagnetic fields from RF or magnets, a vacuum chamber is typically filled with all sorts of contaminants:

residual gases (H_2, H_2O, CO, etc.)

stray electrons (photodesorption, multipactoring, dark currents, etc.)

dust particles

photons (synchrotron radiation, thermal photons, etc.)

microwaves (wakefields, etc.)

ions (trapped, fast ion instability, etc.)

There are various ion effects in electron storage rings and synchrotrons. Most of these are "conventional" effects which occur when ions are trapped by a circulating electron beam for multiple revolutions. To avoid the conventional ion trapping, a gap is introduced in the electron beam by missing bunches in a train of bunches as shown in Fig.4.1. Another way to avoid trapped ions is to introduce clearing electrodes. A conventional ion instability is likely to occur in Fig.4.1(a) and is avoided in Fig.4.1(b). However, the beam in Fig.4.1(b) is not free of instability. It can still suffer from the fast ion instability, which is the topic of this chapter.

We are mainly interested in electron accelerators here because ions are positively charged. A positively charged beam typically will drive the ions to the vacuum chamber walls before they can do significant damage to the beam.

In the fast ion instability, individual ions last only for a single passage of the electron beam and are not trapped for multiple turns. The lifetime of individual ions is therefore very short. Methods to avoid the conventional ion effects, such as a gap in the bunch train, are not applicable. In a fast ion instability, although the ions do not stay long in the accelerator, they still can cause an instability in the electron beam. The growth time of the electron beam is much longer than the lifetime of the ions.[11] In Fig.4.1(a), the electron beam and the trapped ions form an eigen-system. The motions of both the beam and the ions grow exponentially with the same time constant. In Fig.4.1(b), the beam and the ions do not form an eigen-system. The growth of the electron beam, as we will see, is in fact not exponential.

Since ions are not trapped, the problem is conceptually the same whether the accelerator is a storage ring or a very long linac. For conceptual convenience, let us consider an electron beam traveling down a very long linac. Let the beam have a total of N electrons, a transverse distribution of a uniform disc of radius a, and a uniform longitudinal distribution of length ℓ. Let the linac vacuum be such that the residual gas has a volume density n. The gas might be CO. The fast ion instability applies to synchrotrons or storage rings in which the electron beam consists of a long train of bunches with a long gap. (The gap is long enough so that all ions produced in one passage of the beam train are cleared before the bunch train comes back again in the next revolution.) Examples of

---

[11]This is in spite of the fact that we call this effect the *fast* ion instability.
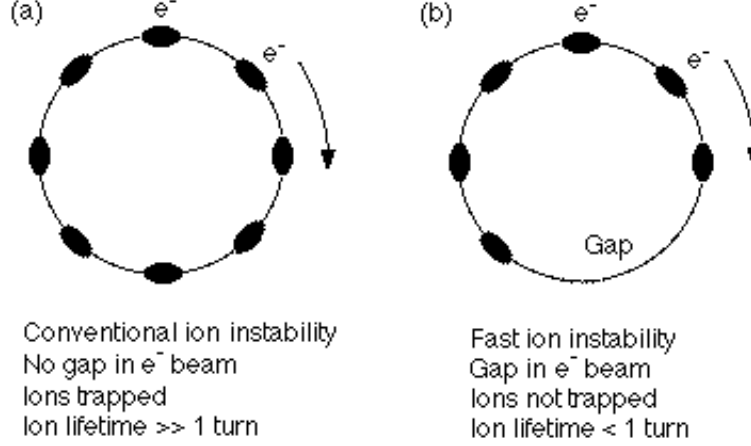
Figure 4.1: Comparison between (a) the conventional ion trapping and (b) the fast ion instability.

such accelerators include the factory-colliders and third generation synchrotron radiation storage rings.

4.1   Ionization

Gas molecules are ionized by the passing electron beam. Let Σ be the ionization cross-section. Each electron ionizes along its path Σn ions per unit length. By the time the tail of the beam passes, the number of ions per unit length is

$$\lambda = \Sigma n N \tag{4.1}$$

We take $\Sigma = 2$ Mbarns $= 2 \times 10^{-18}$ cm^2.[12]

We want to relate n to the vacuum pressure P. This is done by

$$PN_A = nRT, \quad \text{where} \begin{cases} N_A = \text{Avogadro number} = 6.023 \times 10^{23} \\ R = 82.056 \text{ cm}^3 \text{ atm } ^\circ\text{K}^{-1} \\ T = \text{room temperature} = 300^\circ\text{K} \end{cases}$$

$$\implies \quad P[\text{Torr}] = 3.1 \times 10^{-17} \; n[\text{cm}^{-3}] \tag{4.2}$$

where we have used 1 atm = 760 Torr. Using Eq.(4.2), Eq.(4.1) becomes

$$\lambda = \frac{\Sigma N P N_A}{RT} \approx 6.4 \text{ m}^{-1} P[\text{Torr}] N \tag{4.3}$$

---

[12]This is a very large cross-section. The barn unit was introduced by Fermi to denote large cross-sections, "as big as a barn", but that holds for *nuclear* interactions. Nowadays exploring rare *elementary particle* events, we become used to units like nanobarns or picobarns. This is because quarks are much smaller than nuclei. Here we use megabarn unit. This is because we are dealing with *atomic* interactions here, and atoms are much bigger than nuclei.

In a storage ring, we might have $P = 10^{-9}$ Torr and $N = 10^{11}$, then we have an ion line density at the tail of the beam of $\lambda = 6.4$ ions per cm, or one ion per 1.5 mm. If the electron beam consists of a train of bunches, the ion density at the end of the train will be correspondingly larger. Also, in a linac, we might have $P = 10^{-6}$ Torr and $N = 10^{10}$, then we would have 100 times denser ions for a single bunch beam.

We might compare this value of λ with the line density of the residual gas as seen by the beam, which is given by $\lambda_{\text{gas}} = \pi a^2 n$. In this case we have $n = 3.2 \times 10^7$ cm^{-3}, and if $a = 1$ mm, we obtain $\lambda_{\text{gas}} = 1.0 \times 10^6$ molecules per cm. About 10^{-5} of the molecules are ionized by the passing beam.

Figure 4.2 illustrates the situation. As the beam travels down the linac, a fraction of the CO molecules get ionized. The CO$^+$ ions accumulate linearly as the electron beam passes by, until it reaches the level of Eq.(4.1) when the beam tail passes. Figure 4.2 shows of course just the ionization process. The interaction between ions and the beam is not illustrated, and is the subject of this chapter.
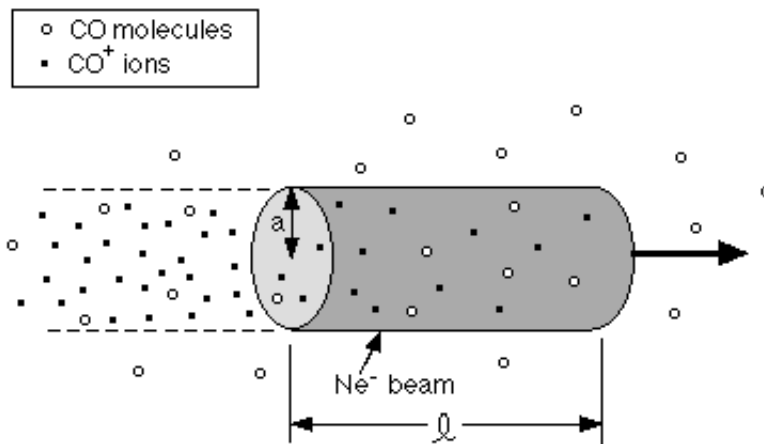
Figure 4.2: Ionization process.

Statistical excitation of beam tail There is in principle a statistical excitation of coherent motion of the tail of the electron beam due to the ions. To see that, consider a beam which consists of two slices, each with $N/2$ electrons and transverse radius a. The two slices are separated longitudinally by a distance ℓ. The slice centroids are free to move, but their shape is considered rigid. The first beam slice produces on the average one ion every distance of $2/\lambda$ with λ given by Eq.(4.1) or (4.3). These ions have random transverse position within the uniform disc of radius a. Consider an ion at transverse location y. Ignoring its ionization electron, this ion kicks the second beam slice centroid by an angle $\Delta y' \approx 2 r_e y / \gamma a^2$ where $r_e = 2.82 \times 10^{-13}$ cm is the classical electron radius.

Since there is one such kick every distance of $2/\lambda$, and the location y is random, there is a statistical growth in the centroid of the beam tail according to

$$\dot{\epsilon}_N = \gamma\dot{\epsilon} \approx \gamma\frac{c\lambda}{2}\beta_y\langle\Delta y'^2\rangle \approx \frac{c\lambda r_e^2}{8\epsilon_N} \tag{4.4}$$

where β_y is the β-function, and we have used the facts that $\langle y^2\rangle = a^2/4$ for a uniform disc and that $\epsilon = a^2/4\beta_y$.

The coherent growth of beam tail (or tail of a beam train), Eq.(4.4), is in addition to the growths due to the incoherent beam-gas scattering or the fast ion instability to be discussed later. Take the storage ring example with $\lambda = 6.4$ /cm, and $\epsilon_N = 10^{-7}$ m, we find $\dot{\epsilon} = 2 \times 10^{-12}$ m/s. The effective emittance doubling time is then about 15 hrs. Note that this emittance growth effect applies regardless of the species of the beam particles. We will not pursue this statistical excitation of beam tail in the following.

4.2 Ion Motion – Unperturbed Electrons

As a zeroth order description of the ion motion, let us first analyse the motion of an ion once it is produced, assuming the electron beam is unperturbed by the ions. We assume that the ion is produced at rest and that its motion is nonrelativistic throughout.[13] It is singly charged to $+e$. The electron beam is considered relativistic.

Let y be the transverse displacement of the ion relative to the electron beam centroid. The electric field due to the passing electron beam and seen by the ion is $-(2Ne/\ell a^2)y$. The ion motion is therefore

$$M\ddot{y} + \frac{2Ne^2}{\ell a^2}y = 0 \tag{4.5}$$

which is simple harmonic. All ions thus oscillate with the same frequency

$$\omega_I = \sqrt{\frac{2Nr_pc^2}{\ell a^2 A}} \tag{4.6}$$

where $M = Am_p$ and $e^2/(m_pc^2) = r_p = 1.54 \times 10^{-16}$ cm is the proton classical radius.

Take $N = 10^{11}, \ell = 1$ cm, $a = 1$ mm, $A = 14$, we find $\omega_I/2\pi = 70$ MHz. The ion oscillation is typically rather rapid!

What is the ion distribution under the focusing of the unperturbed electron beam? Let $\rho(r|z)$ be the radial distribution of the ions at longitudinal location z, where z refers to the distance between the ion and the head of the electron beam, with $\ell > z > 0$. Then (see Fig.4.3)

$$\rho(r|z) = \frac{\Sigma nN}{\pi\ell a^2}\int_{0,\left(|\cos(\frac{\omega_I(z-z')}{c})|>\frac{r}{a}\right)}^{z} dz'\frac{1}{\cos^2(\frac{\omega_I(z-z')}{c})} \tag{4.7}$$

where the integration is over all z'-locations where ions can be produced.
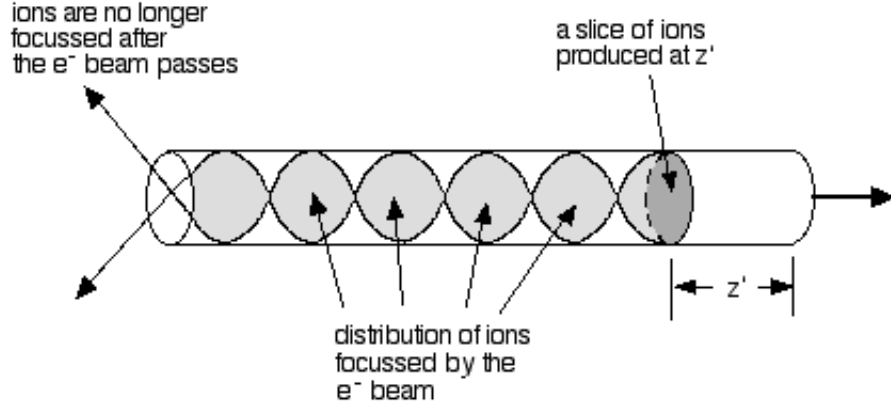
Figure 4.3: Ion distribution after being produced by the electron beam. For each slice of ions produced at z', the distribution at position z is a uniform disc with radius $a|\cos(\omega_I(z-z')/c)|$.
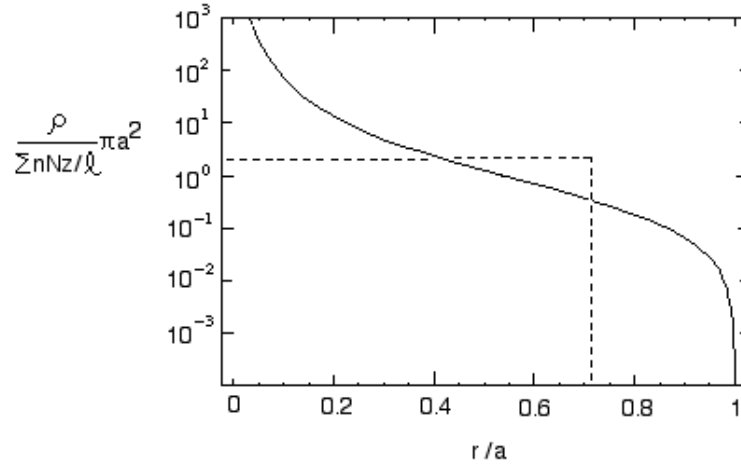
Figure 4.4: Radial distribution of ions by the passing electron beam. The dashed square is its uniform disc approximation.

Ignoring the initial transients (valid when $\omega_I z/c \gg \pi$), this gives

$$\rho(r|z) \approx \frac{2\Sigma nNz}{\pi^2 \ell a^2} \frac{\sqrt{a^2 - r^2}}{r} \tag{4.8}$$

---

[13]The nonrelativistic condition is satisfied if $\omega_I a \ll c$, or equivalently, using Eq.(4.6) below, when the electron line charge density $N/\ell \ll A/r_p$. This is easily satisfied.

Note that there is a divergence at $r = 0$ because the ions are sharply focussed to a point at all the focal points in Fig.4.3. On the other hand, the total number of ions at location z is

$$\int_0^a 2\pi r dr \; \rho(r|z) = \frac{\Sigma nNz}{\ell} \tag{4.9}$$

as it should.

This ion distribution (4.8) has an rms radius

$$\langle r^2 \rangle = \frac{\ell}{\Sigma nNz} \int_0^a 2\pi r^3 dr \; \rho(r|z) = \frac{a^2}{4} \tag{4.10}$$

If we approximate this ion distribution by a uniform disc, the disc radius should perhaps be taken as $a/\sqrt{2}$, which is somewhat smaller than the electron beam cross-secion. Figure 4.4 shows the distribution (4.8). The dashed square in Fig.4.4 is its uniform disc approximation.

> *Exercise* 1 Derive Eqs.(4.7-4.12). Contemplate what physics have we lost by approximating the ion distribution as a uniform disc.

4.3   Electron Motion – Unperturbed Ions

We have now a zeroth order description of ion motion in the presence of the unperturbed electron beam. As the zeroth order description of the electron motion, we approximate the ion distribution as a rigid unmoving uniform cylinder with radius $a/\sqrt{2}$, unperturbed by the electrons.[14] The electron beam and the ion distribution are sketched in Fig.4.5.

An electron at a longitudinal location z relative to the front of the beam sees an electric field of $4(e\Sigma nN/a^2)(z/\ell)y$.[15] The equation of motion for this electron is

$$\ddot{y} + K\frac{z}{\ell}y = 0, \quad \text{where } K \equiv 4\frac{\Sigma nNc^2 r_e}{\gamma a^2} \tag{4.13}$$

The ion focusing for the electron depends on the longitudinal position z of the electron. If $\lambda = \Sigma nN = 6.4/\text{cm}$, $\gamma = 10^4$, and $a = 1$ mm, we have $K = 6.5 \times 10^7$ s^{-2}. The electron at the end of the beam has an ion focusing frequency of $\sqrt{K}/2\pi = 1.3$ kHz. This frequency is much smaller than ω_I. The focusing of

---

[14]The statistical excitation of beam tail discussed earlier is ignored here.

[15]One could ask what is the electric field if we assume the distribution (4.8) instead of a uniform cylinder. The answer is

$$E_y = \frac{4e\Sigma nNz}{\pi\ell} \frac{1}{|y|} \left[\sin^{-1}(\frac{y}{a}) + \frac{y}{a}\sqrt{1 - \frac{y^2}{a^2}} \right] \tag{4.11}$$

To a rather good approximation, this gives

$$E_y \approx \frac{8e\Sigma nNz}{\pi a\ell}\text{sgn}(y) \tag{4.12}$$

In spite of this, we shall approximate the electric field as being linear in y.
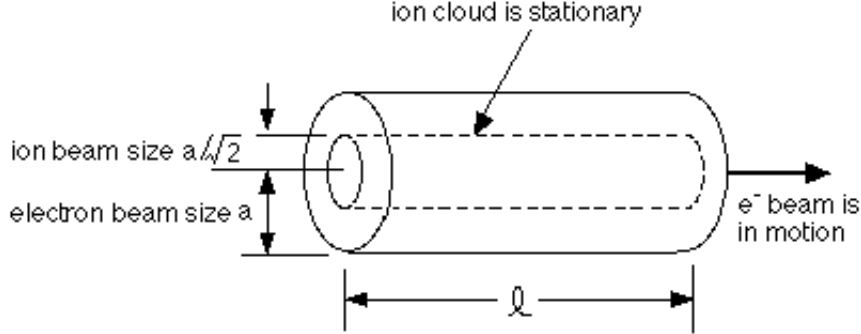
Figure 4.5: The model we use to study the beam-ion interaction. Both the electron beam and the ions have a uniform transverse distribution. The electron beam radius is $\sqrt{2}$ larger than that of the ions. Longitudinally, the electron beam has a uniform distribution, while the ion density is proportional to z, the distance measured from the head of the electron bunch.

the electrons by the ions is much weaker than the focusing of the ions by the electrons.

In addition to the focusing due to the ions, electrons see an additional external focusing from quadrupoles. With a β-function of 10 m, the betatron frequency is $\omega_\beta/2\pi = 5$ MHz, which is much stronger focusing than that due to the ions although it is much slower than the ion oscillation frequency ω_I. Note that in our numerical example, we have $\omega_I \gg \omega_\beta \gg \sqrt{K}/2\pi$.

Exercise 2 Repeat the calculation of electron motion with unperturbed ions for the case of a flat electron beam of height $2a$, width $w \gg 2a$, and length ℓ. Approximate both the electron beam and the ions by uniform ribbons of some finite thickness and length.
Solution

$$\omega_I^2 = \frac{2\pi N r_p c^2}{w\ell a}$$

$$\rho(y|z) = \frac{\Sigma n N z}{\pi w \ell a} \ln\left[\frac{1 + \sqrt{1 - (y/a)^2}}{|y/a|}\right]$$

$$K = \frac{\sqrt{3}\Sigma n N c^2 r_e}{2\gamma w a} \tag{4.14}$$

The ions has a ribbon distribution with height $2a/\sqrt{3}$.

Exercise 3 (a) Consider the case of an electron beam bunch with $a = 100\,\mu$m, $\ell = 1$ mm, $N = 5 \times 10^{10}$, and $E = 1.2$ GeV coasting down a linac of length $L = 3$ km. Let the linac have an average

75

β-function of $\beta = 10$ m, and a CO pressure of $P = 10^{-6}$ Torr. Estimate the difference in betatron phase between the head and the tail of the electron bunch when it reaches the end of the linac. (b) Repeat for an accelerated electron beam from 1.2 GeV to 50 GeV. _Solution_ (a) The bunch head has the equation of motion $y'' + (1/\beta^2)y = 0$. The bunch tail has $y'' + (1/\beta^2 + K/c^2)y = 0$.

4.4   Coupled Ion-Electron Equation of Motion

We have now studied the zeroth order cases (a) the ions are perturbed but the electron beam is rigid, and (b) the electron beam is perturbed but the ions are rigid. We next consider the case when the motions of the electron beam and the ions are coupled and mutually perturbing. Both the electron beam and ion distributions are considered to be uniform discs (electrons with radius a, ions with radius $a/\sqrt{2}$) with centroid motion but no shape distortion.

Note that we ignore the self direct space charge effects, such as the effect of the ion fields on the ions and the effect of electron beam field on the electrons. We are interested mainly nly in the coupled motion of the ions and the electron beam.

Designate the centroid motion of an electron slice by $y_e(s|z)$, where z is the longitudinal position of the electron slice relative to the head of the electron beam $(\ell > z > 0)$, and s is the distance along the accelerator. If the head of the beam passes position $s = 0$ at time $t = 0$, then the electron slice under consideration would have $s = ct - z$.

The ion motion requires a more complicated description. Designate the ion motion by $y_I(s, t|z')$, where z' indicates the ion was produced by an electron which is located at z' relative to the head of the electron beam. Since ions do not move along s like the electrons, we need both s and t to describe their motion. The quantity $y_I(s, t|z')$ is defined only after the ion is born, i.e. when $s < ct - z'$.

Figure 4.6 sketches the situation. As we will show later, y_I is going to be $90°$ out of phase from y_e, and the ions are going to oscillate with a much larger amplitude than the electron beam. In Fig.4.6, the electron beam and the ions are shown separately. In reality, of course, their distributions overlap and their motions are coupled.

The equation of motion for the ions can be obtained by examining Eq.(4.5). Except that now the electron beam is also moving and the focusing force must refer relative to the electron beam centroid. This gives

$$\frac{\partial^2}{\partial t^2} y_I(s, t|z') + \omega_I^2 [y_I(s, t|z') - y_e(s|ct - s)] = 0 \qquad (4.15)$$

The term $y_e(s|ct - s)$ occurs here because it is the electrons with $z = ct - s$ which are interacting with the ions at location s and time t. Eq.(4.15) assumes the oscillation amplitudes are small, with $|y_e| \ll a$ and $|y_I| \ll a$, so that the
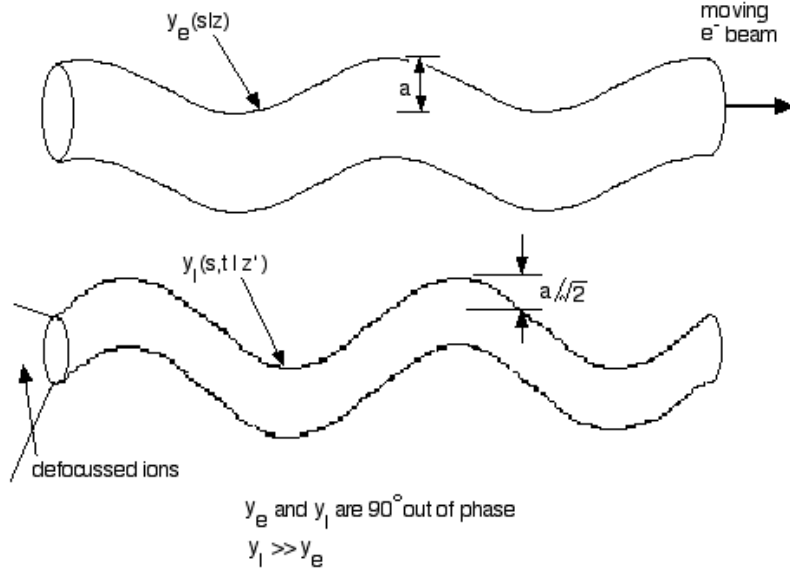
Figure 4.6: Coupled ion-beam oscillation. The snap-shot wavelength of both beam and ion oscillations is given by (4.24).

equations can be linearized. This approximation rules out the study of saturation effects when the oscillation amplitudes become comparable to the beam size a.

Equation (4.15) requires the initial conditions

$$y_I(s, \tfrac{s+z'}{c}|z') = y_e(s|z')$$
$$\left[\tfrac{\partial}{\partial t} y_I(s, t|z')\right]_{t=\frac{s+z'}{c}} = 0 \qquad (4.16)$$

The reason for (4.16) is that the ions at position s were produced at time $t = (s + z')/c$ and when produced, they had the same distribution as the electrons which produced them, and we assume that they were produced with zero velocity.

The equation of motion for the electrons is

$$c^2 \frac{\partial^2}{\partial s^2} y_e(s|z) + \omega_\beta^2 y_e(s|z) + \frac{K}{\ell}\left[z y_e(s|z) - \int_0^z dz'\; y_I(s, \frac{s+z}{c}|z')\right] = 0 \quad (4.17)$$

where the second term describes the external betatron focusing, and K was defined in Eq.(4.13). The second term in the square bracket describes the center of charge of all the ion slices integrated from $z' = 0$ to $z' = z$. The first term in the square bracket gives rise to a betatron frequency shift for the electron beam. We will see later that this first term is not important for the asymptotic behavior and can be dropped for our purpose. Eqs.(4.15-4.17) are the coupled ion-beam equations of motion.

Exercise 4 What modifications in Eqs.(4.15-4.17) are needed if the unperturbed beam cross-section is gaussian elliptical or flat ribbon instead of round uniform disc?

Exercise 5 If the electron beam is in a FODO lattice and is not uniformly focussed as being assumed in Eq.(4.17), the ions see different focussing frequency ω_I depending on where in the FODO structure they are produced. This leads to a spread of ω_I. What modifications in Eqs.(4.15-4.17) are needed in this case? This introduces a stabilizing effect on the fast ion instability.

4.5 Asymptotic Electron Motion

We need to solve Eqs.(4.15-4.17). We are interested only in an asymptotic behavior applicable for a long electron beam bunch or a long train of many electron bunches. Here, for simplicity, we assume a very long electron bunch. The case of a long beam train is discussed in a later section.

Before we solve for the asymptotic behavior of Eqs.(4.15-4.17), we note that there is a resonance between the ion motion and the electron motion. The asymptotic behavior will be dominated by this resonance. To see this resonance, consider an electron motion with

$$y_e(s|z) \sim e^{-i\omega_\beta s/c + ikz} \tag{4.18}$$

for some k, and ask what does this say about the ions? To answer this question, first note that ions execute simple harmonic motion,

$$y_I(s,t|z') \sim y_I(s,t_0|z')e^{\pm i\omega_I(t-t_0)} \tag{4.19}$$

where $t_0 = (s + z')/c$ is the time when the ions are produced. It turns out that in Eq.(4.19) we should keep the $+$ sign for the instability.[16]

At $t = t_0$, the ions have the same displacement as the electrons that produce them, i.e. we can use the initial condition (4.16) to obtain

$$
\begin{aligned}
y_I(s,t|z') &\sim y_e(s|z')e^{i\omega_I(t-t_0)} \\
&\sim e^{-i\omega_\beta s/c + ikz'} e^{i\omega_I t - i\omega_I(s+z')/c}
\end{aligned}
\tag{4.20}
$$

Resonance occurs when $y_I(s,t|z')$ and $y_e(s|z)$ have the same t-dependence when observed at a fixed s. Observed at a fixed location s as a function of time t, we insert $z = ct - s$ in Eq.(4.18) and obtain

$$y_e(s|z) \sim e^{-i\omega_\beta s/c + ikct - iks} \tag{4.21}$$

Comparing Eqs.(4.20) and (4.21), we see that resonance occurs when

$$kc = \omega_I \tag{4.22}$$

---

[16]If we keep the $-$ sign, we will obtain in Eq.(4.38) later a damped solution with J_0 replacing I_0. Since we are concerned only with an instability, we will take the $+$ sign only.

Substituting (21) into (17) and (19) gives

$$
\begin{aligned}
y_e(s|z) &\sim e^{-i\omega_\beta s/c + i\omega_I z/c} \\
y_I(s,t|z') &\sim e^{-i(\omega_\beta+\omega_I)s/c + i\omega_I t}
\end{aligned}
\tag{4.23}
$$

One can make the following observations based on Eq.(4.23):

(i) At resonance, $y_I(s,t|z')$ is independent of z' — all ions at s oscillate in unison regardless of when they were produced. When observed at a fixed s, both the electrons and the ions have a time dependence of $e^{i\omega_I t}$. When observed at a fixed t, they both have the snapshot behavior of $e^{-i(\omega_\beta+\omega_I)s/c}$. The snapshot wavelength of both the electron beam and the ion oscillations is

$$
\lambda = \frac{2\pi c}{\omega_\beta + \omega_I}
\tag{4.24}
$$

The electron beam oscillation has a phase velocity

$$
v_{\mathrm{ph}} = \frac{\omega_I}{\omega_\beta + \omega_I} c
\tag{4.25}
$$

We see that instability occurs for a *slow wave* component with $v_{\mathrm{ph}} < c$.

(ii) In resonance, y_e contains information on ω_I [see Eq.(4.23)]. In practice, this means if we observe the electron beam by a beam position monitor, the signal will contain a frequency peak at the ion frequency ω_I [see Eq.(4.47) later]. This is how the ion frequency ω_I can be observed in the accelerator. It is much easier to observe the electron beam than to look for the ions. Observation of a ω_I signal in the electron beam is one indirect evidence of fast ion instability effect.

We are now ready to examine the asymptotic behavior of the beam-ion coupled motion. We assume

$$
\begin{aligned}
y_e(s|z) &= \tilde{y}_e(s|z)e^{-i\omega_\beta s/c + i\omega_I z/c} \\
y_I(s,t|z') &= \tilde{y}_I(s,t|z')e^{-i(\omega_\beta+\omega_I)s/c + i\omega_I t}
\end{aligned}
\tag{4.26}
$$

where $\tilde{y}_e(s|z)$ is slowly varying in s and $\tilde{y}_I(s,t|z')$ is slowly varying in t.

Substituting Eq.(4.26) into Eqs.(4.15) and (4.17), and dropping small terms $\partial^2\tilde{y}_I/\partial t^2$ and $\partial^2\tilde{y}_e/\partial s^2$, we obtain

$$
\frac{\partial}{\partial t}\tilde{y}_I(s,t|z') + \frac{i\omega_I}{2}\tilde{y}_e(s|ct-s) = 0
\tag{4.27}
$$

$$
\frac{\partial}{\partial s}\tilde{y}_e(s|z) + \frac{iK}{2\omega_\beta c\ell}z\tilde{y}_e(s|z) - \frac{iK}{2\omega_\beta c\ell}\int_0^z dz'\ \tilde{y}_I(s,\frac{s+z}{c}|z') = 0
\tag{4.28}
$$

with the initial condition

$$\tilde{y}_I(s, \frac{s+z'}{c}|z') = \tilde{y}_e(s|z') \tag{4.29}$$

Equations (4.27) and (4.29) give

$$
\begin{aligned}
\tilde{y}_I(s,t|z') &= \tilde{y}_e(s|z') - \frac{i\omega_I}{2} \int_{(s+z')/c}^{t} dt' \; \tilde{y}_e(s|ct'-s) \\
&= \tilde{y}_e(s|z') - \frac{i\omega_I}{2c} \int_{z'}^{ct-s} dz'' \; \tilde{y}_e(s|z'')
\end{aligned}
\tag{4.30}
$$

Substituting Eq.(4.30) into (4.28) and using the identities

$$\int_0^z dz' \int_{z'}^z dz'' \; \tilde{y}_e(s|z'') = \int_0^z dz' \; z'\tilde{y}_e(s|z')$$

$$z\tilde{y}_e(s|z) - \int_0^z dz' \; \tilde{y}_e(s|z') = \int_0^z dz' \; z'\frac{\partial}{\partial z'}\tilde{y}_e(s|z') \tag{4.31}$$

we find

$$\frac{\partial}{\partial s}\tilde{y}_e(s|z) + \frac{iK}{2\omega_\beta c\ell} \int_0^z dz' \; z' \left[\frac{\partial}{\partial z'}\tilde{y}_e(s|z') + \frac{i\omega_I}{2c}\tilde{y}_e(s|z') \right] = 0 \tag{4.32}$$

Taking partial derivative with respect to z gives

$$\frac{\partial^2}{\partial s \partial z}\tilde{y}_e(s|z) + \frac{iK}{2\omega_\beta c\ell}z \left[\frac{\partial}{\partial z}\tilde{y}_e(s|z) + \frac{i\omega_I}{2c}\tilde{y}_e(s|z) \right] = 0 \tag{4.33}$$

The first term in the square bracket is much smaller than the second term because $\tilde{y}_e$ is slowly varying in z compared with the ion frequency ω_I. We shall drop the first term, and later will provide the validity condition (4.41) for making this approximation. Dropping this term is equivalent to dropping the initial condition of ion production.

Equation (4.33) now reads

$$\frac{\partial^2}{\partial s \partial z}\tilde{y}_e(s|z) - \frac{K\omega_I}{4\omega_\beta c^2\ell}z\tilde{y}_e(s|z) \approx 0 \tag{4.34}$$

It is remarkable that a complicated coupled system has yielded a simple equation of motion, Eq.(4.34), at the end. It is even more remarkable that Eq.(4.34) has a simple solution. The solution is that $\tilde{y}_e(s|z)$ depends on s and z through a single dimensionless variable

$$\eta \equiv \frac{z}{c}\sqrt{\frac{K\omega_I s}{2\omega_\beta \ell}} \tag{4.35}$$

with

$$\eta\tilde{y}_e'' + \tilde{y}_e' - \eta\tilde{y}_e = 0 \tag{4.36}$$

80

where $(\ )' = \frac{d}{d\eta}(\ )$. If, for example, the beam has a displacement such that when observed at $s = 0$ behaves in t as

$$\tilde{y}_e(0|0) = y_0 \quad \text{or equivalently} \quad y_e(s = 0|z = ct) = y_0 e^{i\omega_I t} \tag{4.37}$$

then the solution is

$$\tilde{y}_e(s|z) = y_0 I_0(\eta) \tag{4.38}$$

where $I_0(x)$ is the Bessel function. In the asymptotic regime with $\eta \gg 1$, we have

$$\tilde{y}_e(s|z) \approx y_0 \frac{e^\eta}{\sqrt{2\pi\eta}} \tag{4.39}$$

The growth in the electron beam oscillation is exponential in z but behaves like $\sim e^{\sqrt{s}}$ with s. (Recall that z refers to the length along the electron beam bunch or beam train; while s/c is the time the beam has been stored in the accelerator.) The observation that $\eta \propto z$ indicates that one way to fight the fast ion instability is to introduce more gaps within the long bunch train.

In spite of the fact that the instability growth is not exponential in s, one may still define a characteristic growth distance s_0 for which the amplitude of an electron at the tail of the bunch grows by a factor of e,

$$s_0 = \frac{2\omega_\beta c^2}{K\omega_I \ell} \tag{4.40}$$

Fig.4.7 shows $\tilde{y}_e/y_0$ versus s/s_0 for various values of z/ℓ.
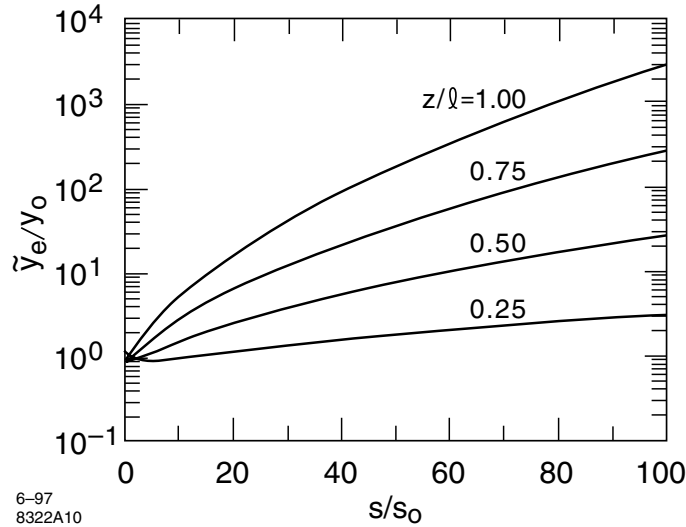
Figure 4.7: Asymptotic amplitude as a function of time, for various electrons along the bunch.

If we consider $K = 6.5 \times 10^7$ s^{-2}, $\omega_\beta = 5$ MHz, $\omega_I = 70$ MHz, and $\ell = 1$ cm, we find $s_0 = 2 \times 10^{10}$ m, or a growth time of about 1 min. This instability is very weak for a single short electron beam bunch. However, as we shall see, this is no longer the case for a long train of intense bunches.

We can check the validity of dropping the first term in Eq.(4.33) here. The approximation was $|\frac{\partial}{\partial z}\tilde{y}_e| \ll \frac{\omega_I}{c}|\tilde{y}_e|$. Together with $\eta \gg 1$, the validity criterion for $z = \ell$ (i.e. an electron at the end of the beam) is

$$\frac{\omega_I \ell}{c} \gg \eta \gg 1 \quad \text{or} \quad \frac{\omega_\beta \omega_I \ell}{K} \gg s \gg s_0 \tag{4.41}$$

This criterion can not be fulfilled unless $\ell\omega_I/c \gg 1$, i.e., there must be many ion oscillations made in the length of the beam. It further says that in order for Eq.(4.39) to be applicable, s has to be limited to the range given by Eq.(4.41).

> *Exercise* 6 (a) Go through the derivation (4.18-4.23) to obtain a feel for the beam-ion resonance process. (b) Go through (4.26-4.39) to see how this type of equation of motion can be analyzed.

4.6   Asymptotic Ion Motion

One may obtain also the asymptotic behavior of the ions by substituting (4.39) into (4.30),

$$\tilde{y}_I(s, t|z') \approx -iy_0 \sqrt{\frac{\omega_\beta \omega_I \ell}{2Ks}} \frac{e^{\bar{\eta}}}{\sqrt{2\pi\bar{\eta}}} \tag{4.42}$$

where

$$\bar{\eta} \equiv (t - \frac{s}{c})\sqrt{\frac{K\omega_I s}{2\omega_\beta \ell}} \tag{4.43}$$

Comparing the electron and ion oscillation amplitudes as they pass by each other, we obtain

$$\frac{y_I(s, \frac{s+z}{c}|z')}{y_e(s|z)} = \frac{\tilde{y}_I(s, \frac{s+z}{c}|z')}{\tilde{y}_e(s|z)} \approx -i\sqrt{\frac{\omega_\beta \omega_I \ell}{2Ks}} \tag{4.44}$$

We note that the ions oscillate $90°$ out of phase relative to the electrons and, using Eq.(4.41), that the ion oscillation amplitude is much larger than that of the electron beam, at least in the regime before the ion amplitude reaches the level comparable to the beam size a. These features were anticipated in Fig.4.6.

> *Exercise* 7 Following the above discussion to show that the beam-ion instability growth begins to saturate after the beam has traveled for a distance s where

$$\frac{e^{\sqrt{s/s_0}}}{(s/s_0)^{3/4}} = \frac{2\sqrt{2\pi}c}{\omega_I \ell} \frac{a}{y_0} \tag{4.45}$$

4.7 Spectrum From Electron Beam

One might be interested in knowing the spectrum of the electron beam as seen by a beam position monitor. Let the monitor be located at $s = 0$. Consider the bunch of length ℓ circulating in a storage ring of circumference $C = cT_0$. The signal seen by the monitor is

$$\text{signal}(t) = \sum_{k=0}^{\infty} y_e(kC|ct - kC)\Big|_{0 < ct - kC < \ell} \tag{4.46}$$

where k sums over multiple turns. The spectrum is then the Fourier transform of the signal,

$$
\begin{aligned}
\text{spectrum}(\Omega) \quad &\propto \quad \int_0^{\infty} dt\, e^{-i\Omega t}\,\text{signal}(t) \\
&= \quad \sum_{k=0}^{\infty} \int_0^{\ell/c} dt'\, e^{-i\Omega(t' + kT_0)} y_e(kC|ct') \\
&= \quad \sum_{k=0}^{\infty} e^{-i(\Omega + \omega_\beta)kT_0} \int_0^{\ell/c} dt'\, e^{-i(\Omega - \omega_I)t'}\, \tilde{y}_e(kC|ct') \\
&= \quad y_0 \sum_{k=0}^{\infty} e^{-i(\Omega + \omega_\beta)kT_0} \int_0^{\ell/c} dt'\, e^{-i(\Omega - \omega_I)t'}\, \frac{e^{\eta'}}{\sqrt{2\pi\eta'}} \tag{4.47}
\end{aligned}
$$

In the last step, $\eta' = t'\sqrt{K\omega_I kC/2\omega_\beta \ell}$ (note it depends on both t' and k).

The integral in Eq.(4.47) can be written as

$$I = \int_0^{\ell/c} dt'\, \frac{e^{(B - iA)t'}}{\sqrt{2\pi B t'}} = \frac{1}{\sqrt{2\pi B}}(-B + iA)^{-1/2}\gamma\left(\frac{1}{2}, (-B + iA)\frac{\ell}{c}\right)$$

where $A = \Omega - \omega_I$ and $B = \sqrt{K\omega_I kC/2\omega_\beta \ell}$, and $\gamma(\alpha, x)$ is the incomplete Gamma function. When $|x| \gg 1$, we have $\gamma(\alpha, x) \approx -x^{\alpha - 1}e^{-x}$, and

$$I \approx \sqrt{\frac{\ell/c}{2\pi B}}\, e^{B\ell/c}\left(\frac{e^{-iA\ell/2c}\sin\frac{A\ell}{2c}}{A\ell/2c}\right)$$

where we have made use of $|A|\ell/c \gg B\ell/c \gg 1$ which is a consequence of Eq.(4.41). Substituting into Eq.(4.47) then leaves us a summation over the revolutions k. This signal of course diverges as $k \to \infty$ because the signal itself diverges. However, if we measure the signal only in a relatively small window around a large $k = \bar{k}$, then the beam spectrum (4.47) gives

$$|\text{spectrum}(\Omega)| \propto y_0\sqrt{\frac{\ell/c}{2\pi\bar{B}}}\, e^{\bar{B}\ell/c}\left|\frac{\sin\frac{(\Omega - \omega_I)\ell}{2c}}{(\Omega - \omega_I)\ell/2c}\right| \sum_{p=-\infty}^{\infty} \delta(\Omega + \omega_\beta - p\omega_0) \tag{4.48}$$

where $\omega_0 = 2\pi/T_0$ is the revolution angular frequency, and $\bar{B} = \sqrt{K\omega_I \bar{k}C/2\omega_\beta \ell}$.

Equation (4.48) says that the electron beam spectrum consists of δ-function peaks located at $\Omega = p\omega_0 - \omega_\beta$, i.e. at the *lower* betatron side-bands of all revolution harmonics. In addition, it contains a broad envelope $\frac{\sin[(\Omega-\omega_I)\ell/2c]}{(\Omega-\omega_I)\ell/2c}$ which peaks around the ion frequency $\Omega = \omega_I$. The width around this broad envelope peak is $\Delta\Omega \approx \pm\pi c/\ell$, where ℓ is the length of the beam bunch (or the beam bunch train). As the length of the bunch (or bunch train) increases, the width of the envelope peak around $\Omega = \omega_I$ shrinks. The width shrinks to as narrow as $\pm\omega_0$ when the bunch train almost fills the accelerator circumference. Finally, the entire spectrum grows with time $\bar{k}$ according to the factor $e^{\bar{B}\ell/c}/\sqrt{2\pi\bar{B}\ell/c}$.

> *Exercise 8* It is instructive to sketch the spectrum, Eq.(4.48), as a function of Ω. Do that for (a) $\ell \ll$ the circumference and (b) ℓ almost equal to the circumference. In both cases, assume $\omega_I \gg \omega_0$.

4.8 The Case of a Train of Bunches

So far we have been considering a beam of a single long electron bunch. The same analysis also applies to a train of short electron bunches in some proper limit. For a train of M bunches, we need to make these replacements:

$$y_e(s|z) \rightarrow y_e(s|j), \qquad y_I(s,t|z') \rightarrow y_I(s,t|j') \tag{4.49}$$

where j and j' refer to the j-th bunch, with $j = 1$ referring to the first bunch, etc. Let S_B be the bunch spacing and N_B be the number of electrons per bunch. Assume $S_B\omega_I/c \ll 1$, so that the bunch train can be approximated as a continuous bunch. We redefine the ion frequency in Eq.(4.6), the parameter K in Eq.(4.13), the η parameter in Eq.(4.35), and the instability characteristic length in Eq.(4.40) as

$$\omega_I = \sqrt{\frac{2N_Br_pc^2}{S_Ba^2A}}$$

$$K = \frac{4\Sigma nN_Bc^2r_e}{\gamma a^2}$$

$$s_0 = \frac{2\omega_\beta c^2}{K\omega_I MS_B}$$

$$\eta = j\sqrt{\frac{s}{Ms_0}} \tag{4.50}$$

then in the asymptotic limit, Eq.(4.34) gives

$$\tilde{y}_e(s|j+1) \approx \tilde{y}_e(s|j) + \frac{j}{2Ms_0}\int_0^s ds'\, \tilde{y}_e(s'|j) \tag{4.51}$$

Equation (4.51) relates the motion of the $(j+1)$th bunch to its previous jth bunch. By iteration, we find (However, see Exercises 10 and 11.)

$$\tilde{y}_e(s|1) = y_0$$

$$\tilde{y}_e(s|2) = y_0 \left[1 + \frac{s}{2Ms_0} \right]$$

$$\tilde{y}_e(s|3) = y_0 \left[1 + \frac{3s}{2Ms_0} + (\frac{s}{2Ms_0})^2 \right], \quad \text{etc.} \tag{4.52}$$

Asymptotically, Eq.(4.52) gives the result of Eq.(4.39) with η given in Eq.(4.50).

Take a numerical example (damping ring for a possible linear collider): $N = 10^{10}, S_B = 10$ cm, $\gamma = 10^4, n = 3.2 \times 10^7$ cm^{-3} (300°K, $P = 10^{-9}$ Torr), $\Sigma = 2 \times 10^{-18}$ cm^2, $A = 14, a = 10$ μm, $r_p = 1.54 \times 10^{-16}$ cm, $\omega_\beta = 2 \times 10^8$ s^{-1}, and $M = 1000$. Then we have $K = 3.5 \times 10^7$ s^{-2}, $\omega_I = 4.4 \times 10^9$ s^{-1}, and $s_0 = 2.3 \times 10^8$ cm, or $s_0/c = 7.6$ ms.

Exercise 9 Perform a self-consistency check by back substitution that Eq.(4.39) does satisfy Eq.(4.51) when $\eta \gg 1$.

Exercise 10 Equation (4.52) is misleading because it was derived by using (4.51), which describes only for the asymptotic behavior, and thus does not apply to the first few bunches, although if the iteration procedure is continued, Eq.(4.52) would apply to later bunches. On the other hand, for the first few bunches, you can solve the problem directly. Do this for the second bunch and compare your result with Eq.(4.52).

Solution For the first bunch, ions have no effect, and we have

$$y_1(t) = y_0 \sin \omega_\beta t \quad (t \geq 0) \tag{4.53}$$

The second bunch sees the ions left behind by the first bunch. Its equation of motion is

$$\ddot{y}_2 + \omega_\beta^2 y_2 + K[y_2(t) - y_1(t - t_0)] = 0 \tag{4.54}$$

where $t_0 = S_B/c$ is the bunch spacing in time. A time lag is introduced in y_1. Substituting (4.53) into (4.54), the solution is found to be $(t \geq t_0)$

$$y_2(t) = y_0 \left\{ \sin[\omega_\beta(t - t_0)] - \frac{\omega_\beta}{\sqrt{\omega_\beta^2 + K}} \sin\left[\sqrt{\omega_\beta^2 + K}(t - t_0)\right] \right\} \tag{4.55}$$

We have assumed the second bunch started initially with $y_2 = 0$. Due to the driving by ions, however, it acquires a maximum amplitude of $\sim 2y_0$ which occurs at time $(t - t_0) \sim 2\pi\omega_\beta/K$. Eq.(4.55) is quite different from Eq.(4.52). In particular, ω_I does not play a role in Eq.(4.55).

If $\omega_\beta t \gg 1, \omega_\beta^2 \gg K$, and $(\sqrt{\omega_\beta^2 + K} - \omega_\beta)t \approx Kt/2\omega_\beta \ll 1$, Eq.(4.55) can be approximated as

$$y_2(t) \approx y_0 \frac{K}{2\omega_\beta}(t - t_0) \cos[\omega_\beta(t - t_0)] \quad (t \geq t_0) \tag{4.56}$$

where the fact that it contains a term $\propto (t-t_0)$ indicates a resonance effect.

Exercise 11 Proceed to calculate the exact expression for $y_3(t)$ and compare with Eq.(4.52). The problem becomes more complicated now because the ions produced by the first bunch and seen by the third bunch has been affected by the second bunch and ω_I begins to play a role.

Solution The ions produced by the first bunch were produced with amplitude $y_1(t - 2t_0)$. When the second bunch comes by, they get a kick with $\Delta y' = -(2N_B r_p/Aa^2)y_1(t - 2t_0)$. When the third bunch arrives, these ions have a displacement

$$\left(1 - \frac{\omega_I^2 S_B^2}{c^2}\right) y_1(t - 2t_0) \tag{4.57}$$

The equation of motion for the third bunch is therefore

$$\ddot{y}_3(t) + \omega_\beta^2 y_3(t) + K\left[2y_3(t) - y_2(t - t_0) - \left(1 - \frac{\omega_I^2 S_B^2}{c^2}\right)y_1(t - 2t_0)\right] = 0 \tag{4.58}$$

where $y_{1,2}(t)$ are given by Eqs.(4.53) and (4.55).

Equation (4.58) can be solved to give

$$y_3(t) = \qquad\qquad (t \geq 2t_0) \tag{4.59}$$

When $\omega_\beta t \gg 1 \gg Kt/2\omega_\beta$, we have

$$y_3(t) \approx \tag{4.60}$$

Note the resonance factor $(t - 2t_0)^2$. Note also that ω_I appears explicitly.

4.9 External Damping

The above analysis applies when the beam or the beam train is injected with a displacement which has a snapshot pattern $\sim e^{-i(\omega_\beta + \omega_I)s/c}$. It also applies if, at injection, there is a displacement at the head of the beam (or the first bunch in the case of a beam train). This initial displacement excites the bunch tail oscillation through ions by the resonance process.

When there is an external damping – radiation damping, for example – the behavior of this instability would be quite different. What happens then is that the entire growth, including the beam head and tail, would be damped by the external damping. This is true even if the damping rate τ_d^{-1} is much weaker than the instability growth rate, i.e. even if $\tau_d^{-1} \ll c/s_0$.

To see this, consider the case of a beam train. The first bunch does not see any ions and executes a free betatron oscillation. The ions it produces excite

the second bunch. However, with an external damping, even a very weak one, the oscillation of the first bunch slowly decays in $t \approx \tau_d$. After the first bunch oscillation damps out, the second bunch is no longer driven, and it starts to damp. It will take another τ_d to damp after the first bunch has been damped; thus its oscillation decays in $t \approx 2\tau_d$. With the first and the second bunches stop oscillating, the third bunch, regardless of the fact that it has been driven to a large amplitude during this time, begins to damp. Eventually, it is damped out, etc. With an external damping, therefore, the fast ion instability is only a transient effect. A small injection error would very quickly grow to a large oscillation, especially towards the tail of the beam train. However, with time, the oscillation of the entire train decays and, if not excited again, will stay quiet.

We see here one more peculiarity of the fast ion instability. To damp out a conventional collective instability, one would need an external damping rate larger than the instability growth rate. But this is not necessary here. The fast ion instability is in this sense not a true instability; it is more a transient effect which is particularly sluggish.

4.10   Feedback System

One might envision therefore that the best way to deal with the fast ion instability is to ignore it, and let radiation damping take care of it. Unfortunately, the beam is constantly excited by various noise effects in an accelerator: power supply ripples, collective instabilities, etc. In fact, we often turn on a strong feedback system to fight just these effects.

A feedback system of course also damps the fast ion instability. However, feedback systems also carry noise, which constantly excite the fast ion instability, and this feedback noise may dominate over all other noise sources. So we now have a situation where the feedback system provides simultaneously the excitation and the damping. The beam responds to it very similarly to a single electron responding to quantum excitation and radiation damping. The net result is that each bunch in a beam train will reach a certain rms oscillation amplitude which is determined by an equilibrium between the feedback damping and the feedback noise. In the following, we analyze this equilibrium.

Let the feedback damping time be τ_d, and its noise be characterized by $\langle y^2 \rangle_{\text{noise}}$, which is the mean square amplitude due to the noise kicks delivered by the feedback to each bunch per revolution. Consider the first bunch $j = 1$ first. Its motion is unaffected by ions. It sees noise excitation of $\langle y^2 \rangle_{\text{noise}}$ on one hand and damping with τ_d on the other hand.[17] A balance is reached when its mean square oscillation amplitude is given by

$$\langle y_1^2 \rangle = \frac{\tau_d}{4T_0} \langle y^2 \rangle_{\text{noise}} \tag{4.61}$$

$\underline{Exercise}$ 12 Derive Eq.(4.61).

---

[17]The following analysis applies even if $\langle y^2 \rangle_{\text{noise}}$ and τ_d do not come from a feedback system, but it is conceptually convenient to assume so for our purpose.

87

$$\langle y_1^2 \rangle = \langle y^2 \rangle_{\text{noise}} \frac{1}{T_0} \int_0^\infty dt \left(\sin \omega_\beta t \; e^{-t/\tau_d} \right)^2$$

$$\approx \langle y^2 \rangle_{\text{noise}} \frac{1}{2T_0} \int_0^\infty dt \, e^{-2t/\tau_d} = \frac{\tau_d}{4T_0} \langle y^2 \rangle_{\text{noise}} \quad (4.62)$$

Now consider the trailing bunches in the asymptotic regime. We will go back to approximating the bunch train as a long continuous bunch of total length ℓ. Let the feedback noise be characterized by a random force $f(s, z)$ acting on the beam. The equation for the amplitude of the electron oscillations is

$$\frac{\partial \tilde{y}_e(s|z)}{\partial s} + \frac{1}{c\tau_d} \tilde{y}_e(s|z) = \frac{1}{2s_0 \ell^2} \int_0^z dz' z' \tilde{y}(s|z') + f(s, z) \quad (4.63)$$

Without the second term on the left hand side and with $f = 0$ we have the case studied in Eqs.(4.32) and (4.34). The new terms take into account the damping caused by the feedback system and the noise modeled by the force $f(s, z)$.

The solution of Eq.(4.63) is

$$\tilde{y}_e(s|z) = \int_{-\infty}^s ds' f(s', z) e^{\frac{s'-s}{c\tau_d}} \quad (4.64)$$

$$- \int_0^z dz' \int_{-\infty}^s ds' f(s', z') e^{\frac{s'-s}{c\tau_d}} \frac{\partial}{\partial z'} I_0 \left(\sqrt{\frac{(z^2 - z'^2)(s - s')}{s_0 \ell^2}} \right)$$

where I_0 is the modified Bessel function. The first term in Eq.(4.64) is the direct response of the beam to the noise kicks. The second term is the response due to coupling to the ions. Our previous analysis is for the case $f(s, z) \propto \delta(s)$, yielding

$$\tilde{y}(s, z) \propto e^{-s/c\tau_d} I_0(\sqrt{z^2 s/s_0 \ell^2}) \quad (4.65)$$

In case we have a constant source of random noise acting on the beam and $f(s, z)$ is a random function, a more adequate description of the beam motion would be in terms of the average square of the amplitude of oscillations. To calculate $\langle \tilde{y}_e^2(s|z) \rangle$ we assume that the force f is a δ-correlated random noise

$$\langle f(s, z) f(s', z') \rangle = F \delta(s - s') \delta(z - z') \quad (4.66)$$

which is appropriate for a wide-band feedback system. The parameter F can be related to the average square of amplitude of the betatron oscillations under the influence of the noise without ions. In this case the amplitude $\tilde{y}_e$ is given by the first term in Eq.(4.64)

$$\tilde{y}_e(s|z) = \int_{-\infty}^s ds' f(s', z) e^{\frac{s'-s}{c\tau_d}} \quad (4.67)$$

and using Eq.(4.66) we have

$$\langle \tilde{y}_e(s|z) \tilde{y}_e(s|z') \rangle = \frac{c\tau_d}{2} F \delta(z - z') \quad (4.68)$$

So far we have assumed a long continuous beam. In case the beam consists of a train of discrete bunches, we will have to identify Eq.(4.68) with

$$\langle \tilde{y}_1^2 \rangle = \frac{c\tau_d}{2} F \frac{1}{S_B} \tag{4.69}$$

where S_B is the bunch spacing, y_1 is the oscillation amplitude of the first bunch, and we have assumed that, in the absence of ions, the amplitudes of different bunches are uncorrelated. Equation (4.61) then gives an expression for F,

$$F = \frac{2S_B}{c\tau_d} \langle \tilde{y}_1^2 \rangle = \frac{S_B}{2cT_0} \langle y^2 \rangle_{\text{noise}} \tag{4.70}$$

Now, returning to the case with the ions, we will assume that the second term in Eq.(4.64) dominates, and neglect the first term. Using Eq.(4.66), we have

$$\langle \tilde{y}_e^2(s|z) \rangle = F \int_0^z dz' \int_0^\infty ds \, e^{-\frac{2s}{c\tau_d}} \left[\frac{\partial}{\partial z'} I_0 \left(\sqrt{\frac{s(z^2 - z'^2)}{s_0 \ell^2}} \right) \right]^2 \tag{4.71}$$

Note that, being the statistical average, this $\langle \tilde{y}_e^2(s|z) \rangle$ is independent of s. We will therefore drop the s in $\langle \tilde{y}_e^2(s|z) \rangle$ from here on.

Let us now consider the bunches in the asymptotic regime with

$$\bar{\eta} \equiv \frac{z}{\ell} \sqrt{\frac{c\tau_d}{s_0}} \gg 1 \tag{4.72}$$

Using the asymptotic representation $I_0(x) \approx (e^x / \sqrt{2\pi x})$, Eq.(4.71) becomes

$$
\begin{aligned}
\langle \tilde{y}_e^2(z) \rangle &\approx \frac{F}{2\pi} \int_0^z dz' \int_0^\infty ds \frac{e^{-2s/c\tau_d}}{\left(\frac{s}{s_0} \frac{z^2 - z'^2}{\ell^2} \right)^{1/2}} \left(\frac{\partial}{\partial z'} e^{\sqrt{s(z^2 - z'^2)/s_0 \ell^2}} \right)^2 \\
&\approx \frac{F}{2\pi} \int_0^z dz' \int_0^\infty ds \, z'^2 \sqrt{\frac{s}{s_0}} \frac{e^{-2s/c\tau_d + 2\sqrt{s(z^2 - z'^2)/s_0 \ell^2}}}{(z^2 - z'^2)^{3/2}}
\end{aligned}
\tag{4.73}
$$

Introducing new variables $\eta = \sqrt{s(z^2 - z'^2)/s_0 \ell^2}$ and $\eta' = (z'/\ell)\sqrt{c\tau_d/s_0}$, we have

$$
\begin{aligned}
\langle \tilde{y}_e^2(z) \rangle &\approx \frac{F(c\tau_d)^{3/2}}{\pi s_0^{1/2} \ell} \int_0^{\bar{\eta}} \eta'^2 \, d\eta' \int_0^\infty \frac{\eta^2 \, d\eta}{(\bar{\eta}^2 - \eta'^2)^3} \exp\left(-2\frac{\eta^2}{\bar{\eta}^2 - \eta'^2} + 2\eta \right) \\
&\approx \frac{F(c\tau_d)^{3/2}}{4\sqrt{2\pi} s_0^{1/2} \ell} \int_0^{\bar{\eta}} d\eta' \frac{\eta'^2}{(\bar{\eta}^2 - \eta'^2)^{1/2}} \exp\left(\frac{\bar{\eta}^2 - \eta'^2}{2} \right) \\
&\approx F \frac{(c\tau_d)^{3/2}}{8 s_0^{1/2} \ell} \frac{e^{\bar{\eta}^2/2}}{\bar{\eta}}
\end{aligned}
\tag{4.74}
$$

Due to the factor $e^{\bar{\eta}^2/2}$, the dependence of $\langle \tilde{y}_e^2(z) \rangle$ on $\bar{\eta}$ for $\bar{\eta} \gg 1$ is very strong.
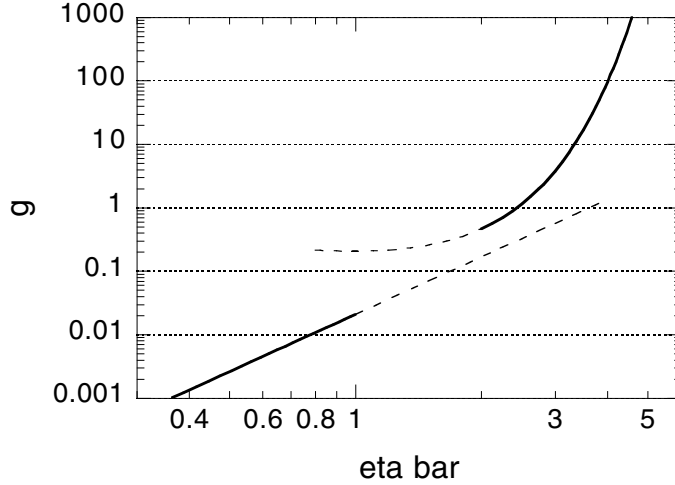
Figure 4.8: Normalized asymptotic mean square amplitude g as a function of $\bar{\eta}$.

We next consider the limit opposite to Eq.(4.72), i.e., when $\bar{\eta} \ll 1$. Using Eq.(4.71), we obtain

$$\langle \tilde{y}_e^2(z) \rangle \approx F \frac{z^3 c^3 \tau_d^3}{48 s_0^2 \ell^4} = F \frac{(c\tau_d)^{3/2}}{48 s_0^{1/2} \ell} \bar{\eta}^3 \qquad (\bar{\eta} \ll 1) \qquad (4.75)$$

Equations (4.74) and (4.75) are our main results. One may relate the average square results Eqs.(4.74) and (4.75) to the average square of the first bunch by using Eq.(4.70).

Figure 4.8 shows the behavior of the normalized mean square amplitude

$$g \equiv \frac{\langle \tilde{y}_e^2(z) \rangle s_0^{1/2} \ell}{F(c\tau_d)^{3/2}} = \frac{\langle \tilde{y}_e^2(z) \rangle}{\langle \tilde{y}_1^2 \rangle} \frac{\ell}{2 S_B} \sqrt{\frac{s_0}{c\tau_d}} \qquad (4.76)$$

versus $\bar{\eta}$. The two curves correspond to the $\bar{\eta} \gg 1$ and $\bar{\eta} \ll 1$ behaviors according to Eqs.(4.74) and (4.75) respectively. The solid portions of the curves represent their respective region of applicability.

In order to avoid an enhancement of beam emittance due to fast ion instability, one should avoid the exponential regime when $\bar{\eta} \gg 1$. If one adopts that as the operating condition, then one is led to require

$$1 < \sqrt{\frac{s_0}{c\tau_d}} \qquad (4.77)$$

or equivalently

$$\tau_{\text{instability}} > \tau_d \qquad (4.78)$$

where $\tau_{\text{instability}} = s_0/c$. Indeed, when Eq.(4.77) [or (4.78)] is satisfied, it follows that the last bunch in the bunch train (with $z = \ell$) has

$$\frac{\langle \tilde{y}_e^2(\ell) \rangle}{\langle y_1^2 \rangle} \approx \frac{\ell}{24 S_B} \left(\frac{c\tau_d}{s_0} \right)^2 \ll 1 \qquad (4.79)$$

90

and the effective emittance growth is negligible. On the other hand, due to the extremely rapid dependence of $\langle \tilde{y}_e(z) \rangle$ on z when $\bar{\eta} \gg 1$, the tolerable value of $\bar{\eta}$ is not far from $\bar{\eta} = 1$.

References

[1] T. Raubenheimer, F. Zimmermann, Phy. Rev. E52, 5487 (1995).

[2] G. Stupakov, T. Raubenheimer, F. Zimmermann, Phys. Rev. E52, 5499 (1995).

[3] J. Byrd et al., Phys. Rev. Lett. 79, 79 (1997).

[4] G. Stupakov, A. Chao, KEK Workshop 1997.

5 Lawson-Woodward Theorem and Laser Acceleration

Consider the plane laser wave propagating in the $\hat{z}$ direction in free space, with

$$
\begin{aligned}
\vec{E} &= E_0 \cos\left(\omega t - \frac{\omega}{c}z + \phi\right)\hat{x} \\
\vec{B} &= E_0 \cos\left(\omega t - \frac{\omega}{c}z + \phi\right)\hat{y}
\end{aligned}
\tag{5.1}
$$

The average laser power per unit cross-sectional area is

$$
\frac{\langle \mathcal{P} \rangle}{A} = \frac{c}{8\pi}E_0^2
\tag{5.2}
$$

Take a 10 TW laser[18] and focus to a spot size of $A = 10\mu\text{m}^2$, the electric field at the focal point is $E_0 = 2.7 \times 10^4$ GV/m. The question is how to harness this huge electric field for the purpose of accelerating particles.

5.1 Lawson-Woodward Theorem

Unfortunately, this huge electric field is basically useless for particle acceleration to high energies. The reason is summarized by the Lawson-Woodward theorem. To illustrate this theorem, one first note that at high energies, the trajectory of a particle, even when perturbed by the laser fields, is a straight line to a good approximation.

Consider a particle whose velocity $\vec{v} = \beta c \hat{v}$ is in the $\hat{v} = \hat{z}$ direction. This particle sees the huge electric field E_0. However this field is useless because it is transverse and does not accelerate the particle.

We then consider making an angle θ between $\vec{v}$ and $\hat{z}$, as shown in Fig.5.1. Now the electric field has a longitudinal component

$$
\frac{d\mathcal{E}}{ds} = e\vec{E}(t)\cdot\hat{v} = eE_0\sin\theta\cos[\omega t(1-\beta\cos\theta)+\phi]
\tag{5.3}
$$

The particle is alternately accelerated and decelerated at a frequency of $\omega(1 - \beta\cos\theta)$. With β necessarily < 1, the particle does not have a *net* acceleration.

How do we circumvent this problem? We may consider to slow down the laser, or to wiggle the particle trajectory so that it is no longer a straight line, or some other ways. Below, we illustrate various ways of using laser to accelerate. As we shall see, in all cases, in one way or another, we are invariably introducing a large reduction factor to the huge potential laser field. The fact that we can never use the full extent of E_0 is the Lawson-Woodward theorem. In other words, we may state the Lawson-Woodward theorem as[19]

$$
E_{\text{effective}} = E_0 \times (\text{reduction factor}), \quad \text{where (reduction factor)} \ll 1 \tag{5.4}
$$

---

[18] If the laser pulse length is 1 ps, it contains 10 Joules per pulse.

[19] This is just my own version of their otherwise scholarly theorem. The Lawson-Woodward reduction factor is usually rather severe. If someone claims he can accelerate by a gradient of $E_0 = 2.7 \times 10^4$ GeV/m using a laser, don't believe him. If the claim is anything larger than 1% of E_0, be skeptical.
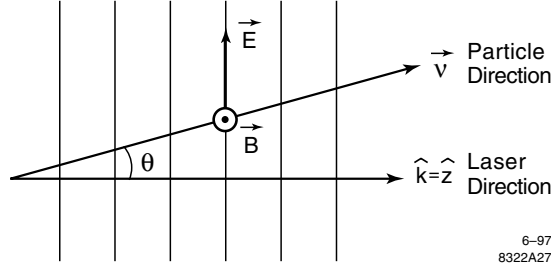
Figure 5.1: A relativistic particle in a plane laser wave.

Exactly which parameters enter the reduction factor depends on the conceived acceleration scheme. Sometimes it is a small crossing angle, sometimes it is the extent of the wiggling of particle trajectory introduced on purpose, and sometimes it is the amount the laser phase velocity slowed down by an index of refraction. Details of these discussions will be the subject of this chapter.

5.2   Slow Down the Laser in a Medium

Operating the acceleration in a medium of index of refraction $n > 1$, the phase velocity of the laser wave slows down, Eq.(5.3) becomes

$$\frac{d\mathcal{E}}{ds} = eE_0 \sin\theta \cos[\omega t(1 - n\beta\cos\theta) + \phi] \tag{5.5}$$

Acceleration becomes possible if we choose parameters to fulfill

$$n\beta\cos\theta = 1 \tag{5.6}$$

As $\beta \to 1$, we require

$$\cos\theta = \frac{1}{n} \tag{5.7}$$

and the acceleration rate is (for $\phi = 0$)

$$\frac{d\mathcal{E}}{ds} = eE_0\sqrt{1 - \frac{1}{n^2}} \tag{5.8}$$

> _Exercise_ 1 To take into account of the effect of phase slippage as the particle's velocity is varied during acceleration, show that Eq.(5.8) is modified to become
>
> $$mc^2\frac{d\gamma}{ds} = eE_0\sqrt{1 - \frac{1}{n^2}}\cos\frac{\omega s(1 - \beta)}{c\beta} \approx eE_0\sqrt{1 - \frac{1}{n^2}}\cos\frac{\omega s}{2\gamma^2 c} \tag{5.9}$$
>
> One then solves for $\gamma(s)$.

94

In the medium, one will need to avoid multiple scatterings. This then requires n to be only slightly larger than 1. Let $n = 1 + \Delta$ with $\Delta \ll 1$, then

$$\frac{d\mathcal{E}}{ds} \approx eE_0\sqrt{2\Delta} \tag{5.10}$$

For H_2 at $0°C$ and 1 atm, we have $\Delta = 0.14 \times 10^{-3}$. At 10^{-4} Torr, it follows that $\Delta = 0.14 \times 10^{-3} \times 10^{-4}/760 = 1.8 \times 10^{-11}$. With $E_0 = 2.7 \times 10^4$ GV/m, we find $d\mathcal{E}/ds = 0.16$ GeV/m, which is not bad, but much smaller than the full E_0.

5.3   Near the Surface of a Medium

Can one improve this by having the beam moving in free space, but immediately next to a medium? The hope is that by doing so, multiple scattering is no longer an issue; one can use a much higher value of n, and thus a much higher acceleration gradient.

Consider the setup shown in Fig.5.2. An incident laser in a medium with index of refraction n and making an angle θ relative to the medium boundary surface has[20]

$$\begin{aligned}
\vec{E}_{\text{in}} &= E_0(\hat{x}\cos\theta - \hat{z}\sin\theta)\ e^{-i\omega t + in(\omega/c)(z\cos\theta + x\sin\theta)} \\
\vec{B}_{\text{in}} &= nE_0\hat{y}\ e^{-i\omega t + in(\omega/c)(z\cos\theta + x\sin\theta)}
\end{aligned} \tag{5.11}$$

After total internal reflection, the reflected wave has

$$\begin{aligned}
\vec{E}_{\text{ref}} &= E_1(\hat{x}\cos\theta + \hat{z}\sin\theta)\ e^{-i\omega t + in(\omega/c)(z\cos\theta - x\sin\theta)} \\
\vec{B}_{\text{ref}} &= nE_1\hat{y}\ e^{-i\omega t + in(\omega/c)(z\cos\theta - x\sin\theta)}
\end{aligned} \tag{5.12}$$

where E_1 is yet to be determined. For total internal reflection, we require

$$n\cos\theta > 1 \tag{5.13}$$

In the free space region, there is a transmitted wave

$$\begin{aligned}
\vec{E}_{\text{tr}} &= B_2(\alpha\hat{x} - i\sqrt{\alpha^2 - 1}\hat{z})\ e^{-i\omega t + i(\omega/c)\alpha z - (\omega/c)x\sqrt{\alpha^2-1}} \\
\vec{B}_{\text{tr}} &= B_2\hat{y}\ e^{-i\omega t + i(\omega/c)\alpha z - (\omega/c)x\sqrt{\alpha^2-1}}
\end{aligned} \tag{5.14}$$

where B_2 and α are yet to be determined.

Eq.(5.14) satisfies Maxwell equations in free space. The parameters yet to be determined are to be found by imposing the boundary conditions: tangential continuity of $\vec{E}, \vec{H}$, and normal continuity of $\vec{D}, \vec{B}$. If we assume $\mu = 1$ and

---

[20] A side remark: note the magnetic field acquires a factor n in Eqs.(5.11-5.12). Since usually $n > 1$, the magnetic field is stronger than the electric field in a medium. In fact it often seems as if magnetic fields prefer the inside a material to the vacuum, while electric fields prefer the opposite. The same tendency occurs inside a resistive metal.
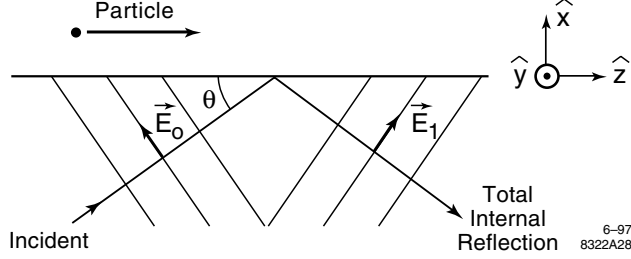
Figure 5.2: Acceleration of a particle using a laser with internal reflection.

$\epsilon = \sqrt{n}$, then $\vec{B} = \vec{H}$ and $\vec{D} = n^2\vec{E}$. To satisfy the boundary conditions at $x = 0$, it is obvious that we must have

$$\alpha = n\cos\theta \tag{5.15}$$

In addition, we have

$$
\begin{aligned}
\text{continuity of } \vec{B} &\implies & B_2 &= n(E_1 + E_0) \\
\text{continuity of } E_z &\implies & -iB_2\sqrt{\alpha^2 - 1} &= (E_1 - E_0)\sin\theta \\
\text{continuity of } n^2 E_x &\implies & B_2\alpha &= n^2(E_1 + E_0)\cos\theta
\end{aligned}
\tag{5.16}
$$

Solution of Eq.(5.16) is

$$
\begin{aligned}
E_1 &= E_0\left(\frac{i\sin\theta + n\sqrt{n^2\cos^2\theta - 1}}{i\sin\theta - n\sqrt{n^2\cos^2\theta - 1}}\right) \\
B_2 &= E_0\left(\frac{2n\sin\theta}{\sin\theta + in\sqrt{n^2\cos^2\theta - 1}}\right)
\end{aligned}
\tag{5.17}
$$

The quantity we are interested in is the electric field in the free space region,

$$
\begin{aligned}
\vec{E}_{\text{tr}} &= E_0\left(\frac{2n\sin\theta}{\sin\theta + in\sqrt{n^2\cos^2\theta - 1}}\right)(\hat{x}n\cos\theta - i\hat{z}\sqrt{n^2\cos^2\theta - 1}) \\
&\quad \times e^{-i\omega t + i(\omega/c)nz\cos\theta}\, e^{-(\omega/c)x\sqrt{n^2\cos^2\theta - 1}}
\end{aligned}
\tag{5.18}
$$

The last factor in (5.18) describes the exponential attenuation in the x-direction. The phase velocity along the z-direction $v_{\text{ph}} = c/(n\cos\theta) < c$ is slowed down so that it can be matched to the velocity of a particle.

Having set up the device, we send a relativistic particle with a fixed distance $x = x_0$ from the surface, and with $z = z_0 + \beta ct$. The energy of this particle changes according to

$$
\begin{aligned}
\frac{d\mathcal{E}}{ds} &= e\vec{E}_{\text{tr}} \cdot \hat{z} = -ieE_0\left(\frac{2n\sin\theta\sqrt{n^2\cos^2\theta - 1}}{\sin\theta + in\sqrt{n^2\cos^2\theta - 1}}\right) \\
&\quad \times e^{-i\omega t + i(\omega/c)n(z_0 + \beta ct)\cos\theta} \times e^{-(\omega/c)x_0\sqrt{n^2\cos^2\theta - 1}}
\end{aligned}
\tag{5.19}
$$

96

In order for this particle to receive energy systematically from the laser acceleration, we must choose the condition (5.6).[21]

Substituting Eq.(5.6) into Eq.(5.19) gives

$$\frac{d\mathcal{E}}{ds} = \left(\frac{-2ieE_0\frac{n}{\beta}}{\gamma + \frac{in^2}{\sqrt{n^2\beta^2 - 1}}} \right) e^{-\omega x_0/\gamma\beta c} e^{i(\omega/c)nz_0\cos\theta} \tag{5.20}$$

When $\beta \rightarrow 1$ or $\gamma = 1/\sqrt{1 - \beta^2} \rightarrow \infty$, we find

$$\frac{d\mathcal{E}}{ds} \rightarrow -2i\frac{eE_0 n}{\gamma} \; e^{-\omega x_0/\gamma c} e^{i(\omega/c)nz_0\cos\theta} \tag{5.21}$$

Only the real part of Eq.(5.21) is to be taken. By keeping the particle close to the surface, we ignore the exponential factor in Eq.(5.21) and we do obtain an accelerating field. Unfortunately, the field is small due to the factor $1/\gamma$.

Both the laser accelerator designs in and near medium suffer from the fact that the electric field seen by the particle is mainly transverse.

> *Exercise* 2 The acceleration efficiency improves somewhat by considering having material on both sides of the particle's path. Two internally reflected lasers then provide the acceleration. Analyze this set-up. Note that by having more material around the particle's path, we are getting closer to the conventional acceleration of rf structures in a linac, except that the rf microwave is replaced by lasers.

5.4 Exact Solution in Plane Wave

So far we have looked at the relativistic case when the particle trajectory is approximated by a straight line. It turns out that it is possible to solve exactly the problem of particle motion in a plane EM field. Let the EM field be given by Eq.(5.1). Let the particle being studied have the initial conditions that at $t = 0$, its coodinates and momenta are given by $x_0, y_0, z_0, p_{x0}, p_{y0}, p_{z0}$. We define

$$\xi = \omega t - \frac{\omega}{c}z + \phi \tag{5.22}$$

The initial value of ξ is $\phi_0 = -(\omega/c)z_0 + \phi$.

The equation of motion is

$$\frac{d\vec{p}}{dt} = eE_0\cos\xi \left(\hat{x} + \frac{1}{mc\gamma}\vec{p} \times \hat{y} \right)$$

$$\Longrightarrow$$

---

[21]It is interesting that the requirements for both designs have the same expression even though the meaning of the symbols are unrelated.

$$\frac{dp_x}{dt} = eE_0(1 - \frac{p_z}{mc\gamma})\cos\xi \qquad (5.23)$$

$$\frac{dp_y}{dt} = 0 \qquad (5.24)$$

$$\frac{dp_z}{dt} = eE_0\frac{p_x}{mc\gamma}\cos\xi \qquad (5.25)$$

We also have

$$\frac{d\gamma}{dt} = \frac{e}{mc}\vec{\beta}\cdot\vec{E} = \frac{eE_0}{m^2c^2\gamma}p_x\cos\xi \qquad (5.26)$$

A constant of the motion follows from Eq.(5.24),

$$p_y = p_{y0} \qquad (5.27)$$

Another constant of the motion follows from Eqs.(5.25) and (5.26),

$$\gamma - \frac{p_z}{mc} \equiv \Gamma = \gamma_0 - \frac{p_{z0}}{mc}, \qquad \gamma_0 = \sqrt{(\frac{\vec{p_0}}{mc})^2 + 1} \qquad (5.28)$$

The constancy of Γ means that the particle gains and loses γ and p_z in a fully correlated manner. The gain/loss of γ is due to $p_x E_x$, while the gain/loss of p_z is due to $p_x B_y$. The full correlation results because E_x and B_y are in phase in a laser.

We next need the expression

$$\frac{d\xi}{dt} = \omega - \frac{\omega}{c}\frac{dz}{dt} = \omega(1 - \frac{p_z}{mc\gamma}) = \omega\frac{\Gamma}{\gamma} \qquad (5.29)$$

Eq.(5.23) then gives

$$\frac{dp_x}{dt} = eE_0\frac{\Gamma}{\gamma}\cos\xi = \frac{eE_0}{\omega}\cos\xi\frac{d\xi}{dt}$$

$$\implies \quad p_x = p_{x0} + \frac{eE_0}{\omega}(\sin\xi - \sin\phi_0) \qquad (5.30)$$

Our strategy is to use Eq.(5.29) to solve all quantities in terms of ξ. After that, we will find an expression of ξ in terms of time t.

Having obtained p_x, we use Eq.(5.26) to obtain γ,

$$\frac{d\gamma}{d\xi} = \frac{eE_0}{m^2c^2\omega\Gamma}\cos\xi\,\left(p_{x0} - \frac{eE_0}{\omega}\sin\phi_0 + \frac{eE_0}{\omega}\sin\xi\right)$$

$$\implies \quad \gamma = \gamma_0 + \frac{eE_0}{m^2c^2\omega\Gamma}p_{x0}(\sin\xi - \sin\phi_0) + \frac{e^2E_0^2}{2m^2c^2\omega^2\Gamma}(\sin\xi - \sin\phi_0)^2 \quad (5.31)$$

The second term on the RHS of (5.31) is what we calculated before, namely the alternating energy gains and losses of the particle in the laser plane wave. The third quadratic term is called the *ponderomotive potential*. It gives rise to an effective force on the particle which is quadratic in E_0. When rapidly oscillating

98

forces are averaged out, this ponderomotive force becomes important. The origin of this term is due to the wobbling (non-straight-line) trajectory of the particle. The laser field has to first bend the particle trajectory, yielding one power of E_0, and secondly accelerate the particle, giving rise to another power of E_0.

Having obtained γ, we obtain p_z by Eq.(5.28). We thus have obtained p_x, p_y, p_z, γ in Eqs.(5.30), (5.27), and (5.31). Next we want to find x, y, z as functions of ξ. This is done as follows:

$$\frac{dx}{dt} = \frac{p_x}{m\gamma} \implies \frac{dx}{d\xi} = \frac{p_x}{m\omega\Gamma}$$

$$\implies x = x_0 + \frac{1}{m\omega\Gamma}\left[(p_{x0} - \frac{eE_0}{\omega}\sin\phi_0)(\xi - \phi_0) - \frac{eE_0}{\omega}(\cos\xi - \cos\phi_0)\right] \quad (5.32)$$

$$\frac{dy}{dt} = \frac{p_{y0}}{m\gamma} \implies \frac{dy}{d\xi} = \frac{p_{y0}}{m\omega\Gamma}$$

$$\implies y = y_0 + \frac{p_{y0}}{m\omega\Gamma}(\xi - \phi_0) \quad (5.33)$$

$$\frac{dz}{dt} = \frac{p_z}{m\gamma} = \frac{c}{\gamma}(\gamma - \Gamma) \implies \frac{dz}{d\xi} = \frac{c}{\omega\Gamma}(\gamma - \Gamma)$$

$$\implies z = z_0 + \frac{c}{\omega\Gamma}\int_{\phi_0}^{\xi} d\xi'(\gamma(\xi') - \Gamma)$$

$$= z_0 + \frac{c}{\omega\Gamma}\left\{\frac{p_{z0}}{mc}(\xi - \phi_0) - \frac{eE_0 p_{x0}}{m^2 c^2 \omega\Gamma}[\cos\xi - \cos\phi_0 + (\xi - \phi_0)\sin\phi_0]\right.$$

$$\left. + \frac{e^2 E_0^2}{2m^2 c^2 \omega^2 \Gamma}\left[(\frac{1}{2} + \sin^2\phi_0)(\xi - \phi_0) - \frac{1}{4}\sin 2\xi + 2\sin\phi_0\cos\xi - \frac{3}{4}\sin 2\phi_0\right]\right\}$$

$$(5.34)$$

We still have to relate ξ to t. This is done using Eq.(5.29), which gives

$$\omega\Gamma t = \int_{\phi_0}^{\xi} d\xi'\gamma(\xi')$$

$$= \gamma_0(\xi - \phi_0) + \frac{eE_0 p_{x0}}{m^2 c^2 \omega\Gamma}[-\cos\xi + \cos\phi_0 - (\xi - \phi_0)\sin\phi_0] \quad (5.35)$$

$$+ \frac{e^2 E_0^2}{2m^2 c^2 \omega^2 \Gamma}\left[(\frac{1}{2} + \sin^2\phi_0)(\xi - \phi_0) - \frac{1}{4}\sin 2\xi + 2\sin\phi_0\cos\xi - \frac{3}{4}\sin 2\phi_0\right]$$

Exercise 3 It may be instructive to fill in the details of the derivation from Eq.(5.23) to (5.35). To build some confidence in these results, at least show that the solution satisfies $\gamma^2 = 1 + (\vec{p}/mc)^2$.

Particle at rest

Consider a particle which at $t = 0$ has $x_0 = y_0 = z_0 = 0$, $p_{x0} = p_{y0} = p_{z0} = 0$, $\gamma_0 = \Gamma = 1$ and $\phi_0 = 0$. It has

$$x = \frac{eE_0}{m\omega^2}(1 - \cos\xi)$$

99

$$y = 0$$

$$z = \frac{e^2 E_0^2}{4m^2 c\omega^3}\left(\xi - \frac{1}{2}\sin 2\xi\right)$$

$$\gamma = 1 + \frac{e^2 E_0^2}{2m^2 c^2 \omega^2}\sin^2 \xi$$

$$t = \frac{\xi}{\omega} + \frac{z}{c}$$

$$= \frac{\xi}{\omega} + \frac{e^2 E_0^2}{4m^2 c^2 \omega^3}\left(\xi - \frac{1}{2}\sin 2\xi\right) \tag{5.36}$$

We note that the leading order of x-motion is linear in E_0 while z-motion is quadratic, as one would expect. The particle energy is indeed accelerated in an oscillatory manner with energy gain proportional to E_0^2. Figure 5.3 shows (a) the trajectory x versus z as the particle moves in the physical space; (b) γ as a function of z; and (c) $t - z/c$ as a function of z. In Fig.5.3, we have shown results for various values of $\lambda = eE_0/m\omega c$. If caught at the right moments, the particle has a maximum energy of $\gamma_{\max} = 1 + \lambda^2/2$. The particle on the average moves with the wave. If we take $E_0 = 2.7\times 10^4$ GV/m and a laser wavelength of $1~\mu$m, one can have a pretty large value of $\lambda = 8$, yielding $\gamma_{\max} = 33$. However, acceleration at this level is no comparison with the raw laser field of 2.7×10^4 GV/m.

Exercise 4 Show that the particle has an average speed in the z-direction given by $\langle v_z\rangle/c = \lambda^2/(4 + \lambda^2)$. This average motion is relativistic if $\lambda \gg 1$.

Exercise 5 Repeat for a stationary particle seeing a different laser phase $\phi_0 = \pi/2$.

Relativistic Particle

We may consider a particle with initial conditions $x_0 = y_0 = z_0 = 0$, $\phi_0 = 0$, $p_{y0} = 0$, $p_{x0} = p_0 \sin\theta$, $p_{z0} = p_0 \cos\theta$, and with $\gamma_0 \gg 1$ and $p_0 \gg eE_0/\omega$. We then find

$$\Gamma \approx \gamma_0\left(1 - \cos\theta + \frac{1}{2\gamma_0^2}\right)$$

$$p_x \approx p_0 \sin\theta + \frac{eE_0}{\omega}\sin\xi$$

$$p_z \approx p_0 \cos\theta + \frac{eE_0}{\omega}\frac{\sin\theta}{1 - \cos\theta + \frac{1}{2\gamma_0^2}}\sin\xi$$

$$\gamma \approx \frac{p_0}{mc} + \frac{eE_0}{mc\omega}\frac{\sin\theta}{1 - \cos\theta + \frac{1}{2\gamma_0^2}}\sin\xi$$

$$\xi \approx \omega t(1 - \cos\theta) \tag{5.37}$$

The maximum energy gain is obtained by choosing $\theta \approx 1/\gamma_0$, with $\Delta\gamma \approx \gamma_0(1 + \frac{eE_0}{mc\omega}\sin\xi)$, which is $\ll \gamma_0$. These expressions are consistent with what we did
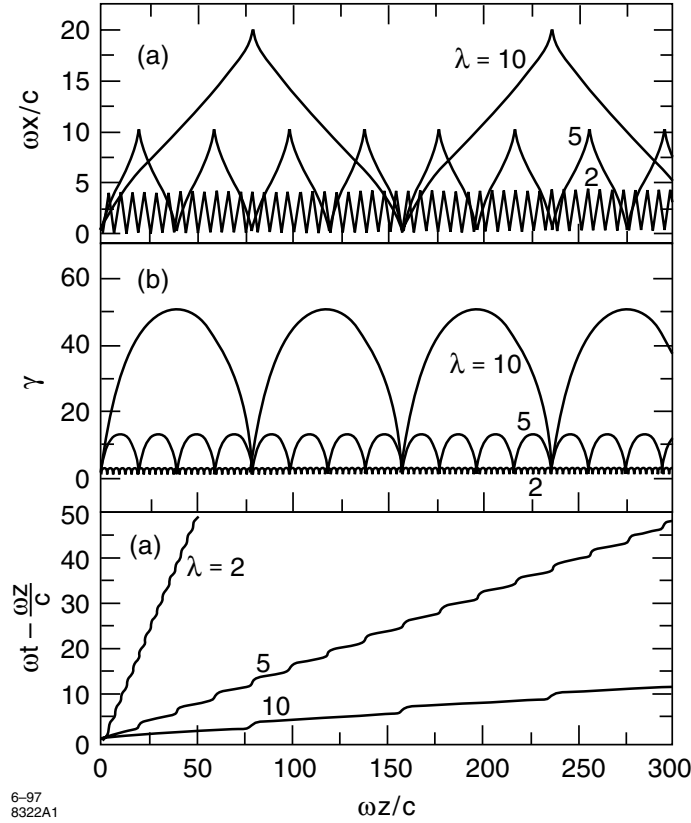
Figure 5.3: Motion of a particle in a plane wave laser. The particle is stationary initially.

before. In particular, if we integrate Eq.(5.3), we obtain the γ expression in (5.37). There is no net energy gain to first order in E_0.

> *Exercise* 6 Find the ponderomotive E_0^2 corrections to Eq.(5.37).

5.5 Auto-resonance Acceleration

We now do a neat trick by adding a static magnetic field to the laser plane wave,

$$
\begin{aligned}
\vec{E} &= E_0 \hat{x} \cos \xi \\
\vec{B} &= E_0 \hat{y} \cos \xi + B_s \hat{z}
\end{aligned}
\tag{5.38}
$$

with ξ given by Eq.(5.22).

Equations (5.25) and (5.26) still apply. It follows that $\gamma - \frac{p_z}{mc} = \Gamma$ is still a constant of the motion, and Eq.(5.29) still holds.

One consequence of $\gamma - \frac{p_z}{mc} = \gamma(1 - \frac{v_z}{c})$ being a constant of the motion is that, if through some mechanism the energy of the particle is increased $\gamma \to \infty$,

101

it follows that $v_z \to c$, i.e. the particle motion is necessarily primarily in the z-direction. This observation would be useful for our discussion later.

There is another much more intriguing observation to be made as follows.[22] As the laser plane wave passes by the moving particle, its frequency seen by the particle (in the laboratory frame) is $\omega(1 - \frac{v_z}{c})$. The fact that this frequency is nonzero – as pointed out before – is the reason why the particle sees alternating acceleration and deceleration. But now we have also a static magnetic field B_s. In the presence of B_s, the particle executes an additional cyclotron motion with cyclotron frequency $eB_s/m\gamma c$. If these two frequencies are made to coincide, one expects some resonance effect to occur in the particle motion. Exactly what will occur is yet to be analyzed, but one sees already now that once the resonance condition is fulfilled at time $t = 0$, it will be fulfilled at all times $t \neq 0$. This is because the resonance condition reads

$$\omega(1 - \frac{v_z}{c}) = \frac{eB_s}{m\gamma c} \quad \Longrightarrow \quad \gamma - \frac{p_z}{mc} = \frac{eB_s}{mc\omega} \tag{5.39}$$

The LHS of Eq.(5.39) is exactly the constant of the motion Γ! Once the resonance is fulfilled at $t = 0$ (e.g. by choosing the right B_s), the resonance is automatic at all other times, thus the term "auto-resonance".

> *Exercise 7* If the plane wave laser is in a medium with index of refraction n, and a static magnetic field $B_s\hat{z}$ is applied. (a) How is the constant of the motion Γ modified? (b) What is the condition for the cyclotron motion to resonate with the laser field? (c) Is the resonance still an auto-resonance?
> *Solution* (a) $\Gamma = \gamma(1 - \frac{v_z}{nc})$. (b) $\gamma(1 - \frac{nv_z}{c}) = \frac{eB_s}{mc\omega}$.

> *Exercise 8* It is instructive to ray trace a particle under (5.38) and observe what the resonance does to the particle's motion.

> *Exercise 9* What if the laser is circularly polarized? Does it make a difference if the laser is right-hand or left-hand polarized?

We now solve the equation of motion. The analysis follows closely the previous section. In particular, we will first try to use ξ as the independent variable. Equations (5.23) and (5.24) now read, using Eq.(5.29),

$$\frac{dp_x}{d\xi} = \frac{eE_0}{\omega}\cos\xi + \frac{eB_s}{mc\omega\Gamma}p_y \tag{5.40}$$

$$\frac{dp_y}{d\xi} = -\frac{eB_s}{mc\omega\Gamma}p_x \tag{5.41}$$

which can be combined into one single complex equation,

$$\frac{dq_\perp}{d\xi} = \frac{eE_0}{\omega}e^{i\alpha\xi}\cos\xi \tag{5.42}$$

<hr>

[22]This phenomenon is well known in plasma physics and is known as cyclotron heating.

where we have defined

$$q_\perp = (p_x + ip_y)e^{i\alpha\xi}, \quad \text{and} \quad \alpha = \frac{eB_s}{mc\omega\Gamma} \tag{5.43}$$

The meaning of $q_\perp$ is that we are observing the motion in a frame rotating with the cyclotron frequency. Note that both the real and imaginary parts of $q_\perp$ have physical meanings. The auto-resonance condition (5.39) occurs when $\alpha = 1$.

The solution to Eq.(5.42) is

$$q_\perp(\xi) = \frac{eE_0}{\omega(1-\alpha^2)}(\sin\xi + i\alpha\cos\xi)e^{i\alpha\xi} + C \tag{5.44}$$

with C some constant to be determined by the initial condition that at time $t = 0$, the particle has $x_0, y_0, z_0, p_{x0}, p_{y0}, p_{z0}$, and $\xi(0) = -(\omega/c)z_0 + \phi = \phi_0$. This gives

$$C = \left[p_{x0} + ip_{y0} - \frac{eE_0}{\omega(1-\alpha^2)}(\sin\phi_0 + i\alpha\cos\phi_0)\right]e^{i\alpha\phi_0} \tag{5.45}$$

It then follows, by substituting (5.45) into (5.44) and separating out the real and the imaginary parts, that

$$\begin{aligned}
p_x &= p_{x0}\cos(\alpha\xi - \alpha\phi_0) + p_{y0}\sin(\alpha\xi - \alpha\phi_0) \tag{5.46}\\
&\quad + \frac{eE_0}{\omega(1-\alpha^2)}[\sin\xi - \sin\phi_0\cos(\alpha\xi - \alpha\phi_0) - \alpha\cos\phi_0\sin(\alpha\xi - \alpha\phi_0)]\\
p_y &= p_{y0}\cos(\alpha\xi - \alpha\phi_0) - p_{x0}\sin(\alpha\xi - \alpha\phi_0) \tag{5.47}\\
&\quad + \frac{eE_0}{\omega(1-\alpha^2)}[\alpha\cos\xi + \sin\phi_0\sin(\alpha\xi - \alpha\phi_0) - \alpha\cos\phi_0\cos(\alpha\xi - \alpha\phi_0)]
\end{aligned}$$

Having obtained p_x and p_y, we obtain p_z and γ by

$$p_z = \frac{mc}{2\Gamma}\left(1 - \Gamma^2 + \frac{p_x^2 + p_y^2}{m^2c^2}\right) \tag{5.48}$$

$$\gamma = \frac{1}{2\Gamma}\left(1 + \Gamma^2 + \frac{p_x^2 + p_y^2}{m^2c^2}\right) \tag{5.49}$$

which can also be written as

$$\gamma - \gamma_0 = \frac{1}{mc}(p_z - p_{z0}) = \frac{p_x^2 + p_y^2 - p_{x0}^2 - p_{y0}^2}{2\Gamma m^2c^2} \tag{5.50}$$

Substituting (5.46-5.47) into (5.50), we obtain

$$2\Gamma m^2c^2(\gamma - \gamma_0) = 2\Gamma mc(p_z - p_{z0}) = p_x^2 + p_y^2 - p_{x0}^2 - p_{y0}^2$$

$$= \frac{2eE_0}{\omega(\alpha^2-1)}\bigg[\alpha p_{y0}\cos\phi_0 - \alpha p_{y0}\cos\xi\cos(\alpha\xi - \alpha\phi_0) + \alpha p_{x0}\cos\xi\sin(\alpha\xi - \alpha\phi_0)$$

$$-p_{y0} \sin \xi \sin(\alpha\xi - \alpha\phi_0) - p_{x0} \sin \xi \cos(\alpha\xi - \alpha\phi_0) + p_{x0} \sin \phi_0 \bigg]$$

$$+ \left(\frac{eE_0}{\omega(\alpha^2-1)} \right)^2 \bigg[\alpha^2 \Big(\cos^2 \xi + \cos^2 \phi_0 - 2 \cos \phi_0 \cos \xi \cos(\alpha\xi - \alpha\phi_0) \Big)$$

$$-2\alpha \sin(\xi - \phi_0) \sin(\alpha\xi - \alpha\phi_0)$$

$$+ \sin^2 \phi_0 + \sin^2 \xi - 2 \sin \phi_0 \sin \xi \cos(\alpha\xi - \alpha\phi_0) \bigg] \tag{5.51}$$

Exercise 10 Prove Eqs.(5.48-5.50).
Solution Use the definition of Γ and the property $|\vec{p}|^2 = (\gamma^2 - 1)m^2c^2$.

We still need to find ξ in terms of t. This is obtained by

$$\omega\Gamma t = \int_{\phi_0}^{\xi} d\xi' \gamma(\xi') \tag{5.52}$$

with γ given by Eq.(5.51). The resulting expression is lengthy and is omitted here.

<u>Case 1</u> A trivial case is when $E_0 = 0$. The particle moves in a pure solenoidal field. We find

$$
\begin{aligned}
p_x &= p_{x0} \cos(\alpha\xi - \alpha\phi_0) + p_{y0} \sin(\alpha\xi - \alpha\phi_0) \\
p_y &= p_{y0} \cos(\alpha\xi - \alpha\phi_0) - p_{x0} \sin(\alpha\xi - \alpha\phi_0) \\
\gamma &= \gamma_0 \\
p_z &= p_{z0} \\
\xi &= \phi_0 + \omega t(1 - \frac{v_{z0}}{c})
\end{aligned} \tag{5.53}
$$

<u>Case 2</u> Another special case is when $B_s = 0$. The particle moves in a pure plane laser wave, and indeed we recover what we did in the previous section.

<u>Case 3</u> A particle starting at rest and with $\phi_0 = 0$ has

$$
\begin{aligned}
p_x &= \frac{eE_0}{\omega(1 - \alpha^2)} [\sin \xi - \alpha \sin(\alpha\xi)] \\
p_y &= \frac{eE_0\alpha}{\omega(1 - \alpha^2)} [\cos \xi - \cos(\alpha\xi)] \\
\gamma - 1 &= \frac{p_z}{mc} = \frac{1}{2\Gamma} \left(\frac{eE_0}{\omega mc(1 - \alpha^2)} \right)^2 \big[\sin^2 \xi - 2\alpha \sin \xi \sin(\alpha\xi) \\
&\qquad + \alpha^2(2 - 2\cos \xi \cos(\alpha\xi) - \sin^2 \xi) \big]
\end{aligned} \tag{5.54}
$$

So far the results look similar to the case studied before when $B_s = 0$. For example, the particle energy given by Eq.(5.51) contains a term linear in

E_0 which oscillates in time, and a term quadratic in E_0 which has some non-zero average value representing the ponderomotive potential. However, an alert reader would note that this is not the case when the auto-resonance condition $\alpha = 1$ is fulfilled. Setting $\alpha = 1$ in the above expressions yields[23]

$$
\begin{aligned}
p_x &= p_{x0}\cos(\xi - \phi_0) + p_{y0}\sin(\xi - \phi_0) \\
&\quad + \frac{eE_0}{2\omega}\left[(\xi - \phi_0)\cos\xi + \frac{1}{2}\sin(\xi - 2\phi_0) + \frac{1}{2}\sin\xi\right] \\
p_y &= p_{y0}\cos(\xi - \phi_0) - p_{x0}\sin(\xi - \phi_0) \\
&\quad - \frac{eE_0}{2\omega}\left[(\xi - \phi_0)\sin\xi - \frac{1}{2}\cos(\xi - 2\phi_0) + \frac{1}{2}\cos\xi\right] \\
\gamma &= \gamma_0 + \frac{eE_0}{2\omega\Gamma m^2 c^2}\Big[(\xi - \phi_0)(p_{x0}\cos\phi_0 - p_{y0}\sin\phi_0) \\
&\quad + \frac{1}{2}(p_{y0}\cos\phi_0 - p_{x0}\sin\phi_0) - \frac{1}{2}(p_{y0}\cos(2\xi - \phi_0) - p_{x0}\sin(2\xi - \phi_0))\Big] \\
&\quad + \frac{1}{2\Gamma}\left(\frac{eE_0}{2\omega mc}\right)^2\left[\frac{1}{2} + (\xi - \phi_0)^2 - \frac{1}{2}\cos(2\xi - 2\phi_0) + (\xi - \phi_0)(\sin 2\xi - \sin 2\phi_0)\right] \\
\omega t &= \frac{\gamma_0}{\Gamma}(\xi - \phi_0) + \frac{eE_0}{48\omega\Gamma^2 m^2 c^2}\Big\{12(\xi - \phi_0)^2(p_{x0}\cos\phi_0 - p_{y0}\sin\phi_0) \\
&\quad + 12(\xi - \phi_0)(p_{y0}\cos\phi_0 - p_{x0}\sin\phi_0) \\
&\quad + 6\big[p_{x0}\cos\phi_0 + p_{y0}\sin\phi_0 - p_{x0}\cos(2\xi - \phi_0) - p_{y0}\sin(2\xi - \phi_0)\big] \\
&\quad + \frac{eE_0}{\omega}(\xi - \phi_0)\big[3 + 2(\xi - \phi_0)^2\big] \\
&\quad - \frac{3eE_0}{\omega}\big[(\xi - \phi_0)^2\sin 2\phi_0 + (\xi - \phi_0)\cos 2\xi + 2\sin\xi\sin\phi_0\sin(\xi - \phi_0)\big]\Big\}
\end{aligned}
$$
(5.55)

We now see terms linear in ξ indicating a resonant response.[24] To be more specific, and to simplify the discussion, we consider a particle which is at rest at $t = 0$ with $\phi_0 = 0$. In this case, Eq.(5.55) becomes

$$
\begin{aligned}
p_x &= \frac{eE_0}{2\omega}(\xi\cos\xi + \sin\xi) \\
p_y &= -\frac{eE_0}{2\omega}\xi\sin\xi \\
\gamma &= 1 + \frac{1}{2}\left(\frac{eE_0}{2\omega mc}\right)^2(\xi^2 + \sin^2\xi + \xi\sin 2\xi) \\
\omega t &= \xi + \frac{\xi}{6}\left(\frac{eE_0}{2\omega mc}\right)^2(\xi^2 - 3\sin^2\xi)
\end{aligned}
$$
(5.56)

---

[23]The apparent divergences with $(1 - \alpha^2)$ in the denominators are not real divergences.

[24]Resonance shows up as a term $\propto \xi$, not $\propto t$. A moment's reflection says this is the right indication of a resonance, recalling that ξ is the oscillation phase seen by a particle.

What is the asymptotic motion of this particle? For $t \to \infty$,[25] we have

$$
\begin{aligned}
\xi &\approx \left(\frac{24\omega t}{\lambda^2}\right)^{1/3} \\
p_x &\approx \frac{eE_0}{2\omega}\xi\cos\xi \\
p_y &\approx -\frac{eE_0}{2\omega}\xi\sin\xi \\
\gamma &\approx \frac{1}{8}\lambda^2\xi^2 \approx \frac{1}{8}(24\lambda\omega t)^{2/3}
\end{aligned}
\tag{5.57}
$$

where $\lambda = eE_0/\omega mc$ is that same parameter defined in Fig.5.3. Equation (5.57) says that the particle energy increases with time as $t^{2/3}$. The fact that $\xi \neq$ constant means the particle sees an alternating laser field; however, the resonance is such that these alternating contributions still add up to a net acceleration.

This acceleration does not violate the Lawson-Woodward theorem. The acceleration results from forcing the particle to move away from a straight line motion due to the solenoidal field B_s. One can show using Eq.(5.57) that the Lawson-Woodward reduction factor is given by

$$
\frac{E_{\text{effective}}}{E_0} = (3\lambda\omega t)^{-1/3}
\tag{5.58}
$$

A similar mechanism is used in an inverse free-electron-laser acceleration, except that here we have one extra feature of auto-resonance.

The transverse cyclotron radius of the particle is

$$
\rho = \frac{p_\perp}{eB_s} \approx \frac{mc^2}{2eB_s}(24\lambda\omega t)^{1/3}
\tag{5.59}
$$

As mentioned before, the existence of Γ as a constant of the motion implies the direction of motion is primarily in the z-direction. Indeed, $p_z = mc(\gamma - 1)$ goes like $t^{2/3}$, while $p_\perp$ goes like $t^{1/3}$ according to Eq.(5.59).

> _Exercise_ 11 Estimate the "transverse emittance" of the auto-resonace accelerated beam. Show that it is independent of time t. It is also independent of the laser parameters.
> _Solution_ Transverse emittance $\sim \rho p_\perp/p_z$.

> _Exercise_ 12 Repeat Eqs.(5.56-5.58) for $\phi_0 = \pi/2$. Is the initial phasing of the laser of importance?
> _Solution_
>
> $$
> \begin{aligned}
> p_x &= \frac{eE_0}{2\omega}(\xi - \frac{\pi}{2})\cos\xi \\
> p_y &= -\frac{eE_0}{2\omega}[\cos\xi + (\xi - \frac{\pi}{2})\sin\xi]
> \end{aligned}
> $$

---

[25]More quantitatively, we need $\xi \gg 1$, or $\omega t \gg \lambda^2/24$.

$$\gamma = 1 + \frac{1}{2}\left(\frac{eE_0}{2\omega mc}\right)^2\left[(\xi - \frac{\pi}{2})^2 + \cos^2\xi + (\xi - \frac{\pi}{2})\sin 2\xi\right]$$

$$\omega t = \xi - \frac{\pi}{2} + \frac{1}{6}(\xi - \frac{\pi}{2})\left(\frac{eE_0}{2\omega mc}\right)^2[3\sin^2\xi + (\xi - \frac{\pi}{2})^2] \quad (5.60)$$

Eq.(5.57) still holds asymptotically.

Exercise 13 Work out the counterpart of Eq.(5.37) for a relativistic particle with initial condition $p_{x0} = p_0\sin\theta, p_{y0} = 0, p_{z0} = p_0\cos\theta$ and $p_0 \gg eE_0/\omega$. Is a spread of initial momentum important?

Exercise 14 Instead of working out special cases one by one, it maybe useful to have a numerical or analytical code which contains Eqs.(5.46), (5.47) and (5.50). One can then study the special cases, the dependences on initial conditions, or if the auto-resonance condition is not exactly satisfied.

Exercise 15 Try to design an auto-resonance laser accelerator. Pay attention to the following considerations: (a) To have a large E_0, we need to focus the laser to a small spot w_0, but w_0 should not be chosen too small. A small w_0 means the laser has a short Rayleigh length (see Eq.(5.69))

$$Z_R = \frac{\omega w_0^2}{2c} = \frac{\pi w_0^2}{\lambda_0} \quad (5.61)$$

where λ_0 is the laser wavelength, thus a short length to interact with the particle, (b) Making B_s large helps. (c) Fulfill the resonance condition $\alpha = 1$. (d) Operate in the asymptotic regime (5.57). (e) The cyclotron radius must stay inside the laser throughout acceleration.

5.6 Focussed laser

So far we have dealt with plane wave laser. One may also consider acceleration with a focussed laser. In free space, the wave equation for the laser is

$$\nabla^2(\vec{E}, \vec{B}) + k^2(\vec{E}, \vec{B}) = \vec{0} \quad (5.62)$$

where $k = \omega/c$. All field components are assumed to behave as $e^{-i\omega t}$.

Let u be any component of $\vec{E}$ or $\vec{B}$. Let

$$u = \psi(x, y, z)e^{ikz} \quad (5.63)$$

where ψ is a slowly varying function in z. Substituting into the wave equation (5.62), and dropping second derivative on z, we obtain

$$\frac{\partial^2\psi}{\partial x^2} + \frac{\partial^2\psi}{\partial y^2} + 2ik\frac{\partial\psi}{\partial z} \approx 0 \quad (5.64)$$

This is called the *paraxial ray approximation*.[26]

Equation (5.64) has the solution

$$
\begin{aligned}
\psi_{mn}(x,y,z) &= H_m\left(\sqrt{2}\frac{x}{w(z)}\right) H_n\left(\sqrt{2}\frac{y}{w(z)}\right) \frac{w_0}{w(z)} \\
&\times \quad \exp\left[-i(m+n+1)\tan^{-1}\frac{2z}{kw_0^2}\right] \\
&\times \quad \exp\left[\frac{ik}{2R(z)}(x^2+y^2) - \frac{x^2+y^2}{w^2(z)}\right]
\end{aligned}
\tag{5.65}
$$

where m and n are mode numbers of the solution, $H_{m,n}(x)$ are the Hermite polynomials, and

$$
\begin{aligned}
R(z) &= z\left[1+\left(\frac{kw_0^2}{2z}\right)^2\right] \\
w^2(z) &= w_0^2\left[1+\left(\frac{2z}{kw_0^2}\right)^2\right]
\end{aligned}
\tag{5.66}
$$

Exercise 16 Show by direct back-substitution that Eqs.(5.65-5.66) satisfies Eq.(5.64).

Reminder Hermite polynomials satisfy

$$
H_n''(x) - 2xH_n'(x) + 2nH_n(x) = 0
\tag{5.67}
$$

We will mostly be interested in the fundamental mode $m = n = 0$ and the mode $m = 1, n = 0$. Note that the higher modes are related to the fundamental mode by

$$
\begin{aligned}
\psi_{mn}(x,y,z) &= \psi_{00}(x,y,z) \times H_m\left(\sqrt{2}\frac{x}{w(z)}\right) H_n\left(\sqrt{2}\frac{y}{w(z)}\right) \\
&\times \quad \exp\left[-i(m+n)\tan^{-1}\frac{2z}{kw_0^2}\right]
\end{aligned}
\tag{5.68}
$$

One sees that most of the z-dependence is the same for all modes. The quantity $R(z)$ is the radius of curvature of the laser wavefront at z. If the laser mode is to be established in a resonator consisting of two perfectly reflecting mirrors, then the laser resonator mirror at location z will need to conform to $R(z)$. At the focus $z = 0$, we have $R = \infty$, indicating the wavefront is a plane, and if one chooses to located one of the mirrors there, this mirror will have to be planar. The quantity $w(z)$ is the transverse laser beam size at location z, while w_0 is the waist size of the beam at the focus.

---

[26]If we replace z by t, Eq.(5.64) is almost identical to the 2-D Schrödinger equation.

The Rayleigh length Z_R is the distance from the focal point when the laser beam size is equal to $\sqrt{2}\,w_0$. The diffraction angle θ_d is the subtending angle made by $w(z)$ toward the focal point, as illustrated in Fig.5.4, and

$$Z_R = \frac{kw_0^2}{2}, \qquad \theta_d = \frac{w_0}{Z_R} = \frac{2}{kw_0} \tag{5.69}$$

Note that $2/kw_0$ is also the characteristic angle of the diffraction pattern formed by an opague screen with a round aperture of size $\sim w_0$.
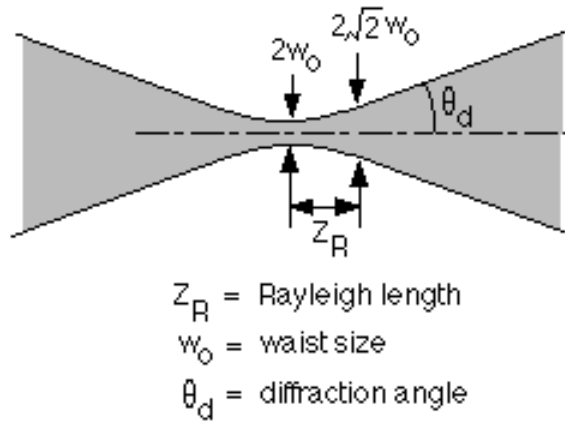
Figure 5.4: Pattern of the envelope of a laser mode.

Validity of the paraxial ray approximation, Eq.(5.64), relies on the assumption that ψ_{mn} does not vary much along z-direction in a distance $1/k = \lambda/2\pi$. An inspection of Eqs.(5.65) and (5.66) indicates that ψ_{mn} varies in a characteristic distance of Z_R. Validity of the paraxial ray approximation therefore requires

$$Z_R \gg \frac{1}{k}, \quad \text{or } R_Z \gg \text{wavelength } \lambda \tag{5.70}$$

which in turn requires

$$kw_0 \gg 1, \quad \text{or } w_0 \gg \text{wavelength } \lambda, \quad \text{or } \theta_d \ll 1 \tag{5.71}$$

For what follows, we will consider a linearly polarized mode with

$$E_x = E_{x0}\,\psi_{mn}\,e^{ikz-i\omega t}, \quad E_y = 0 \tag{5.72}$$

Maxwell equation $\nabla \cdot \vec{E} = 0$ then relates the longitudinal component E_z to the transverse components,

$$E_z \approx \frac{i}{k}\nabla_\perp \cdot \vec{E}_\perp = \frac{i}{k}\frac{\partial E_x}{\partial x} \tag{5.73}$$

109

Once $\vec{E}$ is obtained, $\vec{B}$ can be obtained using $\vec{B} = -\frac{i}{\omega}\nabla \times \vec{E}$. This yields

$$
\begin{aligned}
B_x &= -\frac{i}{\omega}\frac{\partial E_z}{\partial y} \\
B_y &= -\frac{i}{\omega}\left(\frac{\partial E_x}{\partial z} - \frac{\partial E_z}{\partial x}\right) \approx \frac{E_x}{c} + \frac{i}{\omega}\frac{\partial E_z}{\partial x} \\
B_z &= \frac{i}{\omega}\frac{\partial E_x}{\partial y}
\end{aligned}
\tag{5.74}
$$

Exercise 17 Show that $B_z = \frac{i}{k}\nabla_\perp \cdot \vec{B}_\perp$ (a consequence of $\nabla \cdot \vec{B} = 0$) is satisfied by Eq.(5.74).

With ψ_{mn} given by Eq.(5.65), we have, using Eqs.(5.72-5.74),

$$
\begin{bmatrix} E_x \\ E_y \\ E_z \\ cB_x \\ cB_y \\ cB_z \end{bmatrix} = E_{x0}\, e^{ikz-i\omega t}\,\frac{w_0}{w(z)}\,\exp\left[-i(m+n+1)\tan^{-1}\frac{2z}{kw_0^2} + i\frac{kQ}{2}(x^2+y^2)\right]
$$

$$
\times \begin{bmatrix} H_m H_n \\ 0 \\ i\frac{\sqrt{2}}{kw}H_m' H_n - QxH_m H_n \\ \frac{2}{k^2w^2}H_m' H_n' + i\frac{\sqrt{2}Q}{kw}(xH_m H_n' + yH_m' H_n) - xyQ^2 H_m H_n \\ -\frac{2}{k^2w^2}H_m'' H_n - \frac{2\sqrt{2}iQ}{kw}xH_m' H_n + (Q^2x^2 - \frac{iQ}{k} + 1)H_m H_n \\ i\frac{\sqrt{2}}{kw}H_m H_n' - QyH_m H_n \end{bmatrix}
\tag{5.75}
$$

where

$$
Q = \frac{1}{R} + \frac{2i}{kw^2} = \frac{2}{2z - ikw_0^2}
\tag{5.76}
$$

and all the H_m and the H_n functions are taken at $\sqrt{2}x/w(z)$ and $\sqrt{2}y/w(z)$ respectively.

Exercise 18 It maybe instructive to compute the energy flux $\mathcal{P}$ carried by the laser. Form the Poynting vector $S_z = \frac{c}{8\pi}E_x B_y$ on the plane $z = 0$. Integrate $S_z(z=0)$ over x- and y-plane.
Solution Using $kw_0 \gg 1$, one finds

$$
\begin{aligned}
\mathcal{P} &= \frac{c}{8\pi}E_{x0}^2 \int_{-\infty}^{\infty} dx \int_{-\infty}^{\infty} dy\, e^{-2(x^2+y^2)/w_0^2} H_m^2\left(\frac{\sqrt{2}x}{w_0}\right)H_n^2\left(\frac{\sqrt{2}y}{w_0}\right) \\
&= \frac{c}{16}E_{x0}^2 w_0^2 \begin{cases} 1, & \text{fundamental mode} \\ 2, & m=1, n=0 \text{ mode} \end{cases}
\end{aligned}
\tag{5.77}
$$

The Hermite polynomials are $H_0(x) = 1, H_1(x) = 2x, H_2(x) = 4x^2 - 2$. Equation (5.75) have the special cases:

$\underline{m = 0, n = 0}$

$$
\begin{bmatrix}
E_x \\
E_y \\
E_z \\
cB_x \\
cB_y \\
cB_z
\end{bmatrix}
= E_{x0} e^{ikz - i\omega t} \left(\frac{1}{1 + i\frac{2z}{kw_0^2}} \right) \exp\left[i\frac{kQ}{2}(x^2 + y^2) \right]
\begin{bmatrix}
1 \\
0 \\
-Qx \\
-xyQ^2 \\
Q^2 x^2 - \frac{iQ}{k} + 1 \\
-Qy
\end{bmatrix}
\tag{5.78}
$$

$\underline{m = 1, n = 0}$

$$
\begin{bmatrix}
E_x \\
E_y \\
E_z \\
cB_x \\
cB_y \\
cB_z
\end{bmatrix}
= E_{x0} e^{ikz - i\omega t} \left(\frac{1 - i\frac{2z}{kw_0^2}}{1 + i\frac{2z}{kw_0^2}} \right) \frac{\exp\left[i\frac{kQ}{2}(x^2 + y^2) \right]}{\sqrt{1 + \left(\frac{2z}{kw_0^2} \right)^2}}
$$

$$
\times
\begin{bmatrix}
\frac{2\sqrt{2}}{w} x \\
0 \\
i\frac{2\sqrt{2}}{kw} - \frac{2\sqrt{2}Q}{w} x^2 \\
i\frac{2\sqrt{2}Q}{kw} y - \frac{2\sqrt{2}Q^2}{w} x^2 y \\
-\frac{4\sqrt{2}iQ}{kw} x + (Q^2 x^2 - \frac{iQ}{k} + 1)\frac{2\sqrt{2}}{w} x \\
-\frac{2\sqrt{2}Q}{w} xy
\end{bmatrix}
\tag{5.79}
$$

From Eqs.(5.78) anmd (5.79), one notes that the transverse component of the laser electric field is larger than the longitudinal component by a factor kw_0, which is typically $\gg 1$.

Let us consider a laser mode established in free space with mirrors at $z = \pm\infty$. Consider an electron with charge e and moving in the z-direction with a rigid path $x = x_0, y = y_0, z = z_0 + vt$. The energy gain by this electron due to the laser field is given by

$$
\Delta\mathcal{E} = \int_{-\infty}^{\infty} dz\, eE_z(x = x_0, y = y_0, z, t = (z - z_0)/v)
\tag{5.80}
$$

For the fundamental mode, Eq.(5.78) then gives

$$
\begin{aligned}
\Delta\mathcal{E} &= -eE_{x0}\frac{2ix_0}{kw_0^2} e^{ikz_0 c/v} \int_{-\infty}^{\infty} dz\, e^{ikz(1 - \frac{c}{v})} \frac{1}{\left(1 + i\frac{2z}{kw_0^2}\right)^2} \exp\left[-\frac{x_0^2 + y_0^2}{w_0^2\left(1 + i\frac{2z}{kw_0^2}\right)} \right] \\
&= -ieE_{x0}x_0 e^{ikz_0 c/v} \int_{-\infty}^{\infty} d\xi\, \frac{e^{iA\xi}}{(1 + i\xi)^2} \exp\left(-\frac{B}{1 + i\xi} \right)
\end{aligned}
\tag{5.81}
$$

where we have made a change of variables from z to $\xi = 2z/kw_0^2$, and defined

$$A = (1 - \frac{c}{v})\frac{k^2 w_0^2}{2}, \quad B = \frac{x_0^2 + y_0^2}{w_0^2} \qquad (5.82)$$

Physically, $\xi = z/Z_R$, which is natural because z is conveniently measured in units of Z_R.

We need to evaluate the last integral in Eq.(5.81). In particular, we are interested in the acceleration of a relativistic particle by setting $v = c$, i.e. $A = 0$. One first notes that the Lawson-Woodward theorem asserts that the integral vanishes when $v = c$. Indeed when $A = 0$, the integral in Eq.(5.81) can be easily shown to vanish. To first order in laser field, there is no net energy gain for a relativistic particle traversing a laser field in free space. This is regardless of the value of B, i.e. regardless of where the electron is injected.

To accelerate a relativistic particle, one way is to use the fundamental mode but only in the region $z > 0$. This can be provided by a laser resonator established between a planar mirror at $z = 0$ and another mirror at $z = \infty$. The existence of the planar mirror means it is no longer acceleration in free space. In particular, one has to worry about the break down limit at the mirror. See Fig.5.5 for an illustration of the arrangement. The integration (5.81) would then be replaced by an integration from $\xi = 0$ to $\xi = \infty$, yielding, when $A = 0$,

$$\Delta\mathcal{E} = -eE_{x0}\, x_0\, e^{ikz_0}\, \frac{1}{B}(1 - e^{-B}) \qquad (5.83)$$
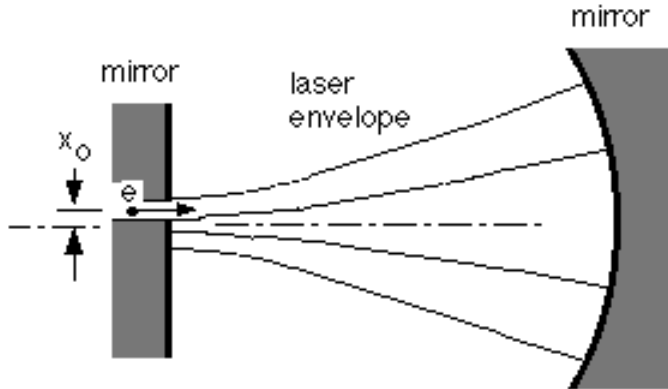
Figure 5.5: An acceleration scheme using a laser resonator.

At this point, we will choose the injection location x_0 and y_0 to maximize the energy gain in Eq.(5.83). We write $\Delta\mathcal{E} \propto F(x_0/w_0, y_0/w_0)$, where $F(x, y) = x(1 - e^{-x^2-y^2})/(x^2 + y^2)$ is shown in Fig.5.6. Maximum of $F(x, y)$ occurs at $x = x_0/w_0 = 1.12, y = y_0/w_0 = 0$, and the maximum value is $F_{\max} = 0.64$. The
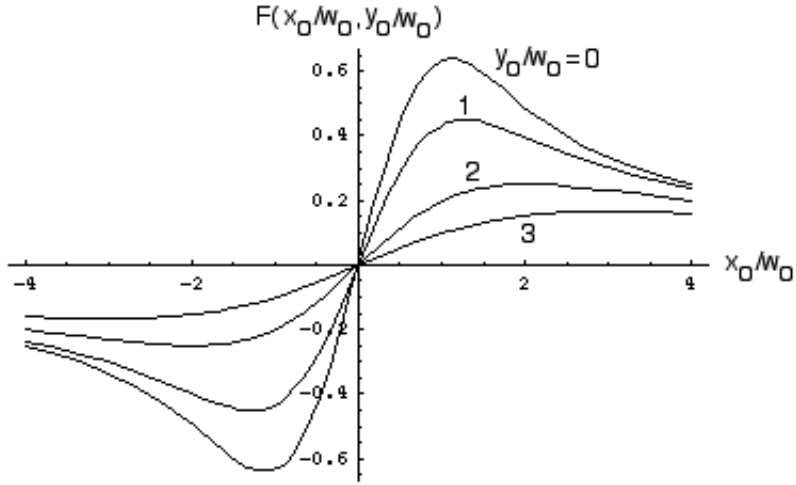
Figure 5.6: Function $F(x, y)$ versus x for $y = 0, 1, 2, 3$.

energy gain of the electron therefore has a magnitude of $\Delta\mathcal{E}_{\max} = 0.64\,eE_{x0}w_0$, and it oscillates with the injection phase relative to the laser.[27]

This acceleration scheme, however, is limited by the breakdown of the mirror at $z = 0$. The maximum electric field at the mirror occurs at $x = y = 0$, and is given by $E_x = E_{x0}$. This means E_{x0} must not exceed the breakdown voltage, which is much smaller than the available laser field. In this sense, Lawson-Woodward theorem applies again.

> *Exercise* 19 Choose the injection location x_0, y_0 and the mirror locations z_1, z_2 to maximize the energy gain. This maybe done first with a fixed E_{x0}. It is then to be repeated by fixing the breakdown voltage of the mirror.
> *Solution* Use the result
>
> $$\Delta\mathcal{E} = ieE_{x0}\,x_0\,e^{ikz_0}\,\frac{1}{B}\left[\exp\left(-\frac{B}{1+i\xi_2}\right) - \exp\left(-\frac{B}{1+i\xi_1}\right)\right] \quad (5.84)$$
>
> where $\xi_{1,2} = 2z_{1,2}/kw_0^2$.

> *Exercise* 20 One may try to accelerate using the x-component of the electric field in a laser fundamental mode. Consider an electron moving in the x-direction following the path $x = x_0 + ct, y = y_0, z = z_0$. Find the energy gain by this electron traversing the laser from $x = -\infty$ to ∞.

---

[27]One might be tempted to focus the laser weakly to increase w_0 in order to increase $\Delta\mathcal{E}_{\max}$. This however lowers E_{x0} for a given laser power. In fact, for a given laser power, $\Delta\mathcal{E}_{\max}$ is basically independent of the setup of the laser focus. See the discussion at the end of section 7.

$$\Delta\mathcal{E} = \frac{\sqrt{\pi}eE_{x0}w_0}{\sqrt{1+i\xi_0}} \exp\left[ik(x_0 + \frac{z_0}{2}) - \frac{k^2w_0^2}{4} - \frac{(y_0/w_0)^2}{1+i\xi_0}\right] \quad (5.85)$$

where $\xi_0 = 2z_0/kw_0^2$. This energy gain is nonzero, but is reduced from $eE_{x0}w_0$ by a factor $\gg 1$. For example, with $z_0 = y_0 = 0$, this reduction factor is $\sqrt{2}e^{-k^2w_0^2/4} = \sqrt{2}e^{-1/\theta_d^2}$.

Exercise 21 One may try to accelerate using the $m = 1, n = 0$ mode. Find an expression of energy gain using Eqs.(5.79) and (5.80). Assume the two mirrors are at z_1, z_2 and $v = c$.
Solution

$$\begin{aligned}
\Delta\mathcal{E} &= i\sqrt{2}eE_{x0}w_0e^{ikz_0} \int_{\xi_1}^{\xi_2} d\xi\, \frac{\exp\left(-\frac{B}{1+i\xi}\right)}{(1+i\xi)^2} \left[1 - \frac{2x_0^2}{w_0^2(1+i\xi)}\right] \\
&= \sqrt{2}eE_{x0}w_0e^{ikz_0} \\
&\quad \times \left\{\frac{1}{B}\left(\frac{y_0^2 - x_0^2}{y_0^2 + x_0^2}\right)\left[\exp\left(-\frac{B}{1+i\xi_2}\right) - \exp\left(-\frac{B}{1+i\xi_1}\right)\right]\right. \\
&\quad \left. - \frac{2x_0^2}{y_0^2 + x_0^2}\left[\frac{\exp\left(-\frac{B}{1+i\xi_2}\right)}{1+i\xi_2} - \frac{\exp\left(-\frac{B}{1+i\xi_1}\right)}{1+i\xi_1}\right]\right\} \quad (5.86)
\end{aligned}$$

This energy gain vanishes if the mirrors are located at $z = \pm\infty$, as dictated by the Lawson-Woodward theorem. When $z_1 = 0, z_2 = \infty$, it reduces to

$$\Delta\mathcal{E} = \sqrt{2}eE_{x0}w_0e^{ikz_0}\left\{e^{-B} + \frac{x_0^2 - y_0^2}{x_0^2 + y_0^2}\left[e^{-B} - \frac{1}{B}(1-e^{-B})\right]\right\} \quad (5.87)$$

One then may optimize the energy gain by choosing x_0 and y_0. Maximum value of the expression in the curly brackets is 1, which occurs at $x_0 = y_0 = 0$.

5.7 Two crossing lasers

Equation (5.80) assumes the accelerated electron follows a rigid path in the z direction. One might ask what happens if the particle moves at an angle to the z-axis so that one can take advantage of the larger transverse electric field component.

Instead of analyzing this problem, however, a somewhat better arrangement is to use two lasers, crossing at their focal points an angles $\pm\theta$ in the x-z plane. Let both lasers be in the fundamental $m = 0, n = 0$ mode, and let them have the complex amplitudes E_{x1} and E_{x2}. The electron to be accelerated is considered to follow the rigid path along the z-axis, namely $x = y = 0, z = z_0 + vt$. The geometry is illustrated in Fig.5.7.
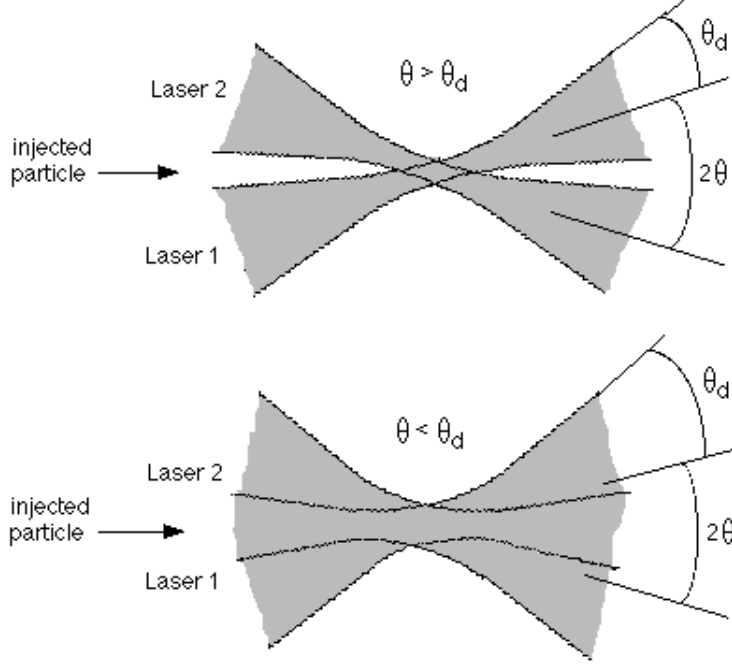
Figure 5.7: Two crossing lasers as an acceleration scheme. Two qualitatively different cases are shown.

Depending on whether $\theta > \theta_d$ or $\theta < \theta_d$, one would have the two cases shown in Fig.5.7, where θ_d is the diffraction angle given by Eq.(5.69). When $\theta > \theta_d$, the two lasers are separated quickly and the region of electron-laser interaction is limited. When $\theta < \theta_d$, the region of interaction will be long.

Consider Laser 1 in Fig.5.7. Its x- and z-components of $\vec{E}$ are given by $E_x = E_{x'} \cos\theta + E_{z'} \sin\theta$ and $E_z = -E_{x'} \sin\theta + E_{z'} \cos\theta$, where $E_{x'}$ and $E_{z'}$ are given by Eq.(5.79) with the substitutions $E_{x0} \to E_{x1}, x \to x\cos\theta - z\sin\theta, z \to x\sin\theta + z\cos\theta$. Similarly for Laser 2, we have $E_x = E_{x'} \cos\theta - E_{z'} \sin\theta$ and $E_z = E_{x'} \sin\theta + E_{z'} \cos\theta$, where $E_{x'}$ and $E_{z'}$ are given by Eq.(5.79) with the substitutions $E_{x0} \to E_{x2}, x \to x\cos\theta + z\sin\theta, z \to -x\sin\theta + z\cos\theta$.

These two laser fields are to be added by superposition to give the total field. For an electron on the z-axis, we set $x = y = 0$. It sees a total electric field

$$
\begin{bmatrix} E_x \\ E_z \end{bmatrix} = e^{ikz\cos\theta - i\omega t} \frac{\exp\left(i\frac{kQ}{2}z^2\sin^2\theta\right)}{1 + i\frac{2z\cos\theta}{kw_0^2}} \left\{ E_{x1} \begin{bmatrix} \cos\theta & \sin\theta \\ -\sin\theta & \cos\theta \end{bmatrix} \begin{bmatrix} 1 \\ Qz\sin\theta \end{bmatrix} \right.
$$
$$
\left. + E_{x2} \begin{bmatrix} \cos\theta & -\sin\theta \\ \sin\theta & \cos\theta \end{bmatrix} \begin{bmatrix} 1 \\ -Qz\sin\theta \end{bmatrix} \right\} \tag{5.88}
$$

115

where $Q = 2/(2z\cos\theta - ikw_0^2), w = w_0\sqrt{1 + \left(\frac{2z\cos\theta}{kw_0^2}\right)^2}$. If we now choose $E_{x2} = -E_{x1}$, i.e. the two lasers have the same amplitude and are exactly out of phase, then the x-components of the two lasers cancel each other along the z-axis, while their z-components add, yielding

$$\begin{bmatrix} E_x \\ E_z \end{bmatrix} = 2E_{x1}e^{ikz\cos\theta - i\omega t}\frac{\exp\left(i\frac{kQ}{2}z^2\sin^2\theta\right)}{1 + i\frac{2z\cos\theta}{kw_0^2}}\begin{bmatrix} 0 \\ -\sin\theta + Qz\sin\theta\cos\theta \end{bmatrix} \quad (5.89)$$

Seen by an ultrarelativistic electron with $z = z_0 + ct$, the accelerating field, written in terms of the familiar variables $\xi = 2z/kw_0^2$ and $\theta_d = 2/kw_0$, is

$$\begin{aligned} E_z &= -2E_{x1}\sin\theta\, e^{ikz_0}\frac{\exp\left[\frac{-i(1-\cos\theta)(2-i\xi+i\xi\cos\theta)\xi}{\theta_d^2(1+i\xi\cos\theta)}\right]}{(1 + i\xi\cos\theta)^2} \\ &\approx -2E_{x1}\theta\, e^{ikz_0}\frac{\exp\left[-i\frac{\theta^2\xi}{\theta_d^2(1+i\xi)}\right]}{(1 + i\xi)^2} \end{aligned} \quad (5.90)$$

where the last step is taking $\theta \ll 1$.

The accelerating electric field seen by the electron is plotted in Fig.5.8 for three values of θ/θ_d. For each value of θ/θ_d, the plot contains the electric fields seen by four electrons with $kz_0 = 0, \pi/2, \pi$, and $3\pi/2$. For each electron, one observes the oscillatory nature of the accelerating field, yielding no total net acceleration if integrated from $-\infty$ to ∞. One also observes that as θ/θ_d increases, the range of particle-laser interaction shrinks, as illustrated in Fig.5.7, while the peak acceleration rate increases. There is of course no acceleration when $\theta/\theta_d = 0$.

Energy gain of the electron from z_1 to z_2 is obtained by integrating Eq.(5.90),

$$\Delta\mathcal{E} = \frac{kw_0^2}{2}\int_{\xi_1}^{\xi_2} eE_z\, d\xi = -2ieE_{x1}w_0 e^{ikz_0}\left(\frac{\theta_d}{\theta}\right)\left[e^{\frac{-i\theta^2\xi_2}{\theta_d^2(1+i\xi_2)}} - e^{\frac{-i\theta^2\xi_1}{\theta_d^2(1+i\xi_1)}}\right]$$
$$(5.91)$$

When $z_{1,2} = \pm\infty$, we find $\Delta\mathcal{E} = 0$. When $z_1 = 0, z_2 = \infty$, we have $\Delta\mathcal{E} = -2ieE_{x1}w_0 e^{ikz_0}F(\theta/\theta_d, 0)$, where $F(x, y)$ is the function shown in Fig.5.6. Its maximum occurs at $\theta/\theta_d = 1.12$ with the maximal value of 0.64.

Exercise 22 repeat the analysis for two crossing lasers of mode $m = 1, n = 0$.
Solution

$$\begin{bmatrix} E_x \\ E_z \end{bmatrix} = e^{ikz\cos\theta - i\omega t}\left(\frac{1 - i\frac{2z\cos\theta}{kw_0^2}}{1 + i\frac{2z\cos\theta}{kw_0^2}}\right)\frac{\exp\left(i\frac{kQ}{2}z^2\sin^2\theta\right)}{\sqrt{1 + \left(\frac{2z\cos\theta}{kw_0^2}\right)^2}} \quad (5.92)$$

$$\times\left\{E_{x1}\begin{bmatrix} \cos\theta & \sin\theta \\ -\sin\theta & \cos\theta \end{bmatrix}\begin{bmatrix} -\frac{2\sqrt{2}}{w}z\sin\theta \\ i\frac{2\sqrt{2}}{kw} - \frac{2\sqrt{2}Q}{w}z^2\sin^2\theta \end{bmatrix}\right.$$

116
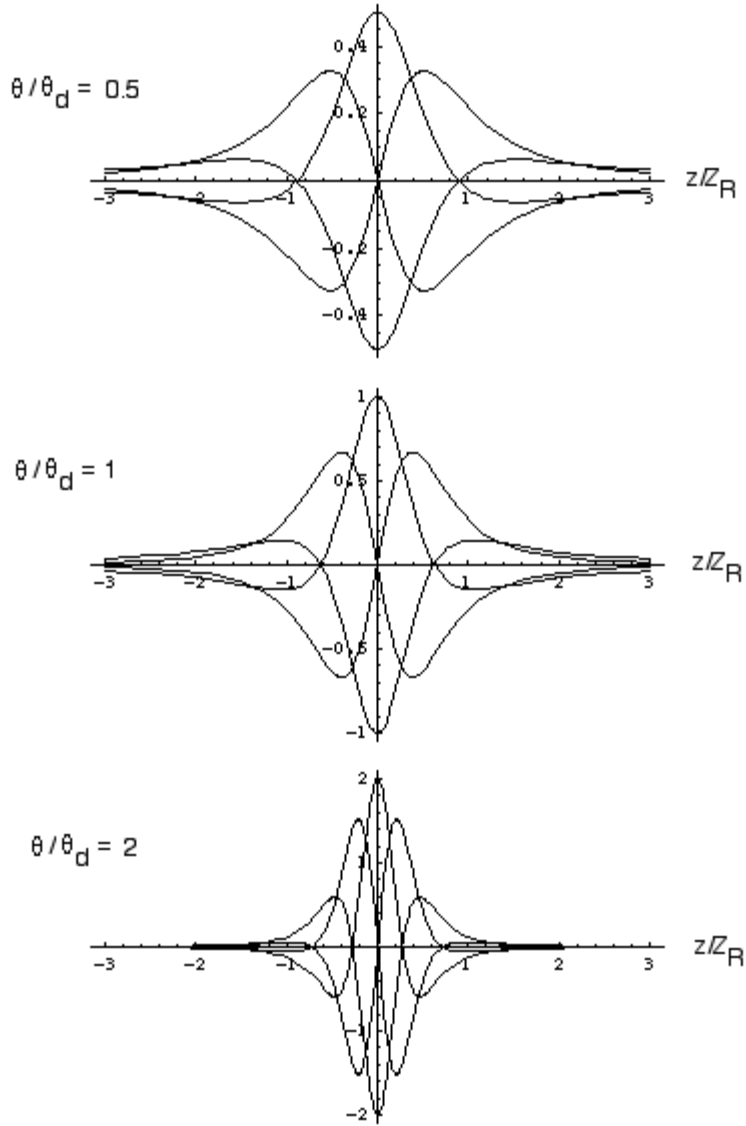
Figure 5.8: Accelerating electric field seen by an electron with various values of θ/θ_d and kz_0. The accelerating field has been normalized by $2E_{x1}\theta_d$.

$$+E_{x2}\left[\begin{array}{cc} \cos\theta & -\sin\theta \\ \sin\theta & \cos\theta \end{array}\right]\left[\begin{array}{c} \frac{2\sqrt{2}}{w}z\sin\theta \\ i\frac{2\sqrt{2}}{kw}-\frac{2\sqrt{2}Q}{w}z^2\sin^2\theta \end{array}\right]\right\}$$

Choose $E_{x2} = E_{x1}$, then the x-components of the two lasers cancel

117

each other along the z-axis, while their z-components add. Seen by an ultrarelativistic electron with $z = z_0 + ct$, the accelerating field is

$$E_z \approx i\frac{4\sqrt{2}E_{x1}}{kw_0}\, e^{ikz_0}\, \frac{\exp\left[-i\frac{\theta^2\xi}{\theta_d^2(1+i\xi)}\right]}{(1+i\xi)^2} \qquad (5.93)$$

This magnitude is smaller than that with two lasers in the fundamental mode by a factor of $2\sqrt{2}/kw_0$.

The following table summarizes the various accelerator configurations using focussed lasers discussed so far.

configuration	Max. energy gain	Optimization
fundamental mode, from $z = 0$ to ∞	$0.64\, eE_{x0}w_0$	$x_0 = 1.12\, w_0,\ y_0 = 0,$ $E_{x0} < $ breakdown
$m = 1, n = 0$ mode, from $z = 0$ to ∞	$\sqrt{2}\, eE_{x0}w_0$	$x_0 = y_0 = 0$
fundamental mode, transversely traversing the focal point	$\sqrt{2}e^{-1/\theta_d^2}\, eE_{x0}w_0$	$y_0 = z_0 = 0$
two crossing lasers, fundamental mode	$1.28\, eE_{x1}w_0$	$\theta = 1.12\, \theta_d,$ $E_{x1} = -E_{x2}$
two crossing lasers, $m = 1, n = 0$ mode	$\sqrt{2}\theta_d \times 1.28\, eE_{x1}w_0$	$\theta = 1.12\, \theta_d,$ $E_{x1} = E_{x2}$

In all cases, the best one can do is an energy gain $\sim eE_{x0}w_0$. This quantity can then be related to the laser power $\mathcal{P}$ using Eq.(5.77), and one gets $eE_{x0}w_0[\text{MeV}] \approx 22\sqrt{\mathcal{P}\,[\text{TW}]}$ for the fundamental mode and $16\sqrt{\mathcal{P}\,[\text{TW}]}$ for the $m = 1, n = 0$ mode. For a 10 TW laser, the energy gain is $\sim$70 MeV for the fundamental mode and $\sim$50 MeV for the $m = 1, n = 0$ mode.

Lawson-Woodward theorem applies to these cases. The length over which the laser acts on the particle $\sim Z_R$. The energy gain $\sim eE_0w_0$. Therefore the acceleration gradient $\sim eE_0w_0/Z_R = eE_0\theta_d \ll eE_0$.

References

[1] J.D. Lawson, RL-75-043 (1975).

[2] E. Esarey, P. Sprangle, and J. Krall, Phys. Rev. E52, 5443 (1995).

[3] C.S. Roberts and S.J.Buchsbaum, Phys. rev. 135, A381 (1964).

6 Spin Dynamics and Siberian Snakes

The motion of spin in an accelerator is of special interest for beam dynamics. The spin can be considered the fourth dimension of the phase space. In addition to the 6 orbital variables $(x, x', y, y', z, \delta)$, we then add two more variables for the spin. The only difference is that the dynamics of the spin variables depend sensitively on the orbital variables, but the orbital variables do not depend (to first order in $\hbar$) on the spin variables.

6.1 Thomas-BMT Equation

Spin of a particle interacts with an EM field through the magnetic moment associated with the spin. Let $\vec{S}$ be the spin represented as a 3-D vector. The associated magnetic moment is

$$\vec{\mu} = \frac{ge}{2mc}\hbar\vec{S} \tag{6.1}$$

where g is the gyromagnetic ratio. For a Dirac particle, g is nominally equal to 2. The deviation of g from 2, attributed to an "anomolous" magnetic moment of the particle, is specified by the parameter

$$a = \frac{g-2}{2} \tag{6.2}$$

For electrons and muons, the value of a is approximately equal to the fine structure constant $1/137$ divided by 2π. More accurately,

$$a = \begin{cases} 0.001160, & \text{electron} \\ 0.001166, & \text{muon} \\ 1.7928, & \text{proton} \end{cases} \tag{6.3}$$

As we shall see, the fact that g is not exactly equal to 2, i.e. the fact that $a \neq 0$, gives rise to all the complications of spin dynamics. Had $a = 0$ been true, the spin will often rotate rigidly with the coordinate system, and spin dynamics would have been much simpler (but much more boring).

Consider a particle at rest in a magnetic field $\vec{B}$. The precession equation of motion for the spin is

$$\frac{d\vec{S}}{dt} = \vec{\Omega} \times \vec{S} \tag{6.4}$$

with the precession angular velocity

$$\vec{\Omega} = -\frac{ge}{2mc}\vec{B} \tag{6.5}$$

Equations (6.4-6.5) describe the precession for a stationary particle, but we need an equation for a relativistic particle moving in an EM field $\vec{E}$ and $\vec{B}$ in an accelerator. Let $c\vec{\beta}$ be the instantaneous velocity of the particle; it is obvious that we need to make a Lorentz transformation to the particle's rest frame.

When doing so, the form of the spin precession equation remains to be (6.4); only $\vec{\Omega}$ needs to be transformed. Note that we are not Lorentz transforming $\vec{S}$, so in the final equation, $\vec{S}$ will be a quantity in the particle's rest frame, while all other quantities, $t, \vec{E}, \vec{B}, \vec{\beta}$ refer to the laboratory frame. This is one of the peculiarities of the Thomas-BMT equation. It is not formally Lorentz covariant. A covariant description of spin motion of course does exist, but we don't need it here.

The magnetic field in the rest frame is given by a Lorentz transformation from the laboratory frame,

$$\vec{B}_R = \gamma \vec{B}_\perp + \vec{B}_\parallel - \gamma \vec{\beta} \times \vec{E} \tag{6.6}$$

with $\vec{B}_\perp$ and $\vec{B}_\parallel$ the components of $\vec{B}$ perpendicular and parallel to $\vec{\beta}$ respectively. The angular velocity $\vec{\Omega}$ in the laboratory frame consists of two terms. The first term is

$$-\frac{1}{\gamma} \frac{ge}{2mc} \vec{B}_R \tag{6.7}$$

where $\vec{B}_R$ is given by Eq.(6.6), and we have included a factor of $1/\gamma$ to take care of the time dilation. The second term is more subtle; it is due to Thomas precession which contributes an additional term to angular velocity when the particle is accelerated sideways,

$$-\frac{\gamma - 1}{\beta^2} \vec{\beta} \times \dot{\vec{\beta}} = -\frac{e\gamma}{mc(\gamma + 1)} (\vec{\beta} \times \vec{E} - \beta^2 \vec{B}_\perp) \tag{6.8}$$

The origin of Thomas precession is relativistic kinematics. Two successive Lorentz transformations along $\vec{\beta}_1$ and $\vec{\beta}_2$ can be combined into one single Lorentz transformation only if $\vec{\beta}_1 \parallel \vec{\beta}_2$. Otherwise, they can be combined into a Lorentz transformation plus a rotation. This additional rotation needed here is the origin of the Thomas precesson.

Adding the two contributions (6.7) and (6.8), we obtain

$$\vec{\Omega} = -\frac{e}{mc} \left[\left(a + \frac{1}{\gamma}\right) \vec{B} - \frac{a\gamma}{\gamma + 1} \vec{\beta}(\vec{\beta} \cdot \vec{B}) - \left(a + \frac{1}{\gamma + 1}\right) \vec{\beta} \times \vec{E} \right] \tag{6.9}$$

which, when substituted into (6.4), is called the Thomas-BMT equation, where BMT stands for Bargman, Michel, and Telegdi (1959).

6.2 Spin Dynamics

To describe the spin motion in a circular accelerator, it is more convenient to change the time variable t to the distance variable $s = \beta ct$. In an accelerator, the electric and magnetic fields seen by a particle depend on the particle's orbital coordinates (x, y, z). A particle on the ideal design orbit, however, sees only the bending magnetic field and the accelerating electric field. The accelerating electric field does not contribute to spin precession according to (6.9) because

it is parallel to the velocity $\vec{\beta}$. The bending magnetic field $\vec{B} = B_0(s)\hat{y}$ with $B_0(s + 2\pi R) = B_0(s)$, on the other hand, does give rise to a precession,

$$\frac{d\vec{S}}{ds} = -\frac{eB_0(s)}{mc^2}\left(a + \frac{1}{\gamma}\right)\hat{y} \times \vec{S} \tag{6.10}$$

With the precession axis along $\hat{y}$, the y-component of the spin S_y is preserved. The spin rotation going through a single bending magnet is sketched in Fig.6.1.
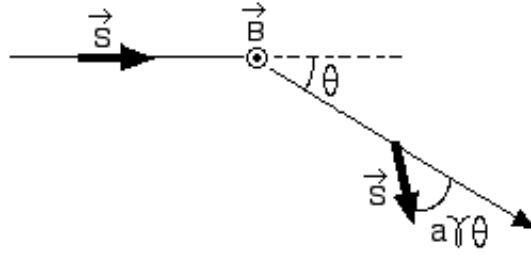
Figure 6.1: Spin rotation going through a single bending magnet.

If we adopt the coordinate system $(\hat{x}, \hat{y}, \hat{z})$ that rotates with the trajectory of the ideal particle, then relative to this rotating frame, the spin components S_x and S_z rotate with the angular speed $a\gamma eB_0/E$ which is $a\gamma$ times the speed at which the coordinate system rotates. As the particle completes one turn, the coordinate system rotates by 2π and the spin of the ideal particle precesses around $\hat{y}$ by an angle $a\gamma 2\pi$ relative to the coordinate system. In analogy to the definition of orbital tunes ν_x, ν_y, ν_s, we define a spin tune

$$\nu_{\text{spin}} = a\gamma = \begin{cases} E/(0.44065 \text{ GeV}), & \text{electron} \\ E/(90.62 \text{ GeV}), & \text{muon} \\ E/(0.5242 \text{ GeV}), & \text{proton} \end{cases} \tag{6.11}$$

We next consider a non-ideal particle executing some betatron motion. It sees a magnetic field

$$\vec{B} = G(s)(x\hat{y} + y\hat{x}) + B_0(s)\hat{y} \tag{6.12}$$

where $G(s)$ is the quadrupole field. We ignore the electric fields in the following because their contribution is small. Substituting into Eq.(6.9) yields

$$\vec{\Omega} \approx -\frac{e}{mc}\left[(a + \frac{1}{\gamma})B_0(s)\hat{y} + (a + \frac{1}{\gamma})G(s)(y\hat{x} + x\hat{y}) - \frac{a\gamma}{\gamma + 1}y'B_0(s)\hat{z}\right] \tag{6.13}$$

where we have used $\vec{\beta} \approx \hat{z} + x'\hat{x} + y'\hat{y}$ and kept terms only up to linear order in x and y.

121

Equations (6.4) and (6.13) describe the spin motion. We rewrite them as

$$\frac{d}{d\theta}\vec{S} = \vec{h} \times \vec{S} \tag{6.14}$$

where the "time" variable is

$$\theta \equiv \int_0^s \frac{ds'}{\rho(s')} = \text{accumulated bending angle} \tag{6.15}$$

and the "angular velocity vector" is

$$
\begin{aligned}
\vec{h} &= h_x\hat{x} + h_y\hat{y} + h_z\hat{z} \\
h_x &= \frac{\rho\Omega_x}{c} = -\frac{e}{mc^2}(a + \frac{1}{\gamma})\rho Gy \\
h_y &= (\frac{\rho\Omega_y}{c} + 1) = -a\gamma + \frac{e}{mc^2}(a + \frac{1}{\gamma})\rho Gx \\
h_z &= \frac{\rho\Omega_z}{c} = \frac{a\gamma^2}{\gamma + 1}y'
\end{aligned}
\tag{6.16}
$$

Among all the terms in $h_{x,y,z}$, the leading term is the $-a\gamma$ term in h_y. It is the spin precession seen by the ideal particle. All other terms contain x or y, and are seen only by particles deviating from the ideal trajectory. The fact that the reference frame is rotating explains the extra term 1 in $1 + \frac{\rho\Omega_y}{c}$ in the definition of h_y,

$$\frac{d\hat{x}}{ds} = \frac{1}{\rho}\hat{z}, \quad \frac{d\hat{y}}{ds} = 0, \quad \frac{d\hat{z}}{ds} = -\frac{1}{\rho}\hat{x} \tag{6.17}$$

Exercise 1 We have been ignoring $\vec{E}$ because most likely $\vec{E}$ is in the longitudinal direction, and is approximately parallel to $\vec{\beta}$, which in turn means it does not contribute much to spin precession according to Eq.(6.9). However, if we use a transverse $\vec{E}$, e.g. electrostatic beam separators, or electrostatic lenses, then we must take into account of its effect. 9a) Show that the reference frame rotation in this case is given by

$$\vec{\Omega} = -\frac{e}{mc}\left(\frac{\vec{B}}{\gamma} - \frac{\gamma}{\gamma^2 - 1}\vec{\beta} \times \vec{E}\right)$$

(b) Show that there is a magic energy given by

$$\gamma = \sqrt{1 + \frac{1}{a}}$$

when even a transverse $\vec{E}$ does not contribute to spin precession. For muons, this magic energy is 3.1 GeV. One can use electrostatic

lenses instead of quadrupole magnets for such a muon storage ring. It allows precise measurement of the muon $g-2$ value.

Exercise 2 We assumed there were no solenoids. Show that the spin precession going through a solenoid $\vec{B} = B_s\hat{z}$ is a rotation around $\hat{z}$ by an angle

$$-\frac{eB_s\ell}{mc^2\gamma}(1+a) = -\frac{B_s\ell}{(B\rho)}(1+a)$$

Exercise 3 It may be useful to have a device which rotates the spin without affecting the particle trajectory. One such device is solenoid $\vec{B} = B_s\hat{z}$. Another consists of transverse $\vec{E}$ and $\vec{B}$ with $\vec{E} = -\beta\hat{z} \times \vec{B}$, where we have assumed the nominal direction of beam motion is along $\hat{z}$. Show that the beam trajectory is unperturbed, while its spin precession is given by

$$\vec{\Omega} = -\frac{eg}{2mc\gamma^2}\vec{B}$$

6.3 Spinor Algebra

To study spin dynamics, one can use Eq.(6.14) to describe the evolution of the three vector components $S_{x,y,z}$. Alternatively, one can also use a spinor algebra language borrowed from quantum mechanics. One first introduces the Pauli matrices,[28]

$$\sigma_x = \begin{bmatrix} 0 & -i \\ i & 0 \end{bmatrix}, \qquad \sigma_y = \begin{bmatrix} 1 & 0 \\ 0 & -1 \end{bmatrix}, \qquad \sigma_z = \begin{bmatrix} 0 & 1 \\ 1 & 0 \end{bmatrix} \qquad (6.18)$$

It is straightforward to show that

$$
\begin{aligned}
\sigma_i^\dagger &= \sigma_i, & \text{i.e. } \sigma_i \text{ is Hermitian} \\
\sigma_i^\dagger\sigma_i &= \sigma_i^2 = I, & \text{i.e. } \sigma_i \text{ is unitary} \\
\vec{\sigma}^\dagger \cdot \vec{\sigma} &= 3I \\
\sigma_x\sigma_y = -\sigma_y\sigma_x = i\sigma_z, & \sigma_y\sigma_z = -\sigma_z\sigma_y = i\sigma_x, & \sigma_z\sigma_x = -\sigma_x\sigma_z = i\sigma_y \\
\sigma_i\sigma_j &= \delta_{ij}I + i\sum_k \epsilon_{ijk}\sigma_k \\
\vec{\sigma} \times \vec{\sigma} &= 2i\vec{\sigma} \\
\det(\sigma_i) &= -1 \\
\det(\vec{\sigma} \cdot \vec{a}) &= -|\vec{a}|^2 \\
(\vec{\sigma} \cdot \vec{a})^2 &= |\vec{a}|^2 I \\
(\vec{\sigma} \cdot \vec{a})(\vec{\sigma} \cdot \vec{b}) &= (\vec{a} \cdot \vec{b})I + i\vec{\sigma} \cdot (\vec{a} \times \vec{b})
\end{aligned}
$$

---

[28] We made a cyclic permutation of the usual convention. This permuted definition is more natural for us because we have $\hat{y}$, instead of the conventional $\hat{z}$, as the rotation axis, at least for the ideal particle.

$$(\vec{\sigma} \cdot \vec{a}) \text{ and } (\vec{\sigma} \cdot \vec{b}) \quad \begin{cases} \text{commute,} & \text{if } \vec{a} \parallel \vec{b} \\ \text{anticommute,} & \text{if } \vec{a} \perp \vec{b} \end{cases}$$

$$\text{tr}(\sigma_i) = 0$$

$$\text{tr}(\vec{\sigma}(\vec{\sigma} \cdot \vec{a})) = \text{tr}((\vec{\sigma} \cdot \vec{a})\vec{\sigma}) = 2\vec{a}$$

$$\vec{\sigma}(\vec{\sigma} \cdot \vec{a}) = \vec{a} - i\vec{\sigma} \times \vec{a}$$

$$(\vec{\sigma} \cdot \vec{a})\vec{\sigma} - \vec{\sigma}(\vec{\sigma} \cdot \vec{a}) = 2i\vec{\sigma} \times \vec{a}$$

$$(\vec{\sigma} \cdot \vec{a})(\vec{\sigma} \cdot \vec{b}) - (\vec{\sigma} \cdot \vec{b})(\vec{\sigma} \cdot \vec{a}) = 2i\vec{\sigma} \cdot (\vec{a} \times \vec{b}) \tag{6.19}$$

In addition, in preparation for the next section, we mention an elegant formula,

$$e^{-\frac{i}{2}\vec{\sigma}\cdot\vec{\phi}} = I \cos \frac{\phi}{2} - i(\vec{\sigma} \cdot \hat{\phi}) \sin \frac{\phi}{2} \tag{6.20}$$

The LHS of Eq.(6.20), as we will see, is a spinor representation (a map) of a rotation around $\hat{\phi}$ with an angle ϕ. This map can be expanded by using Eq.(6.20).

Sometimes one has obtained the spinor map M of a rotation in its complex 2×2 form, and wants to find the rotation angle and rotation axis. The question is then what is $\vec{\phi}$ so that we can express M in the form $e^{-i\vec{\sigma}\cdot\vec{\phi}/2}$. Equation (6.20) can be inverted for that purpose, and the answer is

$$\cos \frac{\phi}{2} = \frac{1}{2}\text{tr}(M)$$

$$\hat{\phi} = \frac{i}{2\sin\frac{\phi}{2}}\text{tr}(M\vec{\sigma}) \tag{6.21}$$

Exercise 4 Show Eq.(6.19) as a good entry practice.

Exercise 5 (a) Prove Eqs.(6.20-6.21). (b) Show that

$$\cos(\vec{\sigma} \cdot \vec{\phi}) = I \cos \phi, \qquad \sin(\vec{\sigma} \cdot \vec{\phi}) = (\vec{\sigma} \cdot \hat{\phi}) \sin \phi$$

Solution (a) Taylor expand $e^{-\frac{i}{2}\vec{\sigma}\cdot\vec{\phi}} = \sum_{k=0}^{\infty} \frac{1}{k!}(-\frac{i}{2}\vec{\sigma} \cdot \vec{\phi})^k$ and then apply Eq.(6.19) to the terms in the expansion. (b) Use $\cos(\vec{\sigma} \cdot \vec{\phi}) = [e^{i\vec{\sigma}\cdot\vec{\phi}} + e^{-i\vec{\sigma}\cdot\vec{\phi}}]/2$ and $\sin(\vec{\sigma} \cdot \vec{\phi}) = [e^{i\vec{\sigma}\cdot\vec{\phi}} - e^{-i\vec{\sigma}\cdot\vec{\phi}}]/2i$

Exercise 6 Show that

$$e^{-\frac{i}{2}\vec{\sigma}\cdot\vec{\phi}}(\vec{\sigma} \cdot \vec{a}) = (\vec{\sigma} \cdot \vec{a}_\perp)e^{\frac{i}{2}\vec{\sigma}\cdot\vec{\phi}} + (\vec{\sigma} \cdot \vec{a}_\parallel)e^{-\frac{i}{2}\vec{\sigma}\cdot\vec{\phi}}$$

$$(\vec{\sigma} \cdot \vec{a})e^{-\frac{i}{2}\vec{\sigma}\cdot\vec{\phi}} = e^{\frac{i}{2}\vec{\sigma}\cdot\vec{\phi}}(\vec{\sigma} \cdot \vec{a}_\perp) + e^{-\frac{i}{2}\vec{\sigma}\cdot\vec{\phi}}(\vec{\sigma} \cdot \vec{a}_\parallel) \tag{6.22}$$

where $\vec{a} = \vec{a}_\parallel + \vec{a}_\perp$ with $\vec{a}_\parallel = (\vec{a} \cdot \hat{\phi})\hat{\phi}$ and $\vec{a}_\perp = (\hat{\phi} \times \vec{a}) \times \hat{\phi}$.

6.4 Spin Dynamics Using Spinor Algebra

In the spinor algebra language, the spin is represented by a complex 2-component vector ψ, with

$$\vec{S} = \psi^\dagger \vec{\sigma} \psi \tag{6.23}$$

Spin dynamics is then described by the time evolution of ψ,

$$\frac{d\psi}{d\theta} = -\frac{i}{2}(\vec{h} \cdot \vec{\sigma})\psi \tag{6.24}$$

Indeed, one can show using the properties (6.19) that Eq.(6.14) follows from Eqs.(6.23-6.24).

> *Exercise 7* (a) Show that Eq.(6.14) follows from Eqs.(6.23-6.24). (b) Show that the scalar quantity $\psi^\dagger \psi$ is conserved. (c) Use Eqs.(6.23-6.24) to show that the magnitude of $\vec{S}$ is conserved.

> *Exercise 8* Consider a particle that enters a region with dipole magnetic field $\vec{B} = B_0 \hat{y}$ with an initial spin $\vec{S}(0)$. Compute the spin at the exit of the magnet $\vec{S}(L)$ using spinor algebra.

> *Exercise 9* Repeat Exercise 8 for a quadrupole magnet with $\vec{B} = Gx\hat{x}$. Consider the case when the particle enters the quadrupole with x_0 (Let $y_0 = 0$, $x_0' = y_0' = 0$).

If $\vec{h}$ is a constant, i.e. independent of θ, Eq.(6.24) has the solution

$$\psi(\theta) = e^{-\frac{i}{2}\vec{\sigma} \cdot \vec{h}\theta}\psi(0) \tag{6.25}$$

Since $\vec{h}$ is the angular velocity, the map in Eq.(6.25) is the spinor representation of a spin rotation by an angle of $\vec{\phi} = \vec{h}\theta$.

It might be curious to note that when $\phi = 2\pi$, meaning a rotation for a full turn, the rotation map is not equal to I, but equal to $-I$, as can be seen by Eq.(6.20). This is not a problem because the spin, given by Eq.(6.23), is quadratic in ψ.

In general, $\vec{h}$ is not a constant but depends on θ. To study the spin dynamics in this general case, we need to examine the quantity

$$
\begin{aligned}
\vec{h} \cdot \vec{\sigma} &= \begin{bmatrix} h_y & h_z - ih_x \\ h_z + ih_x & -h_y \end{bmatrix} \\
&= \begin{bmatrix} -a\gamma + \frac{e}{mc^2}(a + \frac{1}{\gamma})\rho Gx & \frac{a\gamma^2}{\gamma+1}y' + i\frac{e}{mc^2}(a + \frac{1}{\gamma})\rho Gy \\ \frac{a\gamma^2}{\gamma+1}y' - i\frac{e}{mc^2}(a + \frac{1}{\gamma})\rho Gy & a\gamma - \frac{e}{mc^2}(a + \frac{1}{\gamma})\rho Gx \end{bmatrix}
\end{aligned} \tag{6.26}
$$

which appears prominently in Eq.(6.24). We note that the leading terms are the $\pm a\gamma$ terms in the diagonal elements. These are constants, independent of θ. The dominating spin motion is therefore a constant precession around $\hat{y}$ with

spin tune of $a\gamma$ (see Exercise 10). The remaining terms depend linearly on x and y. This means they have a θ dependence of

$$\begin{cases} e^{\pm i\nu_{x,y}\theta + iK\theta}, & \text{for } x, y \text{ due to betatron oscillations} \\ e^{iK\theta}, & \text{for } x, y \text{ due to closed orbit distortions} \end{cases} \tag{6.27}$$

where K is any integer. These terms contribute to perturbations to the spin motion, and the perturbation tunes are $K \pm \nu_{x,y}$ and K. One expects a resonance to occur when one of these perturbation tunes hit the unperturbed tune, i.e. when

$$a\gamma = \begin{cases} K \pm \nu_{x,y}, & \text{for } x, y \text{ due to betatron oscillations} \\ K, & \text{for } x, y \text{ due to closed orbit distortions} \end{cases} \tag{6.28}$$

Exercise 10 In the absence of perturbation, solve the spinor equation

$$\frac{d\psi}{d\theta} = \begin{bmatrix} -a\gamma & 0 \\ 0 & a\gamma \end{bmatrix} \psi$$

Show that it describes a spin motion uniformly precessing around $\hat{y}$ with spin tune $a\gamma$.

Why do we care about these resonances? When a beam is injected into an accelerator, we align its spin along $\hat{y}$. The ideal particle, whose spin motion is simple precession around $\hat{y}$, would keep its spin aligned to $\hat{y}$. The hope is that the spins of the non-ideal particles would not deviate far from $\hat{y}$ so that the net polarization of the whole beam does not suffer. In general, this is not a problem because the perturbations are small. However, when a resonance occurs, these small perturbations cause large deviations of spin from $\hat{y}$ and the beam polarization would be lost. For this reason, resonances (6.28) are called depolarization resonances. They do not affect particle's _orbital_ motions.[29]

A closer examination shows that the perturbation due to x-motion is not important. An x-motion contributes only to diagonal elements of (6.26) and thus perturbs only rotations around $\hat{y}$. Such perturbations do not worry us; we only worry about rotations perpendicular to $\hat{y}$. This means we can drop the x-perturbations from Eq.(6.26).

Next we make an approximation that there is one and only one resonance causing depolarization. Let the depolarization condition (6.28) be written as $a\gamma = \kappa$. Then one can approximate the off-diagonal elements of (6.26) by filtering out their κ-th Fourier components.

After making these approximations, we obtain

$$\vec{h} \cdot \vec{\sigma} \approx \begin{bmatrix} -a\gamma & \epsilon e^{i\kappa\theta} \\ \epsilon^* e^{-i\kappa\theta} & a\gamma \end{bmatrix} \tag{6.29}$$

---

[29]Except when Stern-Gerlach effects are included. These however are small effects proportional to $\hbar$, and will be ignored here.

where

$$\epsilon = \frac{1}{2\pi} \int_0^{2\pi} d\theta \, e^{-i\kappa\theta}(h_z - ih_x)$$

$$= \frac{1}{2\pi} \int_0^{2\pi} d\theta \, e^{-i\kappa\theta} \left[\frac{a\gamma^2}{\gamma+1} y' + i\frac{e}{mc^2}(a + \frac{1}{\gamma})\rho G y \right] \qquad (6.30)$$

where y and y' refer to the betatron contribution if $\kappa = K \pm \nu_y$, and refer to the closed orbit contribution if $\kappa = K$. The integrand of Eq.(6.30) is periodic in θ with period 2π. The important quantity ϵ is independent of θ, and is the complex depolarization resonance strength.

How does the spin move near the resonance $a\gamma = \kappa$? Let $\delta = a\gamma - \kappa$, and observe the spin motion in a rotating frame as

$$\psi_1 = e^{-\frac{i}{2}\kappa\theta\sigma_y}\psi \qquad (6.31)$$

Then the evolution of ψ_1 involves only a constant map,

$$\frac{d\psi_1}{d\theta} = -\frac{i}{2} \begin{bmatrix} -\delta & \epsilon \\ \epsilon^* & \delta \end{bmatrix} \psi_1 \qquad (6.32)$$

where use has been made of Eq.(6.22).

The solution to Eq.(6.32) can be decomposed into two eigen-modes,

$$\psi_\pm = e^{\pm i\lambda\theta/2} \begin{bmatrix} \frac{\epsilon}{|\epsilon|}\sqrt{\frac{\lambda\pm\delta}{2\lambda}} \\ \mp\sqrt{\frac{\lambda\mp\delta}{2\lambda}} \end{bmatrix}, \qquad \lambda = \sqrt{\delta^2 + |\epsilon|^2} \qquad (6.33)$$

The spin of a particle can be decomposed as

$$\psi_1(\theta) = C_+\psi_+ + C_-\psi_-, \qquad |C_+|^2 + |C_-|^2 = 1 \qquad (6.34)$$

The spin projection onto the y-axis is

$$S_y = \psi^\dagger \sigma_y \psi = \psi_1^\dagger \sigma_y \psi_1$$

$$= \frac{\delta}{\lambda}(|C_+|^2 - |C_-|^2) + \frac{2|\epsilon|}{\lambda}\text{Re}[C_+ C_-^* e^{i\lambda\theta}] \qquad (6.35)$$

If we consider a particle which initially is fully polarized along $\hat{y}$, with

$$\psi(\theta = 0) = \begin{bmatrix} 1 \\ 0 \end{bmatrix} \qquad (6.36)$$

then we have

$$C_+ = \frac{|\epsilon|}{\epsilon}\sqrt{\frac{\lambda+\delta}{2\lambda}}, \qquad C_- = \frac{|\epsilon|}{\epsilon}\sqrt{\frac{\lambda-\delta}{2\lambda}} \qquad (6.37)$$

Substituting into Eq.(6.35) yields the time evolution of the spin of the particle. In particular, one finds that S_y oscillates between 1 and $(\delta^2 - |\epsilon|^2)/(\delta^2 + |\epsilon|^2)$,

$$S_y = \frac{\delta^2 + |\epsilon|^2 \cos\lambda\theta}{\delta^2 + |\epsilon|^2} \qquad (6.38)$$

127
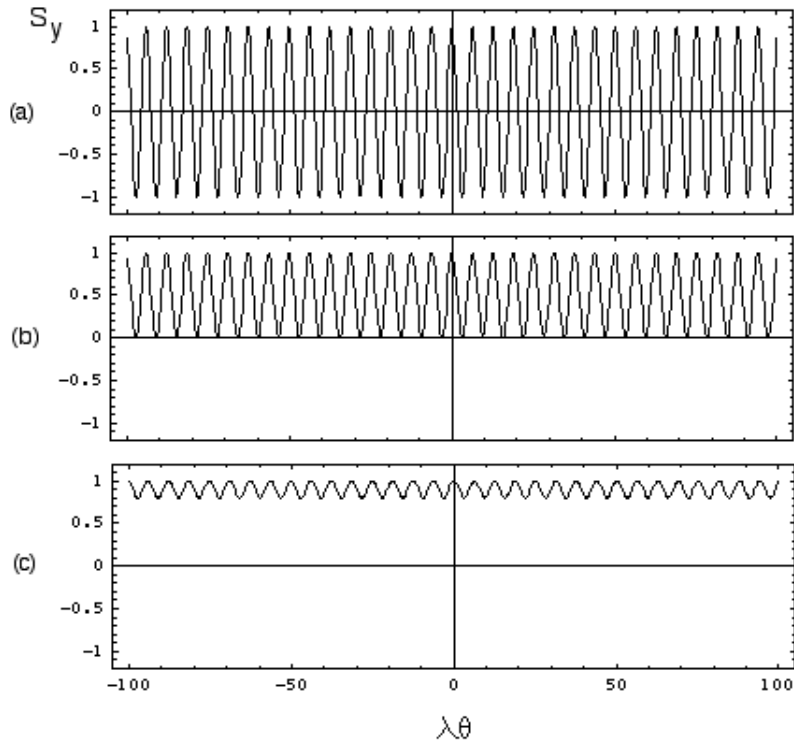
Figure 6.2: Time evolution of spin (a) exactly on resonance $\delta/|\epsilon| = 0$, (b) near resonance $\delta/|\epsilon| = 1$, (c) away from resonance $\delta/|\epsilon| = 3$.

Figure 6.2 shows the time evolution of S_y.

If we ask what is the time averaged polarization of this particle, projected to the $\hat{y}$-axis, we obtain

$$\langle S_y \rangle = \frac{\delta^2}{\delta^2 + |\epsilon|^2} \tag{6.39}$$

which is reduced from the initial polarization of $S_y = 1$.

Away from the resonance, $\delta \to \pm\infty$, we find $\langle S_y \rangle = 1$. The particle is fully polarized. Close to the resonance, the polarization decreases. Right on the resonance, we have $\langle S_y \rangle = 0$. The width of the resonance is given by $|a\gamma - \kappa| = |\epsilon|$. For this reason, $|\epsilon|$ has the meaning of resonance width in tune units.

The $a\gamma = K$ resonances are called *imperfection* resonances. They come from y-orbit distortion which results from imperfections. By a good (and strategic – sometimes called harmonic spin matching) orbit correction, these resonances can be reduced. The $a\gamma = K \pm \nu_y$ resonances are called *intrinsic* resonances. They come from betatron amplitudes of the particles. Since the beam intrinsically has a finite emittance, these resonances can not be avoided by some error

128

correction scheme. Note that all particles have the same strength of imperfection resonances, while the strengths of their intrinsic resonances differ according to their vertical betatron amplitudes.

6.5   Froissart-Stora Equation

We have assumed the particle energy is fixed in the above analysis. In a synchrotron, the beam energy is being changed during acceleration. As a result, the spin tune $a\gamma$ increases with time, and we must consider crossing depolarization resonances. Let us again consider one and only one resonance, and we are crossing it with

$$a\gamma = \kappa + \alpha\theta \qquad (6.40)$$

The resonance is crossed at time $\theta = 0$, and α is the crossing speed.

We make a transformation

$$\psi_1 = e^{-\frac{i}{2}(\kappa\theta+\frac{1}{2}\alpha\theta^2)\sigma_y}\psi \qquad (6.41)$$

Then the evolution of ψ_1 is described by

$$\frac{d\psi_1}{d\theta} = -\frac{i}{2}\begin{bmatrix} 0 & \epsilon e^{-\frac{i}{2}\alpha\theta^2} \\ \epsilon^* e^{\frac{i}{2}\alpha\theta^2} & 0 \end{bmatrix}\psi_1 \qquad (6.42)$$

where use has been made of Eq.(6.22).

To solve Eq.(6.42), let

$$\psi_1(\theta) = \begin{bmatrix} f(\theta) \\ g(\theta) \end{bmatrix}, \quad \text{with } |f|^2 + |g|^2 = 1, \text{ and } |f(\infty)| = 1, \ g(0) = 0 \qquad (6.43)$$

it follows that

$$\frac{d^2 f}{d\theta^2} + i\alpha\theta\frac{df}{d\theta} + \frac{|\epsilon|^2}{4}f = 0 \qquad (6.44)$$

Define $x = \sqrt{\alpha}\theta$, and make a transformation

$$f = e^{-\frac{i}{4}x^2}F \qquad (6.45)$$

then

$$\frac{d^2 F}{dx^2} + \left(\frac{x^2}{4} - a\right)F = 0, \quad \text{with } a = \frac{i}{2} - \frac{|\epsilon|^2}{4\alpha} \qquad (6.46)$$

The solutions to Eq.(6.46) are the parabolic cylindrical functions $E(a,x)$ and $E^*(a,x)$ [5]. With the initial condition $|f(-\infty)| = 1$, the relevant solution is $E(a,x)$. We are interested in the asymptotic behavior of the function $E(a,x)$,

$$\lim_{x\to\infty} E(a,x) = \sqrt{\frac{2}{x}}\exp\left(\frac{i}{4}x^2 - ia\ln x + i\Phi\right)$$

$$\lim_{x\to-\infty} E(a,x) = \sqrt{\frac{2}{|x|}}\exp\left(\frac{i}{4}x^2 - ia\ln|x| - a\pi + i\Phi\right)$$

$$\Phi = \frac{\pi}{4} + \frac{1}{2}\arg\Gamma(\frac{1}{2} + ia) \qquad (6.47)$$

Substituting a from Eq.(6.46) into Eq.(6.47), we obtain

$$f(\theta) = \frac{1}{\sqrt{2}} e^{-\pi|\epsilon|^2/4\alpha} E(\frac{i}{2} - \frac{|\epsilon|^2}{4\alpha}, \sqrt{\alpha}\theta) \qquad (6.48)$$

The polarization is given by $S_y = |f|^2 - |g|^2 = 2|f|^2 - 1$. For $\theta \to -\infty$, we have $S_y = 1$. As the beam is accelerated across the resonance, the polarization is reduced to

$$S_y(\infty) = 2|f(\infty)|^2 - 1 = 2e^{-\pi|\epsilon|^2/2\alpha} - 1 \qquad (6.49)$$

Equation (6.49) was first derived by Froissart and Stora (1960). It says that if a resonance is weak and/or it is crossed quickly ($|\epsilon|^2/\alpha \ll 1$), there is no loss of polarization. When it is strong and/or it is crossed slowly ($|\epsilon|^2/\alpha \gg 1$), the polarization is flipped, and there is, somewhat surprisingly, also no loss of polarization. Loss of polarization occurs when the crossing speed α is comparable to $|\epsilon|^2$, and that is to be avoided. Figure 6.3 shows the dependence of $S_y(\infty)$ on $|\epsilon|/\sqrt{\alpha}$.
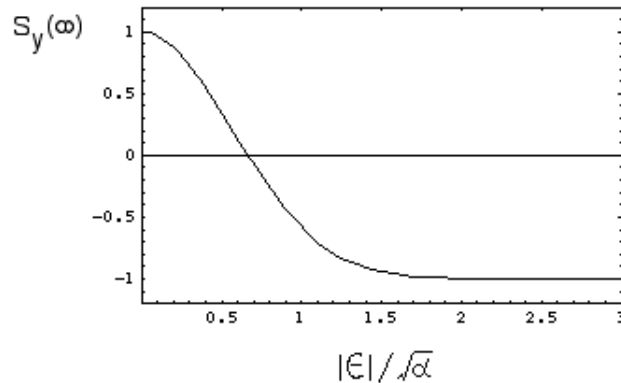
Figure 6.3: Froissart-Stora equation.

Exercise 11 It is instructive to ray trace the spin and observe its behavior as it passes through a resonance. Pay attention to the behavior when the spin tune is far away from the resonance, and then when it is close to the resonance.
Hint Be careful with the $x^2/4$ term in Eq.(6.46) or the $i\alpha\theta df/d\theta$ term in Eq.(6.44) if one chooses to apply these equations. They give troubles at $|x| \to \infty$ or $|\theta| \to \infty$. In fact, these are the subtleties of the parabolic cylindrical functions.

Exercise 12 Equation (6.40) assumes the resonance is crossed linearly in θ. Generalize it to other ways of crossing. Find the generalization for Eq.(6.44). Subsequent application to specific cases will most likely involve numerical solution.

6.6 Siberian Snakes

It takes some effort and some loss of polarization to cross a depolarization resonance. For a high energy synchrotron, there may be many resonances to cross. From Eqs.(6.11) and (6.28), we see that there are at least three resonances to cross for each 0.52 GeV of acceleration (for proton beam). A 1 TeV proton synchrotron therefore requires crossing about 6000 depolarization resonances.

An ingenious invention to avoid all this was made by Derbenev and Kondratenko (1976), and is dubbed the name "Siberian snake" by Courant.

The idea is to somehow make the spin tune independent of energy. Then there is no resonance crossing during acceleration. This fixed spin tune is best chosen to be as far away from the resonances as possible. The best choice is $\nu_{\text{spin}} = K + \frac{1}{2}$. Siberian snake is a device to do just that.

Siberian snake of type 1

This is a magnet or a set of magnets whose net effect on the spin of a particle is to rotate the spin by π around the z-axis as it passes through the device.[30] The rotation in the rest of the accelerator is a rotation by an angle $2\pi a\gamma$ around $\hat{y}$. The total spin rotation for one turn observed at the entrance of the snake is therefore

$$
\begin{aligned}
M_{\text{tot}} &= e^{-\frac{i}{2}\vec{\sigma}\cdot 2\pi a\gamma\hat{y}}e^{-\frac{i}{2}\vec{\sigma}\cdot\pi\hat{z}} = [I\cos(\pi a\gamma) - i\sigma_y\sin(\pi a\gamma)](-i\sigma_z) \\
&= -i[\sigma_z\cos(\pi a\gamma) + \sigma_x\sin(\pi a\gamma)]
\end{aligned}
\tag{6.50}
$$

Equation (6.21) is then used to obtain the net spin precession angle. This angle by definition is $2\pi\nu_{\text{spin}}$. Thus

$$
\cos(\pi\nu_{\text{spin}}) = \frac{1}{2}\text{tr}(M_{\text{tot}}) = 0
$$

$$
\implies \quad \nu_{\text{spin}} = K + \frac{1}{2}
\tag{6.51}
$$

The spin tune is thus made energy independent by this simple device!

One can also calculate the spin rotation axis by using Eq.(6.21). It is found to be

$$
\hat{n} = \frac{i}{2}\text{tr}(M\vec{\sigma}) = \hat{z}\cos(\pi a\gamma) - \hat{x}\sin(\pi a\gamma)
\tag{6.52}
$$

The rotation axis depends on the location of observation. The axis $\hat{n}$ in Eq.(6.52) refers to the entrance of the snake where M was calculated.

Figure 6.4 shows the spin dynamics of a Siberian snake of type 1. It demonstrates why the spin tune is 1/2. The spin direction shown in Fig.6.4(c) is also

---

[30]There is another device called a spin rotator, which is not to be confused with Siberian snakes. A Siberian snake rotates the spins of all particles by a specific angle around a specific axis. The rotation applies to all particles, including those whose spins deviate from the nominal polarization direction. A spin rotator rotates the nominal polarization from one specific incoming direction to a specific outgoing direction. This rotation is important only for the nominal polarization direction. In a spin rotator, how does a deviation from the nominal direction rotate by the action of the device does not matter. A Siberian snake is thus a much more intricate device than a spin rotator.

the spin precession direction $\hat{n}$ at any location in the accelerator.[31] In particular, it shows that $\hat{n}$ at the location exactly opposite to the snake must be longitudinal, $\hat{n} = \hat{z}$. At the entrance to the snake, Fig.6.4 shows $\hat{n}$ is indeed given by Eq.(6.52). Note that $\hat{n}$ has the meaning that if the stored beam has a net polarization, it must be along $\pm\hat{n}$ because any initial polarization perpendicular to $\hat{n}$ will smear out to zero as particles precess around $\hat{n}$ independently of one another. Note also that the spin tune is independent of the choice of observation point in the accelerator.

The simplest type 1 snake is a solenoid. The required strength is $B_s \ell/(B\rho) = \pi/(1-a)$. This means $B_s\ell$ increases as beam energy increases. A solenoid snake therefore works only for low energy beams. For protons higher than several GeV, solenoid snakes become unpractical.

Another type of snake is to use multiple dipole magnets, whose fields are either along $\hat{x}$ or along $\hat{y}$, in such a way that their net effect is a rotation around $\hat{z}$ by an angle π. Compared with solenoid snakes, these snakes have the disadvantage that they distort the closed orbit of the beam. The advantage, however, is that their strengths do not increase with beam energy. There are many practical designs of this type of snakes. We will only mention a couple of designs later. Suffice it to say here that this snake design works at high energies because the needed strengths $B\ell$ are independent of beam energy. On the other hand, they do not work at low energies because the orbit distortion associated with these transverse bending magnets becomes excessive.

Siberian snake of type 2

If the device rotates the spin by an angle π around the $\hat{x}$-axis, this is called Siberian snake of type 2. The total spin rotation observed at the entrance of the snake is

$$M_{\text{tot}} = e^{-\frac{i}{2}\vec{\sigma}\cdot 2\pi a\gamma \hat{y}} e^{-\frac{i}{2}\vec{\sigma}\cdot\pi\hat{x}} = -i[\sigma_x \cos(\pi a\gamma) - \sigma_z \sin(\pi a\gamma)] \qquad (6.53)$$

Again one finds $\nu_{\text{spin}} = K + \frac{1}{2}$. The rotation direction at the point exactly opposite to the snake is $\hat{n} = \hat{x}$.

General Siberian snake

Consider a device that rotates the spin by π around any axis $\hat{\phi}$. The total spin rotation can be found to be

$$M_{\text{tot}} = -i[(\vec{\sigma}\cdot\hat{\phi})\cos(\pi a\gamma) - i(\hat{y}\cdot\hat{\phi})I\sin(\pi a\gamma) + \vec{\sigma}\cdot(\hat{y}\times\hat{\phi})\sin(\pi a\gamma)] \quad (6.54)$$

This device constitutes a Siberian snake (i.e. $\nu_{\text{spin}} = K + \frac{1}{2}$) if and only if $\hat{\phi}\perp\hat{y}$, in which case the middle term on the right hand side of Eq.(6.54) vanishes.

> *Exercise* 13 Find the net polarization direction around the accelerator for the general snake. What is $\hat{n}$ at the point exactly opposite to the snake?

---

[31]The reason we know Fig.6.4(c) has this distinction, and Figs.6.4(a) and (b) do not, is that the spin in Fig.6.4(c) repeats itself turn after turn.
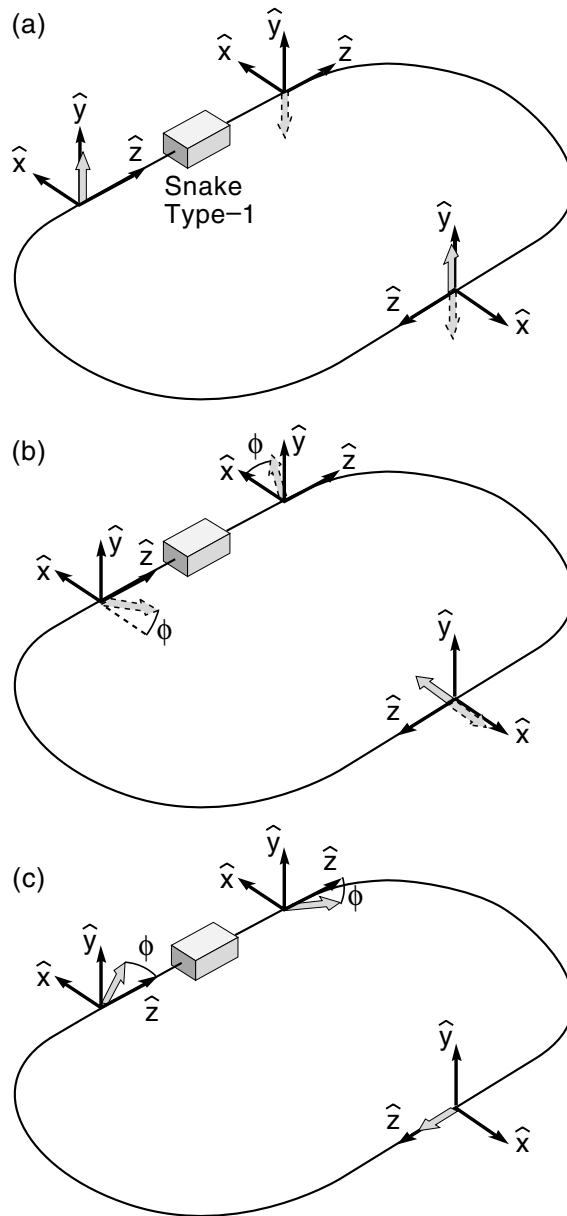
Figure 6.4: Spin motion in a storage ring with Siberian snake of type-1 [2]. (a), (b) are motion of spin perpendicular to the equilibrium direction, demonstrating the spin tune is 1/2. (c) shows the equilibrium spin direction. The angle $\phi = a\gamma/2$ lies in the x-z plane.

$$\hat{n}(\theta) = \hat{\phi}\cos[a\gamma(\theta - \pi)] + \hat{y} \times \hat{\phi}\sin[a\gamma(\theta - \pi)]$$

where $\theta = \pi$ exactly opposite to the snake.

Exercise 14 A special type of snake design utilizes twisted helical dipole magnets. Consider a helical dipole with

$$\vec{B}(s) = B_0(\sin\frac{2\pi s}{\lambda}, 0, \cos\frac{2\pi s}{\lambda})$$

with $0 < s < \lambda$. This magnet constitutes a full twist helical magnet. Show that the spin map for this magnet is

$$M = \cos\frac{\phi}{2} - i(\sigma_2 + \xi\sigma_3)\sin\frac{\phi}{2} \qquad (6.55)$$

where $\xi = (a + \frac{1}{\gamma})\frac{eB_0\lambda}{2\pi}$ and $\phi = 2\pi(\sqrt{1 + \xi^2} - 1)$.

Double Siberian snake

With a single Siberian snake in the accelerator, the equilibrium beam polarization is perpendicular to $\hat{y}$ and executes rapid precession going through the arcs. This is an undesirable arrangement. For one reason, the polarization is going to be sensitive to the energy spread of the beam. It is possible to avoid this by installing two snakes at opposite locations in the accelerator. For example, if we have one type-1 snake and one type-2 snake, we have Fig.6.5, and the equilibrium polarization direction is $\hat{y}$ in one half of the accelerator and $-\hat{y}$ in the other half. The spin rotation of this accelerator is

$$M_{\text{tot}} = e^{-\frac{i}{2}\vec{\sigma}\cdot\pi a\gamma\hat{y}}e^{-\frac{i}{2}\vec{\sigma}\cdot\pi\hat{z}}e^{-\frac{i}{2}\vec{\sigma}\cdot\pi a\gamma\hat{y}}e^{-\frac{i}{2}\vec{\sigma}\cdot\pi\hat{x}} = -i\sigma_y \qquad (6.56)$$

The spin tune is still $K + \frac{1}{2}$.[32]

Exercise 15 Find the spin tune when the type-1 and the type-2 snakes are not located exactly opposite to each other, but by an arc with $2\pi\alpha$ bending and another arc with $2\pi(1 - \alpha)$ bending.

Exercise 16 What if both snakes in the double snake design are of type-1?

6.7 Partial Siberian Snakes

Sometimes there may not be sufficient space (or budget) to install a full Siberian snake. In this case, one may consider a partial snake. It rotates the spin by an

---

[32]Incidentally, Fig.6.5 serves as an illustration of the difference between a Siberian snake and a spin rotator. The two snakes in Fig.6.5 are distinctly different as far as Siberain snakes go, but as spin rotators, they are the same.
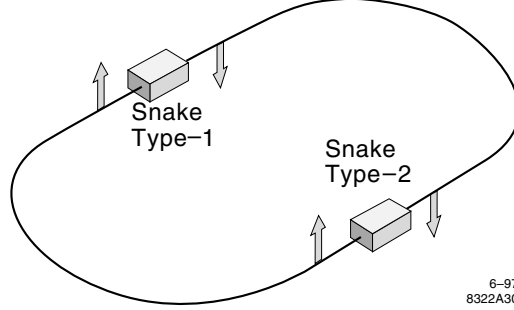
Figure 6.5: A storage ring with double Siberian snakes.

angle ϕ where $\phi < \pi$. Let the rotation axis be $\hat{\phi}$ and consider a single snake in the accelerator. The spin tune is determined by

$$\cos \pi \nu_{\text{spin}} = \cos(\pi a \gamma) \cos \frac{\phi}{2} - (\hat{y} \cdot \hat{\phi}) \sin(\pi a \gamma) \sin \frac{\phi}{2} \qquad (6.57)$$

If the snake rotation axis $\hat{\phi} \perp \hat{y}$, we have

$$\cos \pi \nu_{\text{spin}} = \cos(\pi a \gamma) \cos \frac{\phi}{2} \qquad (6.58)$$

Figure 6.6 shows the spin tune as a function of $a\gamma$. When $\phi = 0$, we have $\nu_{\text{spin}} = a\gamma$. When $\phi = \pi$, we have a full snake with $\nu_{\text{spin}} = K + \frac{1}{2}$. When $\phi < \pi$, we have a partial snake. The spin tune has stopbands around each integer with a stopband width of

$$\Delta \nu_{\text{spin}} = \pm \frac{\phi}{2\pi} \qquad (6.59)$$

It is clear from Fig.6.6 that a partial snake avoid integer (imperfection) resonances even with a rather modest value of ϕ because the spin tune will now never be equal to an integer. A 10% snake for example can help greatly in avoiding the imperfection resonances. If ϕ is sufficiently large, the intrinsic resonances can be avoided as well. A 20% snake for example can be used to avoid intrinsic resonances for ν_y (fractional part) up to ± 0.1. Solenoids become a practical partial snake because the needed strength becomes accessible, up to modestly high energy proton synchrotrons.

Exercise 17 Find the polarization direction with a partial snake.
Solution

$$\hat{n} = \hat{x} \sin[(\pi - \theta)a\gamma] \sin \frac{\phi}{2} + \hat{y} \sin(\pi a \gamma) \cos \frac{\phi}{2} + \hat{z} \cos[(\pi - \theta)a\gamma] \sin \frac{\phi}{2}$$
$$(6.60)$$

135
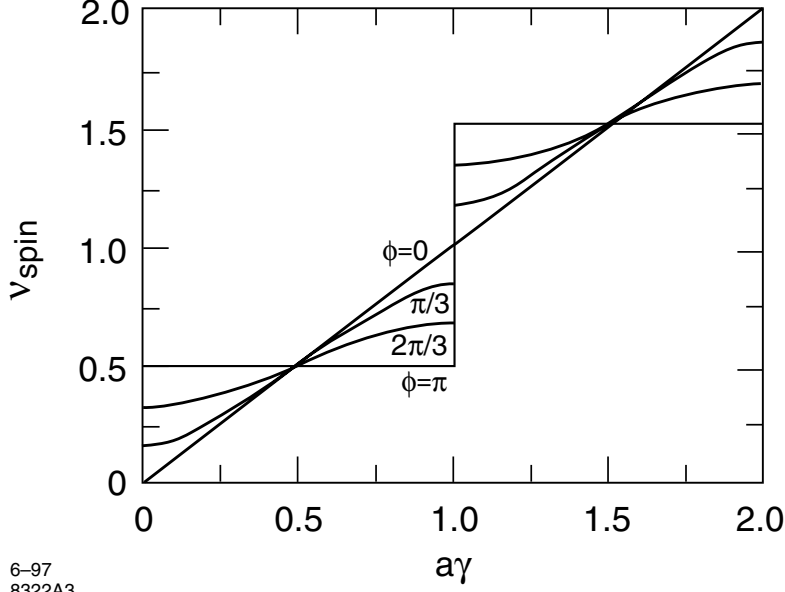
Figure 6.6: Spin tune $\nu_{\rm spin}$ as a function of $a\gamma$ for partial Siberian snakes. The cases $\phi = 0, \pi/3, 2\pi/3$, and π correspond to no snake, 1/3 snake, 2/3 snake, and full snake, respectively.

6.8   Depolarization Due to Snakes

A snake, whether full or partial, however, has also a depolarization mechanism. Each time an integer resonance is crossed, there is some loss of polarization. Even though the spin tune is far away from an integer, the perturbation of a snake – rotation by as much as π! – is huge. To see this quantitatively, consider a type-1 snake with rotation around $\hat{z}$ by an angle ϕ. Spin precession can be described by Eq.(6.14) with

$$\vec{h} = -a\gamma\hat{y} + \phi\hat{z}\delta_p(\theta) \tag{6.61}$$

where $\delta_p(\theta)$ is the periodic δ-function with period 2π. In spinor language, we have Eqs.(6.23-6.24) with

$$\vec{h} \cdot \vec{\sigma} = \begin{bmatrix} -a\gamma & \phi\delta_p(\theta) \\ \phi\delta_p(\theta) & a\gamma \end{bmatrix} \tag{6.62}$$

From Eq.(6.29-6.30), we then find the integer resonance strength

$$\epsilon = \frac{1}{2\pi} \int_0^{2\pi} d\theta e^{-iK\theta} \phi\delta_p(\theta) = \frac{\phi}{2\pi} \tag{6.63}$$

136

We apply the Froissart-Stora equation and find that there is a loss of polarization each time when $a\gamma$ crosses an integer during acceleration,

$$\frac{S(\infty)}{S(-\infty)} = 2e^{-\phi^2/8\pi\alpha} - 1 \qquad (6.64)$$

With a full snake, the resonance strength is very large, $\epsilon = 1/2$, and each crossing means the spin is flipped. The loss of polarization is very small. When the snake is partial, this is no longer true, and one has to be careful not to cross the integer resonances too fast.

Exercise 18 Froissart-Stora equation was derived earlier assuming the initial polarization is in the $\hat{y}$ direction. With a type-1 snake, the initial polarization is no longer along $\hat{y}$. Show that the F-S equation still applies, as we did with Eq.(6.64).

Exercise 19 Equation (6.61) applies when the snake strength is constant. What happens if the snake precession angle is $\phi \sin \nu_1 \theta \delta_p(\theta)$ where ν_1 is the spin modulation tune? Show that there are resonances at $a\gamma = K \pm \nu_1$.

Exercise 20 Consider a snake which is a combination of type-1 and type-2, and whose spin precession angle is time-dependent as $\phi(\hat{x}\cos\nu_1\theta - \hat{z}\sin\nu_1\theta)\delta_p(\theta)$. Show that there are resonances at $a\gamma = K + \nu_1$. What happens to the resonances $a\gamma = K - \nu_1$? What happens if the snake has precession angle $\phi(\hat{x}\cos\nu_1\theta + \hat{z}\sin\nu_1\theta)\delta_p(\theta)$?

6.9 Siberian Snake Designs

A large number of snake designs have been invented. Most of them consist of alternating horizontal and vertical bending dipoles whose net effect on spin is as prescribed for a Siberian snake of the type needed, while its net effect on orbit is made to vanish. We designate a bending magnet by $(\phi, \hat{\phi})$ where ϕ is the spin precession angle, and $\hat{\phi}$ is the spin precession axis, which is the same as the magnetic field direction. Then one possible type-1 snake design is

$$(\frac{\pi}{2},\hat{x})(\frac{\pi}{2},-\hat{x})(\frac{\pi}{2},\hat{y})(\frac{\pi}{2},-\hat{x})(\pi,-\hat{y})(\frac{\pi}{2},\hat{x})(\frac{\pi}{2},\hat{y}) \qquad (6.65)$$

Figure 6.7 shows the design, where H and V means horizontal and vertical bending dipoles, and the orbital angle θ is chosen such that the spin precesses by $\pi/2$. The x- and y-trajectories of the beam are shown. For protons, we have

$$\theta = \frac{B\ell}{(B\rho)} = \frac{\pi}{2a\gamma}, \qquad B\ell = 2.747 \text{ T}-\text{m} \qquad (6.66)$$

Note that, as emphasized before and seen in Fig.6.1, the spin precession is relative to the rotating coordinate system. In absolute space, the spin precesses by $(a\gamma + 1)\theta$. Note also that (also mentioned before) the needed snake magnet strengths are independent of the beam energy.

Figure 6.7: A design of type-1 snake. The middle and the bottom curves are the vertical and the horizontal orbital excursions. The maximum excursions are $\approx 5\ell\theta/2$ horizontally and $\approx 3\ell\theta$ vertically.

Exercise 21 Show that the design (6.65) constitutes a full type-1 Siberian snake.

The condition of no net orbital effect, however, is not necessary for a Siberian snake. To save space for accelerator, for example, it may be useful to incorporate part of the horizontal bends in the snake. We give below one possible type-2 snake design by Derbenev which contains a net horizontal bend. The design consists of four magnets:

$$(\phi, \hat{n}_+)(\phi, \hat{n}_-)(\phi, \hat{n}_-)(\phi, \hat{n}_+)$$
$$\hat{n}_\pm = \pm\hat{x}\sin\alpha + \hat{y}\cos\alpha \tag{6.67}$$

These magnets are tilted in the x-y plane by angles $\pm\alpha$ as sketched in Fig.6.8. Their strengths are all the same, precessing the spin by an angle ϕ. The net spin rotation is

$$M_{\text{tot}} = e^{-\frac{i}{2}\vec{\sigma}\cdot\phi\hat{n}_+}e^{-\frac{i}{2}\vec{\sigma}\cdot\phi\hat{n}_-}e^{-\frac{i}{2}\vec{\sigma}\cdot\phi\hat{n}_-}e^{-\frac{i}{2}\vec{\sigma}\cdot\phi\hat{n}_+} \tag{6.68}$$

Let Φ and $\hat{n}$ be the net precession angle and axis, then Eq.(6.21) gives

$$\hat{n}\sin\frac{\Phi}{2} = 2\cos\alpha\sin\phi\left[-\hat{x}\sin^2\frac{\phi}{2}\sin 2\alpha + \hat{y}\left(\cos^2\frac{\phi}{2} - \cos 2\alpha\sin^2\frac{\phi}{2}\right)\right]$$

$$\cos\frac{\Phi}{2} = \cos^2\phi - \cos 2\alpha\sin^2\phi \tag{6.69}$$

Figure 6.8: A type-2 snake with net horizontal bending.

To make a full Siberian snake of type 2, we require $\Phi = \pi$ and $\hat{n} = \hat{x}$. This means we must choose α and ϕ so that

$$\cot^2 \phi = \cot^2 \frac{\phi}{2} = \cos 2\alpha \tag{6.70}$$

One solution is

$$\phi = \frac{2\pi}{3}, \qquad \alpha = \frac{1}{2}\cos^{-1}\frac{1}{3} = 35°15' \tag{6.71}$$

Exercise 22 Verify Eq.(6.69-6.71).

Exercise 23 In the design of snakes, the following theorem comes handy sometimes: if the magnet arrangement has a mirror symmetry, and if the spin precession axes $\hat{\phi}_i$ of these magnets are all perpendicular to some direction $\hat{k}$, then the axis of the total precession is also perpendicular to $\hat{k}$. (a) Prove this theorem. (b) Use this theorem to explain why design (6.67) cannot be a type-1 snake no matter how α and ϕ are chosen.

References

[1] E.D. Courant and R.D. Ruth, BNL 51270 (1980).

[2] B.W. Bontague, Phys. Reports, 113, 1 (1984).

[3] T. Roser, Proc. Workshop on Siberian snakes and depolarizing techniques, Minneapolis, 1989, p. 1442.

[4] Ya.S. Derbenev, UM HE 97-07 (1997).

[5] Abramowitz and Stegun, Handbook of Mathematical Functions, p.693.

7 Symplectic Approximation of Maps

Linear motion in (x, x', y, y') can be described by maps in matrix form. For example, the map for a quadrupole is

$$M = \begin{bmatrix} \cos kL & \frac{1}{k}\sin kL & 0 & 0 \\ -k\sin kL & \cos kL & 0 & 0 \\ 0 & 0 & \cosh kL & \frac{1}{k}\sinh kL \\ 0 & 0 & k\sinh kL & \cosh kL \end{bmatrix} \tag{7.1}$$

where $k = \sqrt{G/B_0\rho}$.

Often a good approximation can be obtained by letting $L \to 0$, $G/(B_0\rho) \to \infty$, while holding $1/f \equiv GL/(B_0\rho)$ fixed. We then obtain the short-magnet approximation of Eq.(7.1),

$$M \approx \begin{bmatrix} 1 & 0 & 0 & 0 \\ -\frac{1}{f} & 1 & 0 & 0 \\ 0 & 0 & 1 & 0 \\ 0 & 0 & \frac{1}{f} & 1 \end{bmatrix} \tag{7.2}$$

In the absence of x-y coupling, the matrices M degenerate into two 2×2 blocks. One can treat the x and y motions separately by studying their respective 2×2 blocks.

There is a theorem which says that

$$\det M = 1 \tag{7.3}$$

This theorem is true whether M is 2×2, 4×4, or 6×6. It is a consequence of another more powerful theorem of *symplecticity* condition, and is related to the conservation of phase space area. For a linear 1-D case with 2×2 matrices, the symplecticity condition holds if and only if Eq.(7.3) holds. For higher dimensions, the symplecticity condition implies Eq.(7.3), but not vice versa. Note that theorem (7.3) is true in general; it is valid even if the motion is unstable.

Obviously, Eqs.(7.1) and (7.2) satisfy Eq.(7.3). As a check of the internal consistency, note that if a map consists of many segments, the condition that matrices of all segments have det=1 leads to the condition that the total matrix must also have det=1. This is internally consistent because the total matrix must also represent a map of the dynamic system and therefore has to be symplectic.

Consider now a slice of the quadrupole magnet from position s to position $s + \Delta s$. The map for the x motion is

$$M_{s\to s+\Delta s} = \begin{bmatrix} \cos k\Delta s & \frac{1}{k}\sin k\Delta s \\ -k\sin k\Delta s & \cos k\Delta s \end{bmatrix} \tag{7.4}$$

One maybe tempted to Taylor expand this matrix in terms of the small quantity Δs. This leads to

$$M_{s\to s+\Delta s} = \begin{bmatrix} 1 & 0 \\ 0 & 1 \end{bmatrix} + \Delta s \begin{bmatrix} 0 & 1 \\ -k^2 & 0 \end{bmatrix} + \Delta s^2 \begin{bmatrix} -\frac{k^2}{2} & 0 \\ 0 & -\frac{k^2}{2} \end{bmatrix} + \cdots \tag{7.5}$$

141

Keeping only the leading term is not a very interesting thing to do because it loses all the physics introduced by the quadrupole. Keeping up to the Δs term, i.e.

$$M_{s \to s + \Delta s} \approx \begin{bmatrix} 1 & \Delta s \\ -k^2 \Delta s & 1 \end{bmatrix} \tag{7.6}$$

constitutes a problem because it violates theorem (7.3). This exercise says that, if truncations must be performed, then they must be performed carefully. A brute force truncation might lead to violation of fundamental properties.

One reason nonsymplecticity is of concern is because if not used with caution, it may lead to erroneous conclusions. In particular, repeatedly iterating map (7.6) could lead to wrong conclusions in terms of the long term stability of the system. Note there is no objection if the map is approximate. The objection is that the map is nonsymplectic. So we need to explore ways to find approximations without sacrificing symplecticity, i.e. we need *symplectification* techniques.

One trick is to artificially add a $\mathcal{O}(\Delta s^2)$ term to Eq.(7.6) as follows:

$$M_{s \to s + \Delta s} \approx \begin{bmatrix} 1 & \Delta s \\ -k^2 \Delta s & 1 - k^2 \Delta s^2 \end{bmatrix} \tag{7.7}$$

Note that truncating Eq.(7.5) to $\mathcal{O}(\Delta s^2)$ would give a matrix

$$M_{s \to s + \Delta s} \approx \begin{bmatrix} 1 - \frac{1}{2} k^2 \Delta s^2 & \Delta s \\ -k^2 \Delta s & 1 - \frac{1}{2} k^2 \Delta s^2 \end{bmatrix} \tag{7.8}$$

which differs from (7.7). On the other hand, map (7.7) is symplectic (det=1), while map (7.8) is not (det$\neq$1), in spite of the fact that map (7.8) is more accurate than map (7.7).

If we consider a finite-but-thin quadrupole of length L and approximate its map by Eq.(7.6) with $\Delta s = L$, we get $\det M = 1 + \mathcal{O}(L^2)$. If we adopt Eq.(7.8), we get $\det M = 1 + \mathcal{O}(L^4)$. Both maps are nonsymplectic. But $\det M = 1$ exactly if we adopt (7.7). Eq.(7.7) is one way to "symplectify" the map.

Is there a physical meaning to Eq.(7.7)? The answer is yes. In fact, we are at this point launching onto the beginnings of two important topics: map symplectification and canonical integration. Both are active fields of research.

The physical meaning of Eq.(7.7) is seen as follows. One way to assure symplecticity is to model the quadrupole as a combination of interlacing drift spaces and lumped kicks. For example, one might model the quadrupole as sketched in Fig.7.1(a). In the drift region, the map is given by

$$\begin{bmatrix} 1 & L \\ 0 & 1 \end{bmatrix} \tag{7.9}$$

The lumped kick is obtained by concentrating the quadrupole strength to act as a δ-function kick to the passing particles. The matrix that describes that action is

$$\begin{bmatrix} 1 & 0 \\ -k^2 L & 1 \end{bmatrix} \tag{7.10}$$

142

The drift map (7.9) is symplectic — its determinant is equal to 1. It is a general property that lumped kicks give symplectic maps — matrix (7.10) has determinant of 1. By modeling an accelerator element (linear or nonlinear) as combination of drifts and lumped kicks, one obtains a symplectic model of the element. If the quadrupole is modeled as a drift followed by a kick, the total map for the quadrupole is

$$M = \begin{bmatrix} 1 & 0 \\ -k^2 L & 1 \end{bmatrix} \begin{bmatrix} 1 & L \\ 0 & 1 \end{bmatrix} = \begin{bmatrix} 1 & L \\ -k^2 L & 1 - k^2 L^2 \end{bmatrix} \tag{7.11}$$

which obviously has det=1. But Eq.(7.11) has just reproduced Eq.(7.7)! In other words, the artificial symplectification introduced in Eq.(7.7) could be a consequence of the particular *modeling* represented by Fig.7.1(a).
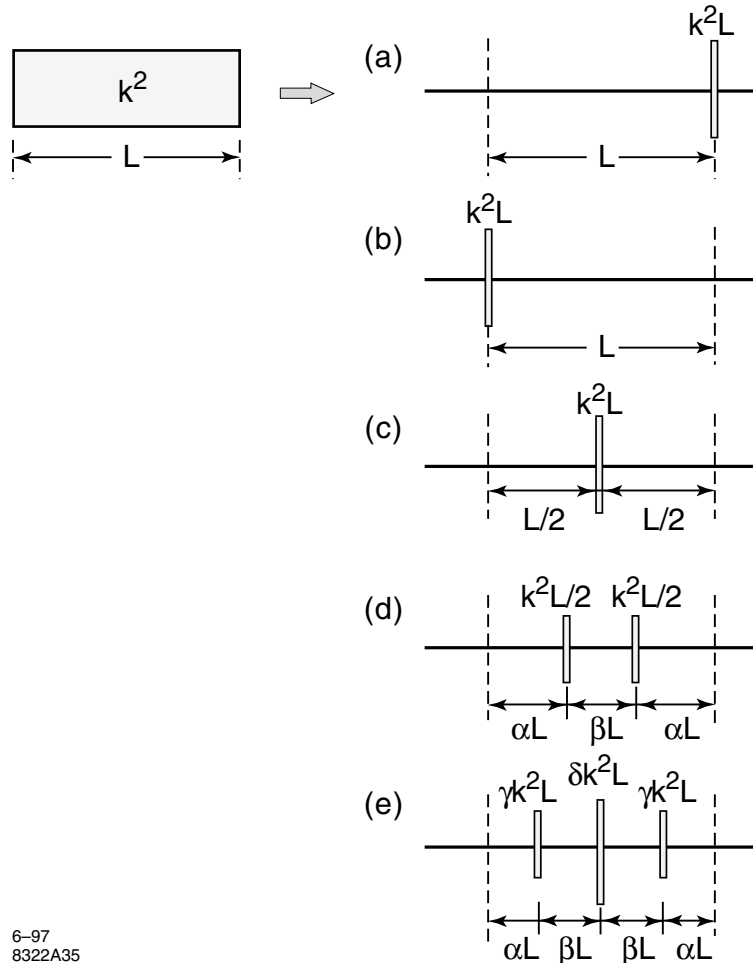
Figure 7.1: Symplectification Models.

143

This observation then opens up to other ways to symplectify. For example, the model of Fig.7.1(b) gives

$$M = \begin{bmatrix} 1 & L \\ 0 & 1 \end{bmatrix} \begin{bmatrix} 1 & 0 \\ -k^2 L & 1 \end{bmatrix} = \begin{bmatrix} 1 - k^2 L^2 & L \\ -k^2 L & 1 \end{bmatrix} \qquad (7.12)$$

which also has det $= 1$, and thus represents another way to symplectify map (7.6).

Both Figs.7.1(a) and (b), although exactly symplectic, give maps that are accurate only up to $\mathcal{O}(L)$ [leading error term is of order $\mathcal{O}(L^2)$]. One way to improve the accuracy of the map while maintaining its symplecticity is to consider Fig.7.1(c), the *thin-lens model*. It gives

$$\begin{aligned} M &= \begin{bmatrix} 1 & \frac{1}{2}L \\ 0 & 1 \end{bmatrix} \begin{bmatrix} 1 & 0 \\ -k^2 L & 1 \end{bmatrix} \begin{bmatrix} 1 & \frac{1}{2}L \\ 0 & 1 \end{bmatrix} \\ &= \begin{bmatrix} 1 - \frac{1}{2}k^2 L^2 & L - \frac{1}{4}k^2 L^3 \\ -k^2 L & 1 - \frac{1}{2}k^2 L^2 \end{bmatrix} \end{aligned} \qquad (7.13)$$

The thin-lens model is accurate up to order $\mathcal{O}(L^2)$, as can be shown by comparing (7.13) with the exact expression (7.1).

Numerical iteration of the maps (7.8), (7.11), (7.12), and (7.13) is shown respectively in Figs.7.2(c) through (f) for $k\Delta s = 0.2$. Fig.7.2(a) is a circle obtained using the exact map (7.4). Fig.7.2(f) is almost, but not quite, a circle. The deviation of Fig.7.2(f) from a circle will be shown in Fig.7.4(a) later. Figure 7.2(c), based on the nonsymplectic map (7.8), exhibits an outward spiral motion, although the spiraling is slower than that shown in Fig.7.2(b), based on Eq.(7.6). For long term stability purposes, enforcing the symplecticity condition is important. If a map is approximate but symplectic, the contours of particle trajectory in phase space maybe slightly distorted, but the long-term stability of the motion is preserved, as shown in Figs.7.2(d,e,f). This is not true if the symplecticity of the map is compromised.

A symplectic model, such as (7.11), (7.12), or (7.13), is extremely useful to model accelerator elements. In the quadrupole example above, these models allow carrying out the mapping without the time-consuming trigonometric functions. But more importantly, when the accelerator element is nonlinear, we often do not have a closed form expression for its map as we do in the quadrupole example. These nonlinear maps have to be obtained by ray tracing. For long-term stability considerations, it is impractical to trace with hundreds of steps per element because of computer limitations. One therefore searches for efficient ways to model an element, which are accurate and, for purpose of long term tracking, are also symplectic. The quadrupole example is just an illustration of this search activity. Models in Fig.7.1 are all applicable to thick nonlinear elements.

One may proceed to consider Fig.7.1(d) with the hope of finding a model that represents the quadrupole to order $\mathcal{O}(L^3)$. Obviously one has the condition
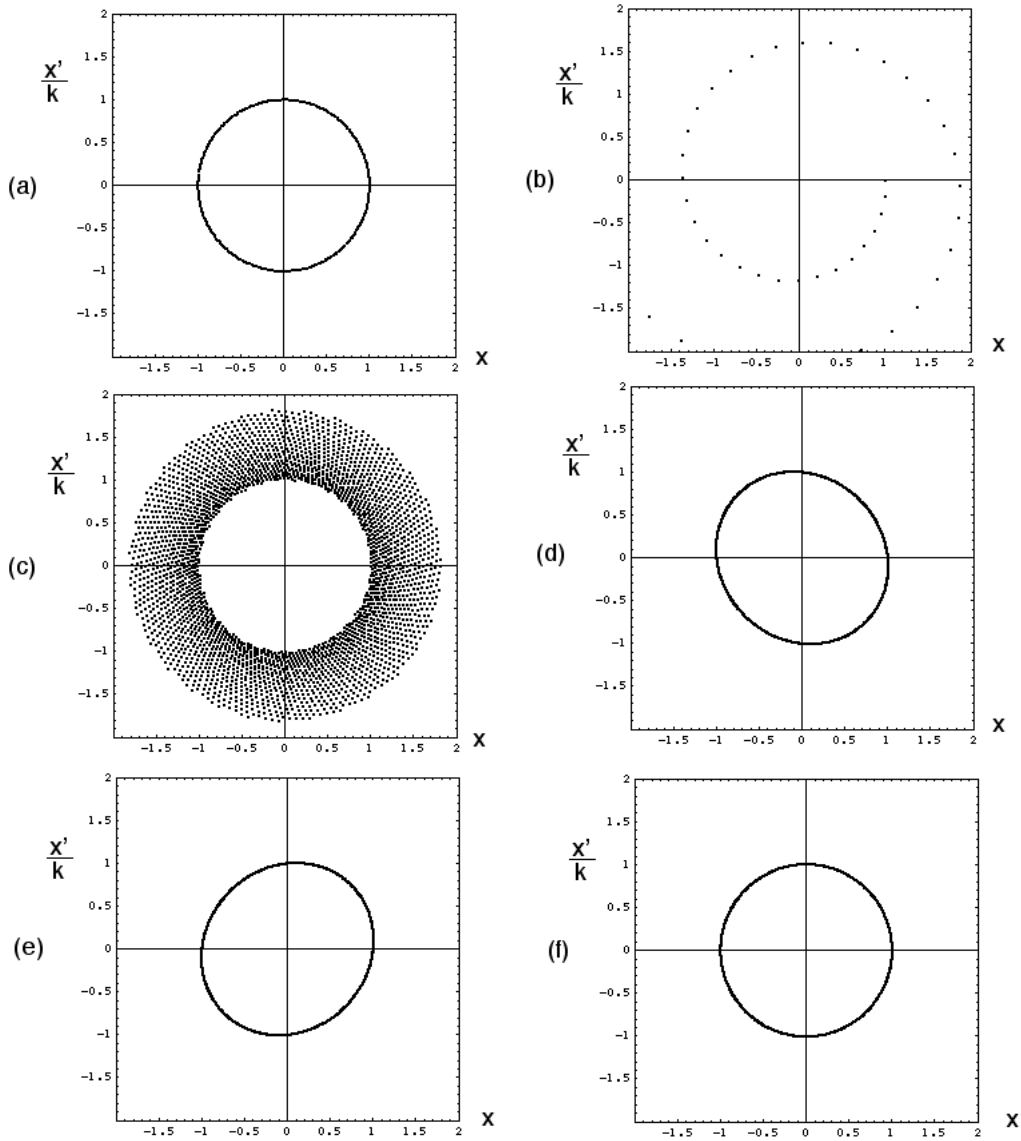
Figure 7.2: Phase space trajectories of a particle traversing a quadrupole as predicted using various tracking algorithms. (a) the exact map (7.4), (b) non-symplectic map (7.6), (c) nonsymplectic map (7.8), (d) symplectic map (7.11), (e) symplectic map (7.12), (f) symplectic thin-lens map (7.13).

$2\alpha + \beta = 1$. The matrix is

$$
M \;=\; \begin{bmatrix} 1 & \alpha L \\ 0 & 1 \end{bmatrix} \begin{bmatrix} 1 & 0 \\ -\frac{1}{2}k^2 L & 1 \end{bmatrix} \begin{bmatrix} 1 & \beta L \\ 0 & 1 \end{bmatrix} \begin{bmatrix} 1 & 0 \\ -\frac{1}{2}k^2 L & 1 \end{bmatrix} \begin{bmatrix} 1 & \alpha L \\ 0 & 1 \end{bmatrix}
$$

$$= \begin{bmatrix} 1 - \frac{1}{2}k^2L^2 + \frac{1}{4}\alpha\beta k^4L^4 & L - \alpha(\alpha+\beta)k^2L^3 + \frac{1}{4}\alpha^2\beta k^4L^5 \\ -k^2L + \frac{1}{4}\beta k^4L^3 & 1 - \frac{1}{2}k^2L^2 + \frac{1}{4}\alpha\beta k^4L^4 \end{bmatrix}(7.14)$$

Eq.(7.14) does give $\det M = 1$. But this map cannot represent the quadrupole to order $\mathcal{O}(L^3)$. Compared with Eq.(7.1), in order to represent the quadrupole to order $\mathcal{O}(L^3)$, we need

$$\alpha(\alpha + \beta) = \frac{1}{6}$$
$$\frac{1}{4}\beta = \frac{1}{6}$$
$$2\alpha + \beta = 1 \qquad (7.15)$$

which, unfortunately, does not have a solution.

Interestingly enough, it is possible to consider Fig.7.1(e) to obtain a map which is correct to order $\mathcal{O}(L^4)$ [errors of order $\mathcal{O}(L^5)$]. We obviously have, to begin with, the conditions

$$2\alpha + 2\beta = 1$$
$$2\gamma + \delta = 1 \qquad (7.16)$$

The map is given by

$$M = \begin{bmatrix} 1 & \alpha L \\ 0 & 1 \end{bmatrix}\begin{bmatrix} 1 & 0 \\ -\gamma k^2 L & 1 \end{bmatrix}\begin{bmatrix} 1 & \beta L \\ 0 & 1 \end{bmatrix}\begin{bmatrix} 1 & 0 \\ -\delta k^2 L & 1 \end{bmatrix}$$
$$\times \begin{bmatrix} 1 & \beta L \\ 0 & 1 \end{bmatrix}\begin{bmatrix} 1 & 0 \\ -\gamma k^2 L & 1 \end{bmatrix}\begin{bmatrix} 1 & \alpha L \\ 0 & 1 \end{bmatrix}$$

$$(7.17)$$

$$= \begin{bmatrix} 1 - \frac{1}{2}k^2L^2 + \beta\gamma(\alpha + \frac{1}{2}\delta)k^4L^4 & L - (\frac{1}{4}\delta + \alpha\gamma + 2\alpha\beta\gamma)k^2L^3 \\ \quad -\alpha\beta^2\gamma^2\delta k^6L^6 & \quad +2\alpha\beta\gamma(\alpha\gamma + \frac{1}{2}\delta)k^4L^5 - \alpha^2\beta^2\gamma^2\delta k^6L^7 \\ & \\ -k^2L + \beta\gamma(1+\delta)k^4L^3 & 1 - \frac{1}{2}k^2L^2 + \beta\gamma(\alpha + \frac{1}{2}\delta)k^4L^4 \\ \quad -\beta^2\gamma^2\delta k^6L^5 & \quad -\alpha\beta^2\gamma^2\delta k^6L^6 \end{bmatrix}$$

The conditions for (7.17) to represent the exact map to order $\mathcal{O}(L^4)$ are, in addition to (7.16),

$$\beta\gamma(\alpha + \frac{1}{2}\delta) = \frac{1}{24}$$
$$\beta\gamma(1 + \delta) = \frac{1}{6}$$
$$\frac{1}{4}\delta + \alpha\gamma + 2\alpha\beta\gamma = \frac{1}{6} \qquad (7.18)$$

Equations (7.16) and (7.18) [4 unknowns, 5 equations] do have solutions! In fact, one finds

$$\beta = \frac{1 - 2^{1/3}}{2(2 - 2^{1/3})} \approx -0.1756$$

$$\alpha = \frac{1}{2} - \beta = \frac{1}{2(2 - 2^{1/3})} \approx 0.6756$$

$$\gamma = \frac{1}{24\beta^2} = \frac{1}{2 - 2^{1/3}} \approx 1.3512$$

$$\delta = 1 - 2\gamma = -\frac{2^{1/3}}{2 - 2^{1/3}} \approx -1.7024 \tag{7.19}$$

Note that β and δ are negative. This means the model involves seven steps as shown in Fig.7.3. Following these 7 steps would yield a symplectic model of a thick quadrupole — or any thick nonlinear element — to order $\mathcal{O}(L^4)$.
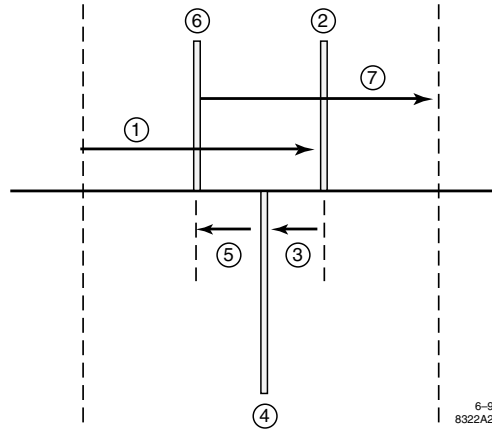
Figure 7.3: Seven steps in the 4-th order symplectic integration.

The map for a quadrupole is then obtained by substituting Eq.(7.19) into Eq.(7.17),

$$M = \begin{bmatrix} 1 - \frac{1}{2}k^2L^2 + \frac{1}{24}k^4L^4 & L - \frac{1}{6}k^2L^3 + \frac{1 - 2^{1/3}}{24(2 - 2^{1/3})^2}k^4L^5 \\ + \frac{2^{1/3}}{48(2 - 2^{1/3})^3}k^6L^6 & + \frac{2^{1/3}}{96(2 - 2^{1/3})^4}k^6L^7 \\ \\ -k^2L + \frac{1}{6}k^4L^3 & 1 - \frac{1}{2}k^2L^2 + \frac{1}{24}k^4L^4 \\ + \frac{2^{1/3}}{24(2 - 2^{1/3})^2}k^6L^5 & + \frac{2^{1/3}}{48(2 - 2^{1/3})^3}k^6L^6 \end{bmatrix} \tag{7.20}$$

It can be explicitly checked that the determinant of (7.20) is 1. This M is correct up to $\mathcal{O}(L^4)$. By introducing artificial terms of the orders of $\mathcal{O}(L^5)$, $\mathcal{O}(L^6)$, and $\mathcal{O}(L^7)$, therefore, we have symplectified the map. See Exercises 11 and 12 for more discussions on this point.

These explicit canonical integration techniques[33] give symplectic models of thick elements, and are most useful for particle tracking purposes. Note that most tracking programs use kick approximation of one kind or another. One

---

[33]These are called *explicit* techniques because all quantities are evaluated directly from previously known quantities and no implicit numerical inversion is required.

often-used example is the thin-lens model, which is a "2nd order explicit canonical integration". Another example is the ray tracing model, which is typically done with a first order integration but acquires accuracy by slicing the element into a large number of steps. As mentioned before, this requires extensive computer time and is not practical for long term stability studies of large accelerators. Table 1 gives the various canonical integration techniques for an accelerator element (linear or nonlinear) of strength S and length L. For a quadrupole, we have $S = k^2$. Exercise 13 shows that the popular Runge-Kutta algorithm is nonsymplectic.

Table 1: Various techniques of explicit canonical integration for an accelerator element of strength S and length L. The symbol (L) means a drift length L. The symbol (SL) means a kick of integrated strength (SL). Values of $\alpha, \beta, \gamma, \delta$ are given by Eq.(7.19). See also Eq.(7.57) for a 6-th order integration.

Integrator	Model	Error
1st order	$(L)(SL)$	$\mathcal{O}(L^2)$
1st order	$(SL)(L)$	$\mathcal{O}(L^2)$
Ray tracing	$(\frac{L}{n})(\frac{SL}{n}) \cdots$ repeat n times	$\mathcal{O}(\frac{L^2}{n})$
2nd order(thin-lens)	$(\frac{L}{2})(SL)(\frac{L}{2})$	$\mathcal{O}(L^3)$
Ray tracing	$(\frac{L}{2n})(\frac{SL}{n})(\frac{L}{2n}) \cdots$ repeat n times	$\mathcal{O}(\frac{L^3}{n^2})$
4th order	$(\alpha L)(\gamma SL)(\beta L)(\delta SL)(\beta L)(\gamma SL)(\alpha L)$	$\mathcal{O}(L^5)$
Ray tracing	$(\frac{\alpha L}{n})(\frac{\gamma SL}{n})(\frac{\beta L}{n})(\frac{\delta SL}{n})(\frac{\beta L}{n})(\frac{\gamma SL}{n})(\frac{\alpha L}{n}) \cdots$ repeat n times	$\mathcal{O}(\frac{L^5}{n^4})$

Note that symmetry always helps in providing one order higher accuracy. Dividing an element into many steps also improves the accuracy. Note also that the technique applies to integration in general, not only to accelerator elements.

In Figs.7.4(a) and (b), we compare the tracking results using the thin-lens map (7.13) and the 4-th order map (7.20). Plotted in Fig.7.4 is the quantity $A = \sqrt{x^2 + (x'/k)^2}$ as a function of iteration number for a particle with initial conditions $(x = 1, x'/k = 0)$ and $kL = 0.2$. The exact map (7.1) would give a constant $A = 1$. Figure 7.4 shows the numerical accuracy of the two approximate maps by computing A. Note the different vertical scales of the two graphs. Note also that in either map — both being symplectic — the stability of the particle motion is not in question; only the numerical accuracy is being compared.

Exercise 1 Still another symplectified form of a quadrupole, valid to order $\mathcal{O}(L^2)$, is

$$\begin{bmatrix} 1 - \frac{1}{2}k^2 L^2 & L \\ -k^2 L + \frac{1}{4}k^4 L^3 & 1 - \frac{1}{2}k^2 L^2 \end{bmatrix} \qquad (7.21)$$

What is its corresponding physical model?

Exercise 2 The two nonsymplectic tracking show exponential growth of spiraling amplitude. Associate the growth rate to the deviation of the matrices from unity.
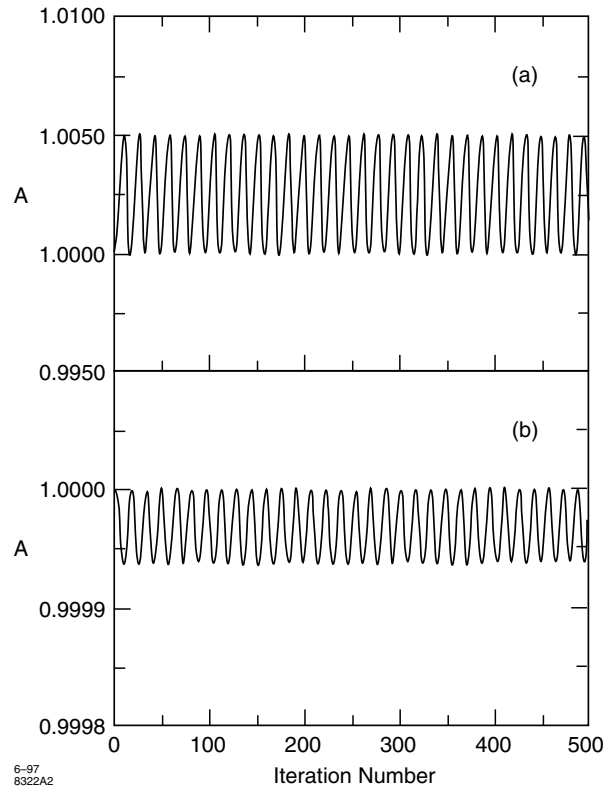
Figure 7.4: Tracking result showing amplitude as a function of time using symplectic integrators, (a) 2-nd order, (b) 4-th order.

<u>Solution</u> Determinant of Eq.(7.6) is $1 + (k\Delta s)^2$. Determinant of Eq.(7.8) is $1 + (k\Delta s)^4/4$. The amplitude grows or damps exponentially depending on whether the determinant is > 1 or < 1.

<u>Exercise</u> 3 Apply the thin-lens approximation to integrate the equation

$$x'' = f(x) \tag{7.22}$$

Show that the result is

$$
\begin{aligned}
x'(L) &\approx x'_0 + Lf(x_0 + \frac{L}{2}x'_0) \\
x(L) &\approx x_0 + \frac{L}{2}(x'_0 + x'(L))
\end{aligned}
\tag{7.23}
$$

Equation (7.23) is also called the *leap-frog algorithm*. Demonstrate explicitly the symplecticity of this map. To what order of L is the leap frog algorithm valid?

149

Solution The exact Taylor map gives

$$x(L) = x_0 + x_0'L + \frac{1}{2}f(x_0)L^2 + \frac{1}{6}x_0'f'(x_0)L^3 + \cdots \qquad (7.24)$$

The leap-frog algorithm gives

$$x(L) = x_0 + x_0'L + \frac{1}{2}f(x_0)L^2 + \frac{1}{4}x_0'f'(x_0)L^3 + \cdots \qquad (7.25)$$

The error terms are $\mathcal{O}(L^3)$.

Exercise 4 Equation (7.22) describes a conservative system. Its leap-frog map is symplectic. Consider a nonconservative system described by $x'' = f(x, x')$. Develop a leap-frog algorithm for this system. Examine its symplecticity.

Exercise 5 Consider a ray tracing model of a thick quadrupole. Let there be n steps, each of length L/n. The total map is given by

$$M = m^n \qquad (7.26)$$

where

$$m = \begin{bmatrix} 1 & 0 \\ -\frac{k^2 L}{n} & 1 \end{bmatrix} \begin{bmatrix} 1 & \frac{L}{n} \\ 0 & 1 \end{bmatrix} = \begin{bmatrix} 1 & \frac{L}{n} \\ -\frac{k^2 L}{n} & 1 - \frac{k^2 L^2}{n^2} \end{bmatrix} \qquad (7.27)$$

(a) Show that the matrix m can be written as

$$m = T \begin{bmatrix} e^{i\mu} & 0 \\ 0 & e^{-i\mu} \end{bmatrix} T^{-1} \qquad (7.28)$$

where $e^{\pm i\mu}$ are the eigenvalues of the matrix m with

$$\sin\frac{\mu}{2} = \frac{kL}{2n} \qquad (7.29)$$

and

$$T = \begin{bmatrix} \frac{1}{\sqrt{2}}e^{-i\mu/2} & i\frac{L}{n}\frac{e^{i\mu/2}}{\sqrt{2}\sin\mu} \\ i\sqrt{2}\frac{n}{L}\sin\frac{\mu}{2} & \frac{1}{\sqrt{2}\cos\frac{\mu}{2}} \end{bmatrix} \qquad (7.30)$$

(b) Use the property (7.28) to show

$$M = \begin{bmatrix} \frac{\cos(n-\frac{1}{2})\mu}{\cos\frac{\mu}{2}} & \frac{L}{n}\frac{\sin n\mu}{\sin\mu} \\ -2\frac{n}{L}\sin n\mu\tan\frac{\mu}{2} & \frac{\cos(n+\frac{1}{2})\mu}{\cos\frac{\mu}{2}} \end{bmatrix} \qquad (7.31)$$

(c) Show that the determinant of (7.31) is 1. Show also that when $n = 1$ and when $n \to \infty$, expression (7.31) becomes the expected results (7.11) and (7.1) respectively.

(d) Show explicitly that for finite n, the error terms are of the order $\mathcal{O}(L^2/n)$, as claimed in Table 1.

Solution Let m be eigenanalyzed as

$$m \begin{bmatrix} u_\pm \\ v_\pm \end{bmatrix} = e^{\pm i\mu} \begin{bmatrix} u_\pm \\ v_\pm \end{bmatrix} \qquad (7.32)$$

and choose normalization $u_+v_- - u_-v_+ = 1$. Then

$$T = \begin{bmatrix} u_+ & u_- \\ v_+ & v_- \end{bmatrix}, \quad \det T = 1 \qquad (7.33)$$

Exercise 6 Repeat the above exercise for the thin-lens model.

Solution Parametrize m as

$$m = \begin{bmatrix} a & b \\ c & a \end{bmatrix} \quad \text{with} \quad a^2 - bc = 1 \qquad (7.34)$$

Eigenanalyze m according to Eq.(7.32), where the eigenvalues are $e^{\pm i\mu}$ with $\cos\mu = a$. The matrix T is found using Eq.(7.33) to be

$$T = \begin{bmatrix} \frac{1}{\sqrt{2}} & i\frac{b}{\sqrt{2}\sin\mu} \\ i\frac{\sin\mu}{\sqrt{2}b} & \frac{1}{\sqrt{2}} \end{bmatrix}, \quad \det T = 1 \qquad (7.35)$$

Matrix m can then be written as (7.28) and we find

$$M = m^n = \begin{bmatrix} \cos n\mu & \frac{b}{\sin\mu}\sin n\mu \\ -\frac{\sin\mu}{b}\sin n\mu & \cos n\mu \end{bmatrix} \qquad (7.36)$$

It follows that $\det M = 1$, and that M reduces to proper limits when $n = 1$ and $n \to \infty$. For the thin-lens model, parameters a, b, and c are given by (7.13). We have $\sin\frac{\mu}{2} = kL/2n$. Substituting this value for μ and $b = \frac{L}{n} - \frac{1}{4n^3}k^2L^3$, it follows that model (7.36) agrees with the exact map with error terms of the order $\mathcal{O}(L^3/n^2)$.

Alternative solution A simpler derivation uses the fact that the map (7.36) can be written as a drift of length $-L/2n$ followed by the map (7.31) followed by a drift of length $L/2n$.

Exercise 7 Repeat the above for the 4th order integrator.

Solution Results (7.34-7.36) still hold. The only difference is the values of a, b, and c. The error terms are of the order $\mathcal{O}(L^5/n^4)$.

Exercise 8 Consider the 1-D motion in a thick sextupole with equation of motion

$$x'' = Sx^2 \qquad (7.37)$$

Work out the exact problem first. Compare the result with those obtained by the thin-lens, and the 4th order integrators.

Solution Integrating (7.37) gives a constant of the motion

$$C = \frac{1}{2}(x')^2 - \frac{1}{3}Sx^3 \tag{7.38}$$

which gives

$$x' = \pm\sqrt{2C + \frac{2}{3}Sx^3} \tag{7.39}$$

With the input coordinates (x_0, x'_0), we have $2C = (x'_0)^2 - \frac{2}{3}Sx_0^3$. The exit coordinates of the particle are described by $(x(L), x'(L))$, where $x(L)$ satisfies

$$\int_{x_0}^{x(L)} \frac{dx}{\pm\sqrt{(x'_0)^2 - \frac{2}{3}S(x_0^3 - x^3)}} = L \tag{7.40}$$

Eqs.(7.39) and (7.40) are the exact solution we are looking for.

Equation (7.39) can be used iteratively to obtain $x(s)$ and $x'(s)$ as Taylor expansion in s. These are approximate expressions for short s. Start with the 0-th order expression $x = x_0$. Insert this expression into (7.39) gives $x'(s) = x'_0$, which can be integrated to yield the 1-st order expression $x(s) = x_0 + x'_0 s$. Inserting this 1-st order expression into (7.39) then yields a 1-st order expression $x'(s) = x'_0 + Sx_0^2 s$, which can be integrated to give a 2-nd order expression of $x(s)$. Repeating this process gives

$$x(s) = x_0 + x'_0 s + \frac{1}{2}Sx_0^2 s^2 + \frac{1}{3}Sx_0 x'_0 s^3 + \frac{S}{12}(x_0'^2 + Sx_0^3)s^4 + \mathcal{O}(s^5)$$

$$x'(s) = x'_0 + Sx_0^2 s + Sx_0 x'_0 s^2 + \frac{S}{3}(x_0'^2 + Sx_0^3)s^3 + \frac{5}{12}S^2 x_0^2 x'_0 s^4 + \mathcal{O}(s^5)$$

$$\tag{7.41}$$

In comparison, the thin-lens approximation gives

$$x(L) = x_0 + x'_0 L + \frac{1}{2}Sx_0^2 L^2 + \frac{1}{2}Sx_0 x'_0 L^3 + \frac{1}{8}Sx_0'^2 L^4$$

$$x'(L) = x'_0 + Sx_0^2 L + Sx_0 x'_0 L^2 + \frac{1}{4}Sx_0'^2 L^3 \tag{7.42}$$

which agrees with (7.41) up to order $\mathcal{O}(L^2)$. Map (7.42) is symplectic. If the $\mathcal{O}(s^5)$ terms are truncated, map (7.41) is not symplectic, even though it is more accurate then Eq.(7.42).

In the 4th order integrator approximation, we use Mathematica to obtain[34]

$$x(L) = x_0 + x'_0 s + \frac{1}{2}Sx_0^2 s^2 + \frac{1}{3}Sx_0 x'_0 s^3 + \frac{S}{12}(x_0'^2 + Sx_0^3)s^4$$

---

[34]Explicit expressions of terms $\mathcal{O}(s^{6-22})$ and $\mathcal{O}(s^{6-22})$ are available but too long to be included in Eq.(7.43).

$$+0.0188747S^2x_0'x_0^2s^5 + \mathcal{O}(s^{6-22})$$

$$x'(L) = x_0' + Sx_0^2s + Sx_0x_0's^2 + \frac{S}{3}(x_0'^2 + Sx_0^3)s^3 + \frac{5}{12}S^2x_0^2x_0's^4$$

$$+ S^2x_0(0.231125x_0'^{\,2} - 0.437566Sx_0^3)s^5 + \mathcal{O}(s^{6-21}) \quad (7.43)$$

These agree with the exact expressions to the appropriate orders respectively but now higher orders (from 5th to 22nd order in s) are added artificially to symplectify the map. Symplecticity of the exact expressions (7.39-7.40), and the symplecticities of maps (7.42-7.43), can be checked by observing

$$\frac{\partial x(L)}{\partial x_0}\frac{\partial x'(L)}{\partial x_0'} - \frac{\partial x(L)}{\partial x_0'}\frac{\partial x'(L)}{\partial x_0} = 1 \qquad \text{exactly} \qquad (7.44)$$

Exercise 9 Show that the sextupole map (7.39-7.40) is symplectic.

Exercise 10 Consider the 1-D motion in a magnet with combined-function quadrupole and sextupole fields. Let the equation of motion be

$$x'' + k^2x = Sx^2 \qquad (7.45)$$

Give the second-order symplectic integration (thin-lens approximation) for the map from the entrance to the exit of this magnet. Let L be the length of the magnet. (a) Model both the quadrupole and the sextupole components as thin-lenses. Does the ordering of these thin-lens kicks matter? (b) Model the quadrupole component as a thick-lens magnet, and the sextupole component as thin-lens. (c) Show explicitly that the results obtained in (a) and (b) are symplectic. This exercise demonstrates the fact that the drifts in the models of Fig.7.1 can be replaced by any map which has exact (symplectic) solution, quadrupole being one example.

Exercise 11 In obtaining Eq.(7.19), we have first obtained an equation for β,

$$48\beta^3 - 24\beta^2 + 1 = 0 \qquad (7.46)$$

Equation (7.19) is then the real solution of (7.46). But there are also two other complex solutions given by

$$\beta_\pm = \frac{1}{4}\left(\frac{1}{2 - 2^{1/3}} \pm \frac{2^{2/3} - 1}{3^{1/2}2^{1/3}}i\right)$$

$$= 0.33780 \pm 0.06729i \qquad (7.47)$$

which in turn gives

$$\alpha = 0.16220 \mp 0.06729i$$
$$\gamma = 0.32441 \mp 0.13458i$$
$$\delta = 0.35118 \pm 0.26916i \qquad (7.48)$$

153

Choosing these complex values are legitimate symplectifications. The total matrix, however, now contains higher order symplectifying terms which are complex! Is this allowed?

Exercise 12 The 3rd order model Fig.7.1(d) assumed a symmetry around the mid-point of the accelerator element and we showed there was no solution. An extra free parameter can be introduced if the symmetry is sacrificed. Is there a solution for this asymmetric 3rd order integrator?

Solution Consider two kicks $-\delta k^2 L$ and $-\epsilon k^2 L$ spaced by three free spaces αL, βL and γL. For the system to describe a third order map, we find two solutions

$$
\begin{aligned}
\alpha &= \frac{\sqrt{3} \mp 3i}{6\sqrt{3} \mp 6i} = 0.25 \mp 0.14434i \\
\beta &= \frac{1}{2} \\
\gamma &= \frac{1}{4} \pm i\frac{1}{4\sqrt{3}} = 0.25 \pm 0.14434i \\
\delta &= \frac{\sqrt{3} \mp 3i}{3\sqrt{3} \mp 3i} = 0.5 \mp 0.28868i \\
\epsilon &= \frac{2\sqrt{3}}{3\sqrt{3} \mp 3i} = 0.5 \pm 0.28868i \qquad (7.49)
\end{aligned}
$$

There is no real solution and the resulting 3rd order map is necessarily complex.

Exercise 13 There are various often-used numerical integration techniques. Some of them are nonsymplectic. Beware! Take the *Runge-Kutta integration* for example. Consider the differential equation

$$
x'' = f(x, x', s) \qquad (7.50)
$$

Given $x(0)$, $x'(0)$ at $s = 0$, Runge-Kutta gives approximate expressions of $x(L)$ and $x'(L)$ at $s = L$ as

$$
\begin{aligned}
x(L) &\approx x(0) + Lx'(0) + \frac{1}{6}L(t_1 + t_2 + t_3) \\
x'(L) &\approx x'(0) + \frac{1}{6}(t_1 + 2t_2 + 2t_3 + t_4) \qquad (7.51)
\end{aligned}
$$

where

$$
\begin{aligned}
t_1 &= Lf[x(0), x'(0), 0] \\
t_2 &= Lf[x(0) + \frac{1}{2}Lx'(0), x'(0) + \frac{1}{2}t_1, \frac{1}{2}L] \\
t_3 &= Lf[x(0) + \frac{1}{2}Lx'(0) + \frac{1}{4}Lt_1, x'(0) + \frac{1}{2}t_2, \frac{1}{2}L] \\
t_4 &= Lf[x(0) + Lx'(0) + \frac{1}{2}Lt_2, x'(0) + t_3, L] \qquad (7.52)
\end{aligned}
$$

(a) Apply the Runge-Kutta technique to the x-motion in a quadrupole and show that

$$x(L) \approx x(0)\left[1 - \frac{1}{2}k^2L^2 + \frac{1}{24}k^4L^4\right] + \frac{1}{k}x'(0)\left[kL - \frac{1}{6}k^3L^3\right]$$

$$x'(L) \approx -kx(0)\left[kL - \frac{1}{6}k^3L^3\right] + x'(0)\left[1 - \frac{1}{2}k^2L^2 + \frac{1}{24}k^4L^4\right] \quad (7.53)$$

(b) Apply it to the case of a sextupole, Eq.(7.37), to obtain

$$
\begin{aligned}
x(L) &\approx x_0 + x_0'L + \frac{1}{2}Sx_0^2L^2 + \frac{1}{3}Sx_0x_0'L^3 + \frac{S}{12}(x_0'^2 + Sx_0^3)L^4 \\
&\quad + \frac{1}{24}S^2x_0^2x_0'L^5 + \frac{1}{96}S^3x_0^4L^6 \\
x'(L) &\approx x_0' + Sx_0^2L + Sx_0x_0'L^2 + \frac{S}{3}(x_0'^2 + Sx_0^3)L^3 + \frac{5}{12}S^2x_0^2x_0'L^4 \\
&\quad + S^2x_0\left(\frac{5}{24}x_0'^2 + \frac{1}{16}Sx_0^3\right)L^5 + \frac{1}{12}S^2x_0'\left(\frac{1}{2}x_0'^2 + x_0^3\right)L^6 \\
&\quad + \frac{1}{16}S^3x_0^2x_0'^2L^7 + \frac{1}{48}S^3x_0x_0'^3L^8 + \frac{1}{384}S^3x_0'^4L^9 \quad (7.54)
\end{aligned}
$$

(c) Show that the determinant of the Jacobian matrix for the transformation (7.53) is

$$1 - \frac{k^6L^6}{72} + \frac{k^8L^8}{576} \neq 1 \quad (7.55)$$

Similarly, for the transformation (7.54), the determinant is

$$
\begin{aligned}
1 &- \frac{1}{72}(2x_0'^2 - 9Sx_0^3)S^2L^6 + \frac{7}{36}x_0^2x_0'S^3L^7 + \frac{1}{144}x_0(7x_0'^2 + 15Sx_0^3)S^3L^8 \\
&+ \frac{1}{288}x_0'(-x_0'^2 + 46Sx_0^3)S^3L^9 + \frac{1}{576}x_p^2(45x_0'^2 + 16Sx_0^3)S^4L^{10} \\
&+ \frac{1}{288}x_0x_o'(4x_o'^2 + 13Sx_0^3)S^4L^{11} + \frac{1}{576}x_0^3(15x_0'^2 + 2Sx_0^3)S^5L^{12} \\
&+ \frac{1}{576}x_0^2x_0'(4x_0'^2 + 3Sx_0^3)S^5L^{13} + \frac{1}{1152}x_0x_0'^2(x_0'^2 + 3Sx_0^3)S^5L^{14} \\
&+ \frac{1}{2304}x_0^3x_0'^3S^6L^{15} \neq 1 \quad (7.56)
\end{aligned}
$$

In both (a) and (b), the Runge-Kutta integration is accurate to order $\mathcal{O}(L^4)$ but is not symplectic. The high order terms beyond 4th order in L in Eq.(7.54) [compare with Eq.(7.43)] do not make the map symplectic as can be checked against Eq.(7.44).

An alert reader might have noted that we have derived all the symplectic integrators in Table 1 using the linear quadrupole map. What if we have used a different map, e.g. a solenoid, or a nonlinear map? Would we get the same

155

integrators? The answer to this question is yes. It does not matter which map we use to derive the integrators. The underlying reason can be seen if one applies *Lie algebra* to the analysis.

I will not explore Lie algebra here, except to say that using Lie algebraic technique allows a systematic way to extend to higher order integrators. For example, a 6th order integrator is found to be as follows (notation the same as in Table 1):

$$(c_1 L)(d_1 SL)(c_2 L)(d_2 SL)(c_3 L)(d_3 SL)(c_4 L)(d_4 SL)(c_5 L)(d_5 SL)$$
$$\times (c_6 L)(d_6 SL)(c_7 L)(d_7 SL)(c_8 L)(d_8 SL)(c_9 L)(d_9 SL)(c_{10} L) \qquad (7.57)$$

where

$$d_1 = d_3 = d_7 = d_9 = \frac{1}{(2 - 2^{1/3})(2 - 2^{1/5})} \approx 1.58722$$

$$d_2 = d_8 = -\frac{2^{1/3}}{(2 - 2^{1/3})(2 - 2^{1/5})} \approx -1.99978$$

$$d_4 = d_6 = -\frac{2^{1/5}}{(2 - 2^{1/3})(2 - 2^{1/5})} \approx -1.82324$$

$$d_5 = \frac{2^{8/15}}{(2 - 2^{1/3})(2 - 2^{1/5})} \approx 2.29714$$

$$c_1 = c_{10} = \frac{1}{2(2 - 2^{1/3})(2 - 2^{1/5})} \approx 0.793612$$

$$c_2 = c_3 = c_8 = c_9 = \frac{1 - 2^{1/3}}{2(2 - 2^{1/3})(2 - 2^{1/5})} \approx -0.206277$$

$$c_4 = c_7 = \frac{1 - 2^{1/5}}{2(2 - 2^{1/3})(2 - 2^{1/5})} \approx -0.118009$$

$$c_5 = c_6 = -\frac{2^{1/5}(1 - 2^{1/3})}{2(2 - 2^{1/3})(2 - 2^{1/5})} \approx 0.23695 \qquad (7.58)$$

One can check that $\sum_i c_i = \sum_i d_i = 1$.

In Table 1, we have kicks interlaced by drifts. This is not necessary. Instead of drifts, one can have any map which has an exact expression. Most likely, this map with exact expression is a linear map. For example, in Exercise 10, we had a combined magnet with quadrupole and sextupole fields. One can have sextupole kicks interlaced by quadrupole maps. The fact that the interlacing map does not have to be drifts is also evident if one uses Lie algebra to hunt for symplectic integrators.

We see that the 2nd order simplectic integrator (thin-lens approximation) requires one lumped kick. The 4th order integrator requires 3 lumped kicks. The 6th order integrator requires 9 lumped kicks.

Exercise 14 Draw the 19-step, 6th order symplectic integration model according to Eqs.(7.57) and (7.58) as we did in Fig.7.3.

156
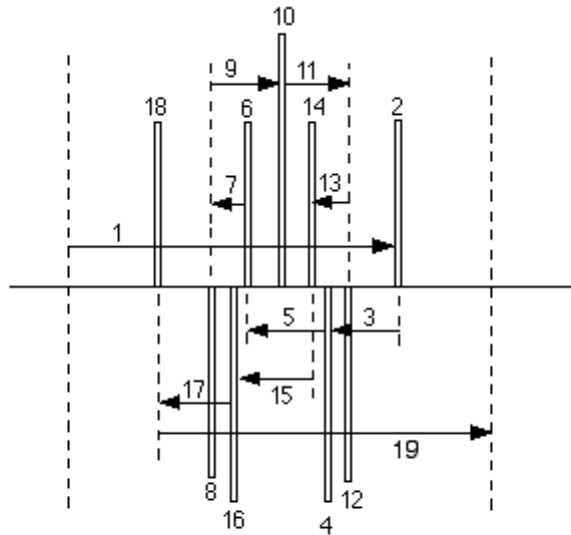
Figure 7.5: Ninteen steps in the 6th order symplectic integrator.

Solution See Fig.7.5.

Exercise 15 It was said that symplecticity of a map is important for its application to long-term stability study. Explore this statement closely to see if long-term stability study requires the complete symplecticity condition, or if it requires only the condition det=1. To study this problem, one will need to study a 2-D or 3-D system.

Solution Consider the special case of a 2-D decoupled system. Its map has the form $M = \begin{bmatrix} A & 0 \\ 0 & B \end{bmatrix}$. Symplecticity requires $\det A = \det B = 1$, while $\det M = 1$ requires only $\det A \, \det B = 1$.

References

[1] Etienne Forest and Ronald D. Ruth, Physica D43, 105 (1990).

[2] Haruo Yoshida, Phys. Lett. A150, 262 (1990).

8 Truncated Power Series Algebra

8.1 Introduction

In the study of nonlinear dynamics in accelerators, one often needs high-order nonlinear maps. Examples: (i) given the maps of sufficiently high order and sufficiently symplectic for all components in the accelerator, one can use them to study the long-term stability of the accelerator system by particle tracking; (ii) given the nonlinear one-turn map, methods (such as Lie algebra) exist to extract various nonlinear dynamics quantities analytically. But for all these applications, question remains as to how to generate high order maps efficiently. Here we describe the truncated power series algebra (TPSA) technique, first introduced for accelerator applications by Berz in 1989. Since then, a large number of computer codes were written on this subject.

The TPSA technique is a powerful, practical calculational technique. It is useful not only for accelerators, but also for any calculational algorithm which relates some output quantities to some input quantities (see Fig.8.1). Once the algorithm is given, TPSA allows one to generate power series expressions of the output quantities in terms of the input quantities. The order of the power series Ω is not limited (other than having sufficient memory space in a computer – see Exercise 11) and can be specified by the user. One should note, however, that TPSA does not contain physics; it is only a calculational technique.

What kind of algorithms are we talking about? The answer is any algorithm that relates outputs to inputs in a well-defined manner. For example, one may have explicit functions

$$y_i = y_i(x_1, x_2, \cdots, x_n), \quad i = 1, 2, \cdots, m \qquad (8.1)$$

or one may have written a computer code with $X = (x_1, x_2, \cdots, x_n)$ as inputs, and $Y = (y_1, y_2, \cdots, y_m)$ as outputs. We are talking about any algorithm that allows one to calculate the numerical values of Y once the numerical values of X are given.

This algorithm, however, may be very complicated (the above computer code may contain 10,000 lines), and to carry it out may be very time consuming. In this case, one would want to approximate the map by something simpler such as a Taylor expansion up to order Ω, or symbolically

$$Y \approx \sum_j^{\Omega} C_j X^j \qquad (8.2)$$

which we recognize as a Taylor map from X to Y. Once we find this map (8.2), we can perform the calculation of the original algorithm much faster, although admittedly only approximately. The TPSA technique is a way to calculate the coefficients C_j once the original algorithm is specified.

For accelerator applications, one may consider X to be the $(x, x', y, y', z, \delta)$ of a particle at some starting position in a storage ring. In a tracking code, this X is followed element by element for one revolution and finally one obtains
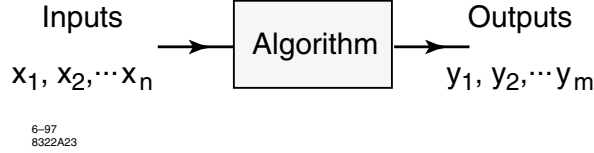
Figure 8.1: A calculation algorithm with inputs and outputs.

Y, which is the $(x, x', y, y', z, \delta)$ of the particle one revolution later. Once this tracking program is written, TPSA allows one to extract the one-turn Taylor map relating Y to X up to some pre-specified order Ω. Subsequent tracking study can then be performed using this Taylor map instead of the original element-by-element tracking. Note that if the original program contains a bug, the TPSA would still work, just that its resulting Taylor map contains the same bug. Note also that the original tracking program relates *numerically* a value of Y to a value of X, while TPSA gives a map which relates Y to X *algebraically*.

The above rosy picture of TPSA sweeps under the rug a problem. The catch lies in how to choose the truncation order Ω. Intricate details such as chaos in phase space can be inadvertently affected by the choice of Ω. This truncation in fact can be rather brutal. In the following, however, we shall not address this subtle problem.

It is obvious from the definition of Taylor series that the coefficients C_j in Eq.(8.2) are related to the derivative of Y with respect to X. So one may also say that the TPSA allows one to calculate the high order derivatives of the outputs with respect to the inputs, e.g.

$$\frac{\partial^{10} y_5}{\partial^3 x_1 \partial^3 x_2 \partial^4 x_8}$$

once the algorithm is known. If $Y = Y(X)$ is a simple analytic expression, one can find derivatives analytically by hand, but such case is unlikely for a 10,000-line tracking code.

Consider the case with a single input x and single output $y = f(x)$, where f may be given as an analytic expression or a 10,000-line code. Let y be expressed as a truncated Taylor series around a reference point $x = a$,

$$y = f(x) = f(a) + (x-a)f'(a) + \frac{1}{2}(x-a)^2 f''(a) + ... \quad + \frac{1}{\Omega!}(x-a)^{\Omega} f^{(\Omega)}(a) \quad (8.3)$$

where $f^{(k)}$ means the kth derivative of $f(x)$. In the simplest application of the TPSA technique, we will illustrate how to obtain the coefficients $f(a)$, $f'(a)$, $f''(a)$, ... Both the order Ω of the power series and the reference point a are specified by the user.

Note that to the extent that a function $f(x)$ can be represented (at least approximately) as a power series in x truncated to the Ω-th order, there is a

160

one-to-one equivalence between the function $f(x)$ and the vector

$$(f(a), f'(a), ... f^{(\Omega)}(a)) \tag{8.4}$$

In particular, the vector can be regarded as the *TPSA representation* of the function around $x = a$. Once the coefficients (8.4) are known using TPSA — there are $\Omega + 1$ of them — the value of $f(x)$ can be calculated using Eq.(8.3) for arbitrary value of x.

One could imagine calculating the derivatives numerically instead of using TPSA. To do so, one first chooses a small number ϵ, and then computes

$$f'(a) \approx \frac{f(a + \epsilon) - f(a)}{\epsilon} \tag{8.5}$$

This procedure, however, loses accuracy rapidly as one proceeds to high order derivatives. As we will see, TPSA is so remarkable because it does not calculate derivatives by subtracting two nearly equal numbers, and offers a way to calculate high order derivatives to computer accuracy![35]

Accelerator application of TPSA is of course not restricted to obtaining one-turn maps. In particular, TPSA allows one to obtain high order Taylor map (of order Ω) relating the exit coordinates $(x, x', y, y', z, \delta)$ to the entrance coordinates of a single magnet element. Before the TPSA days, these high order maps of magnet elements were done by solving the particle's equation of motion. This is clearly a tedious procedure, ending with long expressions, and the results are limited to low orders. These pre-TPSA examples include TRANSPORT for second orders, MARYLIE for third orders, and COSY for fifth orders. Although analytic expressions allow more insight into the problem, TPSA makes the previous approach obsolete, at least as far as efficient generation of high order maps is concerned.

After truncation, the Taylor map is generally nonsymplectic. This Taylor map needs then to be symplectified. One way to do that is to apply Lie algebra. The combined application of TPSA and Lie algebra results in a very powerful modern tool in the study of nonlinear dynamics. This has triggered a revolution on nonlinear dynamics research in accelerators since 1980's.

8.2 TPSA

So far we have not yet described what TPSA does. To do so, let us consider first an example,

$$f(x) = \frac{1}{x + \frac{1}{x}} \tag{8.6}$$

---

[35]This is almost anti-intuitive. We learned in school to compute derivatives like Eq.(8.5). It seems intrinsic, and a matter of definition, that a small quantity ϵ be involved when one calculates derivatives. It therefore seems unavoidable that attempts to calculate high order derivatives numerically contain large numerical errors, but that intuition is apparently wrong.

and suppose we want to find the coefficient $f'(2)$. One way is to do it analytically, i.e. we find first that

$$f'(x) = -\frac{1 - \frac{1}{x^2}}{(x + \frac{1}{x})^2} \qquad (8.7)$$

Substituing $x = 2$ into Eq.(8.7) then gives

$$f'(2) = -\frac{3}{25} \qquad (8.8)$$

The second way is to find it numerically. For example,

$$f'(2) \approx \frac{f(2.1) - f(2)}{2.1 - 2} = \frac{0.38817 - 0.4}{2.1 - 2} = -0.1183 \qquad (8.9)$$

By replacing the value 2.1 by something closer to 2, the accuracy of the calculation improves.

To compute $f'(2)$ using TPSA, let us first form a vector $v = (2, 1)$ and try to find $f(v)$. The reason the first component of v is chosen to be 2 is because we want to compute $f'(2)$. As we shall explain later, the second component of v is always 1. We now have

$$f(v) = \frac{1}{v + \frac{1}{v}} \qquad (8.10)$$

As we will establish later, vectors are manipulated in such a way that

$$\frac{1}{(a_1, a_2)} = (\frac{1}{a_1}, -\frac{a_2}{a_1^2}) \qquad (8.11)$$

$$(a_1, a_2) + (b_1, b_2) = (a_1 + b_1, a_2 + b_2) \qquad (8.12)$$

Thus,

$$\begin{aligned} f(v) &= \frac{1}{(2, 1) + \frac{1}{(2,1)}} = \frac{1}{(2, 1) + (\frac{1}{2}, -\frac{1}{4})} \\ &= \frac{1}{(\frac{5}{2}, \frac{3}{4})} = (\frac{2}{5}, -\frac{3}{25}) \end{aligned} \qquad (8.13)$$

Now notice that the two components in the final vector are miraculously equal to $f(2)$ and $f'(2)$! In the above calculation, nowhere explicit expressions of $f'(x)$ was used, and nowhere subtraction of nearly-equal numbers was needed. The simplest version of the TPSA technique is thus

$$f(v) = (f(a), f'(a)), \qquad \text{for any function } f(x), \quad \text{and } v = (a, 1) \qquad (8.14)$$

Note that in the calculation (8.13), only the input vector v is pre-specified to be equal to $(2, 1)$. In the intermediate steps of the calculation, the vector is of course changed from $(2, 1)$.

The secret of TPSA is contained in these vector manipulation rules. How are those rules established? Let us examine it in 3 steps as follows:

Step 1 Consider the simple identity function $f(x) = x$. We of course want to make sure (8.14) holds for this function. Suppose we take $v = (\alpha, \beta)$, then

$$f(v) = v = (\alpha, \beta) \tag{8.15}$$

We want this to be equal to $(f(a), f'(a))$, but we know $f(a) = a$ and $f'(a) = 1$. This means we must choose $(\alpha, \beta) = (a, 1)$, i.e. the first component of v must be chosen to be equal to the value of x at which the direvative is to be taken, and the second component of v must be 1. This is of course what we have been doing.

We can also apply (8.14) to the constant function $f(x) = c$, i.e. we require $f(v) = c$ to be equal to $(f(a), f'(a)) = (c, 0)$. This gives the identification that

$$\text{constant } c = (c, 0) \tag{8.16}$$

Step 2 Suppose we now have two functions $f(x)$ and $g(x)$, each satisfying (8.14). We now want to establish a rule which allows the new funtion $h(x) = f(x) + g(x)$ to satisfy (8.14) also. The LHS of Eq.(8.14) reads

$$h(v) = f(v) + g(v) = (f(a), f'(a)) + (g(a), g'(a)) \tag{8.17}$$

while the RHS is

$$(f(a) + g(a), f'(a) + g'(a)) \tag{8.18}$$

Obviously $h(x)$ satisfies (8.14) if and only if we establish the vector addition rule (8.12).

We know that the identity function and the constant function satisfy (8.14). By combining them, we now have established (8.14) for all functions of the type $f(x) = c + dx$.

Step 3 With $f(x)$ and $g(x)$ satisfying (8.14), we now want to find the rule for the function $h(x) = f(x)g(x)$ to satisfy (8.14). To do so, we note

$$h(v) = (f(a), f'(a)) \, (g(a), g'(a))$$
$$(h(a), h'(a)) = (f(a)g(a), f(a)g'(a) + f'(a)g(a)) \tag{8.19}$$

Thus (8.14) is assured if and only if we require the vector multiplication rule

$$(a_1, a_2) \, (b_1, b_2) = (a_1 b_1, a_2 b_1 + a_1 b_2) \tag{8.20}$$

If we take $f(x) = g(x) = x$, we can use the vector multiplication rule to assure that the function $h(x) = x^2$ satisfies (8.14). Having established that, we repeat the rule to establish (8.14) for any integer power function $h(x) = x^n$. The vector addition rule then establishes

the validity of (8.14) for any power series of x. We have thus established the TPSA for any arbitrary function which is expandable into a Taylor series just by two simple vector algebraic rules. Just substitute $v = (a, 1)$ into $f(v)$ and follow these simple rules to obtain $f(a)$ and $f'(a)$!

Now how about Eq.(8.11)? One can establish it by applying the vector multiplication rule as follows. Let

$$\frac{1}{(a_1, a_2)} = (x, y) \tag{8.21}$$

then

$$
\begin{aligned}
& (a_1, a_2)\,(x, y) = (1, 0) \\
\Longrightarrow \quad & (a_1 x, a_1 y + a_2 x) = 1 = (1, 0) \\
\Longrightarrow \quad & a_1 x = 1, \quad a_1 y + a_2 x = 0 \\
\Longrightarrow \quad & x = \frac{1}{a_1}, \quad y = -\frac{a_2}{a_1^2}, \qquad \text{Q.E.D.} \tag{8.22}
\end{aligned}
$$

Again by applying the vector multiplication rule, we can also establish

$$c(a_1, a_2) = (c, 0)\,(a_1, a_2) = (ca_1, 0 \times a_1 + ca_2) = (ca_1, ca_2) \tag{8.23}$$

Exercise 1 Show that

$$(a_1, a_2)^{-n} = \left(\frac{1}{a_1^n}, -\frac{na_2}{a_1^{n+1}}\right) \tag{8.24}$$

Solution 1 Mathematical induction.
Solution 2 Identify a function $f(x) \approx f(a) + f'(a)(x - a)$ to the vector $(a_1, a_2)^{-1} = (1/a_1, -a_2/a_1^2)$. This means

$$f(x) \approx \frac{1}{a_1} - \frac{a_2}{a_1^2}(x - a) \tag{8.25}$$

Raising $f(x)$ to n-th power,

$$f^n(x) \approx \left[\frac{1}{a_1} - \frac{a_2}{a_1^2}(x - a)\right]^n \approx \frac{1}{a_1^n} - \frac{na_2}{a_1^{n+1}}(x - a), \qquad \text{Q.E.D.} \tag{8.26}$$

Solution 1 requires n to be an integer. Solution 2 does not have that requirement.

8.3 Higher Orders

To obtain higher derivatives (and thus higher order power series expansions), we need larger dimension for the vectors. Suppose we would like to obtain a power series like (8.3) to the Ω-th order. We first form the vector

$$v = (a, 1, 0, 0, ...0) \tag{8.27}$$

where the number of elements in the vector is $\Omega + 1$. The first component is the reference point a. The second component is always 1. The remaining components are zeros. We would like to have the property that when x is substituted by v in any function $f(x)$, one would obtain

$$f(v) = (f(a), f'(a), f''(a), ... , f^{(\Omega)}(a)) \tag{8.28}$$

As before, the vector (8.27) is chosen in such a way that (8.28) is automatically satisfied for the identity function $f(x) = x$. Indeed, in this case, $f(v) = (a, 1, 0, 0, ...0)$, which is equal to the right hand side of Eq.(8.28) trivially.

Next we need to construct the vector manipulation rules so that (8.28) is satisfied for arbitrary functions $f(x)$ which can be expressed as a truncated power series. Consider first if we have two functions $f(x)$ and $g(x)$, each satisfying (8.28), and would like the functions $h(x) = f(x) + g(x)$ and $h(x) = cf(x)$ also to satisfy (8.28), we need the rules

$$c(a_0, a_1, a_2, ... , a_\Omega) = (ca_0, ca_1, ca_2, ... , ca_\Omega) \tag{8.29}$$

$$(a_0, a_1, a_2, ... , a_\Omega) + (b_0, b_1, b_2, ... , b_\Omega)$$
$$= (a_0 + b_0, a_1 + b_1, a_2 + b_2, ... , a_\Omega + b_\Omega) \tag{8.30}$$

If we consider the function $h(x) = f(x)g(x)$, validity of (8.28) requires

$$h(v) = f(v)g(v)$$
$$= ((f(a), f'(a), f''(a), ... , f^{(\Omega)}(a)) \, (g(a), g'(a), g''(a), ... , g^{(\Omega)}(a)) \tag{8.31}$$

to be equal to

$$(h(a), h'(a), h''(a), ... , h^{(\Omega)}(a))$$
$$= (f(a)g(a), f'(a)g(a) + f(a)g'(a), f''(a)g(a) + 2f'(a)g'(a) + f(a)g''(a),$$
$$... , \sum_{k=0}^{\Omega} \frac{\Omega!}{k!(\Omega - k)!} f^{(k)}(a)g^{(\Omega-k)}(a)) \tag{8.32}$$

This is assured if we choose the vector multiplication rule

$$(a_0, a_1, a_3, ... , a_\Omega) \, (b_0, b_1, b_3, ... , b_\Omega) = (c_0, c_1, c_3, ... , c_\Omega)$$
$$c_m = \sum_{k=0}^{m} \frac{m!}{k!(m - k)!} a_k b_{m-k}$$
$$c_0 = a_0 b_0, c_1 = a_1 b_0 + a_0 b_1, c_2 = a_2 b_0 + 2a_1 b_1 + a_0 b_2, ... \tag{8.33}$$

By identifying a constant c as the vector $(c, 0, 0, ...0)$, Eq.(8.29) follows from Eq.(8.33).

The remarkable thing, again, is that once a vector addition rule (8.30) and a vector multiplication rule (8.33) are established, high order derivatives of an arbitrary function $f(x)$ can be computed by substituting x by $v = (a, 1, 0, 0, ...)$. Once the high order derivatives are obtained, Taylor series expansion follows.

Exercise 2 For the case with $\Omega = 2$, compute $(a_0, a_1, a_2)^{-1}$.

Exercise 3 Show that

$$f((a, \lambda, 0, 0, ...)) = (f(a), \lambda f'(a), \lambda^2 f''(a), ...) \qquad (8.34)$$

The cases $\lambda = 0$ and $\lambda = 1$ are the trivial cases.

Exercise 4 Suppose a function $f(x)$ is identified with the vector $(a_0, a_1, a_2, ...a_\Omega)$, i.e. $f(a) = a_0, f'(a) = a_1$, etc. around $x = a$. What is the vector that identifies with $f(\lambda x)$ around $x = a$? How about $f'(x)$ and $\int_a^x dx' f(x')$?
Solution

$$
\begin{aligned}
f(\lambda x) \quad &\leftrightarrow \quad (f(\lambda a), \lambda f'(\lambda a), ...) & (8.35) \\
&= \quad (b_0, b_1, b_2, ...) \quad \text{where} \quad b_k = \lambda^k \sum_{n=k}^{\Omega} a_n \frac{(\lambda - 1)^{n-k} a^{n-k}}{(n-k)!}
\end{aligned}
$$

8.4 Special Functions

One might question how useful TPSA is in practice because not all operations in the original calculational algorithm are additions and multiplications. What if we have funtions like $e^x, \ln x, \sin x, \cos x$? Surely one can expand them into an infinite power series before we substitute v into them, but that would be computer time consuming and seems to defeat the purpose of TPSA. The answer to this question is that there are useful tricks which allow one to decompose the calculation of these special functions into a *finite* number of vector additions and multiplications. The following exercises are meant to describe these tricks.

Exercise 5 Consider the case with $\Omega = 3$. Show that

$$
\begin{aligned}
(1, 1, 0, 0)^2 &= (1, 2, 2, 0), \quad (1, 1, 0, 0)^3 = (1, 3, 6, 6) \\
(0, 1, 0, 0)^2 &= (0, 0, 2, 0), \quad (0, 1, 0, 0)^3 = (0, 0, 0, 6) \\
(0, 1, 0, 0)^n &= (0, 0, 0, 0) \quad \text{if } n \geq 4 \qquad (8.36)
\end{aligned}
$$

Exercise 6 Apply TPSA to calculate $f'(x), f''(x), f^{(3)}(x), ...$ for the function $f(x) = 1/x$.
Solution Let

$$(x, 1, 0, 0, 0...)^{-1} = (b_0, b_1, b_2, b_3...) \qquad (8.37)$$

166

we require

$$(1, 0, 0, 0, ...) = (x, 1, 0, 0, 0...)(b_0, b_1, b_2, b_3...)$$
$$= (xb_0, xb_1 + b_0, xb_2 + 2b_1, xb_3 + 3b_2, ...)$$
$$\implies \quad b_0 = \frac{1}{x}, \ b_1 = -\frac{1}{x}b_0, \ b_2 = -\frac{1}{x}2b_1, \ ...$$
$$\implies \quad b_{k-1} = (-1)^k \frac{k!}{x^{k+1}}, \quad k = 1, 2, 3...$$
$$\implies \quad (x, 1, 0, 0, 0...)^{-1} = (\frac{1}{x}, -\frac{1}{x^2}, \frac{2}{x^3}, -\frac{6}{x^4}, ...) \tag{8.38}$$

Exercise 7 Repeat the above exercise for the function $f(x) = e^x$.
Solution To find $e^{(x,1,0,0,0,...)}$, first note that

$$e^{(x,1,0,0,0...)} = e^{(x,0,0,0,0...)+(0,1,0,0,0...)} = e^{(x,0,0,0,0...)}e^{(0,1,0,0,0...)}$$
$$= \sum_{k=0}^{\infty} \frac{1}{k!}(x, 0, 0, 0, 0...)^k \sum_{n=0}^{\infty} \frac{1}{n!}(0, 1, 0, 0, 0...)^n \tag{8.39}$$

Then note that

$$(x, 0, 0, 0, 0...)^k = (x^k, 0, 0, 0, 0...)$$
$$(0, 1, 0, 0, 0...)^n = (0, 0, ..., n!, ..., 0, 0...) \tag{8.40}$$

where the term $n!$ on the right-hand-side of the second entry occurs at the $(n+1)$-th element of the vector. When $n \geq \Omega + 1$, the vector $(0, 1, 0, 0, 0...)^n$ vanishes.[36] Substituting (8.40) into (8.39) gives

$$e^{(x,1,0,0,0...)} = (e^x, 0, 0, 0, 0...)(1, 1, 1, 1, 1, ...)$$
$$= (e^x, e^x, e^x, e^x, e^x...) \tag{8.41}$$

which is as expected because all high order derivatives of e^x is e^x.

Exercise 8 Follow a path similar to the previous exercise, show that

$$\ln(x, 1, 0, 0, 0...) = (\ln x, \frac{1}{x}, -\frac{1}{x^2}, ...) \tag{8.42}$$
$$\sin(x, 1, 0, 0, 0...) = (\sin x, \cos x, -\sin x, -\cos x, ...) \tag{8.43}$$
$$\cos(x, 1, 0, 0, 0...) = (\cos x, -\sin x, -\cos x, \sin x, ...) \tag{8.44}$$

The tricks used in the above exercises allow one to evaluate the special function at the vector $(x, 1, 0, 0, 0, ...)$. We still need to extend the trick to evaluate the special functions at an arbitrary vector $(a_1, a_2, a_3, ...)$. This is straightforward to do if we note that the "smallness vector" $(0, 1, 0, 0, ...)$ is not

---

[36]We recognize that $(x, 0, 0, 0, ...)$ is a constant, and that $(0, 1, 0, 0, ...)$ is a "smallness" vector.

the only vector that is small. Any vector whose first component is zero is a "small" vector in the sense that

$$(0, \times, \times, \times, ...)^k = (0, 0, 0, ... \times, \times) \tag{8.45}$$

where each vector contains $\Omega + 1$ components, and an $\times$ means a non-zero component. The RHS of Eq.(8.45) means that, if $k < \Omega + 1$, the leading k components vanishes, while if $k \geq \Omega + 1$, all components vanish.

Using Eq.(8.45), it follows that

$$
\begin{aligned}
e^{(a_0, a_1, a_2, ... \ a_\Omega)} &= e^{a_0} \sum_{k=0}^{\Omega} \frac{1}{k!} (0, a_1, a_2, ... \ a_\Omega)^k &(8.46)\\
\ln(a_0, a_1, a_2, ... \ a_\Omega) &= (\ln a_0, 0, 0, 0..., 0) \\
&\quad + \sum_{k=1}^{\Omega} (-1)^{k+1} \frac{1}{k} (0, \frac{a_1}{a_0}, \frac{a_2}{a_0}, ... \ , \frac{a_\Omega}{a_0})^k &(8.47)\\
\sqrt{(a_0, a_1, a_2, ... \ a_\Omega)} &= \sqrt{a_0} \left[(1, 0, 0, 0...0) + \frac{1}{2} (0, \frac{a_1}{a_0}, \frac{a_2}{a_0}, ... \ , \frac{a_\Omega}{a_0}) \right. \\
&\quad \left. - \sum_{k=2}^{\Omega} (-1)^k \frac{(2k-3)!!}{(2k)!!} (0, \frac{a_1}{a_0}, \frac{a_2}{a_0}, ... \ , \frac{a_\Omega}{a_0})^k \right] &(8.48)\\
\sin(a_0, a_1, a_2, ... \ a_\Omega) &= \sin a_0 \sum_{k=0} \frac{(-1)^k}{(2k)!} (0, a_1, a_2, ..., a_\Omega)^{2k} \\
&\quad + \cos a_0 \sum_{k=0} \frac{(-1)^k}{(2k+1)!} (0, a_1, a_2, ..., a_\Omega)^{2k+1} &(8.49)\\
\cos(a_0, a_1, a_2, ... \ a_\Omega) &= \cos a_0 \sum_{k=0} \frac{(-1)^k}{(2k)!} (0, a_1, a_2, ..., a_\Omega)^{2k} \\
&\quad - \sin a_0 \sum_{k=0} \frac{(-1)^k}{(2k+1)!} (0, a_1, a_2, ..., a_\Omega)^{2k+1} &(8.50)
\end{aligned}
$$

Note that all serieses on the RHSs terminate, and that they can all be evaluated readily by applying the vector addition and multiplication rules. Eqs.(8.47) and (8.48) requires $a_0 > 0$.

> *Exercise 9* Derive Eqs.(8.46-8.50).
> *Exercise 10* Find an expression for $(a_0, a_1, ... a_\Omega)^\lambda$, where λ is a fractional number and $a_0 > 0$.

> *Exercise 11* Consider the function $F(x)$ defined in the following computer code:

$$\text{READ} \quad X$$
$$X1 = X**2 - 1.0$$

$$X2 = X1 * EXP(X1)$$
$$X3 = X1 * X2$$
$$F = COS(X1) * X3$$
$$\text{OUTPUT} \quad F \qquad\qquad (8.51)$$

Use TPSA to compute $F, dF/dx, d^2F/dx^2$ when $x = 1$.

8.5 Multiple Input and Output Variables

So far we discussed the case with a single input variable x and a single output variable y. We will now generalize the algorithm to multiple variables.

It is trivial to generalize to multiple output variables. Each output variable can be treated independently of the other output variables. This means we can concentrate on just one of them each time and consider the case with $y = y(x_1, x_2, ..., x_n)$.

To treat multiple input variables, we need vectors of larger dimension. To keep track of the multiple indices, while using the computer storage efficiently is an extremely complex technical problem when writing TPSA codes.[37] However, to illustrate the principle, we will assume two input variables (x_1, x_2) and one output variable y below.

The TPSA requires that when input x_1 is substituted by vector v_1 and x_2 substituted by v_2, we want to obtain an output vector

$$
\begin{aligned}
y(v_1, v_2) \quad = \quad & \Bigg(y(a_0, b_0), \frac{\partial y}{\partial x_1}(a_0, b_0), \frac{\partial y}{\partial x_2}(a_0, b_0), \\
& \frac{\partial^2 y}{\partial x_1^2}(a_0, b_0), \frac{\partial^2 y}{\partial x_1 \partial x_2}(a_0, b_0), \frac{\partial^2 y}{\partial x_2^2}(a_0, b_0), \\
& .... , \frac{\partial^\Omega y}{\partial x_2^\Omega}(a_0, b_0) \Bigg) \qquad\qquad (8.52)
\end{aligned}
$$

where a_0, b_0 are prespecified reference positions for x_1, x_2 respectively. The first component on the RHS is just y evaluated at the reference positions. The next two terms are first order derivatives. The next three terms are second order derivatives, etc. The last $\Omega + 1$ terms are Ωth order derivatives. All derivatives are evaluated at (a_0, b_0).

It is easy to show that in order for property (8.52) to hold for the identity functions $y(x_1, x_2) = x_1$ and $y(x_1, x_2) = x_2$, we must choose

$$
\begin{aligned}
v_1 \quad &= \quad (a_0, 1, 0, 0, 0, ...0) \\
v_2 \quad &= \quad (b_0, 0, 1, 0, 0, ...0) \qquad\qquad (8.53)
\end{aligned}
$$

---

[37] Remember that the code must be good for *arbitrary* number of input and output variables, as well as *arbitrary* order Ω because these are specified by the user.

The vector addition and multiplication rules are

$$(a_{00}, a_{10}, a_{01}, a_{20}, a_{11}, a_{02}, \dots , a_{0\Omega}) + (b_{00}, b_{10}, b_{01}, b_{20}, b_{11}, b_{02}, \dots , b_{0\Omega})$$
$$= (a_{00} + b_{00}, a_{10} + b_{10}, a_{01} + b_{01}, \dots , a_{0\Omega} + b_{0\Omega}) \tag{8.54}$$
$$(a_{00}, a_{10}, a_{01}, a_{20}, a_{11}, a_{02}, \dots , a_{0\Omega}) \, (b_{00}, b_{10}, b_{01}, b_{20}, b_{11}, b_{02}, \dots , b_{0\Omega})$$
$$= (c_{00}, c_{10}, c_{01}, c_{20}, c_{11}, c_{02}, \dots , c_{0\Omega})$$

$$c_{mn} = \sum_{s=0}^{m} \sum_{t=0}^{n} a_{st} b_{m-s,n-t} \frac{m!n!}{s!(m-s)!t!(n-t)!} \tag{8.55}$$

Once property (8.52) is established, to evaluate a high order derivative, we just have to substitute (8.53) into $y(x_1, x_2)$, processing the calculation using the vector manipulation rules (8.54-8.55), and the output vector contains the result. Once all derivatives are obtained, a Taylor map for y follows.

> *Exercise* 12 Find the total number of elements needed in the TPSA vector to represent one output up to Ωth order when there are M input variables.
> *Solution* Consider M balls in $M+\Omega$ boxes to obtain $(M+\Omega)!/M!\Omega!$.

> *Exercise* 13 Find $f((x, 1, 0, 0, 0, 0...), (y, 0, 1, 0, 0, 0...))$ for the functions $f(x, y) = x + y, xy, 1/xy$ and e^{x+y}.

Applying TPSA to accelerator beam dynamics, we may consider $(x, x', y, y', z, \delta)$ at some starting location in the accelerator as inputs, and the same coordinates one turn later as outputs. A nonlinear Taylor map is then obtained by TPSA. This map can be used to track particles, or to calculate some nonlinear dynamics quantities (such as tune shifts with betatron amplitudes, or nonlinear resonance strengths) analytically.

There may be a case when one is interested in knowing the dependence of the one-turn nonlinear map on the strength S of some special magnet. In such a case, one can include S as one of the input variables. The map is then obtained as a Taylor expansion in terms of S in addition to all the other input variables. This can be useful for example in the study of sensitivity to magnet errors. One can also consider one of the inputs to be a fitting variable strength Q of a quadrupole in a lattice design. This allows varying Q to match the β-functions or the betatron tunes if they are chosen as output variables.

References

[1] Martin Berz, Part. Accel. 24, 109 (1989).

9 Lie Algebra Techniques for Nonlinear Dynamics

9.1 Symplecticity Condition and Poisson Brackets

Consider an n-dimensional ($2n$-dimensional phase space) linear system. Let the canonical coordinates of the system be

$$X = \begin{bmatrix} q_1 \\ p_1 \\ q_2 \\ p_2 \\ . \\ . \\ . \end{bmatrix} \tag{9.1}$$

Let M be the $2n \times 2n$ matrix that describes the map that brings the coordinates of the particles from the initial position $s = 0$ to the position of observation s in this linear dynamical system. Then M must satisfy the *symplecticity condition*

$$\tilde{M} S M = S \tag{9.2}$$

where a tilde means taking the transpose of a matrix, and the matrix S, sometimes called the *symplectic form*,

$$S = \begin{bmatrix} S & 0 & & \\ 0 & S & & \\ & & ... & \\ & & ... & \\ & & & S \end{bmatrix} \tag{9.3}$$

consists of a diagonal array of 2×2 matrices

$$S = \begin{bmatrix} 0 & 1 \\ -1 & 0 \end{bmatrix} \tag{9.4}$$

Note that all symplectic matrices are necessarily even dimensional. Since $S^2 = -I$, S may be thought of as a matrix equivalent of the complex number $i = \sqrt{-1}$.

What is remarkable is that the symplecticity condition (9.2) applies also to a nonlinear system if we identify M to be the Jacobian matrix of the map, whose elements are defined as

$$M_{\alpha\beta} = \frac{\partial X_\alpha}{\partial (X_0)_\beta} \tag{9.5}$$

where $(X_0)_\beta$ is the β-th component of the initial coordinates of a particle at $s = 0$, X_α is the α-th component of the final state X of the particle at an arbitrary position s. In a linear system, the Jacobian matrix is just the transformation matrix, and is independent of the particle coordinates. In a nonlinear system,

the Jacobian matrix M depends on the components of X_0, and the condition (9.2) must be satisfied for all X_0.

The symplecticity condition resembles a "unitarity" condition due to the fact that the left hand side of (9.2) is quadratic in M, while the right hand side is almost a unit matrix. Such a condition obviously imposes a very strong constraint on the matrix M. For example, had the symplectic condition been something like $MS = S\tilde{M}$ with both sides of the equation linear in M, then M could be expanded or shrinked by some factor without consequence. If that were the case, nonlinear dynamics would become very different – most likely much less interesting.

Some of the consequences of the symplecticity condition follow simply from Eq.(9.2). In particular, one observes that (see Exercise 6)

- the matrix S is symplectic. So is the identity matrix I.
- if M is symplectic, then $\det M = \pm 1$. We shall only be interested in those with $\det = +1$.
- if M is symplectic, so are $\tilde{M}$ and M^{-1}.
- if both M are N are symplectic, then MN is symplectic.
- if λ is an eigenvalue of a symplectic matrix M, then so is $1/\lambda$.

Another consequence of a symplectic map is that it obeys the *Liouville theorem*, i.e. the phase space volume is conserved as the system evolves according to the map. Symplectic maps therefore are area-preserving maps. Liouville theorem follows because the Jacobian matrix, being symplectic, has unit determinant, which in turn assures that a volume element in phase space maintains its volume as it evolves with time. Note that the Liouville theorem is a consequence of the symplecticity condition, but the reverse is not necessarily true. (It is true only in a 1-dimensional system.)

We will now introduce the *Poisson bracket*

$$[f,g] = \sum_{i=0}^{n} \left(\frac{\partial f}{\partial q_i} \frac{\partial g}{\partial p_i} - \frac{\partial f}{\partial p_i} \frac{\partial g}{\partial q_i} \right) \tag{9.6}$$

where f and g are arbitrary functions of s and the components of X. Note that although f and g depend on s in general, the Poisson bracket discriminates against these dependences in that no explicit s-derivatives are included in its definition.

Using the notations already introduced, the Poisson bracket can also be written as

$$[f,g] = \sum_{\alpha,\beta} \frac{\partial f}{\partial X_\alpha} S_{\alpha\beta} \frac{\partial g}{\partial X_\beta} \tag{9.7}$$

or in matrix notation,

$$[f,g] = \widetilde{\frac{\partial f}{\partial X}} S \frac{\partial g}{\partial X} \tag{9.8}$$

For what we plan to do, it is necessary to first get familiarized with the Poisson brackets. There are several properties of the Poisson brackets that are

important. For example, let f, g, h be functions of X and s, and let a and b be some constants (independent of X, but can depend on s), we have

$$[f, g] = -[g, f]$$
$$[af + bg, h] = a[f, h] + b[g, h]$$
$$[f, gh] = [f, g]h + g[f, h]$$
$$[f, [g, h]] + [g, [h, f]] + [h, [f, g]] = 0 \qquad (9.9)$$

The last entry is called the *Jacobi identity*. The proofs of Eq.(9.9) are omitted.

We will now prove the symplecticity condition (9.2) for a nonlinear system as follows. The proof for a linear system then follows as a special case. The only information we have at this point is the fact that the system under consideration is Hamiltonian. This means there exists a Hamiltonian H so that the equations of motion can be written as

$$X' = S \frac{\partial H}{\partial X} \qquad (9.10)$$

where a prime means taking derivative with respect to s. We are going to use Eq.(9.10) to calculate the derivative of $\tilde{M}SM$ with respect to s, where M is the Jacobian matrix (9.5). Before doing so, we establish the following:

$$
\begin{aligned}
M'_{\alpha\beta} &= \left(\frac{\partial X_\alpha}{\partial X_{0\beta}} \right)' = \frac{\partial}{\partial X_{0\beta}} \left(S_{\alpha\gamma} \frac{\partial H}{\partial X_\gamma} \right) \\
&= S_{\alpha\gamma} \frac{\partial^2 H}{\partial X_{0\beta} \partial X_\gamma} = S_{\alpha\gamma} \frac{\partial^2 H}{\partial X_\delta \partial X_\gamma} \frac{\partial X_\delta}{\partial X_{0\beta}} \\
&= S_{\alpha\gamma} H_{\delta\gamma} M_{\delta\beta} = (SHM)_{\alpha\beta} \\
\implies \quad M' &= SHM \qquad (9.11)
\end{aligned}
$$

where we have adopted the notation that a repeated index means summation over the index, and we have defined a symmetric matrix H with elements

$$H_{\delta\gamma} = \frac{\partial^2 H}{\partial X_\delta \partial X_\gamma} \qquad (9.12)$$

Note that H is meant to be a function of X, not X_0.

Taking the derivative of the matrix $\tilde{M}SM$ with respect to s yields

$$
\begin{aligned}
(\tilde{M}SM)' &= \tilde{M}'SM + \tilde{M}SM' \\
&= (\widetilde{M'})SM + \tilde{M}SM' \\
&= (\widetilde{SHM})SM + \tilde{M}SSHM \\
&= \tilde{M}\tilde{H}\tilde{S}SM - \tilde{M}HM \\
&= \tilde{M}HM - \tilde{M}HM = 0 \qquad (9.13)
\end{aligned}
$$

This means the matrix $\tilde{M}SM$ is an invariant, independent of s. In particular, its value can be obtained by evaluating it at $s = 0$. At $s = 0$, we have necessarily $M(s|0) = I$, i.e. the identity map. This then completes the proof of the symplecticity condition (9.2).

Note that the Jacobian matrix is symplectic only if we use *canonical* coordinates as the vector X. The transformation matrix for the vector (x, x', y, y'), for example, would not be symplectic in a solenoid, as x' and y' are not the canonical momenta in a solenoid. See Exercise 2, however.]

The symplecticity condition plays an important role in Hamiltonian dynamics. It imposes a strong constraint on the Hamiltonian system. To be more specific, consider an n-dimensional ($2n$-dimensional phase space) linear system with matrix map M. The symplecticity condition (9.2) imposes a total of $n(2n-1)$ conditions.[38] The $2n \times 2n$ matrix M has therefore $4n^2 - n(2n-1) = n(2n+1)$ independent elements. In particular, in a 2-D case, M contains 16 elements, but only 10 of them are independent.

The symplecticity condition imposes an even stronger constraint on nonlinear systems. In a linear system, the map is independent of X_0 or X; the symplecticity condition has only to hold for all s. In a nonlinear system, it has to hold for all s and all X_0.

Consider any function f of s and X. Its value changes with time s either because of its explicit s dependence, or because it depends on X and changes because X changes. The total time derivative of f therefore can be written as

$$
\begin{aligned}
f' &= \frac{\partial f}{\partial s} + \frac{\partial f}{\partial X_\alpha} X'_\alpha \\
&= \frac{\partial f}{\partial s} + \frac{\partial f}{\partial X_\alpha} S_{\alpha\beta} \frac{\partial H}{\partial X_\beta} \\
&= \frac{\partial f}{\partial s} + [f, H]
\end{aligned}
\tag{9.14}
$$

A quantity f is a constant of the motion if it is not explicitly s dependent, and that

$$
[f, H] = 0 \tag{9.15}
$$

Equations (9.14-9.15) are one of the reasons why Poisson brackets play an important role in dynamics; they are intimately related to the time evolution of phase space quantities. At this point, the only relevant Poisson brackets seem to involve the Hamiltonian H. In the next section, however, we will see why the Poisson brackets in general are useful. In fact, we will see that, for our purpose, the Lie[39] algebra technique is basically an algebra of the Poisson brackets.

In later developments, we often compute the Poisson brackets of two Taylor series of X. It is easy to see that if f is an n-th order and g is an m-th order Taylor series, their Poisson bracket is another Taylor series of order $m + n - 2$. For example, the Poisson bracket of two quadratic forms is another quadratic form.

---

[38]To see this, first note that the matrix $\tilde{M}SM$ is necessarily antisymmetric. The diagonal elements of $\tilde{M}SM$ are zeros. The number of free elements is equal to the number of elements in the triangular upper (or lower) off-diagonal region.

[39](Marius) Sophus Lie (1842-1899), Norweigian mathematician, noted for his work in differential equations, for which he developed the theory of continuous groups.

The Poisson bracket of arbitrary functions f and g is given by Eqs.(9.6-9.8). There is one set of Poisson brackets that assumes particular significance, namely the *fundamental Poisson brackets*

$$[X_\alpha, X_\beta] = S_{\alpha\beta} \qquad (9.16)$$

Consider a map from X_0 at $s = 0$ to X at s. The Jacobian matrix M of this map was defined in Eq.(9.5). The symplecticity of M implies that the fundamental Poisson brackets are preserved. To demonstrate this, consider the quantities X at position s as functions of the quantities X_0 at $s = 0$, and compute the Poisson brackets

$$
\begin{aligned}
[X_\alpha, X_\beta] &= \frac{\partial X_\alpha}{\partial X_{0\gamma}} S_{\gamma\delta} \frac{\partial X_\beta}{\partial X_{0\delta}} = M_{\alpha\gamma} S_{\gamma\delta} M_{\beta\delta} \\
&= (MS\tilde{M})_{\alpha\beta} = S_{\alpha\beta} \\
&= [X_{0\alpha}, X_{0\beta}] \qquad (9.17)
\end{aligned}
$$

where again, repeated indices are summed over. In fact, Eq.(9.17) demonstrates that a system is symplectic if and only if all the fundamental Poisson brackets are preserved and are given by Eq.(9.16).

Exercise 1 If M_1 and M_2 are symplectic matrices. Is the matrix $M_1 + M_2$ symplectic?

Exercise 2 Let (q, p) be the canonical variables for a dynamical system with Hamiltonian H. (a) Show that the variables $\bar{q} = aq$ and $\bar{p} = bp$ (a and b are constants) are not canonical unless $ab = 1$. (b) Let $\bar{M}_{\alpha\beta} = \partial \bar{x}_\alpha / \partial \bar{x}_{0\beta}$. Is the matrix $\bar{M}$ symplectic? The issue here is whether the use of noncanonical variables necessarily mean nonsymplecticity.

Exercise 3 Show that, for a Hamiltonian system, if f and g are constants of the motion, so is $[f, g]$.
Solution Let H be the Hamiltonian governing the motion of the system. Use the Jacobi identity to show that if $[f, H] = 0$ and $[g, H] = 0$, then $[[f, g], H] = 0$.

Exercise 4 As an illustration of Exercise 3, consider a degenerate 2-D simple harmonic system described by the Hamiltonian

$$H = \frac{1}{2}(\omega^2 x^2 + p_x^2 + \omega^2 y^2 + p_y^2)$$

Show that

$$f_1 = \omega^2 x^2 + p_x^2 \qquad \text{and} \qquad f_2 = \omega^2 y^2 + p_y^2$$

are constants of the motion. The Poisson bracket $[f_1, f_2] = 0$ gives only a trivial case. However, show that there is another constant of

the motion (the angular momentum)

$$g = xp_y - yp_x$$

By forming the Poisson bracket $[f_1, g]$ or $[f_2, g]$, one then finds another invariant

$$h = \omega^2 xy + p_x p_y$$

The invariant h is not an independent invariant because it is related to the other three invariants according to $\omega^2 g^2 + h^2 = f_1 f_2$.

Exercise 5 As another illustration of Exercise 3, consider the 3-D system with Hamiltonian

$$H = \frac{1}{2}(x^2 + p_x^2 + y^2 + p_y^2 + z^2 + p_z^2) + \epsilon(xy + yz + zx)$$

Show that

$$
\begin{aligned}
f_1 &= (1-\epsilon)(x-y)^2 + (p_x - p_y)^2 \\
f_2 &= (1-\epsilon)(y-z)^2 + (p_y - p_z)^2 \\
f_3 &= (1-\epsilon)(z-x)^2 + (p_z - p_x)^2
\end{aligned}
$$

are constants of the motion. By forming Poisson brackets among $f_1, f_2,$ and f_3, show that

$$g = x(p_y - p_z) + y(p_z - p_x) + z(p_x - p_y)$$

is an invariant. By forming the Poisson brackets of $f_{1,2,3}$ and g, one finds more invariants

$$
\begin{aligned}
h_1 &= (1-\epsilon)(x-y)(2z - x - y) + (p_x - p_y)(2p_z - p_x - p_y) \\
h_2 &= (1-\epsilon)(y-z)(2x - y - z) + (p_y - p_z)(2p_x - p_y - p_z) \\
h_1 &= (1-\epsilon)(z-x)(2y - z - x) + (p_z - p_x)(2p_y - p_z - p_x)
\end{aligned}
$$

Are these invariants all independent?

Exercise 6 (a) Show that, if M is symplectic, so are $\tilde{M}$, M^{-1}, and

$$\bar{M} \equiv -S\tilde{M}S \tag{9.18}$$

The last matrix $\bar{M}$ is called the *symplectic conjugate* of M. (b) Show that if M_1 and M_2 are symplectic, then so is $M_1 M_2$.

Exercise 7 Express a 4×4 symplectic matrix M in 2×2 block form as

$$M = \begin{bmatrix} A & B \\ C & D \end{bmatrix} \tag{9.19}$$

176

(a) Show that

$$M^{-1} = \bar{M} = \begin{bmatrix} \bar{A} & \bar{C} \\ \bar{B} & \bar{D} \end{bmatrix} = \begin{bmatrix} (\det A)A^{-1} & (\det C)C^{-1} \\ (\det B)B^{-1} & (\det D)D^{-1} \end{bmatrix} \quad (9.20)$$

(b) Show that the symplecticity condition gives six conditions

$$\det A + \det C = 1, \quad \det B + \det D = 1, \quad \bar{A}B + \bar{C}D = 0 \quad (9.21)$$

(c) Since $\tilde{M}$ is also symplectic, applying the conditions (9.21) to $\tilde{M}$ gives

$$\det A + \det B = 1, \quad \det C + \det D = 1, \quad A\bar{C} + B\bar{D} = 0 \quad (9.22)$$

The six conditions in Eq.(9.21) and the six conditions in Eq.(9.22) are algebraically equivalent. Combining the first two members of Eq.(9.21) and the first two members of Eq.(9.22) gives the necessary properties

$$\det A = \det D, \quad \det B = \det C \quad (9.23)$$

Results in this exercise are useful when dealing with linearly coupled motions in an accelerator.

Exercise 8 Show that the only way a 4×4 matrix $M = \begin{bmatrix} A & B \\ 0 & D \end{bmatrix}$ is symplectic is when $B = 0$ and A and D are symplectic. A similar conclusion can be made for the matrix $M = \begin{bmatrix} A & 0 \\ B & D \end{bmatrix}$.

Exercise 9 The above exercise can be extended to the 6×6 case. Show that if

$$M = \begin{bmatrix} M_1 & M_2 & M_3 \\ M_4 & M_5 & M_6 \\ M_7 & M_8 & M_9 \end{bmatrix} \quad (9.24)$$

is symplectic, then

$$\det M_1 + \det M_2 + \det M_3 = \det M_4 + \det M_5 + \det M_6$$
$$= \det M_7 + \det M_8 + \det M_9 = \det M_1 + \det M_4 + \det M_7$$
$$= \det M_2 + \det M_5 + \det M_8 = \det M_3 + \det M_6 + \det M_9 = 1 \quad (9.25)$$

9.2 Taylor and Lie Representations

A map can be represented in various ways. Consider an n-dimensional system. One example of this is the *Taylor map*, in which the final canonical variables are expressed as truncated power series in terms of the initial variables,

$$X_\alpha = F_\alpha(X_0) \quad (9.26)$$

where X_α is the α-th component of the final X, and

$$F_\alpha(X_0) = \Omega-\text{th order power series in the components of } X_0 \qquad (9.27)$$

Since there are $2n$ variables, we have $2n$ polynomials like (9.27), each is of order Ω.

Application of Taylor maps to accelerators has a long history. In the linear case, the Taylor map is simply the linear map, which also has a matrix form, as adopted in the Courant-Snyder anaysis.[1] An early version of a nonlinear (2-nd order, i.e. $\Omega = 2$) Taylor map was adopted in the program TRANSPORT.[2] A more recent version of Taylor map scheme is developed in a 5-th order program COSY.[3]

Another way to represent a map is the *Lie map*, which is based on the Lie algebra techniques. Lie algebra techniques are an elegant and powerful tool in the study of nonlinear dynamics in accelerators. It was introduced by Dragt,[4] and extended and applied by many others.[5] It should be noted that the Lie technique is only a tool. No new physics is introduced.

In the Courant-Snyder analysis of linear systems, we saw how matrices are used extensively and effectively. The matrix analysis however is restricted to linear systems. The question is then how to generalize the Courant-Snyder analysis to nonlinear systems. Both the Taylor and the Lie representations can be regarded as ways to provide this generalization. In the case of Taylor maps, this generalization is an obvious one. To appreciate the fact that Lie maps are also a way to generalize the Courant-Snyder analysis, the Courant-Snyder analysis must first be cast in the Lie formulation instead of a matrix formulation. When done, the formulation then allows generalization to nonlinear systems in an elegant and natural manner. Details of these topics will be developed as we proceed.

In the Lie representation, an Ω-th order map is expressed as

$$e^{:G(X):} \qquad (9.28)$$

where

$$G(X) = (\Omega + 1)-\text{th order power series in the components of } X \qquad (9.29)$$

Note the subtle differences between Eq.(9.27) and (9.29): F_α is Ω-th order, while G is $(\Omega + 1)$-th order; there are $2n$ functions of F_α, while there is only one G; F_α is a function of X_0, while G is a function of X.

Equation (9.28) represents an operator. When applied to X, it gives the final coordinates in terms of the initial coordinates. In other words, the way the Lie map is to be used is[40]

$$X = e^{:G(X):} X \Big|_{X=X_0} \qquad (9.30)$$

---

[40] As indicated in Eq.(9.30), the substitution of X by X_0 is to be made *after* the application of the operator. It would be misleading, or at least umbiguous, to write for example $X = e^{:G(X):} X_0$ or $X = e^{:G(X_0):} X_0$.

Its detailed meaning and applications will become clear later.

We assume the map brings the origin $X_0 = 0$ to the origin $X = 0$. This means the lowest order leading terms of F_α are 1-st order in X_0, and the leading terms in $G(X)$ are second order in X.

For a given accelerator system and a pre-determined order Ω, if we compare the expressions of X for the Taylor representation (9.26-9.27) and the Lie representation (9.28-9.29), they coincide up to the Ω-th order terms. There are no terms beyond the Ω-th order in the Taylor map (9.26). All terms beyond the Ω-th order are truncated. With this truncation, Taylor maps are not symplectic in general, although it does maintain its symplecticity up to the Ω-th order. On the other hand, if expanded, the map (9.30) contains higher order terms. These higher order terms, as we will see later, are going to make the Lie map strictly symplectic.

To study the long term stability of a particle in an accelerator, one may encounter the situation when a high order Taylor map (say 12-th order) is needed, while a relatively low order (say 5-th order) Lie map would suffice. The reason one needs a high order Taylor map is not so much to make the map extremely accurate. Rather, it is because the map needs to be extremely symplectic. If one uses Lie maps, which are always symplectic, a lower order map with less accuracy may suffice.

It should be mentioned here that there are still other ways to represent a map. For example, one may choose to introduce a generating function, and then express it as a power series. However, we will discuss only the Taylor and the Lie representations.

Number of coefficients in a Taylor map How many coefficients are needed to describe a Taylor map? Consider the function $F_\alpha(X_0)$ which is a sum of k-th order terms where $k = 1, ..., \Omega$. Exercise 10 shows that the total number of coefficients for the k-th order terms is

$$2n \times \frac{(2n + k - 1)!}{k!(2n - 1)!} \tag{9.31}$$

where the factor $2n$ is because there are $2n$ functions of F_α. By adding the number of coefficients from $k = 1$ to Ω, we obtain Table 2.

> *Exercise* 10 Prove the statement (9.31).
> *Solution* Consider one of the functions $F_\alpha(X_0)$. To find the number of coefficients in F_α that are of k-th order, let us consider k "objects" and $2n - 1$ "partitions". Arrange the collection of objects and partitions in a certain order. Represent an object by a cross, and a partition by a vertical bar, one has for example the following pattern for $n = 2$ and $k = 4$,
>
> $$\times \times \mid \times \mid\mid \times$$
>
> One may identify this pattern with $x_1^2 x_2 x_4$. It is clear that each pattern is in one-to-one correspondence to a term in the polynomial.

The total number of coefficients is then the same as the number of different patterns that can be made with k objects and $2n - 1$ partitions. The answer is

$$\frac{(2n + k - 1)!}{k!(2n - 1)!}$$

Since there are $2n$ functions like F_α, we have proved Eq.(9.31).

Table 2: Total number of coefficients needed to describe a Taylor map of Ω-th order. The phase space is $2n$-dimensional.

	$\Omega = 1$	$\Omega = 2$	$\Omega = 3$	$\Omega = 4$	$\Omega = 5$
$n = 1$	4	10	18	28	40
$n = 2$	16	56	136	276	500
$n = 3$	36	162	498	1254	2766

Taylor maps have the advantage that the final coordinates can be computed straightforwardly from the initial coordinates. However, as mentioned before, Taylor representation is in general nonsymplectic. In addition, it requires more coefficients than necessary to represent the map. To appreciate this, consider the following two exercises.

Exercise 11 Consider the case $n = 1$ and $\Omega = 1$. This linear map can be written as a 2×2 matrix, with 4 elements. The Taylor map therefore has 4 coefficients. On the other hand, the symplecticity condition dictates that this matrix has unit determinant. So the total number of _independent_ coefficients is 3. As we will soon see, the Lie representation indeed requires only 3 coefficients.

Exercise 12 Consider $n = 1$, $\Omega = 2$. The Taylor map reads

$$x = R_{11}x_0 + R_{12}p_0 + T_{111}x_0^2 + T_{112}x_0p_0 + T_{122}p_0^2$$
$$p = R_{21}x_0 + R_{22}p_0 + T_{211}x_0^2 + T_{212}x_0p_0 + T_{222}p_0^2 \quad (9.32)$$

There are 10 coefficients in this representation. The Jacobian matrix of the map is

$$M = \begin{bmatrix} R_{11} + 2T_{111}x_0 + T_{112}p_0 & R_{12} + T_{112}x_0 + 2T_{122}p_0 \\ R_{21} + 2T_{211}x_0 + T_{212}p_0 & R_{22} + T_{212}x_0 + 2T_{222}p_0 \end{bmatrix} \quad (9.33)$$

Due to symplecticity, the determinant of M has to be unity for arbitrary values of x_0 and p_0. This gives the conditions that

$$R_{11}R_{22} - R_{12}R_{21} = 1$$
$$R_{11}T_{212} + 2R_{22}T_{111} - 2R_{12}T_{211} - R_{21}T_{112} = 0$$
$$2R_{11}T_{222} + R_{22}T_{112} - R_{12}T_{212} - 2R_{21}T_{122} = 0 \quad (9.34)$$

where we have dropped terms second order in x_0 or p_0 because information is incomplete for these coefficients after the Taylor map is truncated to second order as done in Eq.(9.32). We have thus obtained 3 conditions constraining the various coefficients. The total number of independent coefficients is therefore 7. As we will show next, 7 is the number of coefficients required in the corresponding Lie representation.

Number of coefficients in a Lie map   Lie map has the minimum number of coefficients to represent a map up to a given order Ω. Lie maps are more concise than Taylor maps. The number of coefficients of the k-th order terms in the function $G(X)$ of Eq.(9.28) is

$$\frac{(2n + k - 1)!}{k!(2n - 1)!} \tag{9.35}$$

By adding the number of coefficients from $k = 2$ to $k = \Omega + 1$, we obtain Table 3 below. Taylor maps are more convenient for numerical tracking; Lie maps are better suited for analysis. One should nevertheless exercise caution when applying Taylor maps for long-term stability tracking studies. The difference between Tables 2 and 3 is of course due to the symplecticity condition.

Table 3: Total number of coefficients needed to describe a Lie map of Ω-th order. The phase space is $2n$-dimensional.

	$\Omega = 1$	$\Omega = 2$	$\Omega = 3$	$\Omega = 4$	$\Omega = 5$
$n = 1$	3	7	12	18	25
$n = 2$	10	30	65	121	205
$n = 3$	21	77	203	455	917

Taylor invariants   For circular accelerators, a type of map of particular significance is the *one-turn map*, which gives the map for one revolution around the accelerator. It is instructive at this point to see how to construct a Taylor expression of an invariant from a Taylor one-turn map. Suppose we are looking

for an invariant of Ω-th order. Consider the vector

$$
Z = \begin{bmatrix} x \\ p \\ x^2 \\ xp \\ p^2 \\ x^3 \\ x^2 p \\ . \\ . \\ . \\ xp^{\Omega-1} \\ p^{\Omega} \end{bmatrix}
$$

Let the one-turn map of the accelerator be written in a matrix form as

$$ Z_{\text{final}} = M Z_{\text{initial}} \tag{9.36} $$

In writing down Eq.(9.36), we have truncated the map at the Ω-th order. Let the invariant be expressed as an Ω-th order Taylor series,

$$ W = \tilde{V} Z \tag{9.37} $$

where V is a vector yet to be found, while the matrix M is assumed known.

Since W is an invariant, we must have

$$
\begin{aligned}
\tilde{V} Z &= \tilde{V} M Z \quad \text{for all } Z \\
\implies \quad \tilde{V} &= \tilde{V} M \\
\implies \quad \tilde{M} V &= V
\end{aligned} \tag{9.38}
$$

This means V is just the eigenvector of $\tilde{M}$ with eigenvalue 1. This is the way V — and therefore the invariant W — can be found. If an eigenvector of eigenvalue 1 cannot be found, it means there is no invariant of the order being considered. Note that even in the linear case, Z must be kept up to the quadratic terms in order to find W.[41]

> *Exercise* 13 Equation (9.32) is a terminated power series because we have performed a truncation. If Eq.(9.32) turns out to be exact, i.e. the higher order terms all vanish exactly, what can we say about this map?
> *Solution* In this case, we can impose the symplecticity condition exactly. Keep all terms including terms second order in X_0, we have in addition to (9.34), three more conditions
>
> $$
> \begin{aligned}
> T_{111}T_{212} - T_{112}T_{211} &= T_{111}T_{222} - T_{122}T_{211} \\
> &= T_{112}T_{222} - T_{122}T_{212} = 0
> \end{aligned} \tag{9.39}
> $$

---

[41] This is except for the trivial case when the map for (x, p) is the identity map, in which case x and p are invariants.

By solving Eqs.(9.34) and (9.39), it follows that the map $(x_0, p_0) \rightarrow (x, p)$ can be written as a two-step process, namely

$$
\begin{aligned}
x_1 &= R_{11}x_0 + R_{12}p_0 \\
p_1 &= R_{21}x_0 + R_{22}p_0
\end{aligned}
\tag{9.40}
$$

followed by

$$
\begin{aligned}
x &= x_1 + T_{111}\left(\frac{T_{111}p_1 - T_{211}x_1}{R_{21}T_{111} - R_{11}T_{211}}\right)^2 \\
p &= p_1 + T_{211}\left(\frac{T_{111}p_1 - T_{211}x_1}{R_{21}T_{111} - R_{11}T_{211}}\right)^2
\end{aligned}
\tag{9.41}
$$

Both steps (9.40) and (9.41) are symplectic. In case either $T_{111} = 0$ or $T_{211} = 0$, we have a kick map.

Exercise 14 Consider the linear one-turn map

$$
\begin{aligned}
x &= x_0 \cos\mu + p_0 \sin\mu \\
p &= -x_0 \sin\mu + p_0 \cos\mu
\end{aligned}
\tag{9.42}
$$

Find Taylor expressions of an invariant up to 2nd order, 3rd order, and 4-th order in (x, p).
Solution There are no 1-st and 3-rd order invariants. The 2-nd order invariant is $x^2 + p^2$. The 4-th order invariant is $(x^2 + p^2)^2$.

Exercise 15 Consider the map that represents a linear map followed by a thin-lens sextupole. The combined map is given by

$$
\begin{aligned}
x &= x_0 \cos\mu + p_0 \sin\mu \\
p &= -x_0 \sin\mu + p_0 \cos\mu + \epsilon x^2
\end{aligned}
\tag{9.43}
$$

Find a Taylor expression of an invariant up to 3rd order in (x, p).
Solution Let $c = \cos\mu$ and $s = \sin\mu$, we find the 3-rd order invariant

$$
W_3 = x^2 + p^2 - \epsilon\frac{sc}{(1 + 2c)(1 - c)}x^3 - \epsilon x^2 p - \epsilon\frac{s}{1 + 2c}xp^2
\tag{9.44}
$$

where x and p are values observed at the exit of the thin-lens sextupole. Note that W_3 diverges when $\cos\mu = 1$ or $-\frac{1}{2}$, i.e. when $\frac{\mu}{2\pi} = \frac{n}{3}$ with n an integer. One may proceed to obtain a 4-th order invariant W_4 and find that it diverges when $\frac{\mu}{2\pi} = \frac{n}{4}$.

One may perform a numerical test of the invariance of $W_2 = x^2 + p^2$ and W_3. Take for example a case with $\mu = 2\pi \times 0.23$ and $\epsilon = 0.05$. A particle with initial conditions $x_0 = 1$ and $p_0 = 0$ is tracked for 1000 iterations. The resulting values of x and p for each iteration are used to calculate the values of W_2 and W_3 and plotted as functions of iteration number in Fig.9.1. It can be seen that W_2 is not a good invariant; its value fluctuates by about 10%. In comparison, W_3 fluctuates only by $< 0.1\%$. Round-off errors are negligible in these calculations.
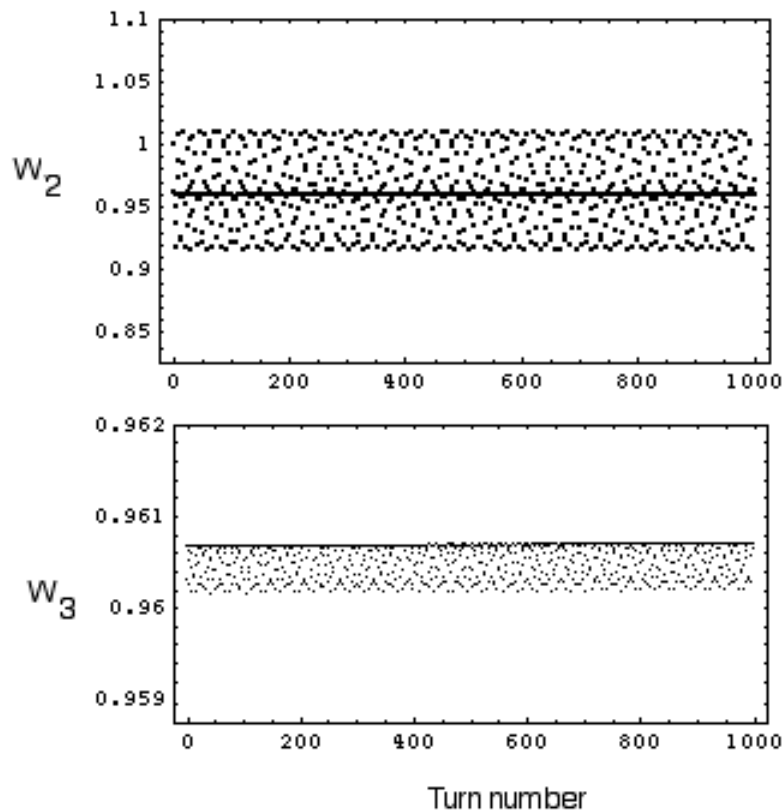
Figure 9.1: Invariants W_2 and W_3.

9.3 Algebra of Operators

In this section, we will describe the techniques of Lie algebra, i.e. the algebra of Poisson brackets. For convenience we rewrite the Poisson bracket (9.6) in another notation, following Dragt,

$$:f:g = [f, g] \tag{9.45}$$

In this notation, the quantity $:f:$ is viewed as an operator — a Lie operator — which operates on the function g. Obviously we have $:f:g = -:g:f$. An identity map will be designated as $1.^{42}$

One can define functions of operators. For example, powers of an operator can be obtained by letting

$$(:f:)^2 g \quad = \quad :f:(:f:g) = [f, [f, g]]$$

_____

[42] Note that :1: is not the identity map. In fact, any function operated on by :1: becomes zero.

184

$$(\mathrel{:}f\mathrel{:})^3 g \;\; = \;\; [f,[f,[f,g]]], \qquad \text{....} \quad \text{etc.} \tag{9.46}$$

It can be shown that

$$(\mathrel{:}f\mathrel{:})^k(gh) = \sum_{n=0}^{k} \frac{k!}{n!(k-n)!}[(\mathrel{:}f\mathrel{:})^n g][(\mathrel{:}f\mathrel{:})^{k-n}h] \tag{9.47}$$

When $k = 1$, it is just the third member of Eq.(9.9). The rest can be proved by induction.

It also follows from the Jacobi identity that the commutator of two operators $\mathrel{:}f\mathrel{:}$ and $\mathrel{:}g\mathrel{:}$, defined as

$$\{\mathrel{:}f\mathrel{:},\mathrel{:}g\mathrel{:}\} \equiv \mathrel{:}f\mathrel{:}\,\mathrel{:}g\mathrel{:} - \mathrel{:}g\mathrel{:}\,\mathrel{:}f\mathrel{:} \tag{9.48}$$

is equal to the operator $\mathrel{:}[f,g]\mathrel{:}$, i.e.

$$\{\mathrel{:}f\mathrel{:},\mathrel{:}g\mathrel{:}\} = \mathrel{:}[f,g]\mathrel{:} \tag{9.49}$$

Equation (9.49) has a useful variation, namely,

$$\{\mathrel{:}f\mathrel{:},\mathrel{:}g\mathrel{:}\}h = \mathrel{:}h\mathrel{::}g\mathrel{:}f \tag{9.50}$$

Equation (9.50) is just another way of writing the Jacobi identity.

Equation (9.49) is the reason Poisson brackets play a prominent role in Lie algebra of operators. The commutators of operators occur often, and Eq.(9.49) relates them to Poisson brackets. In particular, when $[f,g] = 0$, the operators $\mathrel{:}f\mathrel{:}$ and $\mathrel{:}g\mathrel{:}$ commute. [However, see Exercise 19.]

Other functions of operators can then be constructed based on power expansions. Of particular significance are the exponential operators,

$$e^{\mathrel{:}f\mathrel{:}} = \sum_{k=0}^{\infty} \frac{1}{k!}(\mathrel{:}f\mathrel{:})^k \tag{9.51}$$

The leading term on the right-hand-side of Eq.(9.51) is the identity map 1.

Exercise 16 Although $e^{\ln x} = x$ is an identity, show that the maps $e^{\mathrel{:}\ln x\mathrel{:}}$ and $\mathrel{:}x\mathrel{:}$ are quite different.
Solution They are very different:

$$e^{\mathrel{:}\ln x\mathrel{:}}x = x, \qquad e^{\mathrel{:}\ln x\mathrel{:}}p = p + \tfrac{1}{x}$$
$$\mathrel{:}x\mathrel{:}x = 0, \qquad \mathrel{:}x\mathrel{:}p = 1$$

In particular, the map $e^{\mathrel{:}\ln x\mathrel{:}}$ is symplectic as its Jacobian matrix $\begin{bmatrix} 1 & 0 \\ -1/x^2 & 1 \end{bmatrix}$ has determinant of 1. The map $\mathrel{:}x\mathrel{:}$ is nonsymplectic.

Exercise 17 Let $a(s)$ be a function of s and not a function of X. What is the operator $\mathrel{:}a(s)\mathrel{:}$? What is $e^{\mathrel{:}a(s)\mathrel{:}}$?

Exercise 18 To familiarize with the fact that $:f:$ is an operator, establish the following:

$$
\begin{aligned}
:q: &= \frac{\partial}{\partial p}, & :p: &= -\frac{\partial}{\partial q} \\
:q:^2 &= \frac{\partial^2}{\partial p^2}, & :p:^2 &= \frac{\partial^2}{\partial q^2} \\
:qp: &= p\frac{\partial}{\partial q} - q\frac{\partial}{\partial p} \\
:q::p: &= -\frac{\partial^2}{\partial q\partial p} = :p::q: \\
:q^2: &= 2q\frac{\partial}{\partial p}, & :p^2: &= -2p\frac{\partial}{\partial q}
\end{aligned}
\tag{9.52}
$$

Exercise 19 It was mentioned that $:f:$ and $:g:$ commute if $[f,g]=0$. In fact, $:f:$ and $:g:$ commute even if $[f,g]\neq 0$ but $=$ constant (independent of x and p but can depend on s). (a) Although $[ax, bp] = ab \neq 0$, show that

$$:ax::bp: = :bp::ax:$$

(b) Although $[ax^2, \frac{bp}{x}] = 2ab \neq 0$, show that

$$:ax^2::\frac{bp}{x}: = :\frac{bp}{x}:ax^2:$$

Exercise 20 Show that

$$:g::f:^2 g = -:f::g:^2 f \tag{9.53}$$

This identity is of some use later.
Solution Define $h = :f:g$, then

$$
\begin{aligned}
:g::f:^2 g &= :g::f:h = -:f::h:g - :h::g:f \\
&= :f::g:h + :h::f:g = :f::g:h + :h:h \\
&= :f::g:h = :f::g::f:g = -:f::g:^2 f \implies \quad \text{Q.E.D.}
\end{aligned}
$$

Lie operators for accelerator elements   The maps for accelerator elements can be represented as exponential operators. For simplicity, let us consider a 1-D system. A drift space of length L, for example, can be represented as the operator $\exp(:-\frac{1}{2}Lp^2:)$. To show that, let's first establish the following:

$$
\begin{aligned}
:p^2:x &= \frac{\partial p^2}{\partial x}\frac{\partial x}{\partial p} - \frac{\partial p^2}{\partial p}\frac{\partial x}{\partial x} = -2p \\
:p^2:p &= \frac{\partial p^2}{\partial x}\frac{\partial p}{\partial p} - \frac{\partial p^2}{\partial p}\frac{\partial p}{\partial x} = 0 \\
(:p^2:)^2 x &= :p^2:(:p^2:x) = :p^2:(-2p) = 0 \\
(:p^2:)^2 p &= :p^2:(:p^2:p) = :p^2:(0) = 0
\end{aligned}
$$

186

We then apply the operator $\exp(:-Lp^2/2:)$ to (x, p) to obtain

$$
\begin{aligned}
e^{:-Lp^2/2:}x &= x - \frac{1}{2}L:p^2:x + \frac{1}{8}L^2(:p^2:)^2 x + ... \\
&= x - \frac{1}{2}L(-2p) = x + Lp \\
e^{:-Lp^2/2:}p &= p - \frac{1}{2}L:p^2:p + ... = p
\end{aligned}
\tag{9.54}
$$

If we identify the x and p on the right hand sides of Eq.(9.54) as the initial coordinate and momentum of the particle, we recognize that $\exp(:-\frac{1}{2}Lp^2:)x$ and $\exp(:-\frac{1}{2}Lp^2:)p$ give the final coordinate and momentum of the particle. We therefore identify $\exp(:-\frac{1}{2}Lp^2:)$ as the Lie operator of a drift space, and it is to be applied according to Eq.(9.30).

Similarly we can establish the Lie operators for other accelerator elements. A few simpler examples are given in Table 4. [See Exercise 27.]

Table 4: Lie operators of some accelerator elements.

Element	Map	Lie Operator
Drift space	$x = x_0 + Lp_0$	$\exp(:-\frac{1}{2}Lp^2:)$
	$p = p_0$	
Thin-lens Quadrupole	$x = x_0$	$\exp(:-\frac{1}{2f}x^2:)$
	$p = p_0 - \frac{1}{f}x_0$	
Thin-lens Multipole	$x = x_0$	$\exp(:\lambda x^n:)$
	$p = p_0 + \lambda n x^{n-1}$	
Thin-lens kick	$x = x_0$	$\exp(:\int_0^x f(x')dx':)$
	$p = p_0 + f(x)$	
Thick focusing quad	$x = x_0 \cos kL + \frac{p_0}{k}\sin kL$	$\exp[:-\frac{1}{2}L(k^2 x^2 + p^2):]$
	$p = -kx_0 \sin kL + p_0 \cos kL$	
Thick defocusing quad	$x = x_0 \cosh kL + \frac{p_0}{k}\sinh kL$	$\exp[:\frac{1}{2}L(k^2 x^2 - p^2):]$
	$p = kx_0 \sinh kL + p_0 \cosh kL$	
Coordinate shift	$x = x_0 - b$	$\exp(:ax + bp:)$
	$p = p_0 + a$	
Coordinate rotation	$x = x_0 \cos\mu + p_0 \sin\mu$	$\exp[:-\frac{1}{2}\mu(x^2 + p^2):]$
	$p = -x_0 \sin\mu + p_0 \cos\mu$	
Scale change	$x = e^{-\lambda}x_0$	$\exp(:\lambda xp:)$
	$p = e^{\lambda}p_0$	

Exponential Lie operators We will now establish a few formulae of the algebra of exponential operators, which are frequently used in later developments. First, we show that the inverse map of $\exp(:f:)$ is $\exp(-:f:)$, i.e.

$$
(e^{:f:})^{-1} = e^{-:f:}
\tag{9.55}
$$

Proof:

$$
\begin{aligned}
e^{:f:}e^{-:f:} &= \sum_{m=0}^{\infty}\sum_{n=0}^{\infty} \frac{1}{m!n!}(:f:)^m(-:f:)^n \\
&= \sum_{k=0}^{\infty}\sum_{n=0}^{k} \frac{1}{(k-n)!n!}(:f:)^{k-n}(-:f:)^n \\
&= \sum_{k=0}^{\infty}\frac{1}{k!}\sum_{n=0}^{k} \frac{k!}{(k-n)!n!}(:f:)^{k-n}(-:f:)^n \\
&= \sum_{k=0}^{\infty}\frac{1}{k!}(:f:-:f:)^k = 1 \qquad \Longrightarrow \text{Q.E.D.} \qquad (9.56)
\end{aligned}
$$

The derivation in Eq.(9.56) can be repeated to show that if $:f:$ and $:g:$ commute (i.e. if $:f: :g: = :g: :f:$, or if $[f,g] = $ constant depends only on s), then

$$
e^{:f:}e^{:g:} = e^{:f+g:} \qquad (9.57)
$$

In fact, Eq.(9.56), and therefore (9.55), is just a special case of (9.57). When $:f:$ and $:g:$ do not commute, Eq.(9.57) is no longer valid. In that case, the right hand side of Eq.(9.57) will acquire additional terms that relate to the commutators of the operators. The corresponding formula is called the Baker-Campbell-Hausdorff formula, which is an important later subject.

Next we establish the following:

$$
e^{:f:}(gh) = (e^{:f:}g)(e^{:f:}h) \qquad (9.58)
$$

Note that Eq.(9.58) applies for exponential maps (which means all symplectic maps); if one is interested in $:f:(gh)$, one should consider applying the third member of Eq.(9.9). The proof of Eq.(9.58) can be established using Eq.(9.47) and is omitted here. One useful variation of Eq.(9.58) is

$$
e^{:f:}[g,h] = [e^{:f:}g, e^{:f:}h] \qquad (9.59)
$$

It follows from Eq.(9.58) that, for an arbitrary function g of X (X is the vector whose components are the canonical coordinates), one has

$$
e^{:f:}g(X) = g(e^{:f:}X) \qquad (9.60)
$$

The proof of Eq.(9.60) is as follows. Letting $g(X) = h(X) = X$ in Eq.(9.58) gives $e^{:f:}(X^2) = (e^{:f:}X)^2$, i.e. Eq.(9.60) holds if $g(X) = X^2$ including the cross products of the components of X. This can be extended to arbitrary powers of X. Since any function (of interest to us) can be expressed as power series, Eq.(9.60) therefore holds for arbitrary functions of X. Equations (9.58-9.60) establish the fact that the most basic Lie operation is of the type $e^{:f:}X$.

According to Eq.(9.60), the operation by an exponential operator on a function can be propagated to the argument of the function. In other words, exponential Lie operators are "penetrating" in the sense that they penetrate into

the guts of a functions they operate on. Since any symplectic operator can be written as an exponential operator, this property holds for all symplectic operators. This is a very interesting and useful property.[43] Table 5 lists several often-used formulae for Lie operators.

Table 5: Some formulae for Lie operators. Here a is a constant and C is a constant vector, both independent of X, S is given by Eqs.(9.3-9.4), and f, g, and G are arbitrary functions. Square brackets mean Poisson brackets. Curly brackets mean commutators.

$$
\begin{array}{cc}
:a: = 0, & e^{:a:} = 1 \\
:f:a = 0, & e^{:f:}a = a \\
:f:f = 0, & e^{:f:}f = f \\
\multicolumn{2}{c}{\{:f:,:g:\} = :[f,g]:} \\
\multicolumn{2}{c}{e^{:f:}g(X) = g(e^{:f:}X)} \\
\multicolumn{2}{c}{e^{:\tilde{C}X:}g(X) = g(X - SC)} \\
\multicolumn{2}{c}{e^{:f:}G(:g:)e^{-:f:} = G(:e^{:f:}g:)}
\end{array}
$$

Equation (9.60) describes what happens when a symplectic Lie operator is applied to a function. Lie operators can also be applied to other Lie operators. The counterpart of Eq.(9.60) in that case reads

$$ e^{:f:}:g:e^{-:f:} = :(e^{:f:}g): \tag{9.61} $$

Note that it now takes a sandwich form (similarity transformation). Note also the penetrating property of exponential operators into the guts of the operator that being being operated on. Proof of Eq.(9.61) is given in Exercise 23. Similar to Eq.(9.58), Eq.(9.61) is applicable only to symplectic maps.

Exercise 21 Show that the quantity f is invariant under the map $e^{:f:}$.

Solution Consider the map $X = e^{:f:}X\big|_{X=X_0}$. We need to show that $f(X) = f(X_0)$, which is true because

$$ f(X) = f(e^{:f:}X\big|_{X=X_0}) = e^{:f:}f(X)\big|_{X=X_0} = f(X)\big|_{X=X_0} = f(X_0) \tag{9.62} $$

Exercise 22 Show that if $[f, g] = 0$, then g is invariant under $e^{:f:}$. (In particular, if f is the Hamiltonian, then $e^{:f:}$ describes the time evolution of the system, and this exercise says that if $[f, g] = 0$, then g is a constant of the motion.)

Exercise 23 Prove Eq.(9.61).

---

[43] Note again that Eq.(9.60) applies only to symplectic operators. An equation such as $:f:g(X) = g(:f:X)$ does not hold in general. Incidentally, $e^{:f:} = :e^f:$ is also invalid.

Solution Consider an arbitrary function $h(X)$, we have

$$e^{:f:}{:}g{:}h = e^{:f:}[g,h] = [e^{:f:}g, e^{:f:}h] = {:}(e^{:f:}g){:}e^{:f:}h$$
$$\implies \qquad e^{:f:}{:}g{:} = {:}(e^{:f:}g){:}e^{:f:} \qquad\qquad (9.63)$$

where use has been made of Eq.(9.59). Multiplying both sides from the right by $e^{-:f:}$ proves Eq.(9.61).

It follows from Eq.(9.61) that

$$e^{:f:}({:}g{:})^n e^{-:f:} = (e^{:f:}{:}g{:}e^{-:f:})^n = ({:}e^{:f:}g{:})^n \qquad\qquad (9.64)$$

which in turn leads to the property that, for an arbitrary function G that can be expressed as power series, one has

$$e^{:f:}G({:}g{:})e^{-:f:} = G({:}e^{:f:}g{:}) \qquad\qquad (9.65)$$

This property has been listed in Table 5. One particularly useful special case of Eq.(9.65) is

$$e^{:f:}e^{:g:}e^{-:f:} = \exp({:}e^{:f:}g{:}) \qquad\qquad (9.66)$$

Note the difference between Eq.(9.65) — Lie operation on operators — and Eq.(9.60) — Lie operation on functions. In Eq.(9.60), one sees the powerful property for symplectic Lie operators that they *permeate* into the guts of the functions they apply to. In Eq.(9.65), one sees that the application assumes a sandwich form (similarity transformation), and that again, symplectic Lie operators permeate into the guts of the operators being applied to.

The sandwich form in Eq.(9.65) has the consequence that when a string of operators are being transformed, the result can be written as the same string of the transformed operators, i.e.

$$e^{:f:}({:}g_1{:}\,{:}g_2{:}\,...\,{:}g_n{:})e^{-:f:} = ({:}e^{:f:}g_1{:})({:}e^{:f:}g_2{:})\,...\,({:}e^{:f:}g_n{:})$$
$$= [{:}g_1(e^{:f:}X){:}][{:}g_2(e^{:f:}X){:}]\,...\,[{:}g_n(e^{:f:}X){:}] \qquad (9.67)$$

where use has been made of Eq.(9.55). This sandwiching property has been used in Eq.(9.64) and will be used frequently later. Equation (9.67) indicates that the sandwiching transformation is equivalent to substituting the dynamical coordinates X by $e^{:f:}X$ in the arguments of the operators.

There is a subtlety concerning the ordering of operators. Consider an accelerator section consisting of an element F (with operator $e^{:F:}$), followed by an element G (with operator $e^{:G:}$). Let X_0 be the coordinates of a particle entering element F. Let X_1 be the coordinates of the particles exiting element F and entering element G. Then we have

$$X_1 = e^{:F(X):}X\Big|_{X=X_0} \qquad\qquad (9.68)$$

Let X_2 be the coordinates exiting element G, then

$$
\begin{aligned}
X_2 &= \left. e^{:G(X):}X \right|_{X=X_1} = \left. \exp[:G(e^{:F(X):}X):]e^{:F(X):}X \right|_{X=X_0} \\
&= \left. \exp[:e^{:F(X):}G(X):]e^{:F(X):}X \right|_{X=X_0} \\
&= \left. (e^{:F:}e^{:G:}e^{:-F:})e^{:F:}X \right|_{X=X_0} = \left. e^{:F:}e^{:G:}X \right|_{X=X_0}
\end{aligned}
\tag{9.69}
$$

Equation (9.69) indicates that, when a string of elements are connected into an accelerator section, the ordering of the operators is such that operators of the earlier elements appear to the *left* of operators of the later elements. This is opposite to what one might be used to when dealing with the linear systems with matrices!

We are now in a position to show another key property of exponential operators, namely, an operator of exponential form $e^{:f:}$ is necessarily symplectic for an arbitrary function $f(X,s)$. To prove this, consider the quantity $X = \left. e^{:f:}X \right|_{X=X_0}$, and form the fundamental Poisson brackets

$$
\begin{aligned}
[X_\alpha, X_\beta] &= \left. [e^{:f:}X_\alpha, e^{:f:}X_\beta] \right|_{X=X_0} \\
&= \left. (e^{:f:}[X_\alpha, X_\beta]) \right|_{X=X_0} = \left. (e^{:f:}S_{\alpha\beta}) \right|_{X=X_0} = S_{\alpha\beta}
\end{aligned}
\tag{9.70}
$$

Equations (9.16-9.17) then prove that the operator $e^{:f:}$ is symplectic. Conversely, symplectic maps can always be expressed as exponential maps.

The fact that exponential operators are necessarily symplectic has an important practical meaning. In practice, one often has the exponential form $e^{:f:}$ of a symplectic map, and one needs to compute the effect of the map on the motion of a particle, i.e., one needs to find $e^{:f:}X$. For a general f, however, this is often not an easy task. The trick often adopted is to expand f in terms of a power series in the components of X,

$$
e^{:f:} = e^{:(f_2+f_3+f_4+\dots):}
\tag{9.71}
$$

where f_k is a homogeneous power series of k-th order in the components of X. The exponential form allows the possibility that this power series be truncated at will without losing symplecticity. (What one loses is accuracy.) In contrast, had the map been written as $:f:$ instead of an exponential form, a truncation would in general lead to a loss of the symplecticity of the map.

Furthermore, one can also write the map in a different form,

$$
e^{:f:} = e^{:f_2:}e^{:f_3:}e^{:f_4:}\dots
\tag{9.72}
$$

The f_2 in Eq.(9.72) is the same as the f_2 in Eq.(9.71), but all the higher order f_k's differ. Again in this form, exponential factors of higher orders can be truncated at will without losing symplecticity. In either the form (9.71) or (9.72), truncation down to the second order gives the linear map $e^{:f_2:}$.

Applications to Linear Systems Let us apply operator algebra to a linear system. Consider a quadratic form

$$f_2 = -\frac{1}{2}\tilde{X}FX \tag{9.73}$$

where F is a symmetric, positive definite matrix.[44] We have

$$:f_2:X = SFX \tag{9.74}$$

where S is the familiar matrix (9.3). The proof of Eq.(9.74) is as follows:

$$
\begin{aligned}
:f_2:X_\alpha &= \frac{\partial f_2}{\partial X_\beta}S_{\beta\gamma}\frac{\partial X_\alpha}{\partial X_\gamma} \\
&= -\frac{1}{2}\frac{\partial(F_{\ell m}X_\ell X_m)}{\partial X_\beta}S_{\beta\gamma}\delta_{\alpha\gamma} \\
&= -F_{\beta\ell}X_\ell S_{\beta\alpha} = (SFX)_\alpha, \quad \text{Q.E.D.}
\end{aligned}
$$

It follows from Eq.(9.74) that

$$e^{:f_2:}X \leftrightarrow e^{SF}X, \quad \text{or} \quad e^{:f_2:} \leftrightarrow e^{SF} \tag{9.75}$$

There is a reason I use $\leftrightarrow$ instead of $=$ in Eq.(9.75): The left-hand-side of Eq.(9.75) is a Lie operator form, while the right-hand-side is a matrix form. In particular, the left-hand-side can be applied to the components of X individually, while the right-hand-side must be applied simultaneously to all components of X.

Computation of e^{SF} requires taking exponentials of a matrix. Exponentiation of a matrix A is defined in a power series fashion as

$$e^A = \sum_{k=0}^{\infty}\frac{1}{k!}A^k \tag{9.76}$$

To be more specific, consider a 1-D system for which F is a symmetric 2×2 matrix. Let F be

$$F = \begin{bmatrix} a & b \\ b & c \end{bmatrix} \tag{9.77}$$

The positive definiteness of F means the quantity $\tilde{X}FX \geq 0$ for arbitrary X. This leads to

$$b^2 \leq ac \quad \text{and} \quad a \geq 0 \tag{9.78}$$

We now need to compute the matrix e^{SF}. To do so, we apply a theorem called the *Hamilton-Cayley theorem*, which says that, for an $N \times N$ matrix A, and $f(A)$ being any function of A, we have

$$f(A) = \sum_{k=0}^{N-1}a_k A^k \tag{9.79}$$

---

[44]The condition of positive definiteness is for the particle motion to be stable. Examples of exception can be found in Eqs.(9.106) and (9.109).

where a_k are a set of coefficients which satisfy the algebraic conditions

$$f(\lambda) = \sum_{k=0}^{N-1} a_k \lambda^k \quad \text{with} \quad \lambda = \text{eigenvalues of } A \tag{9.80}$$

To appreciate the power of the Hamilton-Cayley theorem, note that the matrix $f(A)$ is a $N \times N$ matrix; it has N^2 elements. However, Eq.(9.79) expresses it with only N (not N^2) "fitting parameters" a_k. Furthermore, these N fitting parameters can be found by solving Eq.(9.80). The prove of the Hamilton-Cayley theorem is given in Exercise 25.

To apply the Hamilton-Cayley theorem to the present problem, we have $N = 2$ and

$$e^{SF} = \exp\left(\begin{bmatrix} b & c \\ -a & -b \end{bmatrix}\right) = a_0 + a_1 \begin{bmatrix} b & c \\ -a & -b \end{bmatrix} \tag{9.81}$$

where a_0 and a_1 are yet to be determined. The eigenvalues of the matrix $SF = \begin{bmatrix} b & c \\ -a & -b \end{bmatrix}$ are

$$\lambda_\pm = \pm i\sqrt{ac - b^2} \tag{9.82}$$

The coefficients a_0 and a_1 therefore satisfy

$$e^{\lambda_+} = a_0 + a_1\lambda_+, \quad e^{\lambda_-} = a_0 + a_1\lambda_-$$

$$\implies \quad a_0 = \cos(\sqrt{ac - b^2}), \quad a_1 = \frac{\sin(\sqrt{ac - b^2})}{\sqrt{ac - b^2}} \tag{9.83}$$

We thus obtain

$$e^{SF} = \cos(\sqrt{ac - b^2}) + \frac{\sin(\sqrt{ac - b^2})}{\sqrt{ac - b^2}} \begin{bmatrix} b & c \\ -a & -b \end{bmatrix} \tag{9.84}$$

Equation (9.84) can be used to find the matrix form of the map when the Lie form of the map $e^{:f_2:} = e^{:-\frac{1}{2}(ax^2 + 2bxp + cp^2):}$ is known. One can also try to find the Lie form, given the matrix form, as follows. Suppose we know that the linear map has a matrix form

$$R = \begin{bmatrix} R_{11} & R_{12} \\ R_{21} & R_{22} \end{bmatrix} \quad \text{with} \quad \det R = 1 \tag{9.85}$$

By identifying the right-hand-side of Eq.(9.84) with Eq.(9.85), the coefficients a, b and c can be related to the R matrix elements according to

$$\cos(\sqrt{ac - b^2}) = \frac{1}{2}\text{tr}R$$

$$\frac{a}{-R_{21}} = \frac{2b}{R_{11} - R_{22}} = \frac{c}{R_{12}} = \frac{\sqrt{ac - b^2}}{\sin(\sqrt{ac - b^2})} \tag{9.86}$$

Knowing a, b, c, the Lie form of the map is readily obtained.

For example, the R matrix may be a one-turn map of the Courant-Snyder form

$$R = \begin{bmatrix} \cos\mu + \alpha\sin\mu & \beta\sin\mu \\ -\gamma\sin\mu & \cos\mu - \alpha\sin\mu \end{bmatrix} \tag{9.87}$$

where β and α are the β- and α-functions at the observation position in the circular accelerator, $\gamma = (1 + \alpha^2)/\beta$, and μ is the betatron phase advance per turn. In terms of α, β, γ and μ, we find

$$a = \mu\gamma, \quad b = \mu\alpha, \quad \text{and} \quad c = \mu\beta$$
$$ac - b^2 = \mu^2 \geq 0 \tag{9.88}$$

This gives, using Eq.(9.73),

$$\begin{aligned} f_2 &= -\frac{\mu}{2}(\gamma x^2 + 2\alpha xp + \beta p^2) \\ &= -\frac{\mu}{2} \times (\text{Courant-Snyder invariant}) \end{aligned} \tag{9.89}$$

The Courant-Snyder map (9.87) has thus acquired a Lie operator form

$$e^{:f_2:} = e^{:-\frac{\mu}{2}(\gamma x^2 + 2\alpha xp + \beta p^2):} \tag{9.90}$$

As we will see later, the one-turn map of a circular accelerator has the general form $e^{-C:H_{\text{eff}}:}$ where C is the accelerator circumference and H_{eff} is the effective Hamiltonian. Equation (9.90) says that in the linear case, the Courant-Snyder invariant has acquired the physical meaning of the effective Hamiltonian that describes the one-turn map, while the betatron phase advance per turn μ has the meaning of the total length of the accelerator (except that it is measured in radians instead of in meters).

In general, linear maps can be described by an exponential operator $\exp(:f_2:)$, where f_2 is a quadratic function of X. In particular, let f_2 be written as Eq.(9.73). We have shown that the map corresponding to the operator $\exp(:f_2:)$ can be written in a matrix notation as

$$X = MX_0 \quad \text{where} \quad M = e^{SF} \tag{9.91}$$

Consider two quadratic forms $f = -\frac{1}{2}\tilde{X}FX$ and $g = -\frac{1}{2}\tilde{X}GX$. Their corresponding maps can be concatenated into another linear map according to

$$e^{:h:} = e^{:f:}e^{:g:} \tag{9.92}$$

where $h = -\frac{1}{2}\tilde{X}HX$ is another quadratic form whose corresponding matrix H satisfies

$$e^{SH} = e^{SG}e^{SF} \tag{9.93}$$

Comparing Eq.(9.92) in the Lie representation and (9.93) in the matrix representation, note that the ordering of the F and G components appear in reversed order. [See discussion following Eq.(9.69).]

The proof of Eq.(9.93) is as follows:

$$
\begin{aligned}
e^{:f:}e^{:g:}X_\alpha &= e^{:f:}(e^{SG}X)_\alpha = e^{:f:}(e^{SG})_{\alpha\beta}X_\beta \\
&= (e^{SG})_{\alpha\beta}e^{:f:}X_\beta = (e^{SG})_{\alpha\beta}(e^{SF}X)_\beta = (e^{SG}e^{SF}X)_\alpha \quad \Longrightarrow \text{Q.E.D.}
\end{aligned}
$$

The map (9.90) can be extended to include the synchrotron motion. Consider a 2-D linear system whose dynamical variables are (x, x', z, δ) where z is the longitudinal coordinate of a particle relative to an ideal reference particle, and $\delta = \Delta P/P$ is the momentum error relative to the reference particle. In the present consideration, we consider $\delta = $ constant in time, i.e., the momentum is an invariant. The motion can be decomposed into a betatron and a synchrotron motion,

$$
x = x_\beta + \eta\delta, \qquad x' = x'_\beta + \eta'\delta \tag{9.94}
$$

where η is the dispersion function. Since x and $p = x'$ in Eq.(9.90) actually are the betatron components x_β and x'_β, the relevant f_2 in the present system is

$$
\begin{aligned}
f_2 &= -\frac{\mu}{2}(\gamma x_\beta^2 + 2\alpha x_\beta x'_\beta + \beta x'^2_\beta) \\
\to f_2 &= -\frac{\mu}{2}[\gamma(x - \eta\delta)^2 + 2\alpha(x - \eta\delta)(x' - \eta'\delta) + \beta(x' - \eta'\delta)^2] + \frac{1}{2}C\alpha_c\delta^2
\end{aligned}
\tag{9.95}
$$

In Eq.(9.95), x and x' refer to the total physical horizontal coordinates (9.94). An extra term $\frac{1}{2}C\alpha_c\delta^2$, where α_c is the momentum compaction factor and C is the accelerator circumference, has been added to f_2; its function will become clear momentarily.

Given the quadratic form (9.95), we then ask what is the 4×4 matrix R for the map $e^{:f_2:}$? This is done by calculating explicitly the quantities $e^{:f_2:}X$ and equating the results with the matrix form RX. Omitting the algebra, the result is $R =$

$$
\begin{bmatrix}
\cos\mu + \alpha\sin\mu & \beta\sin\mu & 0 & \eta - \eta R_{11} - \eta' R_{12} \\
-\gamma\sin\mu & \cos\mu - \alpha\sin\mu & 0 & \eta' - \eta' R_{22} - \eta R_{21} \\
\eta' - \eta' R_{11} + \eta R_{21} & -\eta + \eta R_{22} - \eta' R_{12} & 1 & (\gamma\eta^2 + 2\alpha\eta\eta' + \beta\eta'^2)\sin\mu - C\alpha_c \\
0 & 0 & 0 & 1
\end{bmatrix}
\tag{9.96}
$$

which is a familiar result from basic accelerator optics.

Exercise 24 Consider Eq.(9.75). (a) Show that for any matrix A,

$$
\det(e^A) = e^{\operatorname{tr}A} \tag{9.97}
$$

It follows that, with F any symmetric matrix, $\det(e^{SF}) = 1$. (b) Show that the matrix e^{SF} is symplectic, where F is any symmetric matrix.

Exercise 25 Prove the Hamilton-Cayley theorem (9.79-9.80).

Solution Consider the characteristic polynomial $P(\lambda) = \det(A - \lambda I)$, which is an N-th order polynominal in λ. We have

$$P(\lambda) = (\lambda - \lambda_1)(\lambda - \lambda_2) \ ... \ (\lambda - \lambda_N) \qquad (9.98)$$

where λ_j are the eigenvalues of A. Consider the function of A,

$$P(A) = (A - \lambda_1 I)(A - \lambda_2 I) \ ... \ (A - \lambda_N I) \qquad (9.99)$$

If we apply $P(A)$ to V_j, which is an eigenvector of A, we obtain

$$P(A)V_j = 0 \qquad (9.100)$$

The only way Eq.(9.100) can be true for all $j = 1, 2, ...N$ is when $P(A) = 0$ identically. The fact that $P(A) = 0$ is the Hamilton-Cayley theorem.

   As a consequence of this theorem, when A is raised to a power $\geq n$, the resulting matrix can always be expressed in terms of a summation over lower powers of A with order $\leq n - 1$. If $f(A)$ can be expressed as a power series in A, then it can be expressed as a power series with order $\leq n - 1$. Thus we have proved Eq.(9.79). Having established Eq.(9.79), Eq.(9.80) follows.

Exercise 26 Consider the matrix

$$A = \begin{bmatrix} a & b \\ c & d \end{bmatrix}$$

(a) Demonstrate the Hamilton-Cayley theorem explicitly, i.e. show that
$$P(A) = A^2 - (a + d)A + ad - bc = 0$$

(b) Apply the Hamilton-Cayley theorem to obtain

$$f(A) = \frac{1}{\lambda_+ - \lambda_-} \{ [\lambda_+ f(\lambda_-) - \lambda_- f(\lambda_+)] + [f(\lambda_+) - f(\lambda_-)]A \}$$
$$(9.101)$$

where
$$\lambda_\pm = \frac{1}{2}(a + d) \pm \frac{1}{2}\sqrt{(a - d)^2 + 4bc}$$

are the eigenvalues of A. Given matrix A, Eq.(9.101) gives the matrix $f(A)$ for an arbitrary function $f(x)$. Observe from Eq.(9.101) that if the 2×2 matrix A is triangular (i.e. either $b = 0$ or $c = 0$), the matrix $f(A)$ is necessarily triangular for arbitrary $f(x)$. Similarly, if A is diagonal, so is $f(A)$.
(c) Find the matrices A^2, A^3, A^{-1}, $\sqrt{A}$, and e^A as special cases of Eq.(9.101).
Solution (c) All these matrices can be written in the form $a_0 + a_1 A$, as follows

$$A^2 \quad = \quad -(ad - bc) + (a + d)A$$

$$A^3 = -(a+d)(ad-bc) + (a^2 + ad + d^2 + bc)A$$

$$A^{-1} = \frac{1}{ad-bc}[(a+d) - A] \qquad (9.102)$$

$$\sqrt{A} = \frac{1}{\sqrt{\lambda_+} + \sqrt{\lambda_-}}(\sqrt{ad-bc} + A)$$

$$e^A = e^{(a+d)/2}\left[\frac{\sinh\frac{\sqrt{(a-d)^2+4bc}}{2}}{\sqrt{(a-d)^2+4bc}}(-a-d+2A)\right.$$

$$\left. + \cosh\frac{\sqrt{(a-d)^2+4bc}}{2}\right]$$

Exercise 27 It is possible to establish the connections among Eqs.(9.75), (9.87) and (9.90) differently from the text.
(a) Show by brute force, without using the Hamilton-Cayley theorem, that the quantity $\exp(:f_2:)X$ with f_2 given by Eq.(9.90) gives a transformation according to the matrix (9.87).
(b) Another way is as follows. We have

$$e^{:f_2:}X = RX \quad \implies \quad :f_2:X = (\ln R)X \qquad (9.103)$$

If R has the form (9.87), whose eigenvalues are $e^{\pm i\mu}$, an application of the Hamilton-Cayley theorem gives

$$\ln R = \mu \begin{bmatrix} \alpha & \beta \\ -\gamma & -\alpha \end{bmatrix} \qquad (9.104)$$

This map is to be identified with $:f_2:$. This can be done if f_2 is given by Eq.(9.89).

Exercise 28 Find the Lie operators representing (a) a drift space, (b) a thin-lens quadrupole, (c) a thick focusing quadrupole, and (d) a thick defocusing quadrupole. These results have been given in Table 4.
Solution
(a) Let the operator for a drift space L be written as $e^{:f_2:} = \exp(:-\frac{1}{2}\tilde{X}FX:)$. We need to find F. Let F be written as Eq.(9.77), then we have, using Eq.(9.84),

$$\cos(\sqrt{ac-b^2}) + \frac{\sin(\sqrt{ac-b^2})}{\sqrt{ac-b^2}}\begin{bmatrix} b & c \\ -a & -b \end{bmatrix} = \begin{bmatrix} 1 & L \\ 0 & 1 \end{bmatrix} \qquad (9.105)$$

The solution is found to be, using Eq.(9.86), $a = 0, b = 0, c = L$ which gives $f_2 = -\frac{1}{2}Lp^2$.

(b) Replace the right-hand-side of Eq.(9.105) by $\begin{bmatrix} 1 & 0 \\ -\frac{1}{f} & 1 \end{bmatrix}$ where f = focal length. We have $a = \frac{1}{f}, b = 0, c = 0$, which gives $f_2 = -\frac{1}{2f}x^2$. For a defocusing thin-lens quadrupole, just let $f < 0$.

(c) Replace the right-hand-side of Eq.(9.105) by $\begin{bmatrix} \cos kL & \frac{1}{k}\sin kL \\ -k\sin kL & \cos kL \end{bmatrix}$.

We find $a = k^2 L, b = 0, c = L$, which gives $f_2 = -\frac{1}{2}L(k^2 x^2 + p^2)$.

(d) Replace k in the case above by ik to obtain

$$a = -k^2 L, \quad b = 0, \quad c = L \tag{9.106}$$

which gives $f_2 = \frac{1}{2}L(k^2 x^2 - p^2)$. Note that in this case, $ac - b^2 < 0$.

Exercise 29 If the matrix R is not given by the Courant-Snyder representation (9.87) for a stable system, but is for an unstable system with

$$R = \begin{bmatrix} \cosh\mu + \alpha\sinh\mu & \beta\sinh\mu \\ \frac{1-\alpha^2}{\beta}\sinh\mu & \cosh\mu - \alpha\sinh\mu \end{bmatrix} \tag{9.107}$$

Show that R can also be written as e^{SG}, where

$$G = \mu\begin{bmatrix} \frac{\alpha^2-1}{\beta} & \alpha \\ \alpha & \beta \end{bmatrix} \tag{9.108}$$

and the corresponding Lie representation of the map is

$$\exp\left[: -\frac{\mu}{2}(\frac{\alpha^2-1}{\beta}x^2 + 2\alpha xp + \beta p^2):\right] \tag{9.109}$$

Note that the quadratic form in Eq.(9.109) is not positive definite.

Exercise 30 Lie representation is very useful for generalization to nonlinear systems, but is awkward for a linear system. Linear systems are best studied with matrices. To appreciate this, try to concatenate a drift space followed by a thin-lens quadrupole. This can be easily done in the matrix language. In the Lie language, one needs to concatenate

$$e^{:-\frac{1}{2}Lp^2:}e^{:-\frac{1}{2f}x^2:} \tag{9.110}$$

This can drive you crazy.

Exercise 31 Use Exercise 30 to demonstrate the "reverse" ordering rule of the Lie operators, i.e. Eq.(9.110) describes a quadrupole followed by a drift, and not a drift followed by a quadrupole.

Exercise 32 The Lie map (9.90) gives the one-turn Courant-Snyder map (9.87). The Courant-Snyder map from position 1 (with parameters α_1, β_1) to position 2 (with parameters α_2, β_2) is (ψ is the betatron phase advance from position 1 to position 2)

$$\begin{bmatrix} \sqrt{\frac{\beta_2}{\beta_1}}(\cos\psi + \alpha_1\sin\psi) & \sqrt{\beta_1\beta_2}\sin\psi \\ -\frac{1+\alpha_1\alpha_2}{\sqrt{\beta_1\beta_2}}\sin\psi + \frac{\alpha_1-\alpha_2}{\sqrt{\beta_1\beta_2}}\cos\psi & \sqrt{\frac{\beta_1}{\beta_2}}(\cos\psi - \alpha_2\sin\psi) \end{bmatrix} \tag{9.111}$$

Find the Lie representation of this map.

Solution The Lie map is given by $\exp[-:\frac{1}{2}(ax^2 + 2bxx' + cx'^2):]$, where a, b, and c are determined by Eq.(9.86). In particular,

$$
\begin{aligned}
\sqrt{ac - b^2} \;=\;& \cos^{-1}\left[\frac{1}{2}\left(\sqrt{\frac{\beta_2}{\beta_1}} + \sqrt{\frac{\beta_1}{\beta_2}}\right)\cos\psi \right.\\
& \left. +\frac{1}{2}\left(\alpha_1\sqrt{\frac{\beta_2}{\beta_1}} - \alpha_2\sqrt{\frac{\beta_1}{\beta_2}}\right)\sin\psi\right]
\end{aligned}
\tag{9.112}
$$

Again, one observes that the Lie map is much clumsier than the matrix map for linear problems. One special case occurs when $\alpha_1 = \alpha_2$ and $\beta_1 = \beta_2$. Then the Lie map has a simple form $\exp[-:\frac{1}{2}\psi(\gamma x^2 + 2\alpha xx' + \beta x'^2):]$.

Application to Nonlinear Systems So far we have been considering linear systems, which can be analysed using matrices. Using Lie technique for linear cases in fact is more cumbersome than using matrices. [See Exercises 30 and 32.] Lie technique is not very useful for linear cases, but it is useful for nonlinear cases. In fact, it provides the natural way to generalize the Courant-Snyder analysis to nonlinear systems.

As an application of the operator algebra to a nonlinear problem, consider a map which is known to have a second order Taylor representation

$$
X_\alpha = R_{\alpha\beta}X_{0\beta} + T_{\alpha\beta\gamma}X_{0\beta}X_{0\gamma} + \mathcal{O}(X_0^3)
\tag{9.113}
$$

where the T-coefficients satisfy $T_{\alpha\beta\gamma} = T_{\alpha\gamma\beta}$. We may proceed to find a Lie representation of this map, accurate to order $\mathcal{O}(X^2)$, in the form

$$
e^{:f_2:}e^{:f_3:}
\tag{9.114}
$$

In Eq.(9.114), f_2 and f_3 are homogeneous power series in X,

$$
\begin{aligned}
f_2 \;&=\; -\frac{1}{2}\tilde{X}FX = -\frac{1}{2}F_{\ell m}X_\ell X_m \\
f_3 \;&=\; C_{\ell mn}X_\ell X_m X_n
\end{aligned}
\tag{9.115}
$$

where the F and C coefficients are symmetric with respect to permutations on their respective subscript indices. Our job is to find the F- and C-coefficients in terms of the R- and T-coefficients, and vice versa.

We first note that

$$
\begin{aligned}
:f_3:X_\alpha \;&=\; \frac{\partial f_3}{\partial X_\delta}S_{\delta\gamma}\frac{\partial X_\alpha}{\partial X_\gamma} \\
&=\; \frac{\partial(C_{\ell mn}X_\ell X_m X_n)}{\partial X_\delta}S_{\delta\gamma}\delta_{\alpha\gamma} \\
&=\; C_{\ell mn}(\delta_{\delta\ell}X_m X_n + X_\ell\delta_{m\delta}X_n + X_\ell X_m\delta_{\delta n})S_{\delta\alpha} \\
&=\; -3S_{\alpha\delta}C_{\delta mn}X_m X_n
\end{aligned}
$$

and that
$$(:f_3:)^2 X_\alpha = \mathcal{O}(X^3)$$

It follows that

$$
\begin{aligned}
e^{:f_3:} X_\alpha &= [1 + :f_3: + \frac{1}{2}:f_3:^2 + ...] X_\alpha \\
&= X_\alpha - 3 S_{\alpha\delta} C_{\delta mn} X_m X_n + \mathcal{O}(X^3) \tag{9.116}
\end{aligned}
$$

This then gives

$$
\begin{aligned}
e^{:f_2:} e^{:f_3:} X_\alpha &= e^{:f_2:} X_\alpha - 3 S_{\alpha\delta} C_{\delta mn} e^{:f_2:}(X_m X_n) + \mathcal{O}(X^3) \\
&= (e^{SF} X)_\alpha - 3 S_{\alpha\delta} C_{\delta mn} (e^{:f_2:} X_m)(e^{:f_2:} X_n) + \mathcal{O}(X^3) \tag{9.117}
\end{aligned}
$$

Equation (9.117) then leads to

$$R = e^{SF} \tag{9.118}$$

as expected, and

$$T_{\alpha\beta\gamma} = -3 S_{\alpha\delta} C_{\delta mn} R_{m\beta} R_{n\gamma} \tag{9.119}$$

Equations (9.118-9.119) express the R- and the T-coefficients in terms of the F- and C-coefficients. Their reverses can also be obtained. The procedure of finding F from R is given by Eqs.(9.86) and (9.77). The C-coefficients are found to be

$$C_{\ell mn} = \frac{1}{3} S_{\ell\alpha} (R^{-1})_{\beta m} (R^{-1})_{\gamma n} T_{\alpha\beta\gamma} \tag{9.120}$$

as can be proved by back substitution into Eq.(9.119). This exercise shows an explicit transformation between a Lie map and its corresponding Taylor map. It should be kept in mind that representations (9.113) and (9.114) agree with each other to second order in X, but differ in higher orders.

To be specific, consider a circular accelerator which is otherwise perfectly linear aside from a thin-lens sextupole at $s = 0$. The linear Lie map around $s = 0$ is (consider 1-D motion)

$$e^{:f_2:} \quad \text{where} \quad f_2 = -\frac{\mu}{2}(\gamma x^2 + 2\alpha xp + \beta p^2) \tag{9.121}$$

Let the thin-lens sextupole be (see Table 4)

$$e^{:f_3:} \quad \text{where} \quad f_3 = \lambda x^3 \tag{9.122}$$

The one-turn map from $s = 0^+$, going through the accelerator, then the sextupole, and end up at $s = C^+$, is given by

$$e^{:f_2:} e^{:f_3:} \tag{9.123}$$

As discussed earlier, the ordering of the Lie operators is reversed from that used to in a matrix formulation.

The Taylor representation of the map is given by combining the two steps, i.e., passing through the accelerator,

$$
\begin{aligned}
x_1 &= x_0(\cos\mu + \alpha\sin\mu) + p_0\beta\sin\mu \\
p_1 &= -x_0\gamma\sin\mu + p_0(\cos\mu - \alpha\sin\mu)
\end{aligned}
\tag{9.124}
$$

followed by passing through the sextupole,

$$
x = x_1 \quad\text{and}\quad p = p_1 + 3\lambda x_1^2
\tag{9.125}
$$

The combination of Eqs.(9.124-9.125) gives a Taylor map of the form (9.113) with all higher order terms terminated, and

$$
\begin{aligned}
R_{11} &= \cos\mu + \alpha\sin\mu \\
R_{12} &= \beta\sin\mu \\
R_{21} &= -\gamma\sin\mu \\
R_{22} &= \cos\mu - \alpha\sin\mu \\
T_{211} &= 3\lambda R_{11}^2 \\
T_{212} &= T_{221} = 3\lambda R_{12}R_{11} \\
T_{222} &= 3\lambda R_{12}^2
\end{aligned}
\tag{9.126}
$$

All unlisted T-coefficients vanish. Note that this Taylor map is exactly symplectic and is a special case of the map (9.40-9.41).

As to the Lie representation, the quadratic form f_2 is obtained by implementing Eq.(9.118) and is of course given by Eq.(9.121) as one would expect. The C-coefficients that describe f_3 according to Eq.(9.115) are given by Eq.(9.120). It is found that the only nonvanishing C-coefficient is

$$
C_{111} = \lambda
\tag{9.127}
$$

This leads to the expected Eq.(9.122) for f_3.

Monomial Maps   We now proceed to describe an interesting formula involving monomials. Let x and p be the canonical variables, a, α, and β be arbitrary constants. Consider the exponential operator $\exp(a{:}x^\alpha p^\beta{:})$, where the exponent is a single term in the form of a power of x and p (α and β do not have to be integers). The formula reads

$$
\begin{aligned}
e^{a:x^\alpha p^\beta:}x &= \begin{cases} x[1 + a(\alpha-\beta)x^{\alpha-1}p^{\beta-1}]^{\beta/(\beta-\alpha)}, & \text{if } \alpha \neq \beta \\ x\exp(-a\alpha x^{\alpha-1}p^{\alpha-1}), & \text{if } \alpha = \beta \end{cases} \\
e^{a:x^\alpha p^\beta:}p &= \begin{cases} p[1 + a(\alpha-\beta)x^{\alpha-1}p^{\beta-1}]^{\alpha/(\alpha-\beta)}, & \text{if } \alpha \neq \beta \\ p\exp(a\alpha x^{\alpha-1}p^{\alpha-1}), & \text{if } \alpha = \beta \end{cases}
\end{aligned}
\tag{9.128}
$$

The $\alpha = \beta$ case can be obtained by taking the limit $\alpha \to \beta$ in the $\alpha \neq \beta$ expressions. One way to appreciate Eq.(9.128) is mentioned in Exercise 38.

To prove Eq.(9.128), one first note that the map $e^{a:x^\alpha p^\beta:}$ describes a dynamical system with Hamiltonian [see Eq.(9.178) later.]

$$H = -\frac{a}{T}x^\alpha p^\beta \tag{9.129}$$

where T is the total time period over which the Hamiltonian is being applied to the system. The equations of motion are

$$\begin{aligned}
\dot{x} &= \frac{\partial H}{\partial p} = -\frac{a\beta}{T}x^\alpha p^{\beta-1} \\
\dot{p} &= -\frac{\partial H}{\partial x} = \frac{a\alpha}{T}x^{\alpha-1}p^\beta
\end{aligned} \tag{9.130}$$

Since H is a constant of the motion, we have $x^\alpha p^\beta = x_0^\alpha p_0^\beta$. From the first line of Eq.(9.130), we have therefore

$$\dot{x} = -\frac{a\beta}{T}x_0^{\alpha(\beta-1)/\beta}p_0^{\beta-1}x^{\alpha/\beta}$$

$$\implies \quad x^{-\alpha/\beta}\dot{x} = -\frac{a\beta}{T}x_0^{\alpha(\beta-1)/\beta}p_0^{\beta-1}$$

$$\implies \quad [x(t)]^{(\beta-\alpha)/\beta} = x_0^{(\beta-\alpha)/\beta} - \frac{a(\beta-\alpha)}{T}tx_0^{\alpha(\beta-1)/\beta}p_0^{\beta-1} \tag{9.131}$$

Setting x to be $x(T)$, we obtain

$$x = x_0[1 + a(\alpha-\beta)x_0^{\alpha-1}p_0^{\beta-1}]^{\beta/(\beta-\alpha)} \tag{9.132}$$

which proves the first line of Eq.(9.128).

Similarly,

$$\dot{p} = \frac{a\alpha}{T}x_0^{\alpha-1}p_0^{\beta(\alpha-1)/\alpha}p^{\beta/\alpha}$$

$$\implies \quad p = p_0[1 + a(\alpha-\beta)x_0^{\alpha-1}p_0^{\beta-1}]^{\alpha/(\alpha-\beta)} \tag{9.133}$$

which proves the second identity in Eq.(9.128).

One particular case of Eq.(9.128) is when α and β are integers. Then the exponent is a monomial in x and p. Equation (9.128) then gives the exact result of the evolution of the dynamical variables due to the exponential monomial map. Note that if the exponent contains two monomial terms, then there is in general not an exact expression any more.

Equation (9.128) is exactly symplectic. To demonstrate that, we need only to show that the Poisson brackets of the two expressions in Eq.(9.128) is equal to 1, i.e.,

$$[x,p] = \frac{\partial x}{\partial x_0}\frac{\partial p}{\partial p_0} - \frac{\partial x}{\partial p_0}\frac{\partial p}{\partial x_0} = 1 \tag{9.134}$$

Exercise 33 As mentioned in the text, exponential Lie maps are always symplectic, while Taylor maps are not. However, Taylor maps

202

are symplectic up to the order it is truncated. Show that when Eqs.(9.118) and (9.119) are satisfied, the Taylor map (9.113) is symplectic to order $\mathcal{O}(X)$.

Solution The Jacobian matrix of the map (9.113) is

$$M_{\alpha\delta} = R_{\alpha\delta} + 2T_{\alpha\delta\beta}X_{0\beta} + \mathcal{O}(X^2)$$

This leads to

$$(\tilde{M}SM)_{\alpha\beta} = (\tilde{R}SR)_{\alpha\beta} + 2S_{\ell m}(T_{\ell\alpha n}R_{m\beta} - R_{\ell\alpha}T_{m\beta n})X_{0n} + \mathcal{O}(X^2)$$

We need to prove

$$\tilde{R}SR = S$$
$$S_{\ell m}(T_{\ell\alpha n}R_{m\beta} - R_{\ell\alpha}T_{m\beta n}) = 0 \quad \text{for all } \alpha, \beta, n \quad (9.135)$$

Exercise 34 In this section, we have been considering perturbation in powers of X, i.e. X is the small quantity in the perturbation treatment (assuming we are interested in the region of phase space close to the origin). This is not necessary; the perturbation expansion can be in other small quantities as well. Consider a Taylor map which is first order in the strength ϵ of a certain linear or nonlinear perturbation in such a way that

$$X = X_0 + \epsilon G(X_0) \quad (9.136)$$

where G is a vector function which could be nonlinear in X_0. Find the corresponding Lie map to first order in ϵ.

Solution Let the Lie map be written as $\exp[:\epsilon f(X):]$, then we must have

$$:f(X):X = G(X) \qquad \text{or} \qquad [f(X), X] = G(X) \quad (9.137)$$

Using Eq.(9.7), this gives

$$-S_{ki}\frac{\partial f}{\partial X_i} = G_k \qquad \text{or} \qquad -S\nabla f(X) = G(X) \quad (9.138)$$

By inverting Eq.(9.138), we obtain

$$\nabla f(X) = SG(X)$$
$$\implies \qquad f(X) = \int_0^X dX' SG(X') \quad (9.139)$$

The integral in Eq.(9.139) is along any path from 0 to X in the multi-dimensional phase space. This integral being independent of the path taken is a result of the dynamic system being conservative. Equation (9.138) can be used to obtain the Taylor map once the Lie

map is known (knowing f, one can compute G). Equation (9.139) can be used the other way around (knowing G, one can compute f).

Exercise 35 Kick maps constitute a simple application of Eq.(9.138-9.139). Consider a kick map described by Eq.(9.136) with

$$X = \begin{bmatrix} x \\ p \end{bmatrix}, \qquad G(X) = \begin{bmatrix} 0 \\ g(x) \end{bmatrix} \tag{9.140}$$

where $g(x)$ is a function of x and not p. Find the corresponding Lie map to first order in ϵ.

Solution Equation (9.139) gives

$$\begin{bmatrix} \frac{\partial f(X)}{\partial x} \\ \frac{\partial f(X)}{\partial p} \end{bmatrix} = \nabla f(X) = \begin{bmatrix} 0 & 1 \\ -1 & 0 \end{bmatrix} \begin{bmatrix} 0 \\ g(x) \end{bmatrix} = \begin{bmatrix} g(x) \\ 0 \end{bmatrix}$$

$$\Longrightarrow \quad f(X) = \int_0^x dx' g(x') \tag{9.141}$$

independent of p. Conversely, if one is given the Lie map with $f(X)$ in the form (9.141), then

$$G(X) = -S\nabla f(X) = -\begin{bmatrix} 0 & 1 \\ -1 & 0 \end{bmatrix} \begin{bmatrix} g(x) \\ 0 \end{bmatrix} = \begin{bmatrix} 0 \\ g(x) \end{bmatrix} \tag{9.142}$$

Exercise 36 As another application of Exercise 34, find the Lie map, to first order in ϵ, that gives the Taylor map

$$x = x_0 - \epsilon p_0^2, \qquad p = p_0 + \epsilon x_0^2 \tag{9.143}$$

Solution

$$\exp[:\frac{\epsilon}{3}(x^3 + p^3):] \tag{9.144}$$

Exercise 37 Factorize $\exp[:ax^2 + 2bxp + cp^2:]$ into monomial map factors. Give physical meaning of each of the monomial factor maps. This factorization is exact.

Solution This factorization is not unique. One way is to factorize the map into a drift space of length L_1, followed by a focusing thin-lens quadrupole of focal length f, followed by another drift space L_2, where

$$
\begin{aligned}
L_1 &= \frac{\sqrt{ac - b^2}}{a} \tan \frac{\sqrt{ac - b^2}}{2} + \frac{b}{a} \\
f &= \frac{\sqrt{ac - b^2}}{a \sin \sqrt{ac - b^2}} \\
L_2 &= \frac{\sqrt{ac - b^2}}{a} \tan \frac{\sqrt{ac - b^2}}{2} - \frac{b}{a}
\end{aligned}
\tag{9.145}
$$

204

This means we have factorized

$$e^{:ax^2+2bxp+cp^2:} = e^{:-\frac{1}{2}L_1p^2:}e^{:-\frac{1}{2f}x^2:}e^{:-\frac{1}{2}L_2p^2:} \tag{9.146}$$

A generalization of this factorization into monomial maps to a non-linear system can be found in Exercise 59 after we learn the Baker-Campbell-Hausdorff formula.

Exercise 38 The text mentioned one appreciation of Eq.(9.128) by considering its symplecticity. [See Eq.(9.134).] Another appreciation of Eq.(9.128) is provided by first considering the infinite series representation of the exponential map; application of this map on x or p then leads to infinite series. What Eq.(9.128) says is that the resulting infinite series can be summed exactly. Show this explicitly by first proving that, for $k \geq 1$,

$$(:x^\alpha p^\beta:)^k x = (\beta - \alpha)^k \frac{\Gamma(k + \frac{\beta}{\alpha-\beta})}{\Gamma(\frac{\beta}{\alpha-\beta})} x^{(\alpha-1)k+1} p^{(\beta-1)k}$$

$$(:x^\alpha p^\beta:)^k p = (\beta - \alpha)^k \frac{\Gamma(k - \frac{\alpha}{\alpha-\beta})}{\Gamma(-\frac{\alpha}{\alpha-\beta})} x^{(\alpha-1)k} p^{(\beta-1)k+1} \tag{9.147}$$

Use Eq.(9.147) to prove Eq.(9.128).

Exercise 39 Consider the (x, p) phase space and a map $e^{:pf(x):}$ with some function $f(x)$. Find the explicit expressions of

$$\begin{bmatrix} X \\ P \end{bmatrix} = e^{:pf(x):} \begin{bmatrix} x \\ p \end{bmatrix} \tag{9.148}$$

Solution The map $e^{:pf(x):}$ is a map from $t = 0$ to $t = T$ for a dynamical system with Hamiltonian $H = -pf(x)/T$. The Hamilton equations of motion are

$$\dot{x} = -\frac{1}{T}f(x), \qquad \dot{p} = \frac{1}{T}pf'(x) \tag{9.149}$$

The first member of Eq.(9.149) gives

$$\int_{x_0}^x \frac{dx'}{f(x')} = -\frac{t}{T} \tag{9.150}$$

where (x_0, p_0) are the initial coordinates at time $t = 0$.

Since the Hamiltonian is a constant of the motion, we have

$$pf(x) = p_0 f(x_0) \Longrightarrow x = f^{-1}(\frac{p_0}{p}f(x_0)) \tag{9.151}$$

The second member of Eq.(9.149) then gives

$$\dot{p} = \frac{p}{T}f'[f^{-1}(\frac{p_0}{p}f(x_0))]$$

$$\Longrightarrow \quad \int_1^{p/p_0} \frac{du}{uf'[f^{-1}(\frac{1}{u}f(x_0))]} = \frac{t}{T} \tag{9.152}$$

Knowing $f(x)$, Eq.(9.150) gives the solution for x as a function of t while Eq.(9.152) gives the solution for p. When $t = T$, the solutions give explicit expressions of X and P.

One can apply the result to special cases. Taking $f(x) = ax$ gives the map

$$x(t) = x_0 e^{-at/T}, \qquad p(t) = p_0 e^{at/T} \tag{9.153}$$

Taking $f(x) = ax^2$ gives

$$x(t) = \frac{Tx_0}{T + ax_0 t}, \qquad p(t) = p_0(1 + ax_0\frac{t}{T})^2 \tag{9.154}$$

Taking $f(x) = \alpha e^{ax}$ gives

$$x(t) = -\frac{1}{a}\ln(e^{-ax_0} + \alpha a\frac{t}{T}), \qquad p(t) = p_0(1 + \alpha a\frac{t}{T}e^{ax_0}) \tag{9.155}$$

Taking $f(x) = \alpha\sin(ax)$ gives

$$\tan\frac{ax(t)}{2} = \left(\tan\frac{ax_0}{2}\right)e^{-\alpha at/T}$$

$$p(t) = \frac{p_0 e^{-\alpha at/T}}{2(1 + \cos ax_0)}[(1+\cos ax_0)^2 e^{2\alpha at/T} + \sin^2 ax_0] \tag{9.156}$$

One may check that the Jacobian matrices for the maps (9.153-9.156) have unit determinants. One may also check Eqs.(9.153-9.154) against Eq.(9.128) because they are special cases of Eq.(9.128).

If the map (9.148) is considered to be a change of variables from (x, p) to (X, P), this type of coordinate change is called *contact transformations.* In particular, X and P/p_0 depend only on x_0 and not on p_0. The map (9.155) with $t = T$, for example, is equivalent to a contact transformation with a generating function

$$F(x, P) = -\frac{P}{a}\ln(e^{-ax} + \alpha a) \tag{9.157}$$

Exercise 40 Consider the map $e^{:f(x)g(p):}$. Find expressions for

$$\begin{bmatrix} X \\ P \end{bmatrix} = e^{:f(x)g(p):} \begin{bmatrix} x \\ p \end{bmatrix} \tag{9.158}$$

Solution Follow a similar procedure as in Exercise 39 to obtain

$$\int_{x_0}^{x} \frac{dx}{f(x)g'[g^{-1}(\frac{f(x_0)g(p_0)}{f(x)})]} = -\frac{t}{T}$$

$$\int_{p_0}^{p} \frac{dp}{g(p)f'[f^{-1}(\frac{f(x_0)g(p_0)}{g(p)})]} = \frac{t}{T} \tag{9.159}$$

The map (9.158) is obtained by setting $t = T$ in Eq.(9.159). Equations (9.128), (9.150) and (9.152) are special cases of Eq.(9.159). As a special case, taking $f(x)g(p) = \alpha e^{ax+bp}$ gives

$$
\begin{aligned}
x(t) &= x_0 - \alpha b \frac{t}{T} e^{ax_0 + bp_0} \\
p(t) &= p_0 + \alpha a \frac{t}{T} e^{ax_0 + bp_0}
\end{aligned}
\tag{9.160}
$$

Taking $f(x)g(p) = \alpha x^a e^{bp}$ gives

$$
\begin{aligned}
x(t) &= x_0 - \alpha b x_0^a e^{bp_0} \frac{t}{T} \\
p(t) &= -\frac{a}{b} \ln\left(e^{-bp_0/a} - \alpha b x_0^{a-1} e^{b(a-1)p_0/a} \frac{t}{T} \right)
\end{aligned}
\tag{9.161}
$$

Denoting the coordinate x as ϕ and momentum p as A, and taking $f(\phi)g(A) = \alpha\sqrt{A}\sin\phi$ give

$$
\begin{aligned}
\cot\phi(t) &= \cot\phi_0 + \frac{\alpha}{2\sqrt{A_0}\sin\phi_0} \frac{t}{T} \\
A(t) &= A_0 \sin^2\phi_0 + \left(\sqrt{A_0}\cos\phi_0 + \frac{\alpha t}{2T}\right)^2
\end{aligned}
\tag{9.162}
$$

Similarly, taking $f(\phi)g(A) = \alpha\sqrt{A}\cos\phi$ gives

$$
\begin{aligned}
\tan\phi(t) &= \tan\phi_0 - \frac{\alpha}{2\sqrt{A_0}\cos\phi_0} \frac{t}{T} \\
A(t) &= A_0 \cos^2\phi_0 + \left(\sqrt{A_0}\sin\phi_0 + \frac{\alpha t}{2T}\right)^2
\end{aligned}
\tag{9.163}
$$

One can check the symplecticity of the maps (9.160-9.163) by verifying the Jacobian matrices have unit determinants.

Exercise 41 We learned in Exercise 21 that if

$$
e^{:f(x,p):}x = X(x,p), \quad e^{:f(x,p):}p = P(x,p)
\tag{9.164}
$$

then

$$
f(X(x,p), P(x,p)) = f(x,p)
\tag{9.165}
$$

There is also an inverse relationship to Eq.(9.165). To see that, note that Eq.(9.164) allows us to write

$$
x = X(e^{:-f(x,p):}x, e^{:-f(x,p):}p), \quad p = P(e^{:-f(x,p):}x, e^{:-f(x,p):}p)
\tag{9.166}
$$

Knowing the explicit expressions of the functions $X(x,p)$ and $P(x,p)$, we can solve Eq.(9.166) for the quantities $e^{:-f(x,p):}x$ and $e^{:-f(x,p):}p$ to obtain the expressions

$$
e^{:-f(x,p):}x = \bar{X}(x,p), \quad e^{:-f(x,p):}p = \bar{P}(x,p)
\tag{9.167}
$$

It follows that one has an additional condition

$$f(x,p) = f(\bar{X}(x,p), \bar{P}(x,p)) \qquad (9.168)$$

Check the validity of Eqs.(9.165) and (9.168) for the case of Eq.(9.128).
Solution We have $f(x,p) = ax^\alpha p^\beta$, and $X, P, \bar{X}, \bar{P}$ are given by

$$
\begin{aligned}
X &= x[1 + a(\alpha - \beta)x^{\alpha-1}p^{\beta-1}]^{\beta/(\beta-\alpha)} \\
P &= p[1 + a(\alpha - \beta)x^{\alpha-1}p^{\beta-1}]^{\alpha/(\alpha-\beta)} \\
x &= \bar{X}[1 + a(\alpha - \beta)\bar{X}^{\alpha-1}\bar{P}^{\beta-1}]^{\beta/(\beta-\alpha)} \\
p &= \bar{P}[1 + a(\alpha - \beta)\bar{X}^{\alpha-1}p\bar{P}^{\beta-1}]^{\alpha/(\alpha-\beta)} \qquad (9.169)
\end{aligned}
$$

Conditions (9.165) and (9.168) follow by observing

$$x^\alpha p^\beta = X^\alpha P^\beta = \bar{X}^\alpha \bar{P}^\beta \qquad (9.170)$$

Note that one can solve the last two expressions of Eq.(9.169) to obtain explicit expressions of $\bar{X}$ and $\bar{P}$ in terms of x and p. The result will be the same expressions as X and P except that a is replaced by $-a$, as one expects.

Exercise 42 The canonical transformation $\{x = \sqrt{2A}\sin\phi,\ p = \sqrt{2A}\cos\phi\}$, or $\{A = (x^2 + p^2)/2, \phi = \tan^{-1}(x/p)\}$ can be described by a generating function, as is well known. Can this also be described in Lie language? In other words, look for a function $f(x,p)$ which gives

$$e^{:f:}x = \tan^{-1}\frac{x}{p}, \quad e^{:f:}p = \frac{x^2 + p^2}{2} \qquad (9.171)$$

(a) Find f if possible. (b) If not, at least use Eq.(9.171) to show that

$$e^{:-f:}x = \sqrt{2p}\sin x, \quad e^{:-f:}p = \sqrt{2p}\cos x \qquad (9.172)$$

(c) What is the map $e^{:-\mu(x^2+p^2)/2:}$ expressed in the (ϕ, A) coordinates?
Solution (a) $f(x,p)$ must exist because the Jacobian matrix of the map (9.171) has determinant 1. According to Exercise 41, $f(x,p)$ must satisfy $f(x,p) = f(\tan^{-1}(x/p), (x^2+p^2)/2) = f(\sqrt{2p}\sin x, \sqrt{2p}\cos x)$. How could this be possible? In particular, one must have $f(0,p) = f(0, p^2/2) = f(0, \sqrt{2p})$.
(b) The first member of Eq.(9.171) gives

$$
\begin{aligned}
x &= e^{:-f:}\tan^{-1}\frac{x}{p} = \tan^{-1}\left[e^{:-f:}(\frac{x}{p})\right] = \tan^{-1}\left[\frac{e^{:-f:}x}{e^{:-f:}p}\right] \\
&\Longrightarrow \tan x = \frac{e^{:-f:}x}{e^{:-f:}p} \qquad (9.173)
\end{aligned}
$$

Similarly, the second member of Eq.(9.171) gives

$$2p = (e^{:-f:}x)^2 + (e^{:-f:}p)^2 \qquad (9.174)$$

208

Solving Eqs.(9.173-9.174) for the quantities $e^{:-f:}x$ and $e^{:-f:}p$ gives the needed proof of Eq.(9.172).

(b) The transformation can be described by

$$
\begin{aligned}
e^{:-f:}e^{:-\mu(x^2+p^2)/2:}e^{:f:} &= \exp[:-\frac{\mu}{2}e^{:-f:}(x^2+p^2):] \\
&= e^{:-\mu p:} \rightarrow e^{:-\mu A:}
\end{aligned}
\tag{9.175}
$$

This map is to be applied to coordinates (ϕ, A). Note the ordering on the left hand side of Eq.(9.175). In particular, it is not $e^{:f:}e^{:-\mu(x^2+p^2)/2:}e^{:-f:}$.

Exercise 43 (a) Show that the map

$$
\begin{aligned}
x &= x_0 + bf(ax_0 + bp_0) \\
p &= p_0 - af(ax_0 + bp_0)
\end{aligned}
\tag{9.176}
$$

is symplectic for arbitrary values of a, b, and arbitrary function $f(u)$.

(b) Find the Lie representation of the map. This map can be regarded as the generalized kick map. The usual kick map is obtained when either $a = 0$ or $b = 0$.

Solution (b)

$$
\exp\left[:-\int_0^{ax+bp} f(u)du: \right]
\tag{9.177}
$$

9.4 Baker-Campbell-Hausdorff Formula

In the previous section, we tried to establish some familiarity with the Lie operators. Before we turn attention to accelerator applications in the following sections, we need to introduce a set of formulae — the Baker-Campbell-Hausdorff formula and its variations — which are used repeatedly later.

Single accelerator element An accelerator typically consists of a sequence of elements. Consider one particular element of length L. Let the particle motion in this element be described by the Hamiltonian H which is independent of s inside the element. The map for this element can be written as an exponential operator. Some examples have been given in Table 4. For the element being considered here, the map is

$$
e^{:-LH:}
\tag{9.178}
$$

To prove Eq.(9.178), one only has to note that

$$
\frac{dX}{ds} = -:H:X \quad \Longrightarrow \quad \frac{d^k X}{ds^k} = (-:H:)^k X
\tag{9.179}
$$

It follows that the map

$$
X(s) = \sum_{k=0}^{\infty} \frac{s^k}{k!} \left(\frac{d^k X}{ds^k} \right)_{s=0}
\tag{9.180}
$$

can be represented by the Lie operator

$$\sum_{k=0}^{\infty} \frac{s^k}{k!} (-:H:)^k = e^{:-sH:} \tag{9.181}$$

The operator (9.178) is obtained just by integrating the map to the end of the element $s = L$.

Given below are the Hamiltonians of a few typical accelerator elements:

$$H = \begin{cases} -\frac{x\delta}{\rho} + \frac{1}{2\rho^2}x^2 + \frac{1}{2(1+\delta)}(p_x^2 + p_y^2) & \text{dipole} \\ \frac{1}{2}K(x^2 - y^2) + \frac{1}{2(1+\delta)}(p_x^2 + p_y^2) & \text{quadrupole} \\ \frac{1}{3}S(x^3 - 3xy^2) + \frac{1}{2(1+\delta)}(p_x^2 + p_y^2) & \text{sextupole} \\ \frac{1}{4}\lambda(x^4 - 6x^2y^2 + y^4) + \frac{1}{2(1+\delta)}(p_x^2 + p_y^2) & \text{octupole} \end{cases} \tag{9.182}$$

where $K, S,$ and λ are the strengths of quadrupole, sextupole and octupole elements, ρ is the dipole bending radius. The dynamical variables for the above Hamiltonians are $(x, p_x, y, p_y, z, \delta)$. All elements are considered thick-lens.

In general, for an n-th multipole other than dipole ($n = 1, 2, 3$ for quadrupole, sextupole, octupole, etc), we have

$$H = \frac{1}{n+1}\text{Re}[(\lambda_n + i\bar{\lambda}_n)(x + iy)^{n+1}] + \frac{1}{2(1+\delta)}(p_x^2 + p_y^2) \tag{9.183}$$

where λ_n and $\bar{\lambda}_n$ are the normal and the skew components of the multipole field. Equation (9.182) contains only the normal components with $K = \lambda_1$, $S = \lambda_2$ and $\lambda = \lambda_3$. Explicit equations of motion for the Hamiltonians (9.182) can be found in Exercise 42.

The nonlinear effect of δ through the term $\frac{1}{2(1+\delta)}(p_x^2 + p_y^2)$ in the Hamiltonians (9.182-9.183) is often (although not always) negligible. In those cases, it is a good approximation to make the replacement

$$\frac{1}{2(1+\delta)}(p_x^2 + p_y^2) \rightarrow \frac{1}{2}(p_x^2 + p_y^2) \tag{9.184}$$

In this approximation, the chromatic effects are solely contained in the $-x\delta/\rho$ term of the dipole magnets.

The Hamiltonians (9.182) applies to the 6-D phase space $(x, p_x, y, p_y, z, \delta)$. If one is interested only in the 4-D transverse phase space, it is possible to simplify the Hamiltonians somewhat as follows. One first notes that for the elements described by (9.182), we have $x' = \partial H/\partial p_x = p_x/(1+\delta)$ and similarly $y' = p_y/(1+\delta)$. One then notes that if there are no electric devices (e.g. an rf cavity), δ can be regarded as a numerical constant if one ignores the longitudinal dynamics. It is then easy to show that the Hamiltonian equations of motion hold for the variables (x, x', y, y') with the new Hamiltonians

$$H = \begin{cases} \frac{1}{1+\delta}\left(-\frac{x\delta}{\rho} + \frac{1}{2\rho^2}x^2\right) + \frac{1}{2}(x'^2 + y'^2) & \text{dipole} \\ \frac{1}{2(1+\delta)}K(x^2 - y^2) + \frac{1}{2}(x'^2 + y'^2) & \text{quadrupole} \\ \frac{1}{3(1+\delta)}S(x^3 - 3xy^2) + \frac{1}{2}(x'^2 + y'^2) & \text{sextupole} \\ \frac{1}{4(1+\delta)}\lambda(x^4 - 6x^2y^2 + y^4) + \frac{1}{2}(x'^2 + y'^2) & \text{octupole} \end{cases} \tag{9.185}$$

Hamiltonians (9.185) apply only if one ignores the longitudinal dynamics. In particular, if one wants to find the path length equation of motion by $z' = \partial H/\partial \delta$, he should use Eq.(9.182), not Eq.(9.185).

As mentioned, given the Hamiltonian, the Lie map is simply $e^{:-LH:}$. Exercises 45 and 46 give the matrix representations of the linear maps for quadrupoles and dipoles. On the other hand, although these two exercises are applied to linear cases, the power of Lie technique lies really in nonlinear cases. Take the sextupole case in Eq.(9.182) as an illustration. With the approximation (9.184), we first work out the following:

$$
\begin{aligned}
:H:x &= -\frac{\partial H}{\partial p_x} = -p_x \\
:H:^2 x &= -:H:p_x = -\frac{\partial H}{\partial x} = -S(x^2 - y^2) \\
:H:^3 x &= -S(-\frac{\partial H}{\partial p_x}2x + \frac{\partial H}{\partial p_y}2y) = 2S(xp_x - yp_y) \\
:H:^4 x &= 2S(-\frac{\partial H}{\partial p_x}p_x + x\frac{\partial H}{\partial x} + \frac{\partial H}{\partial p_y}p_y - \frac{\partial H}{\partial y}y) \\
&= 2S[-p_x^2 + p_y^2 + Sx(x^2 + y^2)] \\
:H:^5 x &= \mathcal{O}(S^2)
\end{aligned}
$$

We then obtain the Taylor map

$$
\begin{aligned}
e^{:-LH:}x &= x + p_x L - \frac{1}{2}SL^2(x^2 - y^2) - \frac{1}{3}SL^3(xp_x - yp_y) \\
&+ \frac{1}{12}SL^4[-p_x^2 + p_y^2 + Sx(x^2 + y^2)] + \mathcal{O}(S^2 L^5) \qquad (9.186)
\end{aligned}
$$

where $\mathcal{O}(S^2 L^5)$ means terms same-or-higher order than S^2 in S and same-or-higher order than L^5 in L. Similarly, we have

$$
\begin{aligned}
e^{:-LH:}p_x &= p_x - SL(x^2 - y^2) - SL^2(xp_x - yp_y) - \frac{1}{3}SL^3[p_x^2 - p_y^2 - Sx(x^2 + y^2)] \\
&+ \frac{1}{12}S^2 L^4(5x^2 p_x - y^2 p_x + 6xyp_y) + \mathcal{O}(S^2 L^5) \\
e^{:-LH:}y &= y + Lp_y + SL^2 xy + \frac{1}{3}SL^3(xp_y + yp_x) \\
&+ \frac{1}{12}SL^4[2p_x p_y + Sy(x^2 + y^2)] + \mathcal{O}(S^2 L^5) \\
e^{:-LH:}p_y &= p_y + 2SLxy + SL^2(xp_y + yp_x) + \frac{1}{3}SL^3[2p_x p_y + Sy(x^2 + y^2)] \\
&- \frac{1}{12}S^2 L^4(x^2 p_y - 6xyp_x - 5y^2 p_y) + \mathcal{O}(S^2 L^5) \qquad (9.187)
\end{aligned}
$$

So we have already obtained some useful results! These expressions are of course approximate and nonsymplectic if the higher order terms are truncated.

Chain of Elements So far we have applied Lie operators for single elements. An accelerator typically consists of a sequence of elements. Let the elements be ordered according to the index $i = 1, 2, ..., N$ so that the beam passes through element 1, then element 2, etc. Let the i-th element have length L_i and Hamiltonian H_i. The map for the i-th element is $e^{:-L_i H_i:}$. The one-turn map around the entrance of the first element (call this position $s = 0$) is (note the order of the operators)

$$e^{:-L_1 H_1:} e^{:-L_2 H_2:} \ ... \ e^{:-L_N H_N:} \tag{9.188}$$

which we shall abbreviate as

$$\prod_{i=1}^{N} e^{:-L_i H_i:} \tag{9.189}$$

The situation is illustrated in Fig.9.2. The total one-turn map of the accelerator is obtained by multiplying a sequence of exponential operators. A simple example representing a single thin-lens sextupole in an otherwise perfectly linear accelerator was worked out following Eqs.(9.121-9.122).
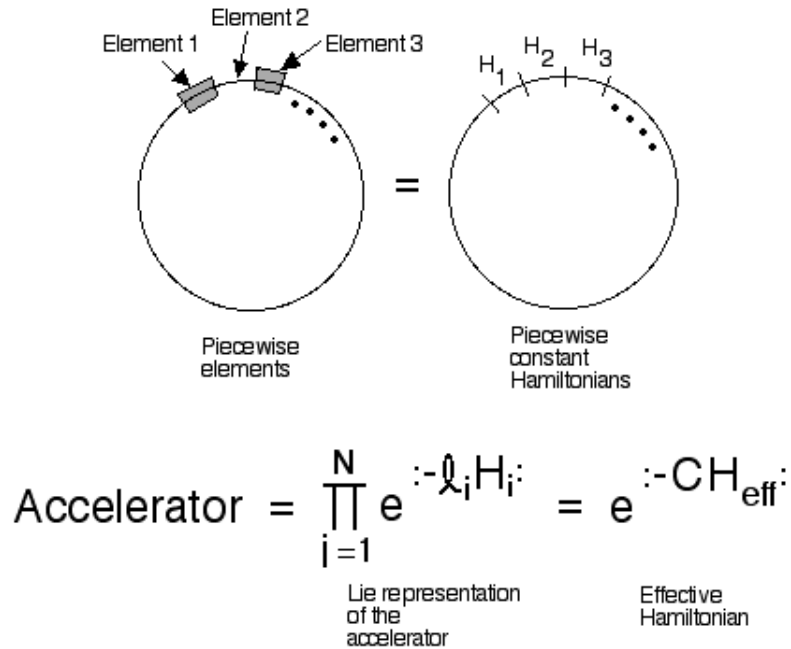

Figure 9.2: The accelerator model viewed in Lie language.

The forms (9.188) or (9.189) are not yet very useful. To proceed, we would like to have the total map represented as a single exponential operator instead of a product of exponential operators. The process of combining exponential

operators is called *concatenation*. After concatenation, the single exponential operator can be written as

$$\text{one turn map} = e^{:-CH_{\text{eff}}:} \tag{9.190}$$

where C is the accelerator circumference.

Drawing an analogy of Eq.(9.190) to Eq.(9.178) for a single element allows the quantity H_{eff} to be identified as the *effective Hamiltonian* of the one-turn map. It describes the one-turn motion of particles in the system. It is a function of the dynamical variables X, but does not depend on s, i.e. it is time-independent. As a consequence, H_{eff} is a constant of the motion when observed at the position $s = 0$. When (or if) one has obtained the one-turn map in the form (9.190) by concatenation, it is impressive that a complex system of an accelerator, which consists of many pieces each having its own Hamiltonian, can be combined into a simple form (9.190) and a constant of the motion can be found this way.

Note that H_{eff} is not only a constant of the motion, but also the Hamiltonian. One can actually derive the equations of motion by applying the Hamilton's equations to it. The condition is that the equations obtained this way apply only if one observes the motion at position $s = 0$.

BCH Formula – First Form The basic formula that allows concatenation of exponential operators is called the Baker-Campbell-Hausdorff (BCH) formula.[6] It can be cast in several forms. We will introduce four forms of this formula. The first form reads

$$e^{:f:}e^{:g:} = e^{:h:} \tag{9.191}$$

where f and g are arbitrary functions of the dynamical variables X, and

$$
\begin{aligned}
h &= f + g + \frac{1}{2}:f:g + \frac{1}{12}:f:^2 g + \frac{1}{12}:g:^2 f + \frac{1}{24}:f::g:^2 f \\
&\quad - \frac{1}{720}:g:^4 f - \frac{1}{720}:f:^4 g + \frac{1}{360}:g::f:^3 g + \frac{1}{360}:f::g:^3 f \\
&\quad + \frac{1}{120}:f:^2:g:^2 f + \frac{1}{120}:g:^2:f:^2 g + \mathcal{O}((f,g)^6)
\end{aligned} \tag{9.192}
$$

where $\mathcal{O}((f,g)^6)$ means terms of the order of $f^m g^n$ where $m + n \geq 6$. If we use the commutator notation of Eq.(9.48) and apply Table 5, Eqs.(9.191-9.192) can be rewritten as

$$
\begin{aligned}
e^{:f:}e^{:g:} &= \exp\Big[:f: + :g: + \frac{1}{2}\{:f:,:g:\} + \frac{1}{12}\{:f:,\{:f:,:g:\}\} + \frac{1}{12}\{:g:,\{:g:,:f:\}\} \\
&\quad + \frac{1}{24}\{:f:,\{:g:,\{:g:,:f:\}\}\} - \frac{1}{720}\{:g:,\{:g:,\{:g:,\{:g:,:f:\}\}\}\} \\
&\quad - \frac{1}{720}\{:f:,\{:f:,\{:f:,\{:f:,:g:\}\}\}\} + \frac{1}{360}\{:g:,\{:f:,\{:f:,\{:f:,:g:\}\}\}\} \\
&\quad + \frac{1}{360}\{:f:,\{:g:,\{:g:,\{:g:,:f:\}\}\}\} + \frac{1}{120}\{:f:,\{:f:,\{:g:,\{:g:,:f:\}\}\}\}
\end{aligned}
$$

$$+ \quad \frac{1}{120} \{ :g:, \{ :g:, \{ :f:, \{ :f:, :g: \} \} \} \} + :\mathcal{O}((f,g)^6): \Big] \tag{9.193}$$

The proof of (9.191-9.193) is somewhat technical. It is given in Exercise 50. There does not seem to be an easy rule of the coefficients in Eq.(9.193). Equations (9.191-9.193) are our first form of the BCH formula. It applies when the two functions f and g are small for the power series to converge. Small f and g means the two operators $e^{:f:}$ and $e^{:g:}$ differ only slightly from identity maps.

When $:f:$ and $:g:$ commute (or when $[f,g] = $ constant depending only on s), we simply have $h = f + g$, as discussed in Eq.(9.57).

BCH Formula – Second Form   The first form has an important variation, which gives the second form of the BCH formula. It is obtained by summing the infinite power series in the first BCH form over either the function f or the function g. If summed over g, then to first order in f, we have

$$e^{:f:} e^{:g:} = \exp \left[:g + \left(\frac{:g:}{e^{:g:} - 1} \right) f + \mathcal{O}(f^2): \right] \tag{9.194}$$

If we choose to sum over f, the summation can be done analytically to first order in g to yield

$$e^{:f:} e^{:g:} = \exp \left[:f + \left(\frac{:f:}{1 - e^{-:f:}} \right) g + \mathcal{O}(g^2): \right] \tag{9.195}$$

The proof of Eqs.(9.194-9.196) are given in Exercises 51 to 53.

Equation (9.195) applies when the function g is small, but f does not have to be small. This expression is particularly useful when we try to concatenate the map for a small perturbation with the map for the rest of the accelerator. In that case, we would obviously choose g to be the perturbation, and f to be the rest of the accelerator. The price to pay in order for f not having to be small is that we have an expression only to first order in the perturbation.[45]

The BCH formula describes how to concatenate two exponential operators into one. It can be inverted to give a formula that describes how to factorize an exponential operator into a product of two exponential operators. In particular, Eq.(9.195) can be inverted to give

$$e^{:f+h:} = e^{:f:} \exp \left[: \left(\frac{1 - e^{-:f:}}{:f:} \right) h: \right] e^{:\mathcal{O}(h^2):} \tag{9.197}$$

---

[45]There is actually an analytic expression to second order in g. It would contribute the following to the $\mathcal{O}(g^2)$ term in Eq.(9.195):

$$\frac{1}{2} \left(\frac{:f:}{1 - e^{-:f:}} \right) \int_0^1 u\,du \int_0^1 dv\, e^{-u:f:} \left[e^{uv:f:} \left(\frac{:f:}{1 - e^{-:f:}} \right) g, \left(\frac{:f:}{1 - e^{-:f:}} \right) g \right] \tag{9.196}$$

A similar statement can be made with Eq.(9.194).

In actual calculations, the opeartion $(1 - e^{-:f:})/:f:$ is not easy to perform as is. In that case, one may prefer an alternative expression for Eq.(9.197) by noting

$$\left(\frac{1 - e^{-:f:}}{:f:}\right) h(X) = \left(\int_0^1 du \; e^{-u:f:}\right) h(X) = \int_0^1 du \; h(e^{-u:f:}X)$$

$$\implies \quad e^{:f+h:} = e^{:f:} \exp\left[: \int_0^1 du \; e^{-u:f:}h:\right] \quad (9.198)$$

What is the physical meaning of Eq.(9.198)? A kick by a slice of h at location $s = uL$ is, to first order in h, equivalent to a kick $h(e^{-:uf:}X)$ at the biginning of the element. The effect of $e^{-:uf:}$ is just to transform the slice kick to the biginning of the element. The integration is then to sum up these kicks of the slices.

BCH Formula – Third Form A third form of the BCH formula which is similar to the first form except that it is more symmetric looking,

$$e^{:f:}e^{:g:}e^{:f:} = e^{:h:} \quad (9.199)$$

where

$$h = 2f + g + \frac{1}{6}:g:^2 f - \frac{1}{6}:f:^2 g + \frac{7}{360}:f:^4 g - \frac{1}{360}:g:^4 f$$

$$+ \; \frac{1}{90}:f::g:^3 f + \frac{1}{45}:g::f:^3 g - \frac{1}{60}:f:^2:g:^2 f + \frac{1}{30}:g:^2:f:^2 g + \mathcal{O}((f,g)^7) \quad (9.200)$$

The symmetry has the consequence that there are no even-order terms on the right hand side of Eq.(9.200). The symmetry makes the algebra simpler. In practice, Eqs.(9.199-9.200) apply when the particle motion is observed at the middle of some element in the accelerator. The proof of Eqs.(9.199-9.200) is provided in Exercise 54.

BCH Formula – Fourth Form Finally the fourth form of the BCH formula is when the right hand side of Eq.(9.200) is summed over g while keeping only to first order in f. This yields

$$e^{:f:}e^{:g:}e^{:f:} = \exp\left[:g: + :\left(\frac{:g:}{e^{:g:} - 1}\right)f: + :\mathcal{O}(f^2):\right]e^{:f:}$$

$$= \exp\left[:g: + :\left(\frac{:g:}{e^{:g:} - 1}\right)f: + :\left(\frac{:g:}{1 - e^{-:g:}}\right)f: + :\mathcal{O}(f^2):\right]$$

$$= \exp\left[:g: + :\left(:g:\coth(\frac{:g:}{2})f\right): + :\mathcal{O}(f^2):\right] \quad (9.201)$$

In other words, if we let

$$e^{:f:}e^{:g:}e^{:f:} = e^{:h:} \quad (9.202)$$

then

$$h = g + :g:\coth(\frac{:g:}{2})f + \mathcal{O}(f^2) \quad (9.203)$$

If g is also small, we can expand Eq.(9.203) in power series in g. The result agrees with Eq.(9.200) as it should. In the first and second lines of Eq.(9.201), we have applied Eqs.(9.194) and (9.195) respectively.

One can also apply the BCH formula to find h in Eq.(9.202) when f is not small but g is small. The result is

$$
\begin{aligned}
e^{:f:}e^{:g:}e^{:f:} &= e^{:2f:}\exp(:e^{-:f:}g:) \\
&= \exp\left[:2f: + :\left(\frac{:2f:}{1-e^{-:2f:}}\right)(e^{-:f:}g): + \mathcal{O}(g^2)\right] \\
&= \exp\left[:2f: + :\left(\frac{:f:}{\sinh:f:}\right)g: + \mathcal{O}(g^2)\right]
\end{aligned}
\tag{9.204}
$$

Again, expanding for small f gives an expression consistent with Eq.(9.200).

We have thus introduced four forms of the BCH formula. The first form is given by Eqs.(9.191-9.193), the second form by (9.194-9.195), the third form by (9.199-9.200), the fourth by (9.202-9.204). These formulae are applied often in later sections.

Exercise 44 Find explicit equations of motion for the Hamiltonians given in Eqs.(9.182) and (9.183).[46]
Solution (a) For dipoles,

$$
\begin{aligned}
x' &= \frac{\partial H}{\partial p_x} = \frac{p_x}{1+\delta} \\
p_x' &= -\frac{\partial H}{\partial x} = \frac{\delta}{\rho} - \frac{x}{\rho^2} \\
y' &= \frac{\partial H}{\partial p_y} = \frac{p_y}{1+\delta} \\
p_y' &= -\frac{\partial H}{\partial y} = 0 \\
z' &= \frac{\partial H}{\partial \delta} = -\frac{x}{\rho} - \frac{p_x^2 + p_y^2}{2(1+\delta)^2} = -\frac{x}{\rho} - \frac{1}{2}(x'^2 + y'^2) \\
\delta' &= \frac{\partial H}{\partial z} = 0 \quad \Longrightarrow \quad \delta = \text{const}
\end{aligned}
\tag{9.205}
$$

Note that $p_x \neq x'$ and $p_y \neq y'$. Equations (9.205) can be combined to yield

$$
x'' + \frac{1}{(1+\delta)\rho^2}x = \frac{\delta}{(1+\delta)\rho}, \quad y'' = 0
\tag{9.206}
$$

Closed form expressions of $x(s)$ and $y(s)$ can be found by solving Eq.(9.206).

---

[46]One should note however that no explicit use of these equations of motion has been made in the text.

(b) For quadrupoles,

$$x'' + \frac{K}{1+\delta}x = 0, \quad y'' - \frac{K}{1+\delta}y = 0 \qquad (9.207)$$

(c) For sextupoles,

$$x'' + \frac{S}{1+\delta}(x^2 - y^2) = 0, \quad y'' - \frac{2S}{1+\delta}xy = 0 \qquad (9.208)$$

(d) For octupoles,

$$x'' + \frac{\lambda}{1+\delta}(x^3 - 3xy^2) = 0, \quad y'' + \frac{\lambda}{1+\delta}(y^3 - 3x^2y) = 0 \quad (9.209)$$

(e) For a general multipole, we have the longitudinal component of the vector potential

$$A_s = -\frac{1}{n+1}\frac{P_0}{e}\text{Re}[(\lambda_n + i\bar{\lambda}_n)(x+iy)^{n+1}] \qquad (9.210)$$

which gives a magnetic field

$$B_y + iB_x = \frac{P_0}{e}(\lambda_n + i\bar{\lambda}_n)(x+iy)^n \qquad (9.211)$$

The Hamiltonian (9.183) is simply

$$H = \frac{eA_s}{cP_0} + \frac{1}{2(1+\delta)}(p_x^2 + p_y^2) \qquad (9.212)$$

and the equations of motion are

$$x'' + \frac{1}{1+\delta}\text{Re}[(\lambda_n + i\bar{\lambda}_n)(x+iy)^n] = 0$$

$$y'' - \frac{1}{1+\delta}\text{Im}[(\lambda_n + i\bar{\lambda}_n)(x+iy)^n] = 0 \qquad (9.213)$$

Exercise 45 Given the Hamiltonian (9.182) of a quadrupole, find the matrix representation of the map $\exp(:-LH:)$ for the vector (x, p_x, y, p_y).

Solution Write the map as $\exp(:f_2:)$, where δ is regarded as a constant. Since x and y motions are decoupled, we can treat them separately with $f_2 = f_{2x} + f_{2y}$. For the x motion, f_{2x} can be written as Eqs.(9.73) and (9.77) with

$$a = KL, \quad b = 0, \quad c = \frac{L}{1+\delta} \qquad (9.214)$$

The matrix form can be obtained by applying Eq.(9.84). Similarly we obtain the matrix for the y motion. By combining the x and y

217

results, we obtain the matrix representation of the map, assuming $K > 0$ and defining $\theta = \sqrt{KL^2/(1+\delta)}$,

$$
\begin{bmatrix}
\cos\theta & \frac{L}{(1+\delta)\theta}\sin\theta & 0 & 0 \\
-\frac{(1+\delta)\theta}{L}\sin\theta & \cos\theta & 0 & 0 \\
0 & 0 & \cosh\theta & \frac{L}{(1+\delta)\theta}\sinh\theta \\
0 & 0 & \frac{(1+\delta)\theta}{L}\sinh\theta & \cosh\theta
\end{bmatrix}
\tag{9.215}
$$

Note that had we used (x, x', y, y') as vector, the transformation matrix would be slightly different:

$$
\begin{bmatrix}
\cos\theta & \frac{L}{\theta}\sin\theta & 0 & 0 \\
-\frac{\theta}{L}\sin\theta & \cos\theta & 0 & 0 \\
0 & 0 & \cosh\theta & \frac{L}{\theta}\sinh\theta \\
0 & 0 & \frac{\theta}{L}\sinh\theta & \cosh\theta
\end{bmatrix}
\tag{9.216}
$$

Using the dynamical variables p_x and p_y, the map (9.215) is actually nonlinear in δ. Note also that the path length variation, determined by the z' equation, is a nonlinear effect, which can not be represented by a matrix.[47] These nonlinear effects, however, are small, and it is often possible to ignore them by making the approximation (9.184).

Exercise 46 Repeat the above exercise for dipole magnets for the vector $(x, p_x, y, p_y, z, \delta)$. In this problem, treat δ as a dynamical variable instead of a constant. Ignore nonlinear effects by making the approximation (9.184).

Solution The y-motion is separated from the x- and z-motions. To describe the y-motion, we have

$$
f_{2y} = -\frac{L}{2}p_y^2
\tag{9.217}
$$

which is just equivalent to a drift space. The remaining f_2 that describes the x- and z-motions is

$$
f_2 = \frac{L}{\rho}x\delta - \frac{L}{2\rho^2}x^2 - \frac{L}{2}p_x^2
\tag{9.218}
$$

Knowing Eqs.(9.217-9.218), the 6×6 transformation matrix is found to be

$$
\begin{bmatrix}
\cos\left(\frac{L}{\rho}\right) & \rho\sin\left(\frac{L}{\rho}\right) & 0 & 0 & 0 & \rho - \rho\cos\left(\frac{L}{\rho}\right) \\
-\frac{1}{\rho}\sin\left(\frac{L}{\rho}\right) & \cos\left(\frac{L}{\rho}\right) & 0 & 0 & 0 & \sin\left(\frac{L}{\rho}\right) \\
0 & 0 & 1 & L & 0 & 0 \\
0 & 0 & 0 & 1 & 0 & 0 \\
-\sin\left(\frac{L}{\rho}\right) & -\rho + \rho\cos\left(\frac{L}{\rho}\right) & 0 & 0 & 1 & -L + \rho\sin\left(\frac{L}{\rho}\right) \\
0 & 0 & 0 & 0 & 0 & 1
\end{bmatrix}
\tag{9.219}
$$

---

[47] The same nonlinear effect appears in a drift space. In this sense, a drift space is a nonlinear element.

Exercise 47 Find the path length change Δz as a particle passes through a quadrupole of strength K and length L to order $\mathcal{O}(L^3)$.
Solution At the exit of the quadrupole, we have

$$
\begin{aligned}
z(L) &= e^{:-LH:}z|_{X=X_0} \\
&= \{z - L[H,z] + \frac{L^2}{2}[H,[H,z]] - \frac{L^3}{6}[H,[H,[H,z]]] + \mathcal{O}(L^4)\}_{X=X_0}
\end{aligned}
$$

With H given in Eq.(9.182), we find

$$
[H,z] = \frac{1}{2(1+\delta)^2}(p_x^2 + p_y^2)
$$

$$
[H,[H,z]] = \frac{K}{(1+\delta)^2}(xp_x - yp_y)
$$

$$
[H,[H,[H,z]]] = \frac{K^2}{(1+\delta)^2}(x^2 + y^2)
$$

$$
\implies \quad \Delta z = z(L) - z_0 = -\frac{L}{2}(x_0'^2 + y_0'^2) + \frac{KL^2}{2(1+\delta)}(x_0 x_0' - y_0 y_0')
$$

$$
-\frac{K^2 L^3}{6(1+\delta)^2}(x_0^2 + y_0^2) + \mathcal{O}(L^4) \tag{9.220}
$$

Equations (9.215) and (9.220) constitute the map for the quadrupole.

Exercise 48 Find the Taylor map, to order $\mathcal{O}(\lambda)$, for (x, p_x, y, p_y) for a thick octupole of strength λ.
Solution The Lie map is

$$
e^{-:LH:}, \quad \text{where} \quad H = \frac{1}{2}(p_x^2 + p_y^2) + \frac{1}{4}\lambda(x^4 - 6x^2 y^2 + y^4) \tag{9.221}
$$

The result is

$$
\begin{aligned}
e^{-:LH:}x &= x + Lp_x - \frac{1}{2}L^2\lambda(x^3 - 3xy^2) + \frac{1}{6}L^3\lambda[3p_x(y^2 - x^2) + 6xyp_y] \\
&+ \frac{1}{4}L^4\lambda(-xp_x^2 + xp_y^2 + 2yp_xp_y) + \frac{1}{20}L^5\lambda(3p_xp_y^2 - p_x^3) + \mathcal{O}(\lambda^2) \\
e^{-:LH:}p_x &= p_x - L\lambda(x^3 - 3xy^2) + \frac{3}{2}L^2\lambda[p_x(y^2 - x^2) + 2xyp_y] \\
&- L^3\lambda(xp_x^2 - xp_y^2 - 2yp_xp_y) + \frac{1}{4}L^4\lambda(3p_xp_y^2 - p_x^3) + \mathcal{O}(\lambda^2)
\end{aligned}
$$

$$
\tag{9.222}
$$

Results for the y-dimension can be obtained by switching x and y in Eq.(9.222).

Exercise 49 Consider a map M that depends on a parameter α, and can be written as $M(\alpha) = e^{:h(\alpha):}$ with some function $h(\alpha)$ [$h(\alpha)$ is

also a function of X]. Show that

$$\frac{dM}{d\alpha}M^{-1} = :\left(\frac{e^{:h:}-1}{:h:}\right)\frac{dh}{d\alpha}: \tag{9.223}$$

Equation (9.223) is a useful formula. It gives an expression of $dM/d\alpha$ when the expression of an exponential map $M(\alpha)$ is known.
Solution Consider the map

$$M = e^{:\beta h(\alpha):} \tag{9.224}$$

where the dummy variable β will set to 1 later. Define

$$A = \frac{dM}{d\alpha}M^{-1} \tag{9.225}$$

Then we have

$$\begin{aligned}
\frac{dA}{d\beta} &= (\frac{d}{d\alpha}\frac{dM}{d\beta})M^{-1} + \frac{dM}{d\alpha}\frac{dM^{-1}}{d\beta} \\
&= [\frac{d}{d\alpha}(:h:M)]M^{-1} - \frac{dM}{d\alpha}M^{-1}:h: \\
&= \frac{d:h:}{d\alpha} + :h:A - A:h: = :\frac{dh}{d\alpha}: - :Ah: \tag{9.226}
\end{aligned}$$

where the last step used Eq.(9.49). The solution to (9.226) is

$$A = :\left(\frac{e^{\beta:h:}-1}{:h:}\right)\frac{dh}{d\alpha}: \tag{9.227}$$

as can be seen by back substitution. Having established Eq.(9.227), Eq.(9.223) follows by setting $\beta = 1$.

Exercise 50 Prove the first form of the BCH formula, Eqs.(9.191-9.193).
Solution Consider

$$e^{:\alpha f:}e^{:\alpha g:} = e^{:h(\alpha):} = M(\alpha) \tag{9.228}$$

which gives

$$\frac{dM}{d\alpha}M^{-1} = :f: + M:g:M^{-1} = :f + Mg: \tag{9.229}$$

Using Eq.(9.223), we obtain

$$f + Mg = \left(\frac{e^{:h:}-1}{:h:}\right)\frac{dh}{d\alpha} \tag{9.230}$$

Let
$$h = \alpha h_1 + \alpha^2 h_2 + \alpha^3 h_3 + \alpha^4 h_4 + \alpha^5 h_5 + ... \tag{9.231}$$

Expand (9.230) in powers of α, the left-hand-side is given by

$$
\begin{aligned}
\text{LHS} \;=\; & f + e^{:h:}g = f + g + :h{:}g + \frac{1}{2}{:}h{:}^2 g + \frac{1}{6}{:}h{:}^3 g + \frac{1}{24}{:}h{:}^4 g + \mathcal{O}(\alpha^5) \\
=\; & f + g + \alpha({:}h_1{:}g) + \alpha^2({:}h_2{:}g + \frac{1}{2}{:}h_1{:}^2 g) \\
& + \alpha^3({:}h_3{:}g + \frac{1}{2}{:}h_1{::}h_2{:}g + \frac{1}{2}{:}h_2{::}h_1{:}g + \frac{1}{6}{:}h_1{:}^3 g) \\
& + \alpha^4({:}h_4{:}g + \frac{1}{2}{:}h_1{::}h_3{:}g + \frac{1}{2}{:}h_2{:}^2 g + \frac{1}{2}{:}h_3{::}h_1{:}g \qquad (9.232) \\
& + \frac{1}{6}{:}h_1{:}^2{:}h_2{:}g + \frac{1}{6}{:}h_2{::}h_1{:}^2 g + \frac{1}{6}{:}h_1{::}h_2{::}h_1{:}g + \frac{1}{24}{:}h_1{:}^4 g)
\end{aligned}
$$

The right-hand-side of Eq.(9.230) is

$$
\begin{aligned}
\text{RHS} \;=\; & (1 + \frac{1}{2}{:}h{:} + \frac{1}{6}{:}h{:}^2 + \frac{1}{24}{:}h{:}^3 + \frac{1}{120}{:}h{:}^4)(h_1 + 2\alpha h_2 \\
& + 3\alpha^2 h_3 + 4\alpha^3 h_4 + 5\alpha^4 h_5) \\
=\; & h_1 + \alpha(2h_2) + \alpha^2(\frac{1}{2}{:}h_1{:}h_2 + 3h_3) + \alpha^3(\frac{1}{6}{:}h_1{:}^2 h_2 + :h_1{:}h_3 + 4h_4) \\
& + \alpha^4(5h_5 + \frac{3}{2}{:}h_1{:}h_4 + \frac{1}{3}{:}h_1{:}^2 h_3 + \frac{1}{2}{:}h_2{:}h_3 - \frac{1}{6}{:}h_2{:}^2 h_1 + \frac{1}{24}{:}h_1{:}^3 h_2) \\
& \hspace{9cm} (9.233)
\end{aligned}
$$

Equating the α coeffiecients of both sides and applying the identity (9.53) give

$$
\mathcal{O}(\alpha^0) \implies \quad h_1 = f + g
$$

$$
\mathcal{O}(\alpha^1) \implies \quad h_2 = \frac{1}{2}{:}f{:}g
$$

$$
\mathcal{O}(\alpha^2) \implies \quad h_3 = \frac{1}{3}({:}h_2{:}g + \frac{1}{2}{:}h_1{:}h_2) = \frac{1}{12}{:}f{:}^2 g + \frac{1}{12}{:}g{:}^2 f
$$

$$
\mathcal{O}(\alpha^3) \implies \quad h_4 = \frac{1}{4}({:}h_3{:}g + \frac{1}{2}{:}h_1{::}h_2{:}g + \frac{1}{6}{:}h_1{:}^3 g - \frac{1}{6}{:}h_1{:}^2 h_2 - :h_1{:}h_3)
$$

$$
= \frac{1}{24}{:}f{::}g{:}^2 f
$$

$$
\begin{aligned}
\mathcal{O}(\alpha^4) \implies \quad h_5 =\; & \frac{1}{5}({:}h_4{:}g + \frac{1}{2}{:}h_1{::}h_3{:}g + \frac{1}{2}{:}h_2{:}^2 g + \frac{1}{2}{:}h_3{::}h_1{:}g + \frac{1}{6}{:}h_1{:}^2{:}h_2{:}g \\
& + \frac{1}{6}{:}h_2{::}h_1{:}^2 g + \frac{1}{6}{:}h_1{::}h_2{::}h_1{:}g + \frac{1}{24}{:}h_1{:}^4 g - \frac{3}{2}{:}h_1{:}h_4 \\
& - \frac{1}{3}{:}h_1{:}^2 h_3 - \frac{1}{2}{:}h_2{:}h_3 + \frac{1}{6}{:}h_2{:}^2 h_1 - \frac{1}{24}{:}h_1{:}^3 h_2) \\
=\; & -\frac{1}{720}{:}f{:}^4 g + \frac{1}{360}{:}g{::}f{:}^3 g + \frac{1}{120}{:}g{:}^2{:}f{:}^2 g + \frac{1}{120}{:}f{:}^2{:}g{:}^2 f \\
& + \frac{1}{360}{:}f{:}g{:}^3 f - \frac{1}{720}{:}g{:}^4 f \hspace{3cm} (9.234)
\end{aligned}
$$

This completes the proof of the first form of BCH formula when α is set to 1.

Prove the second form of the BCH formula, Eq.(9.194).
Solution Consider

$$e^{\alpha:f:}e^{:g:} = e^{:h(\alpha):} = M$$

$$\implies \quad \frac{dM}{d\alpha}M^{-1} = :f: \tag{9.235}$$

With Eq.(9.223), we have

$$f = \left(\frac{e^{:h:} - 1}{:h:}\right)\frac{dh}{d\alpha} \tag{9.236}$$

Define

$$h = g + \alpha h_1 + \alpha^2 h_2 + ...$$

To the leading order in α, Eq.(9.236) gives

$$f = \left(\frac{e^{:g:} - 1}{:g:}\right)h_1$$

or

$$h_1 = \left(\frac{:g:}{e^{:g:} - 1}\right)f \qquad \implies \text{Q.E.D.} \tag{9.237}$$

Exercise 52 Prove the other second form of the BCH formula, Eq.(9.195).
Solution Let

$$e^{:f:}e^{\alpha:g:} = e^{:h(\alpha):} = M$$

$$\implies \quad M^{-1}\frac{dM}{d\alpha} = :g: \tag{9.238}$$

At the same time, it can be shown that

$$M^{-1}\frac{dM}{d\alpha} = :\left(\frac{1 - e^{-:h:}}{:h:}\right)\frac{dh}{d\alpha}: \tag{9.239}$$

Combining Eqs.(9.238-9.239), we have

$$g = \left(\frac{1 - e^{-:h:}}{:h:}\right)\frac{dh}{d\alpha} \tag{9.240}$$

Define

$$h = f + \alpha h_1 + \alpha^2 h_2 + ... \tag{9.241}$$

To the leading order in α, Eq.(9.240) gives

$$g = \left(\frac{1 - e^{-:f:}}{:f:}\right)h_1 \tag{9.242}$$

or

$$h_1 = \left(\frac{:f:}{1 - e^{-:f:}}\right)g \qquad \implies \text{Q.E.D.} \tag{9.243}$$

Solution (*alternative*) Start with Eq.(9.194) which is valid for small f. Sandwitch it by $e^{:g:}$ from the left and $e^{-:g:}$ from the right. This yields

$$
\begin{aligned}
e^{:g:}e^{:f:} &= \exp\left[:e^{:g:}\left(g + (\frac{:g:}{e^{:g:}-1})f\right) + \mathcal{O}(f^2):\right] \\
&= \exp\left[:g + \left((\frac{:g:}{1-e^{-:g:}})f\right) + \mathcal{O}(f^2):\right] \quad (9.244)
\end{aligned}
$$

Exchanging f and g then proves Eq.(9.195).

Exercise 53 Prove the second order expression (9.196).
Solution To deal with the second order terms, instead of Eq.(9.242), we start with

$$
g = \left(\frac{1-e^{-:h:}}{:h:}\right)(h_1 + 2\alpha h_2) \quad (9.245)
$$

The operator in Eq.(9.245) can be written as

$$
\left(\frac{1-e^{-:h:}}{:h:}\right) = \int_0^1 d\beta \; e^{-\beta:f:+\alpha h_1:} \quad (9.246)
$$

If we denote the operator $e^{-\beta:f:+\alpha h_1:}$ by M, then

$$
\left(\frac{1-e^{-:h:}}{:h:}\right) = \int_0^1 d\beta \left(M\Big|_{\alpha=0} + \alpha\frac{dM}{d\alpha}\Big|_{\alpha=0}\right) + \mathcal{O}(\alpha^2) \quad (9.247)
$$

We need to compute $dM/d\alpha$. It follows from Eq.(9.223) that

$$
\frac{dM}{d\alpha} = :\left(\frac{e^{-\beta:f:+\alpha h_1:}-1}{\beta:f:+\alpha h_1:}\right)\beta h_1: \; e^{-\beta:f:+\alpha h_1:} \quad (9.248)
$$

Substituting Eq.(9.248) into Eq.(9.247) yields

$$
\left(\frac{1-e^{-:h:}}{:h:}\right) = \int_0^1 d\beta \left[e^{-\beta:f:} + \alpha :\left(\frac{e^{-\beta:f:}-1}{\beta:f:}\right)\beta h_1: \; e^{-\beta:f:}\right] \quad (9.249)
$$

Substituting Eq.(9.249) into Eq.(9.245) yields

$$
g = \int_0^1 d\beta \left[e^{-\beta:f:} + \alpha :\left(\frac{e^{-\beta:f:}-1}{\beta:f:}\right)\beta h_1: \; e^{-\beta:f:}\right](h_1 + 2\alpha h_2) \quad (9.250)
$$

Terms independent of α and terms first order in α must separately be equal on the two sides of Eq.(9.250). The terms constant in α gives simply Eq.(9.243). Terms linear in α give

$$
0 = \int_0^1 d\beta \; e^{-\beta:f:}2h_2 + \int_0^1 d\beta :\left(\frac{e^{-\beta:f:}-1}{\beta:f:}\right)\beta h_1: \; e^{-\beta:f:}h_1 \quad (9.251)
$$

Substituting h_1 from Eq.(9.243) then gives

$$0 = 2\left(\frac{1-e^{-:f:}}{:f:}\right)h_2 + \int_0^1 d\beta \left[\left(\frac{e^{-\beta:f:}-1}{1-e^{-:f:}}\right)g, e^{-\beta:f:}\left(\frac{:f:}{1-e^{-:f:}}\right)g\right]$$

$$\implies \quad h_2 = -\frac{1}{2}\left(\frac{:f:}{1-e^{-:f:}}\right)\int_0^1 d\beta \left[\left(\frac{e^{-\beta:f:}-1}{1-e^{-:f:}}\right)g, e^{-\beta:f:}\left(\frac{:f:}{1-e^{-:f:}}\right)g\right]$$

$$(9.252)$$

which in turn can be written in the form (9.196). By a change of variables from v to $v' = u(1-v)$, Eq.(9.196) also can be written as

$$\frac{1}{2}\left(\frac{:f:}{1-e^{-:f:}}\right)\int_0^1 du \int_0^u dv \left[e^{-v:f:}\left(\frac{:f:}{1-e^{-:f:}}\right)g, e^{-u:f:}\left(\frac{:f:}{1-e^{-:f:}}\right)g\right]$$

$$(9.253)$$

<u>*Exercise* 54</u> Prove the third form of the BCH formula (9.199-9.200).
<u>*Solution*</u> Consider

$$e^{:\alpha f:}e^{:\alpha g:}e^{:\alpha f:} = e^{:h(\alpha):} \equiv M(\alpha) \qquad (9.254)$$

We have

$$M^{-1}(\alpha) = e^{-:\alpha f:}e^{-:\alpha g:}e^{-:\alpha f:} = M(-\alpha)$$

$$\implies \quad e^{-:h(\alpha):} = e^{:h(-\alpha):}, \quad \text{or} \quad -h(\alpha) = h(-\alpha) \ (9.255)$$

i.e. the function $h(\alpha)$ is an odd function of α. Let

$$h(\alpha) = \alpha h_1 + \alpha^3 h_3 + \alpha^5 h_5 + ... \qquad (9.256)$$

We then consider

$$\frac{dM(\alpha)}{d\alpha} = :f:M + e^{:\alpha f:}:g:e^{:\alpha g:}e^{:\alpha f:} + M:f:$$

$$\implies \quad \frac{dM}{d\alpha}M^{-1} = :f: + e^{:\alpha f:}:g:e^{-:\alpha f:} + M:f:M^{-1}$$

$$= :f: + :e^{:\alpha f:}g: + :Mf: \qquad (9.257)$$

where use has been made of Table 5. We now combine Eqs.(9.223) and (9.257) to obtain

$$f + Mf + e^{:\alpha f:}g = \left(\frac{e^{:h:}-1}{:h:}\right)\frac{dh}{d\alpha} \qquad (9.258)$$

Expand both sides of Eq.(9.258) in powers of α. The left-hand-side reads

$$f + f + :h:f + \frac{1}{2}:h:^2 f + \frac{1}{6}:h:^3 f + \frac{1}{24}:h:^4 f$$

$$+ g + \alpha :f:g + \frac{1}{2}\alpha^2 :f:^2 g + \frac{1}{6}\alpha^3 :f:^3 g + \frac{1}{24}\alpha^4 :f:^4 g + \mathcal{O}(\alpha^5)$$

$$= 2f + g + \alpha(:h_1:f + :f:g) + \frac{1}{2}\alpha^2(:h_1:^2 f + :f:^2 g)$$

$$+ \alpha^3\left(\frac{1}{6}:h_1:^3 f + :h_3:f + \frac{1}{6}:f:^3 g\right)$$

$$+ \alpha^4\left(\frac{1}{2}:h_3::h_1:f + \frac{1}{2}:h_1::h_3:f + \frac{1}{24}:h_1:^4 f + \frac{1}{24}:f:^4 g\right) + \mathcal{O}(\alpha^5) \tag{9.259}$$

The right-hand-side of Eq.(9.258) reads

$$\left(1 + \frac{1}{2}:h: + \frac{1}{6}:h:^2 + \frac{1}{24}:h:^3 + \frac{1}{120}:h:^4\right)(h_1 + 3\alpha^2 h_3 + 5\alpha^4 h_5) + \mathcal{O}(\alpha^5)$$

$$= h_1 + 3\alpha^2 h_3 + \alpha^3\left(\frac{1}{2}:h_3:h_1 + \frac{3}{2}:h_1:h_3\right)$$

$$+ \alpha^4\left(5h_5 + \frac{1}{2}:h_1:^2 h_3 + \frac{1}{6}:h_1::h_3:h_1\right) + \mathcal{O}(\alpha^5) \tag{9.260}$$

We then equate for each order of α on both sides of Eq.(9.258),

$$\mathcal{O}(\alpha^0) \implies \quad h_1 = 2f + g$$

$$\mathcal{O}(\alpha^1) \implies \quad 0 = :h_1:f + :f:g$$

$$\implies \quad 0 = :g:f + :f:g, \text{ satisfied automatically}$$

$$\mathcal{O}(\alpha^2) \implies \quad 3h_3 = \frac{1}{2}:h_1:^2 f + \frac{1}{2}:f:^2 g$$

$$\implies \quad h_3 = \frac{1}{6}:g:^2 f - \frac{1}{6}:f:^2 g$$

$$\mathcal{O}(\alpha^3) \implies \quad \frac{1}{2}:h_3:h_1 + \frac{3}{2}:h_1:h_3 = \frac{1}{6}:h_1:^3 f + :h_3:f + \frac{1}{6}:f:^3 g$$

$$\implies \quad \text{satisfied automatically}$$

$$\mathcal{O}(\alpha^4) \implies \quad 5h_5 + \frac{1}{2}:h_1:^2 h_3 + \frac{1}{6}:h_1::h_3:h_1$$

$$= \frac{1}{2}:h_3::h_1:f + \frac{1}{2}:h_1::h_3:f + \frac{1}{24}:h_1:^4 f + \frac{1}{24}:f:^4 g$$

$$\implies \quad h_5 = \frac{1}{120}:h_1:^4 f + \frac{1}{120}:f:^4 g + \frac{1}{10}:h_3::g:f$$

$$+ \frac{1}{10}:h_1::h_3:f - \frac{1}{15}:h_1:^2 h_3 \tag{9.261}$$

One still needs to substitute h_1 and h_3 into the h_5 expression above. We first note, using property (9.53), that

$$:h_1:^4 f = -8:f:^4 g + 8:f:^2::g:^2 f + 2:f::g:^3 f - 4:g::f:^3 g$$

$$-4:g:^2::f:^2 g + :g:^4 f$$

$$:h_3::g:f = \frac{1}{6}:f::g:^3 f + \frac{1}{6}:g:^2::f:^2 g + \frac{1}{6}:f:^2::g:^2 f + \frac{1}{6}:g::f:^3 g$$

225

$$:h_1::h_3:f \;=\; -\frac{1}{3}:f:^2:g:^2f + \frac{1}{6}:g:^2:f:^2g + \frac{1}{3}:f:^4g + \frac{1}{6}:g::f:^3g$$

$$:h_1:^2h_3 \;=\; \frac{1}{3}:f::g:^3f - \frac{2}{3}:f:^4g + :f:^2:g:^2f + \frac{1}{6}:g:^4f$$

$$-\frac{1}{3}:g::f:^3g - \frac{1}{2}:g:^2:f:^2g \qquad\qquad (9.262)$$

Substituting into Eq.(9.261) and simplifying give

$$h_5 \;=\; \frac{7}{360}:f:^4g - \frac{1}{60}:f:^2:g:^2f + \frac{1}{90}:f::g:^3f + \frac{1}{45}:g::f:^3g$$

$$+\frac{1}{30}:g:^2:f:^2g - \frac{1}{360}:g:^4f \qquad\qquad (9.263)$$

Substituting h_1, h_3 and h_5 into Eq.(9.256) and setting $\alpha = 1$ then give the result (9.200).

Exercise 55 On the right hand side of Eq.(9.197), the ordering of the two factor maps are as chosen. Show that one could choose the reversed ordering to obtain

$$e^{:f+g:} \;=\; \exp\left[:\left(\frac{e^{:f:}-1}{:f:}\right)g:\right]e^{:f:}$$

$$=\; \exp\left[:\left(\int_0^1 du\; e^{u:f:}\right)g:\right]e^{:f:} \qquad\qquad (9.264)$$

A generalization of Eq.(9.264) and several applications can be found following Eqs.(9.421-9.422) later.

Exercise 56 Concatenate the map

$$e^{-:2f_2:}e^{:f_2+f_3:}e^{:f_2+g_3:} \qquad\qquad (9.265)$$

into a form

$$e^{:h_3+\mathcal{O}(X^4):} \qquad\qquad (9.266)$$

Find h_3 in terms of $f_2, f_3,$ and g_3.
Solution

$$h_3 = \int_0^1 du\; e^{-u:f_2:}(e^{-:f_2:}f_3 + g_3) \qquad\qquad (9.267)$$

Exercise 57 (a) Concatenate the map

$$e^{:f+g:}e^{:-f+g:} \qquad\qquad (9.268)$$

to first order in g, assuming g is small but f is not. (b) Consider two short-but-strong sextupoles, each of the same length L but opposite polarity S and $-S$. Consider L to be short, but S strong in such a way that SL is held fixed. Arrange these two sextupoles back to

226

back. The leading effect is that these two sextupoles will cancel each other, but the cancellation is not complete and one ends up with a residual error map. Apply the result in (a) to find this residual error map to leading order in L (but to all orders in LS). Consider on-momentum particles only.

Solution (a) The result is not $e^{:2g:}$ but

$$\exp\left[:2\left(\frac{e^{:f:}-1}{:f:}\right)g+\mathcal{O}(g^2):\right]=\exp\left[:2\left(\int_0^1 du\ e^{u:f:}\right)g+\mathcal{O}(g^2):\right]$$
(9.269)

(b) The map is given by Eq.(9.268) with

$$f=-\frac{LS}{3}(x^3-3xy^2),\quad g=-\frac{L}{2}(p_x^2+p_y^2)$$
(9.270)

and g is small and f is not small. Applying Eq.(9.269) gives the residual map

$$\exp\left[-:L\left(p_x^2+p_y^2-LSp_x(x^2-y^2)+2LSp_yxy\right.\right.$$
$$\left.\left.+\frac{1}{3}L^2S^2(x^2-y^2)^2+\frac{4}{3}L^2S^2x^2y^2\right)+\mathcal{O}(L^2):\right]$$
(9.271)

Exercise 58 Consider a thick-lens sextupole which is represented by the map [see Eq.(9.182)]

$$M=e^{:h_2+h_3:},\quad\text{where}\quad\begin{cases}h_2=-\frac{L}{2}(p_x^2+p_y^2)\\h_3=-\frac{L}{3}S(x^3-3xy^2)\end{cases}$$
(9.272)

The map M can be factorized to read

$$M=e^{:h_2:}e^{:g_3:}e^{:\mathcal{O}(X^4):}$$
(9.273)

where g_3 is a homogeneous 3-rd order polynomial in X. Find g_3. Find the thin-lens limit of the result.
Solution Apply Eq.(9.197-9.198)to obtain

$$\begin{aligned}g_3&=\int_0^1 du\ h_3(e^{-u:h_2:}X)\\&=-\frac{1}{3}SL\int_0^1 du[(x-uLp_x)^3-3(x-uLp_x)(y-uLp_y)^2]\\&=-\frac{1}{3}SL[x^3-\frac{3}{2}Lx^2p_x+L^2xp_x^2-\frac{1}{4}L^3p_x^3-3xy^2+\frac{3}{2}Lp_xy^2\\&\qquad+3Lxyp_y-2L^2yp_xp_y-L^2xp_y^2+\frac{3}{4}L^3p_xp_y^2]\end{aligned}$$
(9.274)

Take the thin-lens limit $L\to0$, $S\to\infty$, while holding LS fixed, this reduces to

$$g_3\to-\frac{SL}{3}(x^3-3xy^2)$$
(9.275)

Exercise 59 Factorize the map

$$\exp[:ax^3 + bx^2p + cxp^2 + dp^3:] \tag{9.276}$$

into the form

$$e^{:Ax^3:}e^{:Bx^2p:}e^{:Cxp^2:}e^{:Dp^3:}e^{:Ex^4:}e^{:Fx^3p:}e^{:Gx^2p^2:}e^{:Hxp^3:}e^{:Ip^4:}e^{:\mathcal{O}(X^5):} \tag{9.277}$$

Apply both Eqs.(9.276-9.277) to x and p. Show that the results agree to order $\mathcal{O}(X^3)$. This factorization can be useful as one can apply the monomial map formula (9.128) to Eq.(9.277). See also Exercise 37.

Solution

$$A = a, \quad B = b, \quad C = c, \quad D = d$$

$$E = -\frac{3}{2}ab, \quad F = -3ac, \quad G = -\frac{3}{2}(3ad + bc)$$

$$H = -3bd, \quad I = -\frac{3}{2}cd \tag{9.278}$$

Exercise 60 The BCH formula can of course be applied to concatenate two linear maps. Take for example the first form, Eq.(9.191-9.192). It follows that given two matrices A and B of the same dimension, they can be concatenated as

$$e^A e^B = e^C \tag{9.279}$$

where

$$C = A + B + \frac{1}{2}\{A, B\} + \frac{1}{12}\{A, \{A, B\}\} + \frac{1}{12}\{B, \{B, A\}\} + ... \tag{9.280}$$

where we have used the curly brackets to mean the commutators of matrices. Note that C contains only A and B and their commutators. No stand-alone terms like A^2, AB or A^2B, etc. appear.

Solution To demonstrate Eq.(9.280), start with the BCH formula. Consider the quadratic forms

$$f_2 = -\frac{1}{2}\tilde{X}FX, \quad g_2 = -\frac{1}{2}\tilde{X}GX \tag{9.281}$$

where F and G are symmetric matrices. Equations (9.92-9.93) and (9.191-9.192) say that

$$e^{SG}e^{SF} = e^{SH} \tag{9.282}$$

where H is a symmetric matrix for which the corresponding quadratic form $h_2 = -\frac{1}{2}\tilde{X}HX$ satisfies

$$h_2 = f_2 + g_2 + \frac{1}{2}[f_2, g_2] + \frac{1}{12}[f_2, [f_2, g_2]] + \frac{1}{12}[g_2, [g_2, f_2]] + ... \tag{9.283}$$

228

where the square brackets are the Poisson brackets. We want to use this property to prove Eq.(9.280), at least for the special case when A and B can be written as SG and SF respectively where F and G are symmetric matrices. To do that, note that

$$
\begin{aligned}
[f_2, g_2] &= \frac{1}{4} \frac{\partial (F_{\alpha\beta} X_\alpha X_\beta)}{\partial X_\ell} S_{\ell m} \frac{\partial (G_{\gamma\delta} X_\gamma X_\delta)}{\partial X_m} \\
&= F_{\alpha\ell} X_\alpha S_{\ell m} G_{\gamma m} X_\gamma = \tilde{X} FSGX = -\frac{1}{2} \tilde{X}(GSF - FSG)X
\end{aligned}
$$

(9.284)

We have therefore demonstrated that $[f_2, g_2]$ is a quadratic form, and its corresponding matrix is given by

$$
GSF - FSG = -S\{SG, SF\} \tag{9.285}
$$

In the last step of Eq.(9.284), we have used the fact that

$$
FSG = -(\widetilde{GSF}) \tag{9.286}
$$

to assure the symmetry of the matrix (9.285). Using Eq.(9.286), it follows that $[f_2, [f_2, g_2]]$ is also a quadratic form, and its corresponding matrix is

$$
-S\{S(-S\{SG, SF\}), SF\} = -S\{SF, \{SF, SG\}\}
$$

The quadratic form h_2 therefore is given by the matrix

$$
\begin{aligned}
H &= F + G - \frac{1}{2} S\{SG, SF\} - \frac{1}{12} S\{SF, \{SF, SG\}\} \\
&\quad - \frac{1}{12} S\{SG, \{SG, SF\}\} + \dots
\end{aligned}
$$

or

$$
\begin{aligned}
SH &= SF + SG + \frac{1}{2}\{SG, SF\} + \frac{1}{12}\{SF, \{SF, SG\}\} \\
&\quad + \frac{1}{12}\{SG, \{SG, SF\}\} + \dots \tag{9.287}
\end{aligned}
$$

which proves Eq.(9.280) if one identifies $A = SF, B = SG, C = SH$.

9.5 Localized rf Cavity

In the following sections, we will apply the Lie algebra techniques to several accelerator applications, including

<div align="center">

localized rf cavities

a single localized sextupole

</div>

distribution of multipoles

multipole correction algorithms

higher order chromaticities

achromats

resonance strengths

To fully address these applications, it turns out there is one more important technique we still need to learn, namely the normal form technique to be covered later. But we will consider a few simpler applications first before we discuss normal forms. As a first application of the techniques developed so far,[7] consider the longitudinal particle motion whose dynamic variables are (z, δ). Consider an rf cavity located at $s = 0$, whose action on particle motion is given by the map

$$z = z_0, \quad \delta = \delta_0 - V \sin k z_0 \qquad (9.288)$$

where V and k are related to the voltage and frequency of the rf cavity. Represent the rest of the accelerator by the simple map

$$z = z_0 + \alpha \delta_0, \quad \delta = \delta_0 \qquad (9.289)$$

where α is related to the momentum compaction factor of the accelerator design. Here, $\alpha > 0$ is below transition; $\alpha < 0$ is above transition.

Strictly speaking, the system described by Eqs.(9.288-9.289) is not integrable. But to the extent that a power series converges, it is at least approximately integrable when some appropriate parameters are "small", and in this sense, there is an invariant of the motion. In this first application of the Lie techniques, we will find this invariant. In fact, we will find several expressions of this invariant, each applicable in its own validity range of the parameters.

We will first find an expression of the invariant when both α and V are small in some sense. The two maps (9.288-9.289) are both close to the identity map. Let us first write them in their Lie algebraic forms (see Table 4),

$$M_{\text{cav}} = \exp(: - \int_0^z dz' V \sin k z' :) = \exp\left[: - \frac{V}{k}(1 - \cos kz): \right]$$

$$M_{\text{acc}} = \exp(: - \frac{1}{2}\alpha\delta^2 :) \qquad (9.290)$$

Observe the particle motion at the exact middle of the rf cavity, the one-turn map is

$$M_{\text{cav}/2} M_{\text{acc}} M_{\text{cav}/2} = \exp\left[: - \frac{V}{2k}(1 - \cos kz): \right] \exp(: - \frac{1}{2}\alpha\delta^2 :)$$

$$\times \exp\left[: - \frac{V}{2k}(1 - \cos kz): \right] \qquad (9.291)$$

This map can be concatenated using the 3rd form of the BCH formula, Eqs.(9.199-9.200), if we identify

$$
\begin{aligned}
f &= -\frac{V}{2k}(1 - \cos kz) \\
g &= -\frac{1}{2}\alpha\delta^2
\end{aligned}
\tag{9.292}
$$

In the concatenation procedure, we note

$$
\begin{aligned}
:g:f &= -\frac{1}{2}V\alpha\delta \sin kz \\
:g:^2 f &= -\frac{1}{2}V\alpha^2 k\delta^2 \cos kz \\
:g:^3 f &= \frac{1}{2}V\alpha^3 k^2 \delta^3 \sin kz \\
:g:^4 f &= \frac{1}{2}V\alpha^4 k^3 \delta^4 \cos kz \\
:f:g &= \frac{1}{2}V\alpha\delta \sin kz \\
:f:^2 g &= -\frac{1}{4}V^2\alpha \sin^2 kz \\
:f:^3 g &= 0 \\
:f::g:^3 f &= -\frac{3}{4}V^2\alpha^3 k^2\delta^2 \sin^2 kz \\
:f::g:^2 f &= \frac{1}{4}V^2\alpha^2 k\delta \sin 2kz \\
:f:^2:g:^2 f &= -\frac{1}{8}V^3\alpha^2 k \sin kz \sin 2kz \\
:g::f:^2 g &= -\frac{1}{4}V^2\alpha^2 k\delta \sin 2kz \\
:g:^2:f:^2 g &= -\frac{1}{2}V^2\alpha^3 k^2\delta^2 \cos 2kz
\end{aligned}
\tag{9.293}
$$

After concatenation, the one-turn map becomes $e^{:h:}$, where

$$
\begin{aligned}
h &= -\frac{1}{2}\alpha\delta^2 - \frac{V}{k}(1 - \cos kz) \\
&\quad -\frac{1}{12}V\alpha^2 k\delta^2 \cos kz + \frac{1}{24}V^2\alpha \sin^2 kz \\
&\quad -\frac{1}{720}V\alpha^4 k^3\delta^4 \cos kz + \frac{1}{120}V^2\alpha^3 k^2\delta^2 (3\sin^2 kz - 2) \\
&\quad +\frac{1}{480}V^3\alpha^2 k \sin kz \sin 2kz + \mathcal{O}((V,\alpha)^7)
\end{aligned}
\tag{9.294}
$$

Why are we interested in h? Because it is an *invariant of the motion*. That is, if we measure (z, δ) of a particle turn after turn as it passes by the middle of the rf cavity, and calculate the value of $h(z, \delta)$, we will find that the value

of h does not vary from turn to turn.[48] More importantly, we are interested in h not only because h is an invariant, but also because $-h$ is the *effective Hamiltonian* of the system. By finding h, we have replaced the discrete system consisting of piecewise constant Hamiltonians by a smooth system which has an s-independent Hamiltonian $-h$. This smooth system is of course much simpler to handle than the original discrete system. In fact, having found h, the problem has been "integrated".

For Eq.(9.294) to be an invariant, the series expansion must converge. This applies when

$$|k\alpha V| \ll 1, \quad |k\alpha\hat{\delta}| \ll 1 \tag{9.295}$$

where $\hat{\delta}$ is the peak value of δ during the evolution of the particle under consideration. For particles inside the rf bucket, $\hat{\delta} <$ bucket height. Since the bucket height $= \sqrt{4V/k\alpha}$, the second condition of (9.295) is satisfied for particles inside the rf bucket if the first condition of (9.295) is satisfied. [For an idea of what does the rf bucket looks like, see Fig.9.3(a).]

One may also try to find an expression of the invariant in case $k\alpha V$ is small but $k\alpha\hat{\delta}$ is not necessarily small by applying the 4-th BCH form (9.202-9.203). With f and g defined in Eq.(9.292), one obtains an invariant to first order in V which holds for particles outside the rf bucket. We note that

$$:g:f = \alpha\delta\frac{\partial f}{\partial z}$$

$$\implies \quad (:g:\coth\frac{:g:}{2})f = -\frac{V}{2k}\left[(\alpha\delta\frac{\partial}{\partial z})\coth(\frac{\alpha\delta}{2}\frac{\partial}{\partial z})\right](1 - e^{ikz})$$

$$= -\frac{V}{k} + \frac{V}{2k}(\alpha\delta ik)\coth(\frac{\alpha\delta}{2}ik)e^{ikz}$$

$$= -\frac{V}{k} + \frac{V}{2k}(\alpha\delta k)\cot\frac{\alpha\delta k}{2}e^{ikz} \tag{9.296}$$

In the above expressions, only the real parts are meaningful, and we have used the fact that $i\coth(ix) = \cot x$. Substituting Eq.(9.296) into Eq.(9.203) gives

$$h = -\frac{1}{2}\alpha\delta^2 - \frac{V}{k} + \frac{1}{2}\alpha\delta V\cot\frac{\alpha\delta k}{2}\cos kz + \mathcal{O}(V^2) \tag{9.297}$$

If $k\alpha\hat{\delta}$ is also small, Eq.(9.297) agrees with (9.294) to first order in V.

The 4-th BCH form also can be used to obtain an expression when $k\alpha\hat{\delta}$ is small, but $k\alpha V$ is not necessarily small. It follows from Eq.(9.204) that

$$\begin{aligned}
h &= 2f + (\frac{:f:}{\sinh:f:})g + \mathcal{O}(\alpha^2) \\
&= 2f + (1 - \frac{1}{6}:f:^2 + \frac{7}{360}:f:^4 + ...)g + \mathcal{O}(\alpha^2) \\
&= 2f + (1 - \frac{1}{6}:f:^2)g + \mathcal{O}(\alpha^2)
\end{aligned}$$

---

[48] provided h exists. If the power series expansion (9.294) does not converge, for example, then h may not exist. In that case, there is not an invariant, and the system is not integrable.

232

$$= -\frac{V}{k}(1 - \cos kz) - \frac{1}{2}\alpha\delta^2 + \frac{1}{24}V^2\alpha\sin^2 kz + \mathcal{O}(\alpha^2) \qquad (9.298)$$

Again, this expression is consistent with Eq.(9.294) in the appropriate limit.

As mentioned, $-h$ also has the meaning of being the one-turn effective Hamiltonian. For example, if one is interested in the one-turn equations of motion to first order in α, one may use Eq.(9.298) to obtain

$$\frac{dz}{dn} = -\frac{\partial h}{\partial\delta} = \alpha\delta + \mathcal{O}(\alpha^2)$$

$$\frac{d\delta}{dn} = \frac{\partial h}{\partial z} = -V[\sin kz - \frac{1}{24}\alpha kV \sin 2kz] + \mathcal{O}(\alpha^2) \qquad (9.299)$$

where n is a turn number index which increases by 1 per turn. What we have shown is that the discrete maps (9.288-9.289) are approximately equivalent to the continuous evolution (9.299), provided the particle motion is observed only at discrete times at the middle of the rf cavity when $n = $ integers.

Sometimes it is more useful to find an invariant which is valid when the dynamical varables z and δ are small, i.e. when the synchrotron motion is close to the origin of the phase space. In this representation, V and α do not have to be small. To do so, let us write the map of half of the the rf cavity as

$$M_{\text{cav}/2} = \exp\left[:-\frac{V}{2k}(1 - \cos kz):\right] = e^{:f_2 + f_{\text{NL}}:} \qquad (9.300)$$

where f_2 is the term in f that is quadratic in the dynamic variables, and f_{NL} contains the remaining, higher order nonlinear terms of f, i.e.

$$f_2 = -\frac{V}{4}kz^2$$

$$f_{\text{NL}} = -\frac{V}{2k}(1 - \cos kz - \frac{1}{2}k^2z^2) \qquad (9.301)$$

Since $:f_2:$ and $:f_{\text{NL}}:$ commute, we have

$$M_{\text{cav}/2} = e^{:f_2:}e^{:f_{\text{NL}}:} = e^{:f_{\text{NL}}:}e^{:f_2:} \qquad (9.302)$$

The one-turn map then reads

$$M = e^{:f_{\text{NL}}:}e^{:f_2:}e^{:g_2:}e^{:f_2:}e^{:f_{\text{NL}}:} \qquad (9.303)$$

where $g = -\frac{1}{2}\alpha\delta^2$ has been designated as g_2 because it is second order in δ.

The three operators in the middle of Eq.(9.303) describe the linearized synchrotron motion, which we designate as

$$M_2 = e^{:f_2:}e^{:g_2:}e^{:f_2:} \qquad (9.304)$$

The action of M_2 on the vector $X = (z, \delta)$ can be described most conveniently by a matrix [see Eqs.(9.288-9.289)]

$$M_2 = \begin{bmatrix} 1 & 0 \\ -\frac{1}{2}kV & 1 \end{bmatrix} \begin{bmatrix} 1 & \alpha \\ 0 & 1 \end{bmatrix} \begin{bmatrix} 1 & 0 \\ -\frac{1}{2}kV & 1 \end{bmatrix}$$

$$= \begin{bmatrix} 1 - \frac{1}{2}kV\alpha & \alpha \\ -kV + \frac{1}{4}k^2V^2\alpha & 1 - \frac{1}{2}kV\alpha \end{bmatrix} \qquad (9.305)$$

233

For sufficiently small z and δ, we can ignore the nonlinear effects described by f_{NL}. The one-turn map is just the linear map M_2. Let us first find the "Courant-Snyder" invariant of this linear system. This means we are looking for a quadratic invariant, which is solely determined by M_2.

Let the Lie representation of M_2 be written as $\exp(:F_2:)$. Let F_2 be written as $-\frac{1}{2}\tilde{X}FX$, where F is a symmetric matrix parametrized as Eq.(9.77). By applying the Hamilton-Cayley technique using Eq.(9.86), we obtain

$$a = \frac{\mu}{\alpha}\sin\mu, \qquad b = 0, \qquad c = \frac{\alpha\mu}{\sin\mu} \tag{9.306}$$

where μ is determined by

$$\cos\mu = 1 - \frac{1}{2}kV\alpha \tag{9.307}$$

For stability of the system, we must have $4 \geq kV\alpha \geq 0$. We will choose μ to be between 0 and π.

The quadratic invariant — the Courant-Snyder invariant — is given by

$$
\begin{aligned}
F_2 &= -\frac{1}{2}(az^2 + 2bz\delta + c\delta^2) \\
&= -\frac{\mu}{2}\left(\frac{\sin\mu}{\alpha}z^2 + \frac{\alpha}{\sin\mu}\delta^2\right)
\end{aligned} \tag{9.308}
$$

We next look for the higher order terms of the invariant. To do this, we will apply Eq.(9.203) to the one-turn map

$$M = e^{:f_{\mathrm{NL}}:}e^{:F_2:}e^{:f_{\mathrm{NL}}:} \tag{9.309}$$

To first order in f_{NL}, the invariant is given by

$$h = F_2 + {:}F_2{:}\coth\left(\frac{{:}F_2{:}}{2}\right)f_{\mathrm{NL}} \tag{9.310}$$

To calculate the invariant, therefore, we need to find ${:}F_2{:}\coth({:}F_2{:}/2)f_{\mathrm{NL}}$. We learned before that an exponential operator operating on a complicated function can be simplified by using (see Table 5) $e^{:f:}g(X) = g(e^{:f:}X)$. But here we have a complicated operator operating on a complicated function, and the question is how to proceed. The answer lies in the idea of *eigenmodes*. To appreciate this, note that the complicated operator is made up of ${:}F_2{:}$, which is a much simpler object. If the function f_{NL} to be operated on can be decomposed into some eigenmodes of the operator ${:}F_2{:}$, then the calculation will simplify considerably. So our first job is to find these eigenmodes of ${:}F_2{:}$.[49]

We first simplify the expression of F_2 by introducing the dynamical variables

$$\bar{z} = z\sqrt{\frac{\sin\mu}{|\alpha|}}, \quad \bar{\delta} = \delta\sqrt{\frac{|\alpha|}{\sin\mu}} \tag{9.311}$$

---

[49] We are touching upon the topic of normal forms.

This is a canonical transformation because the fundamental Poisson brackets are preserved (see Exercise 2):

$$[\bar{z}, \bar{\delta}] = [z, \delta] = 1 \tag{9.312}$$

This means we can treat $(\bar{z}, \bar{\delta})$ as the new dynamical variables. The new F_2 reads

$$F_2 = -\frac{\mu}{2}(\bar{z}^2 + \bar{\delta}^2) \tag{9.313}$$

Applying $:F_2:$ on $\bar{z}$ and $\bar{\delta}$ gives

$$:F_2: \begin{bmatrix} \bar{z} \\ \bar{\delta} \end{bmatrix} = \mu \ \text{sgn}(\alpha) \begin{bmatrix} \bar{\delta} \\ -\bar{z} \end{bmatrix} \tag{9.314}$$

One then notes that if we apply $:F_2:$ to $\bar{z} \pm i\bar{\delta}$, we obtain

$$:F_2:(\bar{z} \pm i\bar{\delta}) = \mp i \ \text{sgn}(\alpha)\mu \ (\bar{z} \pm i\bar{\delta}) \tag{9.315}$$

This means $(\bar{z} \pm i\bar{\delta})$ are eigenmodes of $:F_2:$ with eigenvalues $\mp i \ \text{sgn}(\alpha)\mu$. We have thus found two eigenmodes of $:F_2:$. But we need to find more such modes, as is done next.

To simplify the consideration, below we will consider the case below transition only, with $\alpha > 0$. Make another canonical transformation from $(\bar{z}, \bar{\delta})$ to (ϕ, A) according to[50]

$$\bar{z} = \sqrt{2A} \sin\phi, \quad \bar{\delta} = \sqrt{2A} \cos\phi \tag{9.316}$$

or

$$A = \frac{1}{2}(\bar{z}^2 + \bar{\delta}^2), \quad \phi = \tan^{-1}\frac{\bar{z}}{\bar{\delta}} \tag{9.317}$$

This is a canonical transformation because

$$[\phi, A] = 1 \tag{9.318}$$

The new F_2 is

$$F_2 = -\mu A \tag{9.319}$$

It follows that

$$:F_2:A = 0, \quad :F_2:\phi = \mu \tag{9.320}$$

and that $e^{in\phi}$ is an eigenmode of $:F_2:$ with eigenvalue $in\mu$ for any integer n, i.e.,

$$:F_2:e^{in\phi} = in\mu e^{in\phi} \tag{9.321}$$

Equation (9.315) is just the special case of Eq.(9.321) with $n = \pm 1$. We have thus found a host of eigenmodes of the operator $:F_2:$. Furthermore, $e^{in\phi}$ is also an eigenmode of any function of $:F_2:$, i.e.,

$$G(:F_2:)e^{in\phi} = G(in\mu)e^{in\phi} \tag{9.322}$$

---

[50]Remember that ϕ is the coordinate, A is the momentum, not the other way around.

We are now ready to calculate $:F_2:\coth(:F_2:/2)f_{\rm NL}$. We first note that

$$
\begin{aligned}
f_{\rm NL}(z) &= \frac{1}{48}Vk^3z^4 + \mathcal{O}(z^6) \\
&= \frac{1}{48}Vk^3\frac{\alpha^2}{\sin^2\mu}\bar{z}^4 + \mathcal{O}(\bar{z}^6) \\
&= \frac{1}{12}Vk^3\frac{\alpha^2}{\sin^2\mu}A^2\sin^4\phi + \mathcal{O}(A^3) \qquad (9.323)
\end{aligned}
$$

We then decompose $f_{\rm NL}$ into a linear combination of the eigenmodes of $:F_2:$ as

$$
f_{\rm NL} = \frac{1}{192}Vk^3\frac{\alpha^2}{\sin^2\mu}A^2(e^{i4\phi} - 4e^{i2\phi} + 6 - 4e^{-i2\phi} + e^{-i4\phi}) + \mathcal{O}(A^3) \quad (9.324)
$$

We then find

$$
\begin{aligned}
:F_2:\coth\left(\frac{:F_2:}{2}\right)f_{\rm NL} &= \frac{1}{192}Vk^3\frac{\alpha^2}{\sin^2\mu}A^2[i4\mu\coth(i2\mu)e^{i4\phi} \\
&\quad -i8\mu\coth(i\mu)e^{i2\phi} + 12 + i8\mu\coth(-i\mu)e^{-i2\phi} \\
&\quad -i4\mu\coth(-i2\mu)e^{-i4\phi}] + \mathcal{O}(A^3) \\
&= \frac{1}{48}Vk^3\frac{\alpha^2}{\sin^2\mu}A^2(2\mu\cot 2\mu\cos 4\phi - 4\mu\cot\mu\cos 2\phi + 3) \quad (9.325)
\end{aligned}
$$

where we have used the fact that $x\coth x = 2$ as $x \to 0$ and that $i\coth(ix) = \cot x$.

Equation (9.325) can be expressed in terms of $(\bar{z}, \bar{\delta})$ coordinates as

$$
\begin{aligned}
:F_2:\coth\left(\frac{:F_2:}{2}\right)f_{\rm NL} &= \frac{1}{48}Vk^3\frac{\alpha^2}{\sin^2\mu}[\bar{z}^4(\frac{\mu}{2}\cot 2\mu + \mu\cot\mu + \frac{3}{4}) \\
&\quad + \bar{z}^2\bar{\delta}^2(-3\mu\cot 2\mu + \frac{3}{2}) + \bar{\delta}^4(\frac{\mu}{2}\cot 2\mu - \mu\cot\mu + \frac{3}{4})] \quad (9.326)
\end{aligned}
$$

It can also be expressed in terms of the original coordinates (z, δ). When substituted into the invariant expression (9.310), one obtains finally

$$
\begin{aligned}
h &= -\frac{\mu}{2}(\frac{\sin\mu}{\alpha}z^2 + \frac{\alpha}{\sin\mu}\delta^2) \\
&\quad + \frac{1}{48}Vk^3\frac{\alpha^2}{\sin^2\mu}\Big[\frac{\sin^2\mu}{\alpha^2}z^4(\frac{\mu}{2}\cot 2\mu + \mu\cot\mu + \frac{3}{4}) \qquad (9.327) \\
&\quad + z^2\delta^2(-3\mu\cot 2\mu + \frac{3}{2}) + \frac{\alpha^2}{\sin^2\mu}\delta^4(\frac{\mu}{2}\cot 2\mu - \mu\cot\mu + \frac{3}{4})\Big] + \mathcal{O}((z,\delta)^6)
\end{aligned}
$$

Equation (9.325) gives the effective Hamiltonian in the (ϕ, A) phase space. This expression can be used to calculate the dependence of the synchrotron tune on the longitudinal action A. See Exercise 97.

We can check the various invariants obtained in this section numerically as illustrated in Fig.9.3. Figure 9.3(a) shows the turn-by-turn tracking result of the
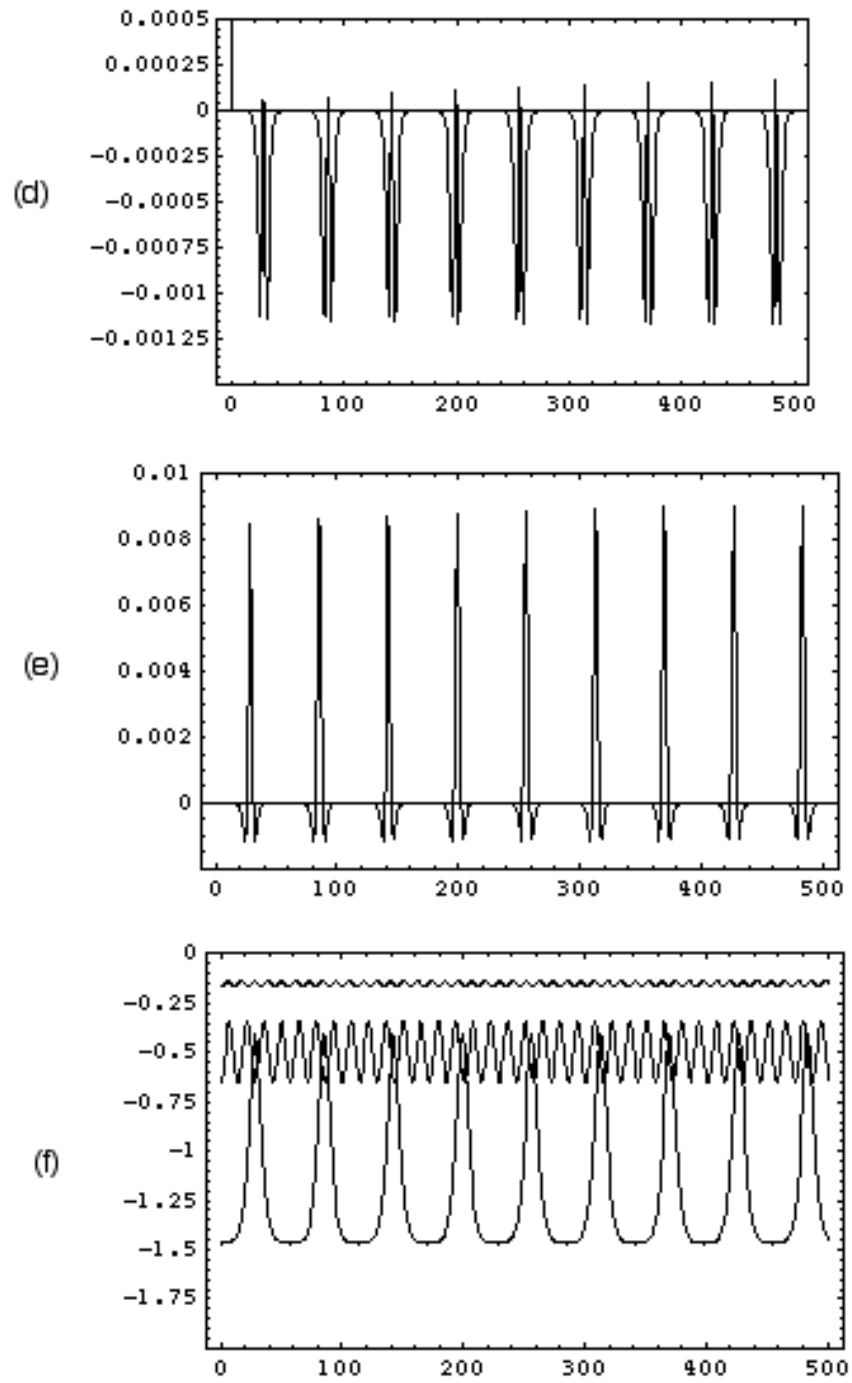
236
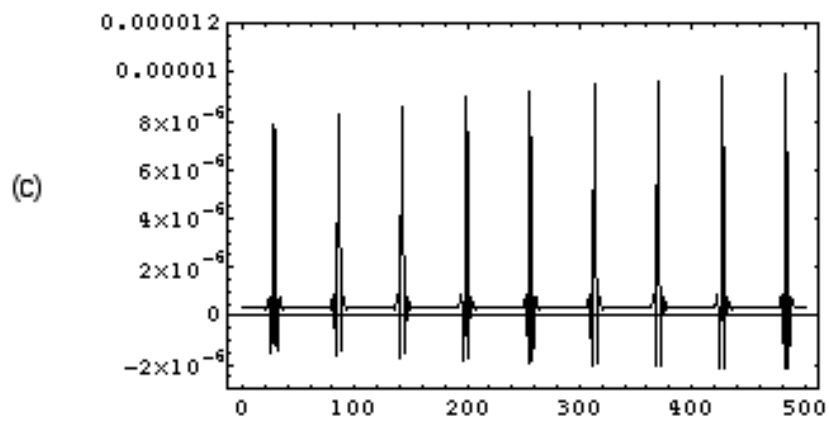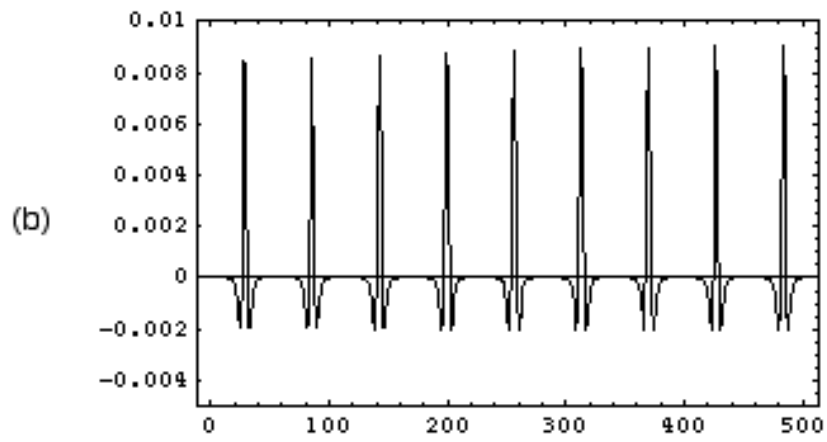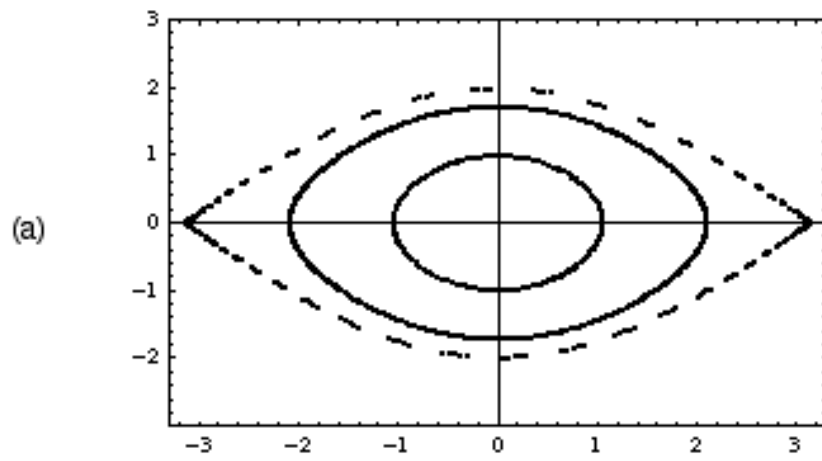
Figure 9.3: Tracking results of various invariants for the case of a localized rf.

system described by Eqs.(9.288-9.289). The motion of a particle is observed as it passes by the middle of the rf cavity turn after turn. The observed coordinates (z, δ) are plotted for 500 turns for three particles whose initial conditions are[51]

$$\text{first particle} : (kz = 3.14 \times \frac{1}{3}, \delta = 0)$$

$$\text{second particle} : (kz = 3.14 \times \frac{2}{3}, \delta = 0)$$

$$\text{third particle} : (kz = 3.14, \delta = 0) \tag{9.328}$$

The parameters used are $k = 1, V = 0.3, \alpha = 0.3$. The small-amplitude synchrotron tune, determined by Eq.(9.307), is $\mu/2\pi = 0.04793$. The trajectory of the third particle approximately traces out the boundary of the rf bucket, within which particle motion is to be confined.

Figure 9.3(b) shows the numerical value of the approximate invariant given by the first two terms [terms linear in (α, V)] of Eq.(9.294) as a function of turn number as the third particle circulates around the accelerator. If it is a true invariant, this quantity would be constant. Figure 9.3(b) shows that it is not an accurate invariant, although the vertical scale is rather expanded. Fig.9.3(c) is the same as Fig.9.3(b) except that all terms in Eq.(9.294) are included, i.e. Fig.9.3(c) is a plot of the 6-th order invariant. For convenience, in Figs.9.3(b) and (c), the vertical coordinates refer to $h+0.6$, instead of the invariant h. It can be seen that the invariant plotted in Fig.9.3(c) is indeed much more accurate than that of Fig.9.3(b). For these figures, conditions (9.295) are reasonably satisfied [$k\alpha V = 0.09$, $k\alpha\hat{\delta} = 0.6$ for the third particle].

Figure 9.3(d) plots the time evolution of $h + 0.6$ where the invariant h is as calculated using Eq.(9.297), an invariant for small $k\alpha V$. Figure 9.3(e) shows the same using Eq.(9.298), an invariant for small $k\alpha\hat{\delta}$. One can also plot the invariant h when it is calculated using Eq.(9.327) for the three particles. This is shown in Fig.9.3(f). In this figure, note that the small-amplitude synchrotron period is given by $2\pi/\cos^{-1}(1 - \frac{1}{2}k\alpha V) \approx 20$ turns. One observes that the invariance holds for small amplitude particles better.

Exercise 61 Show that, when $k\alpha V \ll 1$, the quadratic invariant (9.308) is consistent with Eq.(9.294) for small z and δ.

Exercise 62 For small μ, check that Eq.(9.327) agrees with Eq.(9.294) for small z and δ.

Exercise 63 (a) Consider the invariant (9.308) as the effective Hamiltonian. Derive and solve the effective one-turn equations of motion for z and δ. (b) Derive the equations of motion for the effective Hamiltonian (9.327).

---

[51] In Fig.9.3(a), we are not exploring chaotic motions. Had we looked in great detail in the phase space, there will be small regions where particle motion is chaotic. See Exercise 65.

Exercise 64 Find the Courant-Snyder parameters for the linear motion described by Eq.(9.305). Plot $\beta(s)$ and $\alpha(s)$ as functions of s around the accelerator.

Exercise 65 If one looks closely into Fig.9.3(a), one would notice that there are particles in the neighborhood of the third particle whose turn-to-turn trajectory behaves chaotically. To see this more clearly, consider a case with $V = 0.3$, $\alpha = 0.3$, and $k = 8$. We now have $k\alpha V = 0.72$, which is no longer $\ll 1$, and the series expansions may no longer converge, especially for particles very close to the unstable fixed points. Perform numerical tracking for a particle with initial conditions $(kz = 3.141, \delta = 0)$ to observe this chaotic trajectory.

Solution The portion of the trajectory between $kz = -4$ to $kz = 4$ is shown in Fig.9.4.
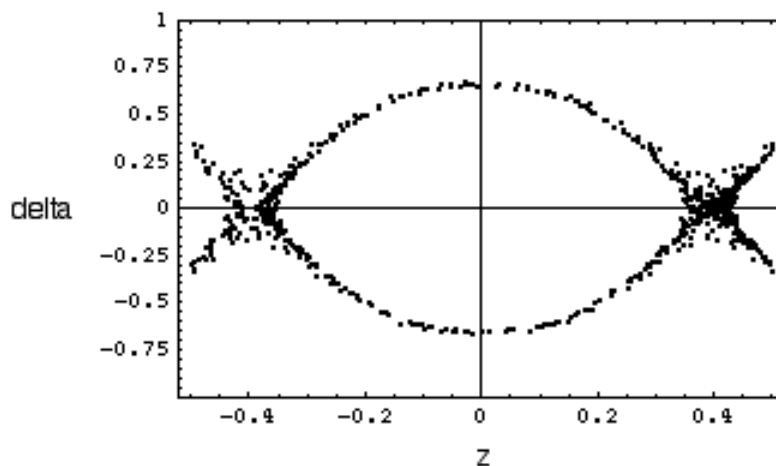
Figure 9.4: Tracking results showing chaos.

Exercise 66 Consider a 1-D motion of a particle going through an accelerator element which has a length L and is described by the equation of motion

$$x'' + \lambda \sin \alpha x = 0 \qquad (9.329)$$

(a) Find the Lie map that describes the motion of a particle through the element.

One may look for Taylor series approximations of this map in different forms. Each form is valid when a certain parameter is small.

(b) Find the Taylor map up to third order in L. [Error terms are $\mathcal{O}(L^4)$.] This expression is valid when the element is short.

(c) Find the Taylor map up to third order in X for arbitrary values

240

of L and λ. This expression holds when particles considered are close to the design orbit.

Solution (a)

$$M = \exp\left[: -\frac{L}{2}p^2 - \frac{\lambda L}{\alpha}(1 - \cos\alpha x):\right] \tag{9.330}$$

(b)

$$
\begin{aligned}
x &= x_0 + Lp_0 - \frac{1}{2}\lambda L^2 \sin\alpha x_0 - \frac{1}{6}\lambda\alpha L^3 p_0 \cos\alpha x_0 + \mathcal{O}(L^4) \\
p &= p_0 - \lambda L \sin\alpha x_0 - \frac{1}{2}\lambda\alpha L^2 p_0 \cos\alpha x_0 \\
&\quad + \frac{1}{6}\lambda\alpha L^3(\lambda\cos\alpha x_0 + \alpha p_0^2)\sin\alpha x_0 + \mathcal{O}(L^4) \tag{9.331}
\end{aligned}
$$

(c) To 4-th order in X, the map (9.330) can be written as

$$M = e^{:f_2:}\exp\left[\frac{L\lambda\alpha^3}{24}:\left(\int_0^1 du\, e^{-u:f_2:}x^4\right):\right] \tag{9.332}$$

where

$$f_2 = -\frac{L}{2}p^2 - \frac{L\lambda\alpha}{2}x^2 \tag{9.333}$$

describes the linearized motion. With

$$e^{-u:f_2:}\begin{bmatrix} x \\ p \end{bmatrix} = \begin{bmatrix} x\cos u\theta - \frac{p}{\sqrt{\lambda\alpha}}\sin u\theta \\ \sqrt{\lambda\alpha}x\sin u\theta + p\cos u\theta \end{bmatrix} \tag{9.334}$$

where $\theta = \sqrt{\lambda\alpha}L$ is the betatron phase advance if only the linear terms are kept, we have

$$
\begin{aligned}
M &= e^{:f_2:}\exp\left[\frac{L\lambda\alpha^3}{24}:\int_0^1 du\left(x\cos u\theta - \frac{p}{\sqrt{\lambda\alpha}}\sin u\theta\right)^4:\right] \\
&= e^{:f_2:}\exp\left[: \frac{\theta p^4}{768\lambda^2 L}(12\theta - 8\sin 2\theta + \sin 4\theta)\right. \\
&\quad + \frac{\alpha x p^3}{192\lambda}(-3 + 4\cos 2\theta - \cos 4\theta) \\
&\quad + \frac{\alpha\theta x^2 p^2}{128\lambda L}(4\theta - \sin 4\theta) + \frac{\alpha^2 x^3 p}{192}(-5 + 4\cos 2\theta + \cos 4\theta) \\
&\quad \left. + \frac{\theta\alpha^2 x^4}{768L}(12\theta + 8\sin 2\theta + \sin 4\theta) :\right] \tag{9.335}
\end{aligned}
$$

The 3rd order Taylor map is found to be

$$x = x_0\cos\theta + \frac{p_0}{\sqrt{\alpha\lambda}}\sin\theta + \frac{\alpha^2 x_0^3}{192}(\cos\theta - \cos 3\theta + 12\theta\sin\theta)$$

$$+\frac{\theta\alpha x_0^2 p_0}{64\lambda L}(-4\theta\cos\theta+7\sin\theta-\sin3\theta)$$

$$+\frac{\alpha x_0 p_0^2}{64\lambda}(-\cos\theta+\cos3\theta+4\theta\sin\theta)$$

$$+\frac{\theta p_0^3}{192\lambda^2 L}(-12\theta\cos\theta+9\sin\theta+\sin3\theta)$$

$$p = -x_0\sqrt{\alpha\lambda}\sin\theta+p_0\cos\theta+\frac{\theta\alpha^2 x_0^3}{192L}(12\theta\cos\theta+11\sin\theta+3\sin3\theta)$$

$$+\frac{\alpha^2 x_0^2 p_0}{64}(3\cos\theta-3\cos3\theta+4\theta\sin\theta)$$

$$+\frac{\theta\alpha x_0 p_0^2}{64\lambda L}(4\theta\cos\theta+5\sin\theta-3\sin3\theta)$$

$$+\frac{\alpha p_0^3}{64\lambda}(-\cos\theta+\cos3\theta+4\theta\sin\theta) \tag{9.336}$$

Equation (9.336) in the limit of small L and Eq.(9.331) in the limit of small x_0 and p_0 can be shown to be consistent.

9.6 Single Sextupole

The previous section considered the synchrotron motion of particles in an accelerator which contains a single nonlinear thin-lens element, i.e. a localized rf cavity. The rest of the accelerator is regarded as perfectly linear. A similar situation occurs in the transverse x- and y-dimensions. In this section, we will consider a single thin-lens sextupole in a circular accelerator whose beam dynamics is otherwise perfectly linear. One difference, however, is that in this section, we are dealing with a 2-D system (4-D phase space). We consider on-momentum particles, so the longitidinal motion is ignored.

The thin-lens sextupole has the map[52]

$$M_{\text{sext}} = e^{:-LH:} = \exp[:\lambda(x^3-3xy^2):] \tag{9.337}$$

where $\lambda=-\frac{1}{3}SL$ is the integrated strength of the thin-lens sextupole with S the quantity that appears in the Hamiltonian (9.182). To relate λ to the physical quantities, we have

$$\lambda = -\frac{1}{6}\frac{L}{B\rho}\frac{\partial^2 B_y}{\partial x^2} \tag{9.338}$$

The rest of the accelerator can be described by the map

$$M_{\text{acc}} = e^{:f_2:} \tag{9.339}$$

where

$$f_2 = -\frac{\mu_x}{2}(\gamma_x x^2+2\alpha_x x p_x+\beta_x p_x^2)-\frac{\mu_y}{2}(\gamma_y y^2+2\alpha_y y p_y+\beta_y p_y^2) \tag{9.340}$$

---

[52]One might compare Eq.(9.337) with Eq.(9.122), which applies when the y-motion is ignored. If a particle has $y=0$ and $y'=0$ initially, it will stay in the horizontal plane at all times. For those particles, ignoring y-motion, applying Eq.(9.122) is legitimate.

The quantities $\alpha_{x,y}$, $\beta_{x,y}$ and $\gamma_{x,y}$ are the unperturbed Courant-Snyder parameters evaluated at the position of the sextupole.

We will observe the motion of a particle at the exit end of the sextupole. The one-turn Lie map is

$$M_{\text{acc}}M_{\text{sext}} \tag{9.341}$$

Effective Hamiltonian away from resonances We now concatenate the two factor maps in Eq.(9.341) to become $\exp(:-CH_{\text{eff}}:)$, where C is the accelerator circumference, and the effective Hamiltonian H_{eff} is an invariant. To first order in the sextupole strength, we apply the BCH form (9.195) to obtain the expression of the invariant as

$$h = f_2 + \left(\frac{:f_2:}{1 - e^{-:f_2:}}\right)\lambda(x^3 - 3xy^2) + \mathcal{O}(\lambda^2) \tag{9.342}$$

The $\mathcal{O}(\lambda^2)$ terms in Eq.(9.342) are small for two reasons. First, they are of the order of λ^2, and are therefore small when the sextupole is weak. Second, These terms are also of order $(x, y)^4$, and are small near the origin of the phase space. In what follows, we will simply drop these terms.[53]

We learned in the previous section that, to evaluate (9.342), we need to find the eigenmodes of the operator $:f_2:$. To do so, we make two successive canonical transformations. The first is

$$\bar{x} = \frac{x}{\sqrt{\beta_x}}, \quad \bar{p}_x = \frac{\alpha_x x + \beta_x p_x}{\sqrt{\beta_x}} \tag{9.343}$$

or

$$x = \sqrt{\beta_x}\bar{x}, \quad p_x = \frac{-\alpha_x \bar{x} + \bar{p}_x}{\sqrt{\beta_x}} \tag{9.344}$$

and similar pairs of expressions with x replaced by y. The function f_2 becomes

$$f_2 = -\frac{\mu_x}{2}(\bar{x}^2 + \bar{p}_x^2) - \frac{\mu_y}{2}(\bar{y}^2 + \bar{p}_y^2) \tag{9.345}$$

The second transformation is

$$\bar{x} = \sqrt{2A_x}\sin\phi_x, \quad \bar{p}_x = \sqrt{2A_x}\cos\phi_x \tag{9.346}$$

and a similar pair of expressions with x replaced by y. Both transformations (9.343-9.344) and (9.346) are canonical. The new expression of f_2 is then

$$f_2 = -\mu_x A_x - \mu_y A_y \tag{9.347}$$

The eigenmodes of $:f_2:$ are, as we found in the previous section, $e^{in_x\phi_x + in_y\phi_y}$ with eigenvalues $in_x\mu_x + in_y\mu_y$. That is,

$$:f_2:A_x = 0, \quad :f_2:A_y = 0$$
$$:f_2:e^{in_x\phi_x + in_y\phi_y} = (in_x\mu_x + in_y\mu_y)e^{in_x\phi_x + in_y\phi_y} \tag{9.348}$$

---

[53]Be reminded that there are subtle nonlinear dynamics effects, such as higher order resonances and chaotic effects, that feed on these higher order terms. Dropping the higher order terms is daring, and must be done with caution.

We now have

$$
\left(\frac{:f_2:}{1 - e^{-:f_2:}} \right) \lambda (x^3 - 3xy^2) \tag{9.349}
$$

$$
= \lambda \left(\frac{:f_2:}{1 - e^{-:f_2:}} \right) [(2\beta_x A_x)^{3/2} \sin^3 \phi_x - 3(2\beta_x A_x)^{1/2}(2\beta_y A_y) \sin \phi_x \sin^2 \phi_y]
$$

We then note that

$$
\left(\frac{:f_2:}{1 - e^{-:f_2:}} \right) \sin^3 \phi_x
$$

$$
= \frac{i}{8} \left(\frac{:f_2:}{1 - e^{-:f_2:}} \right) (e^{i3\phi_x} - 3e^{i\phi_x} + 3e^{-i\phi_x} - e^{-i3\phi_x})
$$

$$
= \frac{i}{8} \left(\frac{i3\mu_x}{1 - e^{-i3\mu_x}} e^{i3\phi_x} - \frac{i3\mu_x}{1 - e^{-i\mu_x}} e^{i\phi_x} + \frac{-i3\mu_x}{1 - e^{i\mu_x}} e^{-i\phi_x} - \frac{-i3\mu_x}{1 - e^{i3\mu_x}} e^{-i3\phi_x} \right)
$$

$$
= -\frac{3}{8} \mu_x \left[\frac{\sin(3\phi_x + \frac{3\mu_x}{2})}{\sin \frac{3\mu_x}{2}} - \frac{\sin(\phi_x + \frac{\mu_x}{2})}{\sin \frac{\mu_x}{2}} \right] \tag{9.350}
$$

and that

$$
\left(\frac{:f_2:}{1 - e^{-:f_2:}} \right) \sin \phi_x \sin^2 \phi_y
$$

$$
= \frac{i}{8} \left(\frac{:f_2:}{1 - e^{-:f_2:}} \right) (e^{i\phi_x + i2\phi_y} - 2e^{i\phi_x} + e^{i\phi_x - i2\phi_y}
$$

$$
- e^{-i\phi_x + i2\phi_y} + 2e^{-i\phi_x} - e^{-i\phi_x - i2\phi_y})
$$

$$
= -\frac{1}{8}(\mu_x + 2\mu_y) \frac{\sin(\phi_x + 2\phi_y + \frac{\mu_x}{2} + \mu_y)}{\sin(\frac{\mu_x}{2} + \mu_y)} + \frac{1}{4}\mu_x \frac{\sin(\phi_x + \frac{\mu_x}{2})}{\sin \frac{\mu_x}{2}}
$$

$$
- \frac{1}{8}(\mu_x - 2\mu_y) \frac{\sin(\phi_x - 2\phi_y + \frac{\mu_x}{2} - \mu_y)}{\sin(\frac{\mu_x}{2} - \mu_y)} \tag{9.351}
$$

Substituting Eqs.(9.349-9.351) into (9.342) gives an expression of the effective Hamiltonian to first order in λ,

$$
h = -\mu_x A_x - \mu_y A_y - \frac{3}{8} \lambda \mu_x (2\beta_x A_x)^{3/2} \left[\frac{\sin(3\phi_x + \frac{3\mu_x}{2})}{\sin \frac{3\mu_x}{2}} - \frac{\sin(\phi_x + \frac{\mu_x}{2})}{\sin \frac{\mu_x}{2}} \right]
$$

$$
- 3\lambda (2\beta_x A_x)^{1/2}(2\beta_y A_y) \left[-\frac{1}{8}(\mu_x + 2\mu_y) \frac{\sin(\phi_x + 2\phi_y + \frac{\mu_x}{2} + \mu_y)}{\sin(\frac{\mu_x}{2} + \mu_y)} \right.
$$

$$
\left. + \frac{1}{4}\mu_x \frac{\sin(\phi_x + \frac{\mu_x}{2})}{\sin \frac{\mu_x}{2}} - \frac{1}{8}(\mu_x - 2\mu_y) \frac{\sin(\phi_x - 2\phi_y + \frac{\mu_x}{2} - \mu_y)}{\sin(\frac{\mu_x}{2} - \mu_y)} \right] \tag{9.352}
$$

Resonances   Note the expression (9.352) contains divergences when one of the following *resonance conditions* is satisfied:

$$
\nu_x = \text{integer}
$$

$$3\nu_x = \text{integer}$$
$$\nu_x + 2\nu_y = \text{integer}$$
$$\nu_x - 2\nu_y = \text{integer} \tag{9.353}$$

where we have defined the tunes

$$\nu_{x,y} = \frac{\mu_{x,y}}{2\pi} \tag{9.354}$$

Away from resonances (9.353), Eq.(9.352) gives the expression of the invariant. Near resonances, the above analysis leading to Eq.(9.352) breaks down. We need to treat the problem differently, which we will do momentarily.

Note also that had we kept some higher order terms in λ, we would have found terms that diverge at higher order resonances. For example, had we kept a term of order X^4, the expression for h would contain a term of the type

$$\left(\frac{:f_2:}{1 - e^{-:f_2:}} \right) \sin 4\phi_x \tag{9.355}$$

which diverges when $\nu_x = \frac{1}{4} \times$integer. When dropping these higher order terms in Eqs.(9.342) and (9.352), therefore, we have inadvertantly dropped effects of higher order resonances. This is of course quite serious. As a result, if one is interested in knowing the effect of a higher order resonance, it is necessary to keep terms of sufficiently high order for the resonance of interest. Even worse, the question arises as to whether the expansion converges at all since there is always some high order resonance of interest even if μ_x and μ_y are irrational numbers. We will not pursue these subtleties however, assuming that the higher order resonances are sufficiently weak to be ignored.

Invariant near a single resonance To proceed, we now consider a 1-D case. This can be obtained by considering only those particles with no y-motion $(y = 0, y' = 0)$ in the 2-D case. We will further drop the subscripts x. The one-turn map then becomes

$$e^{:-\mu A:} e^{:\lambda x^3:} \tag{9.356}$$

The invariant, to first order in λ and away from resonances, is

$$h = -\mu A + \left(\frac{:-\mu A:}{1 - e^{:\mu A:}} \right) \lambda x^3$$

$$= -\mu A - \frac{3}{8} \mu \lambda (2\beta A)^{3/2} \left[\frac{\sin(3\phi + \frac{3\mu}{2})}{\sin \frac{3\mu}{2}} - \frac{\sin(\phi + \frac{\mu}{2})}{\sin \frac{\mu}{2}} \right] \tag{9.357}$$

The effective Hamiltonian is of course given by $H_{\text{eff}} = -h/C$. Equation (9.357) is just Eq.(9.352) when $A_y = 0$.

Particles move in the phase space along contours of constant h. To study the phase space topology, let us go from the (ϕ, A) back to the $(\bar{x}, \bar{p})$ coordinates according to Eq.(9.346). Then Eq.(9.357) becomes

$$h = -\frac{\mu}{2}(\bar{x}^2 + \bar{p}^2) - \frac{3}{8}\mu\lambda\beta^{3/2}\bar{x}[(3\bar{p}^2 - \bar{x}^2)\cot\frac{3\mu}{2} - (\bar{x}^2 + \bar{p}^2)\cot\frac{\mu}{2} - 4\bar{x}\bar{p}] \tag{9.358}$$

Figure 9.5 shows these contours in the $(\bar{x}, \bar{p})$ space for the case with $\nu = \mu/2\pi = 0.17$ and $\frac{3}{8}\lambda\beta^{3/2} = 0.1$. The four contours correspond to $-h/\mu = 0.0137, 0.0515, 0.109,$ and 0.180. As seen in Fig.9.5, a small-amplitude particle traces out a circular contour in phase space. As the amplitude increases, the countour distorts from a circle.
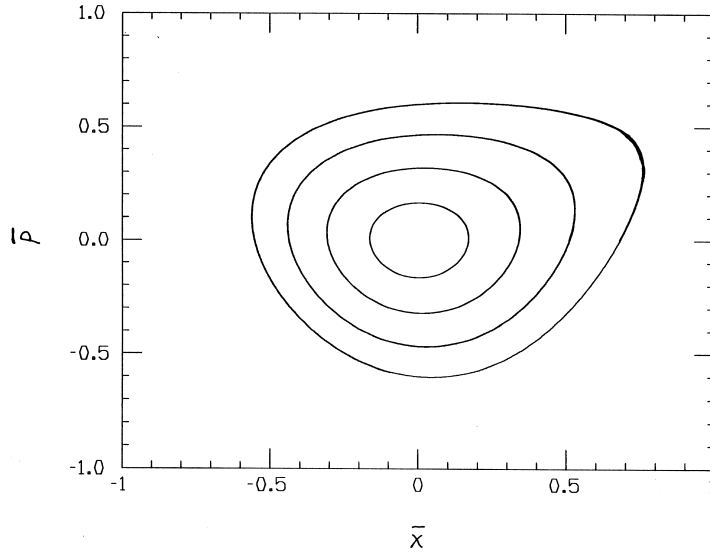
Figure 9.5: Phase space contour plots with a sextupole perturbation, away from resonances.

The invariance of (9.357), and therefore the validity of Fig.9.5, requires ν and 3ν to be away from an integer, i.e., away from resonances. To illustrate how to deal with the situation when there is a resonance near by, consider the case when

$$\nu \approx \frac{p}{3} \tag{9.359}$$

where p is some integer. Let d be the distance of ν from the resonance with

$$\nu = \frac{p+d}{3}, \qquad |d| \ll 1 \tag{9.360}$$

The trick of treating the case near a resonance (9.359) is to observe the system every 3 turns instead of every turn as we have been doing. The motion of particles, when observed every 3 turns, will appear to move slowly. And it is this slow (strobing) motion that we will study. Thus, the 3-turn map is

$$
\begin{aligned}
M^3 &= (e^{:-\mu A:} e^{:\lambda x^3:})^3 \\
&= e^{:-\mu A:} e^{:\lambda x^3:} e^{:-\mu A:} e^{:\lambda x^3:} e^{:-\mu A:} e^{:\lambda x^3:}
\end{aligned}
$$

246

$$
\begin{aligned}
&= e^{:-3\mu A:}e^{:2\mu A:}e^{:\lambda x^3:}e^{:-2\mu A:}e^{:\mu A:}e^{:\lambda x^3:}e^{:-\mu A:}e^{:\lambda x^3:} \\
&= e^{:-3\mu A:}\exp(:e^{:2\mu A:}\lambda x^3:)\exp(:e^{:\mu A:}\lambda x^3:)e^{:\lambda x^3:} \quad (9.361)
\end{aligned}
$$

The first operator $e^{:-3\mu A:}$ in the last line of Eq.(9.361) takes on a different form near the resonance. In fact, this is where the strobing is taking place, i.e.

$$
e^{:-3\mu A:} = e^{:-6\pi\nu A:} = e^{:-2\pi dA:} \quad (9.362)
$$

where the last step is because

$$
e^{:2\pi m A:} = 1 \quad (9.363)
$$

identically for any integer m. The remaining three right-most operators in Eq.(9.361) can be combined to first order in λ easily,

$$
\begin{aligned}
&\exp(:e^{:2\mu A:}\lambda x^3:)\exp(:e^{:\mu A:}\lambda x^3:)e^{:\lambda x^3:} \\
&= \exp[:(e^{:2\mu A:} + e^{:\mu A:} + 1)\lambda x^3 + \mathcal{O}(\lambda^2):] \\
&= \exp\left[:\left(\frac{1 - e^{:3\mu A:}}{1 - e^{:\mu A:}}\right)\lambda x^3 + \mathcal{O}(\lambda^2):\right] \\
&= \exp\left[:\left(\frac{1 - e^{:2\pi dA:}}{1 - e^{:\mu A:}}\right)\lambda x^3 + \mathcal{O}(\lambda^2):\right] \quad (9.364)
\end{aligned}
$$

We then apply the BCH formula to obtain

$$
M^3 = e^{:3h:} \quad (9.365)
$$

where $3h$ is a new expression of the invariant near the resonance (9.359) and is given by

$$
\begin{aligned}
3h &= -2\pi dA + \left(\frac{:-2\pi dA:}{1 - e^{:2\pi dA:}}\right)\left(\frac{1 - e^{:2\pi dA:}}{1 - e^{:\mu A:}}\right)\lambda x^3 \\
&= -2\pi dA + \left(\frac{:-2\pi dA:}{1 - e^{:\mu A:}}\right)\lambda x^3 \quad (9.366)
\end{aligned}
$$

This leads to

$$
h = -\frac{2\pi}{3}dA - \frac{\pi}{12}d\lambda(2A)^{3/2}\left[\frac{\sin(3\phi + \frac{3\mu}{2})}{\sin\frac{3\mu}{2}} - \frac{\sin(\phi + \frac{\mu}{2})}{\sin\frac{\mu}{2}}\right] \quad (9.367)
$$

The expression (9.367) is well-behaved near the resonance as $d \to 0$. Interestingly, it is very similar to the result obtained by the one-turn map, provided one pretends that μ in the one-turn map can be replaced by $2\pi d/3$, the frequency after strobing. To see this, let us consider the invariant (9.357), which was obtained assuming no proximity to resonances. If we insist on applying this invariant even near a 3-rd order resonance $\nu \approx 1/3$, we may keep only the $\sin(3\mu/2)$ term in Eq.(9.357), i.e.

$$
h \approx -\mu A - \frac{3}{8}\mu\lambda(2\beta A)^{3/2}\frac{\sin(\frac{3\mu}{2} + 3\phi)}{\sin\frac{3\mu}{2}} \quad (9.368)
$$

247

Multiplying h by the factor $2\pi d/(3\mu)$ is still an invariant. Thus we write

$$h \approx -\frac{2\pi}{3}dA - \frac{\pi}{4}d\lambda(2\beta A)^{3/2}\frac{\sin(\frac{3\mu}{2} + 3\phi)}{\sin\frac{3\mu}{2}} \tag{9.369}$$

We further note that

$$\sin\frac{3\mu}{2} = -\sin(\pi d) \approx -\pi d$$

$$\sin(\frac{3\mu}{2} + 3\phi) \approx -\sin 3\phi$$

The invariant then becomes

$$h \approx -\frac{2\pi}{3}dA - \frac{1}{\sqrt{2}}\lambda(\beta A)^{3/2}\sin 3\phi \tag{9.370}$$

which is the same as Eq.(9.367) when $d \to 0$.

We can now study the phase space topology. Again make the transformation to the Cartesian coordinates by Eq.(9.346),[54]

$$h \approx -\frac{\pi}{3}d(\bar{x}^2 + \bar{p}^2) - \frac{1}{4}\lambda\beta^{3/2}\bar{x}(3\bar{p}^2 - \bar{x}^2) \tag{9.371}$$

Because the invariant (9.371) has the significance of being the effective Hamiltonian, it gives the fixed points[55] according to

$$\frac{\partial h}{\partial \bar{x}} = -\frac{2\pi}{3}d\bar{x} - \frac{1}{4}\lambda\beta^{3/2}(3\bar{p}^2 - 3\bar{x}^2) = 0$$

$$\frac{\partial h}{\partial \bar{p}} = -\frac{2\pi}{3}d\bar{p} - \frac{1}{4}\lambda\beta^{3/2}6\bar{x}\bar{p} = 0 \tag{9.372}$$

There are four fixed points corresponding to the four solutions to Eq.(9.372). One of them is the origin $(\bar{x}, \bar{p}) = (0, 0)$. The other three are

$$(\bar{x}, \bar{p}) = \begin{cases} (\epsilon, 0) \\ (-\frac{1}{2}\epsilon, \frac{\sqrt{3}}{2}\epsilon) \\ (-\frac{1}{2}\epsilon, -\frac{\sqrt{3}}{2}\epsilon) \end{cases} \tag{9.373}$$

where we have introduced a new parameter

$$\epsilon = \frac{8\pi d}{9\lambda\beta^{3/2}} \tag{9.374}$$

At the three fixed points (9.373), the value of h is given by

$$h = -\frac{\pi}{9}d\epsilon^2 \tag{9.375}$$

---

[54]Note in this case, however, $\bar{x}$ and $\bar{p}$ are not related to the original x and p by Eq.(9.343) because of the strobing.

[55]Fixed points are special points in phase space. A particle located at a fixed point will stay there turn after turn.

Particles move in the phase space along contours of constant Hamiltonian h. The constant-h contour that goes through the fixed points are called the *separatrix*. To find the separatrix, we set h of Eq.(9.371) to be equal to (9.375). This gives

$$(\bar{x} + \frac{1}{2}\epsilon)(\bar{x} - \epsilon + \sqrt{3}\bar{p})(\bar{x} - \epsilon - \sqrt{3}\bar{p}) = 0 \qquad (9.376)$$

The separatrix of the system (9.371), therefore, consists of three straight lines, as shown in Fig.9.6(a).

Comparing Fig.9.6, the phase space contours near resonance, with Fig.9.5, the contours away from resonances, one notes that the contours near resonances are more or less triangular in shape, while the contours away from resonances are more approximately like circles.

In Fig.9.6(a), the dashed straight lines are the separatrices in the $(\bar{x}, \bar{p})$ phase space for the case $\epsilon = 0.5$. The three intersection points are the fixed points (9.373). The solid curves are the constant-h contours. The numerical values next to each curve give the value of $\xi = -8h/3\lambda\beta^{3/2}$. The value of ξ on the separatrices is $\xi = \epsilon^3/3 = 0.0417$.

The topology depends on the parameter ϵ, i.e. the ratio of distance to resonance d to the sextupole strength λ. The topology for the case $\epsilon = -0.5$ is given by the mirror reflection of Fig.9.6(a) with respect to the vertical $\bar{x} = 0$ line. Right on resonance, when $\epsilon = 0$, the phase space looks like Fig.9.6(b). The three fixed points and the origin coincide. Values of ξ are again indicated for each branch of curves. Exactly on resonance, there is no region in the phase space that provides stable motion for the particles. When away from resonances or when the sextupole strength vanishes, $\epsilon = \infty$, we have the unperturbed case where the topology consists of concentric circles.

Invariant away from resonances   We now return to the 2-D case starting with the effective invariant (9.352) away from resonances. The effective Hamiltonian is of course one of the invariants. We first rewrite it as

$$h = -\mu_x W_x - \mu_y W_y \qquad (9.377)$$

where

$$
\begin{aligned}
W_x &= A_x + \frac{3}{8}\lambda(2\beta_x A_x)^{3/2}\left[\frac{\sin(3\phi_x + \frac{3\mu_x}{2})}{\sin\frac{3\mu_x}{2}} - \frac{\sin(\phi_x + \frac{\mu_x}{2})}{\sin\frac{\mu_x}{2}}\right] \\
&\quad + \frac{3}{8}\lambda(2\beta_x A_x)^{1/2}(2\beta_y A_y)\left[-\frac{\sin(\phi_x + 2\phi_y + \frac{\mu_x}{2} + \mu_y)}{\sin(\frac{\mu_x}{2} + \mu_y)}\right. \\
&\quad \left. +2\frac{\sin(\phi_x + \frac{\mu_x}{2})}{\sin\frac{\mu_x}{2}} - \frac{\sin(\phi_x - 2\phi_y + \frac{\mu_x}{2} - \mu_y)}{\sin(\frac{\mu_x}{2} - \mu_y)}\right] \\
W_y &= A_y + \frac{3}{4}\lambda(2\beta_x A_x)^{1/2}(2\beta_y A_y)\left[-\frac{\sin(\phi_x + 2\phi_y + \frac{1}{2}\mu_x + \mu_y)}{\sin(\frac{\mu_x}{2} + \mu_y)}\right. \\
&\quad \left. +\frac{\sin(\phi_x - 2\phi_y + \frac{\mu_x}{2} - \mu_y)}{\sin(\frac{\mu_x}{2} - \mu_y)}\right] \qquad (9.378)
\end{aligned}
$$
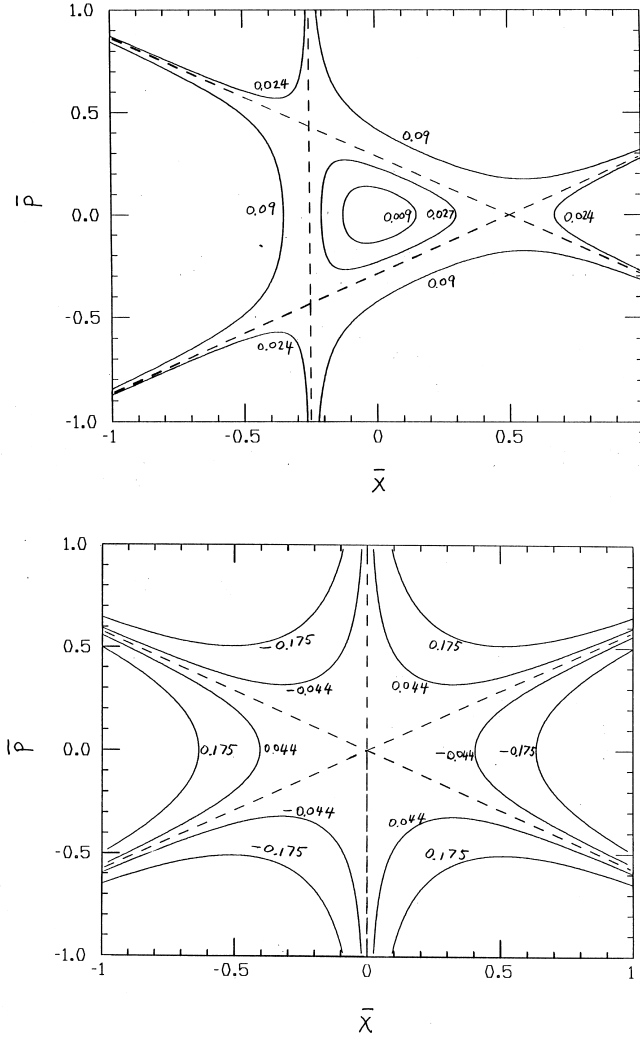
Figure 9.6: Phase space countor plots (a) Top figure: near a third order resonance, (b) Bottom figure: exactly on resonance.

We then make the physical observation that if we make the artificial replacements

$$\mu_x \to \mu_x + 2\pi n_x \quad \text{and} \quad \mu_y \to \mu_y + 2\pi n_y \tag{9.379}$$

for arbitrary integers of $n_{x,y}$, the quantity h in Eq.(9.377) must still be an invariant. This is because the sextupole is located at a fixed location, and it will not know the integer part of the x- and y-tunes. Since the expressions of

250

W_x and W_y in Eq.(9.378) are unchanged by the replacements (9.379), the only way for h to be an invariant is that W_x and W_y are *separately* invariants by their own. That is, there are actually two invariants W_x and W_y, instead of only one invariant h. The important difference between $W_{x,y}$ and h, however, is that h maintains the unique physical meaning of the effective Hamiltonian of the system.

One may try to apply this argument to the 1-D case, but that does not lead to any information of new invariants. The quantity h in 1-D case contains a multiplicative factor μ, which can be simply scaled away, as we did in the step from (9.368) to (9.369).

One can actually prove the invariance of W_x and W_y using the fact that h is the effective Hamiltonian. One first note that the rates of change of W_x per turn is given by

$$\frac{dW_x}{dn} = \frac{\partial W_x}{\partial A_x}\frac{dA_x}{dn} + \frac{\partial W_x}{\partial A_y}\frac{dA_y}{dn} + \frac{\partial W_x}{\partial \phi_x}\frac{d\phi_x}{dn} + \frac{\partial W_x}{\partial \phi_y}\frac{d\phi_y}{dn} \tag{9.380}$$

and a similar expression for dW_y/dn. It then follows straightforwardly from

$$\frac{dA_x}{dn} = \frac{\partial h}{\partial \phi_x}, \qquad \frac{d\phi_x}{dn} = -\frac{\partial h}{\partial A_x}$$
$$\frac{dA_y}{dn} = \frac{\partial h}{\partial \phi_y}, \qquad \frac{d\phi_y}{dn} = -\frac{\partial h}{\partial A_y} \tag{9.381}$$

and the expression of h that $dW_x/dn = dW_y/dn = 0$, i.e., W_x and W_y are invariants.

We will return to the topic of single sextupoles later after we introduce the normal form technique. We will discuss the case of a general distribution of sextupoles. The study of strategically arranged distributions of sextupoles will also be discussed under the subject of achromats.

Exercise 67 Figure 9.5 gives the trajectories of particles when Eq.(9.358) is the effective Hamiltonian. Write a numerical tracking program for the exact system (9.341). Compare the results with those shown in Fig.9.5.

Exercise 68 We worked out an expression of invariant W_3 in Eq.(9.44). Show that it agrees with the invariant h of Eq.(9.358).
Solution Away from resonances, Eqs.(9.358) and (9.44) are identical if one notes $\epsilon = 3\lambda\beta^{3/2}$, and the trigonometric identities

$$\cot\frac{3\mu}{2} + \cot\frac{\mu}{2} = \frac{4sc}{(1+2c)(1-c)}$$
$$3\cot\frac{3\mu}{2} - \cot\frac{\mu}{2} = -\frac{4s}{1+2c} \tag{9.382}$$

where $c = \cos\mu$ and $s = \sin\mu$.

Exercise 69 Equations (9.371-9.374) studied the phase space topology in the Cartesian coordinates. One can do the same in the polar coordinates (ϕ, A) also. Show that the fixed points determined by $\partial h/\partial A = 0$ and $\partial h/\partial \phi = 0$ are indeed given by Eq.(9.373).
Solution Take the case $\epsilon > 0$ for example. The solutions are given by $A = \epsilon^2/4$ and $\phi = 90°, 210°, 330°$.

Exercise 70 Consider the Taylor map (9.43). Find the fixed points in the (x, p) space. What is the connection, if any, between these fixed points and the fixed points found using the effective Hamiltonian (9.358)?
Solution To be a fixed point for the map (9.43), it is necessary that

$$
\begin{aligned}
x &= x \cos \mu + p \sin \mu \\
p &= -x \sin \mu + p \cos \mu + \epsilon x^2
\end{aligned}
\tag{9.383}
$$

There are two solutions of (9.383). One is the trivial case of the origin. The other is located at

$$
x = \frac{2}{\epsilon} \tan \frac{\mu}{2}, \quad p = \frac{2}{\epsilon} \tan^2 \frac{\mu}{2}
\tag{9.384}
$$

The fixed point (9.384) is not a fixed point for Eq.(9.358). The fixed point in Fig.9.5 for example is located at $(x, p) = (0.95, 0.56)$ while Eq.(9.384) gives $(1.48, 0.87)$ using the same parameters.

Exercise 71 Verify the invariance of W_x and W_y in Eq.(9.378) by carrying out the steps (9.380-9.381).

Exercise 72 Consider a thin-lens octupole in an otherwise perfectly linear optics of a circular accelerator. Condiser 1-D motion. The Lie map is $e^{:f_2:}e^{:\lambda x^4:}$. Find the effective Hamiltonian to first order in λ. First do this away from resonances. Then repeat close to a resonance $\nu_x \approx 1/4$.

Exercise 73 Extend the calculation in the text to find an expression of the effective Hamiltonian for a single sextupole to second order in the sextupole strength. Do this for the 1-D case. Results obtained in Exercises 72 and 73 can be used to calculate the tune shift with betatron amplitude, as will be described in a later section.

9.7 Distribution of Multipoles

In the last section, we considered the effects of a single sextupole in an otherwise perfectly linear accelerator. In this section, we will consider the effects of a distribution of multipoles. Sextupoles are of course a special case of multipoles. The special topic of achromats — special distribution of multipoles that minimizes optical abberrations — will be postponed to a later section.

Element maps and one-turn map As illustrated in Fig.9.2, an accelerator elements of piecewise sections, each given by a constant Hamiltonian. Let the i-th element have Hamiltonian H_i and length L_i, then we have the total Lie map M_{tot} of the accelerator given by Eq.(9.189), where N is the total number of elements in the accelerator. For a circular accelerator, this total map gives the one-turn map around the accelerator.

In case there is a distribution of nonlinear elements around the accelerator, these Hamiltonians H_i are in general nonlinear. One way to proceed (done in program MARYLIE, for example) is as follows. First, for each element, the Hamiltonian H_i is Taylor expanded as

$$H_i = H_{2i} + H_{3i} + H_{4i} + ... \tag{9.385}$$

where H_{ki} contains terms k-th order in the components of the dynamic variable X. The leading order is taken to be quadratic in X. If H_i contains only second order terms, i.e. if $H_i = H_{2i}$, we have a linear element. We regard the nonlinear terms to be small, which would be the case if we restrict our attention to phase space regions close to the origin. We will consider Hamiltonians up to $(\Omega + 1)$-th order in X. This means maps are considered up to the Ω-th order. Higher order terms are ignored. The analysis below applies exactly for Hamiltonians quadratic in X, but represents a perturbation analysis as far as the higher order terms are concerned.

Having made the Taylor expansion (9.385), the map of the i-th element reads

$$e^{-:L_i H_i:} = e^{-:L_i[H_{2i} + H_{3i} + ... + H_{(\Omega+1)i}]:} \tag{9.386}$$

The BCH formula can be applied to factorize (9.386) to become

$$e^{-:L_i H_i:} = e^{:f_{2i}:} e^{:f_{3i}:} ... e^{:f_{(\Omega+1)i}:} \tag{9.387}$$

where the function f_{ki} is a k-th order homogeneous polynomial in the components of X. Knowing $H_{2i}, ..., H_{(\Omega+1)i}$, we are looking for expressions for $f_{2i}, ..., f_{(\Omega+1)i}$. The expression for f_{2i} is simply

$$f_{2i} = -L_i H_{2i} \tag{9.388}$$

The next order term f_{3i} follows from Eq.(9.198),

$$f_{3i} = -L_i \int_0^1 du \, e^{:u L_i H_{2i}:} H_{3i} \tag{9.389}$$

The reader is reminded of Eq.(9.120), which gives f_3 when the Taylor map is known. The higher order factors can be obtained by iteration.[8] For example,

$$\begin{aligned} f_4 &= -L_i \int_0^1 du \, e^{:u L_i H_{2i}:} H_{4i} \\ &\quad -\frac{L_i^2}{2} \int_0^1 du \int_0^u dv \, [e^{:v L_i H_{2i}:} H_{3i}, e^{:u L_i H_{2i}:} H_{3i}] \end{aligned} \tag{9.390}$$

Exercise 74 illustrates the procedure of Eqs.(9.387-9.390) by a simple example. Derivation of Eq.(9.390) is given in Exercise 75.

Having obtained the maps of all individual elements in the form (9.387), the total map M_{tot} is expressed as a long string of factor maps. A procedure is followed using the BCH formula to commute the factor maps in M_{tot} in such a way that at the end of the procedure it reads

$$M_{\text{tot}} = e^{:f_2:}e^{:f_3:}...e^{:f_{\Omega+1}:} \qquad (9.391)$$

where again f_k is a k-th order homogeneous polynomial in X. The Courant-Snyder linear one-turn map is just $e^{:f_2:}$. In fact, f_2 is the Courant-Snyder invariant as given by Eq.(9.89).

After M_{tot} has been obtained in the form of Eq.(9.391), the BCH formula can be applied to concatenate all the factors into a single factor,

$$M_{\text{tot}} = e^{:F:} \qquad (9.392)$$

where F is related to the effective Hamiltonian, as was mentioned in Eq.(9.190), by $F = -CH_{\text{eff}}$. This is in fact how the effective Hamiltonian can be obtained explicitly as a Taylor series expansion in X. The quantity F obtained this way is an $(\Omega+1)$-th order Taylor series in X. It is an invariant because (see Exercise 21)

$$M_{\text{tot}}F = F \qquad (9.393)$$

i.e. the value of F does not change by the application of the one-turn map. The leading (quadratic) terms of F is the Courant-Snyder invariant.

The effective Hamiltonian, once obtained, contains a wealth of analytical information on the nonlinear dynamics of the accelerator system. In fact, the procedure described here is a natural way to generalize the Courant-Snyder analysis to a nonlinear system. This point we will elaborate more later.

Particle tracking using Lie maps In passing, Lie maps can also be used for numerical particle tracking. When doing so, it is often necessary to make sure the numerical application keeps the symplecticity of the map. For example, one may consider applying the one-turn map (9.392) for particle tracking. One notes first that F, being truncated to become an $(\Omega+1)$-th order Taylor series, is only an approximate expression; nevertheless, the map (9.392) remains exactly symplectic. One would then attempt to compute

$$(X_j)_{\text{final}} = e^{:F:}X_j\Big|_{X=X_{\text{initial}}} \qquad (9.394)$$

where X_j represents the j-th component of X, and one needs to compute (9.394) for all the components. To do that, one expands the exponential operator into an infinite series,

$$(X_j)_{\text{final}} = \sum_{n=0}^{\infty} \frac{1}{n!}:F:^n X_j\Big|_{X=X_{\text{initial}}} \qquad (9.395)$$

Each of the terms in Eq.(9.395) can be evaluated exactly. This is because F is a Taylor series that terminates. Application of a finite power of :F: on X is therefore a terminated Taylor series, which can be evaluated exactly. However, the series (9.395) is an infinite series. To perform numerical tracking, it is necessary to truncate it to a certain order. This truncation, unlike the one that truncates F to $(\Omega + 1)$-th order, is in general nonsymplectic, and must be done at a sufficiently high order that the nonsymplecticity introduced is negligible numerically.

This inconvenience of having to check symplecticity numerically for tracking can be avoided in several ways. As an illustration, we will mention one way as follows. Instead of tracking with (9.392) or (9.391), one could factorize the map as

$$M_{\text{tot}} = \text{product of } (e^{:\text{monomial}:}) \tag{9.396}$$

Each factor in Eq.(9.396) is a Lie map whose exponent contains a single monomial term in X. The highest order monomial in the representation (9.396) is $(\Omega + 1)$-th order. The number of factors in (9.396) is therefore finite. If all factors in Eq.(9.396) are concatenated into one exponential map, and the exponent is truncated to $(\Omega + 1)$-th order, one re-obtains (9.392). But the form (9.396) now allows exactly symplectic tracking because one can now apply the exact formulae (9.128). The price to pay is that there is a large number of factors in Eq.(9.396) if a high order map is required, which slows down the tracking program.

Concatenating two nonlinear maps We have thus described how a one-turn Lie map can be obtained once the accelerator design is given, and how the one-turn Lie map might be used for particle tracking. To illustrate the concatenation procedure more explicitly, consider the following. Suppose we are interested in a 3-rd order map ($\Omega = 3$), and we have two element-maps which have been factorized into the form (9.387), i.e. we have

$$e^{:f:} = e^{:f_2:}e^{:f_3:}e^{:f_4:} \quad \text{and} \quad e^{:g:} = e^{:g_2:}e^{:g_3:}e^{:g_4:} \tag{9.397}$$

Our job is to concatenate these two maps into the form (9.391). To do so, let us write the total map as

$$e^{:h:} = e^{:f:}e^{:g:} \tag{9.398}$$

We then note that

$$
\begin{aligned}
e^{:h:} &= e^{:f_2:}e^{:f_3:}e^{:f_4:}e^{:g_2:}e^{:g_3:}e^{:g_4:} \\
&= [e^{:f_2:}e^{:g_2:}][e^{-:g_2:}e^{:f_3:}e^{:g_2:}][e^{-:g_2:}e^{:f_4:}e^{:g_2:}]e^{:g_3:}e^{:g_4:} \tag{9.399}
\end{aligned}
$$

The idea of the second line is to commute the lower order maps to the left of the expression. The first pair of square brackets describes the linear map of the combined map, i.e.

$$e^{:f_2:}e^{:g_2:} = e^{:h_2:} \tag{9.400}$$

where the second order h_2 is such that the matrix relation [see Eqs.(9.92-9.93)]

$$e^{SH} = e^{SG}e^{SF} \tag{9.401}$$

holds, where the symmetric matrices F, G and H are related to f_2, g_2 and h_2 by $f_2 = -\frac{1}{2}\tilde{X}FX$, etc.

The second pair of square brackets in Eq.(9.399) can be written as

$$e^{-:g_2:}e^{:f_3:}e^{:g_2:} = \exp\left(:e^{-:g_2:}f_3:\right) = \exp\left[:f_3(e^{-:g_2:}X):\right] = \exp\left[:f_3(e^{-SG}X):\right]$$

i.e. it is a second order map described by $e^{:f_3:}$, except that the arguments of f_3 are transformed from the old coordinates X to the new coordinates according to $e^{:-g_2:}$.

Similarly, maps in the third pair of square brackes in Eq.(9.399) can be combined into

$$\exp\left[:f_4(e^{-SG}X):\right]$$

We therefore have

$$
\begin{aligned}
e^{:h:} &= e^{:h_2:}\exp\left(:f_3(e^{-SG}X):\right)\exp\left(:f_4(e^{-SG}X):\right)e^{:g_3:}e^{:g_4:} \tag{9.402} \\
&= e^{:h_2:}\left[\exp\left(:f_3(e^{-SG}X):\right)e^{:g_3:}\right]\left[e^{-:g_3:}\exp\left(:f_4(e^{-SG}X):\right)e^{:g_3:}\right]e^{:g_4:}
\end{aligned}
$$

The two maps in the first pair of square brackets of Eq.(9.402) are both second order. They can be concatenated to read

$$\exp\left(:f_3(e^{-SG}X):\right)e^{:g_3:} = \exp\left(:f_3(e^{-SG}X)+g_3+\frac{1}{2}[f_3(e^{-SG}X),g_3] + \mathcal{O}(X^5):\right)$$

$$= \exp\left(:f_3(e^{-SG}X) + g_3:\right)\exp\left(:\frac{1}{2}[f_3(e^{-SG}X),g_3]:\right)$$

where the brackets in the last two lines are the Poisson brackets. The term represented by the Poisson brackets is 4-th order in X. Terms higher ordered than 5-th are dropped in the last line. The second pair of square brackets in Eq.(9.402), to 4-th oder in X, is simply

$$
\begin{aligned}
e^{-:g_3:}\exp\left(:f_4(e^{-SG}X):\right)e^{:g_3:} &= \exp\left(:e^{-:g_3:}f_4(e^{-SG}X):\right) \\
&= \exp\left(:f_4(e^{-SG}X) + \mathcal{O}(X^5):\right)
\end{aligned}
$$

Combining the results so far gives

$$e^{:h:} = e^{:h_2:}\exp\left(:f_3(e^{-SG}X)+g_3:\right)\exp\left(:\frac{1}{2}[f_3(e^{-SG}X),g_3]:\right)\exp\left(:f_4(e^{-SG}X):\right)e^{:g_4:} \tag{9.403}$$

If we then write

$$e^{:h:} = e^{:h_2:}e^{:h_3:}e^{:h_4:} \tag{9.404}$$

then we have the explicit final results

$$
\begin{aligned}
h_3 &= f_3(e^{-SG}X) + g_3 \\
h_4 &= \frac{1}{2}[f_3(e^{-SG}X),g_3] + f_4(e^{-SG}X) + g_4 \tag{9.405}
\end{aligned}
$$

A perturbation theory As another illustration, we will develop a particular perturbation theory. Consider the dynamical system described by

$$X' = -:H:X \qquad (9.406)$$

where a prime means derivative with respect to s, and $H(X, s)$ is the Hamiltonian of the system. Let the map that describes the evolution of X be designated formally as M, so that

$$X(s) = MX(0) \qquad (9.407)$$

and

$$f(X(s)) = Mf(X(0)) \qquad (9.408)$$

for any function f of X. The map M is a function of s. We have, by substituting Eq.(9.407) into Eq.(9.406), that

$$
\begin{aligned}
M'X(0) &= -[H(X,s), MX(0)] \\
&= -M[H(X(0),s), X(0)] \qquad (9.409)
\end{aligned}
$$

where the square brackets are the Poisson brackets and use has been made of Eq.(9.408) in the second step. Equation (9.409) can be written symbolically as

$$M' = -M:H: \qquad (9.410)$$

In particular, if the Hamiltonian is independent of s, then we have

$$M' = -M:H: \quad \implies \quad M = e^{-s:H:} \qquad (9.411)$$

which is what one expects.

Now consider a system described by a Hamiltonian which is basically given by an unperturbed Hamiltonian $H_0(X, s)$, but contains in addition a small perturbation,

$$H = H_0(X, s) + \epsilon V(X, s) \qquad (9.412)$$

where ϵ is considered to be small. Let us assume the unperturbed Lie map, $M_0(X, s)$, from position $s = 0$ to position s is known. We will now find an expression for the evolution map $M(X, s)$ from position $s = 0$ to position s for this slightly perturbed system to first order in ϵ.

We know M is approximately given by M_0. Let M be written in the form

$$M = NM_0 \qquad (9.413)$$

where N is approximately equal to the identity map. To first order in ϵ, we let

$$N = e^{:\epsilon f_1:} \qquad (9.414)$$

and we need to find an expression for $f_1(X, s)$.

Using (9.413), the left-hand-side of Eq.(9.410) reads

$$M' = N'M_0 + NM_0' = N'M_0 - NM_0:H_0: \qquad (9.415)$$

The right-hand-side of Eq.(9.410) is given by

$$-M{:}H{:} = -NM_0({:}H_0{:} + \epsilon{:}V{:}) \tag{9.416}$$

Substituting Eqs.(9.415-9.416) into Eq.(9.410) gives

$$N' = -\epsilon N M_0{:}V{:}M_0^{-1} = -\epsilon N{:}(M_0 V){:} \tag{9.417}$$

We need an expression for N' using Eq.(9.414). The result is[56]

$$N' = {:}\left(\frac{e^{:\epsilon f_1:} - 1}{:\epsilon f_1:}\right)\epsilon f_1'{:}N \tag{9.419}$$

To first order in ϵ, however, either one of the expressions in Eq.(9.418) applies. We will take the second of the pair. We then obtain from Eq.(9.417), to first order in ϵ, that

$$\epsilon f_1' = -\epsilon M_0 V \tag{9.420}$$

Solving Eq.(9.420) gives the result we are looking for,

$$
\begin{aligned}
f_1(X, s) &= -\int_0^s ds'\ M_0(X, s')V(X, s') \\
&= -\int_0^s ds'\ V(M_0(X, s')X, s') \tag{9.421}
\end{aligned}
$$

The physical meaning of Eq.(9.421) is described following Eq.(9.198). To first order in ϵ, the effect of errors at position s' can be transformed to the observation position s by the map M_0.

If $H_0 = H_0(X)$ is independent explicitly on s, then $M_0 = e^{-s:H_0:}$, and

$$f_1(X, s) = -\int_0^s ds'\ e^{-s':H_0:}V(X, s') \tag{9.422}$$

Equation (9.422) is just the BCH formula (9.264). This is seen as follows. Consider $H = H_0 + \epsilon V$ where H_0 and V are s-independent. Then, using Eq.(9.422),

$$
\begin{aligned}
M &= e^{-:sH_0 + s\epsilon V:} \\
&= \exp\left[:\int_0^1 du e^{-:usH_0:}(-s\epsilon V):\right]e^{-:sH_0:} \\
&= \exp\left[-\epsilon{:}(\int_0^s ds' e^{-:s'H_0:}V){:}\right]e^{-:sH_0:} \tag{9.423}
\end{aligned}
$$

This means Eq.(9.421) is a generalization of the BCH formula (9.264).

Below, we will consider several applications of Eqs.(9.421) and (9.422).

---

[56]Note that

$$N' \neq \epsilon{:}f_1'{:}N, \quad \text{and} \quad N' \neq N\epsilon{:}f_1'{:} \tag{9.418}$$

as one might be tempted to write using Eq.(9.414). Expressions (9.418) hold only if the operators $:f_1:$ and $:f_1':$ commute, which is not true in general. The correct expression for N' is obtained by Eq.(9.223).

Weak multipole in a long drift space Consider a weak error perturbation uniformly distributed over a drift distance L. Suppose we care only about the optics in 1-D (e.g. we care only about not messing up the x-emittance and don't care much about the y-emittance in this application). Let the perturbed Hamiltonian be

$$H = \frac{1}{2}p^2 + \epsilon v(x) \tag{9.424}$$

Equation (9.422) gives

$$\epsilon f_1 = -\int_0^s ds' e^{-:\frac{s'}{2}p^2:} v(x) = -\int_0^s ds' v(x + s'p) \tag{9.425}$$

For example, the perturbation maybe a multipole. From Eq.(9.183), we have

$$v(x) = \frac{\lambda}{n+1} x^{n+1} \tag{9.426}$$

Then we have

$$\epsilon f_1 = -\frac{\lambda}{(n+1)(n+2)} \frac{(x+sp)^{n+2} - x^{n+2}}{p} \tag{9.427}$$

For a quadrupole error of strength $\lambda = k$, we have $n = 1$ and

$$\epsilon f_1 = -\frac{k}{6}(3sx^2 + 3s^2 xp + s^3 p^2) \tag{9.428}$$

Error multipole correction algorithms We can apply Eqs.(9.421) and (9.422) to error correction algorithms. Suppose we have an uniform error perturbation $v(x)$, and we want to make a correction so that, when observed downstream from position $s = L$, its effect is compensated, at least to first order in the perturbation strength. Suppose we introduce a set of N_c thin-lens multipole correctors (of the same type of multipole as the error multipole). Let the i-th corrector $(i = 1, 2, ..., N_c)$ have location $s = s_i$ and strength α_i. How should we choose the corrector strengths α_i, assuming the corrector positions are given?

Let the Hamiltonian, including the error perturbation and the correctors, be

$$H = \frac{1}{2}p^2 + \epsilon v(x) + \sum_{i=1}^{N_c} \alpha_i \delta(s - s_i) v(x) \tag{9.429}$$

To first order in the perturbation strength, the correction requires

$$\int_0^L ds' e^{-:\frac{s'}{2}p^2:} v(x) \left[\epsilon + \sum_{i=1}^{N_c} \alpha_i \delta(s' - s_i) \right]$$

$$= \int_0^L ds' \, v(x + s'p) + \sum \alpha_i v(x + s_i p) = 0 \tag{9.430}$$

To apply Eq.(9.430), we consider s_i and $v(x)$ to be given, and we need to compute α_i so that Eq.(9.430) is satisfied for all values of x and p. In case

the perturbation is a multipole, $v(x) = \frac{\lambda}{n+1}x^{n+1}$, this correction scheme can be accomplished by having a finite number of correctors. If only 1-D is of interest, there are $n+2$ coefficients to vanish in Eq.(9.430). This requires $n+2$ correctors.

If the error multipole is a weak quadrupole ($n = 1$) of strength k and suppose we introduce three thin-lens quadrupoles of strength $\alpha_{1,2,3}$ at locations $s = 0, \frac{L}{2}$, and L, what should the corrector strengths be?

The correctors Hamiltonian is

$$\frac{\alpha_1}{2}x^2\delta(s) + \frac{\alpha_2}{2}x^2\delta(s - \frac{L}{2}) + \frac{\alpha_3}{2}x^2\delta(s - L) \tag{9.431}$$

To first order in k, the correction requires

$$-\frac{k}{6}(3sx^2 + 3s^2xp + s^3p^2) + \frac{\alpha_1}{2}x^2 + \frac{\alpha_2}{2}(x + \frac{L}{2}p)^2 + \frac{\alpha_3}{2}(x + Lp)^2 = 0 \tag{9.432}$$

where the first term is from Eq.(9.428). Equation (9.432) is to hold for all values of x and p. This means the coefficients of x^2, xp and p^2 must vanish separately. This gives three conditions to determine the three corrector strengths. The solution is found to be

$$\alpha_1 = \alpha_3 = \frac{1}{6}kL, \quad \alpha_2 = \frac{2}{3}kL \tag{9.433}$$

The relative weights of the three corrector strengths are just the Simpson's rule of integral approximation.

In case the perturbation is not a pure multipole, or if the perturbation is a multipole but the number of correctors available is less than $n + 2$, then Eq.(9.430) can not be fulfilled exactly. One can still do it approximately if the function $v(x + s'p)$ does not vary rapidly in the range $s = 0$ to $s = L$ for all values of x and p of interest. The corrector strengths are then determined by

$$\int_0^1 du\ v(x + uLp) = -\frac{1}{L}\sum_i \alpha_i v(x + u_i Lp) \tag{9.434}$$

If we call the function $v(x + uLp) \equiv G(u)$, then it becomes clear that we are just looking for a set of values α_i and s_i which best approximates the integral

$$\int_0^1 duG(u) = -\frac{1}{L}\sum_i \alpha_i G(u_i) \tag{9.435}$$

for any reasonably smooth function $G(u)$. Simpson's rule is then just one way to make this approximation. Simpson's rule is exact if $v(x)$ and H_0 are quadratic in x.

To find other ways to make approximate corrections, let us consider a drift space from $s = 0$ to $s = L$. The Hamiltonian of the drift space is $H_0(X) = \frac{1}{2}p^2$. Now consider some perturbation in this drift space. Let the perturbation be some sextupole fields distributed along the drift space according to the strength

distribution $\alpha(s)$. We consider $\alpha(s)$ to be small. Let the sextupole Hamiltonian be written as $\alpha(s)f(X)$, the Hamiltonian of the system is then[57]

$$H(X, s) = H_0(X) + \alpha(s)f(X) \tag{9.436}$$

We then raise the following question: Suppose we regard the sextupole distribution $\alpha(s)$ to be due to error sextupoles, and suppose one inserts a thin-lens correction sextupole at the middle of the drift space ($s = L/2$) to correct for the effect of this error sextupole distribution, what would be the optimal setting of this thin-lens correction sextupole? To address this question, we assume the optimization is reached when the corrector sextupole removes the effect of the error sextupoles to first order in the strength of the error sextupoles. When the correction sextupole is included, the Hamiltonian can be written as

$$H(X, s) = H_0(X) + \alpha(s)f(X) + \beta\delta(s - \frac{L}{2})f(X) \tag{9.437}$$

where β, yet to be chosen, characterizes the strength of the correction sextupole. In order for the correction sextupole to correct for the effect of the error sextupoles, we want it so that the system behaves as closely as possible to the unperturbed case when the system is observed at the end of the drift space, i.e. at $s = L$. For this to happen, we wish to choose the corrector strength so that [see Eq.(9.422)]

$$f_1 = -\int_0^L ds \ e^{-s:H_0:}[\alpha(s) + \beta\delta(s - \frac{L}{2})]f(X) = 0 \tag{9.438}$$

Equation (9.438) is to be valid for all X. The function $f(X)$ of course describes the sextupole effect. The operation $e^{-s:H_0:}$ is to transform the sextupole effect to position s while observing it at $s = L$. Clearly, the effect of a sextupole at position s is in general not described by the function $f(X)$ when observed at a different position at $s = L$. This means that, in general, the condition (9.438) is impossible to meet exactly, and we do not have a single corrector that entirely removes the first order error effects. But if the drift space is short enough, this can be done because $e^{-s:H_0:} \approx 1$ — which is equivalent to ignoring the difference made on $f(X)$ due to the transport from s to L — and we have the condition

$$\int_0^L ds \ [\alpha(s) + \beta\delta(s - \frac{L}{2})] = 0, \quad \text{or} \quad \beta = -\int_0^L ds \ \alpha(s) \tag{9.439}$$

In other words, the optimal correction is achieved by — not surprisingly — choosing the corrector to be of a sextupole type (reflected by the fact that $f_1 \propto f(X)$), and choosing β to be negative of the total integral of the error sextupole strength. It is easy to see that this choice of β is independent of the location of the corrector sextupole. See Exercise 78.

---

[57]In this application, we assume H_0 is drift space and $v(x)$ is sextupole, but these are not necessary. Same approximate schemes apply for other choices.

If the drift space is not that short, to improve the accuracy of the correction, we can insert two correctors. For example, one might insert one corrector at the entrance $(s = 0)$ and another at the exit $(s = L)$ of the drift space. The condition for correction becomes

$$\int_0^L ds \ [1 - s{:}H_0{:}][\alpha(s) + \beta_1\delta(s) + \beta_2\delta(s - L)]f(X) = 0 \qquad (9.440)$$

where we have kept one more term in $e^{-s:H:}$, i.e., we now use $e^{-s:H_0:} \approx 1 - s{:}H_0{:}$. Regardless of the expression of H_0, Eq.(9.440) can be satisfied if

$$\int_0^L ds \ [\alpha(s) + \beta_1\delta(s) + \beta_2\delta(s - L)] \quad = 0$$
$$\int_0^L ds \ s[\alpha(s) + \beta_1\delta(s) + \beta_2\delta(s - L)] \quad = 0 \qquad (9.441)$$

or

$$\beta_1 \quad = -\int_0^L ds \ (1 - \tfrac{s}{L})\alpha(s)$$
$$\beta_2 \quad = -\tfrac{1}{L}\int_0^L ds \ s\alpha(s) \qquad (9.442)$$

The condition (9.439) and the first condition of Eq.(9.441) have the physical meaning that the total angular kick of the perturbation (errors plus correctors) observed at $s = L$ is zero. The physical meaning of the second condition of Eq.(9.441) is that the total perturbation on the displacement of the particle's trajectory is zero when observed at $s = L$.

In Exercise 79, it is shown that Eq.(9.442) is related to the trapezoidal rule of numerical integration,

$$\int_0^1 dx \ f(x) \approx \frac{1}{2}f(0) + \frac{1}{2}f(1) \qquad (9.443)$$

where $f(x)$ is any smooth function of x. In fact, Eq.(9.439) is simply the cruder approximation $\int_0^1 dx \ f(x) \approx f(1/2)$.

One can further improve the accuracy of correction when the drift space is not too short by having three correctors, located at $s = 0$, $s = L/2$ and $s = L$. The conditions for correction is then

$$\int_0^L ds \ [\alpha(s) + \beta_1\delta(s) + \beta_2\delta(s - \frac{L}{2}) + \beta_3\delta(s - L)] \quad = \quad 0$$
$$\int_0^L ds \ s[\alpha(s) + \beta_1\delta(s) + \beta_2\delta(s - \frac{L}{2}) + \beta_3\delta(s - L)] \quad = \quad 0$$
$$\int_0^L ds \ s^2[\alpha(s) + \beta_1\delta(s) + \beta_2\delta(s - \frac{L}{2}) + \beta_3\delta(s - L)] \quad = \quad 0 \qquad (9.444)$$

or

$$\beta_1 \quad = \quad \int_0^L ds \ \alpha(s)(-1 + \frac{3s}{L} - \frac{2s^2}{L^2})$$

262

$$\beta_2 = \int_0^L ds\ \alpha(s)(-\frac{4s}{L} + \frac{4s^2}{L^2})$$

$$\beta_3 = \int_0^L ds\ \alpha(s)(\frac{s}{L} - \frac{2s^2}{L^2}) \qquad (9.445)$$

Equation (9.445) is related to the Simpson's rule of numerical integration

$$\int_0^1 dx\ f(x) \approx \frac{1}{6}f(0) + \frac{2}{3}f(\frac{1}{2}) + \frac{1}{6}f(1) \qquad (9.446)$$

The proof is described in Exercise 81. Exercises 80 and 81 also ask for generalization of the integration technique to include weight functions.

Equations (9.439), (9.442) and (9.445) give various error correction algorithms for short accelerator sections. It does not matter which type of errors are being considered, sextupole or otherwise. It also does not matter which unperturbed H_0 is being considered (However, see Exercise 85.).

Compensation for the dynamical effects of error multipoles is an important topic for accelerator designs. Depending on the problem at hand, the most effective way to provide the compensation varies. It should be mentioned here that the compensation discussed in this section applies only for the case when the effects of error multipoles are to be compensated locally (or almost locally). In particular, if it is the effect accumulated over one turn of the accelerator that is to be compensated, i.e., if the errors are to be corrected globally, the compensation scheme used would be quite different.

Exercise 74 As an illustration of the factorization procedure described from Eq.(9.387) to Eq.(9.390), factorize the 3-rd order map for a magnet with combined sextupolar and octupolar fields,

$$M = \exp(:-\frac{L}{2}p^2 - Sx^3 - \epsilon x^4:) \qquad (9.447)$$

into a form

$$M = e^{:f_2:}e^{:f_3:}e^{:f_4:}e^{:\mathcal{O}(X^5):} \qquad (9.448)$$

Find expressions for $f_{2,3,4}$. This exercise can be compared with Exercise 58.

Solution

$$f_2 = -\frac{L}{2}p^2$$

$$f_3 = -S\int_0^1 du\ (e^{-u:f_2:}x)^3$$

$$= -S\int_0^1 du\ (x - uLp)^3$$

$$= -S(x^3 - \frac{3}{2}Lx^2p + L^2xp^2 - \frac{1}{4}L^3p^3)$$

$$f_4 = -\epsilon \int_0^1 du [e^{-u:f_2:}x]^4 - \frac{S^2}{2} \int_0^1 du \int_0^u dv [(e^{-v:f_2:}x)^3, (e^{-u:f_2:}x)^3]$$

$$= -\epsilon \int_0^1 du (x - uLp)^4 - \frac{S^2}{2} \int_0^1 du \int_0^u dv [(x-vLp)^3, (x-uLp)^3]$$

$$= -\epsilon(x^4 - 2Lx^3p + 2L^2x^2p^2 - L^3xp^3 + \frac{1}{5}L^4p^4)$$

$$- \frac{S^2L}{2}[-\frac{3}{28}L^4p^4 + \frac{3}{4}L^3xp^3 - \frac{9}{4}L^2x^2p^2 + 3Lx^3p - \frac{3}{2}x^4] \quad (9.449)$$

Exercise 75 Prove Eq.(9.390).
Solution Instead of iteration as suggested in the text, we could apply the second form of the BCH formula, Eqs.(9.195), (9.196) and (9.253). It suffices to show that

$$e^{:-L_iH_{2i}-L_iH_{3i}-L_iH_{4i}:} = e^{:f_2:}e^{:f_3:}e^{:f_4:} = e^{:f_2:}e^{:f_3+f_4:}e^{:\mathcal{O}(X^5):} \quad (9.450)$$

holds when $f_{2,3,4}$ are given by Eqs.(9.388-9.390). Applying Eqs.(9.195-9.196) [or Eq.(9.253)] to the right hand side of Eq.(9.450), keeping terms up to $\mathcal{O}(X^4)$, and substituting $f_{2,3,4}$ by Eq.(9.388-9.390), indeed one obtains $e^{:-L_iH_{2i}-L_iH_{3i}-L_iH_{4i}:}$.

Exercise 76 Find factorized Lie maps to $\mathcal{O}(X^4)$ for thick combined-function magnets, (a) combined quadrupole and sextupole, (b) combined quadrupole and solenoid, (c) combined dipole and quadrupole, (d) combined dipole and sextupole. Do this in 1-D case. Then do it for 2-D. Which of these can be found exactly? Apply the results to obtain 4-th order Taylor maps.

Exercise 77 Equations (9.421) to (9.423) apply when the perturbed map M is written in the form (9.413). Repeat the procedure if M assumes a different form $M = M_0N$. Give the physical meaning as done following Eq.(9.421).

Exercise 78 Equation (9.439) gives the optimal setting of a single sextupole corrector to compensate for a distribution of error sextupoles. Estimate the residual effect of the sextupoles after correction by computing the net Lie or Taylor map.

Exercise 79 Relate the discussions leading to Eq.(9.442) to the trapazoidal rule, Eq.(9.443), of numerical integration.
Solution Identify $e^{-s:H_0:}$ as a function of s and call it $f(s)$. If it behaves sufficiently smoothly in the region between $s = 0$ and $s = 1$, we have shown that the best choice of β_1 and β_2 that makes

$$\int_0^1 ds \; f(s)[\alpha(s) + \beta_1\delta(s) + \beta_2\delta(s-1)] \approx 0 \quad (9.451)$$

is given by Eq.(9.442) regardless of the exact form of $f(s)$. Now if we take $\alpha(s) = 1$, Eq.(9.442) gives

$$\beta_1 = \beta_2 = -\frac{1}{2} \tag{9.452}$$

Substituting back into Eq.(9.451) yields Eq.(9.443).

Exercise 80 The trapezoidal rule (9.443) applies when $f(x)$ is a smooth function of x between 0 and 1. If one is interested in calculating the integral of $f(x)W(x)$ where $f(x)$ is smooth but $W(x)$ is not, we can reconsider Exercise 79 but this time take $\alpha(s) = W(s)$. Show that this leads to

$$\int_0^1 dx\ f(x)W(x) \approx \beta_1 f(0) + \beta_2 f(1) \tag{9.453}$$

where

$$
\begin{aligned}
\beta_1 &= \int_0^1 dx\ (1-x)W(x) \\
\beta_2 &= \int_0^1 dx\ xW(x)
\end{aligned}
\tag{9.454}
$$

As applications of Eqs.(9.453-9.454), show that

$$
\begin{aligned}
\int_{-1}^1 dx\ f(x)(1-x^2) &\approx \tfrac{2}{3}[f(-1) + f(1)] \\
\int_{-1}^1 dx\ f(x)\sqrt{1-x^2} &\approx \tfrac{\pi}{4}[f(-1) + f(1)] \\
\int_{-1}^1 dx\ \frac{f(x)}{\sqrt{1-x^2}} &\approx \tfrac{\pi}{2}[f(-1) + f(1)]
\end{aligned}
\tag{9.455}
$$

Exercise 81 Follow Exercise 79 to prove the Simpson's rule (9.446). Follow Exercise 80 to find the Simpson's rule with a weight function. *Solution* The Simpson's rule with weight function is

$$\int_0^1 dx f(x)W(x) \approx \beta_1 f(0) + \beta_2 f(\tfrac{1}{2}) + \beta_3 f(1) \tag{9.456}$$

where

$$
\begin{aligned}
\beta_1 &= \int_0^1 dx\ (1-x)(1-2x)W(x) \\
\beta_2 &= 4\int_0^1 dx\ x(1-x)W(x) \\
\beta_3 &= -\int_0^1 dx\ x(1-2x)W(x)
\end{aligned}
\tag{9.457}
$$

265

As applications of Eqs.(9.456-9.457), we have

$$\int_{-1}^{1} dx \ f(x)(1 - x^2) \approx \frac{2}{15}f(-1) + \frac{16}{15}f(0) + \frac{2}{15}f(1)$$

$$\int_{-1}^{1} dx \ f(x)\sqrt{1 - x^2} \approx \frac{\pi}{16}f(-1) + \frac{3\pi}{8}f(0) + \frac{\pi}{16}f(1)$$

$$\int_{-1}^{1} dx \ \frac{f(x)}{\sqrt{1 - x^2}} \approx \frac{\pi}{4}f(-1) + \frac{\pi}{2}f(0) + \frac{\pi}{4}f(1) \quad (9.458)$$

Exercise 82 Equation (9.445) describes how to correct for some known nonlinear effects of a short accelerator section from $s = 0$ to $s = L$ using three correctors located at $s = 0, L/2$, and L. The accuracy of this correction is up to order $\mathcal{O}(L^3)$. Free up the locations of the correctors. See if better correction accuracy can be achieved.

Solution To simplify the algebra, change coordinates so that the region of interest is from $s = -L$ to L. The accuracy of correction is $\mathcal{O}(L^4)$ if the correctors are located at

$$s_1 = -\sqrt{\frac{I_3}{I_1}}, \quad s_2 = 0, \quad s_3 = \sqrt{\frac{I_3}{I_1}} \quad (9.459)$$

and the corrector strengths are chosen to be

$$\beta_1 = -\frac{I_1(I_2 - \sqrt{I_1 I_3})}{2 I_3}$$

$$\beta_2 = -I_0 + \frac{I_1 I_2}{I_3}$$

$$\beta_3 = -\frac{I_1(I_2 + \sqrt{I_1 I_3})}{2 I_3} \quad (9.460)$$

where

$$I_k = \int_{-L}^{L} ds \ \alpha(s) s^k \quad (9.461)$$

The residual effect of the errors after correction is given by

$$I_4 - \frac{I_2 I_3}{I_1} = \mathcal{O}(L^5) \quad (9.462)$$

For the special case when $I_1 = 0$ and $I_3 = 0$, a $\mathcal{O}(L^5)$ correction can be achieved with three correctors:

$$s_1 = -s_3 = -\sqrt{\frac{I_4}{I_2}}, \qquad s_2 = 0$$

$$\beta_1 = \beta_3 = -\frac{I_2^2}{2 I_4}, \qquad \beta_2 = -I_0 + \frac{I_2^2}{I_4} \quad (9.463)$$

One can obtain a numerical integration rule from Eq.(9.463) by considering $\alpha(x) = 1$. This leads to

$$\int_{-1}^{1} dx \ f(x) \approx \frac{5}{9}f(-\sqrt{\frac{3}{5}}) + \frac{8}{9}f(0) + \frac{5}{9}f(\sqrt{\frac{3}{5}}) \qquad (9.464)$$

Equation (9.464) is exact if $f(x)$ is a 5-th order Taylor series in x. In contrast, Simpson's rule (9.446) is exact if $f(x)$ is a 3-rd order Taylor series. Compare this with Legendre integration with roots of $P_3(x) = 0$.

One can also include a weight function by considering $\alpha(x) = W(x)$. Equations (9.459-9.461) give for example

$$\int_{-1}^{1} dx \ xf(x) \approx \frac{1}{3}\sqrt{\frac{5}{3}}\left[f(\sqrt{\frac{3}{5}}) - f(-\sqrt{\frac{3}{5}})\right] \qquad (9.465)$$

which is consistent with Eq.(9.464). In case $I_1 = 0$ and $I_3 = 0$, we obtain

$$\int_{-1}^{1} dx \ W(x)f(x) \approx I_0 f(0) + \frac{I_2^2}{2I_4}\left[f(\sqrt{\frac{I_4}{I_2}}) + f(-\sqrt{\frac{I_4}{I_2}}) - 2f(0)\right]$$
$$(9.466)$$

where $I_k = \int_{-1}^{1} dx \ W(x)x^k$. As special cases, we have

$$\int_{-1}^{1} dx \ f(x)(1-x^2) \approx \frac{14}{45}f(-\sqrt{\frac{3}{7}}) + \frac{32}{45}f(0) + \frac{14}{45}f(\sqrt{\frac{3}{7}})$$

$$\int_{-1}^{1} dx \ f(x)\sqrt{1-x^2} \approx \frac{\pi}{8}f(-\sqrt{\frac{1}{2}}) + \frac{\pi}{4}f(0) + \frac{\pi}{8}f(\sqrt{\frac{1}{2}})$$

$$\int_{-1}^{1} dx \ \frac{f(x)}{\sqrt{1-x^2}} \approx \frac{\pi}{3}f(-\sqrt{\frac{3}{4}}) + \frac{\pi}{3}f(0) + \frac{\pi}{3}f(\sqrt{\frac{3}{4}}) \quad (9.467)$$

Compare this with Tsybechev integration.

Exercise 83 Determine the strengths of four correctors located at $s = 0, L/3, 2L/3$, and L to provide a correction accuracy of $\mathcal{O}(L^4)$. Free up the locations of these four correctors to achieve a higher correction accuracy. Compare this with Legendre integration with roots of $P_4(x) = 0$.

Exercise 84 Consider an accelerator transport line consisting of a thin focusing quadrupole at location $s = 0$, followed by two dipoles, each of length D, followed by a thin defocusing quadrupole at location $s = 2D$, followed by another two dipoles, each of length D, followed by a thin focusing quadrupole at $s = 4D$. Suppose that the four dipoles are known to have weak error sextupole fields with strengths of $\alpha_i, i = 1, \dots, 4$, and that it is possible to insert some

thin correctors next to each of the three quadrupoles. Assume the sextupole field within each dipole is uniform over the length of the dipole. (a) Design a single-pass correction scheme and determine the corrector strengths for this transport line. (b) Consider the 2-D motion of on-momentum particles. Give expressions of the Lie and Taylor maps before and after correction to the leading order in α and D.

Solution Three thin sextupoles at the locations next to the quadrupoles serve as the correctors. Apply Eq.(9.445) to obtain their strengths:

$$
\begin{aligned}
\beta_1 &= -\frac{2}{3}\alpha_1 D - \frac{1}{6}\alpha_2 D + \frac{1}{12}\alpha_3 D + \frac{1}{12}\alpha_4 D \\
\beta_2 &= -\frac{5}{12}\alpha_1 D - \frac{11}{12}\alpha_2 D - \frac{11}{12}\alpha_3 D - \frac{5}{12}\alpha_4 D \\
\beta_3 &= \frac{1}{12}\alpha_1 D + \frac{1}{12}\alpha_2 D - \frac{1}{6}\alpha_3 D - \frac{2}{3}\alpha_4 D
\end{aligned}
\tag{9.468}
$$

These corrector settings are independent of the strengths of the quadrupoles or the dipoles.

Exercise 85 Equations (9.431-9.433) are for the case to correct a weak uniform error quadrupole in a free space with three correctors. Consider the case to correct a weak uniform error quadrupole in a not-so-weak, unperturbed quadrupole. Again, we will see that three correctors are needed. Let K and k be the unperturbed and error quadrupole strengths respectively. The Hamiltonian is

$$
H = \frac{1}{2}p^2 + \frac{1}{2}Kx^2 + \frac{k}{2}x^2 + \sum_{i=1}^{3}\frac{\alpha_i}{2}x^2\delta(s-s_i)
\tag{9.469}
$$

We want

$$
\int_0^L ds'\, e^{-:s'(\frac{1}{2}p^2+\frac{1}{2}Kx^2):}[kx^2 + \sum_i \alpha_i x^2\delta(s-s_i)] = 0
$$

$$
\implies \quad k\int_0^L ds'(x\cos\sqrt{K}s' + \frac{p}{\sqrt{K}}\sin\sqrt{K}s')^2
$$

$$
+ \sum_i \alpha_i (x\cos\sqrt{K}s_i + \frac{p}{\sqrt{K}}\sin\sqrt{K}s_i)^2 = 0
$$

$$
\implies \quad
\begin{cases}
k\int_0^L ds'\cos^2\sqrt{K}s' + \sum_i \alpha_i \cos^2\sqrt{K}s_i = 0 \\
k\int_0^L ds'\sin\sqrt{K}s'\cos\sqrt{K}s' + \sum_i \alpha_i \sin\sqrt{K}s_i \cos\sqrt{K}s_i = 0 \\
k\int_0^L ds'\sin^2\sqrt{K}s' + \sum_i \alpha_i \sin^2\sqrt{K}s_i = 0
\end{cases}
$$

$$
\tag{9.470}
$$

Let the three correctors be located at $s_i = 0, \frac{L}{2}$ and L. The

corrector strengths are found to be (with $q = \sqrt{K}L$)

$$\alpha_1 = \alpha_3 = \frac{k}{4\sqrt{K}\sin^2\frac{q}{2}}(-q + \sin q)$$

$$\alpha_2 = \frac{k}{2\sqrt{K}\sin^2\frac{q}{2}}(q\cos q - \sin q) \qquad (9.471)$$

When $K = 0$, this reduces to the Simpson's rule $\alpha_1 = \alpha_3 = -kL/6, \alpha_2 = -2kL/3$. When L is short, this also reduces to Simpson's rule.

9.8 Normal Form

In our discussions so far, linear maps have played an important role. This is not unexpected. We can learn and have learned a lot from linear maps. Linear maps can simultaneously be viewed as Taylor maps and Lie maps and therefore have the advantages of both. In particular, we learned that a lot of the linear system analysis can be handled with matrices. However, we have also learned that an elegant and insightful treatment of linear systems is provided by a Courant-Snyder analysis, and the Courant-Snyder analysis is intimately related to the Lie representation of linear maps. [See Eq.(9.90).]

What we learned from linear systems can be generalized to nonlinear systems. In fact, even the very concept of maps is learned from analysing the linear systems. In a linear system, one speaks of matrices and Courant-Snyder transformation of these matrices without having to think of them as maps. But when considering a nonlinear system, the map concept becomes inevitable. More reasons why maps are useful:

(1) We are interested in observation of particle motion at a fixed location of the accelerator, not the entire time evolution.

(2) Maps are easier to handle mathematically — maps can be multiplied; Hamiltonians can not.

(3) A map allows an algebraic expression of the final coordinates as functions of the initial coordinates, while tracking only establishes their numerical connection.

One then realizes that representing nonlinear maps in their Lie forms provides a natural way to generalize the Courant-Snyder analysis to nonlinear systems, but being able to write the nonlinear maps in Lie forms constitutes only a first step toward completing the analogy to linear analysis. What is missing is the equivalent of the Courant-Snyder transformation, and the analyses of the properties of the linear system subsequent to the transformation. In this section, we will introduce a *normal form* technique which is the nonlinear equivalent of the Courant-Snyder analysis.

Indeed, having obtained the one-turn Lie map such as Eq.(9.190) with the effective Hamiltonian H_{eff}, and transformed it into its normal form, many physical quantities related to the nonlinear dynamics of the system can be extracted.

These physical quantities include:

- closed orbit distortion in the accelerator
- Courant-Snyder α, β, γ functions
- Courant-Snyder functions for off-momentum particles
- strengths for various resonances
- smear or distortion functions
- betatron tunes as functions of momentum deviation and betatron amplitudes
- KAM tori (or KAM invariants)

These quantities are expressed as explicit Taylor expressions in terms of the perturbations up to the order specified by the map.[58]

Note that once one recognizes the significant role maps play, the questions are then (a) how to generate maps efficiently, and (b) once generated, how to analyze those maps. The subject of high-order map generation is addressed by the technique of truncated power series algebra (TPSA) and is not covered here. In this section, we address question (b) using the normal form technique.

Courant-Snyder transformation for 1-D linear systems To introduce the concept of normal forms, let's first consider the nonlinear map for a 1-D system,

$$M = e^{:f_2(X):} e^{:f_3(X):} \ldots \tag{9.472}$$

where X are the physical coordinates $X = (x, p_x)$ with $p_x = x'$. If the system is linear, we have $f_k = 0$ for $k \geq 3$. From the Courant-Snyder analysis, we know it is convenient to transform the physical coordinates to the normalized coordinates

$$U = \begin{bmatrix} \bar{x} \\ \bar{p}_x \end{bmatrix} = \begin{bmatrix} \frac{1}{\sqrt{\beta}} & 0 \\ \frac{\alpha}{\sqrt{\beta}} & \sqrt{\beta} \end{bmatrix} \begin{bmatrix} x \\ p_x \end{bmatrix} \tag{9.473}$$

The question we first ask is how to introduce this transformation in the Lie language.

It is important to realize that the Courant-Snyder transformation (9.473) is not the unique way to lead to normal forms. See Exercise 90.

To proceed, consider the map (in Lie representation)

$$N = A_2 M A_2^{-1} \tag{9.474}$$

---

[58]If the map treats the dynamic variables (components of X) as perturbations, these quantities are expressed to the specified order in terms of the components of X. If the map treats the strength of a certain nonlinear element as the perturbation, explicit expressions of these quantities as functions of this nonlinear element strength can be obtained. It is also possible to simultaneously use X and the strengths of a set of accelerator elements (linear or nonlinear) as perturbations and obtain the corresponding Taylor expressions of these quantities.

where A_2^{-1} is the linear symplectic map[59] whose matrix representation $\mathbf{A_2}^{-1}$ are such that

$$\mathbf{A_2}^{-1}X = U, \quad \text{or} \quad \mathbf{A_2}^{-1} = \begin{bmatrix} \frac{1}{\sqrt{\beta}} & 0 \\ \frac{\alpha}{\sqrt{\beta}} & \sqrt{\beta} \end{bmatrix} \quad \text{or} \quad \mathbf{A_2} = \begin{bmatrix} \sqrt{\beta} & 0 \\ -\frac{\alpha}{\sqrt{\beta}} & \frac{1}{\sqrt{\beta}} \end{bmatrix}$$

(9.475)

The map N operates on coordinates U. We have

$$\begin{aligned} N &= A_2 e^{:f_2(X):} e^{:f_3(X):} .... A_2^{-1} \big|_{X=U} \\ &= A_2 e^{:f_2(X):} A_2^{-1} A_2 e^{:f_3(X):} A_2^{-1} .... \big|_{X=U} \\ &= e^{:A_2 f_2(X):} e^{:A_2 f_3(X):} ... \big|_{X=U} \\ &= e^{:f_2(A_2 U):} e^{:f_3(A_2 U):} ... \end{aligned}$$

(9.476)

where $f_n(A_2 U)$ just means $f_n(X)$ when it is re-expressed in terms of $U = A_2^{-1}X$. For example, [See Eq.(9.90)]

$$f_2(X) = -\frac{\mu}{2}(\gamma x^2 + 2\alpha x p_x + \beta p_x^2) = -\frac{\mu}{2}\left[(\frac{x}{\sqrt{\beta}})^2 + (\frac{\alpha x + \beta x'}{\sqrt{\beta}})^2\right]$$

$$\implies \quad f_2(A_2 U) = -\frac{\mu}{2}(\bar{x}^2 + \bar{p}_x^2)$$

(9.477)

The map N describes the dynamics of the same physical system as described by M, and it has the same form as M except that all coordinates X are transformed into U. If the system is linear, one can use a matrix language. The matrix representation of Eq.(9.474) is, recalling the reversed ordering,

$$\mathbf{N} = \mathbf{A_2}^{-1}\mathbf{M}\mathbf{A_2}$$

(9.478)

If the map M is applied to X, we have

$$\mathbf{M}X = \mathbf{A_2}\mathbf{N}\mathbf{A_2}^{-1}X = \mathbf{A_2}\mathbf{N}U$$

(9.479)

It is also easy to see that applying the map k times gives

$$\mathbf{M}^k X = \mathbf{A_2}\mathbf{N}^k U$$

(9.480)

This means that to study the multi-turn beam dynamics, one can study the effects of the map M on the physical coordinates X, or equivalently, one can study the effects of the map N on the normalized coordinates U. The operation $\mathbf{A_2}$ on the right-hand-side of Eq.(9.480) simply means that after the study, one needs to remember to transform the results back to the physical space, but such transformation needs to be done only once at the end. The *dynamics* of the map M in terms of the X-coordinates and the map N in terms of the U-coordinates are the same.

---

[59] One can consider nonsymplectic transformations as well, but we are not interested in them for our purpose.

3-D linear systems Let us now consider a 3-D case. More specifically let us consider a section of accelerator design that contains only magnetic devices and no electric devices so that δ in an invarinat. For example, if there is only one rf cavity in a circular accelerator, and the cavity is considered to be a thin-lens element located at position $s = 0$, the accelerator section being considered could be the map from $s = 0^+$ to $s = C^-$ for one turn around the accelerator excluding the rf cavity.

We will adopt the dynamic variables $X = (x, x', y, y', z, \delta)$. Let the map through the section be M, which has the form (9.472). Because δ is a constant of the motion, all functions $f_n(X)$ do not depend on z, as one would also expect physically. For a linear system, of course $f_3(X) = 0$, etc.

We then make a transformation according to Eq.(9.474), where A_2 is chosen such that the function $f_2(A_2 U)$ is given by

$$f_2(A_2 U) = -\frac{\bar{\mu}_x}{2}(\bar{x}^2 + \bar{p}_x^2) - \frac{\bar{\mu}_y}{2}(\bar{y}^2 + \bar{p}_y^2) - \frac{\bar{\alpha}_c}{2}\delta^2 \qquad (9.481)$$

where

$$U = \begin{bmatrix} \bar{x} \\ \bar{p}_x \\ \bar{y} \\ \bar{p}_y \\ \bar{z} \\ \delta \end{bmatrix} = A_2^{-1} X \qquad (9.482)$$

and $\bar{\mu}_{x,y}$ (the normal mode frequencies) and $\bar{\alpha}_c$ (the normal mode momentum compaction factor) are constants determined by the system. Note that the variable δ is the same before and after the transformation and that $f_2(A_2 U)$ [and $f_n(A_2 U)$ if the system is nonlinear] do not depend on $\bar{z}$.

How to obtain the normalized coordinates U knowing the one-turn linear map of a circular accelerator? The matrix of the linear map can be written in general as

$$M = \begin{bmatrix} & & & & 0 & R_{16} \\ & & \mathbf{R} & & 0 & R_{26} \\ & & & & 0 & R_{36} \\ & & & & 0 & R_{46} \\ R_{51} & R_{52} & R_{53} & R_{54} & 1 & R_{56} \\ 0 & 0 & 0 & 0 & 0 & 1 \end{bmatrix} \qquad (9.483)$$

where $\mathbf{R}$ is a 4×4 matrix. Couplings among the three dimensions are allowed in Eq.(9.483). As written, Eq.(9.483) contains 25 yet-unspecified elements, but symplecticity of $\mathbf{M}$ imposes strong constraints on these elements. First, it requires that $\mathbf{R}$ be symplectic. This reduces the number of independent elements of $\mathbf{R}$ from 16 to 10. Second, it also requires that the R-elements satisfy

$$\tilde{\mathbf{R}}\mathbf{S} \begin{bmatrix} R_{16} \\ R_{26} \\ R_{36} \\ R_{46} \end{bmatrix} + \begin{bmatrix} R_{51} \\ R_{52} \\ R_{53} \\ R_{54} \end{bmatrix} = 0 \qquad (9.484)$$

where $\mathbf{S}$ is the 4×4 member of the symplectic form (9.3-9.4) and a tilde means taking the transpose of a matrix. Equation (9.484) constitutes 4 more conditions. The total number of independent elements in Eq.(9.483) is 15.

We will make a succession of three canonical transformations. These transformations follows the Courant-Snyder transformation but is its generalization to 3-D linear system. We will obtain a "normal form" result at the end. This discussion then serves as the background to discuss normal forms for nonlinear systems later.

We first make a transformation of coordinates

$$
\text{from} \quad X = \begin{bmatrix} x \\ x' \\ y \\ y' \\ z \\ \delta \end{bmatrix} \quad \text{to} \quad X_1 = \mathbf{B}X \tag{9.485}
$$

where $\mathbf{B}$ is the symplectic matrix

$$
\mathbf{B} = \begin{bmatrix} 1 & 0 & 0 & 0 & 0 & -\eta_x \\ 0 & 1 & 0 & 0 & 0 & -\eta_x' \\ 0 & 0 & 1 & 0 & 0 & -\eta_y \\ 0 & 0 & 0 & 1 & 0 & -\eta_y' \\ \eta_x' & -\eta_x & \eta_y' & -\eta_y & 1 & 0 \\ 0 & 0 & 0 & 0 & 0 & 1 \end{bmatrix} \tag{9.486}
$$

The four components $(\eta_x, \eta_x', \eta_y, \eta_y')$ are the dispersion functions. They form a vector that satisfies a fixed point condition

$$
\mathbf{R} \begin{bmatrix} \eta_x \\ \eta_x' \\ \eta_y \\ \eta_y' \end{bmatrix} + \begin{bmatrix} R_{16} \\ R_{26} \\ R_{36} \\ R_{46} \end{bmatrix} = \begin{bmatrix} \eta_x \\ \eta_x' \\ \eta_y \\ \eta_y' \end{bmatrix} \tag{9.487}
$$

or

$$
\begin{bmatrix} \eta_x \\ \eta_x' \\ \eta_y \\ \eta_y' \end{bmatrix} = -(\mathbf{R} - 1)^{-1} \begin{bmatrix} R_{16} \\ R_{26} \\ R_{36} \\ R_{46} \end{bmatrix} \tag{9.488}
$$

The condition (9.487) allows expressions of the elements $R_{16}, R_{26}, R_{36}, R_{46}$ in terms of $\eta_x, \eta_x', \eta_y, \eta_y'$. The symplecticity condition (9.484) then allows expressions of $R_{51}, R_{52}, R_{53}, R_{54}$ in terms of $\eta_x, \eta_x', \eta_y, \eta_y'$ as

$$
\begin{bmatrix} R_{51} \\ R_{52} \\ R_{53} \\ R_{54} \end{bmatrix} = (1 - \tilde{\mathbf{R}})\mathbf{S} \begin{bmatrix} \eta_x \\ \eta_x' \\ \eta_y \\ \eta_y' \end{bmatrix} \tag{9.489}
$$

273

The transformation matrix for the new coordinates (9.485) is given by

$$\mathbf{N} = \mathbf{BMB}^{-1} = \begin{bmatrix} & & & & 0 & 0 \\ & & \mathbf{R} & & 0 & 0 \\ & & & & 0 & 0 \\ & & & & 0 & 0 \\ 0 & 0 & 0 & 0 & 1 & \bar{\alpha}_c \\ 0 & 0 & 0 & 0 & 0 & 1 \end{bmatrix} \tag{9.490}$$

where

$$\bar{\alpha}_c = R_{56} + \eta'_x R_{16} - \eta_x R_{26} + \eta'_y R_{36} - \eta_y R_{46} \tag{9.491}$$

and use has been made of Eqs.(9.487) and (9.489). The matrix (9.490) is obviously simpler than the matrix (9.483).

We can make the matrix even simpler by introducing a second transformation which deals with the matrix $\mathbf{R}$ in Eq.(9.490). Assuming the betatron motion is stable, $\mathbf{R}$ can be block diagonalized by a 4×4 matrix $\mathbf{T}$:

$$\mathbf{T}^{-1}\mathbf{RT} = \begin{bmatrix} \cos\bar{\mu}_x & \sin\bar{\mu}_x & 0 & 0 \\ -\sin\bar{\mu}_x & \cos\bar{\mu}_x & 0 & 0 \\ 0 & 0 & \cos\bar{\mu}_y & \sin\bar{\mu}_y \\ 0 & 0 & -\sin\bar{\mu}_y & \cos\bar{\mu}_y \end{bmatrix} \tag{9.492}$$

The 6×6 matrix $\mathbf{A}_2^{-1}$ of Eq.(9.482) is given by

$$\mathbf{A}_2^{-1} = \begin{bmatrix} & & & & 0 & 0 \\ & & \mathbf{T} & & 0 & 0 \\ & & & & 0 & 0 \\ & & & & 0 & 0 \\ 0 & 0 & 0 & 0 & 1 & 0 \\ 0 & 0 & 0 & 0 & 0 & 1 \end{bmatrix} \mathbf{B}$$

$$= \begin{bmatrix} & & & & 0 & (A_2^{-1})_{16} \\ & & \mathbf{T} & & 0 & (A_2^{-1})_{26} \\ & & & & 0 & (A_2^{-1})_{36} \\ & & & & 0 & (A_2^{-1})_{46} \\ \eta'_x & -\eta_x & \eta'_y & -\eta_y & 1 & 0 \\ 0 & 0 & 0 & 0 & 0 & 1 \end{bmatrix} \tag{9.493}$$

where

$$\begin{bmatrix} (A_2^{-1})_{16} \\ (A_2^{-1})_{26} \\ (A_2^{-1})_{36} \\ (A_2^{-1})_{46} \end{bmatrix} = -\mathbf{T} \begin{bmatrix} \eta_x \\ \eta'_x \\ \eta_y \\ \eta'_y \end{bmatrix} \tag{9.494}$$

One can also take the inverse of Eq.(9.493) to obtain

$$\mathbf{A}_2 = \begin{bmatrix} & & & & 0 & \eta_x \\ & & \mathbf{T}^{-1} & & 0 & \eta'_x \\ & & & & 0 & \eta_y \\ & & & & 0 & \eta'_y \\ (A_2)_{51} & (A_2)_{52} & (A_2)_{53} & (A_2)_{54} & 1 & 0 \\ 0 & 0 & 0 & 0 & 0 & 1 \end{bmatrix} \tag{9.495}$$

274

where

$$\begin{bmatrix} (A_2)_{51} \\ (A_2)_{52} \\ (A_2)_{53} \\ (A_2)_{54} \end{bmatrix} = -\tilde{\mathbf{T}}^{-1}\mathbf{S} \begin{bmatrix} \eta_x \\ \eta_x' \\ \eta_y \\ \eta_y' \end{bmatrix} \tag{9.496}$$

In terms of the new coordinates (9.482), finally, the transformation matrix assumes a simple form

$$\mathbf{N} = \begin{bmatrix} \cos\bar{\mu}_x & \sin\bar{\mu}_x & 0 & 0 & 0 & 0 \\ -\sin\bar{\mu}_x & \cos\bar{\mu}_x & 0 & 0 & 0 & 0 \\ 0 & 0 & \cos\bar{\mu}_y & \sin\bar{\mu}_y & 0 & 0 \\ 0 & 0 & -\sin\bar{\mu}_y & \cos\bar{\mu}_y & 0 & 0 \\ 0 & 0 & 0 & 0 & 1 & \bar{\alpha}_c \\ 0 & 0 & 0 & 0 & 0 & 1 \end{bmatrix} \tag{9.497}$$

We have thus transformed the complex matrix (9.483) to a much simpler form (9.497) by two coordinate transformations. Application to a special case of 3-D linear system is given in Exercise 86.

Note that $\mathbf{B}$ contains the dispersion function information of the system, while $\mathbf{T}$ contains the betatron functions and $\mathbf{N}$ contains the normal mode frequencies. The dispersion and the betatron functions, and therefore $\mathbf{B}$ and $\mathbf{T}$, depend on the location s of where the one-turn map (9.483) is taken. On the other hand, the normal mode frequencies, and therefore $\mathbf{N}$, are s-independent. [See Exercise 88.]

The components of U are the normalized coordinates which transform the linear part of the map into $e^{:f_2(A_2U):}$ with $f_2(A_2U)$ given by Eq.(9.481). To complete the normal form representation, we still need to introduce a third coordinate transformation. Following what we learned following Eq.(9.346), we introduce the coordinates $(\phi_x, A_x, \phi_y, A_y)$ according to

$$\begin{aligned} \bar{x} = \sqrt{2A_x}\sin\phi_x, \quad &\bar{p}_x = \sqrt{2A_x}\cos\phi_x \\ \bar{y} = \sqrt{2A_y}\sin\phi_y, \quad &\bar{p}_y = \sqrt{2A_y}\cos\phi_y \end{aligned} \tag{9.498}$$

We have

$$f_2(A_2U) = -\bar{\mu}_x A_x - \bar{\mu}_y A_y - \frac{1}{2}\bar{\alpha}_c\delta^2 \tag{9.499}$$

The eigenmodes of $:f_2:$ are given by Eq.(9.348).

What has been described so far since Eq.(9.473) is the normal form formalism for a linear system. Given a general linear map $M = e^{:f_2:}$, we have found a transformation A (or a succession of transformations whose net result is a transformation A) such that the transformed map $N = AMA^{-1}$ has the very simple form $e^{:h_2:}$, where $h_2 = f_2(A_2U)$ is a function only of A_x, A_y, and δ. In contrast, note that in the original map $e^{:f_2:}$, f_2 is a function of 5 variables x, x', y, y', and δ.

Nonlinear systems We are now ready to introduce the idea of normal form for a nonlinear system. For a nonlinear map M such as (9.472), the idea of normal form is to look for a nonlinear symplectic transformation A such that the map

$$N = AMA^{-1} \qquad (9.500)$$

is "as simple as possible". Drawing an analogy to the linear analysis, this means the transformed map N — which has the "simplest possible" form — depends only on A_x, A_y and δ even though the original map M depends on 5 variables x, x', y, y', and δ.[60]

It should be emphasized that, recalling the discussion following Eq.(9.480), A is a coordinate transformation that can be detached from the multi-turn studies. All dynamical effects that involve multi-turns — such as the beam dynamics encountered in circular accelerators — are contained in the map N, and that is why we would like N to be simple.[61] The map A and A^{-1} are applied once and only once before and after the study of the multi-turn effects. We shall see that A has the physical meaning of the Courant-Snyder parameters generalized to the nonlinear systems, that N contains information about tune dependence on the dynamical variables A_x, A_y, δ, and that N also contains information about the resonance strengths.

To demonstrate the normal form formalism for a nonlinear system, consider a second order map

$$M = e^{:f_2:}e^{:f_3:} \qquad (9.501)$$

Again, we are looking for a map N and a transformation A in the form of (9.500) so that N is simple. Let us first consider the second order transformation

$$A = e^{:F_3:}A_2 \qquad (9.502)$$

where A_2 is the linear transformation (9.482) which transforms the X-coordinates to the U-coordinates. Note we have chosen to write the two factor maps in the order as in Eq.(9.502) instead of a reversed order. The function F_3 is yet to be found.

After the transformation, we have

$$
\begin{aligned}
N &= AMA^{-1} = e^{:F_3(X):}A_2 e^{:f_2(X):}e^{:f_3(X):}A_2^{-1}e^{-:F_3(X):}\Big|_{X=U} \\
&= e^{:F_3(U):}e^{:f_2(A_2U):}e^{:f_3(A_2U):}e^{-:F_3(U):} \qquad (9.503)
\end{aligned}
$$

where use has been made of Eq.(9.476). The map $e^{:f_2(A_2U):}$ is a simple rotation map corresponding to Eq.(9.497). The function $f_2(A_2U)$ is a function only of A_x, A_y, and δ if one makes a further transformation (9.498).

We will deal exclusively with the U coordinates in the following developments. At a slight risk of confusion, we write $f_n(A_2U)$ as $f_n(U)$, or simply as

---

[60]This is away from resonances. When there is a resonance near by, there are complications. See later.

[61]Normal forms are not as useful for single pass devices such as a transport line.

f_n. To second order in U,

$$
\begin{aligned}
N &= e^{:f_2:}e^{-:f_2:}e^{:F_3:}e^{:f_2:}e^{:f_3:}e^{-:F_3:} \\
&= e^{:f_2:}\exp(:e^{-:f_2:}F_3:)e^{:f_3:}e^{-:F_3:} \\
&= e^{:f_2:}\exp[:(e^{-:f_2:}-1)F_3 + f_3:] + :\mathcal{O}(U^3): \quad (9.504)
\end{aligned}
$$

An inspection of Eq.(9.504) indicates that, at this point in an effort to make N as simple as possible, one would be tempted to choose F_3 as

$$
F_3 = \left(\frac{1}{1-e^{-:f_2:}}\right)f_3 \quad (9.505)
$$

so that the map N, to second order in U, is simply the linear map $e^{:f_2:}$. It however turns out that this cannot be done in general.[62] On the other hand, we can try to approach Eq.(9.505) as closely as possible as follows.

Consider a function $f_n(U)$, which is an n-th order homogeneous polynomial in the components of U (other than $\bar{z}$). It is possible to express $f_n(U)$ as

$$
f_n = \sum_{\substack{a,b,c,d,e=0 \\ a+b+c+d+e=n}}^{n} C^{(n)}_{abcd,e}|abcd,e\rangle \quad (9.506)
$$

where[9]

$$
\begin{aligned}
|abcd,e\rangle &\equiv (\sqrt{A_x}e^{i\phi_x})^a(\sqrt{A_x}e^{-i\phi_x})^b(\sqrt{A_y}e^{i\phi_y})^c(\sqrt{A_y}e^{-i\phi_y})^d\delta^e \\
&= A_x^{(a+b)/2}A_y^{(c+d)/2}e^{i(a-b)\phi_x}e^{i(c-d)\phi_y}\delta^e \quad (9.507)
\end{aligned}
$$

are the eigenmodes (sometimes referred to as the resonance basis) of $:f_2:$ with

$$
:f_2:\,|abcd,e\rangle = i[(a-b)\bar{\mu}_x + (c-d)\bar{\mu}_y]\,|abcd,e\rangle \quad (9.508)
$$

We have used the fact that $:f_2:$ leaves δ untouched.

It follows from the fact that $f_n(U)$ is a real function that

$$
C^{(n)}_{abcd,e}{}^* = C^{(n)}_{badc,e} \quad (9.509)
$$

In what follows, we will simplify the notations by dropping the bars on the normal mode frequencies $\bar{\mu}_{x,y}$. We will also drop the bars on $\bar{\alpha}_c$ and $\bar{z}$.

For f_3 we have

$$
f_3 = \sum_{a,b,c,d,e=0}^{3} C^{(3)}_{abcd,e}|abcd,e\rangle \quad (9.510)
$$

Using Eq.(9.508) the right-hand-side of Eq.(9.505) reads

$$
\left(\frac{1}{1-e^{-:f_2:}}\right)f_3 = \sum_{a,b,c,d,e} C^{(3)}_{abcd,e}\left[\frac{1}{1-e^{-i(a-b)\mu_x-i(c-d)\mu_y}}\right]|abcd,e\rangle \quad (9.511)
$$

---

[62]If this could be done, all of the nonlinear dynamics are contained simply in the boring coordinate transformation A. There would be no multi-turn effects to speak of any more.

The expression (9.511) is fine except for those terms in the summation when one finds zero demonimators:

$$e^{-i(a-b)\mu_x - i(c-d)\mu_y} = 1$$

$$\text{or} \quad (a-b)\frac{\mu_x}{2\pi} + (c-d)\frac{\mu_y}{2\pi} = \text{integer} \qquad (9.512)$$

There are two circumstances when the condition (9.512) occurs. One is when

$$a = b \quad \text{and} \quad c = d \qquad (9.513)$$

The other occurs only when a "resonance" condition is fulfilled[63], i.e.

$$m\frac{\mu_x}{2\pi} + n\frac{\mu_y}{2\pi} = p \qquad (9.514)$$

where m, n, and p are integers without common denominators. When Eq.(9.514) is satisfied, terms with

$$a - b = km, \quad \text{and} \quad c - d = kn \qquad (9.515)$$

must also be avoided, where k is any integer.

Since the choice of F_3 is at our disposal, we will choose it to be given by Eq.(9.511) *excluding* terms that give us trouble. In other words, we certainly exclude from the summation those terms corresponding to Eq.(9.513) and, when a resonance is uncomfortably close by, also those terms corresponding to Eq.(9.515). We postpone the discussion of the resonance terms till later. For now, let us consider the case away from resonances. In this case, we have

$$F_3 = \sum_{\substack{a,b,c,d,e=0 \\ a+b+c+d+e=3 \\ \text{unless } a=b \text{ and } c=d}}^{3} C_{abcd,e}^{(3)} \left[\frac{1}{1 - e^{-i(a-b)\mu_x - i(c-d)\mu_y}} \right] |abcd, e\rangle$$

$$(9.516)$$

which leads to

$$\begin{aligned}
(e^{-:f_2:} - 1)F_3 + f_3 &= \sum_{a,c,e} C_{aacc,e}^{(3)} |aacc, e\rangle \\
&= \sum_{a,c,e} C_{aacc,e}^{(3)} A_x^a A_y^c \delta^e \\
&= C_{0000,3}^{(3)} \delta^3 + C_{1100,1}^{(3)} A_x \delta + C_{0011,1}^{(3)} A_y \delta \equiv h_3 (9.517)
\end{aligned}$$

We have designated the above function as h_3.

Substituting Eq.(9.517) into Eq.(9.504) gives the simplest form of N, to second order in U, as

$$N = e^{:f_2:} e^{:h_3:} \qquad (9.518)$$

---

[63]Recall that $\mu_{x,y}$ here are really $\bar{\mu}_{x,y}$, the normal mode frequencies, which take into account the linear perturbations of the accelerator.

Both f_2 and h_3 are functions only of A_x, A_y, and δ. Note that h_3 contains only three terms in the summation, each proportional to $A_x\delta, A_y\delta$, and δ^3 respectively. Note also that since $:f_2:$ and $:h_3:$ commute, we can write

$$N = e^{:f_2+h_3:} \tag{9.519}$$

An inspection of Eqs.(9.501) and (9.518) indicates that the normal form transformation basically means dropping the oscillating terms from f_3, and keeping only the 0-th harmonic terms. The reason these 0-th harmonic terms can not be dropped is because it is impossible to find F_3 to transform them away.

The normal form procedure from Eq.(9.501) to Eq.(9.519) can be extended to higher orders. Consider a third order map

$$M = e^{:f_2(X):}e^{:f_3(X):}e^{:f_4(X):} \tag{9.520}$$

By making the transformation with

$$A = e^{:F_4(U):}e^{:F_3(U):}A_2 \tag{9.521}$$

we obtain

$$N = AMA^{-1} = e^{:F_4:}e^{:F_3:}e^{:f_2:}e^{:f_3:}e^{:f_4:}e^{-:F_3:}e^{-:F_4:} \tag{9.522}$$

All functions in Eq.(9.522) are expressed as functions of U. We choose F_3 to be given by Eq.(9.516).

To proceed, we need to go back to Eq.(9.504) and keep terms $\mathcal{O}(U^3)$. Consider the following:

$$
\begin{aligned}
e^{:F_3:}e^{:f_2:}e^{:f_3:}e^{-:F_3:} &= e^{:f_2:}(e^{-:f_2:}e^{:F_3:}e^{:f_2:})(e^{:f_3:}e^{-:F_3:}) \\
&= e^{:f_2:}\exp(:e^{-:f_2:}F_3:)[\exp(:f_3 - F_3 - \frac{1}{2}:f_3:F_3:)+:\mathcal{O}(U^4):] \\
&= e^{:f_2:}\Big\{ \exp[:e^{-:f_2:}F_3 + f_3 - F_3 - \frac{1}{2}:f_3:F_3 \\
&\quad -\frac{1}{2}:(f_3 - F_3):e^{-:f_2:}F_3] + :\mathcal{O}(U^4):\Big\} \\
&= e^{:f_2:}e^{:h_3:}e^{:g_4:} + :\mathcal{O}(U^4): \tag{9.523}
\end{aligned}
$$

where use has been made of the BCH formula (9.192), h_3 is given by Eq.(9.517), and we have introduced

$$g_4 = -\frac{1}{2}(:f_3: + :f_3:e^{-:f_2:} - :F_3:e^{-:f_2:})F_3 \tag{9.524}$$

By definition of h_3 in Eq.(9.517), Eq.(9.524) can also be written as

$$g_4 = -\frac{1}{2}[:f_3:F_3 + :(f_3 - F_3):h_3] \tag{9.525}$$

Having obtained Eq.(9.523), we have

$$
\begin{aligned}
e^{:F_3:}e^{:f_2:}e^{:f_3:}e^{:f_4:}e^{-:F_3:} &= (e^{:F_3:}e^{:f_2:}e^{:f_3:}e^{-:F_3:})(e^{:F_3:}e^{:f_4:}e^{-:F_3:}) \\
&= [e^{:f_2:}e^{:h_3:}e^{:g_4:} + :\mathcal{O}(U^4):][e^{:f_4:} + :\mathcal{O}(U^4):] \\
&= e^{:f_2:}e^{:h_3:}e^{:f_4+g_4:} + :\mathcal{O}(U^4): \tag{9.526}
\end{aligned}
$$

Substituting Eq.(9.526) into Eq.(9.522) gives

$$
\begin{aligned}
N &= e^{:F_4:}e^{:f_2:}e^{:h_3:}e^{:f_4+g_4:}e^{-:F_4:} \\
&= e^{:f_2:}\exp(:e^{-:f_2:}F_4:)e^{:h_3:}e^{:f_4+g_4:}e^{-:F_4:} \\
&= e^{:f_2:}e^{:h_3:}\exp[:(e^{-:f_2:}-1)F_4:+f_4+g_4:]+:\mathcal{O}(U^4): \quad (9.527)
\end{aligned}
$$

Following the steps which are by now familiar, we decompose

$$
f_4 + g_4 = \sum_{a,b,c,d,e}^{4} C^{(4)}_{abcd,e}|abcd,e\rangle \tag{9.528}
$$

and choose F_4 to be (away from resonances)

$$
F_4 = \sum_{\begin{cases} a,b,c,d,e=0 \\ a+b+c+d+e=4 \\ \text{unless } a=b \text{ and } c=d \end{cases}}^{4} C^{(4)}_{abcd,e}\left(\frac{1}{1-e^{-i(a-b)\mu_x-i(c-d)\mu_y}}\right)|abcd,e\rangle
$$

$$
\tag{9.529}
$$

Then, to third order, we have

$$
\begin{aligned}
N &= e^{:f_2:}e^{:h_3:}e^{:h_4:} \\
&= e^{:f_2+h_3+h_4:} \tag{9.530}
\end{aligned}
$$

where

$$
h_4 = \sum_{a,c,e} C^{(4)}_{aacc,e}A_x^a A_y^c \delta^e \tag{9.531}
$$

is a function of A_x, A_y, and δ. In general, h_4 contains six terms, proportional to δ^4, $A_x\delta^2$, $A_y\delta^2$, A_x^2, A_xA_y, and A_y^2, respectively. Knowing A_2, $F_3(U)$, and $F_4(U)$, the coordinate transformation A, given by Eq.(9.521), is obtained.

One can extend the procedure to higher orders and in general obtains an Ω-th order representation

$$
\begin{aligned}
M &= e^{:f_2(X):}e^{:f_3(X):}\ldots e^{:f_{\Omega+1}(X):} \\
A &= e^{:F_{\Omega+1}(U):}\ldots e^{:F_3(U):}A_2 \\
N &= e^{:f_2+h_3+h_4+\ldots\ h_{\Omega+1}:} \tag{9.532}
\end{aligned}
$$

where $f_2, h_3, \ldots, h_{\Omega+1}$ are functions of A_x, A_y, and δ only. Equation (9.532) is the normal form representation of the map M away from resonances.

Applications of normal forms as well as the effect of resonances are later subjects.

Exercise 86 In the absence of x-y coupling, Eqs.(9.483-9.497) have simpler forms. Let the linear part of the accelerator section be rep-

resented by the transformation matrix [see Eq.(9.96)]

$$
\mathbf{M} = \begin{bmatrix}
R_{11} & R_{12} & 0 & 0 & 0 & \eta - \eta' R_{11} - \eta' R_{12} \\
R_{21} & R_{22} & 0 & 0 & 0 & \eta' - \eta' R_{22} - \eta R_{21} \\
0 & 0 & R_{33} & R_{34} & 0 & 0 \\
0 & 0 & R_{43} & R_{44} & 0 & 0 \\
\eta' - \eta' R_{11} + \eta R_{21} & -\eta + \eta R_{22} - \eta' R_{12} & 0 & 0 & 1 & A_\eta \sin \mu_x - C\alpha_c \\
0 & 0 & 0 & 0 & 0 & 1
\end{bmatrix}
$$
$$(9.533)$$

where

$$
\begin{aligned}
R_{11} &= \cos \mu_x + \alpha_x \sin \mu_x \\
R_{12} &= \beta_x \sin \mu_x \\
R_{21} &= -\gamma_x \sin \mu_x \\
R_{22} &= \cos \mu_x - \alpha_x \sin \mu_x \\
R_{33} &= \cos \mu_y + \alpha_y \sin \mu_y \\
R_{34} &= \beta_y \sin \mu_y \\
R_{43} &= -\gamma_y \sin \mu_y \\
R_{44} &= \cos \mu_y - \alpha_y \sin \mu_y \\
A_\eta &= \gamma_x \eta^2 + 2\alpha_x \eta \eta' + \beta_x \eta'^2 \qquad (9.534)
\end{aligned}
$$

Find the matrix $\mathbf{A_2}$ and $f_2(A_2 U)$.

Solution One should first check that the symplectic condition (9.484) is satisfied (and it is) by the matrix M. The matrix map (9.533) has a Lie form $e^{:f_2(X):}$ with [See Eq.(9.95)]

$$
\begin{aligned}
f_2(X) &= -\frac{\mu_x}{2}[\gamma_x(x - \eta\delta)^2 + 2\alpha_x(x - \eta\delta)(x' - \eta'\delta) + \beta_x(x' - \eta'\delta)^2] \\
&\quad -\frac{\mu_y}{2}(\gamma_y y^2 + 2\alpha_y y y' + \beta_y y'^2) - \frac{1}{2}C\alpha_c \delta^2 \qquad (9.535)
\end{aligned}
$$

Following the procedure outlined in the text, we find

$$
U = \mathbf{A_2}^{-1} X = \begin{bmatrix}
\frac{x - \eta\delta}{\sqrt{\beta_x}} \\
\frac{\alpha_x(x - \eta\delta) + \beta_x(x' - \eta'\delta)}{\sqrt{\beta_x}} \\
\frac{y}{\sqrt{\beta_y}} \\
\frac{\alpha_y y + \beta_y y'}{\sqrt{\beta_y}} \\
z + \eta' x - \eta x' \\
\delta
\end{bmatrix}
$$

$$
\bar{\mu}_x = \mu_x, \quad \bar{\mu}_y = \mu_y, \quad \bar{\alpha}_c = \alpha_c
$$

$$
f_2(A_2 U) = -\frac{\mu_x}{2}(\bar{x}^2 + \bar{p}_x^2) - \frac{\mu_y}{2}(\bar{y}^2 + \bar{p}_y^2) - \frac{1}{2}C\alpha_c \delta^2 \quad (9.536)
$$

and

$$
\mathbf{A_2}^{-1} = \begin{bmatrix}
\frac{1}{\sqrt{\beta_x}} & 0 & 0 & 0 & 0 & -\frac{\eta}{\sqrt{\beta_x}} \\
\frac{\alpha_x}{\sqrt{\beta_x}} & \sqrt{\beta_x} & 0 & 0 & 0 & -\frac{\alpha_x\eta+\beta_x\eta'}{\sqrt{\beta_x}} \\
0 & 0 & \frac{1}{\sqrt{\beta_y}} & 0 & 0 & 0 \\
0 & 0 & \frac{\alpha_y}{\sqrt{\beta_y}} & \sqrt{\beta_y} & 0 & 0 \\
\eta' & -\eta & 0 & 0 & 1 & 0 \\
0 & 0 & 0 & 0 & 0 & 1
\end{bmatrix}
$$

$$
\mathbf{A_2} = \begin{bmatrix}
\sqrt{\beta_x} & 0 & 0 & 0 & 0 & \eta \\
-\frac{\alpha_x}{\sqrt{\beta_x}} & \frac{1}{\sqrt{\beta_x}} & 0 & 0 & 0 & \eta' \\
0 & 0 & \sqrt{\beta_y} & 0 & 0 & 0 \\
0 & 0 & -\frac{\alpha_y}{\sqrt{\beta_y}} & \frac{1}{\sqrt{\beta_y}} & 0 & 0 \\
-\frac{\alpha_x\eta+\beta_x\eta'}{\sqrt{\beta_x}} & \frac{\eta}{\sqrt{\beta_x}} & 0 & 0 & 1 & 0 \\
0 & 0 & 0 & 0 & 0 & 1
\end{bmatrix} (9.537)
$$

The matrix representation of the map N is

$$
\mathbf{N} = \mathbf{A_2}^{-1}\mathbf{MA_2} = \begin{bmatrix}
\cos\mu_x & \sin\mu_x & 0 & 0 & 0 & 0 \\
-\sin\mu_x & \cos\mu_x & 0 & 0 & 0 & 0 \\
0 & 0 & \cos\mu_y & \sin\mu_y & 0 & 0 \\
0 & 0 & -\sin\mu_y & \cos\mu_y & 0 & 0 \\
0 & 0 & 0 & 0 & 1 & -C\alpha_c \\
0 & 0 & 0 & 0 & 0 & 1
\end{bmatrix}
$$
$$(9.538)$$

Equation (9.533) gives the 6×6 matrix for one-turn map around a certain position in the circular accelerator. For completeness and later use, we give below the 6×6 matrix from position 1 to position 2:

$$
M = \begin{bmatrix}
R_{11} & R_{12} & 0 & 0 & 0 & \eta_2 - R_{11}\eta_1 - R_{12}\eta_1' \\
R_{21} & R_{22} & 0 & 0 & 0 & \eta_2' - R_{21}\eta_1 - R_{22}\eta_1' \\
0 & 0 & R_{33} & R_{34} & 0 & 0 \\
0 & 0 & R_{43} & R_{44} & 0 & 0 \\
A & B & 0 & 0 & 1 & C - A\eta_1 - B\eta_1' \\
0 & 0 & 0 & 0 & 0 & 1
\end{bmatrix}
$$

$$
R_{11} = \sqrt{\frac{\beta_{x2}}{\beta_{x1}}}[\cos\psi_x + \alpha_{x1}\sin\psi_x]
$$

$$
R_{12} = \sqrt{\beta_{x1}\beta_{x2}}\sin\psi_x
$$

$$
R_{21} = -\frac{1}{\sqrt{\beta_{x1}\beta_{x2}}}[(1 + \alpha_{x1}\alpha_{x2})\sin\psi_x - (\alpha_{x1} - \alpha_{x2})\cos\psi_x]
$$

$$
R_{22} = \sqrt{\frac{\beta_{x1}}{\beta_{x2}}}[\cos\psi_x - \alpha_{x2}\sin\psi_x]
$$

$$R_{33} = \sqrt{\frac{\beta_{y2}}{\beta_{y1}}}[\cos\psi_y + \alpha_{y1}\sin\psi_y]$$

$$R_{34} = \sqrt{\beta_{y1}\beta_{y2}}\sin\psi_y$$

$$R_{43} = -\frac{1}{\sqrt{\beta_{y1}\beta_{y2}}}[(1+\alpha_{y1}\alpha_{y2})\sin\psi_y - (\alpha_{y1}-\alpha_{y2})\cos\psi_y]$$

$$R_{44} = \sqrt{\frac{\beta_{y1}}{\beta_{y2}}}[\cos\psi_y - \alpha_{y2}\sin\psi_y]$$

$$A = R_{21}\eta_2 - R_{11}\eta_1' + \eta_1'$$

$$B = -R_{12}\eta_2' + R_{22}\eta_2 - \eta_1$$

$$C = -\int_{s_1}^{s_2} ds\,\frac{\eta(s)}{\rho(s)} \tag{9.539}$$

where ψ_x and ψ_y are the horizontal and vertical betatron phase advances from position 1 to position 2. As mentioned in Exercise 32, an explicit expression of the corresponding Lie representation can only be done transcendentally.

Exercise 87 Equations (9.506-9.509) are when $f_2(A_2U)$ is given by Eq.(9.499) for stable linear motion. If the system is linearly unstable [see Exercise 29], how are $f_2(A_2U)$ and Eqs.(9.506-9.509) modified? _Solution_ Note that, even though unstable, the system is symplectic. Note also that, unlike the stable case, these eigenmodes do not involve complex quantities.

Exercise 88 Show that in the normal form transformation (9.500) of a one-turn map $M(s)$ around the location s, the map N is s-independent. The s-dependence is contained in the coordinate transformation map A.

Exercise 89 Show that the Poisson bracket

$$[|a_1b_1c_1d_1, e_1\rangle, |a_2b_2c_2d_2, e_2\rangle] \tag{9.540}$$

$$= \frac{i}{2}(a_1b_2 - a_2b_1)\,|a_1+a_2-1, b_1+b_2-1, c_1+c_2, d_1+d_2, e_1+e_2\rangle$$

$$+ \frac{i}{2}(c_1d_2 - c_2d_1)\,|a_1+a_2, b_1+b_2, c_1+c_2-1, d_1+d_2-1, e_1+e_2\rangle$$

In particular, it follows that the operators $:e^{-i\phi_{x,y}}:$ can be regarded as lowering operators, while $:e^{i\phi_{x,y}}:$ have the meaning of raising operators.

Exercise 90 Equation (9.473), the Courant-Snyder transformation, has played a critical role leading to normal forms. However, it is not the only way to reach the normal forms. [more to be added]

9.9 Applications of Normal Forms Away From Resonances

Invariants   In the previous section, we transformed the nonlinear map M by a map A into a normal form N according to

$$N = AMA^{-1} \quad \text{or} \quad M = A^{-1}NA \tag{9.541}$$

We noted that, away from resonances, N has the form $e^{:h:}$ where h depends only on A_x, A_y, and δ out of the phase space coordinates $(\phi_x, A_x, \phi_y, A_y, z, \delta)$ [See Eq.(9.532)]. It follows that the quantities A_x, A_y and δ are invariant under the map N, i.e.,

$$NA_x = A_x, \quad NA_y = A_y, \quad N\delta = \delta \tag{9.542}$$

The quantities A_x, A_y, and δ are the three constants of the motion in the 3-D motion under the map M.

Let us consider the quantities

$$W_x = A^{-1}A_x \quad \text{and} \quad W_y = A^{-1}A_y \tag{9.543}$$

The meaning of the above operation is as follows: in order to obtain an expression of W_x, one first writes $A_x = \frac{1}{2}(\bar{x}^2 + \bar{p}_x^2)$, and then expresses $\bar{x}$ and $\bar{p}_x$ (components of the normalized coordinates U) in terms of the physical X components using $U = A^{-1}X$; the resulting expression in terms of the X coordinates is W_x. Similar meaning applies for W_y.

The two quantities $W_{x,y}$ are invariant under the map M, as can be seen as follows:

$$MW_x = A^{-1}NAW_x = A^{-1}NA_x = A^{-1}A_x = W_x \tag{9.544}$$

and similarly for W_y. As a particle's motion is observed turn after turn, the physical coordinates change but the values of W_x and W_y remain constant.

There is a third invariant, which is simply δ. Its invariance follows from the fact that M is independent of z. Particle motion in the 6-D $(x, p_x, y, p_y, z, \delta)$ phase space must stay on "surfaces" of constant W_x, W_y and δ.

Effective Hamiltonian   We next look for an expression of the effective Hamiltonian of the nonlinear system for the one-turn motion in the $(x, p_x, y, p_y, z, \delta)$ phase space. This is obtained by first writing $N = e^{:h(A_x, A_y, \delta):}$ and then noting

$$
\begin{aligned}
M &= A^{-1}NA = A^{-1}e^{:h(A_x, A_y, \delta):}A \\
&= \exp[:A^{-1}h(A_x, A_y, \delta):] = \exp[:h(A^{-1}A_x, A^{-1}A_y, A^{-1}\delta):] \\
&= e^{:h(W_x, W_y, \delta):}
\end{aligned}
\tag{9.545}
$$

This means $-h(W_x, W_y, \delta)$ is the effective Hamiltonian in the X phase space away from all resonances. The case when a resonance is close by will be addressed later. Suffice it to say here that then the effective Hamiltonian would contain additional terms.

Fixed point for an off-momentum particle For an on-momentum particle, the fixed point in the X space is simply the origin $X = 0$. Consider an off-momentum particle with $\delta = \delta_0 = $ constant. First note that the vector

$$U_0 = \begin{bmatrix} 0 \\ 0 \\ 0 \\ 0 \\ 0 \\ \delta_0 \end{bmatrix} \tag{9.546}$$

is transformed by N according to

$$NU\big|_{U=U_0} = \begin{bmatrix} 0 \\ 0 \\ 0 \\ 0 \\ z_1 \\ \delta_0 \end{bmatrix} \equiv U_1 \tag{9.547}$$

The vector U_1 differs from U_0 only in its z-component, and z_1 is some quantity whose exact form does not matter here. The first four components of U_1 vanish because N does not couple the three normal modes of U. Consider the vector

$$X_0 = AU\big|_{U=U_0} \tag{9.548}$$

We have

$$
\begin{aligned}
MX\big|_{X=X_0} &= AMU\big|_{U=U_0} = AA^{-1}NAU\big|_{U=U_0} \\
&= NAU\big|_{U=U_0} = AU\big|_{U=U_1}
\end{aligned}
\tag{9.549}
$$

In writing down the first step in Eq.(9.549), recall that the earlier Lie operators apply from the left. Since the first four components of the vector on the right hand side of Eq.(9.549) are the same as those of X_0, Eq.(9.549) shows that the first four components of X_0 form a fixed point, i.e. its position does not change turn after turn, in the (x, p_x, y, p_y) space for an off-momentum particle. This fixed point is closly related to the linear and the higher order dispersion functions.

Exercises 91 and 92 apply these analyses to 1-D and 3-D linear systems. Exercies 88 applies them to a nonlinear system.

> *Exercise* 91 Find explicit expressions of the invariant W_x and the effective one-turn Hamiltonian for a 1-D Courant-Snyder system.
> *Solution* The invariant W_x is obtained by substituting
>
> $$\bar{x} = \frac{1}{\sqrt{\beta}}x, \quad \bar{p}_x = \frac{1}{\sqrt{\beta}}(\alpha x + \beta p_x) \tag{9.550}$$

into the expressions

$$A_x = \frac{1}{2}(\bar{x}^2 + \bar{p}_x^2) \qquad (9.551)$$

The result is, as expected,

$$W_x = \frac{1}{2\beta}[x^2 + (\alpha x + \beta p_x)^2] \qquad (9.552)$$

The one-turn map for the system is given by Eq.(9.90). It follows that the effective Hamiltonian is

$$
\begin{aligned}
H &= -f_2 = \mu W_x = \frac{\mu}{2\beta}[x^2 + (\alpha x + \beta p_x)^2] \\
&= \frac{\mu}{2}(\gamma x^2 + 2\alpha x p_x + \beta p_x^2) \qquad (9.553)
\end{aligned}
$$

The effective Hamiltonian can be used to obtain the one-turn behavior of the variables x and p_x as follows:

$$
\begin{aligned}
\frac{dx}{dn} &= \frac{\partial H}{\partial p_x} = \mu(\alpha x + \beta p_x) \\
\frac{dp_x}{dn} &= -\frac{\partial H}{\partial x} = -\mu(\gamma x + \alpha p_x) \qquad (9.554)
\end{aligned}
$$

where n is a turn index which runs from 0 to 1 for one complete turn. Note that although the betatron functions α, β, and γ depend on the location around the accelerator, in the effective Hamiltonian description here, they are taken as constants in the turn index n. The result obtained applies only when the particle motion is observed at this particular location.

Equation (9.554) can be solved to yield

$$
\begin{aligned}
x(n) &= x(0)(\cos n\mu + \alpha \sin n\mu) + p(0)\beta \sin n\mu \\
p_x(n) &= -x(0)\gamma \sin n\mu + p(0)(\cos n\mu - \alpha \sin n\mu) \quad (9.555)
\end{aligned}
$$

When n is set to 1, one recovers map (9.87).

Exercise 92 Consider the 3-D linear system described in Exercise 86. Find expressions of the invariants W_x, W_y, the effective Hamiltonian, and the off-momentum fixed point.
Solution The connection between the physical coordinates $(x, p_x = x', y, p_y = y', z, \delta)$ and the normalized coordinates $(\bar{x}, \bar{p}_x, \bar{y}, \bar{p}_y, \bar{z}, \delta)$ is provided by Eq.(9.536). The two betatron invariants then have the expressions

$$
\begin{aligned}
W_x &= \frac{1}{2\beta_x}\{(x - \eta\delta)^2 + [\alpha_x(x - \eta\delta) + \beta_x(p_x - \eta'\delta)]^2\} \\
W_y &= \frac{1}{2\beta_y}[y^2 + (\alpha_y y + \beta_y p_y)^2] \qquad (9.556)
\end{aligned}
$$

The effective Hamiltonian is

$$
\begin{aligned}
H \;=\; & \frac{\mu_x}{2\beta_x}\{(x-\eta\delta)^2 + [\alpha_x(x-\eta\delta) + \beta_x(p_x - \eta'\delta)]^2 \\
& + \frac{\mu_y}{2\beta_y}[y^2 + (\alpha_y y + \beta_y p_y)^2] + \frac{1}{2}\alpha_c\delta^2
\end{aligned}
\tag{9.557}
$$

A somewhat lengthy but straightforward algebra similar to that of Eqs.(9.554-9.555) verifies that the Hamilton's equations using this effective Hamiltonian in the $(x, p_x, y, p_y, z, \delta)$ phase space recovers the map (9.533).

The off-momentum fixed point in the (x, p_x, y, p_y) space is, according to Eq.(9.548), given by the first four components of the vector $\mathbf{A_2}U_0$. With $\mathbf{A_2}$ given by Eq.(9.537) and U_0 by Eq.(9.546), it follows that the fixed point is simply

$$
\begin{bmatrix} x \\ p_x \\ y \\ p_y \end{bmatrix} = \delta_0 \begin{bmatrix} \eta \\ \eta' \\ 0 \\ 0 \end{bmatrix}
\tag{9.558}
$$

for a particle whose relative momentum error is $\delta = \delta_0$.

Exercise 93 Consider the linear system of Exercise 86. Let there be a static angular kick $\Delta x' = \theta$ at position $s = 0$ of this accelerator. Analyze the steady state motion of the particles.

Solution The one-turn map around $s = 0$ is given by the matrix M of Eq.(9.533), with $\alpha, \beta, \gamma, \eta$, and η' evaluated at the position $s = 0$. The steady state $(x, x', y, y', z, \delta)$ observed at the exit of the angular kick satisfies the condition

$$
M \begin{bmatrix} x \\ x' \\ y \\ y' \\ z \\ \delta \end{bmatrix} + \begin{bmatrix} 0 \\ \theta \\ 0 \\ 0 \\ 0 \\ 0 \end{bmatrix} = \begin{bmatrix} x \\ x' \\ y \\ y' \\ z_1 \\ \delta \end{bmatrix}
\tag{9.559}
$$

The quantity z_1 on the right hand side is not the same as z. This is because z does not have a steady state. We need to analyze the motion described by Eq.(9.559).

Obviously we have $y = 0, y' = 0$. The remaining of Eq.(9.559) can be written as

$$
\begin{aligned}
& R_{11}(x-\eta\delta) + R_{12}(x'-\eta'\delta) = (x-\eta\delta) \\
& R_{21}(x-\eta\delta) + R_{22}(x'-\eta'\delta) + \theta = (x'-\eta'\delta) \\
& (\eta' - \eta'R_{11} + \eta R_{21})x + (-\eta + \eta R_{22} - \eta'R_{12})x' + z \\
& \qquad + (-C\alpha_c + A_\eta \sin\mu_x)\delta = z_1
\end{aligned}
\tag{9.560}
$$

where the definitions of the various quantities can be found with Eq.(9.533).

The first two of Eq.(9.560) can be solved for x and x',

$$
\begin{aligned}
x &= \frac{\theta}{2}\beta_x \cot\frac{\mu_x}{2} + \eta\delta \\
x' &= \frac{\theta}{2}(1 - \alpha_x \cot\frac{\mu_x}{2}) + \eta'\delta
\end{aligned}
\tag{9.561}
$$

These give the closed-orbit displacement of the beam particles in the accelerator observed at the exit of the angular kick. The third equation in (9.560) gives the path length slippage per turn in the "steady state". When x and x' are substituted using Eq.(9.561), one obtains

$$
z_1 - z = -C\alpha_c\delta - \eta\theta
\tag{9.562}
$$

The path length slips by $-C\alpha_c\delta$ due to a momentum error, and by $-\eta\theta$ due to an angular kick θ, and this slippage occurs every turn.

Note that a kick in x' is therefore intrinsically coupled to the longitudinal motion. This intrinsic link is a necessary consequence of the symplecticity of the system. This coupling does not occur in the y-dimension.

Exercise 94 Replace the horizontal angular kick of Exercise 93 by a thin-lens sextupole of strength λ. Find the dispersion functions at the exit of the sextupole to order δ^2.

Tune shift and chromaticity   In the previous two sections, we have developed a normal form scheme away from resonances. In terms of the canonical coordinates $U = (\phi_x, A_x, \phi_y, A_y, z, \delta)$, we showed that, away from resonances, a nonlinear map can be transformed into a simple form

$$
N = e^{-:H(A_x, A_y, \delta):}
\tag{9.563}
$$

where H is the effective Hamiltonian. The Hamilton equations of motion read

$$
\begin{aligned}
\frac{d\phi_x}{dn} &= \frac{\partial H}{\partial A_x}, & \frac{dA_x}{dn} &= -\frac{\partial H}{\partial \phi_x} \\
\frac{d\phi_y}{dn} &= \frac{\partial H}{\partial A_y}, & \frac{dA_y}{dn} &= -\frac{\partial H}{\partial \phi_y} \\
\frac{dz}{dn} &= \frac{\partial H}{\partial \delta}, & \frac{d\delta}{dn} &= -\frac{\partial H}{\partial z}
\end{aligned}
\tag{9.564}
$$

where n is the turn index which runs from 0 to 1 for one turn.

Since H is independent of ϕ_x, ϕ_y, and z, it follows from Eq.(9.564) that A_x, A_y, and δ are constants of the motion. With $H = H(A_x, A_y, \delta)$, the effective Hamiltonian H is a constant of the motion. It then follows that $d\phi_x/dn, d\phi_y/dn$,

and dz/dn are constants independent of n. Integrations over one turn then give the one-turn map which reads

$$\Delta\phi_x = \frac{\partial H}{\partial A_x}, \qquad \Delta A_x = 0$$

$$\Delta\phi_y = \frac{\partial H}{\partial A_y}, \qquad \Delta A_y = 0$$

$$\Delta z = \frac{\partial H}{\partial \delta}, \qquad \Delta\delta = 0 \qquad (9.565)$$

where Δ of a quantity means the change of this quantity over one turn. In particular, the phases $\phi_{x,y}$ and z advance by an amount specified by Eq.(9.565) per iteration of the map. These advances depend on the values of $A_{x,y}$ and δ, which are invariant under the application of the map.

If the map being considered is a one-turn map around a circular accelerator, one can identify the *tunes* to be

$$\nu_x(A_x, A_y, \delta) = \frac{\Delta\phi_x}{2\pi} = \frac{1}{2\pi}\frac{\partial H}{\partial A_x}$$

$$\nu_y(A_x, A_y, \delta) = \frac{\Delta\phi_y}{2\pi} = \frac{1}{2\pi}\frac{\partial H}{\partial A_y} \qquad (9.566)$$

Different particles with different $A_{x,y}$ and δ have dirfferent tunes. The dependences of the tunes on $A_{x,y}$ are called the *detuning* effects. The dependences on δ are called the *chromaticities*.

We showed earlier that, to third order in U, the effective Hamiltonian, away from resonances, can be written as [see Eqs.(9.517) and (9.530-9.531)]

$$
\begin{aligned}
H &= -f_2 - h_3 - h_4 \\
f_2 &= -\mu_x A_x - \mu_y A_y - \frac{1}{2}\alpha_c\delta^2 \\
h_3 &= -C_{x1}A_x\delta - C_{y1}A_y\delta - C_3\delta^3 \\
h_4 &= -C_{xx}A_x^2 - C_{xy}A_xA_y - C_{yy}A_y^2 - C_{x2}A_x\delta^2 - C_{y2}A_y\delta^2 - C_4\delta^4
\end{aligned}
\qquad (9.567)
$$

where $\mu_{x,y}/2\pi$ are the *unperturbed* tunes of the linear system. This gives, using Eq.(9.566),

$$\nu_x(A_x, A_y, \delta) = \frac{1}{2\pi}(\mu_x + C_{x1}\delta + 2C_{xx}A_x + C_{xy}A_y + C_{x2}\delta^2)$$

$$\nu_y(A_x, A_y, \delta) = \frac{1}{2\pi}(\mu_y + C_{y1}\delta + C_{xy}A_x + 2C_{yy}A_y + C_{y2}\delta^2) \quad (9.568)$$

In particular, the chromatic effects are seen by setting $A_x = A_y = 0$:

$$\nu_x(\delta) = \frac{1}{2\pi}(\mu_x + C_{x1}\delta + C_{x2}\delta^2)$$

$$\nu_y(\delta) = \frac{1}{2\pi}(\mu_y + C_{y1}\delta + C_{y2}\delta^2) \qquad (9.569)$$

and the detuning effects are seen by setting $\delta = 0$:

$$
\begin{aligned}
\nu_x(A_x, A_y) &= \frac{1}{2\pi}(\mu_x + 2C_{xx}A_x + C_{xy}A_y) \\
\nu_y(A_x, A_y) &= \frac{1}{2\pi}(\mu_y + C_{xy}A_x + 2C_{yy}A_y)
\end{aligned}
\tag{9.570}
$$

When $A_x = A_y = 0$ and $\delta = 0$, the tunes are of course just given by $\mu_{x,y}/2\pi$. Note that all terms contained in Eq.(9.568) appear in either Eq.(9.569) or Eq.(9.570). This however is not true to higher orders because then there will be synchro-betatron coupling terms that involve both $A_{x,y}$ and δ in the tune expressions. Note also from Eq.(9.570) that the A_x-dependence of ν_y is the same as the A_y-dependence of ν_x — both are described by the coefficient C_{xy}.

The Hamiltonian (9.567) also describes the behavior of the path length according to

$$
\Delta z = \alpha_c \delta + 3C_3 \delta^2 + 4C_4 \delta^3 + C_{x1}A_x + C_{y1}A_y + 2C_{x2}A_x\delta + 2C_{y2}A_y\delta \tag{9.571}
$$

The path length change per revolution depends on the betatron amplitudes $A_{x,y}$ and δ. In particular, the A_x-dependence of Δz is the same as the δ-dependence of ν_x and the A_y-dependence of Δz is the same as the δ-dependence of ν_y. Chromaticities are therefore intimately related to the dynamics of the path length!

Smooth approximation Applications of the results in this section can be found later when we discuss more on single sextupole and the beam-beam interaction. In what follows below, we will introduce a tune shift treatment, sometimes called the *smooth approximation*, which does not use the Lie language. A comparison will then be made with what is obtained using the Lie language. For the tune shift considerations, we will ignore the resonance effects, even though the smooth approximation applies to the case of isolated resonances as well.

Consider a 1-D motion of a particle described by the equation

$$
x'' + K(s)x = f(x, s) \tag{9.572}
$$

where $K(s)$ is the focusing function of the linear, unperturbed accelerator environment, $f(x, s)$ is a perturbation that depends on the instantaneous displacement of the particle x and the position coordinate s. The perturbation $f(x, s)$ is considered to be periodic in s with period $2\pi R$, the circumference of the accelerator. The system can be described by the Hamiltonian[64]

$$
H(x, p_x, s) = \frac{1}{2}p_x^2 + \frac{1}{2}K(s)x^2 - \int_0^x dx' f(x', s) \tag{9.573}
$$

---

[64]Do not write (9.573) with p_x replaced by x'. The fact that $p_x = x'$ is a *consequence* of the Hamiltonian (9.573). Replacing p_x by x' at the Hamiltonian level is a misuse of the Hamiltonian.

Let us start with the equation of motion (9.572). We learned from the Courant-Snyder treatment that the problem simplifies if we introduce the transformation

$$x = \sqrt{\beta(s)}\, u$$
$$\theta = \frac{\psi(s)}{\nu} = \frac{1}{\nu} \int_0^s \frac{ds'}{\beta(s')} \qquad (9.574)$$

where $\beta(s)$ is the unperturbed β-function found in the absence of $f(x,s)$, and ν is the unperturbed tune. With Eq.(9.574), the dynamic variable x is replaced by u, and the independent time-variable s becomes θ. The functions $\beta(s), K(s)$ and $f(x,s)$ become $\beta(\theta), K(\theta)$ and $f(u,\theta)$, and are periodic in θ with period 2π. Equation (9.572) in the new variables reads

$$\frac{d^2 u}{d\theta^2} + \nu^2 u = \nu^2 \beta^{3/2}(\theta) f(u,\theta) \equiv F(u,\theta) \qquad (9.575)$$

In the absence of perturbation, u is described by a simple harmonic motion in θ. This means we can write

$$u = \sqrt{2A} \sin \phi \qquad (9.576)$$

and

$$\frac{du}{d\theta} = \nu \sqrt{2A} \cos \phi \qquad (9.577)$$

where A and $d\phi/d\theta = \nu$ are constants. With a perturbation, we could insist on the action-angle transformation of the form (9.576-9.577) except that A and $d\phi/d\theta$ now depend on θ and we need to solve for them. To do so, first note that by substituting (9.576) into (9.577), one obtains a self-consistency condition

$$\frac{1}{2}\frac{dA}{d\theta}\sin\phi + \left(\frac{d\phi}{d\theta} - \nu\right)A\cos\phi = 0 \qquad (9.578)$$

Secondly, substituting Eqs.(9.576-9.577) into Eq.(9.575) gives another condition

$$\frac{1}{2}\frac{dA}{d\theta}\cos\phi - \left(\frac{d\phi}{d\theta} - \nu\right)A\sin\phi = \frac{\sqrt{A}}{\sqrt{2}\nu}F(\sqrt{2A}\sin\phi, \theta) \qquad (9.579)$$

Equations (9.578-9.579) can be combined to give

$$\begin{aligned}
\frac{dA}{d\theta} &= \frac{\sqrt{2A}}{\nu}\cos\phi\, F(\sqrt{2A}\sin\phi, \theta) \\
\frac{d\phi}{d\theta} &= \nu - \frac{1}{\nu\sqrt{2A}}\sin\phi\, F(\sqrt{2A}\sin\phi, \theta)
\end{aligned} \qquad (9.580)$$

Effectively we have decomposed a second order differential equation (9.575) of one variable u into two first order differential equations (9.580) of two variables A and ϕ. So far no approximations have been made; Eq.(9.580) is exact.

If the perturbation is sufficiently weak, the quantities A and $d\phi/d\theta$ are approximately constants of the motion, i.e. they change slowly with time variable θ. We can approximate the expressions (9.580) by keeping only the slowly varying terms and dropping all fast oscillating terms on the right hand sides. In other words, we make the "smooth approximation"

$$
\begin{aligned}
\frac{dA}{d\theta} &\approx \frac{\sqrt{2A}}{\nu}\langle\cos\phi\ F(\sqrt{2A}\sin\phi,\theta)\rangle \\
\frac{d\phi}{d\theta} &\approx \nu - \frac{1}{\nu\sqrt{2A}}\langle\sin\phi\ F(\sqrt{2A}\sin\phi,\theta)\rangle
\end{aligned}
\tag{9.581}
$$

where the angular brackets mean the smoothing procedure. Fast and slow refer to a comparison with the revolutions. The angular variables θ and ϕ are considered to be fast variables, while the changes in A and $d\phi/d\theta$ per revolution are considered to be slow for sufficiently weak perturbations.

Consider the case when the tune is away from resonances. The smoothing in this case is obtained by a straightforward averaging over the angular variables θ and ϕ, i.e.

$$
\langle\ \rangle = \frac{1}{4\pi^2}\int_0^{2\pi}d\phi\int_0^{2\pi}d\theta
\tag{9.582}
$$

After averaging, Eq.(9.581) becomes

$$
\begin{aligned}
\frac{dA}{d\theta} &\approx 0 \\
\frac{d\phi}{d\theta} &\approx \nu - \frac{1}{4\pi^2\nu\sqrt{2A}}\int_0^{2\pi}d\phi\int_0^{2\pi}d\theta\sin\phi\ F(\sqrt{2A}\sin\phi,\theta)
\end{aligned}
\tag{9.583}
$$

The reason $dA/d\theta$ vanishes is that $F(\sqrt{2A}\sin\phi,\theta)$ is an even function in $\phi' \equiv \phi - \frac{\pi}{2}$; the product $\cos\phi\ F(\sqrt{2A}\sin\phi,\theta)$ is an odd function of ϕ' which averages to zero. The fact that we are averaging θ and ϕ independently of each other assumes that they are not correlated in some way. Such correlations would be a consequence of resonances, which we ignore in this section, but will be discussed following Eq.(9.672).

Equation (9.583) says that the action variable A is approximately a constant of the motion even in the presence of (weak) perturbations provided the unperturbed tune is away from resonances. The quantity $d\phi/d\theta$, which assumes the physical meaning of the perturbed tune, depends on A. The motion of particles in the polar $(\sqrt{2A},\phi)$ phase space is such that particles move along circles of $\sqrt{2A}=$ constant with constant angular speeds. This constant angular speed, however, is different for different particles, creating a sheering effect on the distribution of particles in the phase space. The dependence of the perturbed tune on A specifies the detuning effect. The tune shift is given by

$$
\Delta\nu(A) = -\frac{1}{4\pi^2\nu\sqrt{2A}}\int_0^{2\pi}d\phi\int_0^{2\pi}d\theta\sin\phi\ F(\sqrt{2A}\sin\phi,\theta)
\tag{9.584}
$$

From Eq.(9.584), one notes that if the perturbation $f(x,s)$ is an even function of x, then to first order of the perturbation, the tune shift vanishes. Since

the perturbation due to sextupoles, decapoles, etc. are even in x, these multipoles do not contribute to tune shifts for on-momentum particles to first order of their strengths. Quadrupoles, octupoles, and the beam-beam force, on the other hand, do contribute to first order tune shifts.

Noting the fact that the action and angle variables are canonical variables, one can cast Eq.(9.583) in a Hamiltonian form. Indeed, with the Hamiltonian

$$H = \nu A - \frac{1}{4\pi^2 \nu} \int_0^{2\pi} d\phi \int_0^{2\pi} d\theta \sin\phi \int_0^A \frac{dA'}{\sqrt{2A'}} F(\sqrt{2A'}\sin\phi, \theta) \qquad (9.585)$$

Eq.(9.584) is recovered by the Hamilton equations

$$\frac{d\phi}{d\theta} = \frac{\partial H}{\partial A} \quad \text{and} \quad \frac{dA}{d\theta} = -\frac{\partial H}{\partial \phi} = 0 \qquad (9.586)$$

Since the Hamiltonian H is independent of the time-variable θ, it is a constant of the motion. The system is solvable, or "integrable", away from resonances.[65] The Hamiltonian (9.585) is in fact simply the Hamiltonian (9.573) averaged over θ and ϕ, i.e., (9.585) is (9.573) after smoothing.

Let us consider a few examples. Consider first a thin-lens error quadrupole with focal length f located as the position $s = 0$ in the circular accelerator. In this case, we have

$$f(x, s) = -\frac{x}{f}\delta_p(s) \qquad (9.587)$$

where $\delta_p(s)$ is the periodic δ-function with period $2\pi R$. The kick a particle receives as it traverses the error quadrupole is $\Delta x' = -x/f$. This means

$$F(u, \theta) = \nu^2 \beta^{3/2}(0) f(u, \theta) = -\nu\beta(0)\frac{u}{f}\delta_p(\theta) \qquad (9.588)$$

Substitution into Eq.(9.584) yields

$$\Delta\nu \approx \frac{\beta(0)}{4\pi f} \qquad (9.589)$$

which is a familiar result of accelerator optics. In particular, in this case, $\Delta\nu$ is independent of A.

Now consider a more complex problem, namely the case of a thin-lens error octupole with

$$f(x, s) = \epsilon x^3 \delta_p(s) \qquad (9.590)$$

Substititing into Eq.(9.584) gives

$$\Delta\nu \approx -\frac{1}{2\pi^2}\epsilon\beta^2(0)A \int_0^{2\pi} d\phi \cos^4\phi = -\frac{3}{8\pi}\epsilon\beta^2(0)A \qquad (9.591)$$

This tune shift is proportional to the action A.

---

[65]The fact that H is also independent of ϕ gives the additional nice feature $A = \text{const}$, but this property is not a necessary condition for the system to be called integrable.

Computing tune shifts "physically" It may be instructive at this point to make the following observation. If one is given a perturbation such as that given by Eq.(9.590) and is asked to calculate the tune shift, and had he not known the smooth approximation, what would he do? First, he might note that the focusing effect changes from turn to turn, so some kind of averaging would be unavoidable in order to calculate the tune shift, and he would have to first introduce an "instantaneous" tune and then try to average it over many turns. Naively, the first quantity that comes to mind to be averaged is the force, because the force is what is "physically" applied to the particle. The instantaneous force is given by $f(x, s)$, which is proportional to x^3. Now since x is basically sinusoidal in time s, the average of the force over many turns is zero, which of course gives a wrong answer.

One might then consider perhaps the averaging should be performed over the "gradient" of the force. Although the gradient is not what the particle experience directly, the intuition of averaging over the gradient may be supported by the direct link between tune shift and gradient, as Eq.(9.589) suggests. One then computes the gradient which is connected to an instantaneous focal length f with $1/f = -3\epsilon x^2$. Substituting into Eq.(9.589) and averaging over ϕ give

$$\Delta \nu \approx \frac{\beta(0)}{4\pi} \langle -3\epsilon x^2 \rangle = -\frac{3}{4\pi} \epsilon \beta^2(0) A \tag{9.592}$$

This result gets closer to (9.591) but still is wrong!

The right answer, surprisingly, is effectively to average over the *potential* of the force, i.e. the average should be performed over the integral of the force

$$V(x, s) = -\int_0^x dx' f(x', s) \tag{9.593}$$

instead of either the force itself or the derivative (the gradient) of the force. Noting the fact that the potential is a term contained in the Hamiltonian, one then recognizes that what is being averaged over is the Hamiltonian.[66] In fact, that was what we observed in the smooth approximation developed from Eq.(9.572) to Eq.(9.586). Indeed, the averaged potential is given by

$$\langle V \rangle = -\epsilon \beta^2(0) A^2 \langle \sin^4 \phi \rangle \delta_p(s) = -\frac{3}{8} \epsilon \beta^2(0) A^2 \delta_p(s) \tag{9.594}$$

In terms of the potential V, the tune shift (9.584) can be written as

$$\Delta \nu = \frac{1}{2\pi} \int ds \frac{\partial \langle V \rangle}{\partial A} \tag{9.595}$$

Substituting Eq.(9.594) into Eq.(9.595), we recover the correct tune shift (9.591). As funny looking as Eq.(9.595) is, it gives the right answer.

---

[66]Who says Hamiltonian is merely a mathematical construct?

Tune shift using Lie algebra   Now let us try to connect these results to Lie analysis. Consider the case when the perturbation is localized, i.e., let

$$f(x, s) = \epsilon(x)\delta_p(s) \tag{9.596}$$

The tune shift, Eq.(9.584) or Eq.(9.595), reads

$$\Delta\nu(A) = -\frac{\sqrt{\beta(0)}}{4\pi^2\sqrt{2A}} \int_0^{2\pi} d\phi \sin\phi \, \epsilon(\sqrt{2A\beta(0)}\sin\phi) \tag{9.597}$$

The Hamiltonian (9.585) reads

$$H = \nu A - \frac{1}{4\pi^2} \int_0^{2\pi} d\phi \int_0^{\sqrt{2A\beta(0)}\sin\phi} dx' \epsilon(x') \tag{9.598}$$

This system can also be described in the Lie language. If one observes the particle motion at the exit of the perturbation, the one-turn map, in the (ϕ, A) phase space, is

$$e^{:-2\pi\nu A:} \exp\left[: \int_0^{\sqrt{2A\beta(0)}\sin\phi} dx' \epsilon(x'):\right] \tag{9.599}$$

To first order in the perturbation strength, this map can be concatenated to yield

$$\exp\left[: -2\pi\nu A + \left(\frac{:-2\pi\nu A:}{1 - e^{:2\pi\nu A:}}\right) \int_0^{\sqrt{2A\beta(0)}\sin\phi} dx' \epsilon(x'):\right] \tag{9.600}$$

Let us decompose

$$\int_0^{\sqrt{2A\beta(0)}\sin\phi} dx' \epsilon(x') = \sum_{k=-\infty}^{\infty} C_k(A) e^{ik\phi} \tag{9.601}$$

then we have

$$\left(\frac{:-2\pi\nu A:}{1 - e^{:2\pi\nu A:}}\right) \int_0^{\sqrt{2A\beta(0)}\sin\phi} dx' \epsilon(x') = \sum_{k=-\infty}^{\infty} C_k(A) \left(\frac{2\pi k\nu}{1 - e^{-2\pi k\nu}}\right) e^{ik\phi} \tag{9.602}$$

Away from resonances, terms with $k \neq 0$ can be transformed away by a normal form analysis. After the transformation, the map (9.600) becomes

$$N = \exp[: -2\pi\nu A + C_0(A):] \tag{9.603}$$

where

$$C_0(A) = \frac{1}{2\pi} \int_0^{2\pi} d\phi \int_0^{\sqrt{2A\beta(0)}\sin\phi} dx' \epsilon(x') \tag{9.604}$$

This map is of course described by the effective Hamiltonian (9.598), and it has the tune shift (9.597). The actual normal form transformations are short circuited here. This connects the Lie analysis and the smooth approximation at least away from resonances. Note that it is the 0-th Fourier harmonic of the potential (9.601) that contributes to the tune shift away from resonances.

Exercise 95 As a somewhat trivial exercise of a tune shift effect, consider a simple harmonic oscillator. The map that brings the canonical coordinates (ϕ, A) from $t = 0$ to t is

$$M = e^{:-\omega A t:} \tag{9.605}$$

where ω is the rotation frequency of the oscillator. One has

$$M\phi = \phi + \omega t \qquad \text{and} \qquad MA = A \tag{9.606}$$

which means the map can be written as

$$\phi(t) = \phi(0) + \omega t \qquad \text{and} \qquad A(t) = A(0) \tag{9.607}$$

as expected.

One can also describe the system in terms of the Hamiltonian language with the Hamiltonian

$$H = \omega A \tag{9.608}$$

Indeed, the Hamilton equations read

$$\dot{\phi} = \frac{\partial H}{\partial A} = \omega \qquad \text{and} \qquad \dot{A} = -\frac{\partial H}{\partial \phi} = 0 \tag{9.609}$$

Now describe the system in a rotating frame which has a rotation frequency Ω so that the oscillator has an angular frequency of $\omega - \Omega$. Describe it in both the Lie and the Hamiltonian languages.

Solution In the Hamiltonian language, we introduce a generating function G which transforms the coordinates from (ϕ, A) to (ϕ', A'), where

$$G(\phi, A', t) = (\phi - \Omega t)A' \tag{9.610}$$

The new coordinates are then related to the old ones by

$$\phi' = \frac{\partial G}{\partial A'} = \phi - \Omega t \qquad \text{and} \qquad A = \frac{\partial G}{\partial \phi} = A' \tag{9.611}$$

The new Hamiltonian is

$$H' = H + \frac{\partial G}{\partial t} = (\omega - \Omega)A \tag{9.612}$$

The new equations of motion are

$$\dot{\phi}' = \omega - \Omega \qquad \text{and} \qquad \dot{A}' = 0 \tag{9.613}$$

In the Lie language, the old map is given by Eq.(9.605). The coordinate transformation can be described by the Lie map [See the coordinate shift map of Table 4]

$$R(t) = e^{:\Omega A t:}$$
$$\implies \quad R\phi = \phi - \Omega t = \phi' \quad \text{and} \quad RA = A = A' \tag{9.614}$$

The new map must involve a transformation from the new coordinates to the old ones at time $t = 0$ and from the old coordinates back to the new ones at time t, i.e.,

$$M' = R(t)MR^{-1}(0) \qquad (9.615)$$

Note that because the coordinate transformation depends on time, the map is not transformed according to a similarity transformation as prescribed, e.g., by Eq.(9.61).

Substituting R from Eq.(9.614) and M from Eq.(9.605) into Eq.(9.615) gives

$$M' = e^{:\Omega At:}e^{:-\omega At:} = e^{:-(\omega-\Omega)At:} \qquad (9.616)$$

which is consistent with the new Hamiltonian (9.612). This exercise will be used later when we discuss the effects of resonances.

Exercise 96 Consider an accelerator with uniform focusing and a uniform distribution of octupole error. The equation of motion is

$$\frac{d^2x}{d\theta^2} + \nu^2 x = \epsilon x^3 \qquad (9.617)$$

the tune shift can be obtained from Eq.(9.584),

$$\Delta\nu = -\frac{\epsilon A}{\pi\nu}\int_0^{2\pi} d\phi \sin^4\phi = -\frac{3\epsilon A}{4\nu} \qquad (9.618)$$

But Eq.(9.617) — when the perturbation is uniformly distributed — can be solved exactly. Show that the tune shift (9.618) agrees with this exact solution to first order in ϵ.

Solution Equation (9.617) has a constant of the motion, which we designate as $\nu^2 A$, namely

$$\frac{1}{2}(\frac{dx}{d\theta})^2 + \frac{\nu^2}{2}x^2 - \frac{\epsilon}{4}x^4 = \text{constant} = \nu^2 A \qquad (9.619)$$

Equation (9.619) gives

$$\frac{dx}{d\theta} = \pm\sqrt{2\nu^2 A - \nu^2 x^2 + \frac{\epsilon}{2}x^4} \qquad (9.620)$$

Integrating the periodic motion (9.620) gives a period

$$\Theta = 4\int_0^{\hat{x}} \frac{dx}{\sqrt{2\nu^2 A - \nu^2 x^2 + \frac{\epsilon}{2}x^4}} \qquad (9.621)$$

where $\hat{x}$ is the peak amplitude of the motion with

$$2\nu^2 A - \nu^2 \hat{x}^2 + \frac{\epsilon}{2}\hat{x}^4 = 0 \qquad (9.622)$$

Equation (9.621) gives an exact expression of the tune shift $\Delta\nu$. When $\epsilon = 0$, the unperturbed case has

$$\hat{x}_0 = \sqrt{2A} \quad \text{and} \quad \Theta_0 = \frac{2\pi}{\nu} \qquad (9.623)$$

When $\epsilon \neq 0$, the perturbed tune is related to Θ by

$$\nu + \Delta\nu = \frac{2\pi}{\Theta} \qquad (9.624)$$

To compute $\Delta\nu$, we need to compute Θ of Eq.(9.621). We will do this to first order in ϵ. By a change of variable from x to u, where

$$u = x^2 - \frac{\epsilon}{2\nu^2}x^4$$

$$\implies \quad dx = \frac{du}{2\sqrt{u}}\left(1 + \frac{3\epsilon}{4\nu^2}u + \mathcal{O}(\epsilon^2)\right) \qquad (9.625)$$

we find

$$\begin{aligned} \Theta &= \frac{2}{\nu}\int_0^{2A} du \frac{1 + \frac{3\epsilon}{4\nu^2}u}{\sqrt{u(2A - u)}} \\ &= \frac{2\pi}{\nu}\left(1 + \frac{3\epsilon}{4\nu^2}A\right) \end{aligned} \qquad (9.626)$$

Substituting into Eq.(9.624) gives a tune shift which agrees with Eq.(9.618).

Exercise 97 Refer to Eq.(9.325). Find the dependence of the synchrotron tune on the synchrotron oscillation amplitude.

Exercise 98 Find the tune shifts in the presence of a 1-D single thin-lens octupole.

Exercise 99 3-D analysis of the fringe field effects of a thick quadrupole on tune shifts.

9.10 Isolated Resonances

The normal form analysis so far applies when the betatron frequencies are away from resonances. When a resonance condition [See Eq.(9.514)]

$$m\nu_x + n\nu_y = p \qquad (9.627)$$

is valid or approximately valid, we have to modify our analysis. We will consider the idealized situation when there is one and only one isolated resonance near

298

by. We will not discuss the case with two or more interplaying resonances. This idealization excludes the study of chaos.[67]

First consider a second order map (9.501). We have described a normal form analysis of this map, and shown that it can be transformed into the form of Eq.(9.504). We next decompose f_3 according to Eq.(9.510). Away from resonances, we choose F_3 according to Eq.(9.516). Near a resonance, the normal form analysis as described so far must be modified. In this case, the "simplest possible" form of the map no longer gives an effective Hamiltonian that depends only on A_x, A_y, and δ. In stead, the "simplest" form is now more complicated. Near a resonance, we now choose F_3 similarly to Eq.(9.516) except that terms excluded from the summation are not only those with ($a = b$ and $c = d$), but also those resonant terms satisfying ($a - b = km$ and $c - d = kn$) for some integer k. We then have

$$(e^{-:f_2:} - 1)F_3 + f_3 = h_3 + h_3^{(r)} \tag{9.628}$$

where h_3 has been defined in Eq.(9.517) and is a function of A_x, A_y and δ only. The function $h_3^{(r)}$ is given by

$$h_3^{(r)} = \sum_k \sum_{a,c,e} C_{a,a-km,c,c-kn,e}^{(3)} A_x^{a-\frac{1}{2}km} A_y^{c-\frac{1}{2}kn} e^{ik(m\phi_x + n\phi_y)} \delta^e \tag{9.629}$$

The summations in Eq.(9.629) contains terms that satisfy the conditions

$$k \neq 0$$
$$2a + 2c - k(m + n) + e = 3$$
$$0 \leq a, a - km, \ c, c - kn, e \leq 3 \tag{9.630}$$

The reason the $k = 0$ terms are excluded from the summation is because they have already been included in h_3.

We see now that the "simplest" form depends not only A_x, A_y and δ, but also on ϕ_x, ϕ_y. However, it is important to note that it is only the combined variable $m\phi_x + n\phi_y$ that appears in the normal form.

Take the resonance $3\nu_x = p$ for example. We have $m = 3, n = 0$. There are only two terms that satisfy the conditions (9.630) and therefore contribute to $h_3^{(r)}$. The result is

$$h_3^{(r)} = A_x^{3/2}(C_{3000,0}^{(3)} e^{i3\phi_x} + C_{0300,0}^{(3)} e^{-i3\phi_x}) \tag{9.631}$$

---

[67]All along we have been *assuming* the problem is integrable. This assumption is hidden in that we assumed our expressions of the effective Hamiltonian and the invariants converge in whichever perturbation calculation we have chosen. Chaos is actually a result when the system is nonintegrable. One way to appreciate the convergence of the problem is to look at the map of resonances in the (ν_x, ν_y) plane. As the order of resonances (which is defined as $|m| + |n|$) is raised, we have ever increasingly dense web of resonance lines. Obviously the number of neighboring resonances does not converge as one increases the resonance order. On the other hand, the hope is the strengths (or the width) of resonances decrease sufficiently rapidly with the resonance order, so that the effect on beam dynamics actually converge. As a result, hopefully only one of a relatively low order resonance plays a dominating role, and our analysis of this section approximately applies. In particular, the system then becomes integrable.

Similarly we can work out for all the other resonances excited by this second order map. The results are:

resonance $2\nu_x + \nu_y = p$

$$h_3^{(r)} = A_x A_y^{1/2}(C_{2010,0}^{(3)}e^{i2\phi_x+i\phi_y} + C_{0201,0}^{(3)}e^{-i2\phi_x-i\phi_y})$$

resonance $2\nu_x - \nu_y = p$

$$h_3^{(r)} = A_x A_y^{1/2}(C_{2001,0}^{(3)}e^{i2\phi_x-i\phi_y} + C_{0210,0}^{(3)}e^{-i2\phi_x+i\phi_y})$$

resonance $\nu_x + 2\nu_y = p$

$$h_3^{(r)} = A_x^{1/2} A_y(C_{1020,0}^{(3)}e^{i\phi_x+i2\phi_y} + C_{0102,0}^{(3)}e^{-i\phi_x-i2\phi_y})$$

resonance $\nu_x - 2\nu_y = p$

$$h_3^{(r)} = A_x^{1/2} A_y(C_{1002,0}^{(3)}e^{i\phi_x-i2\phi_y} + C_{0120,0}^{(3)}e^{-i\phi_x+i2\phi_y})$$

resonance $3\nu_y = p$

$$h_3^{(r)} = A_y^{3/2}(C_{0030,0}^{(3)}e^{i3\phi_y} + C_{0003,0}^{(3)}e^{-i3\phi_y})$$

resonance $2\nu_x = p$

$$h_3^{(r)} = A_x\delta(C_{2000,1}^{(3)}e^{i2\phi_x} + C_{0200,1}^{(3)}e^{-i2\phi_x})$$

resonance $\nu_x + \nu_y = p$

$$h_3^{(r)} = A_x^{1/2} A_y^{1/2}\delta(C_{1010,1}^{(3)}e^{i\phi_x+i\phi_y} + C_{0101,1}^{(3)}e^{-i\phi_x-i\phi_y})$$

resonance $\nu_x - \nu_y = p$

$$h_3^{(r)} = A_x^{1/2} A_y^{1/2}\delta(C_{1001,1}^{(3)}e^{i\phi_x-i\phi_y} + C_{0110,1}^{(3)}e^{-i\phi_x+i\phi_y})$$

resonance $2\nu_y = p$

$$h_3^{(r)} = A_y\delta(C_{0020,1}^{(3)}e^{i2\phi_y} + C_{0002,1}^{(3)}e^{-i2\phi_y})$$

resonance $\nu_x = p$

$$h_3^{(r)} = A_x^{1/2}\delta^2(C_{1000,2}^{(3)}e^{i\phi_x} + C_{0100,2}^{(3)}e^{-i\phi_x})$$
$$+A_x\delta(C_{2000,1}^{(3)}e^{i2\phi_x} + C_{0200,1}^{(3)}e^{-i2\phi_x})$$
$$+A_x^{1/2}A_y(C_{1011,0}^{(3)}e^{i\phi_x} + C_{0111,0}^{(3)}e^{-i\phi_x})$$
$$+A_x^{3/2}(C_{3000,0}^{(3)}e^{i3\phi_x} + C_{0300,0}^{(3)}e^{-i3\phi_x})$$
$$+A_x^{3/2}(C_{2100,0}^{(3)}e^{i\phi_x} + C_{1200,0}^{(3)}e^{-i\phi_x})$$

resonance $\nu_y = p$

$$h_3^{(r)} = A_y^{1/2}\delta^2(C_{0010,2}^{(3)}e^{i\phi_y} + C_{0001,2}^{(3)}e^{-i\phi_y})$$
$$+A_y\delta(C_{0020,1}^{(3)}e^{i2\phi_y} + C_{0002,1}^{(3)}e^{-i2\phi_y})$$
$$+A_x A_y^{1/2}(C_{1110,0}^{(3)}e^{i\phi_y} + C_{1101,0}^{(3)}e^{-i\phi_y})$$
$$+A_y^{3/2}(C_{0030,0}^{(3)}e^{i3\phi_y} + C_{0003,0}^{(3)}e^{-i3\phi_y})$$
$$+A_y^{3/2}(C_{0021,0}^{(3)}e^{i\phi_y} + C_{0012,0}^{(3)}e^{-i\phi_y}) \qquad (9.632)$$

The term h_3 is the same for all resonances.

There are a total of 35 C-coefficients of third order. The resonances mentioned above involve 32 C-coefficients (8 of them involved twice). The remaining 3 appeared in the function h_3.

Near the resonance (9.627), we now have

$$N = e^{:f_2:}e^{:h_3+h_3^{(r)}:} \qquad (9.633)$$

where h_3 is given by Eq.(9.517) and $h_3^{(r)}$ is given by Eqs.(9.631-9.632). Given Eq.(9.633), we next try to obtain the effective Hamiltonian of the system. To do so, it seems that we need to concatenate the two factor maps on the right hand side, which gives, to first order in $h_3^{(r)}$,

$$
\begin{aligned}
N &= \exp\left[:f_2 + \left(\frac{:f_2:}{1-e^{-:f_2:}}\right)(h_3 + h_3^{(r)}):\right] \\
&= \exp\left[:f_2 + h_3 + \left(\frac{:f_2:}{1-e^{-:f_2:}}\right)h_3^{(r)}:\right] \qquad (9.634)
\end{aligned}
$$

However, expression (9.634) contains the term

$$
\left(\frac{:f_2:}{1-e^{-:f_2:}}\right)h_3^{(r)} = \sum_{k\neq0}\sum_{ace}C_{a,a-km,c,c-kn,e}^{(3)}
$$
$$
\times\frac{ik(m\mu_x+n\mu_y)}{1-e^{-ik(m\mu_x+n\mu_y)}}A_x^{a-\frac{1}{2}km}A_y^{c-\frac{1}{2}kn}e^{ik(m\phi_x+n\phi_y)}\delta^e \quad (9.635)
$$

which is problematic because it diverges near the resonance.

To get around this problem, we will consider observing the particle motion in a frame which rotates in the phase space. Take the resonance $3\nu_x = p$ for example. We are specifically considering a transformation of coordinates from $U = (\phi_x, A_x, \phi_y, A_y, z, \delta)$ to $U' = (\phi'_x, A_x, \phi_y, A_y, z, \delta)$, where

$$\phi'_x = \phi_x - \frac{2\pi}{3}pk \qquad (9.636)$$

In Eq.(9.636), k is the turn index which increases by one unit per turn and assumes the role of the time variable. The new variable ϕ'_x, the angle variable in the rotating frame, is a slow variable because it increases by $2\pi d/3$ per turn, where $d = 3\nu_x - p$ is a small parameter [see Eq.(9.360)].

To facilitate this change of coordinates, we consider the coordinate shift map [see Exercise 95]

$$R(k) = e^{:\frac{2\pi}{3}pkA_x:}$$
$$\implies \quad R\phi_x = \phi_x - \frac{2\pi}{3}pk = \phi'_x \qquad (9.637)$$

In the new coordinate system, the map for the k-th turn (which takes the particle motion as the turn index increases from k to $k+1$) can be written as

$$
\begin{aligned}
N' &= e^{:\frac{2\pi}{3}p(k+1)A_x:}Ne^{-:\frac{2\pi}{3}pkA_x:} \\
&= [e^{:\frac{2\pi}{3}p(k+1)A_x:}e^{:f_2:}e^{-:\frac{2\pi}{3}pkA_x:}][e^{:\frac{2\pi}{3}pkA_x:}e^{:h_3+h_3^{(r)}:}e^{-:\frac{2\pi}{3}pkA_x:}] \quad (9.638)
\end{aligned}
$$

The two factor maps in the square brackets in Eq.(9.638) can be rewritten in more convenient forms. The first factor map reads

$$e^{:\frac{2\pi}{3}p(k+1)A_x:}e^{:f_2:}e^{-:\frac{2\pi}{3}pkA_x:} = e^{:f_2':}$$

(9.639)

where

$$f_2' = -\frac{2\pi}{3}dA_x - \mu_y A_y - \frac{1}{2}\alpha_c\delta^2$$

(9.640)

Equations (9.639-9.640) follow because A_x commutes with f_2. The other factor map in Eq.(9.638) can be written as

$$
\begin{aligned}
e^{:\frac{2\pi}{3}pkA_x:}&e^{:h_3+h_3^{(r)}:}e^{-:\frac{2\pi}{3}pkA_x:} \\
&= \exp\left[:e^{:\frac{2\pi}{3}pkA_x:}(h_3 + h_3^{(r)}):\right] \\
&= \exp\left[:h_3 + e^{:\frac{2\pi}{3}pkA_x:}h_3^{(r)}:\right] \\
&= \exp\left[:h_3 + 2A_x^{3/2}\mathrm{Re}\left(C_{3000,0}^{(3)}e^{i3\phi_x'}\right):\right]
\end{aligned}
$$

(9.641)

where we have substituted expression (9.631) for $h_3^{(r)}$, and Re[...] means taking the real part of the quantity [...]. We have also applied Eq.(9.509) and used

$$e^{:\frac{2\pi}{3}pkA_x:}e^{i3\phi_x} = e^{i3(\phi_x-\frac{2\pi}{3}pk)} = e^{i3\phi_x'}$$

(9.642)

In the above procedure, note in Eq.(9.640) that the quantity μ_x has been effectively replaced by the small parameter $2\pi d/3$, and in Eq.(9.641), ϕ_x has been replaced by the slow phase ϕ_x'. In the new rotating system, we are now ready to concatenate the map (9.638) without introducing a small denominator, to first order in the nonlinearity strength,

$$
\begin{aligned}
N' &= e^{:f_2':}\exp\left[:h_3 + 2A_x^{3/2}\mathrm{Re}\left(C_{3000,0}^{(3)}e^{i3\phi_x'}\right):\right] \\
&= \exp\left[:f_2' + h_3 + \left(\frac{:f_2':}{1 - e^{-:f_2':}}\right)2A_x^{3/2}\mathrm{Re}\left(C_{3000,0}^{(3)}e^{i3\phi_x'}\right):\right] \\
&= \exp\left\{:f_2' + h_3 + 2A_x^{3/2}\mathrm{Re}\left[C_{3000,0}^{(3)}\left(\frac{i2\pi d}{1 - e^{-i2\pi d}}\right)e^{i3\phi_x'}\right]:\right\}
\end{aligned}
$$

(9.643)

where we have used

$$:f_2':e^{i3\phi_x'} = i2\pi d e^{i3\phi_x'}$$

(9.644)

The expression in Eq.(9.643) is now well-behaved when $d \to 0$. The effective Hamiltonian for the one-turn map is then, in the rotating frame,

$$
\begin{aligned}
H &= \frac{2\pi}{3}dA_x + \mu_y A_y + \frac{1}{2}\alpha_c\delta^2 - C_{0000,3}^{(3)}\delta^3 - C_{1100,1}^{(3)}A_x\delta - C_{0011,1}^{(3)}A_y\delta \\
&\quad -2A_x^{3/2}\mathrm{Re}\left(C_{3000,0}^{(3)}\frac{i2\pi d}{1 - e^{-i2\pi d}}e^{i3\phi_x'}\right)
\end{aligned}
$$

(9.645)

The rotating frame thus avoids the small denominator problem. Alternatively to a rotating frame, one could apply a trick by raising the map to some

302

integer power. This amounts to observing the particle motion not once every turn, but once every few turns. For a third order resonance, for example, one would observe the system once every three turns. By "strobing" the system at three-turn intervals, one expects that the dynamics of the resonance will emerge more visibly.

We thus consider the map $M^3 = (A^{-1}NA)^3 = A^{-1}N^3A$. The dynamics are contained in the map N^3 which reads

$$
\begin{aligned}
N^3 &= (e^{:f_2:}e^{:h_3+h_3^{(r)}:})^3 \\
&= e^{3:f_2:}(e^{-2:f_2:}e^{:h_3+h_3^{(r)}:}e^{2:f_2:})(e^{-:f_2:}e^{:h_3+h_3^{(r)}:}e^{:f_2:})e^{:h_3+h_3^{(r)}:} \\
&= e^{3:f_2:}\exp[:e^{-2:f_2:}(h_3+h_3^{(r)}):]\exp[:e^{-:f_2:}(h_3+h_3^{(r)}):]e^{:h_3+h_3^{(r)}:} \quad (9.646)
\end{aligned}
$$

To first order in h_3 and $h_3^{(r)}$, this gives

$$
N^3 = e^{3:f_2:}\exp\left[:\sum_{k=0}^{2}e^{-k:f_2:}(h_3+h_3^{(r)}):\right] \quad (9.647)
$$

Since f_2 and h_3 both depend only on A_x, A_y, and δ, we have

$$
\sum_{k=0}^{2}e^{-k:f_2:}h_3 = 3h_3 \quad (9.648)
$$

The other quantity in Eq.(9.647) reads

$$
\begin{aligned}
\sum_{k=0}^{2}e^{-k:f_2:}h_3^{(r)} &= 2A_x^{3/2}\mathrm{Re}\left[C_{3000,0}^{(3)}e^{i3\phi_x}(\sum_{k=0}^{2}e^{-i3k\mu_x})\right] \\
&= 2A_x^{3/2}\mathrm{Re}\left[C_{3000,0}^{(3)}e^{i3\phi_x}\frac{1-e^{-i9\mu_x}}{1-e^{-i3\mu_x}}\right] \\
&= 2A_x^{3/2}\mathrm{Re}\left[C_{3000,0}^{(3)}e^{i3\phi_x}\frac{1-e^{-i6\pi d}}{1-e^{-i2\pi d}}\right] \quad (9.649)
\end{aligned}
$$

We next note that the factor $e^{:3f_2:}$ in Eq.(9.647) can be written as [See Eq.(9.363)]

$$
e^{:3f_2:} = e^{:3f_2':} \quad (9.650)
$$

Combining the results gives, to first order in h_3 and $h_3^{(r)}$,

$$
\begin{aligned}
N^3 &= e^{:3f_2':}\exp\left[:3h_3+2A_x^{3/2}\mathrm{Re}\left(C_{3000,0}^{(3)}e^{i3\phi_x}\frac{1-e^{-i6\pi d}}{1-e^{-i2\pi d}}\right):\right] \\
&= \exp\left\{:3f_2'+3h_3+2A_x^{3/2}\mathrm{Re}\left[C_{3000,0}^{(3)}\frac{1-e^{-i6\pi d}}{1-e^{-i2\pi d}}\left(\frac{3:f_2':}{1-e^{-3:f_2':}}\right)e^{i3\phi_x}\right]:\right\} \\
&= \exp\left\{:3f_2'+3h_3+2A_x^{3/2}\mathrm{Re}\left[C_{3000,0}^{(3)}\frac{i6\pi d}{1-e^{-i2\pi d}}e^{i3\phi_x}\right]:\right\} \quad (9.651)
\end{aligned}
$$

303

Equation (9.651) obtained by strobing agrees with Eq.(9.643) obtained by rotating the phase space. In particular, the small denominator is removed. Note that at three-turn intervals, the difference between ϕ_x and ϕ_x' disappears.

Let k be the turn index which runs from 0 to 1 per turn. The one-turn Hamilton equations of motion are, using the effective Hamiltonian (9.645),

$$\frac{d\phi_x}{dk} = \frac{\partial H}{\partial A_x} = \frac{2\pi}{3}d - C_{1100,1}^{(3)}\delta - 3A_x^{1/2}\text{Re}\left[C_{3000,0}^{(3)}\frac{i2\pi d}{1 - e^{-i2\pi d}}e^{i3\phi_x'}\right]$$

$$\frac{dA_x}{dk} = -\frac{\partial H}{\partial \phi_x'} = -2A_x^{3/2}\text{Re}\left[C_{3000,0}^{(3)}\frac{6\pi d}{1 - e^{-i2\pi d}}e^{i3\phi_x'}\right]$$

$$\frac{d\phi_y}{dk} = \frac{\partial H}{\partial A_y} = \mu_y - C_{0011,1}^{(3)}\delta$$

$$\frac{dA_y}{dk} = -\frac{\partial H}{\partial \phi_y} = 0$$

$$\frac{dz}{dk} = \frac{\partial H}{\partial \delta} = \alpha_c\delta - 3C_{0000,3}^{(3)}\delta^2 - C_{1100,1}^{(3)}A_x - C_{0011,1}^{(3)}A_y$$

$$\frac{d\delta}{dk} = -\frac{\partial H}{\partial z} = 0 \tag{9.652}$$

Take the first member of Eq.(9.652) for example. There are three terms on the right hand side. The first term describes the unperturbed betatron phase advance per turn. The second term gives the nonlinear effect which is not driven by resonance. The third term is the nonlinear resonance driven term.

There are three constants of the motion: δ, A_y, and

$$h_x = \frac{2\pi}{3}dA_x - C_{1100,0}^{(3)}A_x\delta - 2A_x^{3/2}\text{Re}\left[C_{3000,0}^{(3)}\frac{i2\pi d}{1 - e^{-i2\pi d}}e^{i3\phi_x'}\right] \tag{9.653}$$

The quantity h_x can be regarded as the effective Hamiltonian in the x phase space. For small d, and consider on-momentum particles with $\delta = 0$, we have

$$h_x \approx \frac{2\pi}{3}dA_x - 2A_x^{3/2}\text{Re}(C_{3000,0}^{(3)}e^{i3\phi_x'}) \tag{9.654}$$

In the next section [See Eq.(9.681)], we will show that for the case of a single thin-lens sextupole and observing the particle motion at the exit point of the sextupole, $C_{3000,0}^{(3)} = \frac{i}{8}\lambda(2\beta_x)^{3/2}$, where λ is the sextupole strength. For this case,

$$h_x = \frac{2\pi}{3}dA_x + \frac{\lambda}{\sqrt{2}}(\beta_x A_x)^{3/2}\sin 3\phi_x' \tag{9.655}$$

which agrees with Eq.(9.370).

From the first member of Eq.(9.652), it follows that, as ϕ_x' varies on the right hand side, $\frac{1}{2\pi}\frac{d\phi_x'}{dk}$ oscillates around the value $d/3$ with an amplitude $\Delta/3$, where, for small d,

$$\Delta = \frac{9}{2\pi}A_x^{1/2}|C_{3000,0}^{(3)}| \tag{9.656}$$

This quantity Δ can be loosely associated with a "tune resonance width" in the sense that the "tune" of the particle oscillates in time slowly with a half-width of $\Delta/3$. If a particle has $\Delta \gtrsim d$ (which happens when the particle has an unperturbed tune close to $1/3$, and its amplitude A_x is sufficiently large), its motion will exhibit a pronounced resonance response. When $\Delta \lesssim d$, the resonance behaviour would be weak. In this sense, the quantity Δ can be loosely associated with the "width" of the resonance.

So far we have been considering the resonance $3\nu_x \approx p$ which involves only the x-motion. The analysis can be extended to the coupling resonances such as the $2\nu_x + \nu_y \approx p$ resonance. The corresponding $h_3^{(r)}$ is given by Eq.(9.632). Let us define two reference tunes ν_{x0} and ν_{y0} in such a way that $\nu_x \approx \nu_{x0}$ and $\nu_y \approx \nu_{y0}$, where $\nu_{x0,y0}$ satisfy the resonance condition $2\nu_{x0} + \nu_{y0} = p$ exactly. (This definition does not give $\nu_{x0,y0}$ uniquely, but this ambiguity does not matter.) Let $2\nu_x + \nu_y = p + d$ with a small d, $|d| \ll 1$. Consider then a frame that "rotates" with frequency ν_{x0} in the x phase space and frequency ν_{y0} in the y phase space. The change of coordinates from $(\phi_x, A_x, \phi_y, A_y, z, \delta)$ to $(\phi'_x, A_x, \phi'_y, A_y, z, \delta)$, where

$$\phi'_x = \phi_x - 2\pi\nu_{x0}k, \qquad \text{and} \qquad \phi'_y = \phi_y - 2\pi\nu_{y0}k \qquad (9.657)$$

can be facilitated by the map

$$R(k) = e^{:2\pi(\nu_{x0}A_x + \nu_{y0}A_y)k:} \qquad (9.658)$$

The new map is then

$$\begin{aligned} N' &= e^{:2\pi(\nu_{x0}A_x+\nu_{y0}A_y)(k+1):} N e^{-2\pi(\nu_{x0}A_x+\nu_{y0}A_y)k:} \\ &= e^{:f'_2:} \exp\left[:h_3 + e^{:2\pi(\nu_{x0}A_x+\nu_{y0}A_y)k:} h_3^{(r)}:\right] \\ &= e^{:f'_2:} \exp\left[h_3 + 2A_x A_y^{1/2} \mathrm{Re}(C_{2010,0}^{(3)} e^{i2\phi'_x + i\phi'_y})\right] \end{aligned} \qquad (9.659)$$

where

$$f'_2 = -2\pi(\nu_x - \nu_{x0})A_x - 2\pi(\nu_y - \nu_{y0})A_y - \frac{1}{2}\alpha_c\delta^2 \qquad (9.660)$$

Concatenating the two factor maps in Eq.(9.659) gives

$$N' = e^{:-H:} \qquad (9.661)$$

where H is the effective Hamiltonian

$$\begin{aligned} H &= 2\pi(\nu_x - \nu_{x0})A_x + 2\pi(\nu_y - \nu_{y0})A_y + \frac{1}{2}\alpha_c\delta^2 \\ &\quad - C_{0000,3}^{(3)}\delta^3 - C_{1100,1}^{(3)}A_x\delta - C_{0011,1}^{(3)}A_y\delta \\ &\quad - 2A_x A_y^{1/2}\mathrm{Re}\left[C_{2010,0}^{(3)}\frac{i2\pi d}{1 - e^{-i2\pi d}}e^{i2\phi'_x + i\phi'_y}\right] \end{aligned} \qquad (9.662)$$

305

The Hamilton equations give

$$
\begin{aligned}
\frac{d\phi'_x}{dk} &= \frac{\partial H}{\partial A_x} = 2\pi(\nu_x - \nu_{x0}) - C^{(3)}_{1100,1}\delta \\
&\quad -2A_y^{1/2}\mathrm{Re}\left[C^{(3)}_{2010,0}\frac{i2\pi d}{1-e^{-i2\pi d}}e^{i2\phi'_x + i\phi'_y}\right] \\
\frac{dA_x}{dk} &= -\frac{\partial H}{\partial \phi'_x} = -2A_x A_y^{1/2}\mathrm{Re}\left[C^{(3)}_{2010,0}\frac{4\pi d}{1-e^{-i2\pi d}}e^{i2\phi'_x + i\phi'_y}\right] \\
\frac{d\phi'_y}{dk} &= \frac{\partial H}{\partial A_y} = 2\pi(\nu_y - \nu_{y0}) - C^{(3)}_{0011,1}\delta \\
&\quad -A_x A_y^{-1/2}\mathrm{Re}\left[C^{(3)}_{2010,0}\frac{i2\pi d}{1-e^{-i2\pi d}}e^{i2\phi'_x + i\phi'_y}\right] \\
\frac{dA_y}{dk} &= -\frac{\partial H}{\partial \phi_y} = -2A_x A_y^{1/2}\mathrm{Re}\left[C^{(3)}_{2010,0}\frac{2\pi d}{1-e^{-i2\pi d}}e^{i2\phi'_x + i\phi'_y}\right] \quad (9.663)
\end{aligned}
$$

The equations for dz/dk and $d\delta/dk$ are the same as those in Eq.(9.652).

As can be seen from Eq.(9.663), the resonance affects both x and y motions. There is an apparent divergence of $d\phi'_y/dk$ when $A_y \to 0$, but this does not cause problem in actual beam dynamics. There are three constants of the motion. The first two are δ and H. An inspection of Eq.(9.663) gives a third constant, i.e.,

$$
\frac{d}{dk}(A_x - 2A_y) = 0 \quad \Longrightarrow \quad A_x - 2A_y = \text{constant} \qquad (9.664)
$$

One can obtain a resonance width by associating it to the amplitude of variation of the quantity $\frac{1}{2\pi}d(2\phi'_x + \phi'_y)/dk$, which according to Eq.(9.663), for small d and $\delta = 0$, is given by

$$
\frac{1}{2\pi}\frac{d(2\phi'_x + \phi'_y)}{dk} = d - \frac{1}{2\pi}(4A_y^{1/2} + A_x A_y^{-1/2})\mathrm{Re}(C^{(3)}_{2010,0}e^{i2\phi'_x + i\phi'_y}) \qquad (9.665)
$$

In analogy to the tune width defined in Eq.(9.656), one may be tempted to introduce

$$
\Delta = (4A_y^{1/2} + A_x A_y^{-1/2})|C^{(3)}_{2010,0}| \qquad (9.666)
$$

This definition of resonance width, however, has the drawback of a divergence as $A_y \to 0$.

One can repeat the above analysis for a general resonance described as $\nu_x \approx \nu_{x0}, \nu_y \approx \nu_{y0}$ with $m\nu_{x0} + n\nu_{y0} = p$. The one-turn effective Hamiltonian, observed in the rotating frame defined by Eq.(9.657), would have the general form

$$
\begin{aligned}
H &= 2\pi(\nu_x - \nu_{x0})A_x + 2\pi(\nu_y - \nu_{y0})A_y + \frac{1}{2}\alpha_c\delta^2 \\
&\quad -h(A_x, A_y, \delta) - A_x^{|m|/2}A_y^{|n|/2}\mathrm{Re}(\epsilon e^{im\phi'_x + in\phi'_y}) \qquad (9.667)
\end{aligned}
$$

where h is some function developed in the normal form analysis and depends on A_x, A_y, and δ only, ϵ is some complex coefficient related to the strength of the resonance-driving nonlinearity.

It follows from the Hamilton equation with the Hamiltonian (9.667) that

$$\frac{d}{dk}(nA_x - mA_y) = -(n\frac{\partial H}{\partial \phi'_x} - m\frac{\partial H}{\partial \phi'_y}) = 0 \qquad (9.668)$$

This property (9.668) means the quantity $nA_x - mA_y$ is a constant of the motion. The quantity (9.664) is just its special case. In this system, the three constants of the motion are δ, H, and $nA_x - mA_y$. Property (9.668) follows because ϕ'_x and ϕ'_y appear in H as a combined quantity $m\phi'_x + n\phi'_y$.

The invariance of $nA_x - mA_y$, valid to first order in the nonlinearity strength, is an important observation. When m and n have opposite signs, i.e. the resonance is a "difference resonance", the invariance of $nA_x - mA_y$ imposes a constraint on both of the oscillation amplitudes A_x and A_y. The particle motion is then necessarily bounded and is therefore necessarily stable. For the "sum resonances", on the other hand, the invariance of $nA_x - mA_y$ does not impose a constraint on either A_x or A_y. The particle motion is not necessarily stable.

For resonances of third order and lower, the one-turn effective Hamiltonian can be written as

$$\begin{aligned} H &= 2\pi(\nu_x - \nu_{x0})A_x + 2\pi(\nu_y - \nu_{y0})A_y + \frac{1}{2}\alpha_c\delta^2 \\ &\quad -C^{(3)}_{0000,3}\delta^3 - C^{(3)}_{1100,1}A_x\delta - C^{(3)}_{0011,1}A_y\delta + H' \end{aligned} \qquad (9.669)$$

where H' has the same expression as $-h_3^{(r)}$ in Eqs.(9.631-9.632) for the corresponding resonance, except that $\phi_{x,y}$ are replaced by $\phi'_{x,y}$.

A general expression for the tune width is, for the system with effective Hamiltonian (9.667),

$$\Delta = \frac{1}{2}(\frac{m|m|}{A_x} + \frac{n|n|}{A_y})A_x^{|m|/2}A_y^{|n|/2}|\epsilon| \qquad (9.670)$$

where we have set $d = m\nu_x + n\nu_y - p$ and $\delta = 0$. For resonances of third order, for example, we have

$$|\epsilon| = \begin{cases} |C^{(3)}_{3000,0}|, & 3\nu_x = p \\ |C^{(3)}_{2010,0}|, & 2\nu_x + \nu_y = p \\ |C^{(3)}_{2001,0}|, & 2\nu_x - \nu_y = p \\ |C^{(3)}_{1020,0}|, & \nu_x + 2\nu_y = p \\ |C^{(3)}_{1002,0}|, & \nu_x - 2\nu_y = p \\ |C^{(3)}_{0030,0}|, & 3\nu_y = p \end{cases} \qquad (9.671)$$

If one would like a geometric definition of a width in the ν_x-ν_y plane around the resonance line $m\nu_x + n\nu_y = p$, it may be more appropriate to call $\Delta/\sqrt{m^2 + n^2}$ the resonance width as illustrated in Fig.9.7. It should be mentioned here that a careful examination of a strict definition of a resonance width or resonance stopband can be rather involved [see comment following Eq.(9.666)]. For our purpose, the simplistic definition seems to suffice.
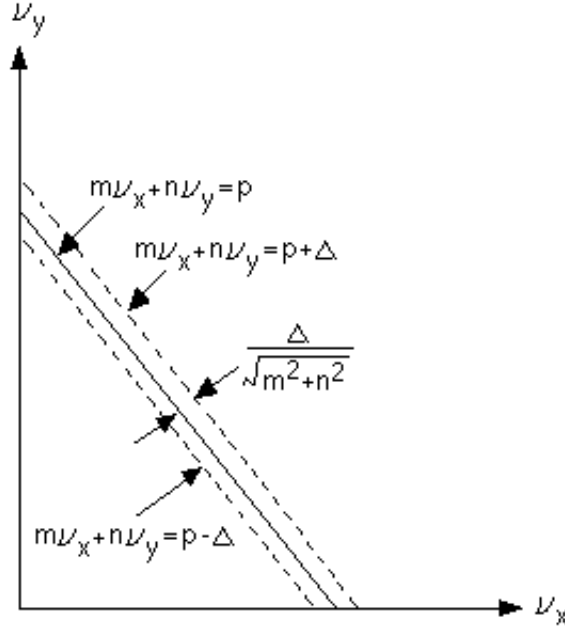
Figure 9.7: A resonance with width in the tune plot.

Smooth approximation near an isolated resonance   In the previous section, we introduced a smooth approximation for an 1-D system, under which the equations of motion of a particle can be approximately written as Eq.(9.581), where the brackets mean keeping the slowly varying terms. Away from resonances, the slowly varying terms are extracted by (9.582). When the tune is close to a rational number n/p, there are additional slow terms to be included in the smoothing process. To see this, let us first change variable from ϕ to

$$\psi = \phi - \frac{n}{p}\theta \qquad (9.672)$$

Since ϕ advances by $2\pi\nu$ per turn, and θ advances by 2π per turn, and ν is close to n/p, it is easy to see that ψ is slowly varying. We further Fourier decompose[68]

$$F(\sqrt{2A}\sin\phi, \theta) = \sum_{m=-\infty}^{\infty} \sum_{k=-\infty}^{\infty} f_{mk}(A)e^{ik\phi+im\theta} \qquad (9.673)$$

then

$$\langle \cos\phi\, F \rangle = \frac{1}{2} \sum_{q=-\infty}^{\infty} e^{iqp\psi}[f_{(-nq)(qp-1)} + f_{(-nq)(qp+1)}]$$

---

[68]This is possible because F is periodic in both θ and ϕ with period 2π.

$$\langle \sin \phi \, F \rangle = \frac{1}{2i} \sum_{q=-\infty}^{\infty} e^{iqp\psi}[f_{(-nq)(qp-1)} - f_{(-nq)(qp+1)}] \qquad (9.674)$$

In fact, Eq.(9.674) follows from the Hamiltonian

$$H(\psi, A, \theta) = (\nu - \frac{n}{p})A - \frac{\sqrt{2A}}{2\nu} \sum_{q=-\infty}^{\infty} \frac{e^{iqp\psi}}{iqp}(f_{-nq,qp-1} + f_{-nq,qp+1}) \qquad (9.675)$$

This Hamiltonian is independent of s, and is a constant of the motion. Away from resonances, only the $q = 0$ term in the summation would remain.

> *Exercise* 100 Prove Eq.(9.668) using Eq.(9.667).

> *Exercise* 101 Apply the smooth approximation to a single sextupole problem near the resonance $\nu_x = p/3$. The result should agree with Eq.(9.645) when the C-coefficients are substituted from Eq.(9.681).

Single sextupole, away from resonances We can apply the normal form results to a simple nonlinear system as an illustration of the normal form technique. The system we will study next is an otherwise-perfectly-linear circular accelerator which contains a single thin-lens sextupole. Observed at the exit point of the sextupole, the one-turn Lie map is

$$M = e^{:f_2(X):}e^{:f_3(X):} \qquad (9.676)$$

where $f_2(X)$, given by Eq.(9.535) with $\alpha, \beta, \gamma, \eta$, and η' the unperturbed lattice functions evaluated at the exit of the sextupole, describes the linear transformation of the accelerator and

$$f_3(X) = \lambda(x^3 - 3xy^2) \qquad (9.677)$$

is due to the thin-lens sextupole whose strength is given by Eq.(9.338).

We first carry out a third order normal form transformation according to

$$A = e^{:F_3(U):}A_2 \qquad (9.678)$$

where A_2 is the linear map whose matrix representation is given by Eq.(9.537). The transformed map reads

$$N = AMA^{-1} = e^{:f_2+h_3:} \qquad (9.679)$$

where f_2 here is given by Eq.(9.536). To find expressions for F_3 and h_3, we follow the normal form procedure. First, we need to express f_3 as

$$
\begin{aligned}
f_3(A_2U) &= \lambda(x^3 - 3xy^2)\big|_{x=\sqrt{\beta_x}\bar{x}+\eta\delta, \ y=\sqrt{\beta_y}\bar{y}} \\
&= \lambda(\sqrt{\beta_x}\bar{x} + \eta\delta)^3 - 3\lambda(\sqrt{\beta_x}\bar{x} + \eta\delta)(\sqrt{\beta_y}\bar{y})^2 \\
&= \lambda(\sqrt{2\beta_x A_x}\sin\phi_x + \eta\delta)^3 \\
&\quad - 3\lambda(\sqrt{2\beta_x A_x}\sin\phi_x + \eta\delta)(\sqrt{2\beta_y A_y}\sin\phi_y)^2 \qquad (9.680)
\end{aligned}
$$

We need to express the above in terms of the eigenmode functions $|abcd, e\rangle$ defined by Eq.(9.507). The result is given by Eq.(9.510) with coefficients

$$C^{(3)}_{0000,3} = \lambda\eta^3$$

$$C^{(3)}_{1000,2} = -C^{(3)}_{0100,2} = -\frac{3i}{2}\lambda\sqrt{2\beta_x}\eta^2$$

$$C^{(3)}_{2000,1} = C^{(3)}_{0200,1} = -\frac{3}{2}\lambda\beta_x\eta$$

$$C^{(3)}_{1100,1} = 3\lambda\beta_x\eta$$

$$C^{(3)}_{0020,1} = C^{(3)}_{0002,1} = \frac{3}{2}\lambda\beta_y\eta$$

$$C^{(3)}_{0011,1} = -3\lambda\beta_y\eta$$

$$C^{(3)}_{3000,0} = -C^{(3)}_{0300,0} = \frac{i}{8}\lambda(2\beta_x)^{3/2}$$

$$C^{(3)}_{2100,0} = -C^{(3)}_{1200,0} = -\frac{3i}{8}\lambda(2\beta_x)^{3/2}$$

$$C^{(3)}_{1020,0} = -C^{(3)}_{0102,0} = C^{(3)}_{1002,0} = -C^{(3)}_{0120,0} = -\frac{3i}{4}\lambda\sqrt{2\beta_x}\beta_y$$

$$C^{(3)}_{1011,0} = -C^{(3)}_{0111,0} = \frac{3i}{2}\lambda\sqrt{2\beta_x}\beta_y \quad (9.681)$$

The unlisted coefficients vanish.

Away from resonances, we have then from Eq.(9.517),

$$
\begin{aligned}
h_3 &= C^{(3)}_{0000,3}\delta^3 + C^{(3)}_{1100,1}A_x\delta + C^{(3)}_{0011,1}A_y\delta \\
&= \lambda\eta^3\delta^3 + 3\lambda\beta_x A_x\eta\delta - 3\lambda\beta_y A_y\eta\delta
\end{aligned}
\quad (9.682)
$$

and by working out the expression (9.516), we find

$$
\begin{aligned}
F_3 &= -\frac{3}{2}\lambda\sqrt{2\beta_x A_x}\eta^2\delta^2\frac{\cos(\phi_x + \frac{\mu_x}{2})}{\sin\frac{\mu_x}{2}} \\
&\quad -\frac{3}{2}\lambda\eta\delta\left[A_x\beta_x\frac{\sin(2\phi_x + \mu_x)}{\sin\mu_x} - A_y\beta_y\frac{\sin(2\phi_y + \mu_y)}{\sin\mu_y}\right] \\
&\quad +\frac{1}{8}\lambda(2\beta_x A_x)^{3/2}\left[\frac{\cos(3\phi_x + \frac{3}{2}\mu_x)}{\sin\frac{3\mu_x}{2}} - 3\frac{\cos(\phi_x + \frac{\mu_x}{2})}{\sin\frac{\mu_x}{2}}\right] \\
&\quad -\frac{3}{4}\lambda\sqrt{2\beta_x A_x}\beta_y A_y\left[\frac{\cos(\phi_x + 2\phi_y + \frac{\mu_x}{2} + \mu_y)}{\sin(\frac{\mu_x}{2} + \mu_y)}\right. \\
&\quad \left.+\frac{\cos(\phi_x - 2\phi_y + \frac{\mu_x}{2} - \mu_y)}{\sin(\frac{\mu_x}{2} - \mu_y)} - 2\frac{\cos(\phi_x + \frac{\mu_x}{2})}{\sin\frac{\mu_x}{2}}\right] \quad (9.683)
\end{aligned}
$$

The effective Hamiltonian, to first order in λ and away from resonances, is

$$
\begin{aligned}
H &= -f_2 - h_3 \\
&= \mu_x A_x + \mu_y A_y + \frac{1}{2}\alpha_c\delta^2 - \lambda\eta^3\delta^3 - 3\lambda\beta_x A_x\eta\delta + 3\lambda\beta_y A_y\eta\delta \quad (9.684)
\end{aligned}
$$

This gives the betatron tunes as

$$\nu_x(A_x, A_y, \delta) = \frac{1}{2\pi}\frac{\partial H}{\partial A_x} = \frac{1}{2\pi}(\mu_x - 3\lambda\beta_x\eta\delta)$$

$$\nu_y(A_x, A_y, \delta) = \frac{1}{2\pi}\frac{\partial H}{\partial A_y} = \frac{1}{2\pi}(\mu_y + 3\lambda\beta_y\eta\delta) \qquad (9.685)$$

The terms proportional to δ of the above expressions are contributions of the sextupole to the linear chromaticities of the accelerator design.

The effective Hamiltonian also gives an expression of the path length change per turn as

$$\Delta z(A_x, A_y, \delta) = \frac{\partial H}{\partial \delta} = \alpha_c\delta - 3\lambda\eta^3\delta^2 - 3\lambda\eta(\beta_x A_x - \beta_y A_y) \qquad (9.686)$$

As pointed out after Eq.(9.571), the linear chromaticities also appear in the path length dependences on the betatron amplitudes.

One can understand Eq.(9.685) physically as follows. As a particle passes through the sextupole with transverse displacements x and y, it receives angular kicks

$$\Delta x' = -\frac{B_y L}{B\rho} = 3\lambda(x^2 - y^2)$$

$$\Delta y' = \frac{B_x L}{B\rho} = -6\lambda xy \qquad (9.687)$$

For an off-momentum particle, the particle executes betatron oscillation relative to a displaced position $x = \eta\delta$. This makes the sextupole behave as if it is a quadrupole with strength $(L/B\rho)\frac{\partial B_y}{\partial x} = -6\lambda\eta\delta$. This leads to the chromatic part of the tune shifts as described in Eq.(9.685).

To understand Eq.(9.686), substitute

$$x = \sqrt{2\beta_x A_x}\sin\phi_x + \eta\delta, y = \sqrt{2\beta_y A_y}\sin\phi_y$$

into Eq.(9.687), and recognize the fact that $\sin\phi_{x,y}$ are rapidly oscillating from turn to turn, which means we can take averages over ϕ_x and ϕ_y to obtain

$$\Delta x' = 3\lambda(\eta^2\delta^2 + \beta_x A_x - \beta_y A_y)$$

$$\Delta y' = 0 \qquad (9.688)$$

Eq.(9.686) then follows by noting that the path length change Δz is related to $\Delta x'$ by $\Delta z = -\eta\Delta x'$ [see Exercise 93].

Having obtained Eq.(9.683), one can calculate the two betatron invariants $W_{x,y}$ in terms of the linear amplitudes $A_{x,y}$ and the phases $\phi_{x,y}$ as follows.

$$W_{x,y} = A^{-1}A_{x,y} = e^{-:F_3:}A_{x,y} = A_{x,y} - :F_3:A_{x,y} + \mathcal{O}(\lambda^2 X^4) \qquad (9.689)$$

Noting that

$$:F_3:A_{x,y} = [F_3, A_{x,y}] = \frac{\partial F_3}{\partial\phi_{x,y}} \qquad (9.690)$$

we obtain the results

$$
\begin{aligned}
W_x &= A_x - \frac{3}{2}\lambda\sqrt{2\beta_x A_x}\eta^2\delta^2\frac{\sin(\phi_x + \frac{\mu_x}{2})}{\sin\frac{\mu_x}{2}} + 3\lambda\beta_x A_x\eta\delta\frac{\cos(2\phi_x + \mu_x)}{\sin\mu_x} \\
&\quad -\frac{3}{4}\lambda\sqrt{2\beta_x A_x}\beta_y A_y\left[\frac{\sin(\phi_x + 2\phi_y + \frac{\mu_x}{2} + \mu_y)}{\sin(\frac{\mu_x}{2} + \mu_y)}\right. \\
&\qquad \left. +\frac{\sin(\phi_x - 2\phi_y + \frac{\mu_x}{2} - \mu_y)}{\sin(\frac{\mu_x}{2} - \mu_y)} - 2\frac{\sin(\phi_x + \frac{\mu_x}{2})}{\sin\frac{\mu_x}{2}}\right] \\
&\quad -\frac{3}{8}\lambda(2\beta_x A_x)^{3/2}\left[\frac{\sin(\phi_x + \frac{\mu_x}{2})}{\sin\frac{\mu_x}{2}} - \frac{\sin(3\phi_x + \frac{3\mu_x}{2})}{\sin\frac{3\mu_x}{2}}\right] + \mathcal{O}(\lambda^2 X^4) \\
W_y &= A_y - 3\lambda\beta_y A_y\eta\delta\frac{\cos(2\phi_y + \mu_y)}{\sin\mu_y} \\
&\quad -\frac{3}{2}\lambda\sqrt{2\beta_x A_x}\beta_y A_y\left[\frac{\sin(\phi_x + 2\phi_y + \frac{\mu_x}{2} + \mu_y)}{\sin(\frac{\mu_x}{2} + \mu_y)} - \frac{\sin(\phi_x - 2\phi_y + \frac{\mu_x}{2} - \mu_y)}{\sin(\frac{\mu_x}{2} - \mu_y)}\right] \\
&\quad +\mathcal{O}(\lambda^2 X^4)
\end{aligned}
\tag{9.691}
$$

These expressions are identical to Eq.(9.378) if we drop the terms proportional to δ. We have another derivation of these results later by Eq.(9.695).

How are the normalized coordinates related to the physical coordinates? We have obtained an expression of F_3 in terms of the coordinates ϕ_x, A_x, ϕ_y, A_y, and δ. One may also express it in terms of $\bar{x}, \bar{p}_x, \bar{y}, \bar{p}_y$, and δ. [See Eq.(9.498).] We first find that

$$
\begin{aligned}
F_3 &= \frac{3}{2}\lambda\sqrt{\beta_x}(\bar{x} - \cot\frac{\mu_x}{2}\bar{p}_x)\eta^2\delta^2 \\
&\quad +\frac{3}{4}\lambda[\beta_x(\bar{x}^2 - 2\cot\mu_x\bar{x}\bar{p}_x - \bar{p}_x^2) - \beta_y(\bar{y}^2 - 2\cot\mu_y\bar{y}\bar{p}_y - \bar{p}_y^2)]\eta\delta \\
&\quad +\frac{3}{8}\lambda\sqrt{\beta_x}\beta_y[-4\bar{x}\bar{y}^2 + 2\bar{p}_x(\bar{y}^2 + \bar{p}_y^2)\cot\frac{\mu_x}{2} \\
&\qquad -(2\bar{x}\bar{y}\bar{p}_y + \bar{p}_x\bar{p}_y^2 - \bar{p}_x\bar{y}^2)\cot(\frac{\mu_x}{2} - \mu_y) \\
&\qquad +(2\bar{x}\bar{y}\bar{p}_y - \bar{p}_x\bar{p}_y^2 + \bar{p}_x\bar{y}^2)\cot(\frac{\mu_x}{2} + \mu_y)] \\
&\quad +\frac{1}{8}\lambda\beta_x^{3/2}[4\bar{x}^3 - 3\bar{p}_x(\bar{x}^2 + \bar{p}_x^2)\cot\frac{\mu_x}{2} - \bar{p}_x(3\bar{x}^2 - \bar{p}_x^2)\cot\frac{3\mu_x}{2}]
\end{aligned}
\tag{9.692}
$$

The normalized coordinates U are given by

$$
\begin{aligned}
U &= A^{-1}X = e^{-:F_3:}A_2 X \\
&= e^{-:F_3:}\begin{bmatrix}\bar{x}\\\bar{p}_x\\\bar{y}\\\bar{p}_y\\\bar{z}\\\delta\end{bmatrix} = \begin{bmatrix}\bar{x}\\\bar{p}_x\\\bar{y}\\\bar{p}_y\\\bar{z}\\\delta\end{bmatrix} - :F_3:\begin{bmatrix}\bar{x}\\\bar{p}_x\\\bar{y}\\\bar{p}_y\\\bar{z}\\\delta\end{bmatrix} + \mathcal{O}(\lambda^2 X^3)
\end{aligned}
\tag{9.693}
$$

Substituting Eq.(9.692) into Eq.(9.693) gives explicit expressions of the U-coordinates, i.e. the final normal form coordinates, in terms of the coordinates $(\bar{x}, \bar{p}_x, \bar{y}, \bar{p}_y, \bar{z}, \delta)$. By relabelling $(\bar{x}, \bar{p}_x, \bar{y}, \bar{p}_y, \bar{z}, \delta)$ as $(\bar{x}_1, \bar{p}_{x1}, \bar{y}_1, \bar{p}_{y1}, \bar{z}_1, \delta)$ and substituting for $(\bar{x}_1, \bar{p}_{x1}, \bar{y}_1, \bar{p}_{y1}, \bar{z}_1, \delta)$ by Eq.(9.536), and reserving the symbols $(\bar{x}, \bar{p}_x, \bar{y}, \bar{p}_y, \bar{z}, \delta)$ for the components of U, we obtain the relation between the final normal form coordinates in terms of the original physical coordinates $(x, p_x, y, p_y, z, \delta)$ as follows:

$$
\begin{aligned}
\bar{x} &= \bar{x}_1 - \frac{3}{2}\lambda\sqrt{\beta_x}\eta^2\delta^2 \cot\frac{\mu_x}{2} - \frac{3}{2}\lambda\beta_x\eta\delta(\bar{x}_1 \cot\mu_x + \bar{p}_{x1}) \\
&\quad + \frac{3}{8}\lambda\sqrt{\beta_x}\beta_y\{2(\bar{y}_1^2 + \bar{p}_{y1}^2)\cot\frac{\mu_x}{2} \\
&\qquad\qquad + (\bar{y}_1^2 - \bar{p}_{y1}^2)[\cot(\frac{\mu_x}{2} + \mu_y) + \cot(\frac{\mu_x}{2} - \mu_y)]\} \\
&\quad - \frac{3}{8}\lambda\beta_x^{3/2}[(\bar{x}_1^2 + 3\bar{p}_{x1}^2)\cot\frac{\mu_x}{2} + (\bar{x}_1^2 - \bar{p}_{x1}^2)\cot\frac{3\mu_x}{2}] + \mathcal{O}(\lambda^2 X_1^3) \\
&= \frac{x - \eta\delta}{\sqrt{\beta_x}} - \frac{3}{2}\lambda\sqrt{\beta_x}\eta^2\delta^2 \cot\frac{\mu_x}{2} \\
&\quad - \frac{3}{2}\lambda\sqrt{\beta_x}\eta\delta[(x - \eta\delta)\cot\mu_x + \alpha_x x + \beta_x x' - \alpha_x\eta\delta - \beta_x\eta'\delta] \\
&\quad + \frac{3}{8}\lambda\sqrt{\beta_x}\{2[y^2 + (\alpha_y y + \beta_y y')^2]\cot\frac{\mu_x}{2} \\
&\qquad\qquad + [y^2 - (\alpha_y y + \beta_y y')^2][\cot(\frac{\mu_x}{2} + \mu_y) + \cot(\frac{\mu_x}{2} - \mu_y)]\} \\
&\quad - \frac{3}{8}\lambda\sqrt{\beta_x}\{[(x - \eta\delta)^2 + 3(\alpha_x x + \beta_x x' - \alpha_x\eta\delta - \beta_x\eta'\delta)^2]\cot\frac{\mu_x}{2} \\
&\qquad\qquad + [(x - \eta\delta)^2 - (\alpha_x x + \beta_x x' - \alpha_x\eta\delta - \beta_x\eta'\delta)^2]\cot\frac{3\mu_x}{2}\} + \mathcal{O}(\lambda^2 X^3)
\end{aligned}
$$

$$
\begin{aligned}
\bar{p}_x &= \bar{p}_{x1} - \frac{3}{2}\lambda\sqrt{\beta_x}\eta^2\delta^2 - \frac{3}{2}\lambda\beta_x\eta\delta(\bar{x}_1 - \bar{p}_{x1}\cot\mu_x) \\
&\quad + \frac{3}{4}\lambda\sqrt{\beta_x}\beta_y\{2\bar{y}_1^2 + \bar{y}_1\bar{p}_{y1}[\cot(\frac{\mu_x}{2} - \mu_y) - \cot(\frac{\mu_x}{2} + \mu_y)]\} \\
&\quad - \frac{3}{4}\lambda\beta_x^{3/2}\bar{x}_1[2\bar{x}_1 - \bar{p}_{x1}(\cot\frac{\mu_x}{2} + \cot\frac{3\mu_x}{2})] + \mathcal{O}(\lambda^2 X_1^3) \\
&= \frac{\alpha_x(x - \eta\delta) + \beta_x(x' - \eta'\delta)}{\sqrt{\beta_x}} - \frac{3}{2}\lambda\sqrt{\beta_x}\eta^2\delta^2 \\
&\quad - \frac{3}{2}\lambda\sqrt{\beta_x}\eta\delta[(x - \eta\delta) - (\alpha_x x + \beta_x x' - \alpha_x\eta\delta - \beta_x\eta'\delta)\cot\mu_x] \\
&\quad + \frac{3}{4}\lambda\sqrt{\beta_x}\{2y^2 + y(\alpha_y + \beta_y y')[\cot(\frac{\mu_x}{2} - \mu_y) - \cot(\frac{\mu_x}{2} + \mu_y)]\} \\
&\quad - \frac{3}{4}\lambda\sqrt{\beta_x}(x - \eta\delta)[2(x - \eta\delta) \\
&\qquad\qquad - (\alpha_x x + \beta_x x' - \alpha_x\eta\delta - \beta_x\eta'\delta)(\cot\frac{\mu_x}{2} + \cot\frac{3\mu_x}{2})] + \mathcal{O}(\lambda^2 X^3) \\
\bar{y} &= \bar{y}_1 + \frac{3}{2}\lambda\beta_y\eta\delta(\bar{y}_1 \cot\mu_y + \bar{p}_{y1})
\end{aligned}
$$

$$-\frac{3}{4}\lambda\sqrt{\beta_x}\beta_y[-2\bar{p}_{x1}\bar{p}_{y1}\cot\frac{\mu_x}{2}+(\bar{x}_1\bar{y}_1+\bar{p}_{x1}\bar{p}_{y1})\cot(\frac{\mu_x}{2}-\mu_y)$$
$$-(\bar{x}_1\bar{y}_1-\bar{p}_{x1}\bar{p}_{y1})\cot(\frac{\mu_x}{2}+\mu_y)]+\mathcal{O}(\lambda^2 X_1^3)$$
$$=\quad\frac{y}{\sqrt{\beta_y}}+\frac{3}{2}\lambda\sqrt{\beta_y}\eta\delta(y\cot\mu_y+\alpha_y y+\beta_y y')$$
$$-\frac{3}{4}\lambda\sqrt{\beta_y}\{-2(\alpha_x x+\beta_x x'-\alpha_x\eta\delta-\beta_x\eta'\delta)(\alpha_y y+\beta_y y')\cot\frac{\mu_x}{2}$$
$$+[(x-\eta\delta)y+(\alpha_x x+\beta_x x'-\alpha_x\eta\delta-\beta_x\eta'\delta)(\alpha_y y+\beta_y y')]\cot(\frac{\mu_x}{2}-\mu_y)$$
$$-[(x-\eta\delta)y-(\alpha_x x+\beta_x x'-\alpha_x\eta\delta-\beta_x\eta'\delta)(\alpha_y y+\beta_y y')]\cot(\frac{\mu_x}{2}+\mu_y)\}$$
$$+\mathcal{O}(\lambda^2 X^3)$$

$$\bar{p}_y\quad=\quad\bar{p}_{y1}+\frac{3}{2}\lambda\beta_y\eta\delta(\bar{y}_1-\bar{p}_{y1}\cot\mu_y])+\frac{3}{4}\lambda\sqrt{\beta_x}\beta_y[4\bar{x}_1\bar{y}_1-2\bar{p}_{x1}\bar{y}_1\cot\frac{\mu_x}{2}$$
$$+(\bar{x}_1\bar{p}_{y1}-\bar{p}_{x1}\bar{y}_1)\cot(\frac{\mu_x}{2}-\mu_y)-(\bar{x}_1\bar{p}_{y1}+\bar{p}_{x1}\bar{y}_1)\cot(\frac{\mu_x}{2}+\mu_y)]$$
$$+\mathcal{O}(\lambda^2 X_1^3)$$
$$=\quad\frac{\alpha_y y+\beta_y y'}{\sqrt{\beta_y}}+\frac{3}{2}\lambda\sqrt{\beta_y}\eta\delta[y-(\alpha_y y+\beta_y y')\cot\mu_y]$$
$$+\frac{3}{4}\lambda\sqrt{\beta_y}\{4(x-\eta\delta)y-2(\alpha_x x+\beta_x x'-\alpha_x\eta\delta-\beta_x\eta'\delta)y\cot\frac{\mu_x}{2}$$
$$+[(x-\eta\delta)(\alpha_y y+\beta_y y')-(\alpha_x x+\beta_x x'-\alpha_x\eta\delta-\beta_x\eta'\delta)y]\cot(\frac{\mu_x}{2}-\mu_y)$$
$$-[(x-\eta\delta)(\alpha_y y+\beta_y y')+(\alpha_x x+\beta_x x'-\alpha_x\eta\delta-\beta_x\eta'\delta)y]\cot(\frac{\mu_x}{2}+\mu_y)\}$$
$$+\mathcal{O}(\lambda^2 X^3)$$

$$\bar{z}\quad=\quad\bar{z}_1+3\lambda\eta^2\delta\sqrt{\beta_x}(\bar{x}_1-\bar{p}_{x1}\cot\frac{\mu_x}{2})+\frac{3}{4}\lambda\beta_x\eta(\bar{x}_1^2-2\cot\mu_x\bar{x}_1\bar{p}_{x1}-\bar{p}_{x1}^2)$$
$$-\frac{3}{4}\lambda\beta_y\eta(\bar{y}_1^2-2\cot\mu_y\bar{y}_1\bar{p}_{y1}+\bar{p}_{y1}^2)+\mathcal{O}(\lambda^2 X_1^3)$$
$$=\quad z+\eta'x-\eta x'+3\lambda\eta^2\delta[x-\eta\delta-(\alpha_x x+\beta_x x'-\alpha_x\eta\delta-\beta_x\eta'\delta)\cot\frac{\mu_x}{2}]$$
$$+\frac{3}{4}\lambda\eta[(x-\eta\delta)^2-2\cot\mu_x(x-\eta\delta)(\alpha_x x+\beta_x x'-\alpha_x\eta\delta-\beta_x\eta'\delta)$$
$$-(\alpha_x x+\beta_x x'-\alpha_x\eta\delta-\beta_x\eta'\delta)^2$$
$$-y^2+2\cot\mu_y y(\alpha_y y+\beta_y y')-(\alpha_y y+\beta_y y')^2]+\mathcal{O}(\lambda^2 X^3)\quad(9.694)$$

One can calculate the invariants W_x and W_y to order $\mathcal{O}(\lambda^2 X^4)$ by substituting the expressions of $\bar{x}$ and $\bar{p}_x$ in terms of $(\bar{x}_1,\bar{p}_{x1},\bar{y},\bar{p}_{y1},\bar{z}_1)$ in Eq.(9.694) into $W_x=\frac{1}{2}(\bar{x}^2+\bar{p}_x^2)$ and $W_y=\frac{1}{2}(\bar{y}^2+\bar{p}_y^2)$. This gives

$$W_x\quad=\quad\frac{1}{2}(\bar{x}_1^2+\bar{p}_{x1}^2)-\frac{3}{2}\lambda\sqrt{\beta_x}\eta^2\delta^2(\bar{x}_1\cot\frac{\mu_x}{2}+\bar{p}_{x1})$$
$$-\frac{3}{2}\lambda\beta_x\eta\delta[(\bar{x}_1^2-\bar{p}_{x1}^2)\cot\mu_x+2\bar{x}_1\bar{p}_{x1}]$$

314

$$+\frac{3}{8}\lambda\sqrt{\beta_x}\beta_y\{4\bar{p}_{x1}\bar{y}_1^2+2\bar{x}_1(\bar{y}_1^2+\bar{p}_{y1}^2)\cot\frac{\mu_x}{2}$$

$$+\bar{x}_1(\bar{y}_1^2-\bar{p}_{y1}^2)[\cot(\frac{\mu_x}{2}+\mu_y)+\cot(\frac{\mu_x}{2}-\mu_y)]$$

$$-2\bar{p}_{x1}\bar{y}_1\bar{p}_{y1}[\cot(\frac{\mu_x}{2}+\mu_y)-\cot(\frac{\mu_x}{2}-\mu_y)]\}$$

$$-\frac{3}{8}\lambda\beta_x^{3/2}\{\bar{x}_1(\bar{x}_1^2+3\bar{p}_{x1}^2)\cot\frac{\mu_x}{2}+\bar{x}_1(\bar{x}_1^2-\bar{p}_{x1}^2)\cot\frac{3\mu_x}{2}$$

$$+2\bar{x}_1\bar{p}_{x1}[2\bar{x}_1-(\cot\frac{\mu_x}{2}+\cot\frac{3\mu_x}{2})\bar{p}_{x1}]\}+\mathcal{O}(\lambda^2X_1^4)$$

$$W_y = \frac{1}{2}(\bar{y}_1^2+\bar{p}_{y1}^2)+\frac{3}{2}\lambda\beta_y\eta\delta[(\bar{y}_1^2-\bar{p}_{y1}^2)\cot\mu_y+2\bar{y}_1\bar{p}_{y1}]$$

$$+\frac{3}{4}\lambda\sqrt{\beta_x}\beta_y\{4\bar{x}_1\bar{y}_1\bar{p}_{y1}$$

$$-[\bar{y}_1(\bar{x}_1\bar{y}_1+\bar{p}_{x1}\bar{p}_{y1})-\bar{p}_{y1}(\bar{x}_1\bar{p}_{y1}-\bar{p}_{x1}\bar{y}_1)]\cot(\frac{\mu_x}{2}-\mu_y)$$

$$+[\bar{y}_1(\bar{x}_1\bar{y}_1-\bar{p}_{x1}\bar{p}_{y1})-\bar{p}_{y1}(\bar{x}_1\bar{p}_{y1}+\bar{p}_{x1}\bar{y}_1)]\cot(\frac{\mu_x}{2}+\mu_y)\}$$

$$+\mathcal{O}(\lambda^2X_1^4) \tag{9.695}$$

If we substitute $\bar{x}_1, \bar{p}_{x1}, \bar{y}, \bar{p}_{y1}$ in Eq.(9.695) respectively by $\sqrt{2A_x}\sin\phi_x$, $\sqrt{2A_x}\cos\phi_x$, $\sqrt{2A_y}\sin\phi_y$, and $\sqrt{2A_y}\cos\phi_y$, it follows that one recovers Eq.(9.691). As was mentioned there, these results also agree with those obtained in Eq.(9.378) by manipulating the BCH formula. Note also that one can obtain the connections between the invariants and the physical coordinates $(x, x', y, y', z, \delta)$ by substituting $\bar{x}_1, \bar{p}_{x1}, \bar{y}, \bar{p}_{y1}$ in Eq.(9.695) using Eq.(9.536).

So far we have looked at the second order effects. One can also explore the third order effects of this accelerator with a single sextupole. This accelerator is modeled by Eq.(9.520) with f_2 given by Eq.(9.535), f_3 given by Eq.(9.677), and $f_4 = 0$. Substituting Eq.(9.680) for f_3, (9.683) for F_3 and (9.682) for h_3 into Eq.(9.525), and after performing some algebra, one obtains, using Eq.(9.531),

$$h_4 = \frac{9}{16}\lambda^2\beta_x\beta_y^2A_y^2[4\cot\frac{\mu_x}{2}+\cot(\frac{\mu_x}{2}+\mu_y)+\cot(\frac{\mu_x}{2}-\mu_y)]$$

$$-\frac{9}{4}\lambda^2\beta_x\beta_yA_xA_y[2\beta_x\cot\frac{\mu_x}{2}+\beta_y\cot(\frac{\mu_x}{2}-\mu_y)-\beta_y\cot(\frac{\mu_x}{2}+\mu_y)]$$

$$+\frac{9}{16}\lambda^2\beta_x^3A_x^2(3\cot\frac{\mu_x}{2}+\cot\frac{3\mu_x}{2})$$

$$-\frac{9}{2}\lambda^2\beta_yA_y\eta^2\delta^2(\beta_x\cot\frac{\mu_x}{2}-\beta_y\cot\mu_y)$$

$$+\frac{9}{2}\lambda^2\beta_x^2A_x\eta^2\delta^2(\cot\frac{\mu_x}{2}+\cot\mu_x)+\frac{9}{4}\lambda^2\beta_x\eta^4\delta^4\cot\frac{\mu_x}{2} \tag{9.696}$$

The effective Hamiltonian is $-f_2-h_3-h_4$. The betatron tunes can now be carried to include terms higher order than Eq.(9.685). This gives

$$\nu_x(A_x, A_y, \delta) = \frac{1}{2\pi}\mu_x - \frac{3}{2\pi}\lambda\beta_x\eta\delta$$

$$
+\frac{9}{8\pi}\lambda^2\beta_x\beta_y A_y[2\beta_x\cot\frac{\mu_x}{2}+\beta_y\cot(\frac{\mu_x}{2}-\mu_y)-\beta_y\cot(\frac{\mu_x}{2}+\mu_y)]
$$
$$
-\frac{9}{16\pi}\lambda^2\beta_x^3 A_x(3\cot\frac{\mu_x}{2}+\cot\frac{3\mu_x}{2})
$$
$$
-\frac{9}{4\pi}\lambda^2\beta_x^2\eta^2\delta^2(\cot\frac{\mu_x}{2}+\cot\mu_x)+\mathcal{O}(\lambda^3 X^3)
$$
$$
\nu_y(A_x,A_y,\delta)=\frac{1}{2\pi}\mu_y+\frac{3}{2\pi}\lambda\beta_y\eta\delta
$$
$$
-\frac{9}{16\pi}\lambda^2\beta_x\beta_y^2 A_y[4\cot\frac{\mu_x}{2}+\cot(\frac{\mu_x}{2}+\mu_y)+\cot(\frac{\mu_x}{2}-\mu_y)]
$$
$$
+\frac{9}{8\pi}\lambda^2\beta_x\beta_y A_x[2\beta_x\cot\frac{\mu_x}{2}+\beta_y\cot(\frac{\mu_x}{2}-\mu_y)-\beta_y\cot(\frac{\mu_x}{2}+\mu_y)]
$$
$$
+\frac{9}{4\pi}\lambda^2\beta_y\eta^2\delta^2(\beta_x\cot\frac{\mu_x}{2}-\beta_y\cot\mu_y)+\mathcal{O}(\lambda^3 X^3) \tag{9.697}
$$

As mentioned before, the leading terms in the shifts of the betatron tunes from the ideal values are proportional to δ, and these are the linear chromaticity terms. In particular, on-momentum particles do not experience betatron tune shifts due to sextupoles to first order in the sextupole strength. The higher order terms, on the other hand, contains terms that do not vanish for $\delta=0$. Also as pointed out before, the ν_x dependence on A_y is the same as the ν_y dependence on A_x.

One also obtains a higher order counterpart of Eq.(9.686) for the path length,

$$
\begin{aligned}
\Delta z(A_x,A_y,\delta) &= \alpha_c\delta-3\lambda\eta^3\delta^3-3\lambda\eta(\beta_x A_x-\beta_y A_y)\\
&\quad +9\lambda^2\beta_y A_y\eta^2\delta(\beta_x\cot\frac{\mu_x}{2}-\beta_y\cot\mu_y)\\
&\quad -9\lambda^2\beta_x^2 A_x\eta^2\delta(\cot\frac{\mu_x}{2}+\cot\mu_y)\\
&\quad -9\lambda^2\beta_x\eta^4\delta^3\cot\frac{\mu_x}{2}+\mathcal{O}(\lambda^3 X^4)
\end{aligned} \tag{9.698}
$$

So far we have studied the case of perturbation by a single sextupole. What happens when there is a distribution of sextupoles is a straightforward extension [more to be added].

Smear and distortion function Equation (9.691) can be used to extract the "smears" and the "distortion functions". The x-smear S_x is the relative variation of the Courant-Snyder invariant A_x (which is a true invariant only in the linear case without the sextupole perturbation) as a function of time for an on-momentum particle. Let the peak-to-peak variation of A_x be $2\Delta A_x$. Similarly we define the y-smear S_y. To first order in λ, since W_x are W_y are true invariants, the smears are given by

$$
\begin{aligned}
S_x = \frac{\Delta A_x}{A_x} &= \frac{3}{4}\lambda\sqrt{\frac{2\beta_x}{A_x}}\beta_y A_y\left(\frac{1}{|\sin(\frac{\mu_x}{2}+\mu_y)|}+\frac{1}{|\sin(\frac{\mu_x}{2}-\mu_y)|}+\frac{2}{|\sin\frac{\mu_x}{2}|}\right)\\
&\quad +\frac{3}{8}\lambda(2\beta_x)^{3/2}A_x^{1/2}\left(\frac{1}{|\sin\frac{\mu_x}{2}|}+\frac{1}{|\sin\frac{3\mu_x}{2}|}\right)
\end{aligned}
$$

$$S_y = \frac{\Delta A_y}{A_y} \;\; = \;\; \frac{3}{2}\lambda\sqrt{2\beta_x A_x}\beta_y\left(\frac{1}{|\sin(\frac{\mu_x}{2}+\mu_y)|} + \frac{1}{|\sin(\frac{\mu_x}{2}-\mu_y)|}\right) \qquad (9.699)$$

The smears also contain the resonance denominators. Near resonances, the smears become large. The smears are sometimes used as indicators of how the system deviates from a perfectly linear system.

Smears for a distribution of sextupoles can also be found.

> *Exercise* 102 One may repeat the analysis in the text for the case of a single octupole. Consider 1-D motion. The one-turn map around the exit of the octupole is
>
> $$e^{-:\mu A:}e^{:\lambda x^4:} \qquad (9.700)$$
>
> where λ is the octupole strength, and $A = \frac{1}{2}(\gamma x^2 + 2\alpha xp + \beta p^2)$. (a) Find the invariant of the motion to first order in λ. Express it in terms of the action-angle coordinates (ϕ, A). Assume there are no resonances nearby. (b) Find the tune shift with amplitude A to first order in λ. (c) Find the invariant when the tune is close to a resonance $\nu = \frac{p}{4}$.

> *Exercise* 103 Consider a circular accelerator, which has a perfectly linear optics in its x and y motions, but is perturbed by a thin, weak quadrupole of strength $k = \frac{\partial B_y}{\partial x}\ell/B\rho$. Perform a normal form analysis to obtain the x- and y-tune shifts to second order in k. Also calculate the perturbation on the Courant-Snyder β- and α-functions to second order in k at the exit location of the perturbing quadrupole. Compare the results with an exact calculation using matrices.
> *Exercise* 104 Consider a weak thin-lens skew quadrupole with strength $k = \frac{\partial B_y}{\partial y}\ell/B\rho$. Compute the tune shifts to order $\mathcal{O}(k^2)$ (a) away from resonances, (b) near a $\nu_x \pm \nu_y = p$ resonance.

9.11   Achromats

Accelerator lattice is often constructed from building blocks. One very useful building block is a section of magnets arranged in such a way that it is transparent to particle motion, i.e. the section is there only to physically transport the beam but otherwise as if it does not exist. In particular, this section can be "unit transformations". However there is a question of how accurately the section acts as a unit transformation. An array of quadrupoles can easily make a unit transformation, but only to first order in $X = (x, x', y, y', z, \delta)$. Particularly, the higher order δ-dependence of the map often contributes to chromatic abberrations that must be compensated for. Adding sextupoles to this array of quadrupoles can make the section to act as a unit transformation to second order in X, thus providing a more accurate unit transformation section, which

we will call an achromat — in this case, a second order achromat. Similarly, if the array includes octupoles, the unit transformation can be made into a third order achromat.

First consider two thin-lens sextupoles of strengths λ_1 and λ_2 at locations 1 and 2 in an accelerator. Let us consider only the 1-D x-motion for now. Let ψ be the betatron phase advance between these two locations. Let $\alpha_{1,2}, \beta_{1,2}$, and $\gamma_{1,2}$ be the Courant-Snyder parameters at these two locations. See Fig.9.8(a). The map from the entrance of sextupole 1 to the exit of the sextupole 2 is

$$M = e^{:\lambda_1 x^3:} e^{:f_2:} e^{:\lambda_2 x^3:} \qquad (9.701)$$

where f_2 is the linear transformation from location 1 to location 2. We have

$$M = e^{:f_2:} \exp(:e^{-:f_2:} \lambda_1 x^3:) e^{:\lambda_2 x^3:} \qquad (9.702)$$
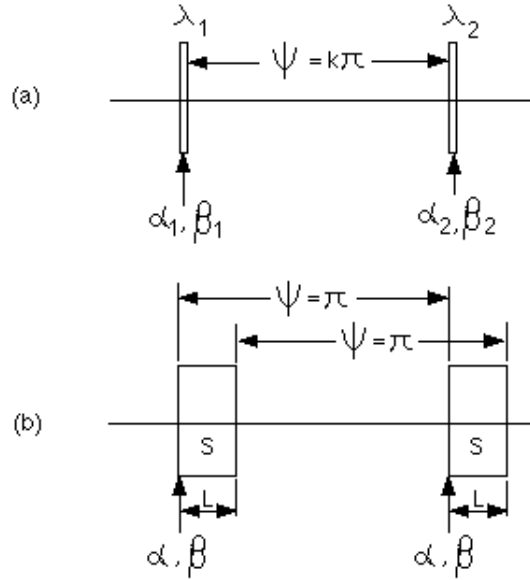

Figure 9.8: Optimal arrangement of two sextupoles.

Using Eq.(9.111), we have

$$e^{-:f_2:} x = x \sqrt{\frac{\beta_1}{\beta_2}} (\cos \psi - \alpha_2 \sin \psi) - x' \sqrt{\beta_1 \beta_2} \sin \psi \qquad (9.703)$$

This leads to

$$M = e^{:f_2:} \exp \left\{ :\lambda_1 \left[x \sqrt{\frac{\beta_1}{\beta_2}} (\cos \psi - \alpha_2 \sin \psi) - x' \sqrt{\beta_1 \beta_2} \sin \psi \right]^3 : \right\} e^{:\lambda_2 x^3:}$$

$$(9.704)$$

We now observe that the two factor exponential maps on the right of Eq.(9.704) —those involving the sextupoles — commute if $\sin\psi = 0$. In other words, if $\psi = k\pi$ for some integer k, the total map of this section reads

$$M = e^{:f_2:}\exp\left[:\lambda_1 x^3\left(\frac{\beta_1}{\beta_2}\right)^{3/2}(-1)^{3k} + \lambda_2 x^3:\right] \qquad (9.705)$$

If we further choose the sextupole strengths so that

$$\lambda_1\left(\frac{\beta_1}{\beta_2}\right)^{3/2}(-1)^{3k} + \lambda_2 = 0 \qquad (9.706)$$

then the map of the section is $e^{:f_2:}$ just as if the sextupoles were not there. Effects of the two sextupoles have cancelled each other, and the section is made optically transparent when observed outside the section.

Note that the cancellation is exact, i.e. Eq.(9.704) is not a perturbation treatment, and that the cancellation is not true if observed inside the section. Note also that in the special case when $\beta_1 = \beta_2$, the cancellation condition reads

$$\begin{cases} \lambda_1 = \lambda_2 & \text{if } \psi = \text{odd multipole of } \pi \\ \lambda_1 = -\lambda_2 & \text{if } \psi = \text{even multipole of } \pi \end{cases} \qquad (9.707)$$

Let us make a detour concerning what would affect the exact cancellation mentioned above. One situation occurs when the condition $\sin\psi$ is not exactly 0. This will be studied in Exercise 105. Another situation occurs when the sextupoles are thick, as shown in Fig.9.8(b). To be specific, let ψ — measured from the entrace of sextupole 1 to the entrance of sextupole 2 (or measured between the two exits) — be exactly equal to π, and let $\beta_1 = \beta_2$ and $\alpha_1 = \alpha_2$. Let the two sextupoles both have strength S and length L. Let us still consider 1-D motion. Inside the sextupole, the equation of motion is

$$x'' = Sx^2, \qquad \lambda = \frac{1}{3}SL \qquad (9.708)$$

The map from the entrance of sextupole 1 to the exit of sextupole 2 is

$$M = e^{:-\frac{L}{2}x'^2 + \frac{1}{3}SLx^3:}e^{:\frac{L}{2}x'^2:}e^{:f_2:}e^{:-\frac{L}{2}x'^2 + \frac{1}{3}SLx^3:} \qquad (9.709)$$

where $e^{:f_2:}$ is the linear map from the entrance of sextupole 1 to the entrance of sextupole 2. We would like to know what is the residual error of the map, to order $\mathcal{O}(L^2)$, when sextupoles are thick.

We have

$$\begin{aligned} M &= e^{:f_2:}(e^{-:f_2:}e^{:\frac{L}{2}x'^2:}e^{:f_2:})(e^{-:f_2:}e^{-:\frac{L}{2}x'^2:}e^{-:f_2:}) \\ &\times(e^{-:f_2:}e^{:-\frac{L}{2}x'^2 + \frac{1}{3}SLx^3:}e^{:f_2:})(e^{-:f_2:}e^{:\frac{L}{2}x'^2:}e^{:f_2:})e^{:-\frac{L}{2}x'^2 + \frac{1}{3}SLx^3:} \end{aligned} \qquad (9.710)$$

Using the fact that

$$e^{-:f_2:}x = -x, \qquad e^{-:f_2:}x' = -x' \qquad (9.711)$$

it follows

$$
\begin{aligned}
M &= e^{:f_2:}e^{:\frac{L}{2}x'^2:}e^{-:\frac{L}{2}x'^2:}e^{:-\frac{L}{2}x'^2-\frac{1}{3}SLx^3:}e^{:\frac{L}{2}x'^2:}e^{:-\frac{L}{2}x'^2+\frac{1}{3}SLx^3:} \\
&= e^{:f_2:}e^{:-\frac{L}{2}x'^2:}\left(e^{:\frac{L}{2}x'^2:}e^{:-\frac{L}{2}x'^2-\frac{1}{3}SLx^3:}\right)\left(e^{:\frac{L}{2}x'^2:}e^{:-\frac{L}{2}x'^2+\frac{1}{3}SLx^3:}\right) \quad (9.712)
\end{aligned}
$$

The left-most two exponential factor maps $e^{:f_2:}e^{:-\frac{L}{2}x'^2:}$ give the intended map if the scheme has worked perfectly. The "error map" due to the fact that the sextupoles are thick is therefore given by

$$
E = \left(e^{:\frac{L}{2}x'^2:}e^{:-\frac{L}{2}x'^2-\frac{1}{3}SLx^3:}\right)\left(e^{:\frac{L}{2}x'^2:}e^{:-\frac{L}{2}x'^2+\frac{1}{3}SLx^3:}\right) \quad (9.713)
$$

and we need to compute E to order $\mathcal{O}(L^3)$. To do so, one writes

$$
e^{:\frac{L}{2}x'^2:}e^{:-\frac{L}{2}x'^2+\frac{1}{3}SLx^3:} = e^{:h:} \quad (9.714)
$$

where, h can be found by applying the BCH formula Eq.(9.192) as

$$
h = \frac{1}{3}SLx^3 - \frac{1}{2}SL^2x'x^2 + \frac{1}{3}SL^3x'^2x + \frac{1}{12}S^2L^3x^4 \quad (9.715)
$$

Inserting this into Eq.(9.713) then yields

$$
\begin{aligned}
E &= e^{:-\frac{1}{3}SLx^3+\frac{1}{2}SL^2x'x^2-\frac{1}{3}SL^3x'^2x+\frac{1}{12}S^2L^3x^4:} \\
&\quad \times e^{:\frac{1}{3}SLx^3-\frac{1}{2}SL^2x'x^2+\frac{1}{3}SL^3x'^2x+\frac{1}{12}S^2L^3x^4:} \\
&= e^{:\frac{1}{6}S^2L^3x^4+\mathcal{O}(L^4):} \quad (9.716)
\end{aligned}
$$

The leading term in the error map is of the order $\mathcal{O}(L^3)$ and it behaves like an octupole.

The achromat analysis can be extended to 6-D phase space $(x, x', y, y', z, \delta)$ [more to add].

> *Exercise* 105 Consider the 1-D motion for the system shown in Fig.9.8(a) with thin-lens sextupoles. What happens if the conditions $\psi = k\pi$ or (9.706) are not satisfied exactly? Consider the case when $k = 1$, (a) what if $(\beta_1/\beta_2)^{3/2}\lambda_1 = \lambda_2 + \Delta\lambda$? (b) what if $\psi = \pi + \Delta\psi$? Give the error map to first order in $\Delta\lambda$ and $\Delta\psi$.
> *Solution* (a) The error map is
>
> $$
> E = e^{:-\Delta\lambda x^3:} \quad (9.717)
> $$
>
> The net effect is as if there is a thin-lens sextupole of strength $-\Delta\lambda$ at position 2.
> (b) Here we assume condition (9.706) is satisfied. To first order in $\Delta\psi$,
>
> $$
> M = e^{:f_2:}\exp\left[:-\lambda_2x^3 - 3x^2\Delta\psi\lambda_2(\alpha_2x + \beta_2x'):\right]e^{:\lambda_2x^3:} \quad (9.718)
> $$

An application of Eq.(9.264) then gives

$$
\begin{aligned}
M &= e^{:f_2:} \exp\left\{ : \int_0^1 du \ e^{u:-\lambda_2 x^3:} \left[-3x^2 \Delta\psi\lambda_2(\alpha_2 x + \beta_2 x') \right] : \right\} \\
&= e^{:f_2:} \exp\left\{ : -3\Delta\psi\lambda_2 \int_0^1 du \ \left[\alpha_2 x^3 + \beta_2 x^2 (x' - 3u\lambda_2 x^2) \right] : \right\} \\
&= e^{:f_2:} \exp\left[: -3\Delta\psi\lambda_2 x^2 (\alpha_2 x + \beta_2 x' - \frac{3}{2}\beta_2\lambda_2 x^2) : \right] \quad (9.719)
\end{aligned}
$$

At the exit end of sextupole 2, the trajectory of a particle gets an additional kick, to order $\mathcal{O}(\Delta\psi)$, of

$$
\begin{aligned}
\Delta x &= 3\beta_2\Delta\psi\lambda_2 x^2 \\
\Delta x' &= -3\Delta\psi\lambda_2(3\alpha_2 x^2 + 2\beta_2 xx' - 6\beta_2\lambda_2 x^3) \quad (9.720)
\end{aligned}
$$

Exercise 106 If we trace a particle with initial conditions (x_0, x_0') through the thick-sextupole achromat system of Fig.9.8(b), the particle coordinate at the exit of the system, to order $\mathcal{O}(X^3)$, is determined by

$$
\begin{cases}
x_1 = x_0 + x_0'L + \frac{1}{2}Sx_0^2 L^2 + \frac{1}{3}Sx_0 x_0' L^3 \\
x_1' = x_0' + Sx_0^2 L + Sx_0 x_0' L^2 + \frac{1}{3}S(x_0'^2 + Sx_0^3)L^3
\end{cases}
$$

$$
\begin{cases}
x_2 = -x_1 \\
x_2' = -x_1'
\end{cases}
$$

$$
\begin{cases}
x_3 = x_2 - Lx_2' \\
x_3' = x_2'
\end{cases}
$$

$$
\begin{cases}
x_4 = x_3 + x_3'L + \frac{1}{2}Sx_3^2 L^2 + \frac{1}{3}Sx_3 x_3' L^3 \\
x_4' = x_3' + Sx_3^2 L + Sx_3 x_3' L^2 + \frac{1}{3}S(x_3'^2 + Sx_3^3)L^3
\end{cases} \quad (9.721)
$$

where $(x_1, x_1'), (x_2, x_2'), (x_3, x_3')$, and $(x_4 x_4')$ are the coordinates of the particle at different stages in passing through the system with (x_4, x_4') the coordinates at the exit of sextupole 2. The connection between (x_1, x_1') and (x_0, x_0') and the connection between (x_4, x_4') and (x_3, x_3') are according to Eq.(47.41).

Equation (9.721) can be processed to give (x_4, x_4') in terms of the initial coordinates (x_0, x_0') as

$$
\begin{cases}
x_4 = -x_0 - x_0'L + \mathcal{O}(L^4) \\
x_4' = -x_0' - \frac{2}{3}S^2 L^3 x_0^3 + \mathcal{O}(L^4)
\end{cases} \quad (9.722)
$$

Compare this result with that obtained using Lie language, Eq.(9.716). _Solution_ In the Lie language, the map is given by

$$
M = e^{:f_2:} e^{:-\frac{1}{2}Lx'^2:} E \quad (9.723)
$$

where E is the error map (9.716). We need to find X_{final} where

$$X_{\text{final}} = MX\Big|_{x=x_0, x'=x'_0} \tag{9.724}$$

Note the ordering of factor maps of M is such that earlier maps occur to the left, but when performing the computations, operators to the right are applied first. After computation is completed, x and x' are set to x_0 and x'_0.

We first find

$$
\begin{aligned}
E \begin{bmatrix} x \\ x' \end{bmatrix} &= \begin{bmatrix} x \\ x' + \frac{1}{6}S^2 L^3 : x^4 : x' \end{bmatrix} + \mathcal{O}(L^4) \\
&= \begin{bmatrix} x \\ x' + \frac{2}{3}S^2 L^3 x^3 \end{bmatrix} + \mathcal{O}(L^4) \tag{9.725}
\end{aligned}
$$

This then leads to

$$X_{\text{final}} = M \begin{bmatrix} x \\ x' \end{bmatrix} = \begin{bmatrix} -x_0 - Lx'_0 \\ -x'_0 + \frac{2}{3}S^2 L^3 x_0^3 \end{bmatrix} \tag{9.726}$$

which agrees with Eq.(9.722).

9.12 Beam-beam Interaction

One of the sources of nonlinear perturbation in the storage ring collider accelerators is the beam-beam interaction. Particles in one beam, as it circulates around the storage ring, encounters the electromagnetic fields generated by the on-coming beam every time it passes by the point of collision (let it be designated $s = 0$). These fields perturb the motion of the particle being considered. This perturbation is localized at the point of collision and is very nonlinear. The beam-beam interaction perturbation is one of the main limitations on the beam intensity in colliders.

Consider first the 1-D motion. In the absence of the beam-beam perturbation, the one-turn map of the accelerator around $s = 0$ can be written as

$$
\begin{aligned}
x &= x_0 \cos \mu + \beta p_0 \sin \mu \\
p &= -\frac{x_0}{\beta} \sin \mu + p_0 \cos \mu \tag{9.727}
\end{aligned}
$$

where β is the β-function at $s = 0$, $\nu = \mu/2\pi$ is the betatron tune, and we have assumed the parameter $\alpha = 0$ at $s = 0$. Both β and μ are the nominal values unperturbed by the beam-beam interaction. In matrix form, we can represent (9.727) by the Courant-Snyder map

$$\begin{bmatrix} \cos \mu & \beta \sin \mu \\ -\frac{1}{\beta} \sin \mu & \cos \mu \end{bmatrix} \tag{9.728}$$

In Lie algebraic form, we can write the map as

$$e^{:f_2:}, \quad \text{where} \quad f_2 = -\frac{\mu}{2}\left(\frac{x^2}{\beta} + \beta p^2\right) \tag{9.729}$$

i.e.,

$$x = e^{:f_2:}x\Big|_{x=x_0,p=p_0}, \quad \text{and} \quad p = e^{:f_2:}p\Big|_{x=x_0,p=p_0} \tag{9.730}$$

We now introduce the beam-beam interaction. Consider the case when there is only one collision point around the circumference. The beam-beam perturbation is represented as a δ-function kick at $s = 0$,

$$x = x_0 \quad \text{and} \quad p = p_0 + f(x_0) \tag{9.731}$$

where $f(x)$ is the nonlinear beam-beam kick. The form of $f(x)$ depends on how particles are distributed in the on-coming beam at the collision point. For example,

$$f(x) = \frac{Nr_0}{\gamma} \begin{cases} \frac{2}{x}(1 - e^{-x^2/2\sigma^2}), & \text{round gaussian of rms radius } \sigma \\ \frac{\sqrt{2\pi}}{W}\int_{-x}^{x}\frac{dx'}{\sigma}e^{-x'^2/2\sigma^2}, & \text{flat gaussian of width } W \\ \frac{2x}{a^2} \text{ if } x < a, \quad \frac{2}{x} \text{ if } x > a, & \text{uniform disc of radius } a \end{cases} \tag{9.732}$$

where N is the number of particles in the on-coming beam, r_0 is the classical radius of the particle, γ is the relativistic Lorentz factor. We have assumed the two beam particles have the same sign of charge so that the beam-beam kick is repulsive.

The beam-beam map (9.731) can be written in Lie form as

$$e^{:F:} \quad \text{where} \quad F = \int_0^x dx' f(x') \tag{9.733}$$

The quantity $-F$ is just the potential due to the beam-beam force.

Observe the particle motion at the exit of the collision point, the one-turn map of the particle motion, in the Lie formulation, reads

$$e^{:f_2:}e^{:F:} \tag{9.734}$$

If the beam-beam perturbation is weak, we can apply the BCH formula (9.195) to concatenate the map (9.734) to obtain the effective Hamiltonian of the system. To proceed, we introduce the action-angle variables (ϕ, A) according to

$$x = \sqrt{2A\beta}\sin\phi, \quad p = \sqrt{\frac{2A}{\beta}}\cos\phi \tag{9.735}$$

and decompose $F(x)$ as a Fourier series in ϕ as

$$F(x) = \sum_{n=-\infty}^{\infty} c_n(A)e^{in\phi} \tag{9.736}$$

323

Note that in previous studies we have $c_n(A)$ as A to some power. This does not have to be the case. For the beam-beam problem, for example, as we will soon see, $c_n(A)$ are more related to the Bessel functions.

The function f_2 becomes $f_2 = -\mu A$, and we have the properties

$$:f_2:g(A) = 0, \quad :f_2:e^{in\phi} = in\mu e^{in\phi} \tag{9.737}$$

for arbitrary function $g(A)$. We then have, to first order in the beam-beam perturbation strength,

$$
\begin{aligned}
h &= f_2 + \left(\frac{:f_2:}{1 - e^{-:f_2:}} \right) F + \mathcal{O}(F^2) \\
&= -\mu A + \sum_n c_n(A) \left(\frac{in\mu}{1 - e^{-in\mu}} \right) e^{in\phi} \\
&= -\mu A + \sum_n c_n(A) \frac{n\mu}{2 \sin \frac{n\mu}{2}} e^{in\phi + i\frac{n\mu}{2}} \tag{9.738}
\end{aligned}
$$

where the one-turn map (9.734) has been concatenated into the form $e^{:h:}$.

Equation (9.738) is the expression of the beam-beam perturbed invariant, to first order of perturbation, away from resonances. Resonances appear at

$$\nu = \frac{\mu}{2\pi} = \frac{p}{n} \tag{9.739}$$

for all integers p and n, as long as $c_n \neq 0$. Near resonances, the expansion (9.738) diverges.

Away from resonances, one can make a normal form transformation which removes the oscillating terms in Eq.(9.738). The only term left will be the zero-th Fourier harmonic term, and the effective Hamiltonian becomes

$$h = -\mu A + c_0(A) \tag{9.740}$$

The tune shift due to the beam-beam perturbation is given by

$$\Delta\nu = -\frac{1}{2\pi} \frac{dc_0(A)}{dA} \tag{9.741}$$

This tune shift is a function of the amplitude A.

If we take the round gaussian beam distribution in Eq.(9.732), we have

$$F(x) = \frac{Nr_0}{\gamma} \int_0^{A\beta/2\sigma^2} \frac{d\alpha}{\alpha} (1 - e^{-2\alpha \sin^2 \phi}) \tag{9.742}$$

The decomposition coefficients c_n are

$$
\begin{aligned}
c_n(A) &= \frac{1}{2\pi} \int_0^{2\pi} d\phi\, e^{-in\phi} F(x) \\
&= \frac{Nr_0}{\gamma} \int_0^{A\beta/2\sigma^2} \frac{d\alpha}{\alpha} \frac{1}{2\pi} \int_0^{2\pi} d\phi e^{-in\phi} (1 - e^{-2\alpha \sin^2 \phi})
\end{aligned}
$$

324

$$= \frac{Nr_0}{\gamma} \int_0^{A\beta/2\sigma^2} \frac{d\alpha}{\alpha} \frac{1}{2\pi} \int_0^{2\pi} d\phi \, e^{-in\phi} [1 - e^{-\alpha} \sum_k I_k(\alpha) e^{2ik\phi}]$$

$$= \frac{Nr_0}{\gamma} \int_0^{A\beta/2\sigma^2} \frac{d\alpha}{\alpha} \begin{cases} 1 - e^{-\alpha} I_0(\alpha), & \text{if } n = 0 \\ -e^{-\alpha} I_{n/2}(\alpha), & \text{if } n = \text{even} \neq 0 \\ 0 & \text{otherwise} \end{cases} \quad (9.743)$$

In the derivation of (9.743), we have used

$$e^{x \cos y} = \sum_{k=-\infty}^{\infty} I_k(x) e^{iky} \quad (9.744)$$

where $I_k(x)$ is the Bessel function.

One observes that due to the symmetry of the beam-beam force, only even order resonances with even n are excited. Figure 9.9 shows the behavior of c_n as functions of A.
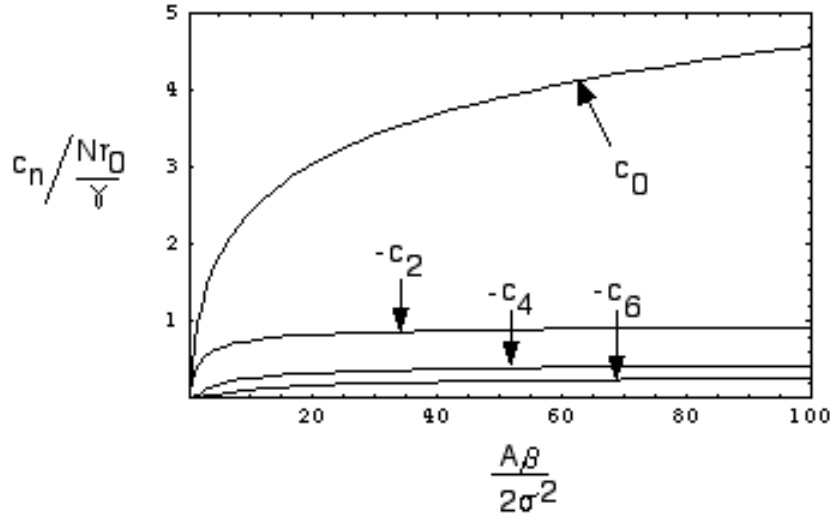

Figure 9.9: Beam-beam detuning functions. The vertical scale is $\pm c_n / \frac{Nr_0}{\gamma}$. The horizontal scale is $A\beta/2\sigma^2$.

The tune shift (9.741) reads, for a round gaussian beam,

$$\Delta\nu(A) = -\frac{1}{2\pi} \frac{Nr_0}{\gamma} \frac{d}{dA} \left[\int_0^{A\beta/2\sigma^2} \frac{d\alpha}{\alpha} (1 - e^{-\alpha} I_0(\alpha)) \right]$$

$$= -\frac{1}{2\pi} \frac{Nr_0}{\gamma A} [1 - e^{-A\beta/2\sigma^2} I_0(A\beta/2\sigma^2)] \quad (9.745)$$
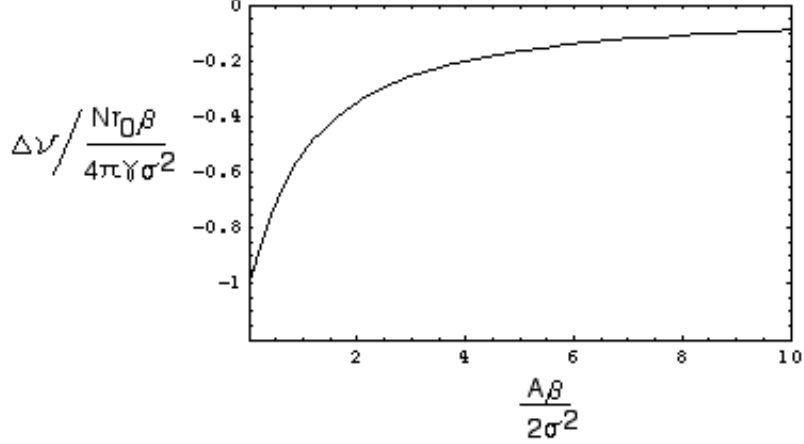
325

Figure 9.10: Beam-beam tune shift.

Plotted in Fig.9.10 is the function

$$y(x) = \Delta\nu \Big/ \frac{Nr_0\beta}{4\pi\gamma\sigma^2} = \frac{1}{x}(e^{-x}I_0(x) - 1) \tag{9.746}$$

where $x = A\beta/2\sigma^2$. For small betatron amplitudes, the tune shift is given by

$$\Delta\nu(A = 0) = -\frac{Nr_0\beta}{4\pi\gamma\sigma^2} \tag{9.747}$$

This parameter is called the *beam-beam tune shift* parameter, although it refers only to the tune shift of small-amplitude particles. As can be seen in Fig.9.10, particles with large amplitudes do not experience much tune shift. This is because, unlike forces due to magnet multipoles, the beam-beam force decreases rapidly with amplitude. An inspection of Fig.9.10 indicates that the beam-beam tune shift also has the physical meaning of the beam-beam induced tune spread of the beam.

In case the tune is close to the resonance (9.739) for some integers n and p, let

$$\nu = \frac{p}{n} + d, \quad |d| \ll 1 \tag{9.748}$$

As mentioned, the expansion (9.738) diverges. The way to proceed is to consider an n-turn map. Following the development similar to Eqs.(9.646-9.651), the n-turn map can be written as

$$e^{:n\bar{h}:} \tag{9.749}$$

where the n-turn effective Hamiltonian is given by

$$\bar{h} = \frac{d}{\nu}f_2 + \frac{d}{\nu}\left(\frac{:f_2:}{1 - e^{-nd:f_2:/\nu}}\right)[1 + e^{-:f_2:} + ...e^{-(n-1):f_2:}]F + \mathcal{O}(F^2) \tag{9.750}$$

326

After some algebraic manipulations, we arrive at

$$\bar{h} = -2\pi dA + \sum_k c_k(A) \frac{i2\pi kd}{1 - e^{-i2\pi knd}} \left(\frac{1 - e^{-ikn\mu}}{1 - e^{-ik\mu}} \right) e^{ik\phi} \qquad (9.751)$$

This expression is well-behaved at the resonance, i.e. when $d \to 0$. As pointed out before, it can be obtained by considering the expression (9.738) and taking the limit approaching the resonance.

These results are to be compared with those obtained by the smooth approximation. The phase space topology is shown in Fig.**??**. One can carry the analysis to second order in the beam-beam strength. A more elaborate application to 2-D case can also be done.

References

[1] E. D. Courant and H. S. Snyder, Ann. Phys. 3, 1 (1958).

[2] K. L. Brown, SLAC Report 75 (1967).

[3] M. Berz, H. C. Hofmann, and H. Wollnick, Nucl. Instru. Meth. A258, 402 (1987).

[4] A. Dragt, AIP Proc. 87, Phys. High Energy Accel., Fermilab, 1981, p.147.

[5] E. Forest, SSCL Report 29 (1985); E. Forest, M. Berz, and J. Irwin, Part. Accel. 24, 91 (1989); J. Irwin, SSCL Report 228 (1989); Y. Yan, AIP Proc. 249, Phys. Part. Accel., 1993, p.378.

[6] J. E. Campbell, *Proc. London Math. Soc.*, 29, 14 (1898); H. F. Baker, *London Math. Soc.*, 34, 347 (1902); F. Hausdorff, Ber. Verhandl. Akad. Wiss. Leipzig, *Math-nauturwiss*, 58, 19 (1906); V.S.Varadarajan, *Lie Groups, Lie Algebras, and Their Representations*, Prentice-Hall, Englewood Cliffs, NJ, 1974.

[7] Etienne Forest, Beat Leemann, and Swapan Chattopadhyay, SSC-N-118 (1986).

[8] Alex J. Dragt and Etienne Forest, J. Math. Phys. 24(12), 2734 (1983).

[9] Etienne Forest, David Douglas, and Beat Leemnann, Nucl. Instr. Meth. in Phys. Res. A258, 355 (1987).